

Raising Questions in the Central Mojave Desert

Robert E. Reynolds, editor



California State University Desert Studies Center
2013 Desert Symposium

April 2013

Table of contents

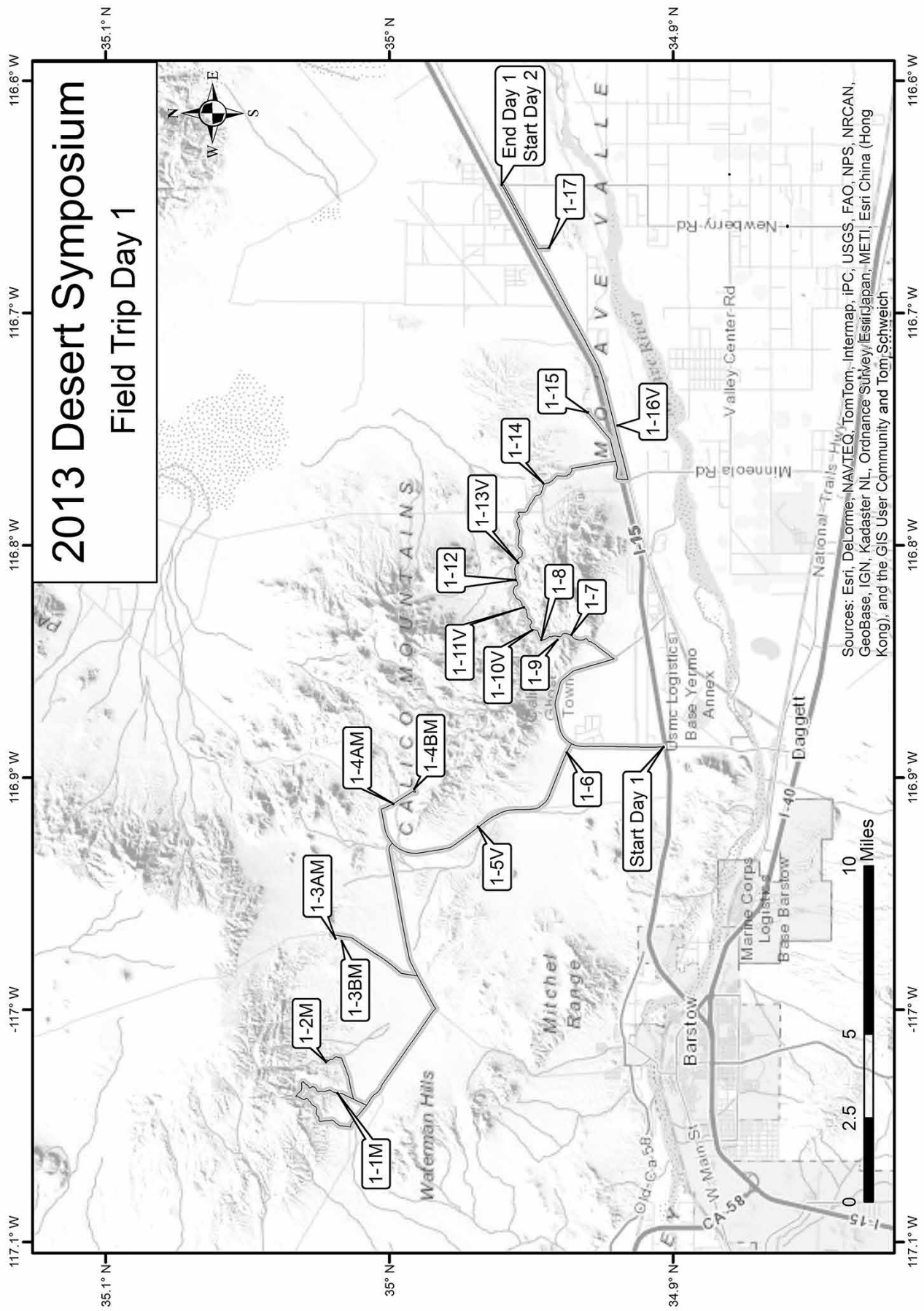
Raising questions in the central Mojave: the field trip	5
<i>David M. Miller, Peter Sadler, Kevin Schmidt, and Robert E. Reynolds, trip leaders</i>	
Paleogeographic insights based on new U-Pb dates for altered tuffs in the Miocene Barstow Formation, California	31
<i>D. M. Miller, J. E. Rosario, S. R. Leslie, and J. A. Vazquez</i>	
The Rainbow Loop Flora from the Mud Hills, Mojave Desert, California	39
<i>Robert E. Reynolds and Thomas A. Schweich</i>	
Global warming and fluctuating adult body size in the oreodont <i>Brachyerus</i> (Mammalia, Artiodactyla, Oreodontidae) during the Middle Miocene climatic optimum	49
<i>E. Bruce Lander</i>	
Nonmarine gastropods from the Temblor and Barstow formations of California	68
<i>Austin S. Pyley, Don L. Lofgren, and Andrew A. Farke</i>	
History of the Barstow Formation cricetid record	73
<i>Everett H. Lindsay and David P. Whistler</i>	
Review of <i>Megahippus</i> and <i>Hypohippus</i> from the Middle Miocene Barstow Formation of California	78
<i>Bobby Gonzalez and Don L. Lofgren</i>	
Calico—a brief overview of mining history	90
<i>Larry M. Vredenburg</i>	
The High Road to Borate	95
<i>Robert E. Reynolds</i>	
Non-vertebrate fossils in the Miocene Barstow Formation, central Mojave Desert, California	99
<i>R. E. Reynolds</i>	
Iron ore deposits of the Johnson Valley	103
<i>Douglas C. Shumway and Dinah O. Shumway</i>	
Rock avalanche setting of the Cave Mountain (Baxter Mine) iron deposits, Afton Canyon, California	107
<i>Kim M. Bishop</i>	
<i>Parapliohippus carrizoensis</i> (Perissodactyla: Equidae) from early Miocene (Hemingfordian NALMA) Barstow Formation outcrops in the southwestern Cady Mountains, Mojave Desert, California	114
<i>Robert E. Reynolds</i>	
New mammal tracks and invertebrate ichnites from Early Miocene Barstow Formation sediments on Daggett Ridge, Mojave Desert, California	117
<i>Robert E. Reynolds</i>	
Recognized, zoned, active and potentially active faulting in the Mojave Desert	121
<i>Frank F. Jordan, Jr</i>	
Vegetation lineaments near Pearblossom, CA: possible indicators of secondary faulting subparallel to the San Andreas Fault	138
<i>David K. Lynch and Frank Jordan</i>	
Population dynamics of the Joshua tree (<i>Yucca brevifolia</i>): twenty-three-year analysis, Queen Valley, Joshua Tree National Park	146
<i>James W. Cornett</i>	
Kelso Dunes mining claim validity examination	147
<i>Gregg Wilkerson</i>	
Dinosaur and arthropod tracks in the Aztec Sandstone of Valley of Fire State Park, Nevada	159
<i>Heather M. Stoller, Stephen M. Rowland, and Frankie D. Jackson</i>	

New records of fish from southern exposures of the Imperial Formation of San Diego County, California	165
<i>Mark A. Roeder</i>	
Hydrographic significance of fishes from the Early Pliocene White Narrows Beds, Clark County, Nevada	171
<i>Gerald R. Smith, Robert E. Reynolds, and Joseph D. Stewart</i>	
The terror bird, <i>Titanis</i> (Phorusrhacidae), from Pliocene Olla Formation, Anza-Borrego Desert State Park, southern California	181
<i>Robert M. Chandler, George T. Jefferson, Lowell Lindsay, and Susan P. Vescera</i>	
Persistent drought lowers estimated survival in adult Agassiz's desert tortoises (<i>Gopherus agassizii</i>) in Joshua Tree National Park: a multi-decadal perspective	184
<i>Jeffrey Lovich, Charles B. Yackulic, Jerry Freilich, Mickey Agha, Meaghan Meulblok, Kathie Meyer, . Terence R. Arundel, Jered Hansen, Michael Vamstad, and Stephanie Root</i>	
Changes in the paleogeographic distribution of <i>Mammut</i> in the southwestern United States and northwestern Mexico during the Pliocene and Pleistocene epochs	186
<i>George T. Jefferson</i>	
Halloran Springs and pre-Columbian turquoise trade	198
<i>Sharon Hull and Mostafa Fayek</i>	
Weathering climatic change: signs of prehistoric peoples	206
<i>Amy Leska</i>	
Sites I would like to see: historic Native American refugee sites in southern California	209
<i>Frederick W. Lange, Ph.D., RPA</i>	
Owlshead GPS Project	216
<i>Randy Banis</i>	
Recent meteorite falls in California	221
<i>R. S. Verish</i>	
Abstracts from the 2013 Desert Symposium	226
<i>Robert E. Reynolds, editor</i>	

Front cover: Mule Canyon

Back cover: Folded sediments in Big Borate Canyon

Title page: Mule team hauling borax ore in Mule Canyon



2013 Desert Symposium

Field Trip Day 1

Sources: Esri, DeLorme, NAVTEQ, TomTom, Intermap, IPC, USGS, FAO, NPS, NRCAN, GeoBase, IGN, Kadaster NL, Ordnance Survey, Esri/Japan, METI, Esri China (Hong Kong), and the GIS User Community and Tom, Schweich

Raising questions in the central Mojave Desert: the field trip

David M. Miller,¹ Peter Sadler,² Kevin Schmidt,¹ and Robert E. Reynolds,³ trip leaders

¹ U.S. Geological Survey

² Department of Earth Sciences, University of California, Riverside

³ Redlands, CA 92373

Day 1

More questions than constraints

Trip Leaders: David Miller, Peter Sadler, and Robert E. Reynolds

On Day 1, we will examine the well-dated type section of the Barstow Formation (Fm) in the Mud Hills. We will attempt to use that framework as the basis for interpreting the sedimentary structures and lacustrine sediments that ring the Yermo Volcanic Domes in the Calico Mountains. Trip leaders will use stratigraphy, biostratigraphy and dates on volcanic ashes to show the relation of the Barstow Fm in the Calico Mountains to the type section in the Mud Hills. Stops along route are labeled: **M**=Miocene; **Q**=Pleistocene; **V**= view without stopping; **A**, **B**, **C**=Sequence of related stops.

Convene at the Desert Studies Center in Zzyzx. Arrive with a full tank of gas in your high clearance vehicle. Carpooling is recommended, as we will be returning to the Center in the evening. Bring snacks and water; dress for cold or hot and sunny, windy weather.

Proceed north toward I-15.

Enter I-15 westbound.

Pass Afton Road.

Pass Harvard Road.

Pass under Minneola Road and through the California Agricultural Inspection Station.

Pass East Yermo exit.

Pass Calico Road.

EXIT I-15 at Ghost Town Road.

00.0 (0.0) Stop at Ghost Town Road; **Reset** trip meter. TURN RIGHT (north) on Ghost Town Road.

2.2 (2.2) TURN LEFT (west) at Yermo Cutoff.

3.9 (1.7) Stop at Ft. Irwin Road. Watch for traffic. TURN RIGHT (north).

7.9 (4.0) TURN LEFT (west) at Old Irwin Road and proceed west toward Rainbow Basin.

11.3 (3.2) Continue past Copper City Road.

12.2 (0.9) TURN RIGHT (west) on Fossil Bed Road.

15.1 (2.9) TURN RIGHT (north) on Rainbow Loop Road.

15.5 (0.4) Slow; continue past the road to Owl Canyon Camp.

15.8 (0.3) PARK on the far right side of Rainbow Loop Road.

STOP 1-1M. Walk westerly to look at outcrops¹ containing, from lowest:

Pale gray lenses in red sandstone mark a reworked tuffaceous deposit, possibly the stratigraphic position of the **Red Tuff** (19.3 Ma; NAD 83, UTM Zone 11S, 496681mE/3875311mN; Figure 1). Another exposure is located 720 feet west on the west wall of a major drainage. Greenish gray siltstone down section suggests an even earlier lacustrine incursion than the MSL (below) into the Miocene Barstow Basin, at a time somewhat contemporaneous with lacustrine sediments farther east at Harvard Hill.

Massive Stromatolite Limestone (MSL 16.7 Ma) in red sandstone (NAD 83, UTM Zone 11S, 496654mE/3875333mN; Fig. 2) consists of round calcite "heads" precipitated by blue-green algae in shallow water (Reynolds and others, 2010)..

Rak Tuff at the base of a gray mudstone section (16.3 Ma; NAD 83, UTM Zone 11S, 496527mE/3875456mN)

Brown Platy Limestone (Lowest BPL, 16.3 Ma) of marker beds (NAD 83, UTM Zone 11S 496533mE/3875458mN) consist of sheets of sandy limestone (Reynolds and others, 2010).

The short physical distance between tuffs dated 3 Ma apart (McFadden and others, 1990) may require a fault in this section, or might be attributed to an unidentified unconformity or slow basin-filling by pulses of fanglomeratic sandstone. Walk back to vehicles. Drive through Rainbow Loop Road, and RETRACE to the junction of Rainbow Loop and Owl Canyon roads.

¹ For citations, see Woodburne and Reynolds, 2010; Reynolds and others, 2010.

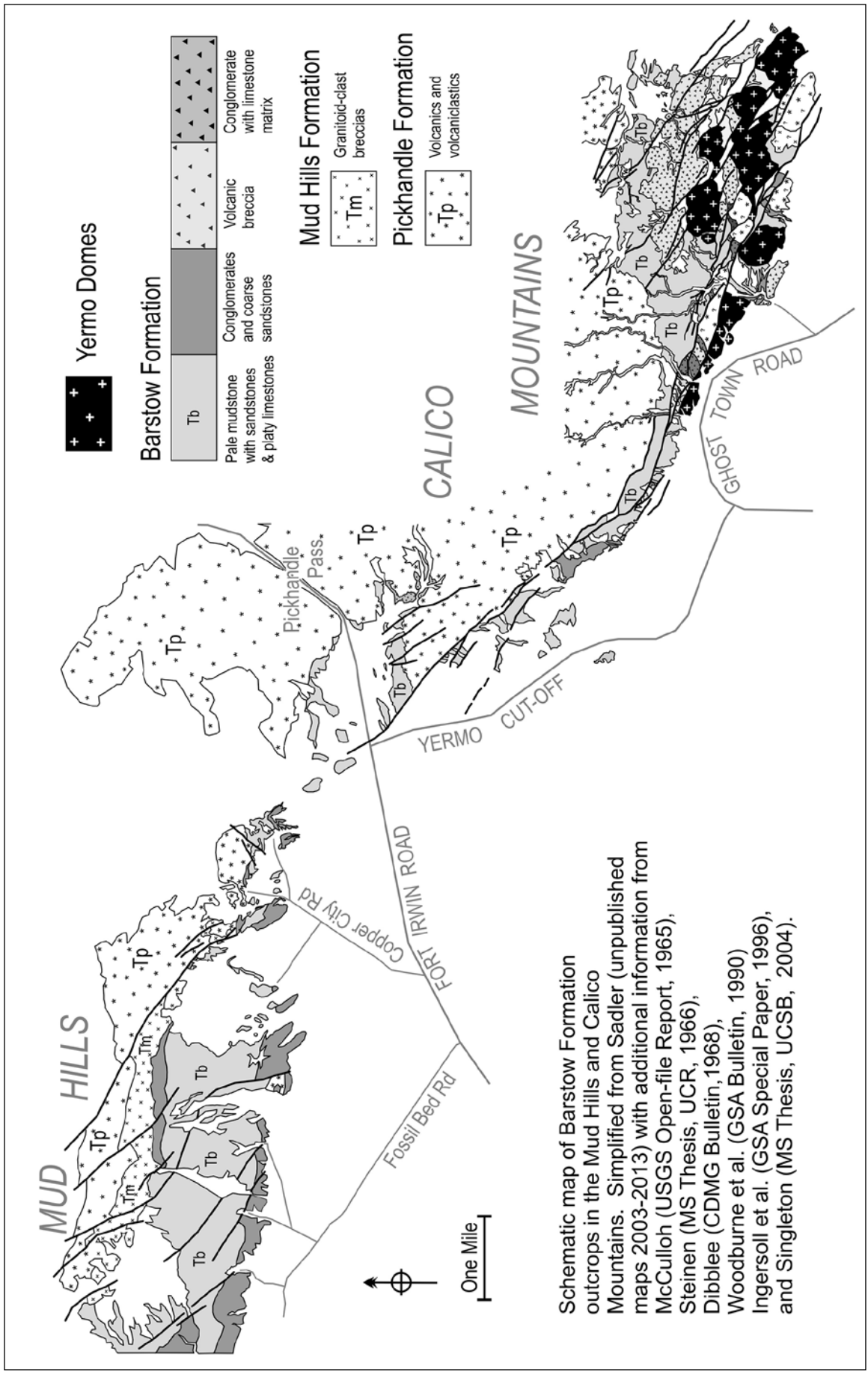


Figure 1. Schematic map of the Barstow Fm outcrops in the Mud Hills and Calico Mountains.

0.0 (00.0) Reset trip meter at the junction of Owl Canyon Road and Rainbow Loop Road. TURN RIGHT (east) toward Owl Canyon Campground.

1.0 (1.0) Continue past a right turn to the group camp and BEAR LEFT (north) after crossing the stream.

1.3 (0.3) STAY RIGHT while entering campground.

1.4 (0.1) PARK at camp #26 across from the rest rooms.

STOP 1-2M. Hike west into the wash, then south, then upslope west. This traverse will take you past the lowest BPL in green silts and upslope to the MSL. At this locality, the MSL facies is different than we saw at Stop 1-1. Here, the MSL consists of layered tufa coating large, multi-branched bushes that may have been rooted in gravel and inundated by the first local incursion of lake water constrained in an internally drained basin. The bushes were covered first with tufa and then with silt as the lake filled. Cole and others (2005) used U-Pb methods to date branching tufa mounds. Results from three dated localities are 15.39 ± 0.15 Ma and 15.30 ± 0.25 Ma at Owl Canyon Campground, and 16.25 ± 0.25 Ma on the north limb of the Barstow Syncline. Apparently, the MSL was actively depositing over nearly 1 million years along the south and north margins of the basin. This would be expected during the lacustrine deposition of an expanding basin event in tandem with alluvial fans developing from rising highlands to the north and south. The U-Pb dates may be useful in providing relative ages of lacustrine carbonates deposited across different portions of the basin. In summary, dates on tubular stromatolites and phytoherms of the MSL from the Mud Hills span a period from 16.2–15.3 Ma along a N-S line across the Barstow Syncline at this point. For one mile west, along the south limb of the syncline, the marker sequence (MSL, BPL, SrB) spans 0.5 Ma, with the MSL dating older than the comparable MSL on the north limb and approximately 1.3 Ma years older than here in Owl Canyon (Reynolds and others, 2010). These different dates reinforce the marker sequence acting as time-transgressive depositional indicators along the margins of an expanding basin. We will continue to see this time-transgressive deposition for the marker bed sequence (MSL/BPL/SrB) as we continue east through the Calico Mountains to Harvard. Walk back to vehicles. RETRACE to Fossil Bed Road.

2.9 (1.5) Slow, TURN LEFT (south) on Rainbow Loop Road.

3.3 (0.4) Stop at Fossil Bed Road. TURN LEFT (east) and proceed toward Old Irwin Road.

6.2 (2.9) Stop at Old Irwin Road. Look both directions for oncoming traffic. TURN LEFT (east) toward Copper City Road.

7.1 (0.9) TURN LEFT (north) on Copper City Road.

8.5 (1.4) Continue past a left turn to a zeolite mine pit excavated in the Skyline Tuff (Dibblee, 1968).

8.8 (0.3) View northwest of Skyline Tuff along strike from the zeolite pit.

9.4 (0.4) Watch for oncoming traffic and prepare to turn left.

9.5 (0.1) TURN LEFT. Drive southwest to the low hills south of green andesite hills (Figure 2).

9.6 (0.1) PARK between low hills.

STOP 1-3M. Walk to MSL on north (**1-3AM**) and BPL on south (**1-3BM**). Notice the change in appearance as we examine equivalent facies laterally and at different water depths along the lake shoreline.

PROCEED southwest.

9.8 (0.2) **STOP 1-3CM** “Yellow Tuffs” (16.5 Ma). This tuff is similar to one of a pair 1.5 km east along strike in Gypsum Basin, dated by Miller and others (2013). Color, physical characteristics, and position in the section suggest that the tuff here correlates with those to the east. The date on this tuff suggests that the MSL and BPL are similar in age to marker units at Owl Canyon and along Rainbow Loop road. As the trip proceeds east through the Calicos, we will not find the same tuffs as we have seen in the Mud Hills. However, we will be able to keep track of geologic events by additional tuff dates and biostratigraphic age control.

RETRACE to Copper City Road.

10.1 (0.3) STOP at Copper City Road. Watch for traffic, TURN RIGHT (south) toward Old Irwin Road.

12.4 (2.3) Stop at Old Irwin Road. TURN LEFT (east) toward Ft. Irwin Road.

15.8 (3.4) Stop at Ft. Irwin Road. Watch for traffic. TURN LEFT (northeast) toward Pickhandle Pass.

16.5 (0.7) Prepare to turn right.

16.6 (0.1) TURN RIGHT (southeast) toward the BLM kiosk; proceed on BLM Route 7615.

17.0 (0.4) PARK on right side of road.

STOP 1-4AM. Examine north-dipping Barstow Fm succession deposited on Pickhandle Fm surface along the northwestern margin of the Calico Mountains, south of Fort Irwin Road (Figure 3). PARK on dirt road outboard of mountains and proceed down section across strike (southeast). Note some similarities with the succession at Copper City Road (1-3BM) and Gypsum Basin (1-3AM). 1) The youngest unit is a thick sequence of immature, dark-colored, conglomeratic sandstones. 2) Microbialite mounds occur sporadically along an older horizon that parallels the basal unconformity. 3) The basal lithology,

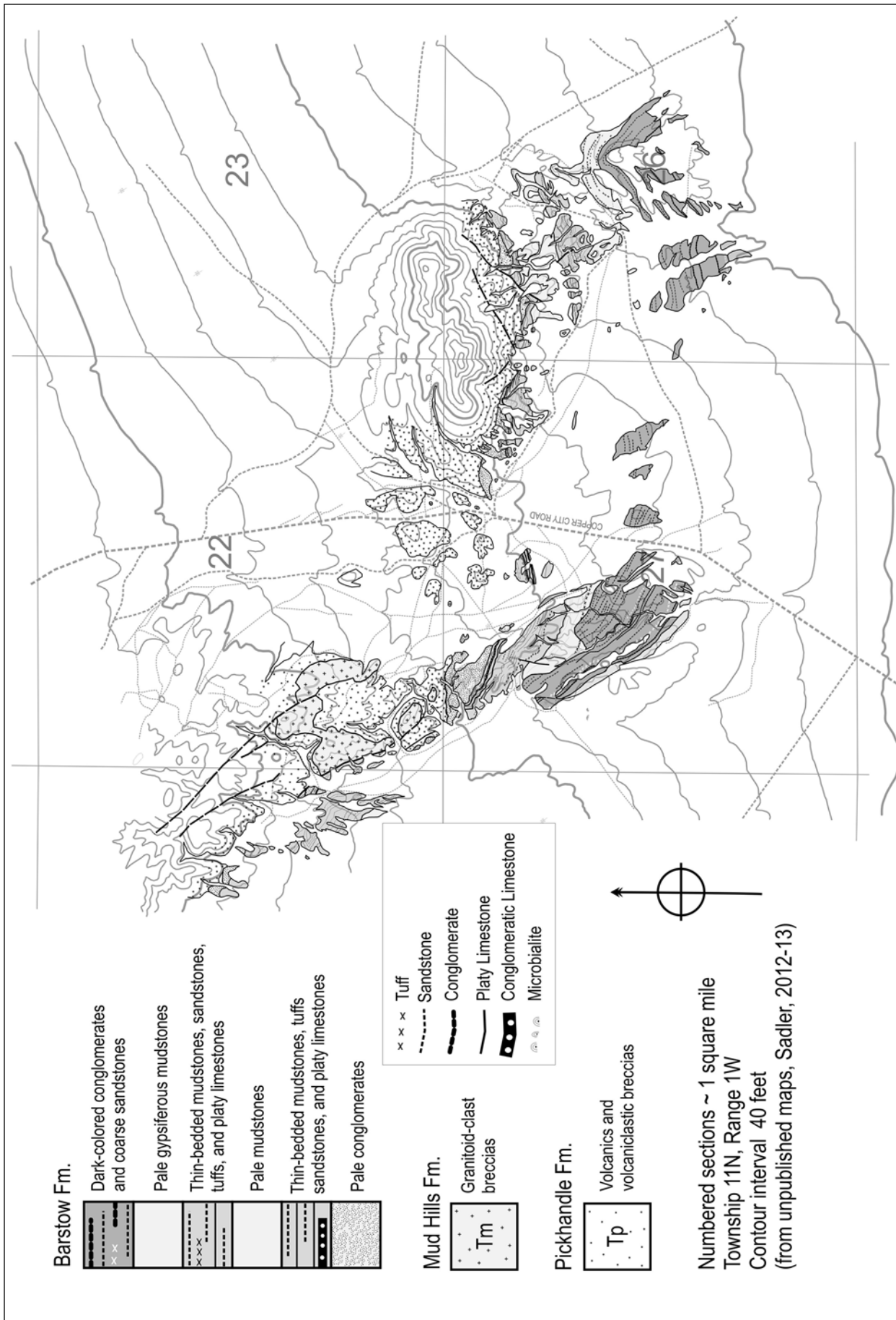


Figure 2. The Barstow, Mud Hills, and Pickhandle formations near Copper City Road.

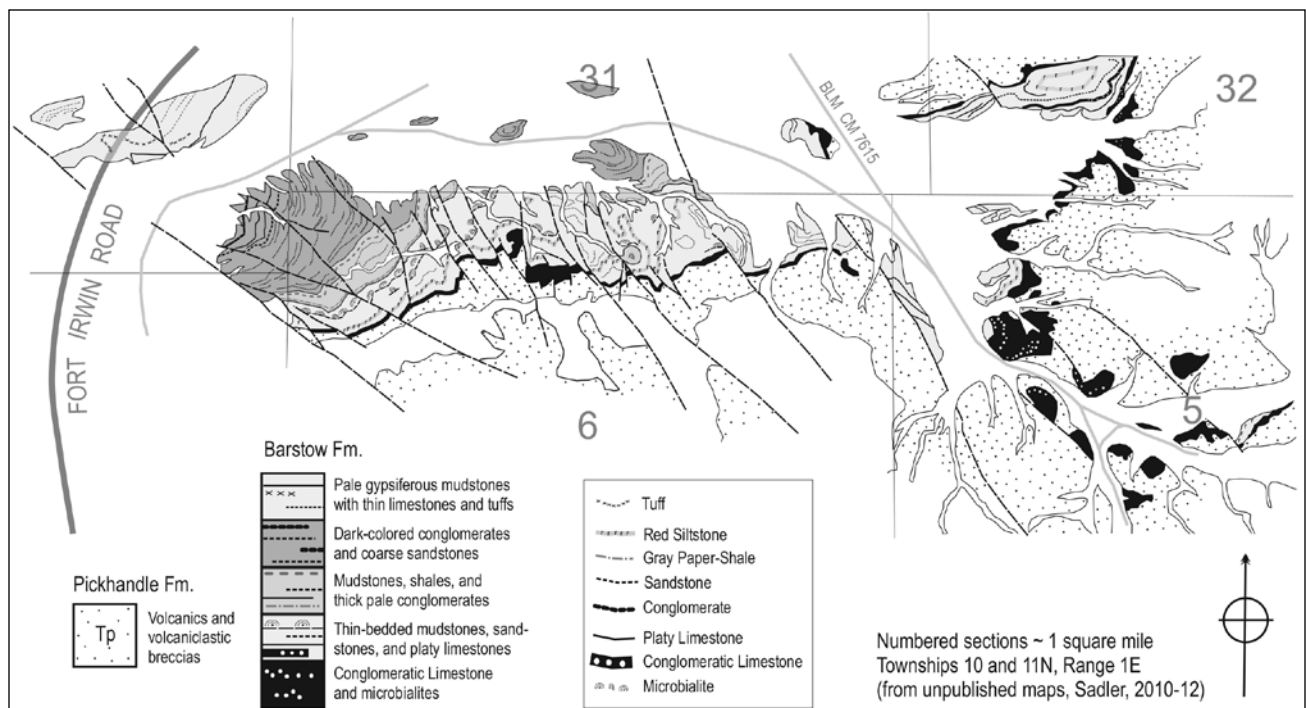


Figure 3. The Pickhandle Fm, south near Fort Irwin Road.

in contact with Pickhandle Fm breccias, is a persistent brown limestone of variable thickness with local microbial structures or volcanic clasts. Many small faults at a high angle to strike displace the Barstow sequence; some are lined with travertine. Other features are unlike Copper City Road and Gypsum basin: the pale-colored basal conglomeratic sandstones are missing; the interval between the conglomeratic sandstones and the basal limestones contains red beds and pale-colored, more mature conglomerates; tuffs are not such a prominent component.

17.1 (0.1) DIP! Drive left around a gully.

17.5 (0.4) The road bears left (east) past turns to the right (south).

17.6 (0.1) PARK on the left side of the road.

STOP 1-4BM. Russ' Mailbox Locality in Northwest Calico Mountains. At the eastern end of the Barstow Fm outcrop in the northwestern Calico Mountains, the basal brown limestone is thickest and hosts large cobbles. The thick limestone interval lies directly on ~19Ma Pickhandle dacite. The rounded and sub-rounded pebbles suggest a substantial period of weathering; the age of the limestone host may therefore be significantly younger than the weathered Pickhandle substrate. The brown limestone contains approximately 50% pebbles at its base, but becomes finer upward and has vertically oriented pores that resemble the texture of the tufa at Travertine Point (Salton Sea). This five meter thick limestone section may represent a lacustrine onlap facies. A very similar, but coarser, limestone-hosted conglomerate is locally developed at the Pickhandle contact between Copper City

Road and Gypsum Basin; dips are much steeper there and the limestone conglomerate can be traced laterally away from the Pickhandle where it becomes a thinner brown platy limestone. In the area around Stop 1-4BM, dips are gentler and brown limestone can be seen resting on the Pickhandle over a large area. The lesson from these two relationships is that the brown limestones and conglomerates, while forming the local base of the Barstow Formation, are not necessarily the oldest Barstow beds in the region, or even of the same age everywhere.

RETRACE to Ft. Irwin Road.

18.6 (1.0) Stop at Ft. Irwin Road, watch for traffic, and TURN RIGHT (west).

19.4 (0.8) Continue past Old Irwin Road; proceed south.

21.8 (2.4) **MP VIEW 1-5V**—Strachan Road to Langtree area. Sandstones to the east contain imprints of horse hooves that measure 50% smaller than those present in the Barstovian land mammal age (LMA) sediments of the Mud Hills (Reynolds, 2006). This may indicate that sediments in this portion of the Calico Mts. are from a (pre-Barstovian) Hemingfordian age greater than 16 Ma.

23.4 (1.6) Watch oncoming traffic and prepare for left turn.

23.6 (0.1) TURN LEFT (east) at Yermo Cutoff.

25.0 (1.4) PARK off the pavement on the right side of the road at the west end of the concrete block fence.

STOP 1-6M View north of the Waterloo Mine. The Waterloo narrow gauge railroad grade is located immediately northwest (Myrick, 1966). View northeast: Cemetery



Figure 4. White ashes at Cemetery Ridge. (Stop 1-6).

Ridge is a narrow swath of Barstow Fm beds that are folded between two strands of the Calico fault. A fossil flamingo egg was recovered from these sediments (Reynolds, 1998). It includes beds similar to the BPL in a sandstone sequence, and two white tuffaceous beds near the BPL sequence. Miller and others (2013) report a maximum age of 18.6 Ma for one of these ash beds. Because only six zircon grains were used in the analysis, there is uncertainty about the age, but no younger zircons were evident. This tuff age makes the BPL older here than we saw farther to the west in the Mud Hills. The ghost town of Calico is perched on a younger terrace that overlies the Barstow Fm

on the east side of Wall Street Canyon. Fossils from the west side of Wall Street (Tb-mc of McCulloh and perhaps Tbc3-4 of Singleton) include phalanges from a Hemingfordian NALMA size horse and the edentulous jaw of a small bear dog (*Amphicyon* sp.), suggesting that these sediments are late Hemingfordian.

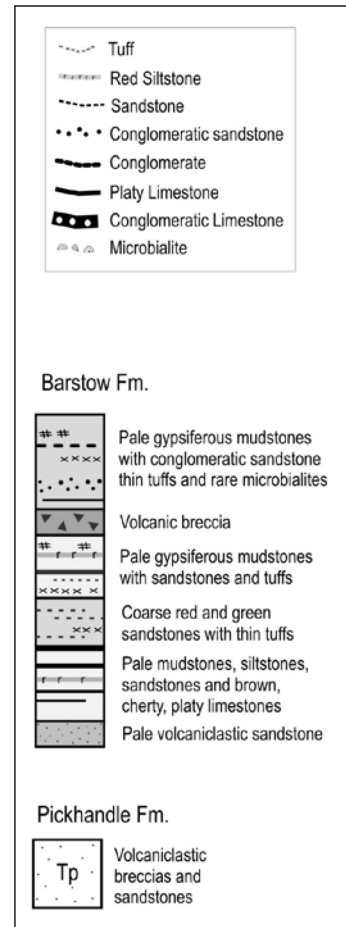
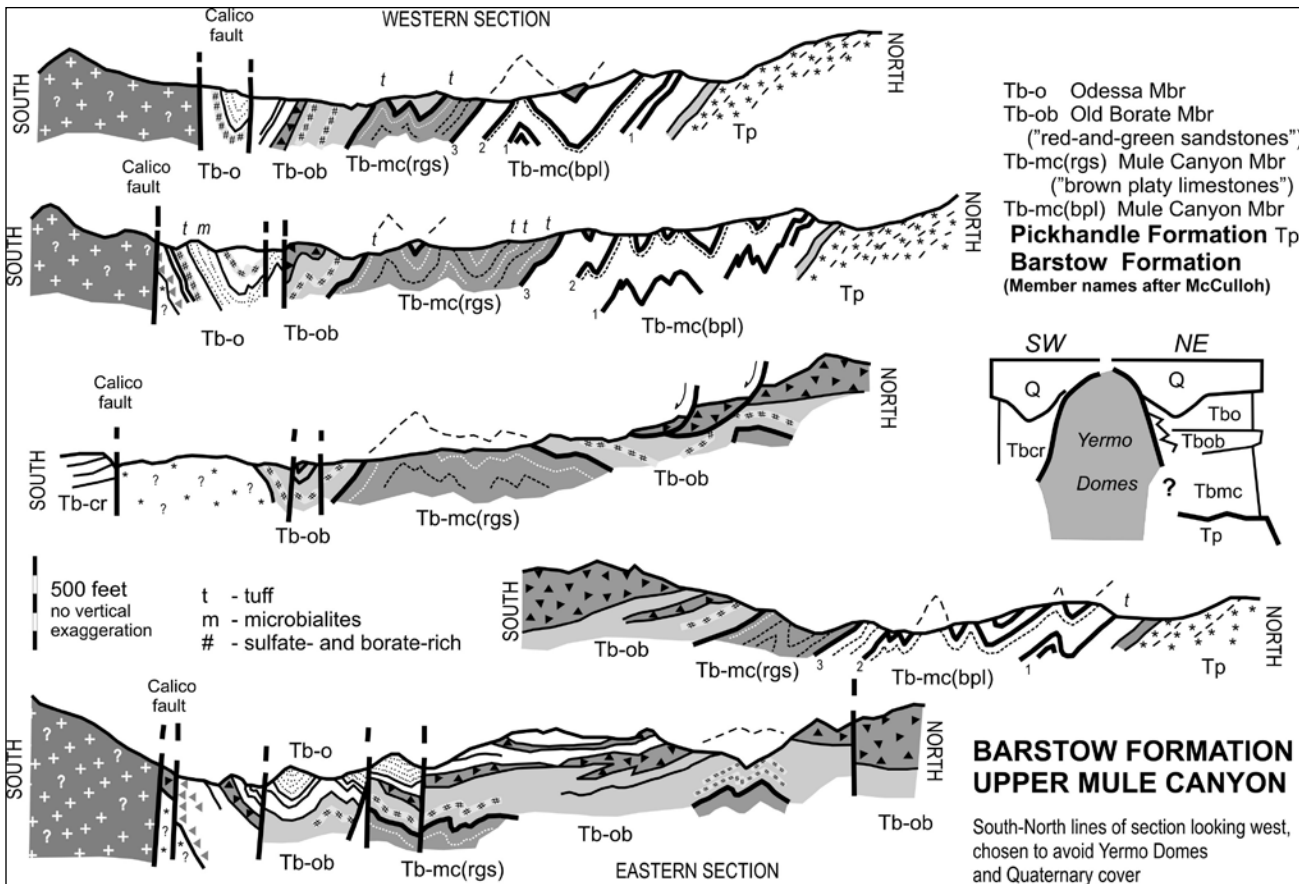
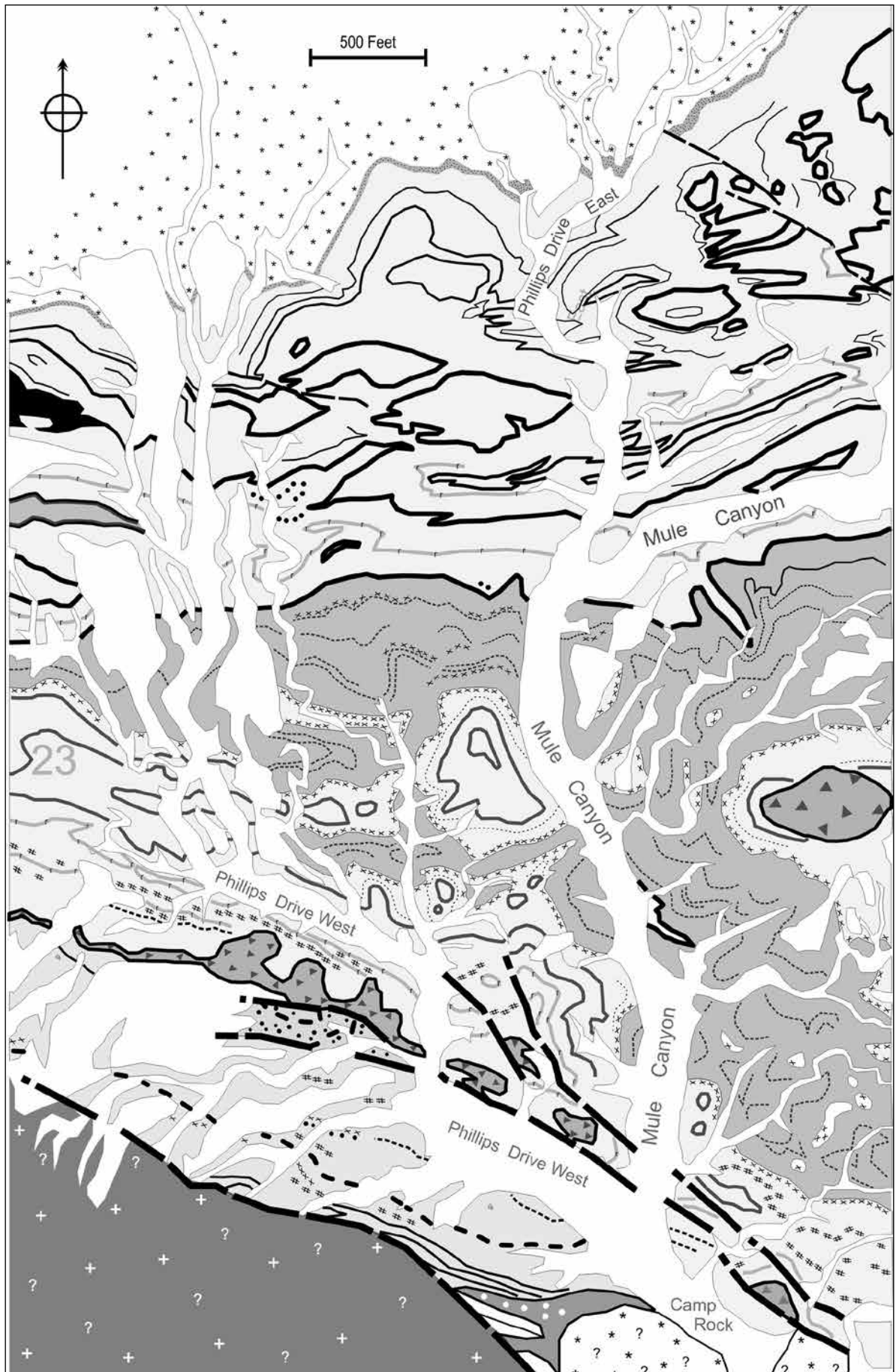


Figure 5 a, b, c. The Barstow and Pickhandle formations in Mule Canyon: schematic map, key, and cross sections.





PROCEED EAST to Ghost Town Road.

25.5 (0.2) Stop at Ghost Town Road and watch for traffic. TURN LEFT (northeast).

26.3 (1.1) Pass the entrance to Calico Ghost Town and Wall Street Canyon.

26.5 (0.2) Pass the Garfield (Silver King) mill structure from the 1880s on the left (north; Weber, 1966); pink mill tailings are to the right.

26.8 (0.3) Continue past a left turn (north) into Doran Scenic Drive.

27.2 (0.45) Pass Barber's mill site (1880s; Weber, 1966) and tailings on the right (southwest).

28.3 (1.1) TURN LEFT (northeast) on Mule Canyon Road.

28.9 (0.6) Enter Mule Canyon. Continue past the closed route to the Calico Lace Onyx Mine on the left.

29.5 (0.6) **STOP 1-7M View: Kill Bill Movie Site.** The sequence of Barstow Fm facies observed while driving north from the entrance of Mule Canyon to Camp Rock is not readily correlated with the sections exposed at the earlier stops. These beds crop out between strands of the Calico Fault. Coarse volcanic breccias form the walls of the gorge at the canyon mouth. Next come coarse conglomerates exposed in the south limb and core of an open anticline seen to the south of the road. Erosion of the conglomerate outcrop has left a small cylindrical stack-like landform near the fold core. Similar structures account for the name "Chimney Rock" in a canyon farther southeast; there the coarse conglomerates form the base of the Barstow Formation. The conglomerates in Mule Canyon lie beneath the volcanic breccia and on top of a sequence of pale red and mustard-colored sandstones and siltstones that includes brown platy limestones. The mustard-colored facies crops out behind the site of Bud's trailer in the Kill Bill movies!

29.6 (0.1) Cross the trace of the Camp Rock fault running east-southeast to west-northwest.

29.8 (0.2) Camp Rock is on the left. This massive rock was the overnight stop for the 20 mule team borax freight wagons running between the railhead at Daggett and the borax mining town of Borate via Mule Canyon in late 1880s (Hildebrand, 1982).

29.9 (0.1) We are at the junction with West Phillips Drive, and will return here (Stop 1-9M) after the next stop. Proceed north on Mule Canyon Road.

30.3 (0.4) PARK at junction with East Phillips Drive.

STOP 1-8M . Fork left from Mule Canyon Road onto the east end of Phillips Drive. PARK next to folded brown slabby limestones exposed in the walls of the wash. Walk north (upstream, down section) to the

Pickhandle-Barstow Fm contact. Red-brown volcaniclastic sandstones and breccias of the Pickhandle Fm are readily distinguishable in the hills to the north. At the contact with overlying, pale yellow Barstow Formation, there is a coarse, pale, lithic sandstone. Above this sandstone come the soft pale yellow sandstone and mudstone slopes that characterize so much of the Barstow Formation. There is no basal limestone and no microbialite in this region. Up section, three distinctive brown slabby limestones crop out in laterally ridges, separated by pale sandstones and siltstones. The oldest of the three is a red-brown, cherty, hematitic limestone; the second is a yellow-brown, cherty limestone that locally includes crinkly laminations; and the youngest is a brown sandy limestone with numerous intraclasts. The trio may be traced west to Odessa Canyon and Calico Ghost Town. Midway between the limestones are thin red beds; very rarely there are also small lenses of cobbles of crystalline basement rocks. Thin impersistent limestone beds in this interval have wrinkle mark attributable to microbial films. The youngest of the ridge-forming brown slabby limestones crops out repeatedly across the landscape to the west in a series of chevron folds. Up-section, to the south of the limestone ridges, lies a wide outcrop of immature red and green sandstones and three or more very thin tuffs. Exposed bedding planes reveal wave-ripples. Farther south comes a pale colored interval of gypsiferous mudstones, sandstones, and thin tuffs.

RETRACE south to Camp Rock (Stop 1-9).

30.7 (0.4) **STOP 1-9M** Camp Rock. To see the youngest part of the section, drive south back to Camp Rock and turn right along the west end of Phillips Drive (Figure 5). PARK where the road follows strike after right and left turns. Lateral equivalents of the commercial borate interval crop out south of the road. The ridge to the south is capped by a dacite breccia bed usually attributed to a source among the volcanic Yermo Domes (~17.0 Ma, Singleton and Gans, 2008). The breccia bed thins westward. Follow it west to a low dry waterfall where the overlying section of pale sandstones, siltstones, and brown platy limestones is exposed. Locally, these youngest beds of the Barstow Fm in Upper Mule Canyon include thin tuffs and microbialites.

Follow the dacite breccia bed to the east, toward Camp Rock, or drive back along Phillips Drive. Where the road turns to pass between breccia outcrops, the breccia is folded. Upsection, to the south, are exposures of coarse conglomeratic sands and brown platy limestones within pale green gypsiferous mudstones and sandstones. Clambering up the boulder-strewn slopes immediately northwest of Camp Rock reveals exposures of breccias, limestone-hosted conglomerates, and brown platy limestones. This facies association is reminiscent of the Barstow-Pickhandle onlap elsewhere. It is seen next to several volcanic dome(?) outcrops east and west of Mule



Figure 6. West end of High Road to Borate used by empty wagons.

Canyon along the Calico fault. This introduces the possibility that some volcanic outcrops attributed to the intrusive Yermo Domes may be part of an older Pickhandle relief. The marginal facies would be talus and landslide deposits, perhaps in the moat of an older dacite dome. We might examine the interbedded dacite breccia to try to determine whether it was a blocky ash flow from an active dome or a landslide deposit formed by sector collapse of an older volcanic edifice.

In order to explain the range of radio-isotopic dates and the estimated ages of vertebrate fossil finds in the Calico Mountains, we have three freedoms to depart from the simple model of a layer-cake Barstow Fm that rests on



Figure 7. West end of downhill route for loaded borax wagons.

Pickhandle Fm and is intruded by younger Yermo Domes. First, we should surely imagine substantial relief on the Pickhandle surface. Second, we may allow the brown limestones and microbialites to be an onlap facies of variable age at the edge of the Barstovian lake. Third, we might admit the possibility that some dacite outcrops are not younger Yermo Domes but may be part of the relief that predates some of the Barstow beds in the Mule Canyon area.

PROCEED northeast through Mule Canyon (BLM CM7630) toward Little Borate Canyon.

31.2 (0.5) Continue past Stop 1-8 and the junction with East Phillips Drive.

31.5 (0.3) **VIEW 1-10H.** The road to the left (Figure 6) is the High Road to Borate (Reynolds, 2013). Empty borax freight wagons going to Little Borate and Borate apparently took this northern route, possibly to avoid loaded freight wagons returning from Borate on the way to Camp Rock and Daggett. This northern route gained 310 feet within half a mile, quite a feat for 20 mules pulling two wagons that each weighed 7800 pounds even without a load of ore, as well as the water wagon!

31.6 (0.1) Continue past a left turn into the canyon (Figure 7) that served as a downhill route for loaded borax freight wagons returning west, downhill from the borate mines.

We will pass the east end of this route at the summit.

32.2 (0.5) **SUMMIT: VIEW 1-11H:** Summit of Mule Canyon Road. The canyon immediately north contains wagon wheel ruts running west, downhill from the borate mines to Camp Rock. This suggests that the graded portion of Mule Canyon Road that we traveled, with road cuts that removed large volumes of rock, was not built until 1894–98 (Hildebrand, 1982; Myrick, 1963) when stream tractors and, later, a narrow gauge railroad were employed to haul ore from the borate mines.

VIEW EAST of the level Borate to Daggett narrow gauge railroad grade (Myrick, 1963). Engineers attempted to balance the waste rock removed from large railroad cuts by filling

canyons. When too deep, canyons were crossed with trestles. The railroad was designed to reach the portals of the mine adits, thereby reducing the manpower necessary to load ore and the amount of lumber to support ore shoots, and cutting the cost of transportation (Hildebrand, 1982). PROCEED EAST.

32.5 (0.3) Pass the junction on left with the High Road to Borate which merges from the northwest.

33.0 (0.5) Pass the mouth of Little Borate Canyon. The blue-gray waste rock on the canyon wall upstream from here was placed to stabilize the trestle supports. Stubs of sawn timbers remain, but all usable wood from trestles and buildings at Borate was hauled to the richer borax operations in Death Valley in 1907 (Hildebrand, 1982). The canyon leads west to the Happy Hollow Camp at the Little Borate mines.

33.1 (0.1) **STOP 1-12M. PARK.** Note the recumbent folds of less competent siltstone between competent massive silty sandstone to the north.

Walk east to a thin tuff bed in sandstone to discuss its stratigraphic position. The tuff is about 17.6 Ma (Miller and others, 2013) and lies below a gray limestone with sparse stromatolitic structures that may represent the MSL. However, thin brown limestones lie down section toward the top of the Pickhandle Fm, raising ambiguity in correlation of the marker beds. A much thicker section of BPL is up section from the MSL at the entrance to Little Borate canyon, where they support remains of the railroad trestle. A proboscidean track is located at the top of that BPL section, and suggests a date 16.2 Ma (Reynolds and Woodburne, 2002). PROCEED EAST.

33.4 (0.2) Continue past Tin Can Alley on the left. The mining town of Borate was operated in a very wholesome and sanitary fashion. Trash from the town to the south was hauled out and dumped in this canyon.

33.6 (0.2) **VIEW 1-13H:** Pass Big Borate Canyon on the right. The Borax Consolidated, Ltd. company town contained a dining hall, recreation room, store, and bunk houses (Hildebrand, 1986; Reynolds, 1999). Mining at Borate and Little Borate is significant because it was the first attempt at underground, hard-rock mining of borax. Previously, water soluble sodium borates were gathered from dry playas. Underground mining recovered large volumes of relatively insoluble calcium borate (colemanite) which needed cleaning from clay matrix, roasting/ calcining, and then dissolution to become marketable. Shafts deepened, ore became scarce, and the entire operation, including the narrow gauge railroad, was moved in 1907 from Borate to Death Valley (Hildebrand, 1986).

33.8 (0.2) Pass the Sulfur Hole on the right. Unusual hydrous iron sulfates (Cooper and others, 2002) were precipitated along fractures by ground water leaching metallic sulfides in the silicified BPL (Schuiling, 1999).

34.1 (0.3) Look back southwest to the blue-gray dumps of the eastern Reserve Claims in the borate zone. Pick-handle Fm andesite outcrops on the north side of the road have been quarried for decorative yard and roofing rock. The andesite porphyry is a good example of a massive to flow-banded intrusive volcanic rock with phenocrysts of plagioclase, sanidine, biotite, and hornblende to 3 mm.

34.8 (0.7) Stay left at a fork in road.

34.9 (0.1) **TURN RIGHT** (south) at the pole line road.

35.1 (0.2) **TURN LEFT** (southeast) where the road divides, and proceed toward Minneola Road. At this point we cross the buried trace of the Tin Can Alley fault, an active right-lateral fault (Dudash, 2006).

35.9 (0.8) **TURN LEFT** into Emerald Basin after passing the toe of the ridge.

36.1 (0.2) **PARK** in **Emerald Basin.**

STOP 1-14M: Discuss dated ashes. This section of the Barstow Fm is younger than it is at Little Borate. It includes a lower conglomerate, lime and emerald colored tuffs, succeeded by a sandstone section, and then a mudstone section. A meter-thick chalcedony horizon connects this section westward to about MP 34.1. The prominent white cliff at the top is a soil and groundwater discharge deposit formed at the base of the overlying Yermo Gravel. The highest thick tuff in the mudstone section yielded an age of 15.5 Ma and one near the base of the mudstone section is 16.2 Ma (Miller and others, 2013). No marker beds are present in this section, despite being of similar age to the lower part of the lacustrine section in the Mud Hills, where the limestones occur.

RETRACE south.

36.2 (0.1) Proceed south toward Minneola Road.

37.0 (0.9) Stop at Collection Center Road. Directly ahead is the road to the Calico Mountains Archaeological Excavation. **TURN RIGHT** (south) toward Sunrise Canyon Road and Minneola Road.

38.1 (1.1) Stop at paved Sunrise Canyon Road. **TURN LEFT** (east).

38.3 (0.2) Pavement ends. **BEAR RIGHT** onto dirt road.

38.5 (0.2) Continue right through the Y junction.

38.7 (0.2) Proceed northeast along power line road.

39.5 (0.9) **PARK** at Toomey Hills. The abrupt rise of the hills is caused by the Manix fault, which lies near our location. The hills are primarily a fold complex caused by a restraining bend of the fault.

STOP 1-15M: Toomey Hills. **STOP 1-15M:** Toomey Hills. The stratigraphy at this exposure (conglomerate, lime and emerald colored tuffs) is very similar to that in Emerald

Basin, but no tuffs have been dated. This locality has produced the Yermo Hills Local Fauna, the lower section containing the small three-toed horse *Parapliohippus carrizoensis*, while a larger horse, *Acritohippus stylodontis*, occurs at the top of the section, demonstrating faunal change across the He/Ba transition at 16 Ma (Woodburne and Reynolds, 2010). Stickleback fish at this outcrop suggest that the drainage connected to the Pacific Ocean (Bell and Reynolds, 2010). RETRACE to Sunrise Canyon Road.

40.3 (0.8) The power line road turns right (west).

40.7 (0.4) Proceed west on pavement of Sunrise Canyon Road.

41.3 (0.6) TURN LEFT (south) on Minneola Road and cross over I-15.

41.5 (0.2) Continue past the eastbound ramp of I-15. The road cut exposes a sharp vertical contact between gray Lake Manix beach sands and tan gravels from the Mojave River delta and the Calico Mountains. The contact marks the trace of the Calico fault (Bortugno and Spittler, 1986), which curves in a restraining bend here, causing shortening and uplift of the sediments.

41.6 (0.1) Stop, TURN LEFT (east) onto Yermo Road.

42.7 (1.1) **VIEW 1-16Q** We are starting across the fluvial plain built by the Mojave River after Lake Manix drained (~24 ka; Reheis et al., 2007) and before the river entrenched its modern channel (after ~12 ka; Reynolds and Reynolds, 1996). This plain obscures underlying sediments and geomorphic features, but it also provides a nearly flat surface that can be examined for Holocene tectonic deformation. We passed one scarp associated with the Calico fault, and will cross more associated with the Dolores Lake fault. Day 2 will visit normal faults that deform the fluvial plain. Even without detailed topography, several playas and stream channels that postdate the plain can provide information. Near here, two stream channels zig-zag across the plain through the primary channel topography of the plain to the Mojave River. These channels drain water from stream flow in alluvial fans that lead east and south from the Calico Mountains. Farther east, we cross a few small stream channels that connect tiny fans at the east end of the Toomey Hills to the Mojave River, and farther north there are channels that lead from fans of the Yermo Hills to low areas of Coyote Lake. Several questions arise: Why do some drainages into Coyote Lake wander east across the plain when past Mojave River channels ran west of Agate Hill, then north into Coyote Lake? Was there regional tilt after development of the fluvial plain? Was the block west of Dolores Lake fault tilted? Playas at the toes of big fans shed north from the Newberry Mountains and Daggett Ridge suggest there never was enough stream flow to carve channels to the Mojave River. Why were streams on those

big fans less active in the Holocene than those on much smaller fans from the Calico–Yermo–Toomey hills area? Perhaps there is greater runoff and little infiltration into a bentonitic Barstow Fm substrate, so that the latter hills have greater stream flow response to rainfall events, while the former only respond with stream flow to big rainfall events. If so, there were few big events since the Mojave River carved its channel and stopped building the fluvial plain.

43.9 (1.2) Pass Coyote Lake Road and the I-15 overpass.

45.9 (2.0) On the right (south), the Lake Dolores fault (Meek, 1994) is represented by down-to-the-west, N 20° W trending scarps heading toward Agate Hill. At this location, it is represented by two scarps, indicating two one-meter+ steps to the east. These faults are covered by Holocene alluvium along the west side of Harvard Hill, where they appear to be cut by the through-going strands of the Manix fault (Leslie and others, 2010). The Dolores Lake fault cuts Mojave River gravels on the upper part of the Mojave River plain, which vary in age, but are dated closer to Yermo at about 11 ka (Reynolds and Reynolds, 1991). Harvard Hill lies to the south as we proceed along Yermo Road.

48.4 (2.5) Stop at Harvard Road. TURN RIGHT (south). Cross railroad tracks and immediately TURN RIGHT on a dirt road paralleling the south side of tracks. Proceed west on the dirt road.

49.5 (1.1) Pass tamarisk trees at a railroad siding.

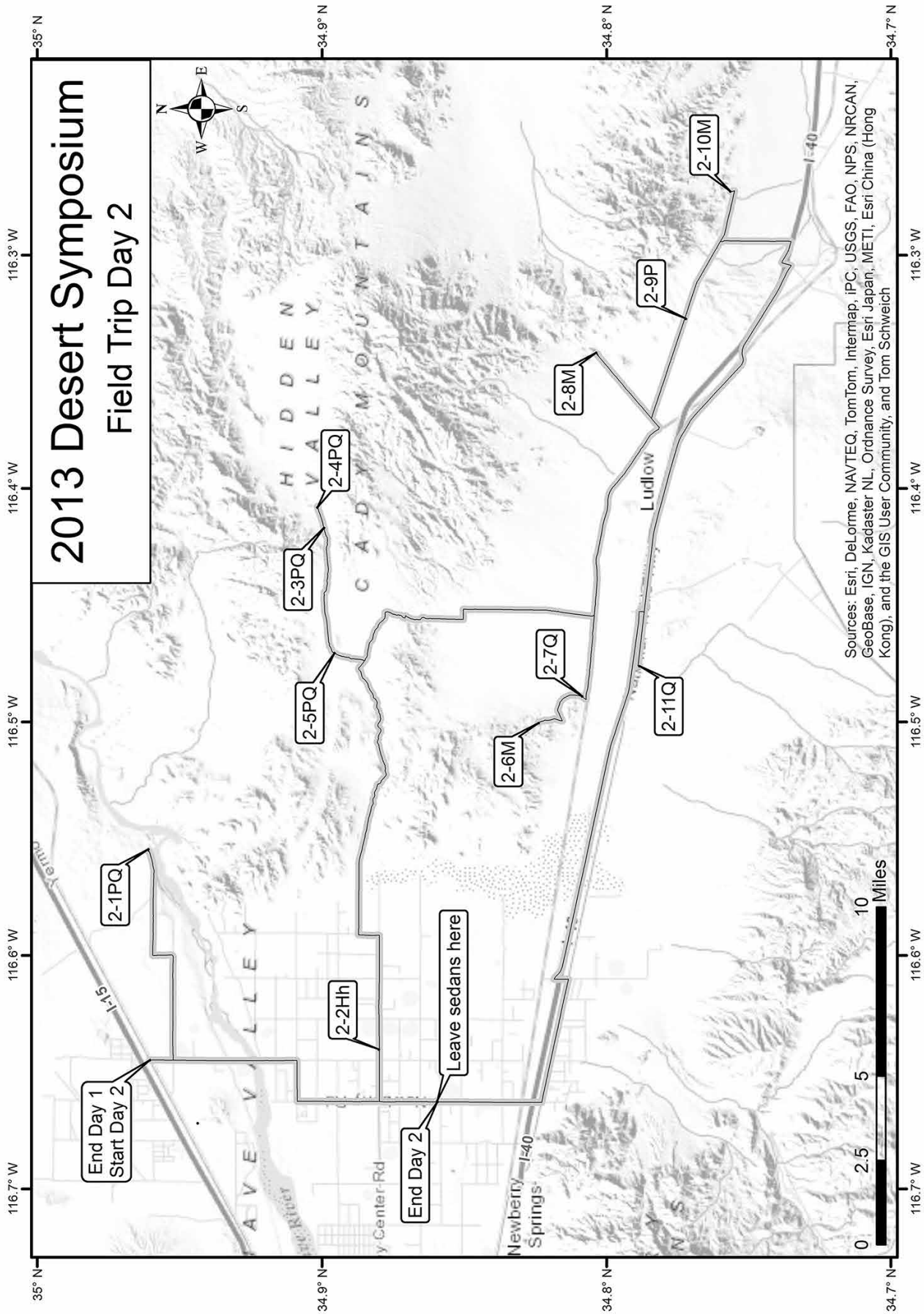
50.1 (0.6) TURN LEFT (south) toward Harvard Hill.

50.3 (0.2) PARK and hike to Harvard Hill just to the south.

STOP 1-17M: The Peach Spring Tuff (18.8 Ma, Hillhouse and others, 2011) lies at the base of the exposed section, a pale green tuff that is over 11 m thick. It is not welded here, unlike many exposures, perhaps because it was deposited in a lake. Green color comes from zeolitic alteration. The top of the tuff is reworked in thin beds that are made up entirely of the tuff, apparently as lake levels rose following tuff emplacement (Leslie and others, 2010). Above the tuff and interbedded with reworked tuff are thick limestone beds of the MSL, strongly silicified here. Higher, and out of sight, is a thin alluvial conglomerate and then a thick section of BPLs. The marker beds here are much older than we saw at Calico Mountains and Mud Hills, but comparable in age to limestone at Cemetery Ridge. The Manix fault bisects the south portion of Harvard Hill, and trends west toward the Toomey Hills. RETRACE to Harvard Road.

50.6 (0.3) TURN RIGHT (east) toward Harvard Road.

52.3 (1.7) Stop at Harvard Road. Day 2 will reconvene near here tomorrow.



TURN LEFT (north) to I-15. Enter the eastbound lanes and proceed to Baker, bypassing for now the Zzyzx exit. Fill gas tank at Baker for tomorrow's 200 mile trip, gather snacks and water, and return to I-15 westbound. Proceed west to Zzyzx Road and return to CSUF Desert Studies Center.

Day 2

Valleys on mountain tops: the Cady Mountains

Trip leaders: Kevin Schmidt, David Miller, and Robert E. Reynolds

On today's route we can compare different styles of faulting that have occurred over the last 20 million years in and around the Cady Mountains: extensional tectonics with listric normal faults, west-striking, left-lateral strike-slip faults, and the Pisgah fault as an example of a Pleistocene northwest-striking, right-lateral strike-slip fault. Our focus will then turn to the north-striking faults of the Landers–Hector regime that may have been active over the last several centuries. Tectonic activity has left valleys perched on the tops of mountains at many summits around the Mojave Valley east of Barstow.

Abbreviations for stops:

M Miocene extensional structure

P Pliocene structure

QP early Pleistocene structure

Q late Pleistocene structure

H Holocene structure

Hh Holocene historic structure

Convene in Zzyzx at the Desert Studies Center. Arrive with a full tank of gas (from Baker) for the 200 mile trip in your high clearance vehicle. Arrange carpool rides in high clearance 4WD vehicles before leaving the center. We will park and return to sedans on Newberry Road. Bring snacks and water; dress for cold or hot and sunny, windy weather.

Proceed north to I-15.

0.0 (0.0) Enter I-15 westbound. To the east are several strands of the Soda–Avawatz fault, the eastern boundary of the Eastern California Shear Zone (ECSZ).

5.9 (5.9) Pass the Razor Road interchange.

9.7 (3.8) Pass the Basin Road interchange. Miocene-aged rock avalanches have emplaced Paleozoic iron deposits at the Baxter Mine to the south (Bishop, 2013). East Cronese playa, visible to the north, is fed by the Mojave River during floods. It has an extensive record of past lakes and human occupations (Schneider, 1989; Warren and Schneider, 2000). A recent paper (Miller and others, 2010) demonstrates that late Holocene lakes were present here

during the Little Ice Age (~ AD 1650) and Medieval Warm Period (~AD 1290).

17.3 (7.6) Pass through faulted Pliocene sediments in the road cut. Note the mineralized faults in the western part of the cut. View west into Afton Basin, which was filled by Lake Manix in late Pleistocene time. Much of the hilly country south of the Mojave River is underlain by Pliocene and possibly Quaternary gravel. The badlands topography is caused primarily by the relatively recent, rapid downcutting of the basin through which the Mojave River currently flows.

18.3 (1.0) Continue past the Afton Road exit.

20.6 (2.3) The unnamed hill north of the freeway is composed of Mesozoic rocks against which, in the dissected foreground of the hill, are Pliocene or Pleistocene gravels. The gravels are cut by several faults, considered by Miller (2011) to be part of the Cave Mountain fault zone. Pliocene gravels at the south base of the hill are of different lithologies than the hill and are offset from bedrock in the hill by the fault (Miller, pers. comm., 2013).

26.2 (5.6) Continue past the Field Road exit. We are on the crest of a broad dome or fold in Pliocene and Pleistocene gravel. Southward, the gravels appear to interfinger with beds of Lake Manix sediments. Gravel in Buwalda Ridge contains Pliocene ash beds and underlies the Early Pleistocene Mojave River Fm (Miller and others, 2011).

30.2 (4.0) Pass under Alvord Mountain Road.

31.9 (1.7) The highway cuts through eastern Lime Hill east of Harvard Road. The tilted (but unfaulted), medium- to thick-bedded gravels are well exposed in this cut and in quarries south of the road. Lime Hill is made up of Miocene Barstow Fm sediments that contain an ash dated at 14.89 Ma (Miller and others, 2013). The Miocene sediments are overlain by a thick gravel sequence. Two prominent white silicified limestone beds, each thin but resistant, are located near the top of the exposure of the Barstow. Cut into the Barstow and crossing the limestone beds is a channel that contains white limestone-boulder conglomerate, presumed to be Pliocene. This deposit appears to have a local source of silicified Barstow limestone and only sparse clasts from other rock types. Above this white resistant deposit, which continues to the hill crest and beyond, is a brown-weathering sequence of gravels that is continuous with the Pliocene deposits viewed in the road cut just east of Harvard Road. Clasts in the brown gravels are derived from many sources north, south, and west of here. They are considered by Miller and others (2011) to represent valley-axis deposits of east-flowing streams that drained several distant mountains during Pliocene time. Evidently, the future basin that Lake Manix would occupy during the middle and late Pleistocene did not exist. All of the Miocene and Pliocene beds

dip eastward in these hills, and only a few faults have been mapped.

41.6 (1.0) EXIT at Harvard Road.

41.9 (0.3) Stop at Harvard Road. Reset odometer. TURN LEFT (south) onto Harvard Road. .

0.3 (0.3) Stop at Yermo Road. Proceed south across railroad tracks. To the west is Harvard Hill (Stop 1-11). Harvard Hill contains Barstow Fm marker beds MSL and BPL, and a waterlaid facies of the Peach Spring Tuff (18.8 Ma; Leslie and others, 2010). Folding of the sediments is a response to Pliocene left-lateral strike slip along the Manix fault. PROCEED SOUTH on Harvard Road

0.5 (0.5) Prepare for a left turn: watch for oncoming traffic.

0.6 (0.1) TURN LEFT (east) at Cherokee Road.

3.4 (2.8) TURN LEFT (north) before reaching the first house on either side of Cherokee Road.

3.9 (0.5) TURN RIGHT (east) and proceed easterly along the north fence line of the Ironwood Ranch.

4.4 (0.5) Pass pole line road.

4.7 (0.3) Pass west road to Vortac navigational station.

4.9 (0.2) Pass east road to Vortac.

6.0 (1.1) PARK on bluff with view of Lake Manix badlands.

STOP 2-1Q —Wetterman (Blaire) Ranch. Quaternary faults strike NNE on the south side of the Manix fault. These faults do not offset the youngest lake deposits, but several do offset “Q17” (upper C) and older units. One fault is well exposed under this bluff, cutting all Lake Manix units but not the upper 3 m of Mojave River gravels, suggesting that the fault became inactive about the time that Lake Manix drained (23,500 years, Reheis and others, 2007). RETRACE toward Harvard Road.

Note the abundant vegetation in the river bottom at Fort Cady. Does a geologic structure, such as the Cady fault or the Newberry graben, cause water to rise to the surface?

7.1 (1.1) Pass the east road to Vortac.

7.3 (0.2) Pass the west road to Vortac.

7.6 (0.3) Pass the pole line road.

8.1 (0.5) TURN LEFT (southwest) toward houses.

8.6 (0.5) TURN RIGHT (west) on Cherokee Road.

11.4 (2.8) Stop at Harvard Road. Watch for cross traffic. TURN LEFT (south).

12.8 (1.4) Drop into the Mojave River channel. Watch for oncoming traffic. Bluffs on both sides of the river channel expose sediments very similar to Unit D fluvial-deltaic deposits of Lake Manix. Active blowing sands from the channel often force closure of the road during high winds.

13.6 (0.8) Pass Cady Springs/Mojave Trail road crossing.

14.4 (0.8) Slow as road curves right (west) and becomes Riverside Road.

15.4 (1.0) Stop at Newberry Road. TURN LEFT (south).

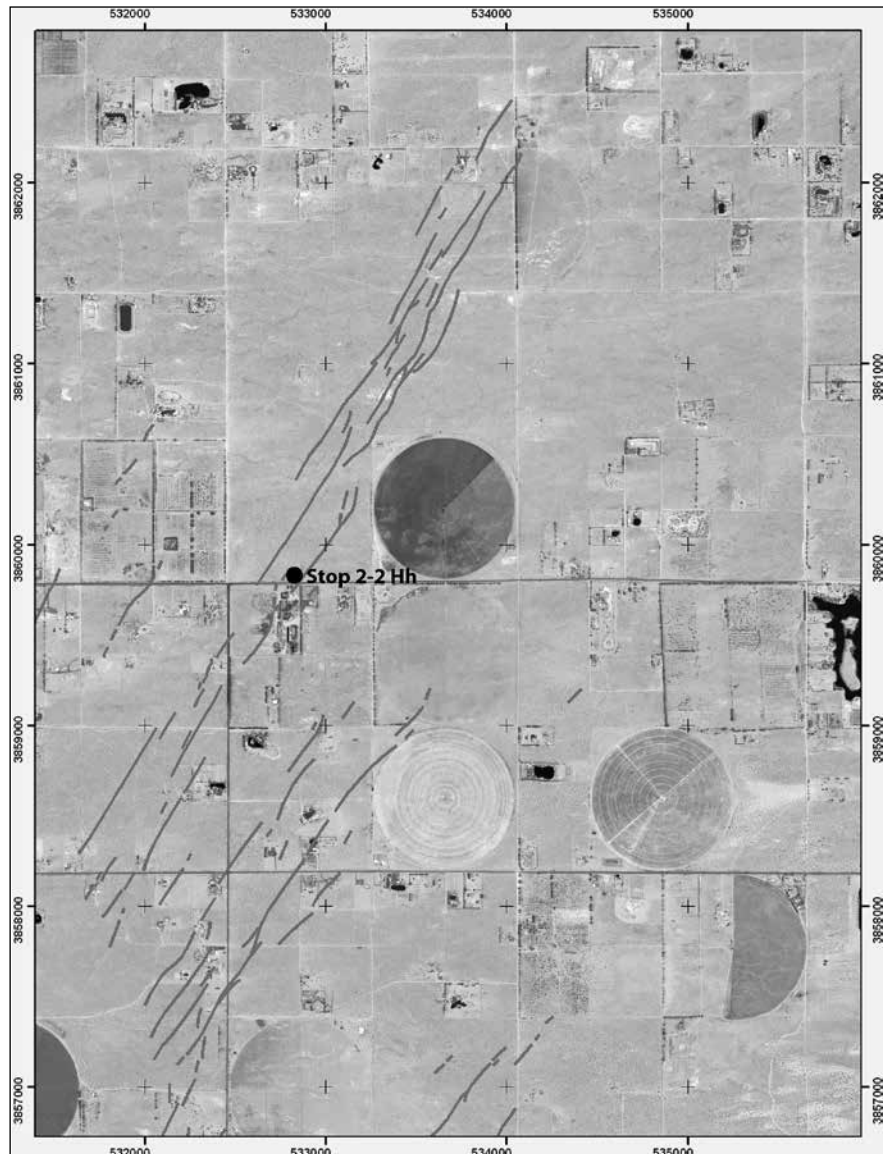


Figure 1: Newberry fracture zone faults and grabens as mapped after the 1992 Landers earthquake in the USGS Quaternary fault and fold database (<http://earthquake.usgs.gov/hazards/qfaults/>) overlain on Digital Globe imagery with UTM NAD83 coordinates.

17.4 (2.0) Pass Valley Center Road. We will return to Valley Center for the next stops.

17.9 (0.5) Pass Palos Verdes Road.

18.4 (0.5) Pass Silver Valley Road.

18.7 (0.3) Watch for oncoming traffic. Prepare for left turn across traffic.

18.8 (0.1) TURN LEFT (east) into Silver Valley Senior Center. If you reach Black Butte Road you have gone too far. We will leave sedans in the Senior Center parking lot since carpooling in high clearance vehicles is necessary.

Retrace north to Valley Center Road.

19.2 (0.4) Pass Silver Valley Road.

20.2 (1.0) TURN RIGHT (east) on Valley Center Road.

21.2 (1.0) Slow as you pass Harvard Road. Look for 1992 asphalt patches in the road. We are at the western margin of the Newberry graben that showed open fractures along its west and east walls resulting from the 1992 (Mw 7.3) Landers earthquake.

21.4 (0.2) **STOP 2-2Hh**: PARK off asphalt. We are at the east margin of the Newberry graben that reactivated in the Mw 7.3 1992 Landers Earthquake (Lettis and Kelson, 1992; Reynolds, 1993; Unruh and others, 1994) (Figure 1). This earthquake produced almost 50 miles of surface rupture terminating at this reactivated graben, trending ~N 40° E and extending for 4.5 miles, called the Newberry fracture zone. The reactivation of these fractures is not considered to be generated by primary fault rupture, but rather forming in response to the earthquake as coseismic triggered slip. Mapping after the Landers earthquake noted that these fractures had a normal dip-slip separation by as much as 12 cm and apparent lateral offsets of 5 cm or less. The mean slip direction was nearly perpendicular to general strike of the fractures, hence they accommodated almost pure northwest-southeast extension. Open fractures remain one-half mile north, and can be accessed by driving north on Harvard Road for 0.2 miles, then 0.4 miles west on a dirt track to the southern tip of the fractures.

Projection of the trend for an additional mile reaches historic Fort Cady. From where we stand, 200 feet east is a northeast-trending dirt road (Mojave Trail: Google Earth; Thompson, 1921, 1929) that parallels the east side of the graben. It runs southwest to Newberry Springs. Although not currently passable because of private property boundaries, it trends northeasterly, crossing the Mojave River at a shallow slope, and proceeds northeast across the west Vortac Road to Manix Wash. The position and direction of this pre-1920 road may have been determined by the presence of this graben, suggesting that the Landers stress regime was present historically. Elsewhere, unmapped breaks in slope that were ruptured along the Johnson

Valley fault north of the Landers epicenter also support historic activity of the Landers system (Reynolds, 1993).

Why did the Newberry fracture zone terminate where it did? This coseismic slip possibly terminated by structural interactions with westward projections of the Cady fault truncating the distal end of these fractures at a high angle. At its western extent, the Cady fault is occluded by pervasive young (decadal to century scale) and active eolian deposits sourced from the nearby Mojave River sink. Although mantled by sandy deposits younger than the last date of fault rupture, aeromagnetic anomalies help indicate that the trace of the Cady fault does not coincidentally end under the ample cover of Holocene eolian and fluvial deposits south of the Mojave River. Rather, the primary structure continues under the eolian deposits and may change orientation to a more northwesterly strike, likely diverges into two strands, and approaches the Manix fault to the north near Interstate 15 and Harvard Road. The westward extension of the Cady fault beneath the active eolian deposits is inferred to follow the linear aeromagnetic gradient that separates high magnetic values to the south and low magnetic values to the north. This gradient results from the juxtaposition of two magnetically different rock packages, and fault displacement is consistent with this abrupt juxtaposition. These two strands, extending the fault to the west, represent a possible structure responsible for the abrupt truncation of the Newberry fracture zone. Proceed east on Valley Center Road.

22.3 (0.7) Pass Fremont Street.

23.3 (1.0) Pass Fort Cady Road.

24.3 (1.0) TURN LEFT (north) on Troy Road.

24.8 (0.5) TURN RIGHT (east) at Lani Kai & Mauka Roads.

27.2 (2.4) Pass through a complex intersection and posts marking a fence line. PROCEED EAST on BLM 9470 road. Miocene volcanics (primarily andesite and basalt) partially mantled by active and Holocene eolian and alluvial units are to left (N). East-West trending structural grain to bedrock outcrops may be related to pre-Quaternary tectonic or volcanic structure. Unfaulted Quaternary sediments here reveal a dominant eolian contribution in deposits ranging in age from Pleistocene to active.

27.8 (0.6) Pass smaller untraveled two-track oblique turn on left.

28.3 (0.5) Junction of BLM 9470 and 9476. Proceed easterly on BLM 9470 through active wash.

Note the continued influence of pervasive wind-blown sands sourced from the Mojave River and Newberry Springs plain. An abundant source of available sand and the prevailing easterly wind direction generate sand

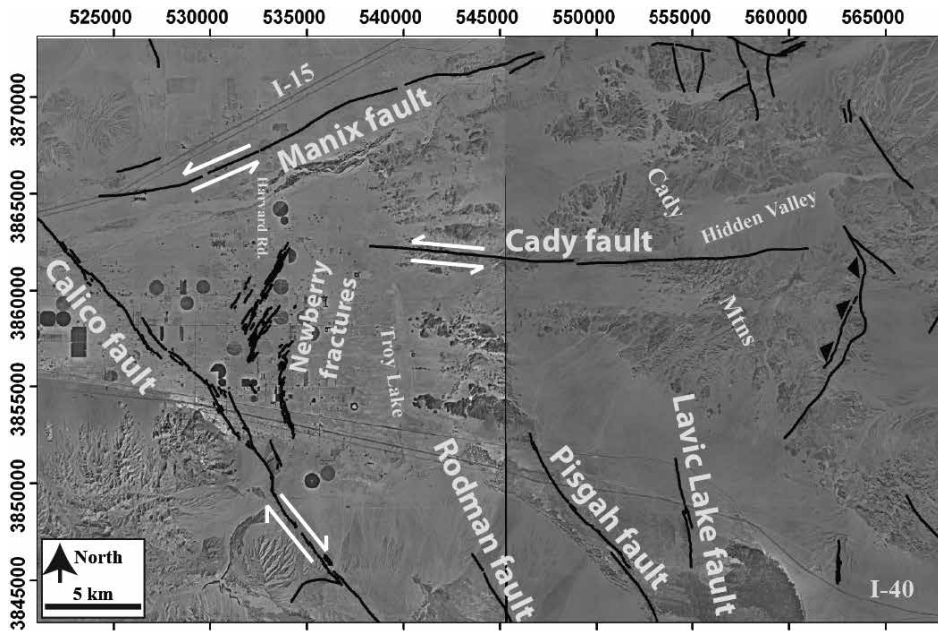


Figure 2: Map of regional faults overlain on USGS digital ortho-photoquadrangle base with UTM NAD83 coordinates. Red arrows denote predominant sense of fault slip. Barstow lies ~20 km to west from edge of map.



Figure 3: View west, oblique to trace of Cady fault, where buried sediments faulted against Miocene andesitic breccia were dated using infrared-stimulated luminescence (IRSL) techniques.

sheets on gentle topography, largely composed of older Pleistocene alluvial deposits, and ramps mantling steeper bedrock topography all with overall east-west trending margins. Bordering the meandering wash through which the road traverses are Miocene fanglomerates of andesitic source rocks, volcanic fanglomerates, as well as andesitic and basaltic breccias. Some of the smaller, lower lying bedrock outcrops are of the Hector formation, largely non-marine fluvial, volcaniclastic, and pyroclastic units that began depositing about 23 Ma and continued to about 16.5 Ma. No dates approximating 16 Ma or Barstovian mammalian fossils have been recovered from the Hector Fm (Woodburne, 1988). These deposits lie above a stratigraphic unconformity with the larger, older and underlying sequence of Miocene extrusive volcanic rocks.

The Hector Fm contains well-studied sections containing mammalian camel and oreodont fossils of Arikareean to early and late Hemingfordian age (Woodburne and Reynolds, 2010).

32.2 (3.9) Intersection at wells. TURN sharply to the LEFT, northeast on BLM 9470

33.1 (0.9) Proceed north-east on BLM 9470 at junction with BLM 9472. To the south of this road intersection are abrupt east-west trending distinct edges to older Pleistocene alluvial fan deposits expressing darker, more varnished surfaces than adjacent Holocene light-colored alluvial sediments. These east-trending edges are oblique to the regional surface-water flow direction typified by southwest oriented drainages.

36.2 (3.1) **STOP 2-3Q:** Saddle: (NAD 83, UTM Zone 11S; 553258mE/3862025mN)

PARK in active wash crossing the road; pull far in to wash on either side of road as parking is tight. We are nearing the subtle saddle entering Hidden Valley to the east. At this location, both the active drainages and the Pleistocene deposits preserve records of westward-flowing sediment. Just to the east, though, the active and Pleistocene fans flow eastward. To the south lie traces of the Cady fault, cropping out at the slope break between Quaternary sediments and the bedrock uplands composed of Miocene volcanic rocks and older crystalline intrusive rocks. To the southwest, overlying the volcanic rocks, are more sediments from the Hector formation. These deposits are non-marine fluvial conglomeratic beds, locally with imbricated clasts, interfingered with packages of poorly sorted, matrix-supported sediments. This unit likely represents a depositional setting similar to the present geography, but those Miocene alluvial fans accumulated sediment from the ancestral Cady Mountains and are now exposed and uplifted south of the Cady fault.

Walk south (0.3 mi) along active wash to a diffused trench revealing numerous traces of the Cady fault. The Cady fault forms a significant structural boundary separating northwest-striking dextral faults such as the Calico,

Walk south (0.3 mi) along active wash to a diffused trench revealing numerous traces of the Cady fault. The Cady fault forms a significant structural boundary separating northwest-striking dextral faults such as the Calico,

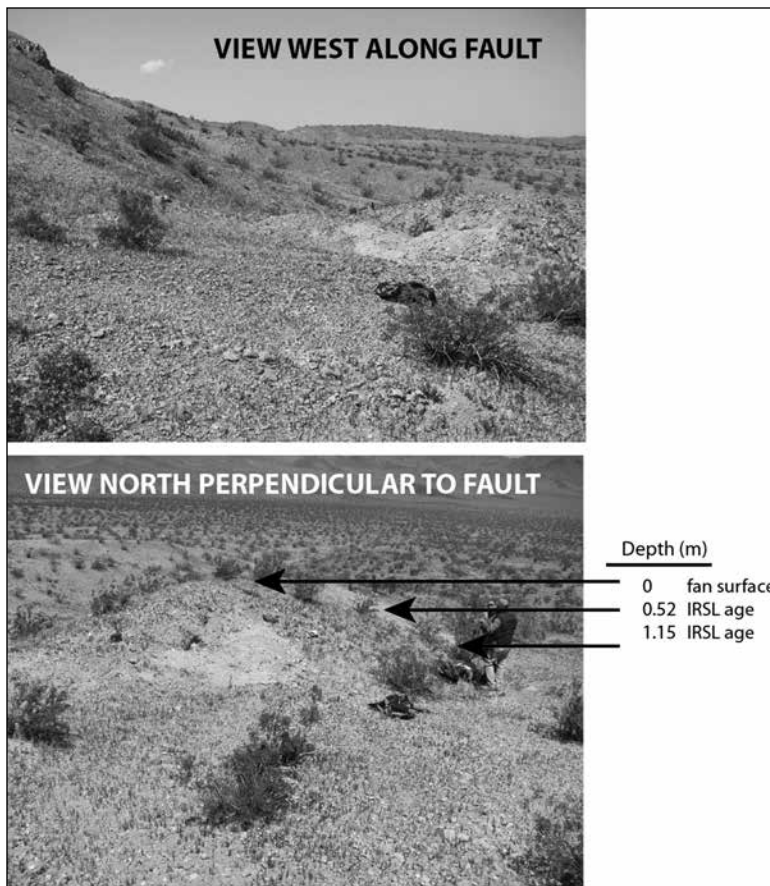


Figure 4: View parallel and orthogonal to trace of Cady fault where buried sediments were dated using infrared-stimulated luminescence (IRSL) techniques.

Rodman, Pisgah, and Lavic Lake to the south, from east-northeast-striking faults to the north such as the Manix (Figure 2).

This exposure (Fig. 3) shows six secondary fault strands and lesser shear zones over an 11-m long trench exposure. These are likely wedged between larger, more primary strands of the Cady fault. Fault orientations range from

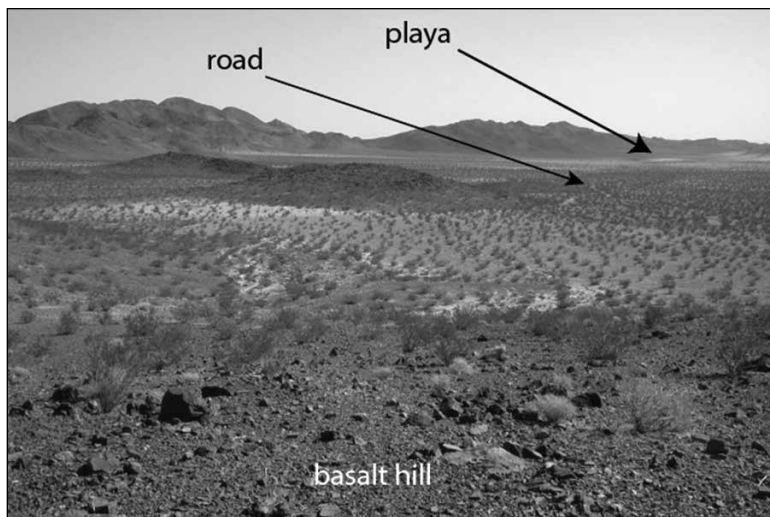


Figure 5: The view eastward from the basalt hill adjacent to the topographic saddle and flow divide affords a good view for discussing possible origins of the playa.

62° to 118° azimuth with predominant southerly dips of 58° to 89°. Fault gouge and shear zones range in thickness from 1-7 cm. The thickest splay exposed, possibly representing the largest amount of shear displacement, is oriented 118° with a 78°SW dip—generally consistent with regional structure observed along Cady fault. Luminescence dating of sediments sampled at this location indicate deposits as young as ~30–35,000 years old have been displaced against other Quaternary sediments as well as juxtaposition with Miocene andesitic breccia. Similar aged Quaternary sediments show significant pedogenic development near the ground surface. Since the neighboring bedrock ridge appears disconnected from the regional drainage, this site is probably a small shutter ridge with a relative sense of upward vertical motion resulting in exhumation of the soil horizons.

Approximately half a mile to the east is a Holocene–Pleistocene aged alluvial fan deposit that is beheaded at its upslope extent by the Cady fault (Figure 4) and juxtaposed against sheared Miocene andesite separated by a clay-rich fault gouge. Fault generated slickensides denote left-lateral slip with an oblique up-to-the-south component. Additionally, the clast lithology in the beheaded fan differs from that of the proximal watershed source bedrock. To preclude sampling of younger alluviated post-deposition fines, two horizons were sampled below the weak Stage I calcic Bk horizon for dating. Infrared-stimulated luminescence (IRSL) dates were used to estimate numeric ages of alluvial sediment and an aggradation rate. Adopting an extrapolated deposit age and a measured offset results in a Holocene time-averaged sinistral offset rate of <1 mm/yr. Therefore, the tectonic block-bounding Cady fault is an active feature that may have similar offset rates using short- and long-term slip indicators.

PROCEED EAST to a small basalt hill.

36.7 (0.5) **STOP 2-4PQ:** (NAD 83, UTM Zone 11S; 554097mE/3862296mN) Topographic saddle at Miocene basalt outcrop adjacent to road to left (north).

PARK at the drainage divide by the basalt hill. WALK to the top of the hill for a view eastward into Hidden Valley playa and south along the trace of the Cady fault (Figure 5). Ask these questions:

Q1 : Why does a valley traverse through the top of the Cady Mountains?

Q2: Why there is a playa 2 miles northeast at a cul-de-sac in the valley, only 70 ft lower than this drainage divide?

A1 : Note the regional flow directions of the channels as they are oriented away, or bifurcate, from this small hill.

A2: The topographic sink at the playa could be caused by: i) a concealed normal fault north of the Cady fault with a relative downward sense of offset in the block with the playa, ii) a downwarp related to folding sub-parallel to the Cady fault, iii) a depression caused by regional clockwise rotation at the corner of a tectonic block, or iv) northward progradation of alluvial fans from the south at a rate faster than those from the north, in a basin where deposition rates exceed rate at which drainages are able to remove sediment. Or, likely some combination of these factors?

Looking 0.5 mi to the south, the east-west striking Cady fault generated a prominent topographic break between the stack of increasing aged Quaternary alluvial fans over the Miocene volcanic rocks to the south, composed largely of andesite and dacite, and Mesozoic crystalline intrusive rocks. Long-term fault slip is left-lateral with an oblique component responsible for the pronounced bedrock topography south of the fault, consistent with the uplift and exhumation of the basin sediments in the Hector Fm as well as the most recent offset record interpreted by slickensides observed in fault zones. The sequence of early Pleistocene to active Holocene alluvial fan deposits also supports the assertion that relative down-to-the-north displacement is responsible for the progressively older, uplifted, and highly crowned fans that are well preserved with increasing height above the active channel.

Discussion: age of the Cady fault

Q1: When did slip on the Cady fault originate?

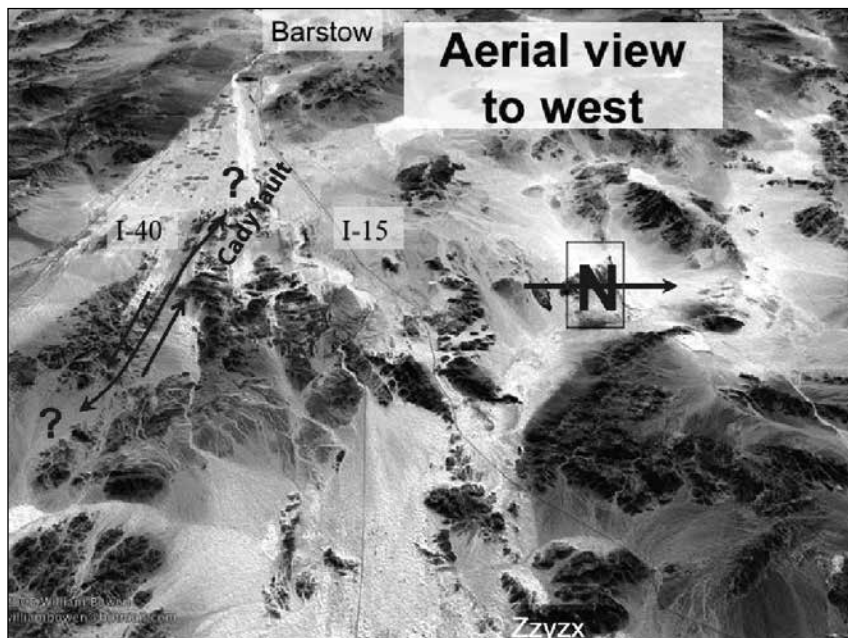


Figure 6. NASA base map showing westward oblique aerial view of Cady fault. Note topographically stranded Hidden Valley in the center of the Cady Mountains.

Q2: What is the total amount of slip over its life in the current tectonic framework?

To address these questions, we interpreted bedrock and surficial geologic mapping in conjunction with potential-field anomalies and recently acquired luminescence dates of alluvial sediments. We estimated total sinistral offset of ~6 km along the Cady fault based upon reconstruction of displaced bedrock outcrops and magnetic anomalies. As the timing for the onset of slip on the structure is not known, we can conservatively assume that extensional strain in the region began ~10 Ma, as recorded by interbedded sediments and volcanics of the Ricardo Group exposed in the Basin-Range Province north of the Garlock fault. If correct, the long-term offset rate is ~0.6 mm/yr. Assuming that, onset of strain along the Cady fault can be dated by the far afield opening of the Gulf of California by rifting associated with the San Andreas fault system at ~ 6 Ma. The long-term offset rate is roughly 1 mm/yr.

Time-averaged sinistral offset rates through the Quaternary decrease with older deposit age. These dates are estimated from field mapping of displaced alluvial deposits, from regional age constraints obtained through luminescence, from radiocarbon dating techniques. Deposits from the late Pleistocene/Holocene transition yield rates exceeding 1 mm/yr, whereas minimum rates for middle to early Pleistocene deposits may be as low as 0.02 mm/yr, assuming this time-averaged fault offset ensued immediately following deposit formation. This suggests that offset rates on the Cady fault have increased into the present day.

Where does the Cady fault go to the east?

Similar to the east-west striking sinistral Garlock fault changing orientation to a more northerly strike at its eastern termination, the Cady fault also breaks into numerous splays as it rolls over to the south (Figure 6), forcing crystalline basement rock up to the surface in a compressive regime. In a sinistral fault domain, this change in orientation increases the thrust component of slip with an eastward vengeance. The Cady fault does not extend as far east as Broadwell Lake, but there is increasing evidence that similar east-west striking faults are present near this eastern boundary of the Eastern California shear zone. Ongoing field mapping will focus on these relations.

RETRACE west on BLM 9470 to wells.

37.5 (0.8) The Cady fault scarp is to the south, paralleling the road. To the south (left), note sharp topographic breaks with linear margins between

Quaternary alluvial fans and Miocene volcanics and Hector Fm sediments.

38.8 (1.3) Drop into wash. Note thick red-brown paleosols exposed on the north bank of the wash. Similar paleosols in Broadwell Valley to the east contain vertebrate fossils suggesting a Pleistocene age. The exposure afforded by the wash cut reveals pedogenic development such that the top of the oxidized and calcic B-horizon is present at ~0.3 m below the ground surface with the top of the Stage III-IV calcic horizon is located at ~1.2 m below the ground surface. This advanced calcic soil displays massive accumulations of CaCO₃ between clasts of sediment cementing them in place. Locally there are exposures of carbonate laminae that drape into fractures. These features are thought to indicate a mid-Pleistocene timeframe of deposition. As many of the Quaternary sediments in the Cady Mountains have abundant sand in the upper horizon, exposures such as these are critical to determine the maturity of soils at depth. The last 0.4 miles has crossed this higher stable unit, and it continues until the next road intersection.

40.1 (1.3) Take LEFT FORK on BLM 9470 at junction with BLM 9472

40.3 (0.2) **STOP 2-5Q** The low hill cored with Miocene volcanic fanglomerate (Hector formation) and basalt on the left (south) marks the trace of the Cady fault. These volcanic rocks and fanglomerates are overlain by early Pleistocene alluvial deposits and are displaced and uplifted on the south side of the fault. Late Pleistocene alluvial deposits are permeated with oxidized sand-sized particles indicating long-lived influence of eolian sand in the Cady Mountains. Furthermore, the clasts composing the desert pavement on these Pleistocene deposits commonly display ventifact characteristics. On the south side of the small hill are small late Pleistocene fans beheaded by the Cady fault as they currently are not connected to source watersheds. No offset Holocene deposits have been observed in this area.

From here, the Cady fault projects westerly through a narrow valley and small drainage divide, bifurcating into at least two divergent strands, and projects into the Mojave River plain towards Harvard Road south of I-15. The two strands change orientation from the primary east-west strike to a more northwesterly strike and possibly form a northerly structural break to the northern extent of the Newberry fracture zone. Because of the mantle of younger sediment and ample Holocene sand derived from the Mojave River bed, surface mapping of these features is not possible. The location and extent of the strands was determined by interpreting aeromagnetic and gravity anomaly maps. It does not appear as if these strands extend across the Mojave River towards Harvard Hill.

41.0 (0.7) Junction with wells. PROCEED LEFT (south-east) on BLM 9489 (San Bernardino County Road #20795). Although not currently used, the wells and watering troughs here supported cattle grazing with numerous trails radiating away from this site.

42.4 (1.4) TAKE RIGHT (south) FORK at junction and proceed south toward Hector.

IMPORTANT: DO NOT continue east due to treacherous loose sand.

43.2 (0.8) Drop into wash.

43.3 (0.1) TURN LEFT (east) out of wash.

43.9 (0.6) Pass a road to the right (west). Proceed south.

44.4 (0.5) Road bears left (east).

44.6 (0.2) Road bears right (south) between young and active wash crossings. We are driving over late Pleistocene alluvial fan deposits with strong vesicular Av horizons under the desert pavement. Many of these fan surfaces appear light in color on imagery because of abundant thin sand sheets, bioturbation, and vegetation associated with coppice mounds. Coppice mounds are vegetated sand mounds scattered throughout lowland areas with a shrub (typically creosote, *Larrea tridentata*) as the trap for the blowing sand. Small burrowing animals often focus burrows in this loose sand and shade.

44.9 (0.3) Cross a wash.

46.1 (1.2) BLM 8599. Pass a road from the right (west).

46.6 (0.5) Pass Hector Road on the left (east) just north of a large southwest-flowing wash.

47.8 (1.2) Stop at railroad tracks. BLM 8590. Hector Crossing (closed) is immediately east. PROCEED RIGHT (west) along the railroad maintenance road.

49.9 (2.1) TURN RIGHT (north) on BLM 8591.

50.0 (0.1) Cross the trace of the Pisgah fault, offsetting Miocene sediments in the southwestern Cady Mountains.

50.5 (0.5) TURN LEFT (west) at junction with BLM 8592.

50.7 (0.2) Stay left at fork.

51.0 (0.3) TURN RIGHT (north) on bladed mine road.

51.4 (0.4) Drop into wash.

51.5 (0.1) **STOP 2-6M.** Park and walk north across terrace to Barstow Fm markers (MSL, BPL). Previous geologic research (MacFadden and others, 1990a; Ross, 1995) noted large amounts of vertical axis clockwise rotation in the Cady Mountains, in contrast to lack of such rotation in the Mud Hills over the last 19 Ma (MacFadden and others, 1990b). The model suggests that paleomagnetic signatures of the Hector Fm in the northern Cady Mountains

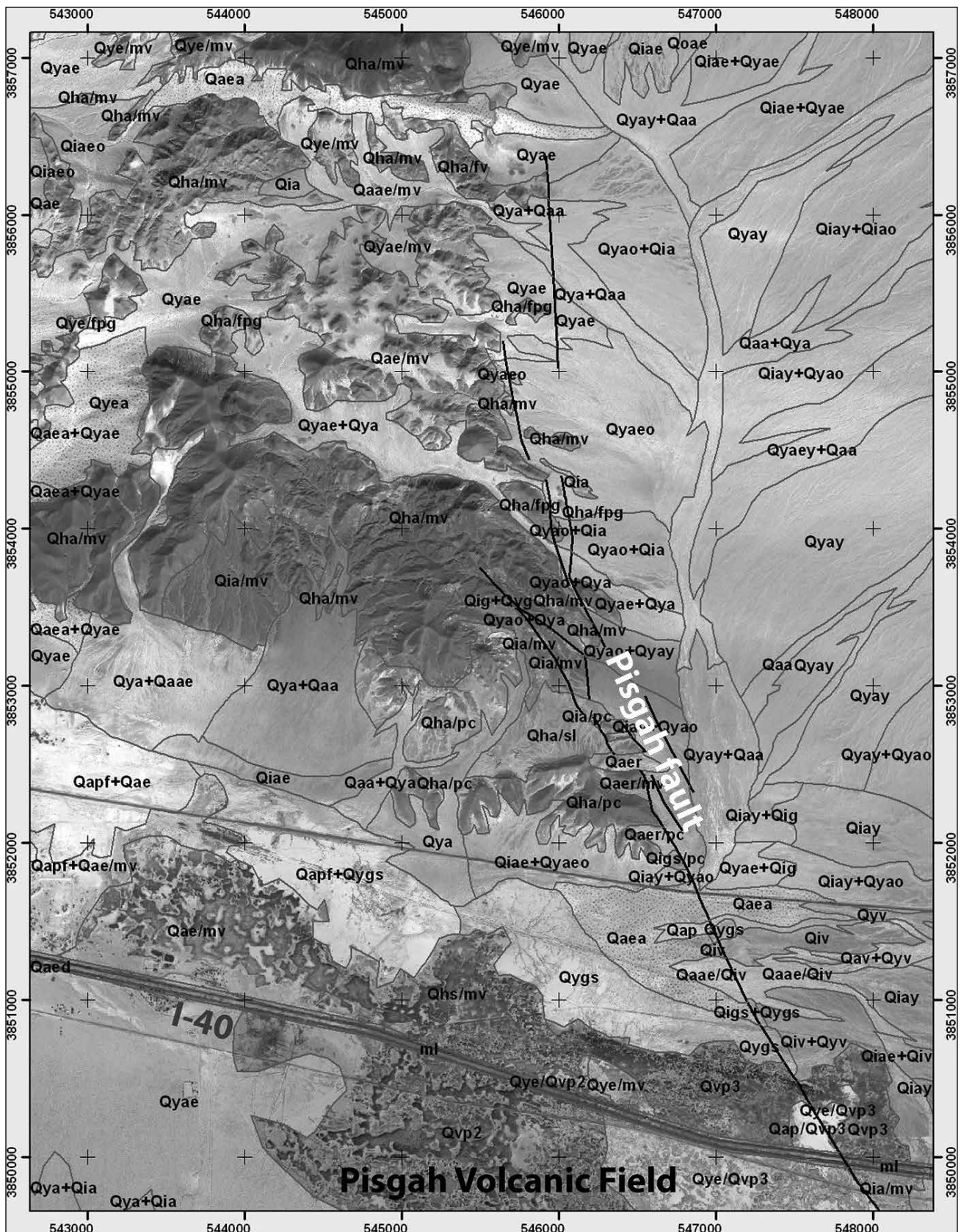


Figure 7. Quaternary geology map (Phelps and others, 2011) showing multiple strands of Pisgah fault north of the Pisgah Volcanic Field. DigitalGlobe base map with UTM NAD83 coordinates. Primary map units depicted are: Qaa, active alluvial sediments; Qya, young largely Holocene alluvial fan deposits; Qia, Pleistocene alluvial fan deposits; Qae, active sand; Qye, young Holocene sand; mv, mafic volcanic rocks; and Qvp, Quaternary basalt of the Pisgah crater. See Phelps and others (2011) for full description of map units.

indicate 26° of clockwise rotation after about 16 Ma (MacFadden and others, 1990a). Consistent with that model, the left-lateral Manix and Cady faults bound the north and central portions (respectively) of the Hector block. In support, Ross and others (1989) describe terranes of the central Mojave Desert associated with left-lateral and northwest trending faults undergoing as much as 50° of clockwise rotation after early Miocene deposition.

51.6 (0.1) Pass dozer road to left (east).

52.0 (0.4) TURN LEFT (east) at BLM 8592.

52.6 (0.6) TURN RIGHT (south) at junction with BLM 8590.

53.1 (0.5) **STOP 2-7Q:** The Pisgah fault runs south-southeast for more than 20 miles through the Lava Bed District into the Bullion Mountains, south of Lavic Lake. Where the fault cuts Sunshine Peak, an approximately 100-m, down-to-the-east vertical topographic escarpment is present. The Pisgah fault is one of the northwest striking dextral strike slip faults, similar to the Calico and Rodman faults to the west and the Lavic Lake fault to the east (Figure 2). Ross (1992) studied the southwest Cady Mountains, which, according to his paleomagnetic data, have rotated clockwise ~83° since ~16 ma. He attributes the rotation to dextral shearing of the southwestern Cady Mountains Block between the Pisgah and Rodman Faults. Ross inferred that 15 ± 4 km of slip has occurred on the Pisgah–Rodman fault system to account for the rotation of the southwestern Cady Mountains Block. This is in rough agreement with the 6.3 km of slip suggested for the Pisgah fault based on the alignment of magnetic anomalies (Jachens and others, 2002), combined with a possible 20 km total offset on the Bullion–Pisgah–Rodman fault system. This result would imply roughly 14 km of slip on the Bullion–Rodman fault system and between 5 and 13 km of slip on the Rodman fault.

The Pisgah fault cuts the western part of the Pisgah Field (Qvp on Figure 7) and, therefore, the latest activity on the fault is no older than about 20 ka. The Pisgah cone and associated lava flows were mapped in detail by Wise (1966), who distinguished three distinct flows for Pisgah crater and two flows for Sunshine crater, using basalt rheology. He separated the Sunshine crater basalts into the Lavic Flow and the Sunshine Flow, suspecting the lavas were late Quaternary in age. Recent analytical ages obtained from the lavas (Sylvester and others, 2002) obtained an $^{40}\text{Ar}/^{39}\text{Ar}$ plateau age of 18.3 ± 2.6 ka and an isochron age of 23.4 ± 4.3 ka for the second of the three eruptive phases that flowed from the Pisgah Cone. Phillips (2003) obtained a mean age of 22.5 ± 1.3 ka using cosmogenic ^{26}Cl , sampling within the first (oldest) Pisgah Flow. This age assumes an erosion rate of 1 mm/yr. Age



Figure 8. Black Butte Mine northwest trending fault with barium and manganese oxides.

estimates based on calibrated desert varnish microstratigraphy yield a similar age range of 24 to 30 ka (Liu, 2003). The various dating methods yield similar ages and place the age of the oldest Pisgah flow at very late Pleistocene with younger deformation by the Pisgah fault cutting these relatively young flows.

The Lavic Lake fault ruptured during the 1999 Mw 7.1 Hector Mine earthquake. Many of the railroad structures nearby were significantly damaged from this quake. Triggered slip was also recognized on the Calico fault generated by the 1992 Landers earthquake. We are presently near the northernmost extent of the Pisgah fault as it feathers out into multiple strands (Figure 7) as it approaches the Cady fault, the latter representing the southernmost block boundary of the sinistral domain to the north.

53.3 (0.2) TURN LEFT (east) at BLM 8590 at railroad tracks.

55.3 (2.0) Pass San Bernardino County Road 20795 and BLM 9489 on the left, and proceed east past Hector Crossing (closed) on the right.

58.2 (2.9) Utility road bears southeast along railroad.

59.7 (1.5) Pass under powerline. Access to I-40 is gained by crossing the tracks to the railroad maintenance road, proceeding under the bridge to the south side of I-40, then west on National Trails Highway to the Hector Road offramp.

60.1 (0.4) Pisgah Road, BLM 8570. TURN LEFT (north-east) through fence line toward Black Butte Mine.

60.4 (0.3) Pass gas line road, BLM 8687; we will return to this spot.

62.1 (1.7) Pass a right turn to mines.



Figure 9. The exposed upper surface of the beheaded fan exhibits round vesicular basalt cobbles indicating long transport from a non-local source.

62.4 (0.3) **STOP 2-8M:** Northwest-trending Miocene fault at Black Butte Mine (Figure 8), where fault conduits have allowed hot springs to deposit manganese oxide minerals romanechite and psilomelane: $(\text{Ba}, \text{H}_2\text{O})(\text{Mn}^{++4}, \text{Mn}^{+3})_5\text{O}_{10}$; pyrolusite, Mn^{+4}O_2 ; and goethite, $\text{Fe}^{+30}(\text{OH})$. These ores were mined during WWI and WWII for manganese (Wright and others, 1953). Retrace to gas line road.

64.5 (2.1) **TURN LEFT** at gas line road BLM 8670 and proceed northeast.

65.3 (0.8) The gas line road is joined by a powerline.

67.1 (1.8) **STOP 2-9PQ:** Beheaded Fan (NAD 83, UTM Zone 11S; 561601mE/3848041mN). **PARK** at wash. Walk south to examine young Holocene gravel clasts deposited against older Pleistocene (?) fan. The South Cady frontal fault (SCFF) truncates the upslope northern watershed source of the fan. The wash at the base of the fan exposes young fanglomeratic gravels consist of clasts of pale gray, green, dark red, purple and black Miocene volcanic and shallow intrusives of flow-banded and brecciated porphyritic andesite, dacite and non-vesicular basalt. These clasts are subangular, indicating a relatively short transport distance. No Peach Spring Tuff (PST), olivine basalt, Jurassic volcanics or granitic rocks are apparently present. This suite of clasts would be expected from a source area immediately north.

In contrast, the top of the fan (4WD access to microwave station via BLM 8660) exhibits clasts exposed by erosion that are subrounded to round (Figure 9), indicating a longer distance of transport. In addition to variegated Miocene volcanics, 40+ percent of the clasts are round cobbles of vesicular to scoriaceous basalt with white (feldspar?) phenocrysts from a source not currently recognized in the Cady Mountains to the north. No PST, olivine basalt, Jurassic volcanics or granitic rocks are present. When the source of clasts in the fan is determined, they might assist in determining the amount or timing of movement on the SCFF.

Additionally, the surface of the fan has had all desert pavement and upper soil horizons removed by erosion. This geomorphology suggests that it might fall into the same age range as the north-dipping fans on the north slopes of the Rodman Mountains (Dibblee and Bassett, 1966) and the Yermo Fan on the east slope of the Calico Mountains. Miller and others (2011), discussing the Yermo gravel, suggested an early Pleistocene to Pliocene age, and described the characteristics of these deposits that make them generally mapped as QT in age: A): provenance disrupted from present; B):no surface remains of the original deposit; C): no original soils remaining.

In some cases, QT deposits are structurally isolated, such as indicated by transport directions different than present slope, or dips tilted more steeply than the adjacent drainages. The crests of ridges that make up the fan slope downward to the south. The question remains as to whether this is an original slope, or one altered by tectonic deformation associated with the SCFF.

68.0 (0.9) Summit; powerline road (BLM 8670) starts downhill

69.1 (1.1) Pass through intersection with BLM 8655, we will return to this intersection. Proceed east on BLM 8670. Pink boulders on south side of road are PST. The DuPont strontium claim (Durrell, 1953) on the right exhibits red and green mine dumps.

69.3 (0.2) The road bears easterly.

69.7 (0.4) Pass the first left turn (north) to the DuPont strontium mines.

70.0 (0.3) Pass a second turn left (north) to the strontium mines.

70.1 0.1 Pass a right turn for BLM 8706.

70.2 0.1 Pass a third left turn to the strontium mines.

70.3 (0.1) **TURN LEFT** (north).

70.4 (0.1) **PARK** at **STOP 2-10M:** (NAD 84, UTM Zone 11; 566626mE/3846371mN) Barstow Fm marker strata MSL, BPL, SrB, & PST south of the SCFF. The PST (#40 of Wells and Hillhouse, 1989) has been rotated $11.6 \pm 4.2^\circ$ clockwise. In contrast, to the south where the PST is flat-lying on Pacific Mesa, on the Marine Base, the inferred rotation is $10.1 \pm 3.7^\circ$ counterclockwise (#38 of Wells and Hillhouse, 1989). Farther north in the Cady Mts, at Baxter Wash, the PST shows a rotation of $30.0 \pm 6.3^\circ$ clockwise (Hillhouse and others, 2010). The differing degrees of rotation suggest different histories for each of the blocks within which the PST outcrop lies. Examine the overturned Miocene section (Durrell, 1953). Retrace to the powerline road.

70.5 (0.1) **TURN RIGHT** (west) at powerline road.

70.7 (0.2) Pass east DuPont road.

71.2 (0.5) Pass west DuPont road.

71.8 (0.6) TURN LEFT (south) on BLM 8655, Sleeping Beauty Road.

71.9 (0.1) Pass through intersection with BLM 8660. The road west provides 4WD access to top surface of the beheaded fan.

73.0 (1.1) Cross buried gas lines.

73.5 (0.5) Stop at National Trails Highway. Ludlow is six miles east. TURN RIGHT (west).

74.0 (0.5) Slow at overpass. TURN LEFT (south) over I-40.

74.3 (0.3) TURN RIGHT (west) on the south side of I-40. Proceed west on National Trails Highway (Route 66).

76.8 (2.5) Slow; cross over railroad tracks at East Pisgah crossing.

79.0 (2.2) Pass the left turn under I-40 and over the tracks to Pisgah Crater Road North and Black Butte Mine.

80.7 (1.7) View left of north-northwest trending vegetation and outcrop lineations mapped as tentative faults (Bortugno and Spittler, 1986).

83.2 (2.5) Pass road south to Hector Mine, which produces a bentonitic clay called hectorite composed of montmorillonite (smectite group) that is high in magnesium and lithium: $\text{Na}^{0.3}(\text{Mg, Li})_3\text{Si}_4\text{O}_{10}(\text{F,OH})_2$. This colloidal, waxy, gel-forming bentonitic clay is used for oil well drilling mud to float rock particles, as well as other specialty products. It was apparently formed as an alteration product of volcanic ash. The mine has been in continuous production since 1931 (Wright and others, 1953). A pictorial history of initial development by National Lead Company and expansion of the Newberry processing plant is available at the Mojave River Valley Museum (NL Chemicals, 1982).

83.6 (0.4) Pass the Hector onramp to I-40.

85.0 (1.3) **STOP 2-11Q:** The Pisgah fault cuts the late Pleistocene Pisgah basalt flow (Figure 10). The basalt flowed north onto the southern (Troy Lake) arm of Lake Manix within the period of the late Pleistocene before the lake drained (Meek, 2000, 2004). There are no pillow structures developed in the basalt, as one would expect if warm basalt flowed into lake water. Evidently, basalt flowed across dry lake mud flats, and was later submerged during lake rises. Meek (1999) demonstrated that the upstream Mojave River was diverted into Harper Lake Basin at 30,000 and 25,000 years BP, possibly by activity on the Lenwood/Lockhart fault zone (Reynolds and Reynolds, 1994; Reynolds and others, 1994). If the upstream Mojave



Figure 10. View northwest toward Cady Mountains showing buckled basalt blocks that mark the trace of the Pisgah Fault.

River flowed into Harper Lake, it would leave portions of the Manix Basin dry, which possibly helps constrain the timing of basalt flows. RETRACE east.

86.3 (1.3) TURN LEFT (north) at Hector Road to the west bound I-40 onramp. Proceed west toward Barstow.

87.5 (1.2) Buckled basalt slabs mark the trace of the Pisgah fault.

89.8 (2.3) Pass the rest area.

94.9 (5.1) **EXIT** at Newberry Springs/ Fort Cady Road offramp.

95.2 (0.3) Stop at Fort Cady Road. TURN LEFT (south) and proceed over I-40.

View south. Perched on the skyline of the Newberry Mountains is the Pipkin basalt flow (770±40 ka., Oskin and others, 2007) in a “valley on a mountain top.” The upper valley has been truncated on the north side by a steep escarpment. The flow occupies a paleovalley floor, and starts at 4,200 feet, runs downhill to the west, then northwest along Kane Springs Wash and ends at 2,050 feet, where the toe is cut by the Calico fault. The flow spans an elevational difference of 2,150 feet. Obviously, the upper end of the flow was constrained by rocks that are missing. Where did they go? The Calico fault crosses the east end of the flow, and erosion removed rocks to create the exposure.

95.5 (0.3) Stop at National Trails Highway. TURN RIGHT (west) toward Newberry Springs.

98.0 (2.5) **View west-southwest** of the Newberry Mountains. Paleomagnetism of volcanic rocks in the central Mojave Desert indicates that large fault-bounded blocks rotated clockwise in Early Miocene time (18.8–21 Ma), as a consequence of regional extension. Improved geologic mapping in the Newberry Mountains, California, has afforded tight stratigraphic control for paleomagnetic

study, allowing calculation of a paleomagnetic pole that represents the axial dipole field. Volcanic rocks span at least two polarity zones (>22-21.3 Ma), revealing several large swings in paleodeclination and a transition to normal polarity. Paleomagnetic data from basalts define a polarity transition with a pole path that passes through eastern South America, where previous studies show a preferred clustering of transitional poles. After excluding these transitional directions from the 55 flows sampled, we used 21 independent readings of the ancient field to define the paleomagnetic pole (Lat.= -60.9°; Long.= 151.4°E, a95= 10.0°). We infer a clockwise vertical-axis rotation of $42.7^\circ \pm 10.3^\circ$ by comparing the Newberry paleomagnetic pole with central North America data. The rotation is substantial, but 30° less than the previously reported rotation of 72.7° . The rotation affects rocks as young as ~21 Ma, but the unconformably overlying Peach Spring Tuff (18.8 Ma) shows little or no rotation. We conclude that the rotation occurred during an early Miocene extensional event and is not the result of Pliocene or younger strike-slip faulting in the region (Hillhouse and others, 2010).

98.5 (0.5) TURN RIGHT (north) on Newberry Road. Cross over I-40.

98.8 (0.3) Pass Pioneer Road and cross the railroad tracks.

100.9 (2.1) Pass Black Butte Road, TURN RIGHT into Silver Valley Senior Center and retrieve vehicles. For those returning to Las Vegas, retrace north along Newberry Road to the start of Day 2 at I-15.

Proceed south on Newberry Road toward I-40.

102.5 (1.6) Pass Fairview Road.

103.1 (0.6) TURN RIGHT (west) at Pioneer Road toward I-40.

105.0 (1.9) Stop at National Trails Highway. TURN LEFT (south).

105.1 (0.1) TURN RIGHT and enter I-40 westbound.

125 (20.0) **End of trip** in central Barstow. Highway I-40 joins I-15 which runs southwest to San Bernardino. Highway 247 (Barstow Road) runs south to Lucerne Valley and the San Bernardino Mountains. Three miles ahead, Highway 58 leads to Mojave and Bakersfield.

References cited

- Bell, M. A. and R. E. Reynolds. 2010. Miocene and Late Pleistocene stickleback spines from the Mojave Desert, California. In *Overboard in the Mojave: 20 million years of lakes and wetlands*, R. E. Reynolds and D. M. Miller, eds. Desert Studies Consortium, p. 162-168.
- Bishop, K. M. 2013. Rock avalanche setting of the Cave Mountain (Baxter Mine) iron deposits, Afton Canyon, California, in *Raising Questions in the Central Mojave*, R.E. Reynolds, ed. California State University Desert Studies Consortium, this volume.
- Bortugno, E. J. and T. E. Spittler. 1986. Geologic map of the San Bernardino quadrangle, scale 1:250,000. Regional Geologic Map Series, Map No. 3A, California Division of Mines and Geology.
- Byers, F. M. 1960. Geology of the Alvord Mountain quadrangle, San Bernardino County, California. U.S. Geological Survey Bulletin 1089-A, 71 p.
- Cole, J. M., E. T. Rasbury, G. N. Hanson, I. P. Montanez, and V. A. Pedone. 2005. Using U-Pb ages of Miocene tuffa for correlation in a terrestrial succession, Barstow Formation, California. *Geological Society of America Bulletin*, 117, p. 276–287.
- Cooper, J. F. Jr., G. E. Dunning, T. A. Hadley, W. P. Moller, and R. E. Reynolds. 2002. The Sulfur Hole, Calico District, San Bernardino County, California. California State University Desert Studies Consortium, p. 29-36.
- Dibblee, T. W. Jr. 1967. Geologic map of the Broadwell Lake quadrangle, San Bernardino County, California. U.S. Geological Survey. Misc. Geologic Investigations Map I-478.
- Dibblee, T. W. Jr. 1968. Geology of the Opal Mountain and Fremont Peak quadrangles, California. California Division of Mines and Geology, Bulletin 188: 64p.
- Dibblee, T. W. Jr. 1970. Geologic map of the Daggett quadrangle, San Bernardino County, California. U.S. Geological Survey Misc. Geologic Investigations Map I-592.
- Dibblee, T. W. Jr. and A. M. Bassett. 1966a. Geologic map of the Newberry quadrangle, San Bernardino County, California. U.S. Geological Survey Miscellaneous Geological Investigations Map I-461.
- Dibblee, T. W. Jr. and A. M. Bassett. 1966b. Geologic map of the Cady Mountains quadrangle, San Bernardino County, California. U.S. Geological Survey Miscellaneous Geological Investigations Map I-467.
- Dudash, S.L. 2006. Preliminary surficial geologic map of a Calico Mountains piedmont and part of Coyote Lake, Mojave desert, San Bernardino County, California: U.S. Geological Survey Open-File Report 2006-1090, scale 1:24,000. <http://pubs.usgs.gov/of/2006/1090/>
- Durrell, C. 1953. Geological investigations of strontium deposits in southern California. California Division of Mines and Geology Special Report 32, p. 23-36.
- Grose, L. T. 1959. Structure and petrology of the northeast part of the Soda Mountains, San Bernardino County, California: *Geological Society of America Bulletin*, v. 70, p. 1509–1548.
- Hamilton, P. and S. Biehler. 1982. A geophysical study of the Mojave Valley, San Bernardino County, California. *San Bernardino County Museum Association Quarterly*, v. 29 (3, 4), p. 15-24.
- Hildebrand, G. H. 1982. *Borax Pioneer: Francis Marion Smith*. San Diego, Howell-North Books, 318p.
- Hillhouse, J. W., and D. M. Miller. 2011. Magnetostratigraphy and tectonic rotation of the Miocene Spanish Canyon Formation at Alvord Mountain, California, in *The Incredible Shrinking Pliocene*, R. E. Reynolds, ed. California State University Desert Studies Consortium, p. 49-52.

- Hillhouse, J. W., D. M. Miller, and B. D. Turrin. 2010. Correlation of the Miocene Peach Spring Tuff with geomagnetic polarity time scale and new constraints on tectonic rotations in the Mojave Desert, *in* *Overboard in the Mojave*, R. E. Reynolds, ed. California State University Desert Studies Consortium, p. 105-121.
- Hillhouse, J. W., R. E. Wells, and B. F. Cox, 2010. Paleomagnetism of Miocene volcanic rocks in the Newberry Mountains, California: vertical-axis rotation and a polarity transition. Desert Studies Consortium, California State University, Fullerton, p. 177-195.
- Jachens, R. C., V. E. Langenheim and J. C. Matti. 2002. Relationship of the 1999 Hector Mine and 1992 Landers fault ruptures to offsets on Neogene faults and distribution of late Cenozoic basins in the Eastern California Shear Zone. *Bulletin of the Seismological Society of America*, v. 92 (4) p. 1592-1605.
- Laiety, J. E. 2000. Ventifacts in the Mojave River corridor and at "Ventifact Hill." *San Bernardino County Museum Association Quarterly*, v. 47 (2), p. 37-39.
- Leggitt, V. Leroy, 2002. Preliminary report on the stratigraphic setting and microstructure of Avian eggshell fragments from the Calico Mountains: Barstow Formation, Mojave Desert, California. CSU Desert Studies Consortium, p. 51-57.
- Leslie, S. R., D. M. Miller, J. L. Wooden and J. A. Vazquez. 2010. Stratigraphy, age, and depositional setting of the Miocene Barstow Formation at Harvard Hill, central Mojave Desert, California, *in* *Overboard in the Mojave*, R. E. Reynolds and D. M. Miller, ed. Desert Studies Consortium, California State University, Fullerton, p. 85-104.
- Lettis, W. R. and K. I. Kelson. 1992. Patterns of surficial deformation in the Newberry Springs area and the Johnson Valley- Homestead Valley step over associated with the 1992 Landers earthquake. EOS, Fall Meeting Abstract Supplement, p. 363.
- Liu, T. 2003. Blind testing of rock varnish microstratigraphy as a chronometric indicator; results on late Quaternary lava flows in the Mojave Desert, California. *Geomorphology*, v. 53 (3-4) p. 209-234.
- MacFadden, B. J., N. D. Opdyke and M. O. Woodburne. 1990a. Paleomagnetism and Neogene clockwise rotation of the northern Cady Mountains, Mojave Desert of Southern California. *Journal of Geophysical Research* 95(B4), p. 4597-4608.
- MacFadden, B. J., N. D. Opdyke, C. C. Swisher III and M. O. Woodburne. 1990b. Paleomagnetism, geochronology and possible tectonic rotation of the middle Miocene Barstow Formation, Mojave Desert, California. *Geological Society of America Bulletin* 102: 478-493.
- Meek, N. 1994. The stratigraphy and geomorphology of Coyote Basin, central Mojave Desert, California. *San Bernardino County Museum Association Quarterly*, vol. 47(2) p. 32-34.
- Meek, N. 1999. New discoveries about the Late Wisconsinan history of the Mojave River. *San Bernardino County Museum Association Quarterly*, vol. 46(3), p. 113-117.
- Meek, N. 2000. The late Wisconsinan history of the Afton Canyon area, Mojave Desert, California, in *Empty Basins, Vanished Lakes: The Year 2000 Desert Symposium Field Guide*, R. E. Reynolds and J. Reynolds, eds. San Bernardino County Museum Association Quarterly, vol. 47(2), p. 32-34.
- Meek, N. 2004. Mojave River history from an upstream perspective, in *Breaking Up--the 2004 Desert Symposium Field Trip and Abstracts*, R. E. Reynolds, ed. California State University, Desert Studies Consortium, p. 41-49.
- Mendenhall, W. C. 1909. Some desert watering places in southeastern California and southwestern Nevada. U. S. Geol. Survey, Water Supply Paper 224, p. 98.
- Miller, D. M. and S. R. Leslie. 2011. Geologic mapping of the Harvard Hill 7.5' topographic map. US Geological Survey, in press.
- Miller, D. M., S. R. Leslie, J. W. Hillhouse, J. L. Wooden, J. A. Vazquez and R. E. Reynolds. 2010. Reconnaissance geochronology of tuffs in the Miocene Barstow Formation; implications for basin evolution and tectonics in the central Mojave Desert. Desert Studies Consortium, California State University, Fullerton, p. 70-84.
- Miller, D. M., M. C. Reheis, E. Wan, D. B. Wahl, and H. Olson. 2011. Pliocene and early Pleistocene paleogeography of the Coyote Lake and Alvord Mountain area, Mojave Desert, California, in *The Incredible Shrinking Pliocene*, R. E. Reynolds, ed. California State University Desert Studies Consortium, p. 53-67.
- Miller, D. M., J. E. Rosario, S. R. Leslie and J. A. Vazquez. 2013. Paleogeographic insights based on new U-Pb dates for altered tuffs in the Miocene Barstow Formation, California. Desert Studies Consortium, California State University, Fullerton, this volume. Miller D. M., K. M. Schmidt, S. A. Mahan, J. P. McGeehin, L. A. Owen, J. A. Barron, F. Lehmkuhl, and R. Lohrer. 2010. Holocene landscape response to seasonality of storms in the Mojave Desert. *Quaternary International*, vol. 215, p. 45-61.
- Myrick, David F. 1963. *Railroads of Nevada and Eastern California*. Berkeley, Howell North Books.
- NL Chemicals. 1982. A pictorial history of Hectorite mining and processing in the Mojave Desert, 1930s-1960s, Hector and Newberry Springs, California, p. 23.
- Oskin, M., L. Perg, D. Blumentritt, S. Mukhopadhyay, and A. Iriondo. 2007. Slip rate of the Calico fault: implications for geologic versus geodetic rate discrepancy in the Eastern California Shear Zone, *J. Geophys. Res.*, 112, B03402, doi:10.1029/2006JB004451.
- Phelps, G. A., D. R. Bedford, D. J. Lidke, D. M. Miller and K. S. Schmidt. 2011. Preliminary Quaternary geologic map and database of the Newberry Springs 30' x 60' quadrangle, California. U.S. Geological Survey Open-File Report 2011-1044, 59 pp. <http://pubs.usgs.gov/of/2011/1044/>
- Phillips, F. M. 2003. Cosmogenic (super 36) Cl ages of Quaternary basalt flows in the Mojave Desert, California, USA. *Geomorphology*, vol. 53 (3-4), p. 199-208.
- Reheis, M.C., D. M. Miller and J. L. Redwine. 2007. Quaternary stratigraphy, drainage-basin development, and geomorphology of the Lake Manix basin, Mojave Desert—Guidebook for fall field trip, Friends of the Pleistocene, Pacific Cell. U.S. Geological Survey Open-File Report 2007-1281, 31 p.
- Reynolds, R. E. 1993. Road log through the 1992 Landers surface rupture; in: *Landers: Earthquakes and Aftershocks*. San

- Bernardino County Museum Association Quarterly, vol. 40(1) p. 3-39.
- Reynolds, R. E. 1998a. Flamingo egg from the Miocene sediments of the Calico Mountains, San Bernardino County, California, in Abstracts of Proceedings, 1998 Desert Research Symposium, J. Reynolds, ed. San Bernardino County Museum Association Quarterly, 45(1, 2), p. 106.
- Reynolds, R. E. 1999. A walk through Borate, rediscovering a Borax mining town in the Calico Mountains. San Bernardino County Museum Association Quarterly, vol. 46(1): 31.
- Reynolds, R. E., B. Lemmer and F. Jordan. 1994. The Landers rupture zone and other faults in the Central Mojave Desert Province, California, Field Trip 11 in Geological investigations of an active margin, S.F. McGill and T.M. Ross, eds. 27th Annual Meeting, Geological Society of America, Cordilleran Section Guidebook, p. 258-271.
- Reynolds, R. E., D. M. Miller, M. O. Woodburne, and L. B. Albright. 2010. Extending the boundaries of the Barstow Formation in the central Mojave Desert. CSU Desert Studies Consortium, p. 148-161.
- Reynolds, R. E., and D. M. Miller, eds. 2010. Overboard in the Mojave: the field guide. Desert Studies Consortium, California State University, Fullerton, p.7-23.
- Reynolds, R.E. and R. L. Reynolds, R.L. 1991. Structural implications of late Pleistocene faunas from the Mojave River Valley, California, in Inland southern California: the last 70 million years, M.O. Woodburne, R.E. Reynolds, and D.P. Whistler, ed. Redlands, San Bernardino County Museum Association Quarterly 38(3,4) p.100-105.
- Reynolds, R. E., and R. L. Reynolds. 1994. The isolation of Harper Lake Basin, in Off limits in the Mojave Desert, R.E. Reynolds, ed. San Bernardino County Museum Association Special Publication, 94(1), p. 34-37.
- Reynolds, R. E. and M. O. Woodburne. 2002. Review of the Proboscidean datum within the Barstow Formation, Mojave Desert, California [abs], in Between the basins: exploring the western Mojave and southern Basin and Range Province, R. E. Reynolds, ed. California State University, Desert Studies Consortium, p. 82-83.
- Ross, T. M. 1992. Geologic and paleomagnetic constraints on the timing of initiation and amount of slip on the Rodman and Pisgah faults, central Mojave Desert, California. San Bernardino County Museum Association Special Publication, 92(1), p. 75-77.
- Ross, T. M. 1995. North-south directed extension and timing of extension and vertical-axis rotation in the southwestern Cady Mountains, Mojave Desert, California. Geological Society of America Bulletin 107, p. 793-811.
- Schmidt, K. M. and V. E. Langenheim. 2012. Quaternary offset of the Cady fault, eastern California shear zone, southern California. Searching for the Pliocene: southern exposures, R. E. Reynolds, ed. CSU Fullerton Desert Studies Consortium, p. 144-150.
- Schneider, J. S. 1989. Fresh water bivalves as paleoenvironmental indicators. San Bernardino County Museum Association Quarterly, vol. 36(2), p. 65.
- Schuiling, W. T. 1999. A Miocene hot spring exhalite in the southern Calico Mountains. San Bernardino County Museum Association Quarterly vol. 46(3), p. 89-94.
- Singleton, J. S., and P. B. Gans. 2008. Structural and stratigraphic evolution of the Calico Mountains: Implications for early Miocene extensions and Neogene transpression in the central Mojave Desert, California. Geosphere, vol. 4, p. 459-479.
- Sylvester, A. G., K. C. Burmeister and W. S. Wise. 2002. Faulting and effects of associated shaking at Pisgah Crater Volcano caused by the 16 October 1999 Hector Mine earthquake (M_w 7.1), central Mohave Desert, California. Bulletin of the Seismological Society of America, v. 92 (4) p. 1333-1340.
- Thompson, D. G. 1921. Routes to desert watering places in the Mohave Desert region. . U. S. Geological Survey Water Supply Paper 490-B, p. 183.
- Thompson, D. G. 1929. The Mohave Desert region, California, a geographic, geologic, and hydrologic reconnaissance. U. S. Geological Survey Water Supply Paper 578.
- Unruh, J. R., W. R. Lettis and J. M. Sowers. 1994. Kinematic interpretation of the 1992 Landers earthquake: Bulletin of the Seismological Society of America, vol. 84(3) p. 537-546.
- Vredenburg, L. M. 2013. Calico: a brief overview of mining history. Desert Studies Consortium, California State University, Fullerton, this volume.
- Walker, J. D., M. W. Martin, J. M. Bartley, and D. S. Coleman. 1990. Timing and kinematics of deformation in the Cronese Hills, California, and implications for Mesozoic structure of the southwestern Cordillera. Geology, vol. 18, p. 554-557.
- Warren, C. N., and J. S. Schneider. 2000. Archaeology in Cronese Basin: a history. San Bernardino County Museum Association Quarterly, vol. 47(2), p. 40-41.
- Weber, H. F. Jr. 1966. Silver mining in Old Calico. Mineral Information Service, Calif. Div. Mines & Geol., vol. 19(5), p. 71-80.
- Wells, R. E. and J. W. Hillhouse. 1989. Paleomagnetism and tectonic rotation of the lower Miocene Peach Springs Tuff: Colorado Plateau, Arizona, to Barstow, California. Geol. Soc. Am. Bull., v. 101, p. 846-863.
- Wise, W. S. 1968. Geologic map of the Pisgah and Sunshine Cone lava fields. NASA Technical Letter, NASA-11, p. 8.
- Woodburne, M. O. 1998. Arikareean and Hemingfordian faunas of the Cady Mountains, Mojave Desert province, California. In Depositional environments, lithostratigraphy, and biostratigraphy of the White River and Arikaree Gouups (late Eocene to early Miocene, North America, D. O. Terry Jr, H. E. LaGarry, and R. M. Hunt Jr, eds. Geological Society of America Special Paper 325: 197-201.
- Woodburne, M. O. and R. E. Reynolds. 2010. Litho- and biochronology of the Mojave Desert Province, California. California State University, Fullerton Desert Studies Consortium, p. 124-147.
- Wright, L. A., R. M. Stewart, T. E. Gay and G. C. Hazenbush. 1953. Mines and minerals of San Bernardino County, California. California Journal of Mines and Geology, vol. 49 (1, 2), p. 93.

Paleogeographic insights based on new U-Pb dates for altered tuffs in the Miocene Barstow Formation, California

D. M. Miller,¹ J. E. Rosario¹, S. R. Leslie,² and J. A. Vazquez¹

¹ U.S. Geological Survey, 345 Middlefield Road, Menlo Park, CA 94025

² NCAR, University of Colorado, Boulder, Colorado, 80309

ABSTRACT: The type section of the Barstow Formation in the Mud Hills, north of Barstow, is a reference section for early to middle Miocene paleontology, magnetostratigraphy, and dated volcanic episodes. Thanks to this robust chronologic framework, much of the interpretation of the paleogeography of the region from about 18 Ma to 13 Ma is based on study of the rocks in the Mud Hills. Eastward from the type section, the Barstow Formation typically is altered and structurally complex, and therefore it is hard to fit into the patterns inferred for sedimentation at the type section. We have studied ten tuff beds in five locations, extracting zircons that are partly eruptive components of the volcanic ash and partly detrital. Ion microprobe dating of the zircons associated with the ashes allows us to improve stratigraphic correlations. Dated tuffs range from 19.3 Ma to ~14.8 Ma. In several of the sections, we dated tuffs in the range 16.2-16.5 Ma, about the same age as the ~16.3 Ma Rak Tuff in the type section. The beginning of lacustrine limestone, shale, and siltstone deposition varies significantly, from ~16.3 Ma in the type section to ~18.5 Ma in hills to the east and the Calico Mountains, and greater than 19.3 Ma at Harvard Hill. At ~16.3 Ma, the sedimentary rocks ranged (west to east) from silty sandstone and limestone, to mudstone with gypsum, to massive mudstone, and then to sandstone. If the sections have not been greatly shuffled by subsequent faulting, the picture that emerges is one of a broad basin whose center near the Yermo Hills was occupied by a lake that was much longer lived and deeper than to the east and west.

Introduction

As part of an investigation into neotectonics in the Mojave Desert part of the Eastern California Shear Zone (Dokka and Travis, 1990; ECSZ), we have been studying the Barstow Formation and its basins (Fig. 1) to establish a pre-ECSZ template that could be used for reconstructing faults and distributed deformation in the central Mojave Desert. The Barstow Formation has been described as a post-extension basinal deposit (e.g., Fillmore 1993; Fillmore and Walker, 1996) and therefore should not require restoration for early Miocene extension associated with the central Mojave metamorphic core complex. Our studies (Miller et al., 2010) have shown that extensional tectonism, although less profound, continued into the time span of the Barstow Formation deposition, spurring more study of the Barstow Formation.

This report provides preliminary zircon U-Pb geochronologic results for the Barstow Formation, and summarizes these results in terms of paleogeography of the northwestern part of the Barstow basin. Because the strata are significantly altered by hydrothermal processes in much of this area, age control relies on methods other than the commonly used ⁴⁰Ar/³⁹Ar method. Using an ion microprobe, we have dated individual zircon grains in altered tuff beds to place stratigraphic sections into a temporal context with the type Barstow Formation.

Geochronology and stratigraphy of the Barstow Formation.

The Barstow Formation is a ~1-km thick sedimentary sequence of conglomerate and lacustrine rocks at its type section (MacFadden et al., 1990) in the Mud Hills (Fig. 1, 2) but it is entirely lacustrine in many of the locations we studied. Rocks are commonly silicified, and in many places also show alteration to gypsum, clays, iron-oxide, and celadonite; as a result of the extensive alteration, correlation across the basin has been difficult. The formation has been well dated at its type section in the Mud Hills (Fig. 2), where six tuff and tuffaceous sandstone beds have been dated by K-Ar and ⁴⁰Ar/³⁹Ar methods and magnetostratigraphy (McFadden et al., 1990). The tuffs in the Barstow Formation type section previously have been given informal names; therefore, to maintain continuity with the previous literature these names have been retained, but the informal status is indicated as “tuff”. The lower part of the formation is dated by the locally interstratified ~19.3 Ma Red tuff and the uppermost part is dated by the ~13.4 Ma Lapilli Sandstone. This sequence is well-characterized for vertebrate fossils and serves as the reference section for the Barstovian land mammal stage (e.g., Woodburne et al., 1990) of the upper Miocene. Woodburne et al. (1990) and Woodburne (1991) divide the

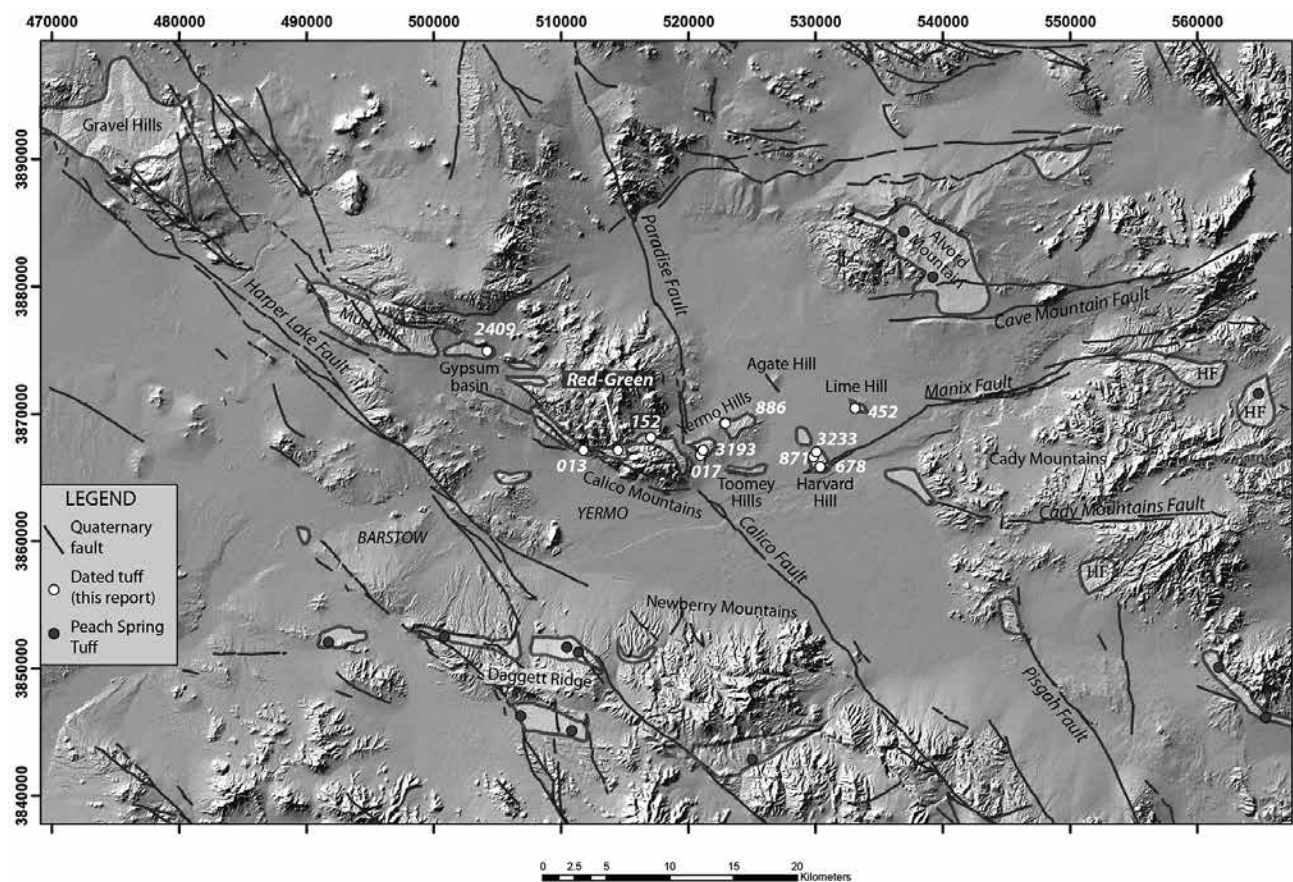


Figure 1. Location map of the Barstow, California, area, showing areas where the Barstow Formation and similar-age stratigraphic sequences are exposed. HF=Hector Formation. Dots include one tephrochronology sample along with 10 zircon samples. Peach Spring Tuff sites are from Hillhouse et al. (2010) and Miller et al. (2010), with a few added sites from studies by the authors.

type section into a lower unit of fluvial conglomerate (Owl Conglomerate member) succeeded by a thick lacustrine interval of sandstone to mudstone, and locally limestone. The lacustrine interval is approximately bracketed by the ~16.3 Ma Rak tuff and the ~13.4 Ma Lapilli Sandstone.

Singleton and Gans (2008) studied the Barstow Formation and volcanic rocks in the Calico Mountains, establishing that the underlying Pickhandle Formation is as young as 19.0 Ma and that intrusive and volcanic rocks dated at 17.1 to 16.8 Ma intrude and are deposited on the Barstow Formation. Reynolds (2000, 2004,) and Reynolds et al. (2010) established a sequence of marker units in the Barstow Formation at the type section and in many other exposures, providing an opportunity to correlate strata across the basin. Two of the markers we refer to in many sections. They are a lower, gray thick-bedded to massive limestone that typically carries many stromatolite buildups (massive stromatolitic limestone, MSL), and an upper series of brown thin-bedded limestones with characteristic plant fossils (brown platy limestone, PBL). However, the marker units were shown by Miller et al. (2010) to be strongly time-transgressive. Using the Peach Spring Tuff (~18.8 Ma; Ferguson et al., 2013), these workers showed that the marker units both underlie and overlie the distinctive tuff, and as a group range in age

from place to place by as much as 3 million years (Reynolds et al., 2010).

Methods

We attempted to date tuffs within altered lacustrine sequences by use of U-Pb geochronology, using the joint Stanford-USGS SHRIMP-RG ion microprobe. Tuff samples were crushed and ground, and heavy minerals were separated by use of heavy liquids, sieving, and magnetic sorting. Zircons were hand-picked under a binocular microscope, embedded in epoxy mounts along with standards, and polished and imaged with cathodoluminescence. The images were used as guides for locating the SHRIMP probe spots for analysis; individual analyses used a 5–6 nA primary beam of O_2^- to sputter an approximately 15–30 micrometer wide pit, allowing for separate zones in zircon crystals to be analyzed. In addition to radiogenic daughter products of the U-Pb system, we collected data on several trace and rare-earth elements (not reported in this paper). Concentrations for U, Th and all of the measured trace elements are standardized against the well-characterized, homogeneous zircon standard MAD, and U-Pb ages are referenced to zircon standard R33 (419 Ma, Black et al., 2004). Data were reduced using programs SQUID 1 and Isoplot (Ludwig, 2001, 2002). All U-Pb ages are reported with 2-sigma errors that

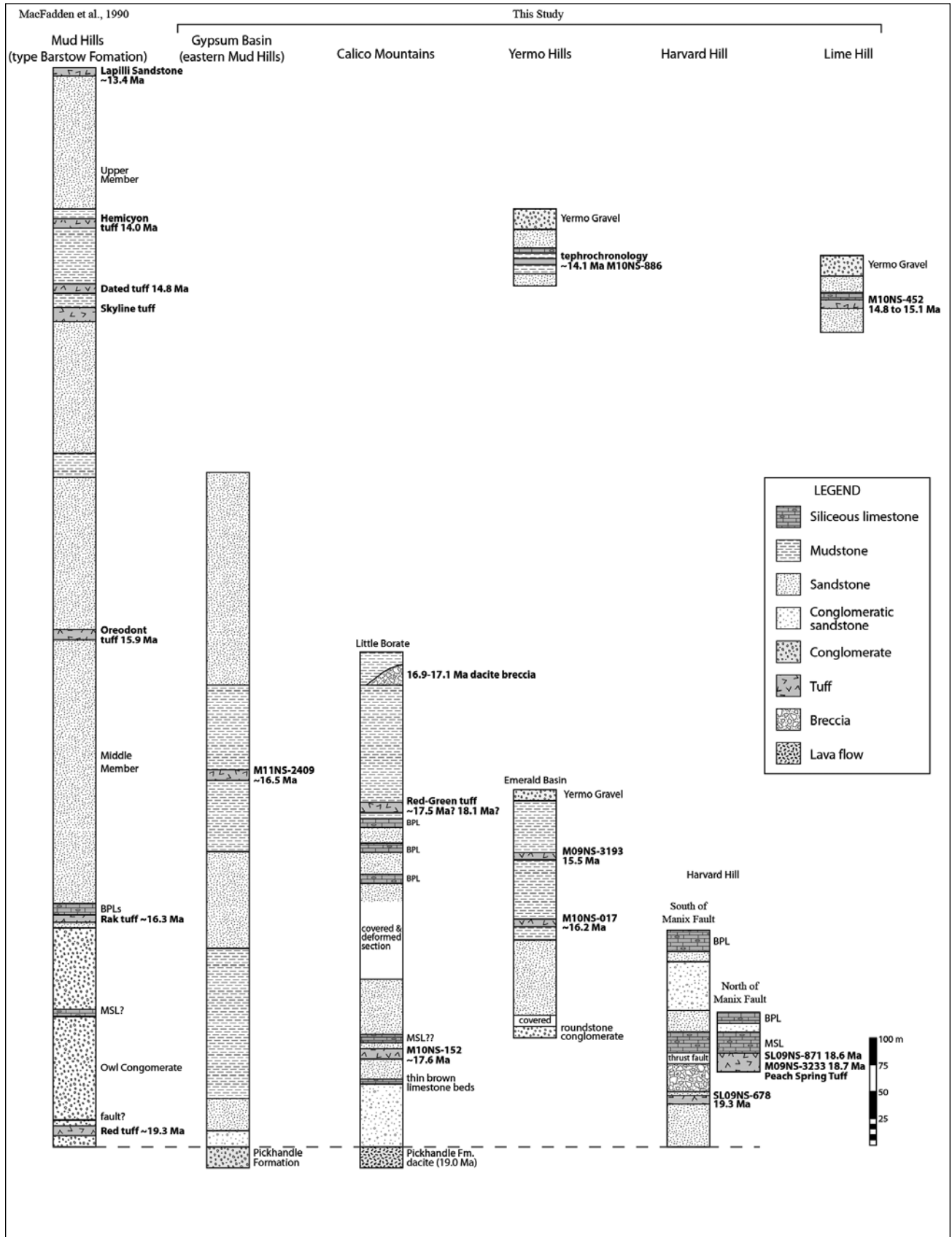


Figure 2. Generalized stratigraphic columns for eight sections of the Barstow Formation in six locations, showing context for dated tuff beds. BPL, brown platy limestone; MSL, massive stromatolitic limestone. The deformed Cemetery Ridge section is not shown.

Table 1. Summary of U-Pb data for zircon from 10 Miocene tuff samples. Weighted mean ages and errors are for the youngest coherent groups of zircons that are chemically similar and excludes outlier zircons with the Mesozoic and Proterozoic ages.

StationID	UTM_E	UTM_N	Date collected	Comments	Age	error	n	N
M11NS-2409	504201	3874903	10-Nov-11	yellow tuff in Gypsum Basin	16.5	0.2	4	7
M10NS-013	511728	3867132	13-Jan-10	white biotite tuff, Cemetery Ridge	18.6	0.4	6	10
M10NS-152	517048	3868098	8-Apr-10	thin white tuff in sandstone section, Little Borate	17.6	0.2	7	11
Red-Green	514470	3867074	10-Nov-11	tuff in Red-Green section, Mule Canyon	18.1	0.2	25	26
M10NS-017	521002	3866844	13-Jan-10	lower white tuff in Emerald Basin section	16.2	0.1	13	34
M09NS-3193	521084	3867068	16-Nov-09	white tuff high in Emerald Basin section	15.5	0.5	20	29
SL09NS-871	529970	3866740	11-May-09	Peach Spring Tuff, green tuffaceous sandstone	18.7	0.2	32	35
M09NS-3233	530048	3866896	19-Nov-09	Peach Spring Tuff, pale green massive tuff	18.6	0.1	39	39
SL09NS-678	530359	3865815	8-May-09	Harvard Hill white tuff, feldspar-quartz-biotite	19.3	0.4	30	39
M10NS-452	533078	3870438	1-May-10	Lime Hill tuff sandy to platy clean tuff	14.8	0.2	12	21

Notes: UTM coordinates in NAD 83. Age in Ma, error as 2σ . N = total number of grains analyzed; n = number of grains used for age reduction.

include both uncertainties in the zircon grain statistics and uncertainties associated with the standards (Table 1).

Results

We studied zircons from tuff beds sampled in five locations ranging from hills east of the Mud Hills (“Gypsum basin”) to Lime Hill (Fig. 1). Results are shown in Figure 2 as generalized stratigraphic sections. Although many sections are only partial, they provide a chronostratigraphic framework for the deposits and facies of the Barstow Formation.

Gypsum basin

Although Gypsum basin is less than 10 km east of the type section of the Barstow Formation in the Mud Hills, strata are strikingly different (Fig. 2). Lacustrine conglomerate, sandstone, and siltstone lie directly on the Pickhandle Formation, with no intervening Owl Conglomerate seen at Gypsum basin. Thin limestone beds in the lower part resemble the brown platy limestone (BPL) marker unit of Reynolds (2001). The middle part of the section is composed of gypsiferous mudstone, with a central part of this interval being sandstone. The upper part is sandstone that is locally conglomeratic. A thick yellowish tuff bed high in the gypsiferous mudstone section is altered to apatite, zeolite, and clay, but yielded sparse (see Table 1 for grain counts) zircons that are 16.5 ± 0.2 Ma (M11NS-2409; Table 1). The bed is not firmly dated because zircon yield was low. Other tuff beds in the section are possible targets for dating.

Calico Mountains

The interpretation of ages for the Barstow Formation in the Calico Mountains sections of the Barstow Formation is not straightforward. Difficulties arise from

segmentation of the formation by several strands of the Calico Fault, by tight folding of strata in many exposures, and by lateral changes in facies and alteration characteristics. In addition, the base of the formation was probably irregular, since it was deposited in places on ~ 19.0 Ma lava flows and domes of the Pickhandle Formation (Singleton and Gans, 2008), and the Barstow Formation was intruded by and overlain by dacite dome-flow complexes that range from 17.1 ± 0.1 Ma to 16.8 ± 0.2 Ma, as determined by $^{40}\text{Ar}/^{39}\text{Ar}$ (Singleton and Gans, 2008). We targeted four beds of altered tuff, three of which were nearly entirely altered to apatite. One sample was in a section between two strands of the Calico Fault (Cemetery Ridge), and three are in the Mule Canyon to Little Borate area. One tuff bed yielded no zircons and will not be discussed.

Cemetery Ridge. A section of sandstone, conglomerate, and mudstone lies between two strands of the Calico Fault at this location. It is structurally complex, so we did not create a stratigraphic section. Two white tuff beds about 2 m thick occur in mudstone and sandstone. Each tuff bed includes beds of sandstone, suggesting that the tuff is detrital. We sampled the upper white tuffaceous sandstone, which contains feldspar and biotite, and lies in a section of brown limestone and tan sandstone. Sample M10NS-013 yielded sparse zircons, but the youngest group of grains forms a population with a weighted mean age of 18.6 ± 0.4 Ma (Table 1). Some of the zircon grains are chemically similar to the 18.8 Ma Peach Spring Tuff (e.g., Miller et al., 2010).

Little Borate tuff. At Little Borate, a calcareous sandstone sequence contains a thin (2-5 cm) tuff bed that is pale gray with visible biotite and feldspar phenocrysts and is in part reworked and laminated (Figs 1 and 2). The tuff bed (sample M10NS-152) is dated on the basis of 7 zircon

grains. Others we measured were Mesozoic. The 7 grains are very similar in appearance, age, and chemistry and yielded a weighted mean age of 17.6 ± 0.2 Ma. The tuff lies approximately 70 m above the base of the Barstow Formation, which was deposited on a 19.0-19.1 Ma Pickhandle rhyodacite (Singleton and Gans, 2008). The section of calcareous sandstone was folded and faulted in a soft-sediment environment, but it lies below a pale ledge of limestone considered to be the MSL (R.E. Reynolds, 2009, oral communication). The tuff bed lies well below three prominent ledges of brown limestone considered to be the BPL sequence. Some ambiguity in applying the marker bed terminology exists because a few thin brown platy limestones also underlie this tuff (Fig. 2)

Red-Green tuff. The Red-Green tuff was sampled from a 3-cm thick bed in a section southwest of Little Borate, causing ambiguity with correlations between the locations. Detailed mapping by Sadler (this volume) allows the Red-Green sandstone interval, within which the tuff occurs, and underlying brown limestones to be traced from the sample site to Little Borate, placing it higher in the section than sample M10NS-152. The Red-Green tuff had 25 grains that are similar texturally and compositionally, and that vary fairly smoothly from 17.0 to 19.0 Ma. One (#26) is an outlier at 15.8 Ma. There are three possible interpretations of the age data. (1) The full population of 25 grains yields an age of 18.1 ± 0.2 Ma, seemingly too old given its position ~220 m above the Little Borate tuff (M10NS-152). If the Red-Green tuff is ~18.1 Ma, it lies in a stratigraphic section that is sharply time-transgressive, with brown platy limestone (BPL) marker beds becoming younger to the east. (2) It is possible to pick breaks such that the youngest three and oldest three grains are distinct, and discard them for the analysis. The remaining grains form an age distribution without significant gaps. However, eliminating 6 outlier grains changes the age only slightly to 18.0 ± 0.2 Ma. (3) If we acknowledge that the tuff must be younger than ~17.6 Ma, and only use the youngest zircon grains in the analysis, we can select populations of the young grains that yield weighted means ranging from 17.5 to 17.6 Ma (± 0.4). For this to be the case, we have to argue that most of the juvenile-appearing, fairly abundant, fragile zircon grains are derived from the erupting magma but represent earlier-formed crystal mush or sidewall plucked material.

The Red-Green tuff must be older than the 17.1 Ma dacite domes. The lowest stratigraphic interval in which debris from those domes was deposited is 130 m above the BPLs (Fig. 2) and the Red-Green tuff is therefore likely to be much older, best fitting with the entire zircon grain data at 18.1 ± 0.2 Ma. The dated tuffs suggest that stratigraphic and/or structural complexities exist in the Calico Mountains.

Difficulty in determining and interpreting unique ages for the Little Borate and Red-Green tuffs results in geochronologic uncertainties for these rocks. Although there appears to be consistent stratigraphy across the two

sections, such as a gradational fining upward sequence in grain size, there are still many stratigraphic and/or structural complexities that must be solved.

Yermo Hills

East of the Calico Mountains, the Yermo Hills (Fig. 1) contain several exposures of the Barstow Formation. The thickest exposure, at "Emerald basin", is about 220 m thick. Exposures 2 km to the east at Calico Early Man Site are similar, but those 10 km east of the Emerald basin are different and are shown in Figure 2 as a separate section.

The sequence at Emerald basin, greater than 200 m thick, consists of a lower roundstone conglomerate, which is distinguished from other conglomerates such as the Owl Conglomerate by its well-rounded and distinctly bedded pebble-rich stream deposits that appear to represent a big stream. The conglomerate is overlain by a covered interval and then a thick lacustrine sandstone interval followed by thick mudstone (Fig. 2). Much of the section is altered and green-colored with celadonite or other secondary minerals. It contains no limestone beds. Southern exposures of the section have recognizable ash beds, although the materials are variably altered to silica. We sampled the two beds with apparent phenocrysts in this area, and provide approximate positions for these tuff beds in the more complete section shown in Figure 2, which lies north of the sampled beds by about 1 km.

Upper Emerald. The uppermost tuff beds are a pair of thin white beds, below which is a thicker (~1 m) white to pale green bed with biotite phenocrysts that we sampled. The whiter, finer, and most shard-rich lower part of the bed (sample M09NS-3193) contains numerous acicular zircons that give an age of 15.5 ± 0.5 Ma (Table 1). Parts of the bed are altered to white silica.

Lower Emerald. Approximately 80 m lower in the section than sample M09NS-3193 is the lowest well exposed white tuff. It contains vestiges of feldspar phenocrysts and sparse biotite (sample M10NS-017), and yielded a moderate number of zircon grains that group tightly to give an age of 16.2 ± 0.1 Ma (Table 1). The transition from sandstone to mudstone is about 13 m below this sample.

Tephrochronology of eastern exposures. A sample from an unaltered thin white ash bed (M10NS-886) interbedded with green thin bedded sandstone and siltstone was examined for chemical correlations (Fig. 2). One bed of white limestone altered to lacey textured opal occurs above the ash bed. The firmest correlation was with an ash sampled at Point of Rocks (Miller et al., 2011) with an interpolated age of 14.1 Ma. This ash, derived from the southern Nevada volcanic field, occurs elsewhere in the Mojave Desert from a sedimentary sequence in the Piute Range and the Muddy Creek Formation in Arizona Rocks (Miller et al., 2011).

Harvard Hill

Rocks at Harvard Hill (Fig. 1) were thoroughly described by Leslie et al. (2010), who showed that Miocene strata north and south of a strand of the Manix Fault differed

significantly (Fig. 2). South of the fault, lacustrine and alluvial materials underlie a thick avalanche breccia deposit. North of the fault, limestone and other rocks lie on a thick altered tuff. Limestone beds in the two sections are similar. Leslie et al. (2010) presented preliminary dates for two tuff units, which we later improved by dating more grains in each sample.

White tuff of Harvard Hill. The southern section includes the MSL and BPL, and intervening mudstone and alluvial conglomerate and sandstone. A thrust (?) fault places a section with a thick white tuff in a thin-bedded sandstone and shale onto the BPL (shown on Fig. 2 as older than, and below, the limestone section). This white tuff (sample SL09NS-678, Table 1) contains biotite, quartz, and feldspar, and yielded numerous zircons grains that form a broad peak at about 19.3 ± 0.4 Ma. Lacustrine sandstone and shale must be older than this.

Peach Spring Tuff. The 18.8 Ma Peach Spring Tuff (Ferguson et al., 2013) is pale green-colored and thicker than about 11 m in exposures at the north end of Harvard Hill. We dated the Peach Spring Tuff (initially called the Shamrock tuff by Leslie et al., 2010) in two places, one near the base of the exposure (sample M09NS-3233) in massive tuff containing feldspar, quartz, and sphene, and one near the top, where it is bedded and apparently reworked by waves (SL09NS-871). The lower sample is of rock with oriented ash particles, pumice lumps, and lithic clasts. Both samples yielded many zircon grains that have distinctive high Th/U chemistry (Miller et al., 2010) and that yield an age of 18.7 ± 0.2 Ma. The upper sample has several grains that are as young as 18.2 Ma, but which are not statistically distinct; these may represent Pb loss in this part of the deposit (M. Lidzbarski, 2011, personal communication). Overlying MSL and BPL units must be somewhat younger.

The limestone units at southern Harvard Hill may be similar in age to those in northern Harvard Hill, as shown in Fig. 2, but Peach Spring Tuff cannot be confirmed beneath the MSL in the southern exposures to establish age equivalence (the limestone is underlain by a thrust fault). The date on the white tuff demonstrates that lacustrine deposition began before 19.3 Ma.

Lime Hill

A section of the upper part of the Barstow Formation underlies the Yermo gravel (or its correlative; Miller et al., 2011) in a hill, which is informally named Lime Hill for its triangulation station “Lime”, and is located northeast of the Harvard Road exit at Interstate 15, (Fig. 1). Much of the section consists of thin bedded green tuffaceous and calcareous sandstone (Fig. 2). Pumice and the presence of biotite and feldspar mark pale-colored sandstone beds as tuffaceous. Other beds range to arkose with grains derived from Mesozoic granitic rocks. Sample M10NS-452 was collected from a white tuff bed with platy texture. This bed grades downward into calcareous sandstone that is only slightly tuffaceous, and these relations suggest

that, although little altered and fairly pure, the tuff is reworked. The tuff sample yielded abundant zircon. Of the 21 grains analyzed, 9 ranged from 18 Ma to Proterozoic in age. The remaining 12 grains make up a population with a weighted mean age of 14.8 ± 0.2 Ma (Table 1). This tuff also was studied for tephrochronologic correlations (Miller et al., 2011) and yielded possible correlations with 9.9 Ma ash and several ashes from 6.3 to 3.1 Ma. Absence of zircon grains younger than ~ 14.8 Ma indicates that the ash is older than the chemical correlations imply.

About 6 m above the tuff bed is a resistant ledge of silicified limestone about 1 m thick. The limestone contains plant fragments and cigar-size stromatolites, with some hints of larger stromatolites in opaline masses, and thus is similar in some respects to the MSL, but it bears closer resemblance to the lacey-textured silicified limestone in the eastern Yermo Hills (Fig. 2).

Discussion of paleogeography

The U-Pb dates on tuff beds we report bear out other studies of the northern Barstow Formation exposures that concluded the onset of lacustrine deposits was variable in age, ranging from >19.3 Ma (Harvard Hill) to ~ 16 Ma (Mud Hills). Using the dated, full and partial sections summarized in Figure 2, it is possible to infer depositional setting at several time slices. At ~ 19 Ma, distal alluvial fan gravel was deposited near lake margins (Mud Hills), lake waters were reworking surface materials on lava domes (Calico Mountains), and shallow lake sediments were overridden by the Peach Spring Tuff pyroclastic flow (Harvard Hill). By 16.5 to 16 Ma, lacustrine conditions were beginning in the west (Mud Hills), while shallow water (Calico Mountains) to deeper water conditions (mudstone in Gypsum Basin and Emerald Basin) held farther east. By ~ 15 Ma, lacustrine deposits were coarsening to sandstone (representing a nearshore environment along the periphery of the lake) in the Mud Hills and Lime Hill, but there was still mudstone in the central parts of the lake (Yermo Hills), and these relations are consistent with an areal contraction of the lake.

The paleogeographic pattern that emerges is one of lacustrine conditions beginning earliest in the Yermo and Harvard Hills area, and also persisting longest in that area as basin-center facies. Deeper water environments in this area were maintained for longer than 4 million years. Limestone marker beds represent nearshore depositional environments (Reynolds et al., 2010), that range in age by more than 2 million years, generally being oldest in the basin center area of Harvard and Yermo Hills and younger toward the margins. The MSL ranges from ~ 18.8 Ma at Harvard Hill to younger than 19.3 at Mud Hills to slightly younger than 17.6 Ma at Little Borate. The BPL ranges from ~ 18.6 Ma to ~ 18.1 Ma to much younger than ~ 17.6 Ma in the Calico Mountains and ~ 16.3 Ma in the Mud Hills. Nearby steep basin margins are inferred from avalanche breccias at Harvard Hill and coarse alluvial

fan conglomerate in the Mud Hills, but other sections do not show evidence for nearby steep terrain. The lake was apparently reworking detritus off of volcanic domes of the Pickhandle Formation in parts of the Calico Mountains where the domes might have formed islands within or promontories into the lake. The top of the Barstow Formation is eroded at all locations we have studied, so little information is available for understanding how and when the lacustrine deposition ended. However, in most sections, sediment younger than ~15 to 14 Ma is coarser grained than underlying sediment, suggesting that the lake was diminishing in size.

Evidence from dated tuffs in the Calico Mountains suggests sharply time-transgressive limestone beds, in that the BPL package lies under an ~18.1 Ma tuff in one location and just 3 km to the east the BPL package overlies a 17.6 Ma tuff. Although structural complexities are possible in this highly folded section, the time-transgressive nature of the limestone package seems to be required by the dated tuffs. Studies near Daggett Ridge previously showed similar time-transgressive changes in the limestones of the lower Barstow Formation, which lie under the Peach Spring Tuff in the east and above it in the west, although the distance over which the transgressive changes take place is 12 km (Miller et al., 2010).

With more dating of tuffs in southern and eastern parts of the Barstow Basin, paleogeographic history of the basin could be clarified. Questions such as the lateral extent of lacustrine facies through time, and the timing of mineralization events such as Sr-B (Reynolds et al., 2010) could be examined more thoroughly.

Acknowledgements

Discussions with Brett Cox, Phil Gans, Bob Reynolds, Pete Sadler, and Kevin Schmidt about their unpublished studies in the area have aided our work substantially. Discussion about limestones in the Barstow Formation with Vicki Pedone was illuminating, as were discussions about the Peach Spring Tuff with David Buesch, Jack Hillhouse, Marsha Lidzbarski, Jonathan Miller, Calvin Miller and Jim Riehle. We thank Dean Miller for his help with the mineral separations and Joe Wooden, Matt Coble, and Eric Gottlieb for their superb help at the SHRIMP laboratory. We also thank Jack Hillhouse, David Buesch, and Dave Lynch for helpful comments on earlier drafts of this paper.

References

- Black, L.P., Kamo, S.L., Allen, C.M., Davis, D.W., Aleinikoff, J.N., Valley, J.W., Mundil, R., Campbell, I.H., Korsch, R.J., Williams, I.S., and Foudoulis, C., 2004, Improved $^{206}\text{Pb}/^{238}\text{U}$ microprobe geochronology by the monitoring of a trace-element-related matrix effect; SHRIMP, ID-TIMS, ELA-ICP-MS and oxygen isotope documentation for a series of zircon standards: *Chemical Geology*, v. 205, p. 115-140.
- Dokka, R.K., and Travis, C.J., 1990, Late Cenozoic strike-slip faulting in the Mojave Desert, California: *Tectonics*, v. 9, p. 311-340.
- Ferguson, C.A., McIntosh, W.C., and Miller, C.F., 2013, Silver Creek Caldera—The tectonically dismembered source of the Peach Spring Tuff: *Geology*, v. 41, p. 3-6.
- Fillmore, R.P., 1993, Sedimentation and extensional basin evolution in a Miocene metamorphic core complex setting, Alvord Mountain, central Mojave Desert, California, USA: *Sedimentology*, v. 40, p. 721-742.
- Fillmore, R.P., and Walker, J. D., 1996, Evolution of a supradetachment extensional basin: The lower Miocene Pickhandle Basin, central Mojave Desert, California: *Geological Society of America Special Paper 303*, p. 107-126.
- Hillhouse, J.W., Miller, D.M., and Turrin, B.D., 2010, Correlation of the Miocene Peach Spring Tuff with the geomagnetic polarity time scale and new constraints on tectonic rotations in the Mojave Desert, *in* Reynolds, R.E., and Miller, D.M., ed., *Overboard in the Mojave: Desert Studies Consortium*, California State University, Fullerton, p.105-121.
- Leslie, S.R., Miller, D.M., Wooden, J.L., and Vazquez, J.A., 2010, Stratigraphy, age, and depositional setting of the Miocene Barstow Formation at Harvard Hill, central Mojave Desert, California, *in* Reynolds, R.E., and Miller, D.M., ed., *Overboard in the Mojave: Desert Studies Consortium*, California State University, Fullerton, p. 85-104.
- Ludwig, K., 2001, Isoplot/EXversion 2.49: a geochronological toolkit for Microsoft Excel. Berkeley Geochronology Center Special Publication, v. 1a.
- Ludwig, K., 2002, SQUID 1.02, A Users Manual: Berkeley Geochronology Center Special Publication, v. 2.
- MacFadden, B.J., Swisher, C.C. III, Opdyke, N.D., and Woodburne, M.O., 1990, Paleomagnetism, geochronology, and possible tectonic rotation of the middle Miocene Barstow Formation, Mojave desert, southern California: *Geological Society of America Bulletin*, v. 102, p. 478-493.
- Miller, D.M., Leslie, S.R., Hillhouse, J.W., Wooden, J.L., Vazquez, J.A., and Reynolds, R.E., 2010, Reconnaissance geochronology of tuffs in the Miocene Barstow Formation: implications for basin evolution and tectonics in the central Mojave Desert, *in* Reynolds, R.E., and Miller, D.M., ed., *Overboard in the Mojave: Desert Studies Consortium*, California State University, Fullerton, p.70-84.
- Miller, D.M., Reheis, M.C., Wan, E., Wahl, D.B., Olson, H., 2011, Pliocene and early Pleistocene paleogeography of the Coyote Lake and Alvord Mountain area, Mojave Desert, California, *in* Reynolds, R.E., ed., *The incredible shrinking Pliocene: Desert Studies Consortium*, California State University, Fullerton, p. 53-67.
- Reynolds, R.E., 2000, Marker units suggest correlation between the Calico Mountains and the Mud Hills, central Mojave Desert, California: *San Bernardino County Museum Quarterly*, v. 47, no. 2, p. 1-10.
- Reynolds, R.E., 2004, Widespread early Miocene marker beds unite the Barstow Formation of the central Mojave Desert: *Inland Geological Society*, p. 1-10.

- Reynolds, R.E., Miller, D.M., Woodburne, M.O., and Albright, L.B., 2010, Extending the boundaries of the Barstow Formation in the central Mojave Desert, *in* Reynolds, R.E., and Miller, D.M., ed., *Overboard in the Mojave: Desert Studies Consortium*, California State University, Fullerton, p.148-161.
- Singleton, J.S., and Gans, P.B., 2008, Structural and stratigraphic evolution of the Calico Mountains: Implications for early Miocene extensions and Neogene transpression in the central Mojave Desert, California: *Geosphere*, v. 4, p. 459-479.
- Woodburne, M.O., 1991, The Mojave Desert Province, *in* *Inland Southern California: the last 70 million years*: San Bernardino County Museum Association Quarterly, v. 38, p. 60-78.
- Woodburne, M.O., Tedford, R.H., and Swisher, C.C., III., 1990, Lithostratigraphy, biostratigraphy and geochronology of the Barstow Formation, Mojave Desert, southern California. *Geological Society of America Bulletin*, v. 102, p. 459-477.

The Rainbow Loop Flora from the Mud Hills, Mojave Desert, California

Robert E. Reynolds¹ and Thomas A. Schweich²

¹Redlands, CA 92373, rreynolds220@verizon.net

²University of California, University and Jepson Herbaria, tomas@schweich.com

ABSTRACT: The Rainbow Loop Flora contains at least 13 plant taxa representing four sub-adjacent communities: aquatic with water reeds; riparian with streamside plants; oak woodland or parkland with a shrub understory and interspersed grassland; and a dry upland community. The age of the flora is about 16.3 Ma, falling just past the first trough of the Mid-Miocene Climactic Optimum. Associated tracks of shore birds and invertebrates help provide a picture of the depositional environment.

Introduction

The Barstow Flora was initially reported by Raymond Alf (1970), who wrote “...it is hoped that others will continue the [floral] work better to understand the ecological conditions of the upper Miocene times in Southern California.” The flora he described included specimens from two different areas in the Barstow Fossil Beds approximately two and one-half miles apart, at different stratigraphic horizons. The “petrified wood” locality (Alf, 1970), is located in the Sky Line Tuff exposed in the southern portion of Solomon’s Canyon (Durrell, 1953). The “leaf” locality is located along the Rainbow Basin Loop Road in slightly older sediments, at a spot where Alf and his students (“Peccaries”) camped (Fig 1). Due to the difference in stratigraphic position of the floras, this paper separates them by naming the former the Solomon Skyline Flora, and the latter the Rainbow Loop Flora. The well-preserved leaves figured by Alf (1970) prompted a search for the Rainbow Loop Flora locality in 2012 by volunteers working under BLM Permit.

Stratigraphy

The Rainbow Loop Flora (RLF) is located at the top of the Brown Platy Limestones (BPL) sequence and below the Strontium–Borate (Sr-B) horizon (Reynolds and others, 2010), the former dated magnetostratigraphically between 16.4–16.2 Ma at a locality half a mile west. No celestine (SrSO₄) was detected in concretions (R. Housley p. c. to Reynolds, 2013) at the RLF outcrops, suggesting a position below the Sr-B horizon, perhaps closer to 16.3 Ma. The flora lies in middle Rak Division strata below the Oredont Tuff (15.8 Ma), reinforcing an earlier age. Alternating layers of sand, silt, and silty claystone are repeated through the fossiliferous section. Bedding plane surfaces show ripple marks, flute marks, and drag marks, the latter being parallel over a length of 30 cm. These structures suggest water flowing as a sheet or

current around the margins of a shallow lake. Plant fossils range in size from limbs 5 cm in diameter to microscopic, found individually, in small clumps, or as small mats. The leaves apparently became saturated in moving water and were buried in sand. Seeds floated and are found in fine sand or silt.

Methods

Taxa were identified using visible characters such as leaf shape, margin type, vein patterns, and surface expression. Comparisons were made to existing published paleofloras, e.g., Alf (1970) and Axelrod (1940, 1985), and to modern plant material to confirm the diagnosis, e.g., Specimen 6-19, *Fraxinus*. Several of the more promising, or vexing, specimens were reviewed with University of California Museum of Paleontology staff to obtain guidance.

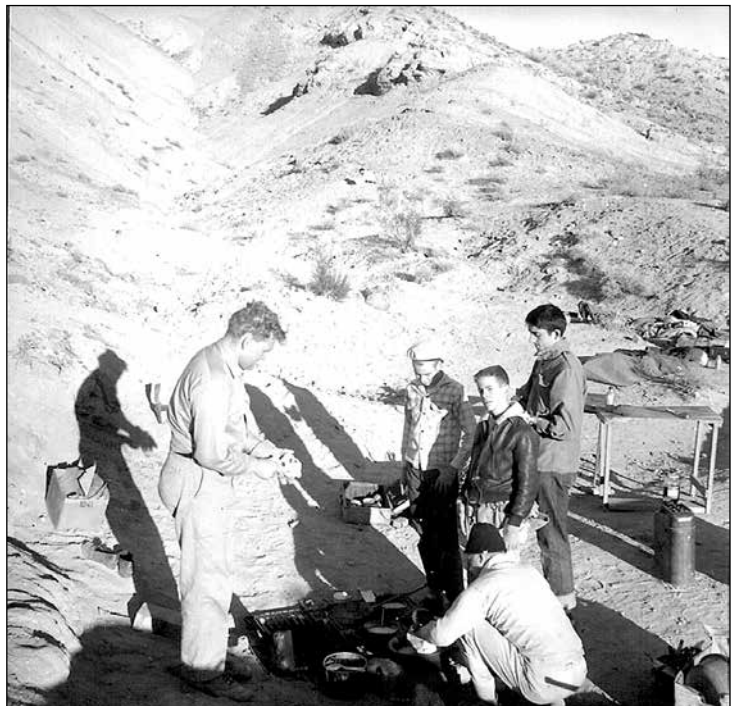


Figure 1. Raymond Alf and his student Peccaries camped near the Rainbow Loop Flora locality. Photo courtesy D. Lofgren, Alf Museum.

However, many well preserved specimens remain unidentified. They are included in this paper as figures (Fig 13-Fig. 19) and descriptions with the hope that they will be recognized by readers. Habitats are suggested by analogy to modern taxa, resting on the basic assumption that modern taxa do not differ substantially in their ecological relations from those of the past (Chaney, 1938; Cain, 1944; cited in Axelrod, 1958).

Rainbow Loop Flora descriptions

Gymnosperms

Cupressaceae, cf. *Juniperus* (Fig. 2)

Specimen 7-20 is a linear feature approximately 11 mm long and 1.5 mm wide. Lines diagonally crossing the linear feature are regularly spaced. These are most strongly visible in the central portion, and faintly visible near the ends. There are no branching features from the central feature as seen in Specimen 7-5.

Possibilities considered: This is likely a stem covered by regularly spaced scales, and is strongly reminiscent of the scale-like leaves of the genus *Juniperus*.

Dicots

Fagaceae, *Quercus* (oak), leaf. (Fig. 3)

Specimen 8-1 is a leaf, elliptical in shape. The tip is missing, but projecting curvature of the margins yields a

length of about 5.5 cm. The width is 2 cm. Margins are entire. The petiole, seen in part and counterpart, is at least 6 mm; the proximal end is not seen. Primary veins are more or less alternate, straight, and unbranched. Secondary veins cannot be seen. The overall shape, margin, vein patterns, and existence of a petiole suggest *Quercus*. There are two other similar leaves from the same location: 8-2a and 8-2b.

Fagaceae, *Quercus* (oak), acorn (Fig. 4)

Specimen 7-1 is part and counterpart of a smooth-surfaced spheroid, 11 mm diameter at the widest part, and possibly slightly flattened perpendicular to the bedding plane. The smooth surface has light longitudinal striations, but they are not prominent enough to be reticulations.

Associated material on one side could be surrounding part of the object, or could wrap around a part of the spheroid, such as a fleshy pericarp or the cup of an acorn. There are fine parallel reticulations ~1/2 mm, but it is not clear whether these are texture of the original material, such as scales, or artifacts of preservation.

Possibilities considered: Fruit, c.f., *Quercus* acorn with cup.

Possibilities considered and rejected:

- Fruit, cf. *Ginkgo*, is rounded, flattened spheroid with marginal ridge. Unfortunately, the irregularity of the

Table 1. Rainbow Loop Flora taxa, characters, and habitats

Taxa	Common name	Key Characters	Habitats Suggested
Cupressaceae, c.f., <i>Juniperus</i>	Juniper or cypress?	See text.	Warm, dry, exposed.
Fagaceae, <i>Quercus</i>	Oak	See text.	Mesic woodland.
Oleaceae, <i>Fraxinus</i>	Ash	See text.	Mesic woodland.
Rosaceae, c.f., <i>Cercocarpus</i>	Mountain mahogany	See text.	Mesic woodland or dry upland.
Rosaceae, c.f., <i>Prunus</i>	Rose family	Fruit, dense smooth center surrounded by a less-dense covering.	Mesic woodland
Rosaceae, <i>Purshia</i>	Bitterbrush	Reduced leaf, deeply lobed, pinnate veins, rolled margins.	Warm, dry, exposed.
Rubiaceae, seed.	Madder	Seed, one of a pair, adaxial groove, hemispheric shape.	Streamside to mesic woodland.
Undetermined, sclerophyllous shrub or tree, Specimen 7-15, Rhamnaceae (<i>Ceanothus</i> or <i>Rhamnus</i> ?)	Buck thorn?	Petiole, thick leaf, strong mid vein, stiff?, convex adaxially.	Mixed, warm, dry scrub,
Undetermined leaf Specimen 7-13b	?	Petiole, thick leaf, crenate base, broad flat mid vein proximally, proximal margins rolled, leathery?	Mixed, warm, dry scrub.
Undetermined leaf Specimen 7-31	?	Soft, wrinkled surface, pinnate orientation,	Mesic woodland, partial shade.
Undetermined leaf., e.g., Specimen 7-9, <i>Acer</i> .	Maple?	Thin leaf tissue, palmate veins.	Streamside.
Undetermined, numerous small leaves, <i>Salix</i> ?	Willow?	Short petioles, small, flat, pinnate veins, rounded tips.	Streamside.
Aracaceae	Palm root		Stream or wetland.
<i>Carex</i> ?	Sedge?	Leafy monocots are likely aquatic, and probably represent <i>Carex</i> and	
<i>Typha</i> ?	Cat tail?	<i>Typha</i>	

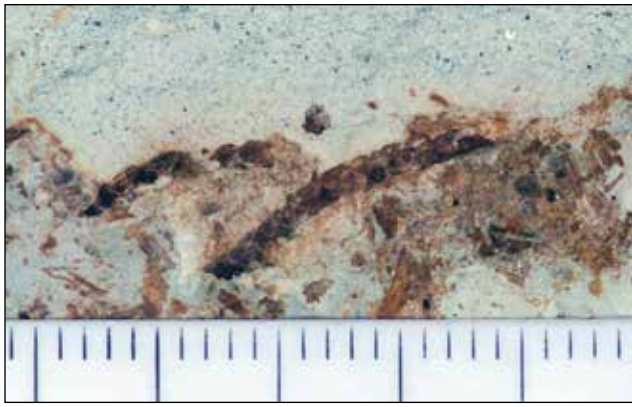


Figure 2. Cupressaceae, c.f. *Juniperus*, juniper twig.



Figure 3. Fagaceae, *Quercus*, oak leaf.

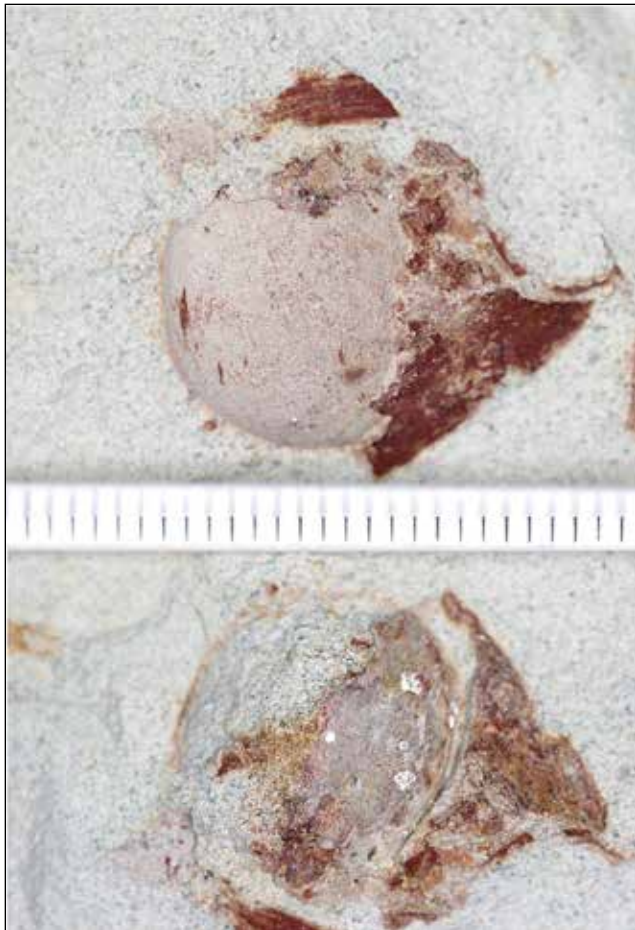


Figure 4. Fagaceae, *Quercus*, oak acorn.



Figure 5. Oleaceae, *Fraxinus*, wing of ash seed.



Figure 6. Rosaceae, c.f. *Cercocarpus*, mountain mahogany leaf.

Figure 7. Rosaceae, c.f. *Prunus*, fruit.



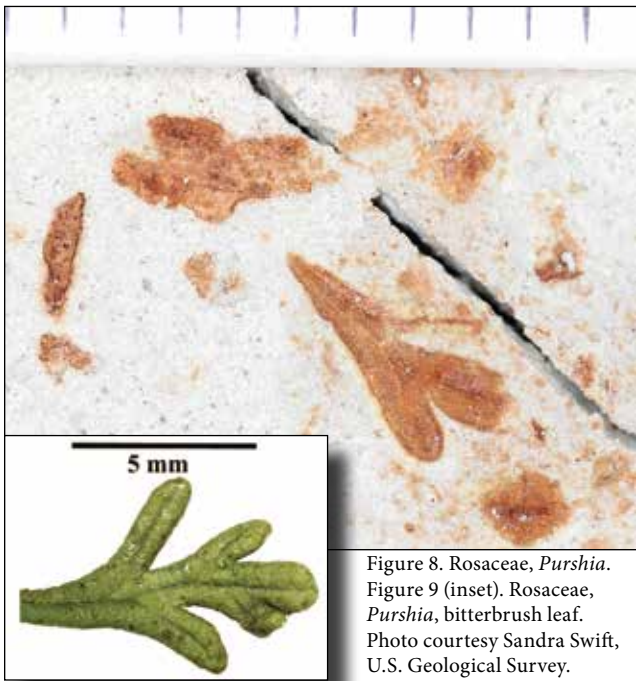


Figure 8. Rosaceae, *Purshia*.
 Figure 9 (inset). Rosaceae, *Purshia*, bitterbrush leaf.
 Photo courtesy Sandra Swift, U.S. Geological Survey.



Figure 10. Rubiaceae, madder family seed.

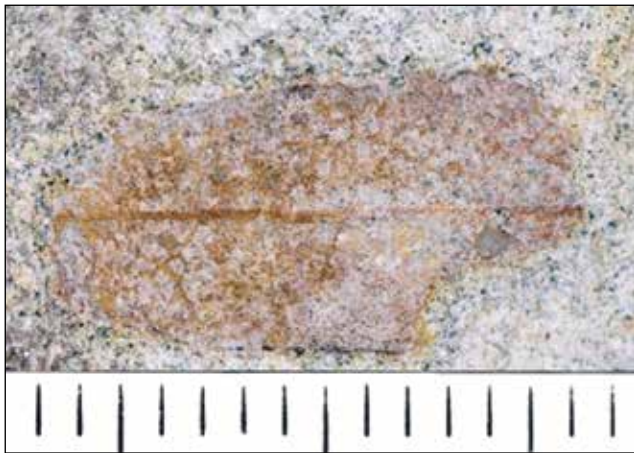


Figure 11. Undetermined, possible Rhamnaceae (*Ceanothus?* or *Rhamnus?*)

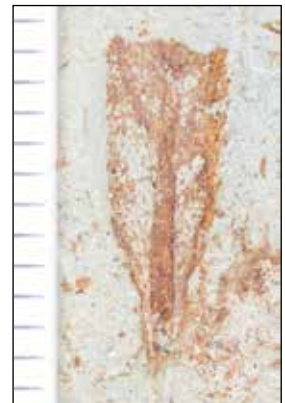


Figure 12. Undetermined, leaf.



Figure 13. Undetermined, leaf.



Figure 14. Undetermined, ?*Acer*, maple leaf

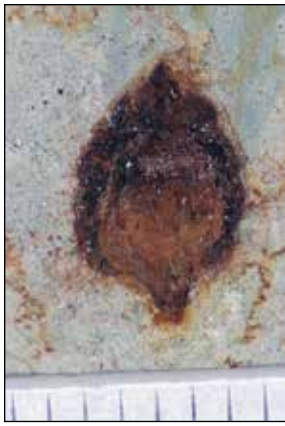


Figure 15. Undetermined, fruit.



Figure 16. Undetermined, fruit or seed.



Figure 18. *Carex?*, sedge.



Figure 17. Undetermined, interior of seed.



Figure 19. *Typha?*, cattail

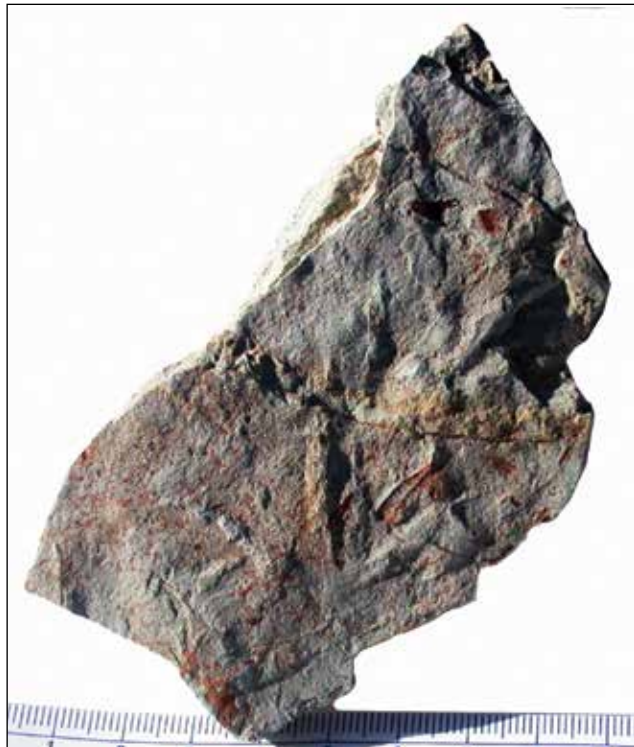


Figure 20. Tracks of *Avipeda gryponyx*, made by a bird similar to a sanderling that forages in shallow water.



Figure 21. Invertebrate tracks.

shape is insufficient to suggest the marginal ridge of the modern ginko fruit.

- Fruit, c.f., a drupe, other family.

Oleaceae, *Fraxinus*, wing of samara. (Fig. 5)

Specimen 6-19 is a fragment 20 mm in length by 9 mm wide. It appears to be thin tissue, with primary sub-parallel longitudinal veins and some secondary net veins. The edge seen at left appears to be mainly intact and shows the shape. The right edge is not intact. The proximal tip (at top) is broken and cannot be seen. The distal tip is also broken, as some additional fragments are seen above the broken edge.

Possibilities considered: Oleaceae, *Fraxinus* (ash) samara wing, see example of modern ash samaras.

Possibilities considered and rejected: Sapindaceae, *Acer* (maple) samara. Veins in the samara of modern maple are uniformly curved.

Rosaceae: c.f., *Cercocarpus* (Fig. 6)

Specimen 3-1 is a leaf with a blade about 9 mm in length by 5 mm in width. The shape is elliptic. A portion of the petiole about 2 mm in length is seen at left. The base is cuneate. The margin of the leaf can be seen for about ¼ of the circumference of the leaf. It appears to be entire and turned down, but it is not clear whether or not the margin is rolled. The tip of the leaf is not preserved, although the texture of the matrix suggests the tip might be acute. The surface of the leaf is flat proximally and undulates distally. The mid vein is strongly expressed. The blade veins cannot be seen but the leaf appears pinnate, as suggested by the patterns of the undulating surface of the leaf.

Possibilities: Rosaceae, c.f., *Cercocarpus antiquus* Lesq., see Axelrod (1985).

Rosaceae cf. *Prunus* (Fig. 7)

Specimen 6-10 is an ovate dense smooth body surrounded by a less-dense covering of more or less uniform width. The dense body appears to be circular in cross-section, and slightly elongated at opposite ends. The surface is smooth, and not textured or angled. The elongation is very nearly acute at one end, and this is assumed to be the distal end. The elongation is obtuse at the opposite, and assumed to be proximal end. The dense body is 6 mm in width and 7 mm in "length." The less-dense covering surrounds the entire dense body. It now varies from 1 mm to 2 mm in width, but could have been uniform in width originally.

This is likely a drupe, i.e., a fleshy fruit with a soft pericarp surrounding a stone. However, a single-seeded bacca (berry) such as seen in Lauraceae (*Persea*, avocado) cannot be ruled out. The Rose family, e.g., *Prunus*, would seem a likely candidate for this fossil fruit, given their ubiquity of the family and previous recognition in the Tehachapi and Mint Canyon beds.

Possibilities considered and rejected:

- Ginkgoaceae (*Ginko*, ginko). The spermidium of *Ginko* looks very much like a drupe. However, there is no kind of ridge on the dense body that would be expected if this were a *Ginko*.

- Cupressaceae (*Juniperus*, juniper). The arceuthida (berry) of a juniper can appear like a drupe, and there are some single-seeded junipers. However, the ratio of seed to pericarp is too high to be a juniper, and the seed (dense body) is too round.

- Cannabaceae (*Celtis*, hackberry). The fruits of the hackberry are classified as drupes. However, the stones of *Celtis* (hackberry) are textured (in the one image found), and the stone of the fossil at hand appears to be smooth.

- Rhamnaceae (*Rhamnus*) While the fruit of *Rhamnus* is a drupe, it is described as two-seeded, and there is nothing in this specimen to suggest a parting line between two seeds.

- Ulmaceae (*Ulmus*, elm). The samaras of the elms have this general shape. However, the apparent density of the central body and the small size of the surrounding tissue relative to the central body does not appear consistent with an elm samara.

Rosaceae, *Purshia* (bitterbrush). (Fig. 8); modern *Purshia* leaf (Fig. 9)

Specimen 7-30 is a fragment of a pinnately lobed leaf about 4.5 mm long and 3 mm wide. Three lobes are seen. It is not clear whether this is the entire leaf, or whether more, proximal, lobes have been lost. Nor is it clear whether the leaf has a petiole. There is also a central structure visible. This could be a mid-vein, or, it could be a cast of the central portion between rolled margins. See also Specimen 7-16, which is similar.

Possibilities considered: Rosaceae: *Purshia*. The leaves of modern *Purshia*, which now includes *Cowanina*, have three to five lobes and rolled margins. The oldest known collections of *Purshia* are Pliocene (McArthur et al., 1983). However, the same article also suggests that ancestral forms of *Purshia* might date from the Eocene.

Possibilities considered and rejected: Cupressaceae: *Thuja* (cedar). The branching pattern suggests the flattened stem and leaves of genus *Thuja*. However, joints between the stem and leaves should be visible, and no such joints can be seen on this specimen. Therefore, a diagnosis of *Thuja* seems unlikely.

Rubiaceae, seed, one of a pair found in a fruit. (Fig. 10)

Specimen 7-4 is a slightly flattened hemisphere with a longitudinal groove on the flat side. The flat side is assumed to be the adaxial side. There is a possible indentation at the visible end of the groove. Seen in cross section the object is flattened and not quite hemispheric. It appears to be symmetric both longitudinally and laterally.

Possibilities considered: Rubiaceae. Somewhat reminiscent of a modern coffee berry; however, the body is not nearly so full (Graham, 2009). Axelrod (1940) reported *Chiococca* (Rubiaceae) from the Mint Canyon flora.

Possibilities considered and rejected: Apiaceae. Most seeds in the Apiaceae are symmetrical longitudinally, but not laterally, and the adaxial surface is more likely to be a ridge than a groove.

Undetermined, sclerophyllous shrub or tree. (Fig. 11)

Specimen 7-15 is a partial leaf. The widest section is 6 mm wide, and the exposed portion of the specimen is 12 mm. The overall length of the leaf is probably 30–40 mm. The cross-section of the leaf is convex relative to the adaxial surface. The mid vein of the leaf is strong. Primary veins are poorly preserved, but appear to be pinnate. The margins of the leaf appear entire and do not appear to be rolled under. The leaf appears to be relatively thick and was probably stiff as opposed to soft, which suggests a sclerophyllous shrub or tree such as those found in Rhamnaceae, genus *Rhamnus*.

Undetermined leaf (Fig. 12)

Specimen 7-13b is a leaf fragment with narrow lanceolate or oblanceolate shape. The base is cuneate. Seen from the abaxial side, it has a prominent, broad, and flat mid vein, and alternate pinnate veins. Margins appear to be thickened (or possibly rolled). Leaves with these characters are also seen in other specimens, e.g., 7-18b.

Undetermined leaf (Fig. 13)

Specimen 7-31 is a fragment 5 mm by 3 mm, with a mid-vein, relatively strong pinnate veins, and an undulatory surface parallel to the veins. Specimens 7-5B and 8-6A & B are very similar; however this is the best example.

Undetermined leaf. *Acer?* (maple) (Fig. 14)

Specimen 7-9 is a poorly preserved fragment, or fragments, of a large thin leaf with possible palmate veins. Neither margins nor the petiole are preserved. It is also possible that there are two leaves superimposed on each other.

Possibilities considered: Possible Sapinadaceae, *Acer* (maple).

Undetermined fruit, drupe. (Fig. 15)

Specimen 7-8 is a fruit showing a receptacle, two densities of tissue, interior and exterior, and an acute tip.

Possibilities considered and rejected: Rosaceous fruit, cf., *Prunus*.

Undetermined fruit or seed. (Fig. 16)

Specimen 7-10 is a roughly circular object about 9 mm in diameter. There is an area of higher density about 4 mm in diameter located in the center of the object. Fine detail, such as that which would permit identification

of proximal or distal end or of placentation, has been destroyed.

Possibilities considered and rejected: Ulmaceae, *Ulmus* (elm) seed. If this were an elm seed, additional detail such as the receptacle at the base should be visible.

Undetermined, interior of seed. (Fig. 17)

Specimen 6-12 appears to be a fragment of something seen from the inside. The fragment is 6 mm in length. Assuming the object has a regular shape, the curvature of the margins suggests the fragment is just less than one-half of the total object length. Therefore, the estimated length of the object is 14–15 mm. The fragment is 2.5 mm wide. The depth of the fragment, about 1 mm, and the minor folding, suggests the fragment has been compressed in depth since deposition. There is a small channel or groove at left, which may represent a scar or attachment point, and this is likely the proximal end.

There is a deep “groove” or fold seen at the right end of the fragment. It probably extends the full length of the fragment to the left, but it is obscured by other material. It is not clear whether the groove was a feature in the original object, or was created by compression of the object. If it was a feature in the original object, then it could be the inside of a seed with a ridged margin.

Possibilities considered: interior of seed.

Possibilities considered and rejected:

- Poaceae: keeled glume. This could be the lower portion of a keeled glume, assuming that the glumes of Miocene grasses were similar to modern glumes. However, if this is a glume, it is a very well-developed and strong glume, which seems unlikely.
- Ginkgoaceae, ginkgo seed. The “seed coat” of a modern ginkgo seed is quite brittle. It seems unlikely to deform evenly when compressed. It is also smoothly curved on the inside, notwithstanding two to four sharp-angled ridges on the outside.
- Eudicot, seed. It could be a seed with a ridged margin that would be reflected as the deep groove on the inside. Normally one would expect a seed with a ridged margin to be wider than thick, such as that seen in a pumpkin seed. So, if this is a seed, then it has been compressed laterally to much less than its original width. To accomplish that, the seed would have to be deposited on its edge. This seems unlikely, and therefore, the possibility of it being a seed is rejected.

Monocots

Aracaceae palm: root fragments

Multiple undetermined monocot leaves, parallel veins, some folded or keeled, likely: *Carex?* (Fig. 18) and/or *Typha?* (Fig. 19)

Ichnites

Bird tracks preserved in claystone suggest a shallow water environment.

Avipeda gryponyx (Fig. 20), Figure 3a, RAM14742, Figure 3b. RAM14742,

Diagnosis: Avian footprints of small size, having three slender digits, the outer ones (II and IV) curving forward, the central digit (III) curving in toward the track axis. Digits acuminate, but claws not distinct; interpad spaces not evident. Claws acute, attached to digit. Digits united proximally, and lack webbing or an intertarsal pad. Interdigital span (at base) around 95°. Length of digits III and IV almost uniform (15 mm); Digit II 10 mm); interdigital angle between II and III less than that between III and IV.

Holotype: Sarjeant and Reynolds, 2001. (Plates 2, 3, 4; Figures 4, 5) V94021/110 (P. 4, Fig. 4). Raymond M. Alf Museum of Paleontology, Claremont, California.

Additional Localities. Avawatz Formation, Miocene (Clarendonian), Avawatz Mountains, San Bernardino County, California; Bouse Fm., early Pliocene, Amboy, San Bernardino County, CA. (RAM# V201208-RAM14742, RAM14742.).

Discussion: The curvature of the digits, their thinness and their proximal union combine to differentiate *A. gryponyx* from all other ichnospecies of *Avipeda*. *A. gryponyx* is distinguished by its slightly curving digits.

The footprints of *Avipeda gryponyx* are similar to those figured for the sanderling (Elbroch and Marks, 2001, p. 105, 106). The legs of sanderlings are short, approximately two inches long, and they typically forage in shallow water. The length of legs suggests that water was less than two inches deep.

Invertebrate track: A possible arthropod tracks (Fig. 21) is preserved on a bedding plane covered with fragments of plant debris. The track consists of a central drag furrow that “plows under” fragments of plant debris, perhaps while the animal was feeding. On both sides of the central furrow are impressions from multiple legs, oriented at a 25 degree angle from the central furrow. The maximum width of individual “leg” impressions is 0.7 mm, the width of the central furrow is approximately two millimeters, and the overall width of the trackway is 13 mm. Similar, but larger invertebrate trackways have been reported from stratigraphy dating to 15 Ma. in Owl Canyon (Howe and Eby, 2006) in the Mud Hills.

Overall impression

Habitats are suggested by analogy to modern taxa, resting on the basic assumption that modern taxa do not differ substantially in their ecological relations from those of the past (Chaney, 1938; Cain, 1944; cited in Axelrod, 1958). Some fruits are large (1 cm+) with well-developed pericarps. Unfortunately, most of the fruit detail is lost. One

well-preserved seed is very likely one of a pair. Present are many smaller, seed-like objects, without preserved detail to permit determination.

All the material appears to have been deposited after transportation by water, resulting in a “hash” of plant material and generally poor preservation. Only first-order blade veins are visible, higher order veins being obscured by poor preservation. Often vein patterns are only suggested by leaf surface expression. Transportation distance could conceivably be measured in miles or tens of miles. Such examples can be found in the Miocene Puente Formation and Round Mountain Silt where continental floras have been transported along streams and rivers and deposited in marine sediments (Kinoshita, n. d.; Reynolds, 2011).

Some generalizations can be made about plant habitat from the material found so far. The thin, soft, small veined leaves could represent willows and maples in a stream-side habitat. Rainfall was sufficient to maintain at least small streams and wetlands. Typically, rainfall estimates of 15-20 inches per year are made for similar floras in southern California (Axelrod, 1976), and such may also be reasonable for the Rainbow Loop Flora. However, the possibility of long distance transport argues for caution when estimating rainfall at the deposition site. The larger leathery and hard surface leaves represent oaks, ashes, and buckthorns in a woodland habitat away from the streamside. The larger fruits would be expected in the well-watered habitats at streamside or nearby. Finally, the reduced leaves of *Purshia* and scale-like leaves of *Juniperus* could represent dry, upland vegetation. Palm is the only identified species from the RLF that suggests frost-free requirements.

Floral comparisons

The Rainbow Loop Flora, its plant communities, and its environment of deposition can be compared to other described Miocene floras: from older to younger, Tehachapi (17 Ma), Solomon Skyline (14.8 Ma), Mint Canyon (12 Ma), and Ricardo (10 Ma).

The **Tehachapi Flora**, with more than seventy taxa (Axelrod, 1939; 1976), was recovered from andesitic mudflows of the Kinnick Formation (17.6 Ma; Evernden and others, 1964). These mudflows were later referred to the andesitic mudflows (Tbi; Quinn, 1987) that occur in the lower Bopesta Formation, above the 17.6 Ma date from the upper Kinnick Formation (Tk 10; Quinn, 1987), suggesting that the flora falls within the biostratigraphic range of *Parapliohippus carrizoensis* (Kelly, 1995). Floral communities include woodland, a shrub understory, chaparral, and thorn-scrub. “The assemblage indicates rainfall was near 25 inches...in the warm season, and ..semi-desert where dry tropic scrub live [with] under 15 inches precipitation. Temperatures were mild in summer and frost free, ...from the occurrence of... *Ficus*, *Persea*, and *Sabal*” (Axelrod, 1976). The Rainbow Loop Flora shares



Figure 22. Fossil limb -Solomon Skyline Locality (14.8 Ma). Photo courtesy D. Lofgren.

seven taxa with the Tehachapi Flora: *Prunus*, *Ceanothus*, *Quercus*, *Salix*, *Cupressus*, and palm.

Solomon Skyline is a new name for the “Petrified Wood” locality (Alf, 1970) east of Owl Canyon in the Mud Hills. This locality yields stems and branches up to 5 cm in diameter (Fig 22). The mode of preservation within an air-fall volcanic ash (Skyline Tuff; 14.8 Ma; Woodburne and Reynolds, 2010) apparently was not conducive to the preservation of leaf material. Plant taxa include juniper (*Juniperus* sp.), poison oak (*Rhus* sp.) and buckthorn (*Ceanothus* sp.). The Rainbow Loop Flora has juniper and *Ceanothus* in common with the Solomon Skyline Flora.

Mint Canyon produced a robust flora with at least 100 woody species. Zircon crystal dates of 10.1 and 11.6 Ma

Table 2. Plant taxa by community

Community	Genus	Common name
Aquatic	<i>Carex</i> ?	Sedge
	<i>Typha</i> ?	Cat tail
Riparian	<i>Acer</i> ?	Maple
	<i>Salix</i> ?	Willow
	Aracaceae	palm
Woodland	<i>Quercus</i>	Oak
	<i>Fraxinus</i>	Ash
	Rhamnaceae (<i>Ceanothus</i> ? or <i>Rhamnus</i> ?)	Buck thorn
	Rosaceae, c.f., <i>Prunus</i>	Rose family
	Rubiaceae	Madder
	Rosaceae, c.f., <i>Cercocarpus</i>	Mountain mahogany
Upland	Cupressaceae, c.f., <i>Juniperus</i>	Juniper
	<i>Purshia</i>	Bitterbrush

(Terres and Luyendyk, 1985) are reported from the upper part (Clarendonian) of the Mint Canyon Formation. Floral communities are dominated by live oak woodland with associated understory shrubs. The lower and more xeric portions of the basin contained dry tropic scrub. “Rainfall occurred chiefly in the summer months, and winters were mild and frostless” (Axelrod, 1940). The Rainbow Loop Flora shares Rubiaceae, Rosaceae?, *Quercus* sp., *Ceanothus* sp., *Salix* sp., and *Brahea* (Syn: *Erythea*, palm) with the Mint Canyon flora.

Ricardo was known for its fossil forest until its standing tree stumps were removed by collectors. The wood indicates oak-pine woodland and includes palm (*Sabal*), piñon, evergreen oak, and locust (Webber, 1933). This woodland received up to 30 inches of summer rain and winters were frost-free. Recent work indicates the flora is located in the middle of Member 2 of the Dove Springs Formation (Whistler and others, 2009, Table 1, Fig. 4; Whistler p. c. to Reynolds March 2013) and falls between the Ibex Hollow tephra (12.01 ± 0.03 Ar/Ar, Ma) and the Cougar point Tuff V tephra (12.15 ± 0.04 Ar/Ar, Ma). *Quercus* sp., *Cupressus* sp., and palm are found in both the Rainbow Loop Flora and the Ricardo forest.

The Rainbow Loop Flora (about 16.3 Ma) contains the only described California Miocene continental aquatic component—probably including sedges and cattail. Taxa that have not been described elsewhere in the early to middle Miocene of California include ?*Acer*, Aracaceae, and possibly *Carex*. Floral communities present in addition to the aquatic plants include riparian (*Acer*?, *Salix*?), oak woodland or parkland (*Quercus*, *Fraxinus*, palm) with a shrub understory (*Ceanothus*? or *Rhamnus*?, *Fraxinus*, *Prunus*, Rubiaceae), in which grasses (Poaceae) might be expected, and a distant upland community (*Juniperus*, *Purshia*, and possibly *Pinus*). The presence of palm suggests that winters were frost free. Summer rainfall was probably limited, as the taxa represented in woodland and upland vegetation are able to withstand at least short periods of drought.

Significance

Recent work has expanded the taxa known from the Rainbow Loop Flora to a point where climatic conditions can be inferred. The RLF is about 16.3 Ma, a time just past the first peak of the Mid-Miocene Climactic Optimum (16.2 Ma; see Fig. 3 in Lander, this volume.).

As Alf (1970) stated “... the [flora allows paleontologists] better to understand the ecological conditions of the upper Miocene times.” Associated tracks of birds and invertebrates assist with description of the depositional environment.

Acknowledgements

This work was conducted under the authorization of Jim Shearer, archaeologist, Bureau of Land Management, Barstow Field Office (BLM Permit No. CA-10-00-007P).

This study could not have been carried out without the help of volunteers from the Mojave River Valley Museum (Bob Hilburn, President), Inland Geological Society, Riverside Metropolitan Museum, Jurupa Mountain Discovery Center, and Western Mojave Subgroup members. Valuable assistance was provided by Diane Erwin, University of California Museum of Paleontology; and Mark Roeder. Dr. Robert Housley, Caltech, tested samples for strontium.

Thanks also go to Don Lofgren, Alf Museum, Claremont, CA, for references to the works of Raymond Alf, for supplying the Fig. 1 image of the 1958 Alf Museum party camping in the Mud Hills, and for accepting plant specimens for curation. Photos were taken by the authors except as noted in the captions. The *Purshia* leaf image was taken by Sandra Swift. Constructive comments regarding information in this paper were provided by Mike Woodburne and Don Lofgren.

References

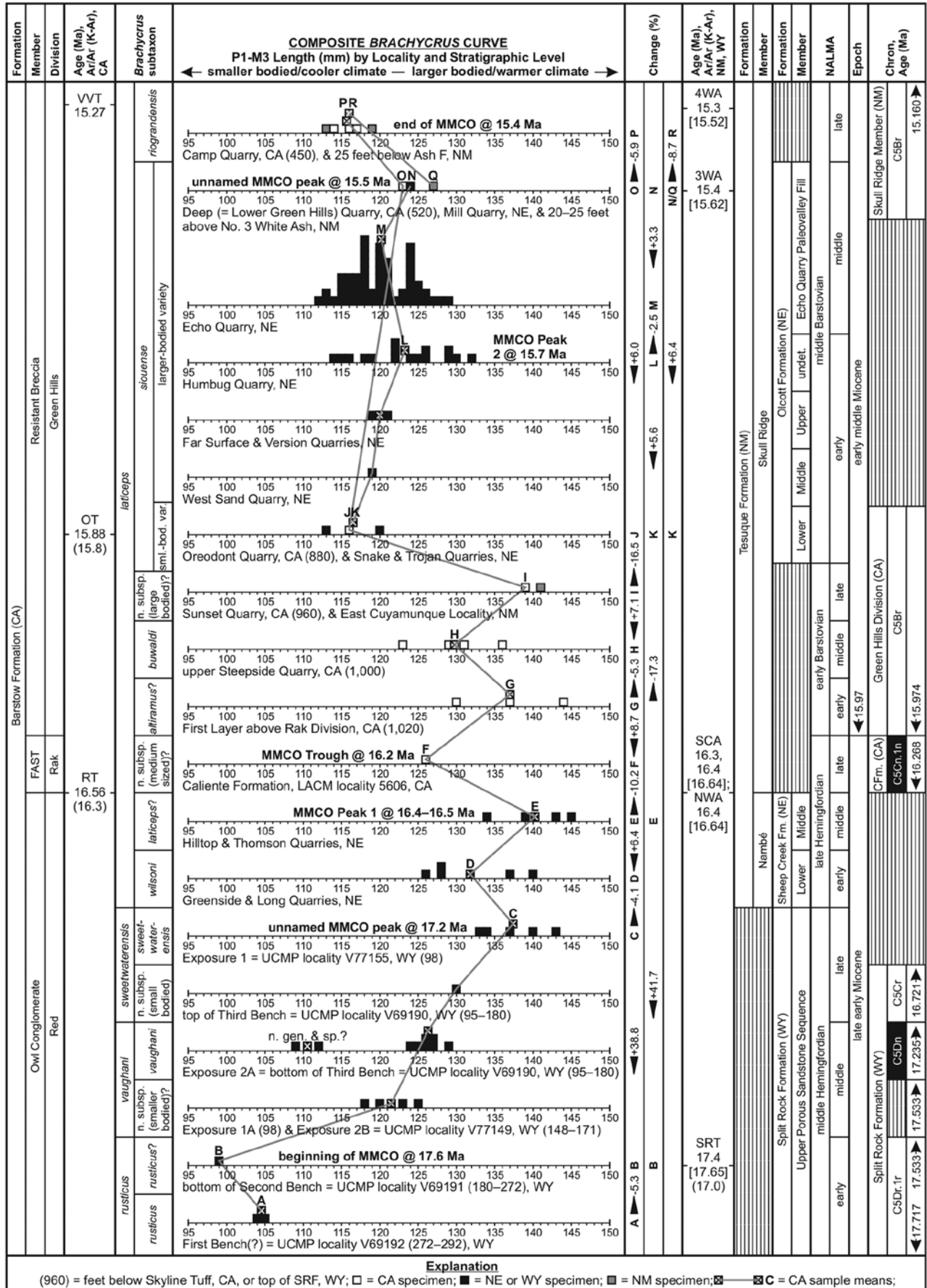
- Alf, Raymond M., 1970. A preliminary report on a Miocene Flora from the Barstow Formation, Barstow, California. *Southern California Academy of Science*, 69(3-4): 183-189.
- Axelrod, D. I., 1939. A Miocene floras from the western border of the Mojave Desert. *Carnegie Inst. Wash.*, Publ. 516: 1-129.
- Axelrod, D. I., 1940. The Mint Canyon flora of southern California: a preliminary statement. *Amer. Jour. Sci.*: 238: p. 577-585.
- Axelrod, D. I., 1958 Evolution of the Madro-Tertiary Geoflora, *Bot. Rev.*, vol. 24, pp.433-509.
- Axelrod, D. I., 1976. Fossil Floras of the California Desert Conservation Area. Manuscript (CDD No. 206) submitted to Hyrum Johnson, BLM, Riverside, California. p. 41.
- Axelrod, Daniel I., 1985. Miocene floras from the Middlegate Basin, West-Central Nevada. *University of California Publications in Geological Sciences*, Volume 129, January 1985.
- Cain, S. A., 1944. *Foundations of Plant Geography*. Harper and Bros., New York, 556 pp.
- Chaney, Ralph W., 1938. Paleoecological interpretations of Cenozoic plants in western North America. *Botanical Review*. 4: 371-396.
- Durrell, Cordell. 1953. Geological Investigations of strontium deposits in southern California. *California Division of Mines and Geology Special Report* 32:23-36.
- Elbroch, Mark and E. Marks, 2001. *Bird tracks and sign*. Stackpole Books, Mechanicsburg, PA., p. 456.
- Evernden, J.F., D.E. Savage, G.H. Curtis, and G.T. James. 1964. Potassium-argon dates and the Cenozoic mammalian geochronology of North America. *American Journal of Science*, 262:145-198.
- Graham, Alex, 2009. Fossil Record of the Rubiaceae. *Annals of the Missouri Botanical Garden* 96(1):90-108.
- Howe, Tom, and Margaret Eby, 2006. Miocene invertebrate trackways in the Owl Canyon area, Barstow, California. *CSU Desert Symposium Vol. 2006*, p. 63-64.
- Kinoshita, Glen, n.d. Late Miocene floral assemblages of Chino Hills, CA. California State Polytechnic University, Pomona, Department of Geological Sciences. Unpublished Master's Thesis, p. 78
- Lander, E. B., 2013, Global warming and fluctuating adult body size in the oreodont *Brachycrus* (Mammalia, Artiodactyla, Oreodontidae) during the Middle Miocene Climatic Optimum, this vol.
- McArthur, E. D., H. C. Stutz, and S. C. Sanderson, 1983. Taxonomy, distribution, and cytogenetics of *Purshia*, *Cowania*, and *Fallugia* (Rosoidae, Rosaceae). Pp 4-24 in *Proceedings of the Symposium on Research and Management of Bitterbrush and Cliffrose in Western North America*, ed., A. R. Tiedemann and K. L. Johnson (Gen. Tech. Rep. 152, USDA, Forest Service, Ogden, Utah.
- Reynolds, R. E., 2011. A new Miocene flora from the Round Mountain Silt. *CSU Desert Symposium Volume, 2011*; p. 114-118.
- Reynolds, R. E., D. M. Miller, M. O. Woodburne, L. B. Albright, 2010. Extending the boundaries of the Barstow Formation in the central Mojave Desert. *CSU Desert Symposium Volume, 2010*; p. 148-161.
- Terres, R. R., and B. P. Luyendyk (1985), Neogene tectonic rotation of the San Gabriel Region, California, suggested by paleomagnetic vectors, *J. Geophys. Res.*, 90(B14), 12,467-12,484, doi:10.1029/JB090iB14p12467.
- Webber, I. E., 1933. Woods from the Ricardo Pliocene of Last Chance Gulch, California. *Carnegie Inst. Wash.*, Publ. 412: 115-134..
- Woodburne, M. O., and R. E. Reynolds, 2010. The mammalian litho- and biochronology of the Mojave Desert Province. *CSU Desert Symposium Volume, 2010*; p. 124-147.

Global warming and fluctuating adult body size in the oreodont *Brachycrus* (Mammalia, Artiodactyla, Oreodondontidae) during the Middle Miocene climatic optimum

E. Bruce Lander

Paleo Environmental Associates, Inc., 2248 Winrock Avenue, Altadena, California 91001-3205, paleo@earthlink.net

ABSTRACT—Average adult body size, as represented by mean upper cheek tooth-row or P1–M3 length, fluctuated dramatically through stratigraphically superposed samples of the tapir-like oreodontid lineage *Brachycrus* from the western half of the United States. The *Brachycrus* biochron spanned the earliest middle Hemingfordian to the late middle Barstovian North American Land Mammal Ages (NALMAs) or the interval from approximately 17.72–15.30 million years (Ma) ago, and lasted for as long as 2.42 Ma. The graphical representation of those fluctuations in body size is termed the *Brachycrus* Curve. The swings in body size are referred to as the Haws-Berkeley Effect and are considered to have been largely non-evolutionary or dominantly phenotypic responses to climatically induced changes in the volume of the taxon's food supply, but, in contrast to Bergmann's Rule, were not necessarily tied to temperature shifts. Smaller body size likely corresponded to a reduction in forage that resulted from a more seasonal climate characterized by summer drought, whereas larger body size probably accompanied an increased food supply as climate moderated. The *Brachycrus* Curve comprises of two cycles. Following a slight initial decrease in adult body size at the beginning of the middle Hemingfordian NALMA that resulted in very small size, body size increased substantially (nearly 40%) and then fluctuated between medium and large or from approximately 4–10%, with body size peaking prominently four times during the late middle Hemingfordian to the late early Barstovian NALMAs before a marked (over 16%) diminution in size at the beginning of the early middle Barstovian, a span of roughly 1.52–1.85 Ma. In contrast, adult body size fluctuated between small and medium or about 3–6% and peaked slightly only twice during the second cycle before a final diminution in size approaching 9% and the eventual extinction of the genus during the late middle Barstovian, a span lasting perhaps about 0.28–0.58 Ma. Although such changes in *Brachycrus* have never been ascribed previously to any temperature-related global climate event, the Middle Miocene Climatic Optimum (MMCO) now appears to have substantially overlapped and virtually coincided with the two cycles documented by the *Brachycrus* Curve or perhaps even the entire *Brachycrus* biochron. The beginning of the MMCO probably corresponds to the onset of increasing adult body size during the middle Hemingfordian NALMA, whereas two of the four peaks characterized by large body size in *Brachycrus* during the first cycle or the late middle Hemingfordian to the late early Barstovian NALMAs likely correlate with the unnamed MMCO peak and MMCO Peak 1 at 17.2 and 16.4–16.5 Ma before the present (BP), respectively, whereas the reduction in body size during the latest Hemingfordian might be related to the MMCO Trough, which occurred 16.2 Ma ago. In contrast, the two lesser peaks of moderate body size during the second cycle and the middle Barstovian NALMA appear to correspond to MMCO Peak 2 and the ensuing unnamed peak at 15.7 and 15.5 Ma BP, respectively, whereas the final diminution in body size and subsequent extinction of the genus are probably related to the end of the MMCO 15.4 Ma ago. Because the peaks in the *Brachycrus* Curve and that for the MMCO appear to be correlated, it is possible that larger adult body size in *Brachycrus* was ultimately the result of global warming and the accompanying reductions in the extent of the Antarctic Ice Sheet. Conversely, smaller body size and the eventual extinction of *Brachycrus* might be correlated with periods of cooler climate and advances of the ice sheet.



deepening markedly, the preorbital portion of the fossa penetrating ever more deeply behind the anterior rim of the orbit (Figure 2; Lander 1977, 1985, Munthe 1979, Kelly and Lander 1988b). Accompanying those changes in the facial area of the skull were substantial changes to the basicranium, particularly the tympanic bulla. The ventral surface of the bulla in *B. rusticus* is decidedly flattened and even slightly convex or basined medially, that surface sloping anteromedially from a prominent posterolateral apex that is enclosed posteriorly by the anteriorly opening, paroccipital fold, with the bulla resembling those of other ticholeptine oreodontids, including *Ticholeptus*, all but the earliest forms of *Merychylus*, and early Hemingfordian *Mediochoerus johnsoni*, the ancestor of *Brachycrus* (Lander 1977, 1985). In contrast, the bulla is much more inflated in *B. vaughani* and the ventral surface is comparatively convex, but still slopes strongly in a medial direction, whereas the bulla is taller, rather erect, and comparatively conical or cylindrical in *B. sweetwaterensis*, but, in contrast to *B. laticeps*, the bulla is a bit less erect and, consequently, its apex is still in the paroccipital fold (Lander 1977, 1985, Kelly and Lander 1988b). In *B. laticeps*, the tympanic bulla is decidedly cylindrical and erect, with the entire posterior surface being aligned with and closely appressed to the anterior edge of medial blade of the paroccipital process instead of being mostly enclosed by the paroccipital fold (Lander 1977, 1985, Kelly and Lander 1988b). Lander (1985, 1998, 2003, 2005, 2011), Kelly and Lander (1988a–b), Lander and Kelly (1989), and Pagnac (2009) have rejected all other late Hemingfordian (of this report) and Barstovian species of *Brachycrus* in favor *B. laticeps*, which has priority on the basis of its earlier publication date.

Average adult body size, as represented by mean upper cheek tooth-row or P1–M3 length, changed dramatically and even reversed direction, as documented in a composite sequence comprising numerous superposed samples and well over one hundred individuals of *Brachycrus* from four stratigraphic successions in California, Nebraska, New Mexico, and Wyoming (Figure 3, Table 1; Schultz and Falkenbach 1940, 1968, Lander 1977, 1985, 1998, 2003, Kelly and Lander 1988a–b, 1992, Lander and Kelly 1989). Such fluctuations were particularly well documented between successive samples of the lineage by Lander (1985, fig. 4) and Kelly and Lander (1988b, fig. 4), who determined that those changes occurred in parallel fashion in *Brachycrus laticeps* from the early late Hemingfordian to the late middle Barstovian NALMAS in southern California and approximately 875 miles to the northeast in northwestern Nebraska. However and as documented below, the size changes so documented are now believed to have represented discontinuous and even disparate parts from just the latter half of one much longer cycle that spanned the early late Hemingfordian to the earliest middle Barstovian NALMAS, and most of a subsequent cycle, which covered much of the middle Barstovian. Only some of the samples in one state that were

regarded as correlatives of those in the other by Lander (1985) and Kelly and Lander (1988b) are still considered herein to have been contemporaneous.

Reconstruction of the two cycles and the preceding diminution of body size in *Brachycrus rusticus* described in this contribution and depicted in Figure 3 relied very heavily on more refined stratigraphic documentation of samples containing *Brachycrus* remains. Chronologic constraints for essentially all samples were provided by radiometric and/or magnetostratigraphic data that also allowed the temporal ordering of the samples. With the exceptions of the earliest record of the genus (*B. rusticus rusticus*) and a highly questionable occurrence of *Brachycrus* of earliest late Barstovian age, the entire known *Brachycrus* biochron is covered by the two cycles, as illustrated in Figure 3. The composite graphical depiction of changes in average adult body size through the interval spanned by both cycles along with the preceding biochron of *B. rusticus rusticus* is referred to in this report as the *Brachycrus* Curve (Figure 3).

Those segments of the composite *Brachycrus* curve in Figure 3 that cover *B. laticeps siouense* and *B. laticeps riograndensis* from the middle Barstovian NALMA of California, Nebraska, and New Mexico virtually coincide, indicating that the corresponding points or apices along the curve represent correlative assemblages and that the environmental parameters influencing adult body size were perhaps of continental scale (Figures 1, 3). Lander (1977, 1984, 1988, 1989, 1998, 2008), Lander and Hanson (2006), and Morgan et al. (2009) regarded diminishing body size in *Brachycrus* and other oreodontoid lineages as a non-evolutionary or strictly phenotypic response (i.e., stunting) to a progressive, geographically wide-spread, and comparatively long-term reduction in a taxon's resource base. An increasingly seasonal climate characterized by summer drought was considered to have been the primary cause of a deteriorating food supply, with the full-growth potential of an immature individual not being realized because of the reduced availability of forage when that individual would have achieved much of its growth (Lander 1977, 1984, 1988, 1989, 1998, Morgan et al. 2009). In contrast, increasing body size would have reflected a corresponding growth in the taxon's food supply during a period of moderating climate, when summer drought did not occur and forage was not a factor limiting adult body size. Consequently, average adult body size in *Brachycrus* during such periods would have been greater than in its immediate ancestors and/or descendants who existed under more severe climatic regimes. Such changes are referred to informally herein as the Haws-Berkeley Effect. On the other hand, variations in body size have never been ascribed to any specific temperature-related global climatic event with regard to *Brachycrus*. In contrast to Bergmann's Rule, in which species living in colder climates and/or at higher latitudes tend to be larger bodied than closely related species living in warmer climates and/or at lower latitudes, the Haws-Berkeley Effect can be

Table 1. Upper cheek tooth-row (P1–M3) lengths and sample means (mm) for *Brachycrus*. See Figure 3.

CALIFORNIA—BARSTOW FORMATION AND CALIENTE FORMATION	<i>B. l. siouense</i> (larger-bodied variety), Middle Member: West Sand Quarry: uncat. F:AM specimen (119).
Barstow Formation, Resistant Breccia or Middle Member, Green Hills Division—Green Hills Fauna	<i>B. l. siouense</i> (larger-bodied variety), Upper Member: Quarry B = Far Surface Quarry (Skinner et al. 1977): AMNH 18333 (119); Version Quarry: F:AM 34212 (121), uncat. F:AM specimen (120) (M = 120.0).
<i>Brachycrus laticeps altiramus?</i> , First Layer above Rak (= Third) Division: F:AM 42374 (137), 42377 (130); 40 feet above Rak Division: uncat. F:AM specimen (144) (M = 137).	<i>B. l. siouense</i> (larger-bodied variety), Olcott Formation, undifferentiated: Humbug Quarry: F:AM 42422 (116), 42424 (122), 42426 (126), 42427 (119), 42460 (118), 42461 (130), 42462 (132), 42463 (126), 42467 (122), uncat. F:AM specimens (114, 115, 118, 122, 124, 125, 129, 129) (M = 123.1, OR = 114–129, N = 16).
<i>B. laticeps buwaldi</i> , upper level of Steepside Quarry: F:AM 34466 (131), 34467 (129), uncat. F:AM specimens (123, 136) (M = 129.8);	<i>B. l. siouense</i> (larger-bodied variety), Echo Quarry Paleovalley Fill, Echo Quarry: F:AM 24513 (128), 33554 (127), 33572 (120), 35550 (121), 36109 (118), 36111 (117), 36112 (121), 36113 (124), 36114 (125), 36115 (121), 36116 (119), 36117 (126), 36118 (124), 36119 (120), 36120 (124), 36122 (116), 36124 (125), 36125 (120), 36126 (119), 36127 (120), 36128 (115), 36131 (118), 36132 (115), 36135 (117), 36139 (123), 36140 (124), 36141 (121), 36147 (120), 36152 (118), 36153 (118), 36169 (122), 36171 (120), 36176 (118), 36185 (124), 36186 (113), 37552 (116), 37553 (117), 37554 (118), 37555 (118), 37556 (117), 37558 (121), 37559 (115), 42317 (125), uncat. F:AM specimens (112, 113, 114, 115, 116, 116, 118, 118, 118, 120, 120, 121, 122, 123, 124, 124, 124, 126, 129) (M = 120.0, OR = 112–129, N = 60).
<i>B. l. buwaldi</i> (probably includes following records): Ness Quarry: F:AM 42372 (135); First or Second Layer above Third [= Rak] Division: F:AM 42402 (<i>B. buwaldi barstowensis</i> holotypic specimen) (125); lower Green Hills Division: uncat. F:AM specimen (131); UCMP locality 2057 (800–1,000 feet below Skyline Tuff): UCMP 21350 (holotypic specimen) (126).	<i>B. l. siouense</i> (larger-bodied variety), Echo Quarry Paleovalley Fill, Mill Quarry: uncat. F:AM specimen (124).
<i>B. laticeps</i> , new large-bodied subspecies?: Sunset Quarry: uncat. F:AM specimen (139).	Sand Canyon Formation
<i>B. laticeps siouense</i> (smaller-bodied variety), Oreodont Quarry: uncat. F:AM specimen (116.0).	<i>B. laticeps siouense</i> (larger-bodied variety), 45 feet above black ash bed: uncat. F:AM specimen (125).
<i>B. laticeps siouense</i> (larger-bodied variety), Deep (= Lower Green Hills) Quarry: F:AM 42379 (123).	New Mexico—Nambé and Skull Ridge Members of Tesuque Formation
<i>B. laticeps riograndensis</i> , Camp Quarry: uncat. F:AM specimens (114, 116, 117) (M = 115.7).	<i>Brachycrus laticeps</i> , new large-bodied subspecies?, probably Nambé Member or lower part of Skull Ridge Member below No. 3 White Ash, East Cuyamunque locality: uncat. F:AM specimen (141).
<i>B. l. siouense</i> (smaller-bodied variety) or <i>B. l. riograndensis</i> , Green Hills Quarry: uncat. F:AM specimens (112, 117) (M = 114.5).	<i>B. laticeps siouense</i> (smaller-bodied variety), 20–25 feet above No. 3 White Ash, lower (but not lowermost) part of Skull Ridge Member: uncat. F:AM specimen (127).
Caliente Formation—Upper West Dry Canyon Local Fauna of West Dry Canyon Fauna	<i>B. laticeps riograndensis</i> , lower (but not lowermost) part of Skull Ridge Member: 25 feet below Ash F (= 90–90 feet above No. 3 White Ash): F:AM 72326 (holotypic specimen) (113); probably between No. 3 White Ash and Ash F: uncat. F:AM specimen (119) (M = 116).
<i>Brachycrus laticeps</i> , new medium-body-sized subspecies?, Upper West Dry Canyon Local Fauna, LACM locality 5606: uncat. LACM specimen (126).	Wyoming—Upper Porous Sandstone Sequence of Split Rock Formation—Split Rock Fauna
MONTANA—SIXMILE CREEK FORMATION	<i>B. rusticus rusticus</i> (genotypic species), First Bench or base of Second Bench: USNM 145 (holotypic specimen) (105), UW 3163 (99) (M = 102).
<i>Brachycrus laticeps laticeps</i> , Sixmile Creek Formation, Montana: Flint Creek Local Fauna, Flint Creek Beds: CM 796 (holotypic specimen) (141), F:AM 34482 (134) (M = 137.5).	<i>B. r. rusticus?</i> , Exposure 2A, ca. 10 feet above base of Second Bench: CM 13592 (104).
<i>Brachycrus laticeps altiramus</i> , Sixmile Creek Formation, Montana: Madison Valley Fauna, Madison Valley Formation: AMNH 9746 (<i>B. altiramus</i> holotypic specimen) (150); Deep River Beds: possibly includes F:AM 21321 (<i>B. laticeps mooki</i> holotypic specimen) (145).	<i>B. vaughani</i> , new subspecies (smaller bodied)?: Exposure 1A: F:AM 34499 (120), 361061 (125); Exposure 2B = UCMP locality V77149: UCMP 165899 (118), 165900 (123) (M = 121.50).
NEBRASKA—HEMINGFORD GROUP	<i>B. vaughani vaughani</i> , Exposure 2A: F:AM 34492 (holotypic specimen) (129), 36101 (126), 37583 (127), 37586 (126), 37589 (127), KUVV 16481 (several feet above base of Third Bench) (125), UCMP 162477 (124) (M = 126.3).
Hemingford Group, undifferentiated	<i>B. sweetwaterensis</i> , new subspecies (smaller bodied), top of Third Bench = UCMP locality V69190: UCMP 163023 (130).
<i>Brachycrus vaughani vaughani</i> or <i>B. sweetwaterensis</i> new subspecies (small)?, Ginn Quarry: uncat. F:AM specimens (124, 132) (M = 128).	<i>B. sweetwaterensis sweetwaterensis</i> , Exposure 1: F:AM 34493 (134), 34494 (137), 34495 (133), 34498 (holotypic specimen) (143), 34500 (140) (M = 137.4).
Sheep Creek Formation—Sheep Creek Fauna	New genus and species?, Exposure 2A: F:AM 36105 (112), KUVV 16476 (several feet above base of Third Bench) (109) (M = 110.5).
<i>Brachycrus laticeps wilsoni</i> , Lower Sheep Creek Local Fauna, Lower Member: Greenside Quarry: F:AM 34202 (holotypic specimen) (140), uncat. F:AM specimen (126); Long Quarry: F:AM 33574 (<i>B. wilsoni longensis</i> holotypic specimen) (128), 34203 (128), 34205 (137) (M = 131.8).	
<i>B. laticeps laticeps?</i> , Upper Sheep Creek Local Fauna, Middle Member (= Horizon A or <i>Merychippus primus</i> Zone; Skinner et al. 1977): Hilltop Quarry: F:AM 36188 (139); Thomson Quarry: AMNH 18344 (134), F:AM 34201 (143), uncat. F:AM specimen (145) (M = 140.3).	
Olcott Formation (= Lower Snake Creek Beds; Skinner et al. 1977)—Lower Snake Creek Fauna	
<i>Brachycrus laticeps siouense</i> (smaller-bodied variety), Lower Member: Sheep Creek Quarry = Trojan Quarry (Skinner et al. 1977): AMNH 18338 (120); Sinclair Quarry 4 = Snake Quarry (Skinner et al. 1977): F:AM 33576 (113) (M = 116.5).	

documented among superposed samples of one lineage from the same place and stratigraphic sequence and is not necessarily linked directly to temperature change.

However, there appears to have been substantial overlap and perhaps even virtual coincidence between the time period covered by the MMCO on one hand and the two cycles of changing body size recorded by the *Brachycrus* Curve or possibly the entire *Brachycrus* biochron, on the other. Like the *Brachycrus* biochron, the MMCO also spanned the early middle Hemingfordian to late middle Barstovian NALMAs and the boundary between the early and middle Miocene Epoch. That boundary is 15.97 Ma in age (Lourens et al. 2004). The MMCO was a period of pronounced global warming that (1) began approximately 17.6 Ma ago, (2) climaxed at 17.2, 16.4 (MMCO Peak 1), 15.7 (MMCO Peak 2), and 15.5 Ma, and (3) ended about 15.4 Ma ago (Warny et al. 2009, Foersterling 2011, Browning 2012, Feakins et al. 2012). MMCO Peaks 1 and 2 were separated by a short-term excursion informally termed in this report the MMCO Trough, during which global temperatures dipped slightly to a low point approximately 16.2 Ma ago (Foersterling 2011, Feakins et al. 2012). The peaks and troughs in the curve characterizing the MMCO appear to coincide temporally with only some of those observed in the more complex *Brachycrus* Curve, which is based entirely on mean P1–M3 lengths (Figure 3). This paper evaluates the possible relations between the MMCO and fluctuating body size in *Brachycrus*.

Acronyms and abbreviations

3WA, No. 3 White Ash; **4WA**, No. 4 White Ash; **AMNH**, American Museum of Natural History Division of Paleontology; **Ar/Ar**, ⁴⁰argon/³⁹argon; **B.**, *Brachycrus*; **BP**, before the present; **CA**, California; **CFm.**, Caliente Formation; **CM**, Carnegie Museum of Natural History, Section of Vertebrate Paleontology; **F:AM**, Frick American Mammals (collection now at AMNH); **FAST**, Fine Ashy and Shaly Tuff; **Fm.**, Formation; **K-Ar**, ⁴⁰potassium-⁴⁰argon; **KUVP**, University of Kansas Museum of Natural History, Division of Vertebrate Paleontology; **L.**, *laticeps*; **LACM**, Natural History Museum of Los Angeles County Vertebrate Paleontology Department; **M**, mean; **Ma**, megannum (million years); **mm**, millimeter; **MMCO**, Middle Miocene Climatic Optimum; **N**, sample size; **n. gen. & sp.**, new genus and species; **n. subsp.**, new subspecies; **NALMA**, North American Land Mammal Age; **NE**, Nebraska; **NWA**, Nambé White Ash; **OR**, observed range; **OT**, Oreodont Tuff; **P1–M3**, upper cheek tooth row; **p1–m3**, lower cheek tooth row; **PUM**, Princeton University Museum of Natural History (collection now at Yale University Peabody Museum of Natural History, Vertebrate Paleontology Division); **RT**, Rak Tuff; **SCA3**, Sheep Creek Ash No. 3; **sml.-bod. var.**, smaller-bodied variety; **SRF**, Split Rock Formation; **SRT**, Split Rock Tuff; **UCM**, University of Colorado Museum of Natural History; **UCMP**, University of California Museum of Paleontology;

uncat., uncataloged; **undet.**, undetermined; **undif.**, undifferentiated; **USNM**, United States National Museum, Smithsonian Institution, Department of Paleobiology; **UW**, University of Wyoming Department of Geology and Geophysics, Departmental Scientific Collections, Collection of Fossil Vertebrates; **v.**, *vaughani*; **VVT**, Valley View Tuff; **WY**, Wyoming.

Methods and materials

Upper cheek tooth-row or P1–M3 length (in millimeters) is used in this report as a reliable indicator of adult body size in *Brachycrus* and other oreodonts because that parameter is strongly correlated with skull length, which, in turn, is proportional to body size (Lander 1977, 2008, Stevens and Stevens 1996, Lander and Hanson 2006). Each measurement was acquired parallel to the occlusal surface using the outside jaws of a caliper and extended from the anterior surface of the P1 (or anterior rim of anterior alveolus when tooth missing) to the base of the posterior edge of the M3 metastyle (see Figure 2F). Following Kelly and Lander (1988a–b, 1992), Lander and Kelly (1989), and Lander (1998, 2011), successive and morphologically similar samples *Brachycrus* that differ substantially (i.e., at least 5 percent) from one another only in terms of their mean P1–M3 lengths are retained in the same species, but are assigned to different subspecies because such differences are not thought to reflect any evolutionary change (see below). Similar mean P1–M3 lengths have allowed the correlation of *Brachycrus* samples from quarries in southern California and northwestern Nebraska that are separated by approximately 875 miles (Figure 1; Lander 1985, Kelly and Lander 1988b, Lander and Kelly 1989; see below).

Most of the *Brachycrus* specimens measured for this contribution are F:AM specimens from the Barstow Formation of southern California, the Sheep Creek and Olcott Formations of the Hemingford Group in northwestern Nebraska, the Tesuque Formation of north-central New Mexico, and the Split Rock Formation of central Wyoming (Figure 1). Those specimens comprise many cataloged individuals published by Schultz and Falkenbach (1940), but include numerous uncataloged F:AM specimens from several of the same formations, as well. Those stratigraphic units yielded most of the holotypic specimens for species assigned to *Brachycrus laticeps* by Lander (1998). A number of UCMP specimens and a few CM, KUVP, USNM, and UW specimens from the Split Rock Formation were also incorporated into this study for completeness, as were two uncataloged F:AM specimens from the undifferentiated Hemingford Group at Ginn Quarry in northwestern Nebraska. The stratigraphic levels of the F:AM quarries in the Barstow Formation are based on Galusha et al. (1966), whereas the positions of the F:AM quarries in the Sheep Creek and Olcott Formations follow Skinner et al. (1977). In some cases, the relative stratigraphic levels of Ginn Quarry and

several quarries (e.g., Echo, Humbug, and Mill Quarries) in the Olcott Formation were based on the stages of evolution of their respective faunas. Galusha (1975) compared some faunal elements from Ginn Quarry with those from the Sheep Creek Formation and the Red Valley Member of the Box Butte Formation, which preceded the Sheep Creek Formation, whereas Skinner et al. (1977) compared some species from Echo, Humbug, and Mill Quarries with similar ones from quarries in the Olcott Formation of known stratigraphic position. The stratigraphic intervals occupied by various F:AM and UCMP localities in the Split Rock Formation of Wyoming are mostly after Munthe (1979). Stratigraphic data for many specimens, particularly those from the Split Rock Formation, were reviewed and verified or corrected, as necessary. Size and stratigraphic data for the *Brachycrus* records from all of the stratigraphic units cited above provided documentation of the conclusions presented herein regarding changes in body size between stratigraphically superposed samples of *Brachycrus*.

The *Brachycrus* specimens measured for this study and their respective P1–M3 lengths are listed by state, subtaxon, faunal assemblage, stratigraphic level, and locality in Table 1. The P1–M3 lengths for most of those specimens are graphed in Figure 3. Also presented in Table 1 are similar data for a number of other critical specimens and quarry samples from less securely documented levels in the same stratigraphic units (e.g., Barstow Formation) and from correlative units in Montana that produced additional holotypic specimens for some of the species now assigned to *Brachycrus laticeps* (Figure 1). The identifications of the *Brachycrus* specimens cited in this report and the systematics of *Brachycrus* are modified from Lander (1985, 1998) and Kelly and Lander (1988b).

Ar/Ar and K-Ar radiometric age determinations cited in this report and provided in Figure 3 are after MacFadden et al. (1990), Woodburne et al. (1990), and Woodburne (1991, 1996) for the Barstow Formation; Woodburne et al. (1990), Woodburne (1991), and Izett and Obradovich (2001) for the Sheep Creek Formation; Izett and Obradovich (2001) for the Skull Ridge Member of the Tesuque Formation of north-central New Mexico; and Munthe and Coombs (1979) and Izett and Obradovich (2001) for the Split Rock Formation. However, the Ar/Ar determinations provided by Izett and Obradovich (2001) have been corrected as recommended therein to comply with internationally adopted calibration standards used by Ogg (2012) and Hilgen et al. (2012). The age of the boundary between the early and middle Miocene Epoch (15.97 Ma) is after Lourens et al. (2004). Magnetostratigraphic data cited herein and provided in Figure 3 are from Lander et al. (2008) as modified by Lander (2011) for the Split Rock Formation, MacFadden et al. (1990) for the Barstow Formation (however, see alternative interpretation provided by Woodburne 1996), Prothero et al. (2008) for the Caliente Formation of California, and Barghoorn (1981) for the Tesuque Formation, whereas corresponding

chronologic data regarding the Geomagnetic Polarity Timescale are after Ogg (2012) and Hilgen et al. (2012).

Samples of Middle Hemingfordian to Middle Barstovian Age—compiling a comprehensive database

Upper cheek tooth-row or P1–M3 lengths for individual specimens and sample means for that parameter are provided by state, stratigraphic unit, and taxon in Table 3. Those data are portrayed graphically and in vertical succession in Figure 3. Biostratigraphic, lithostratigraphic, radiometric, and magnetostratigraphic data have been used extensively to determine the geologic ages of various specimens and samples and to arrange them in chronological order. As a consequence, the systematics of *Brachycrus* recognized in this report differs markedly with the taxonomic schemes presented previously by Schultz and Falkenbach (1940, 1968), Lander (1977, 1985, 1998, 2003, 2005, 2011), Kelly and Lander (1998a–b), Lander and Kelly (1989), and Stevens and Stevens (2007), particularly with regard to the subspecies subsumed under *Brachycrus laticeps*.

Sheep Creek and Olcott formations, Nebraska

Wood et al. (1941) based the Hemingfordian NALMA on the fossil land mammal assemblages from the Hemingford Group of northwestern Nebraska (Figure 1), particularly the Sheep Creek Fauna from the Lower Sheep Creek Beds as recognized by Cook and Cook (1933) (= Upper Sheep Creek Local Fauna of this report). Matthew (1924) recorded the large-bodied taxon *Pronomotherium siouense*, variety (= a large-bodied form of *Brachycrus laticeps*, AMNH 18344; Lander 1985, Kelly and Lander 1988b) from Horizon A (= *Merychippus primus* Zone) or the lower part of the Sheep Creek Beds as recognized by Matthew (1924) in Stonehouse Draw. Cook and Cook (1933), in turn, listed the same record as *P. cf. siouense* from the Lower Sheep Creek Beds. Skinner et al. (1977) recognized three superposed units of the Sheep Creek Formation that are referred to as the Lower, Middle, and Upper Members in this report. The specimens from the *Merychippus primus* Zone in Stonehouse Draw were recovered from the future site of Thomson Quarry at the base of the Middle Member (Skinner et al. 1977). Hilltop Quarry is also at the base of the Middle Member (Skinner et al. 1977) and, along with Thomson Quarry, produced additional large-bodied examples of *B. laticeps* (Figures 2–3, Table 1; Lander 1977, 1985, 1998, Kelly and Lander 1988b). The holotypic specimen of *B. laticeps laticeps* is from the Sixmile Creek Formation of southwestern Montana and, for reasons presented below, is considered questionably to include the large-bodied sample from the Middle Member of the Sheep Creek Formation, following Lander (1977, 1985, 1998, 2003), Kelly and Lander (1988b), and Lander and Kelly (1989). Skinner et al. (1977) included

the assemblages from the Lower Member of the formation (= Lower Sheep Creek Local Fauna of this study) in the Sheep Creek Fauna, which they regarded as late Hemingfordian in age. Tedford et al. (1987, 2004) and essentially all other recent workers have also considered the Sheep Creek Fauna to be late Hemingfordian in age. The Lower Member produced a medium-body-sized subspecies of *B. laticeps* at Greenside and Long Quarries, which (Schultz and Falkenbach 1940) yielded the holotypic specimens of the *B. laticeps* junior synonyms, *B. wilsoni* and *B. wilsoni longensis*, respectively (Figure 3, Table 1; Lander 1977, 1985, 1998, 2003, Kelly and Lander 1988b, Lander and Kelly 1989). *Brachycrus laticeps* underwent a slight (6.4%) increase in mean P1–M3 length from the Lower to the Middle Member of the Sheep Creek Formation (Figure 3, Table 1).

Sheep Creek Ash No. 3 lies near the top of the Middle Member of the Sheep Creek Formation (Skinner et al. 1977). That ash is 16.3 or 16.4 Ma old on the basis of Ar/Ar radiometric dating analysis (Figure 3; C.C. Swisher III unpublished data in Woodburne et al. 1990, Woodburne 1991, and Woodburne and Reynolds 2010, Izett and Obradovich 2001). The latter determination is 16.64 Ma when recalculated using the correction factor provided by Izett and Obradovich (2001) (Figure 3). The younger of two determinations based on fission-track dating analysis of zircon crystals from the same ash is 16.5 Ma (Figure 3; Naeser et al. 1980). On the other hand, the age of the Sheep Creek Ash No. 3 is only 15.55 Ma old by interpolation (Perkins and Nash 2002). Nevertheless, the Lower Sheep Creek Local Fauna on one hand and the Upper Sheep Creek Local Fauna on the other are regarded herein as early late and middle late Hemingfordian in age, respectively, based strictly on the preponderance of radiometric data indicating that the Sheep Creek Fauna is at least 16.3 Ma old (figure 3). Magnetostratigraphic data presented below indicate that medium-bodied sized *B. laticeps buwaldi* from the Green Hills Division of the Barstow Formation at Steepside Quarry in southern California and the large-bodied subspecies from overlying Sunset Quarry are younger than 15.974 Ma in age. Correspondingly, those subspecies cannot be the same as the medium-body-sized subspecies of *B. laticeps* from the Lower Member of the Sheep Creek Formation at Greenside and Long Quarries and *B. laticeps laticeps?* from Hilltop and Thomson Quarries from the overlying Middle Member, respectively, contrary to Lander (1977, 1985, 2003, 2005), Kelly and Lander (1988a–b), and Lander and Kelly (1989) (Figure 3). For that reason, *B. wilsoni* is resurrected as the earliest subspecies of *B. laticeps* rather than as a species of *Brachycrus* (contrary to Stevens and Stevens 2007), with *B. wilsoni longensis* being regarded as a junior synonym of *B. laticeps wilsoni* (Figure 3). The first appearance of *B. l. wilsoni* in the Lower Member of the Sheep Creek Formation is regarded in this report as marking the beginning of the late Hemingfordian NALMA, whereas

the Sheep Creek Fauna is considered to be early late to latest Hemingfordian in age (Figure 3).

The unfossiliferous Upper Member of the Sheep Creek Formation is unconformably overlain by the Lower Snake Creek Beds (= Olcott Formation; Skinner et al. 1977). The Olcott Formation, which comprises three successive subcycles (herein termed Lower, Middle, and Upper Members) and the Echo Quarry Paleovalley Fill, yielded the Lower Snake Creek Fauna (Skinner et al. 1977). Matthew (1924) recorded *Pronomotherium siouense* (= small-bodied subspecies *Brachycrus laticeps siouense*; Schultz and Falkenbach 1940, 1968, Lander 1977, 1985, 1998, 2003, Kelly and Lander 1988a–b, Lander and Kelly 1989) from the Lower Snake Creek Beds (= Horizon A of Snake Creek Beds = *Merychippus paniensis* Zone). Cook and Cook (1933) listed that taxon from the same unit and from the underlying Upper Sheep Creek Beds (= lower part of Lower Snake Creek Beds; McKenna 1965), as well. The holotypic specimen of *B. l. siouense* (PUM 12057) is from an unspecified level in the Olcott Formation (Skinner et al. 1977). The stratigraphic relations of the Echo Quarry Paleovalley Fill and Humbug Quarry with respect to the three members of the Olcott Formation have not been determined, nor have the relative stratigraphic positions of Echo and Mill Quarries within the paleovalley fill (Skinner et al. 1977). However, Skinner et al. (1977) considered the Mill Quarry assemblage to be slightly younger than that from Echo Quarry, whereas the equids from Humbug Quarry appeared to be slightly older (i.e., more primitive) than those from either Echo or Mill Quarry (Figure 3). Moreover, the mean P1–M3 lengths for the *B. l. siouense* samples from the Lower (Snake and Trojan Quarries), Middle (West Sand Quarry), and Upper Members (Far Surface and Version Quarries) of the Olcott Formation fall in the lower half of the observed range of the parameter for the Humbug Quarry sample of the same taxon (Figure 3, Table 1). Consequently, the Humbug Quarry assemblage is considered herein to be younger than those from the three members of the Olcott Formation. In general, the samples from the Middle and Upper Members and from Humbug, Echo, and Mill Quarries appear to represent a somewhat larger-bodied variety of *B. l. siouense* and to have undergone a slight increase in size relative to the preceding, smaller-bodied variety of the same subspecies from the Lower Member (Figures 2–3, Table 1; Lander 1985, 2003, Kelly and Lander 1988b). In stratigraphic succession, *B. l. siouense* underwent (1) a slight (5.6%) increase in mean P1–M3 length from the Lower Member of the Olcott Formation to Humbug Quarry in the undifferentiated Olcott Formation, (2) a lesser (4.0%) decrease from Humbug Quarry to Echo Quarry in the Echo Quarry Paleovalley Fill, and (3) an even smaller increase from Echo Quarry to Mill Quarry, also in the paleovalley fill (Figure 3, Table 1). All mean and individual P1–M3 lengths for *B. laticeps wilsoni* and *B. laticeps laticeps?* from the Sheep Creek Formation are greater than 125 mm, whereas all means and most

individual lengths for *B. laticeps siouense* are below 125 mm (Figure 3, Table 1).

Perhaps following Cook and Cook (1933), Lugn (1939) extended the concept of the Sheep Creek Formation upward stratigraphically by considering the Lower Snake Creek Beds to be the upper part of the Sheep Creek Formation (McKenna 1965, Skinner et al. 1977, Tedford et al. 1987, Woodburne et al. 1990). However, Wood et al. (1941) excluded the Lower Snake Creek Fauna from their definition of the Hemingfordian NALMA when they included the fauna from the lower part of the Sheep Creek Formation in the land mammal age, but explicitly rejected also including the succeeding assemblage (i.e., Lower Snake Creek Fauna) from the upper part of the formation as recognized by Lugn (1939) (McKenna 1965, Tedford et al. 1987, Woodburne et al. 1990). Consequently, Woodburne and Tedford (1982), Woodburne et al. (1990), Woodburne (1991), and Tedford et al. (1987) extended the concept of the Barstovian NALMA backwards temporally to include the post-type Hemingfordian Lower Snake Creek Fauna, which they regarded as early Barstovian rather than late Hemingfordian in age (see below). In contrast, Wilson (1960), Schultz and Stout (1961), Evander (1986), and Lander (2005) considered the Lower Snake Creek Fauna to be late Hemingfordian in age. On the other hand, Lander (1985) deemed the fauna to be post-Hemingfordian and pre-Barstovian in age because it represented a time interval that had not been included in the original definition of either land mammal age by Wood et al. (1941). For reasons presented below, the Lower Snake Creek Fauna is regarded as middle Barstovian in age herein (Figure 3). The majority of radiometric age determinations for Sheep Creek Ash No. 3 indicate that *B. laticeps siouense* and the Lower Snake Creek Fauna are younger than 16.3 Ma in age (Figure 3). However, biostratigraphic and radiometric data from the Green Hills Division of California and the Skull Ridge Member of the Tesuque Formation in north-central New Mexico suggest that (1) the smaller-bodied variety of *B. l. siouense* from the Lower Member of the Olcott Formation at Snake and Trojan Quarries corresponds to the individual from the Green Hills Division at Oreodont Quarry, (2) the larger-bodied variety from the Echo Quarry Paleovalley Fill at Mill Quarry is the same taxon as the individuals from the Green Hills Division at Camp Quarry and 20–25 feet above the No. 3 White Ash in the Skull Ridge Member, and, therefore, (3) *B. l. siouense* is between 15.62 and 15.52 Ma in age (Figure 3). Consequently, the Sheep Creek and Lower Snake Creek Faunas might be separated in time by at least 680,000 years.

Woodburne (1969) and Tedford et al. (1987) considered the assemblage of presumed early Barstovian age from the Sand Canyon Formation at Observation Quarry in northwestern Nebraska to be intermediate in age between those from the Sheep Creek and Olcott Formations. Unfortunately, the *Brachycrus* remains from Observation Quarry that Schultz and Falkenbach (1940) referred to

B. siouense are too incomplete to be assigned confidently to any subspecies of *B. laticeps*. Moreover, the age of the quarry assemblage is not constrained by radiometric or magnetostratigraphic data. However, if the quarry sample represents a smaller-bodied form than *B. laticeps laticeps*, the assemblage might instead be regarded as earliest middle Barstovian in age.

Barstow and Caliente formations, California

The Green Hills Fauna comprises a number of stratigraphically superposed quarry assemblages from the Green Hills Division of the Barstow Formation in the Mud Hills of the southern California Mojave Desert (Figure 1; Galusha et al. 1966). Most of the quarries were developed along the southwestern margin of the Mud Hills on the divide between Coon Canyon and Rainbow Basin (Galusha et al. 1966, Woodburne et al. 1990, fig. 3). There, the Green Hills Division is about 740 feet thick and extends from approximately 320–1,060 feet below the Skyline Tuff at the base of the overlying First Division (= Fossiliferous Tuff or Upper Member) of the Barstow Formation (Galusha et al. 1966, Woodburne et al. 1990, fig. 3). The Green Hills (or Third) Division is equivalent to the lower part of the Resistant Breccia Member or the middle part of the Middle Member of the Barstow Formation, whereas the lower part of the Middle Member corresponds to the Fine Ashy and Shaly Tuff Member or the Rak Division and the upper portion is the same as the Second Division, the Red (or Fourth) Division is equivalent to the Lower Member, and the upper part of the member is the same as the Second Division, which underlies the First Division (Woodburne et al. 1990, fig. 2). The Barstovian NALMA was based specifically on the Barstow Fauna from the Fossiliferous Tuff Member by Wood et al. (1941).

Remains of *Brachycrus laticeps* have been recovered from a number of superposed F:AM quarries that are located stratigraphically with regard to their distances below the Skyline Tuff. Stratigraphically constrained records of *B. laticeps* from the Green Hills Division include (1) a large-bodied subspecies (*B. laticeps altiramus*?; see below) from the First Layer above the Rak Division in the lower 60 feet of Green Hills Division (roughly 1,000–1,060 feet below Skyline Tuff), with one unusually large individual documented from 40 feet above the Rak Division and, contrary to Lander (1985) and Kelly and Lander (1988b), not from the same level as Sunset Quarry, (2) a medium-body-sized subspecies (*B. laticeps buwaldi*) from the upper level of Steepside Quarry or approximately 1,000 feet below Skyline Tuff and 60 feet above the base of the Green Hills Division, (3) an unnamed large-bodied subspecies from 100 feet above the base of the division at Sunset Quarry (about 960 feet below Skyline Tuff), (4) a small-bodied sample from Oreodont Quarry (around 880 feet below Skyline Tuff) that is comparable in its mean P1–M3 length to

the smaller-bodied variety of small-bodied to medium-body-sized *B. laticeps siouense* from the Lower Member of the Olcott Formation in northwestern Nebraska, (5) a medium-body-sized individual from Deep (= Lower Green Hills) Quarry (R.L. Evander 2013 personal communication) (roughly 520 feet below the Skyline Tuff) with a P1–M3 length that is similar to those for individuals from the Echo Quarry Paleovalley Fill of the Olcott Formation at Mill Quarry and 20–25 feet above the No. 3 White Ash in the Skull Ridge Member of the Tesuque Formation in north-central New Mexico, and (6) a small-bodied sample from Camp Quarry (approximately 450 feet below Skyline Tuff) that is comparable in its mean P1–M3 length to that for the small-bodied subspecies (*B. laticeps riograndensis*) from 25 feet below Ash F of the Skull Ridge Member (Figure 3, Table 1; Galusha et al. 1966, Lander 1977, 1985, 1998, 2003, 2011, Kelly and Lander 1988a–b, Lander and Kelly 1989, Pagnac 2009). In stratigraphic succession, *B. laticeps* underwent (1) a slight (5.3%) decrease in mean P1–M3 length from the First Layer to Steepsides Quarry, (2) a slightly greater (7.1%) increase from Steepsides to Sunset Quarry, (3) a substantial (16.5%) reduction from Sunset to Oreodont Quarry, (4) a small (6.0%) increase from Oreodont to Deep Quarry, and (5) a comparable (5.9%) decrease in length before going extinct (Figure 3, Table 1). The lowest and highest local occurrences of *Brachycrus* in the Green Hills Division are separated by at least 570 to as many as 610 feet of strata.

All mean and nearly all individual P1–M3 lengths for medium-body-sized and large-bodied *B. laticeps* from the First Layer and Steepsides and Sunset Quarries are greater than 125 mm, whereas all such lengths for *B. laticeps siouense* from Oreodont and Lower Green Hills (= Deep) Quarries and *B. laticeps riograndensis* from Camp Quarry are below 125 mm (Figure 3, Table 1). Based on their P1–M3 lengths (Table 1), a specimen from Ness Quarry (F:AM 42372), F:AM 42402 (*B. buwaldi barstowensis* holotypic specimen) from the First or Second Layer above the Third (= Rak) Division, an uncataloged F:AM specimen from the lower part of the Green Hills Division, and UCMP 2057 (*B. laticeps buwaldi* holotypic specimen) are probably from about the same level as Steepsides Quarry and, therefore, referable to *B. l. buwaldi*, whereas two uncataloged F:AM specimens from Green Hills Quarry are probably from a level at or near that of Oreodont or Camp Quarry (Table 1; Lander 1977, 1985, fig. 4, 1998; see Kelly and Lander 1988b, fig. 4).

The occurrence of the medium-body-sized sample of *B. laticeps buwaldi* at Steepsides Quarry and stratigraphically between the large-bodied records of the species from the First Layer and Sunset Quarry indicates that body size in *B. laticeps* peaked twice during the period of time represented by the lower 100 feet of the Green Hills Division (Figure 3). Consequently, the large-bodied samples are referable to different subspecies. Based on their respective P1–M3 lengths, the uncataloged F:AM specimen from 40 feet above the Rak Division in the First Layer represents

the largest individual of *Brachycrus* recorded from the Barstow Formation, whereas the holotypic specimen of *B. laticeps altiramus* from the Madison Valley Formation (= Sixmile Creek Formation) of southwestern Montana is the largest-bodied record for the genus overall (Figure 3, Table 1). Therefore, the First Layer sample assigned questionably to *B. l. altiramus* herein, following Lander (2011) (see below), but the uncataloged F:AM specimen from Sunset Quarry perhaps represents an unnamed subspecies. On the other hand and as in the Skull Ridge Member, the small-bodied sample of *B. laticeps* at Camp Quarry occurred above an individual referable to the larger-bodied variety of *B. laticeps siouense* from Deep Quarry and, therefore, is assignable to *B. laticeps riograndensis* (Figure 3; see above). Moreover, the occurrence of the larger-bodied variety of *B. l. siouense* at Deep Quarry stratigraphically between the comparatively small-bodied records of the species from Oreodont and Camp Quarries indicates that the latter records are not referable to the same subspecies. *Brachycrus l. riograndensis*, like the smaller-bodied variety of *B. l. siouense* from Oreodont Quarry and the Lower Member of the Olcott Formation in Nebraska represents one of the two smallest-bodied records of the species (Figure 3, Table 1).

The Oreodont Tuff lies only a few feet below (not above) Oreodont Quarry, contrary to Woodburne et al. (1990), and has been determined to be 15.80 and 15.88 Ma old on the basis of K-Ar and Ar/Ar radiometric dating analyses, respectively (Figure 3; Tedford et al. 1987, MacFadden et al. 1990, R.E. Reynolds 2013 personal communication to M.O. Woodburne). The Valley View Tuff is 15.27 Ma in age, based on Ar/Ar analysis, and lies roughly 2,165 feet above the base of the Barstow Formation (C.C. Swisher III unpublished data in Woodburne 1991, 1996, and Woodburne and Reynolds 2010). Therefore, the latter tuff probably lies about 340 feet below the Skyline Tuff, 20 feet below the top of the Green Hills Division, and perhaps 150 feet above Camp Quarry (Figure 3; see Galusha 1966, Woodburne et al. 1990, fig. 6, MacFadden et al. fig. 7). On the other hand, the larger-bodied variety of *B. laticeps siouense* and *B. laticeps riograndensis* from of the Skull Ridge Member of New Mexico are bracketed stratigraphically by the No. 3 and 4 Whites Ashes, which are 15.4 and 15.3 Ma old, respectively (see below; Figure 3). Consequently, the smaller-bodied variety of *B. l. siouense* from Oreodont Quarry and the Lower Member of the Olcott Formation is about 15.80 or 15.88 Ma in age, whereas the larger-bodied variety of that subspecies from Deep Quarry and the Echo Quarry Paleovalley Fill of the Olcott Formation on one hand and *B. l. riograndensis* from Camp Quarry on the other are between 15.4 and 15.3 Ma old (Figure 3).

The Rak Tuff, which lies at the base of the Rak Division, is 16.30 and 16.56 Ma old on the basis of K-Ar and Ar/Ar dating analyses, respectively (MacFadden et al. 1990). The top of the Rak Division and the Green Hills Division up to a level above those of Oreodont Quarry and the Oreodont

Tuff occur in a reversed magnetozone assignable to Chron C5Br (see above, Woodburne et al. 1990, fig. 6, MacFadden et al. 1990, fig. 8). The beginning of Chron C5Br is 15.974 Ma in age (Ogg 2012, Hilgen et al. 2012). Those data suggest that (1) the medium-body-sized and large-bodied subspecies of *B. laticeps* from the First Layer and Steepside and Sunset Quarries are between 15.974 and 15.88 Ma in age and (2) those subspecies are younger than the ones in the Sheep Creek Fauna, which (2a) is found in the Lower and Middle Members of Sheep Creek Formation in northwestern Nebraska, (2b) underlies Sheep Creek Ash No. 3, and, therefore, (2c) is at least 16.3 Ma old (see above; Figure 3). Consequently, the subspecies of *B. laticeps* from the Green Hills Division are not the same as those from the Sheep Creek Formation and perhaps are best regarded as early Barstovian in age, contrary to Lander (1977, 1985, 1998, 2003, 2005, Kelly and Lander (1988a–b), Lander and Kelly (1989) (see below). Available radiometric and magnetostratigraphic data for the Barstow Formation and the Skull Ridge Member (see below) indicate that the biochron of *B. laticeps* in the Barstow Formation spanned 0.454–0.674 Ma. Unfortunately, the chron assignments by Woodburne et al. (1990), MacFadden et al. (1990), and Woodburne (1991) for the magnetozone in the stratigraphic interval that includes the Deep and Camp Quarry levels and the Valley View Tuff have been disputed by Woodburne (1996) and Woodburne and Reynolds (2010), who also assigned the latter interval to Chron C5Br (Figure 3). Accordingly, the magnetozone containing Camp Quarry and the last local occurrence of the smaller-bodied variety of *B. laticeps siouense* has not been established with certainty. However, correlative strata of reversed polarity in the Skull Ridge Member that include the No. 3 and 4 White Ashes have also been assigned to Chron C5Br (see below; Figure 3; Barghoorn 1981, Tedford and Barghoorn 1993).

Following Galusha et al. (1966), Woodburne (1969, 1991, 1996) and most subsequent workers (e.g., Woodburne et al. 1982, 1990, Woodburne and Tedford 1982, Tedford et al. 1987, 2004, Pagnac 2009, Woodburne and Reynolds 2010, etc.) extended the concept of the Barstovian NALMA downward stratigraphically to embrace the entire post-type Hemingfordian and pre-type Barstovian Green Hills Fauna, including the Steepside Quarry assemblage and those faunal elements from the lower 60 feet (i.e., the First Layer) of the Green Hills Division between the quarry level and the top of the underlying Rak Division. The Hemingfordian-Barstovian NALMA boundary was placed between the Rak and Green Hills Divisions and their respective faunas by those authors because (1) some of the index taxa used by Wood et al. (1941) to define the Barstovian (e.g., the ursid *Hemicyon* [*Plithocyon*]) were also occurred in the Green Hills Fauna (with *Hemicyon* [*Plithocyon*] first appearing at Steepside Quarry) and principal correlatives of the overlying, type Barstovian Barstow Fauna, and (2) some of the faunas regarded as principal correlatives of the Barstow Fauna were instead

found to be correlatives of the Green Hills Fauna. The Green Hills Fauna, including those faunal elements from the First Layer (Galusha et al. 1966, Woodburne et al. 1990), were regarded as early Barstovian rather than late Hemingfordian in age because the presumably correlative Lower Snake Creek Fauna from the Olcott Formation of Nebraska was specifically excluded the Hemingfordian NALMA by Wood et al. (1941). However, no medium-body-sized or large-bodied sample of *Brachycrus* is recorded from the Olcott Formation. Consequently and as noted by Lander (1977, 1985) and Kelly and Lander (1988b), the assemblages from Steepside and Sunset Quarries and the First Layer (i.e., 40 feet above the Rak Division) are older than the Lower Snake Creek Fauna (Figure 3). It was partly for that reason that Lander (1977, 1985, 2003, 2005), Kelly and Lander (1988a–b), and Lander and Kelly (1989) regarded the assemblages from Steepside and Sunset Quarries as late Hemingfordian and age and correlatives of the type Hemingfordian Sheep Creek Fauna from the Lower and Middle Members of the Sheep Creek Formation in Nebraska, respectively, conclusions not accepted herein (see above). Unfortunately, Wood et al. (1941) did not consider assemblages intermediate in age between the Sheep Creek and overlying Lower Snake Creek Faunas when defining the Hemingfordian and Barstovian NALMAs. Because *B. laticeps siouense* and *B. laticeps riograndensis* were comparatively common taxonomic elements in correlative, geographically widely-distributed assemblages of early Barstovian age and succeeded the even earlier Barstovian biochrons of larger-bodied subspecies of *B. laticeps*, the two smaller-bodied subspecies are regarded herein as middle rather than early Barstovian in age, with the boundary between the early and middle Barstovian NALMA lying between Sunset and Oreodont Quarries (Figure 3).

The holotypic specimen of *Brachycrus altiramus* (AMNH 9746) is from the Madison Valley Beds (= Sixmile Creek Formation) of southwestern Montana and represents the largest known individual of the genus in terms of its P1–M3 length, whereas the holotypic specimen of *B. laticeps mooki* (F:AM 21321) from the Deep River Beds (= Sixmile Creek Formation) of southwestern Montana and the specimen from 40 feet above the base of the Green Hills Division represent individuals that were nearly as large (Table 1). Following Lander (2011), *B. altiramus* is resurrected herein and tentatively subsumed under *B. laticeps* as a large-bodied subspecies (*B. laticeps altiramus*) that questionably (1) includes *B. l. mooki* and the three specimens from the First Layer of the Green Hills Division (including the individual from 40 feet above the Rak Division), (2) preceded the similarly large-bodied unnamed subspecies of *B. laticeps* from Sunset Quarry, (3) succeeded comparatively large-bodied *B. laticeps laticeps*? from the Middle Member of the Sheep Creek Formation, and (4) is early Barstovian rather than late Hemingfordian in age (Figure 3). Lander (1977, 1998) had earlier rejected *B. altiramus*, assigning it to *B. laticeps laticeps*.

The late Hemingfordian Lower West Dry Canyon Local Fauna of the Caliente Formation at LACM locality 5607 and UCMP locality V6766 produced remains assigned questionably to *B. laticeps buwaldi* by Kelly and Lander (1988a–b, 1992). Those and other localities yielding assemblages referable to the same local fauna occur below the lower of two closely spaced and comparatively thick, resistant, and coarse-grained sandstone beds (Kelly and Lander 1988b, fig. 5). The localities were shown too high in the section by Prothero et al. (2008, fig. 6) and should have been placed below the lower sandstone bed lying at the 1,500-foot level. The overlying Upper West Dry Canyon Local Fauna at LACM locality 5606 contains a medium-body-sized form of *Brachycrus* referred to *B. l. buwaldi* by Kelly and Lander (1988b, 1992), Prothero et al. (2008), and Lander (1998, 2011) (Figure 3, Table 1). LACM locality 5606 occurs in a less-resistant finer-grained sequence between the two sandstone beds (Kelly and Lander 1988b, fig. 5; locality not shown in Prothero et al. 2008, fig. 6) (Table 1). However, the latter interval and the one lying immediately below the lower sandstone bed and containing the Lower West Dry Canyon Local Fauna occur at the top of a normal magnetozone assignable to Chron C5Cn (Prothero et al. 2008, fig. 6), presumably Chron C5Cn.1n (Figure 3). Chron C5Cn.1n is 16.268–15.974 Ma in age (Ogg 2012, Helgen et al. 2012). Therefore and contrary to Kelly and Lander (1988a–b) and Lander (1998, 2011), the entire West Dry Canyon Fauna is regarded herein as a correlative of the Rak Division Fauna, following Prothero et al. (2008), and not the Green Hills Fauna which occurs in the succeeding reversed magnetozone, Chron C5Br, and, consequently, is younger than 15.974 Ma in age (see above). Correspondingly, *B. laticeps* in the West Dry Canyon Fauna cannot be the same subspecies as *B. laticeps buwaldi* from the Green Hills Division at Steepside Quarry because it is older and separated in time from the latter subspecies by the large-bodied subspecies *B. laticeps altiramus?* from the First Layer of the Green Hills Division (Figure 3). Similarly, the West Dry Canyon Fauna is younger than the late Hemingfordian Sheep Creek Fauna of Nebraska. The latter fauna occurs below the Sheep Creek No. 3 Ash and, therefore, is older than 16.3 Ma in age (see above; Figure 3). Consequently, *B. laticeps wilsoni* and *B. laticeps laticeps?* from the Lower and Middle Members of the Sheep Creek Formation are regarded herein as early late and middle late Hemingfordian in age, respectively, whereas the unnamed subspecies of *B. laticeps* in the Upper West Dry Canyon Local Fauna is considered to be latest Hemingfordian (Figure 3).

On the other hand, a small-bodied subspecies of *B. laticeps* is found in the overlying Lower Dome Spring Fauna at LACM locality 5604 and UCMP localities V5670, V5824, V6414, and V6768, which occur above the upper 65-foot-thick sandstone bed and only a short distance above the interval containing the Upper West Dry Canyon Local Fauna (Lander 1977, 1998, Kelly and

Lander 1988a–b, Prothero et al. 2008). The Lower Dome Spring Fauna is in the lower part of a reversed magnetozone referable to Chron C5Br (Prothero et al. 2008), which is 15.974–15.160 Ma old (Ogg 2012, Helgen et al. 2012). Consequently, the Lower Dome Spring Local Fauna is comparable in age to the assemblages from the Green Hills Division at Oreodont and Camp Quarries. However, based on its stratigraphic proximity to the underlying Upper West Dry Canyon Local Fauna, the Lower Dome Spring Fauna is probably a correlative of the Oreodont Quarry assemblage and, therefore, is assignable to *B. laticeps siouense* and between 15.80 and 15.62 Ma in age (see above; Figure 3; Lander 1977, Kelly and Lander 1988b, 1992). The overlying Upper Dome Spring Fauna, which occurs in the upper part of the magnetozone as the Lower Dome Spring Fauna, has been correlated with the Second Division Fauna of the Barstow Formation (Prothero et al. 2008). Consequently, the upper part of the Green Hills Division, including the Camp Quarry level, is probably assignable to Chron C5Br, too (Woodburne 1996, Woodburne and Reynolds 2010) (Figure 3).

Lander (1985, 2003, 1998), Kelly and Lander (1988b), and Lander and Kelly (1989) assigned an uncataloged F:AM dentary from the late Barstovian Barstow Fauna at New Year Quarry to *B. laticeps siouense*. New Year Quarry is in the Upper Member of the Barstow Formation, approximately 35 feet above the Skyline Tuff and perhaps about 20 feet below the Dated Tuff (Galusha et al. 1966, Evander 1986). The Skyline Tuff is as old as 15.0 Ma in age, based on Ar/Ar analysis, whereas the Dated Tuff has been determined to be 14.8 Ma in age on the basis of both Ar/Ar and K-Ar dating analyses (MacFadden et al. 1990, WoldeGabriel et al. 1996, Cole et al. 2005). A p1–m3 length of 128 mm suggests that the specimen represents an individual slightly larger than those from Camp Quarry. However, the comparatively shallow horizontal ramus suggests that the specimen might be assignable to *Mediochoerus mohavensis* instead of *Brachycrus* and that the last local occurrence of the latter genus is from Camp Quarry. The *M. mohavensis* holotypic specimen (F:AM 34464) is from the *Hemicyon* Stratum, roughly 260 feet above the Skyline Tuff (Schultz and Falkenbach 1941, Galusha et al. 1966). The P1–M3 length of F:AM 34464 (114 mm) suggests that the specimen represents an individual slightly smaller than that represented by the dentary from New Year Quarry.

Skull Ridge Member of Tesuque Formation, New Mexico

Brachycrus laticeps occurs between the No. 3 and 4 White Ashes in the Skull Ridge Member of the Tesuque Formation in north-central New Mexico (Figure 1). The No. 3 White Ash has been determined to be 15.4 Ma old on the basis of Ar/Ar radiometric dating analysis (Izett and Obradovich 2001), but that determination is 15.62 Ma when recalculated using the correction factor provided

by Izett and Obradovich (2001) (Figure 3). On the other hand, the No. 4 White Ash is as old as 15.3 Ma in age, based on the Ar/Ar dating analysis of sanidine crystals (Izett and Obradovich 2001), but the latter determination is 15.52 Ma when recalculated. The two ash beds are separated by about 7–75 feet of strata and occur in a reversed magnetozone assignable to Chron C5Br (Galusha and Blick 1971, fig. 17, Barghoorn 1981, Tedford and Barghoorn 1993). The age determinations for the No. 3 and 4 White Ashes indicate that the *B. laticeps* remains from between the two ashes postdate the assemblage from the Green Hills Division of the Barstow Formation at Oreodont Quarry in southern California, but are no younger than those from higher in the division at Deep (= Lower Green Hills) and Camp Quarries (Figure 3).

The P1–M3 length of an uncataloged F:AM specimen from 20–25 feet above the No. 3 White Ash indicates that the individual probably represents the same late record of the larger-bodied variety of *B. laticeps siouense* as those from Deep Quarry and the Echo Quarry Paleovalley Fill of the Olcott Formation at Mill Quarry in northwestern Nebraska (Figure 3, Table 1). The holotypic specimen of *Brachycrus rusticus riograndensis* (F:AM 72326) is from 25 feet below Ash F or about 45–50 feet above the No. 3 White Ash, 20–30 feet above the uncataloged F:AM specimen, and 155 feet below the No 4 White Ash. Based on its diminutive P1–M3 length and geologic age, the specimen is probably the same small-bodied subspecies of *B. laticeps* as that found in the Green Hills Division at Camp Quarry (but not Oreodont Quarry), following Lander (1977, 1998), but probably younger than any record of *Brachycrus* from the Olcott Formation in northwestern Nebraska (Figure 3, Table 1). Therefore and contrary to Lander (1977, 1998), *B. r. riograndensis* is resurrected herein for those two occurrences and subsumed under *B. laticeps* as the second small-bodied subspecies of that species and the last record of the genus. The P1–M3 length of another uncataloged F:AM specimen, this one presumably also from between the No. 3 White Ash and Ash F, is just above the observed range of that parameter for the Camp Quarry sample and, along with the length for F:AM 72326, closely brackets that observed range (Figure 3, Table 1). Consequently, the latter uncataloged F:AM specimen is regarded as a topotypic specimen of *B. laticeps riograndensis*.

Lander (1977, 1998) assigned a third uncataloged F:AM specimen, that one representing a large-bodied individual of *Brachycrus* from an unspecified level in the Tesuque Formation of the East Cuyamunque locality, to *B. laticeps laticeps*. However, the last specimen, presumably from the Nambé Member or the lower part of the Skull Ridge Member below the No. 3 White Ash, might instead be referable to *B. laticeps altiramus* or (Figure 3, Table 1) the same unnamed large-bodied subspecies of *B. laticeps* as the one from Sunset Quarry in the Green Hills Division.

Split Rock Formation, Wyoming

Three consecutive, comparatively primitive, but progressively more-derived and larger-bodied species of *Brachycrus* (very small-bodied *B. rusticus*, medium-body-sized *B. vughani*, and large-bodied *B. sweetwaterensis*) were described from the Upper Porous Sandstone Sequence of the Split Rock Formation in central Wyoming by Schultz and Falkenbach (1940) (Figures 1–3, Table 1). Those species are members of the Split Rock Fauna or Local Fauna (Munthe 1979, Tedford et al. 2004). All three species are represented by remains from Exposure 2A (Schultz and Falkenbach 1940, Munthe 1979). In stratigraphic succession, Exposure 2A comprises the First, Second, and Third Benches (= UCMP localities V69192, V69191, and V69190, respectively) (Munthe 1979). Additional examples of *B. vughani* and *B. sweetwaterensis* are recorded from Exposures 1, 1A, and 2B (Schultz and Falkenbach 1940, Munthe 1979). With the exception of any specimen from UCMP locality V77144, examples of *Brachycrus* were recovered from 98–292 feet below the top of the Split Rock Formation (Munthe 1979). UCMP locality V77144 lies roughly 440–480 feet below the top of the formation. However, contrary to Munthe (1979), no specimen of *Brachycrus* or any other large-bodied land mammal taxon is recorded from that locality, a microvertebrate fossil site, in the UCMP online database.

Brachycrus rusticus represents the earliest, most primitive, and smallest-bodied species of the genus (Figure 3, Table 1). The ventral surface of the tympanic bulla is decidedly flattened or even slightly basined in CM 13592 and UW 3163 and is unlike those of all later and more-derived species of *Brachycrus* (see above). UW 3163 (figured by Hager 1970, fig. 44-2) is the smallest individual of the genus on the basis of its P1–M3 length and is from about 10 feet above the base of the Second Bench (Figure 3, Table 1; J. Munthe personal communication). The p2–m3 length (112 mm) of a mandible (UCM 29917) from the underlying First Bench P.O. McGrew personal communication to J. Munthe suggests an individual similar in size to, or slightly larger than the holotypic specimen (USNM 145) and CM 13592, but one clearly larger than that represented by UW 3163. Presumably, therefore, one or both of CM 13592 and USNM 145 are from the First Bench (Figure 3, Table 1) or the bottom of the overlying Second Bench.

The holotypic (F:AM 34492) and four measured F:AM topotypic specimens of *Brachycrus vughani* are from Exposure 2A (Schultz and Falkenbach 1940), as are two referred specimens (KUVV 16481, UCMP 162477). The P1–M3 lengths of the latter two specimens are immediately below the bottom of the observed range of that parameter for the five F:AM specimens (Figure 3, Table 1). KUVV 16481 is from a few feet above the base of the Third Bench (C.C. Black personal communication to J. Munthe). Consequently, UCMP 62477 and the F:AM specimens are most likely from about the same level (J. Munthe personal communication) and, correspondingly, KUVV 16481

and UCMP 62477 are probably topotypic specimens of *B. vaughani* (Figure 3, Table 1). UCMP 62477 is recorded as having been collected from the First Bench at UCMP locality V69192 in 1980. However, that specimen was not collected by UCMP personnel, who (J. and K. Munthe) last collected *Brachycrus* material from the First Bench in 1972. Moreover, the P1–M3 length of UCMP 62477 is much greater than that for any specimen of *B. rusticus* (Figure 3, Table 1). Furthermore, the tympanic bulla of that specimen is somewhat inflated, in contrast to those of *B. rusticus rusticus* from the bottom of the Second Bench and perhaps the First Bench (see above), and essentially identical morphologically to those of other specimens of *B. vaughani*. It is probable that the collector of UCMP 62477 inverted the locality terminology and misidentified the Third Bench at the top of the sequence as the First Bench. On the other hand, the composite observed range of the P1–M3 lengths for the F:AM and UCMP referred specimens of *B. vaughani* from Exposures 1A and 2B (= UCMP locality 77149) is almost entirely below that for the type and topotypic specimens of *B. vaughani vaughani* from Exposure 2A (Figure 3, Table 1). Therefore, the samples from Exposures 1A and 2B are presumed in this report to represent an unnamed earlier and smaller-bodied subspecies of *B. vaughani*.

Schultz and Falkenbach (1940) recorded both *B. rusticus* and *B. vaughani* from Exposure 2A, although noting that the referred F:AM specimens of *B. rusticus* apparently came from a lower stratigraphic level than those referred to in this report as *B. vaughani vaughani*. However, the P1–3 length for one of the *B. rusticus* referred specimens (F:AM 36105) falls midway between the observed ranges of that parameter for the smaller-bodied sample comprising the type and presumed topotypic specimens of the species all presumed to be from the base of the Second Bench and perhaps the First Bench on one hand and the sample representing the smaller-bodied subspecies of *B. vaughani* from Exposure 2B on the other (Figure 3, Table 1). Unfortunately, the taxonomically diagnostic tympanic bullae of F:AM 36105 are not preserved. Although KUVV 16476 is from a few feet above the base of the Third Bench (C.C. Black personal communication to J. Munthe), its P1–M3 length is substantially less than that for the type and topotypic specimens of *B. vaughani vaughani*, including the other specimen (KUVV 16481) from the bottom of the Third Bench, but only slightly less than that for F:AM 36105 (Figure 3, Table 1). On the other hand, the tympanic bulla of KUVV 16476 is relatively tall and inflated rather than ventrally flattened as in *B. rusticus* and resemble those of *B. vaughani*. This information suggests that F:AM 36105 is from the same stratigraphic level as KUVV 16481 and the type and topotypic specimens of *B. vaughani* from Exposure 2A, and, therefore, might represent the same comparatively small-bodied taxon as KUVV 16481 (but not *B. rusticus*) (Figure 3, Table 1). For those reasons, the two specimens are considered tentatively herein to represent a previously

unrecognized and short-lived lineage that arose from the smaller-bodied subspecies of *B. vaughani* and was characterized by its substantially smaller body size relative to contemporary *Brachycrus* (i.e., *B. v. vaughani*). If this conclusion is correct, then the two specimens should be assigned to a new genus and species.

A referred specimen of *Brachycrus sweetwaterensis* (UCMP 163023) from Exposure 2A at UCMP locality V69190 was collected at the top of the Third Bench (Munthe 1979, Lander 2011, J. Munthe personal communication). The P1–M3 length of UCMP 163023 is a bit below the observed range of that parameter for the type and topotypic specimens of *B. sweetwaterensis* from Exposure 1 (Figure 3, Table 1). Consequently, UCMP 163023 is considered in this report to represent an earlier and smaller-bodied subspecies of *B. sweetwaterensis* than the type and topotypic specimens of *B. sweetwaterensis sweetwaterensis* from Exposure 1. *Brachycrus sweetwaterensis* was regarded as ancestral to *B. laticeps wilsoni* from the Lower Member of the Sheep Creek Formation in northwestern Nebraska, based on its somewhat more primitive facial and basicranial anatomies (Munthe and Lander 1973, Lander 1977, 1985, 2011, Munthe 1979, Munthe and Coombs 1979), as described in detail by Lander (1977, 1985) and Kelly and Lander (1988b) (see above). Therefore and contrary to Munthe (1979), the Split Rock Fauna is not a correlative of the Sheep Creek Fauna. Consequently, Lander (1977, 1985, 2011), Munthe and Coombs (1979), and Kelly and Lander (1988b) regarded the Split Rock Fauna or Local Fauna as middle rather than late Hemingfordian in age, an age assignment at variance with that of Tedford et al. (2004) and Litter et al. (2008) (Figure 3). Similarly and in opposition to Litter et al. (2008), the uppermost Split Rock Local Fauna from the top of the Third Bench at UCMP locality V69190 is clearly not early Barstovian in age (Lander 2011). The much more primitive cranial anatomy of *B. sweetwaterensis* compared with that of early late Hemingfordian *B. laticeps wilsoni* indicates that the Split Rock Fauna is substantially older than the Sheep Creek Fauna (Figure 2).

The local stratigraphic range of *B. rusticus* brackets the Split Rock Tuff, which is exposed at the base of the Second Bench or UCMP locality V69191 and has been determined to be 17.65 Ma (recalculated from 17.4 Ma) in age on the basis of Ar/Ar radiometric dating analysis (Figure 3; Munthe 1979, Izett and Obradovich 2001, Litter et al. 2008, Lander 2011). The tuff, UCMP locality V69191, and the underlying First Bench (= UCMP locality V69192) lie in a reversed magnetozone, with the succeeding normal magnetozone occurring higher on the Second Bench (still UCMP locality V69191) and at the base of the Third Bench or UCMP locality V69190, and the following reversed magnetozone present still higher on the Third Bench (still UCMP locality V69190) (Litter et al. 2008). Litter et al. (2008) assigned the magnetozones to Chron C5Cr, C5Cn, and C5Br, respectively. However and based on the recalculated age of the Split Rock Tuff, Lander (2011)

recalibrated the magnetostratigraphic record for the Split Rock Formation at Exposure 2A, reassigning the magnetozones to Chron C5Dr.1r, C5Dn, and C5Cr, respectively (Figure 3). The beginning of Chron C5Dr.1r is 17.717 Ma in age, whereas the end of Chron C5Cr is 16.721 Ma old (Ogg 2012, Helgen et al. 2012). Therefore, the lowest local occurrence of *B. rusticus* at the First Bench, the earliest record of the genus, and, correspondingly, the boundary between the early and middle Hemingfordian NALMA are between 17.717 and 17.650 Ma old, whereas the biochron of *Brachycrus* in the Split Rock Local Fauna at Exposure 2A is 17.717–16.721 Ma in age (Figure 3). The late early Hemingfordian NALMA is characterized partly by the last occurrence of *Merycochoerus* (i.e., *M. proprius*) in the upper part of the Runningwater Formation in northwestern Nebraska (Lander 1985, 2011, Lander and Lindsay 2011). Moreover, the Split Rock Local Fauna and probably *Brachycrus sweetwaterensis sweetwaterensis* from Exposure 1 are substantially older than the early late Hemingfordian Lower Sheep Creek Local Fauna and *B. laticeps wilsoni* from the Lower Member of the Sheep Creek Fauna in Nebraska, as corroborated by the much more primitive cranial anatomy of *B. sweetwaterensis* (Figures 2–3).

The primitive comparatively small-bodied example of *Brachycrus* (F:AM 95553) recorded from the Red Valley Member of the Box Butte Formation at Dry Creek Prospect A in northwestern Nebraska by Galusha (1975) and Munthe (1979) was regarded as assignable to *B. rusticus* or *B. vaughani* by Lander (1985, 1998, 2011) and Kelly and Lander (1988b). Contrary to Galusha (1975), F:AM 95553 does not represent an individual smaller than *B. rusticus* (i.e., F:AM 35106) from the Split Rock Formation. For example, the P2–M2 length of F:AM 95553 (96 mm) is the same as that for a topotypic specimen (F:AM 36101) of *B. vaughani vaughani* from the Split Rock Formation, but is actually less than that (98 mm) for the specimen (F:AM 35106) assigned questionably above to an unnamed small-bodied genus that is closely related to *B. vaughani*. Therefore, the Box Butte Fauna from the Red Valley Member is considered herein to be a correlative of the Split Rock Fauna and middle (not late) Hemingfordian in age, following Munthe (1979, 1988), Munthe and Coombs (1979), Lander (1985), and Kelly and Lander (1988b).

The sample of the canid *Tomarctus* from Ginn Quarry in the undifferentiated Hemingford Group of northwestern Nebraska is intermediate in its stage of evolution between those of the same genus from the Red Valley Member of the Box Butte Formation and the Lower Member of the Sheep Creek Formation (Galusha 1975). The mean P1–M3 length of the *Brachycrus* sample from Ginn Quarry is similar to that for *B. vaughani vaughani* from the Split Rock Formation (Figure 3, Table 1). Contrary to Lander (1977, 1985, 1998) and Kelly and Lander (1988b), the Ginn Quarry sample is too small bodied for that sample to be assignable to *B. sweetwaterensis* and probably too old to be referable to *B. laticeps*. Consequently, the Ginn Quarry sample is assigned in this

report to *B. vaughani vaughani*, whereas the Ginn Quarry assemblage, following Lander (1977), is considered to be middle Hemingfordian in age rather than early late Hemingfordian, an assignment counter to that of Lander (1985) and Kelly and Lander (1988b).

Sixmile Creek Formation, Montana

Brachycrus laticeps laticeps is considered in this report to be the earliest of three successive large-bodied subspecies of *B. laticeps* because the holotypic specimen of the species (CM 796), the holotypic and topotypic specimens of *Ticholeptus smithi* (CM 766 and 845 [= *Poatrephes paludicola* holotypic specimen], respectively), and a referred example of *Merychius relictus* (CM 8893) were all found in the Flint Creek Beds (= Sixmile Creek Formation) east of New Chicago in Granite County, southwestern Montana (Figure 1). The observed range of P1–M3 lengths for the type and topotypic specimens of *B. laticeps* (134–141 mm) is nearly bracketed by that for the sample from the Middle Member of the Sheep Creek Formation at Hilltop and Thomson Quarries in northwestern Nebraska (Figure 3, Table 1), the latter sample representing the earliest record of large body size in *B. laticeps* from the central Great Plains. The observed range of P1–M3 lengths for *T. smithi* (includes *Poatrephes paludicola*, contrary to Lander 1977, 1998, Kelly and Lander 1988) (88–92 mm) is below the P1–M3 length for the holotypic specimen of *Ticholeptus zygomatiscus* (AMNH 8112, 96 mm) from the Deep River Beds (= Sixmile Creek Formation) in Lewis and Clark County, southwestern Montana, and is mostly below the observed range of that parameter (92–99 mm) for the early Barstovian *T. zygomatiscus* sample from the Olcott Formation at Jenkins Quarry in northwestern Nebraska. In contrast, the P1–M3 length for CM 8893 (79 mm) is only slightly above the observed ranges of the parameter (72–77 and 74–77 mm) for the samples of *M. relictus* from the Lower Member of the Sheep Creek at Long Quarry and the Olcott Formation at Humbug Quarry. Contrary to Kelly and Lander (1988b) and Lander (1998), *T. smithi* is not regarded as a junior synonym of *Merychius elegans* because it was probably a contemporary of *M. relictus*, which was much smaller bodied. Moreover, the relative length of the rostral premaxillary suture of CM 8893 is similar to an example of *M. relictus* (F:AM 34319) from the Lower Member of the underlying Sheep Creek Formation at Long Quarry.

Summary

As illustrated in Figure 3 and recorded in Table 1, the *Brachycrus* biochron comprised two lengthy cycles that recorded changes in mean upper cheek tooth-row or P1–M3 length, a proxy for average adult body size. Each cycle began with an increase in P1–M3 length and ended with a decrease (Figure 3). In chronologic order and following a slight (perhaps about 5%) reduction in mean cheek tooth-row length in *B. rusticus* during the early middle

Hemingfordian NALMA and about 17.65 Ma ago, the first cycle was characterized by (1) a dramatic (38.8%) increase in P1–M3 length that began with *B. rusticus* about 17.4 Ma ago (recalculated as 17.65 Ma) and peaked with *B. sweetwaterensis* in the latest middle Hemingfordian NALMA, (2) a slight (4.1%) decrease in length from *B. sweetwaterensis* to early late Hemingfordian *B. laticeps wilsoni*, (3) three minor subcycles, in which P1–M3 length in *B. laticeps* diminished moderately and then peaked a comparable amount from the early late Hemingfordian to the late early Barstovian NALMAs, with changes in mean P1–M3 length ranging from about 5.3–10.2%, and (4) a substantial (16.5%) reduction in length from the latest early to the earliest middle Barstovian NALMA and ending with the smaller-bodied variety of *B. laticeps siouense* (Figure 3). The first cycle spanned roughly 1.52–1.85 Ma. Such shifts were less pronounced in the subsequent or second cycle, which was characterized by (1) a slight (5.6%) increase in mean cheek tooth-row length in *B. l. siouense* during the early middle Barstovian NALMA, (2) a lesser (only 2.5%) decrease and a subsequent but comparable (3.3%) increase during the middle middle Barstovian (an overall increase of just 6.0–6.4% for *B. l. siouense* from the early middle to middle middle Barstovian), and (3) a final decrease of 5.9–8.7% in P1–M3 length that ended with *B. laticeps riograndensis* and the apparent extinction of the genus during the late middle Barstovian or a bit over 15.3 Ma ago (recalculated as 15.52 Ma) (Figure 3).

Those data indicate that body size in *Brachycrus* peaked a total of six times, (1) once during the middle Hemingfordian NALMA with large-bodied *B. sweetwaterensis* after a dramatic increase in mean P1–M3 length, (2) three times with large-bodied *B. laticeps* (once during middle late Hemingfordian NALMA and twice during early Barstovian) following moderate increases in P1–M3 length, and (3) twice in the medium-body-sized, larger-bodied variety of *B. l. siouense* during the early middle and middle middle Barstovian and subsequent to decreases in P1–M3 length (Figure 3). On average, *Brachycrus* was much larger bodied during the middle Hemingfordian to the late early Barstovian NALMAs than during the middle Barstovian. P1–M3 lengths for individual specimens and mean P1–M3 lengths for samples of *B. sweetwaterensis* and medium-body-sized to large-bodied *B. laticeps* are very nearly always greater than 125 mm, whereas the mean lengths for that parameter are very nearly always less than 125 mm, as are most individual P1–M3 lengths (Figure 3, Table 1).

Relations of the *Brachycrus* Curve, the Haws-Berkeley Effect, and the Middle Miocene Climatic Optimum

The *Brachycrus* biochron spanned the earliest middle Hemingfordian to late middle Barstovian NALMAs and lasted from about 17.72–15.30 Ma ago, or about 2.42

Ma (Figure 3). Fluctuating average adult body size in that genus through time, as recorded by the *Brachycrus* Curve (Figure 3) and referred to herein as the Haws-Berkeley Effect, probably reflected shifts in its food supply. Four pronounced and two lesser peaks in body size are recorded by the *Brachycrus* Curve (Figure 3). Following an initial decrease in body size, two curves of increasing-decreasing body size are documented by the *Brachycrus* Curve. Smaller body size likely corresponded to a reduction in forage as a result of a more seasonal climate characterized by summer drought, whereas larger body size probably accompanied an increased food supply as climate moderated (see above). Although such changes with regard to *Brachycrus* had not been tied previously to any temperature-related global climatic event, there now appears to have been substantial overlap and perhaps even virtual coincidence between the time period covered by the MMCO on one hand and the two cycles of changing body size recorded by the *Brachycrus* Curve or possibly the entire *Brachycrus* biochron, on the other.

Like the *Brachycrus* biochron, the MMCO also spanned the early middle Hemingfordian to late middle Barstovian NALMAs and the boundary between the early and middle Miocene Epoch. That boundary is 15.97 Ma in age (Lourens et al. 2004). Based largely on palynological and geochemical data, the MMCO was a period of pronounced global warming, that (1) began approximately 17.6 Ma ago, (2) climaxed at 17.2, 16.4 (MMCO Peak 1), 15.7 (MMCO Peak 2), and 15.5 Ma, and (3) ended about 15.4 Ma ago (Warny et al. 2009, Foersterling 2011, Browning 2012, Feakins et al. 2012). MMCO Peaks 1 and 2 were separated by a short-term excursion (Foersterling 2008) informally termed in this report the MMCO Trough, during which global temperatures dipped slightly to a low point approximately 16.2 Ma ago (Foersterling 2011). The peaks and troughs in the curve characterizing the MMCO appear to coincide temporally with some of those observed in the *Brachycrus* Curve, which is based entirely on mean upper cheek tooth-row or P1–M3 lengths and calibrated by radiometric and magnetostratigraphic data (Figure 3). As illustrated in Figure 3, (1) the beginning of the MMCO 17.6 Ma ago appears to coincide with the onset of increasing adult body size in *Brachycrus*, as documented in early middle Hemingfordian *B. rusticus rusticus*? at the bottom of the Second Bench and immediately above the Split Rock Tuff in the Split Rock Formation of central Wyoming, (2) an unnamed or undesigned peak in global warming 17.2 Ma before the present (BP) might correspond to the first peak in body size for the genus, as observed in latest middle Hemingfordian *B. sweetwaterensis sweetwaterensis* in the Split Rock Formation at Exposure 1, (3) MMCO Peak 1, which occurred 16.5–16.4 Ma ago, seems to be correlated with the second peak in body size, as represented by middle late Hemingfordian *B. laticeps laticeps*? in the Middle Member of the Sheep Creek Formation of northwestern Nebraska, (4) the MMCO Trough at 16.2 Ma BP perhaps is related to

the third reduction in body size for the genus and the second for *B. laticeps*, as documented in the unnamed, latest Hemingfordian, medium-body-sized subspecies from the Upper West Dry Canyon Local Fauna in the Caliente Formation of southern California, (5) MMCO Peak 2, which occurred 16.7 Ma ago, presumably is correlated with either (5a) the fourth peak in body size for the genus and the third for *B. laticeps*, as documented in the unnamed, late early Barstovian, large-bodied subspecies from the Barstow Formation at Sunset Quarry in southern California, or, more likely, (5b) the fifth peak in body size for the genus and the first for the early middle Barstovian, larger-bodied variety of *B. laticeps siouense* from the Olcott Formation at Humbug Quarry in northwestern Nebraska, and (6) a second unnamed peak in global warming 15.5 Ma BP might correspond to the sixth peak in body size for the genus and the second for the middle middle Barstovian, larger-bodied variety of *B. l. siouense* from Echo Quarry Paleovalley Fill of the Olcott Formation at Mill Quarry, whereas (7) the end of the MMCO 15.4 Ma is probably related to the seventh or final reduction in body size for the genus and its subsequent extinction, and the sixth such decrease for *B. laticeps*, as represented by late middle Barstovian *B. laticeps riograndensis* from the Barstow Formation at Camp Quarry and 25 feet below Ash F in the Skull Ridge Member of the Tesuque Formation in north-central New Mexico. If these correlations are correct, then periods of smaller body size and comparatively seasonal climate might also have been intervals of cooler climate that accompanied Antarctic glacial advances, whereas periods of larger body size and relatively uniform climate perhaps were also intervals of warmer climate and glacial melting (Figure 3).

Acknowledgments

J. Munthe supplied the author with unpublished stratigraphic data on the KUVF, UCM, UCMP, and UW specimens of *Brachycrus* from the Split Rock Formation in the late 1970s, whereas T.J. Meehan and S. Tomiya provided measurements and digital images of some of the KUVF and UCMP specimens, respectively, from the same unit. R.L. Evander and R. O'Leary sent stratigraphic data and measurements for the F:AM specimens from the Barstow Formation. The illustrations of the F:AM *Brachycrus* skulls in Figure 2 were reproduced with the permission of T. Fischelis, the daughter of the late C.B. Schultz. T.S. Kelly and R.E. Reynolds reviewed early drafts of this paper and offered constructive criticisms.

Literature cited

- Barghoorn, S. 1981. Magnetic-polarity stratigraphy of the Miocene type Tesuque Formation, Santa Fe Group, in the Española Valley, New Mexico, *Bulletin of the Geological Society of America* 92 (12):1027–1041.
- Browning, E. 2012. Calcareous nannofossils records of Miocene sea level at the Marion Plateau (northeastern Australia); and Pliocene–formation of cold water carbonate mounds (northeastern Atlantic continental margin. University of Massachusetts, Amherst, unpublished Ph.D. dissertation.
- Cole, J.M., E.T. Rasbury, G.N. Hanson, I.P. Montanez, and V.A. Pedone. 2005. Using U-Pb ages of Miocene tufa for correlation in a terrestrial succession, Barstow Formation, California. *Bulletin of the Geological Society of America* 117(3–4):276–287.
- Cook, H.J., and M.C. Cook. 1933. Faunal lists of the Tertiary Vertebrata of Nebraska and adjacent areas. *Nebraska Geological Survey Paper* 5:9–58.
- Douglass, E. 1900. New species of *Merycochoerus* in Montana. Part 1. *The American Journal of Science* 4/10(60[41]):428–438.
- Evander, R.L. 1986. Formal redefinition of the Hemingfordian-Barstovian Land Mammal Age boundary. *Journal of Vertebrate Paleontology* 6(4):374–381.
- Feakins, S.J., S. Warny, and J.-E. Lee. 2012. Hydrologic cycling over Antarctica during the middle Miocene warming. *Nature Geoscience* 5:557–560.
- Foersterling, L.R. 2008. Antarctic plant and phytoplankton response to the first phase of the Mid Miocene Climatic Optimum at South McMurdo Sound. Louisiana State University and Agricultural and Mechanical College, unpublished M.S. thesis.
- Galusha, T. 1975. Stratigraphy of the Box Butte Formation, Nebraska. *Bulletin of the American Museum of Natural History Bulletin* 156(1):7–68.
- Galusha, T., and J.C. Blick. 1971. Stratigraphy of the Santa Fe Group, New Mexico. *Bulletin of the American Museum of Natural History Bulletin* 144(1):7–127.
- Galusha, T., M.F. Skinner, B.E. Taylor, and R.H. Tedford. 1966. Preliminary analysis of the lithostratigraphy and biostratigraphy of the Barstow Formation in the Mud Hills, San Bernardino County, California. Society of Vertebrate Paleontology 1966 Annual Meeting Field Trip and Guidebook, Riverside, California.
- Hager, M.W. 1970. Fossils of Wyoming. *Wyoming Geological Survey Bulletin* 54:1–51.
- Hilgen, F.J., L.J. Lourens, and J.A. Van Dam. 2012. The Neogene Period. Pp. 923–978. In Gradstein, F.M., J.G. Ogg, M.D. Schmitz, and G.M. Ogg, editors. *The Geologic Time Scale 2012*. Elsevier, Oxford, UK.
- Izett, G. A., and J. D. Obradovich. 2001. ⁴⁰Ar/³⁹Ar ages of Miocene tuffs in basin fill deposits (Santa Fe Group, New Mexico, and Troublesome Formation, Colorado) of the Rio Grande system. *Mountain Geologist* 38(2):77–86.
- Kelly, T.S., and E.B. Lander. 1988a. Correlation of Hemingfordian and Barstovian land mammal assemblages, lower part of Caliente Formation, Cuyama Valley area, California. *American Association of Petroleum Geologists Bulletin* 72(3):384.
- Kelly, T.S., and E.B. Lander. 1988b. Biostratigraphy and correlation of Hemingfordian and Barstovian land mammal assemblages, Caliente Formation, Cuyama Valley area, California. In W.J.M. Bazeley, editor. *Tertiary Tectonics and Sedimentation in the Cuyama Basin, San Luis Obispo, Santa Barbara, and Ventura Counties, California. Society of Economic Paleontologists and Mineralogists Pacific Section* 59:1–19.
- Kelly, T.S., and E.B. Lander. 1992. Miocene land mammal faunas from the Caliente Formation, Cuyama Valley, California. *PaleoBios* 14(1):3–8.
- Lander, E.B. 1977. A review of the Oreodonta (Mammalia, Artiodactyla), Parts I, II and III. University of California, Berkeley, unpublished Ph.D. dissertation.

- Lander, E.B. 1984. Biochronologic implications of climatically induced changes in mammalian adult body through time. Page 47. *In* Society of Economic Paleontologists and Mineralogists Abstracts, First Annual Midyear Meeting.
- Lander, E.B. 1985. Early and middle Miocene continental vertebrate assemblages, central Mojave Desert, San Bernardino County, California. Pages 127–144. *In* R.E. Reynolds, compiler. Geological Investigations Along Interstate 15, Cajon Pass to Manix Lake. San Bernardino County Museum.
- Lander, E.B. 1988. Faunal events in the North American continental Tertiary mammalian herbivore record and their implications regarding the causes of extinction and diminishing average adult body size in late Quaternary mammalian herbivores. *In* J. Reynolds, compiler. Quaternary history of the Mojave Desert, Proceedings and Abstracts of the Mojave Desert Quaternary Research Center Second Annual Symposium, San Bernardino County Museum, Redlands, California, June 25–26, 1988. *San Bernardino County Museum Association Quarterly* 35(3&4):36–38.
- Lander, E.B. 1989. Climatically induced fluctuations in average adult body size through successive generations of Oligocene oreodonts (Mammalia, Artiodactyla, Oreodonta, Agriocheridae and Oreodontidae). *Geological Society of America Abstracts with Programs* 21(6):A115.
- Lander, E.B. 1998. Oreodontoidea. Pages 402–425. *In* C.M. Janis, K.M. Scott, and L.L. Jacobs, editors. Evolution of Tertiary Mammals of North America, Volume 1: Terrestrial Carnivores, Ungulates, and Ungulate-like Mammals. Cambridge University Press, United Kingdom.
- Lander, E.B.. 2003. Stratigraphically documented fluctuations in average adult body size through successive generations of *Brachycrus laticeps* (Mammalia, Artiodactyla, Oreodontidae) and a reevaluation of the Hemingfordian-Barstovian North American Land Mammal Age “boundary” in California and Nebraska. Western Association of Vertebrate Paleontologists Annual Meeting Abstracts and Program. Mojave River Valley Museum.
- Lander, E.B. 2005. Revised correlation and age assignments of fossil land mammal assemblages of late Hemingfordian to earliest Hemphillian (early Middle to early Late Miocene) age in California, Nebraska, and Texas, based on occurrences of ticholeptine oreodonts (Mammalia, Artiodactyla, Oreodontidae, Ticholeptinae) and other land mammal taxa. *Bulletin of the Southern California Academy of Sciences* 104(2 supplement):29–30.
- Lander, E.B. 2008. Early Clarendonian (late middle Miocene) fossil land mammal assemblages from the Lake Mathews Formation, Riverside County, southern California; and a preliminary review of *Merychys* (Mammalia, Artiodactyla, Oreodontidae). *In* X. Wang and L.G. Barnes, editors. Geology and Vertebrate Paleontology of Western and Southern North America. *Natural History Museum of Los Angeles County Science Series* 41.181–212.
- Lander, E.B., compiler. 2011. Western Association of Vertebrate Paleontologists 2011 annual meeting field trip volume and guidebook—Stratigraphy, biostratigraphy, biochronology, geochronology, magnetostratigraphy, and plate tectonic history of the early middle Eocene to late early Miocene Sespe, Vaqueros, and Lower Topanga Formation, east-central Santa Monica Mountains, Los Angeles County, southern California. Natural History Museum of Los Angeles County Department of Vertebrate Paleontology and Paleo Environmental Associates, Inc.
- Lander, E.B., and C.B. Hanson. 2006. *Agriocherus matthewi crassus* (Artiodactyla, Agriocheridae) of the late middle Eocene Hancock Mammal Quarry Local Fauna, Clarno Formation, John Day Basin, north-central Oregon. *PaleoBios* 26(3):19–34.
- Lander, E.B., and T.S. Kelly. 1989. Reassessment of the age and correlation of the type Barstow Formation in the Rainbow Basin area of southern California, based on changes in average adult body size through time in *Brachycrus laticeps* (Mammalia, Artiodactyla, Oreodontidae). *In* J. Reynolds, compiler. Abstracts of papers presented at the Mojave Desert Quaternary Research Center Third Annual Symposium. *San Bernardino County Museum Association Quarterly* 36(2):60–61.
- Lander, E.B., and E.H. Lindsay. 2011. *Merychys calaminthus* (Mammalia, Artiodactyla, Oreodontidae) of probable early late Arikareean (late Oligocene to late early Miocene) age from the lower part of the Chalk Canyon Formation, Maricopa and Yavapai counties, central Arizona. *Journal of Vertebrate Paleontology* 31(1): 215–226.
- Liter, M.R., D.R. Prothero, and S.S.B. Hopkins. 2008. Magnetic stratigraphy of the late Hemingfordian–Barstovian (lower to middle Miocene) Split Rock Formation, central Wyoming. *In* S.G. Lucas, G.S. Morgan, J.A. Spielmann, and D.R. Prothero, editors. Neogene mammals. *New Mexico Museum of Natural History & Science Bulletin* 44:25–30.
- Lourens, L.J., F.J. Hilgren, N.J. Shackleton, J. Laskar, and D.S. Wilson. 2004. The Neogene Period. Pages 409–440. *In* F.M. Gradstein, J.G. Ogg, and A.G. Smith, editors. A geologic time scale 2004. Cambridge University Press, Cambridge, United Kingdom.
- Lugn, A.L. 1939. Classification of the Tertiary System in Nebraska. *Bulletin of the Geological Society of America* 50(8):1245–1276.
- Matthew, W.D. 1924. Third contribution to the Snake Creek Fauna. *Bulletin of the American Museum of Natural History* 50(2):59–210.
- MacFadden, B.J., C.C. Swisher III, N.D. Opdyke, and M.O. Woodburne. 1990. Paleomagnetism, geochronology, and possible tectonic rotation of the middle Miocene Barstow Formation, Mojave Desert, southern California. *Bulletin of the Geological Society of America* 102(4):478–493.
- McKenna, M. C. 1965. Stratigraphic nomenclature of the Miocene Hemingford Group, Nebraska. *American Museum Novitates* 2228:1–21.
- Morgan, G.S., E.B. Lander, C. Cikoski, R.M. Chamberlin, D.W. Love, and L. Peters. 2009. The oreodont *Merychys major major* (Mammalia: Artiodactyla: Oreodontidae) from the Miocene Popotosa Formation, Bosque del Apache National Wildlife Refuge, Socorro County, central New Mexico. *New Mexico Geology* 31:91–103.
- Munthe, J. 1979. Summary of Miocene vertebrate fossils of the Granite Mountains Basin, central Wyoming. *University of Wyoming Contributions to Geology* 18:33–46.
- Munthe, J. 1988. Miocene mammals of the Split Rock area, Granite Mountains basin, central Wyoming. *University of California Publications in Geological Sciences* 126:1–136.
- Munthe, J., and M.C. Coombs. 1979. Miocene dome-skulled chalicotheres (Mammalia, Perissodactyla) from the western United States: A preliminary discussion of a bizarre structure. *Journal of Paleontology* 53(1):77–91.

- Munthe, J., and E.B. Lander. 1973. A reevaluation of the age of the Split rock vertebrate fauna, Wyoming. *Geological Society of America Abstracts with Programs* 5(6):497.
- Naeser, C.W., G.A. Izett, and J.D. Obradovich. 1980. Fission-track and K-Ar ages of natural glasses. *United States Geological Survey Bulletin* 1489:1–31.
- Ogg, J.G. 2012. Geomagnetic polarity time scale. Pp. 85–113. In Gradstein, F.M., J.G. Ogg, M.D. Schmitz, and G.M. Ogg, editors. *The Geologic Time Scale 2012*. Elsevier, Oxford, UK.
- Pagnac, D. 2009. Revised large mammal biostratigraphy and biochronology of the Barstow Formation (middle Miocene), California. *PaleoBios* 29(2):48–59.
- Perkins, M.E., and B.P. Nash. 2002. Explosive silicic volcanism of the Yellowstone hotspot: The ash fall tuff record. *Geological Society of America Bulletin* 114(3):367–381.
- Prothero, D.R., T.S. Kelly, K.R. McCardel, and E.L. Wilson. 2008. Magnetostratigraphy, biostratigraphy, and tectonic rotation of the Miocene Caliente Formation, Ventura County, California. In S.G. Lucas, G.S. Morgan, J.A. Spielmann, and D.R. Prothero, editors. *Neogene mammals. New Mexico Museum of Natural History & Science Bulletin* 44:255–272.
- Schultz, C.B., and C.H. Falkenbach. 1940. Merycochoerinae, a new subfamily of oreodonts. *Bulletin of the American Museum of Natural History* 77(5):213–306.
- Schultz, C.B., and C.H. Falkenbach. 1941. Ticholeptinae, a new subfamily of oreodonts. *Bulletin of the American Museum of Natural History* 79(1):1–105.
- Schultz, C.B., and C.H. Falkenbach. 1968. The phylogeny of the oreodonts, Parts 1 and 2. *Bulletin of the American Museum of Natural History* 139:1–498.
- Schultz, C.B., and T.M. Stout. 1961. Field conference on the Tertiary and Pleistocene of western Nebraska (Guide book for the Ninth Field Conference of the Society of Vertebrate Paleontology). *Special Publication of the University of Nebraska State Museum* 2:1–55.
- Skinner, M. F., S. M. Skinner, and R. J. Gooris. 1977. Stratigraphy and biostratigraphy of late Cenozoic deposits in central Sioux County, western Nebraska. *Bulletin of the American Museum of Natural History* 158:263–370.
- Stevens, M.S., and J.B. Stevens. 1996. Merycooidontinae and Miniocoherinae. Pp. 498–573 in D.R. Prothero and R.J. Emry, editors. *The Terrestrial Eocene–Oligocene Transition in North America*. Cambridge University Press, Cambridge, United Kingdom.
- Stevens, M. S., and J. B. Stevens. 2007. Family Merycooidontidae; Pages 157–168. In D. R. Prothero and S. E. Foss, editors. *The Evolution of Artiodactyls*. Johns Hopkins University Press, Baltimore, Maryland.
- Tedford, R.H., L.B. Albright III, A.D. Barnosky, I. Ferrusquía-Villafranca, R.M. Hunt Jr., J.E. Storer, C.C. Swisher III, M.R. Voorhies, S.D. Webb, and D.P. Whistler. 2004. Mammalian biochronology of the Arikareean through Hemphillian interval (late Oligocene through early Pliocene Epochs). Pages 169–231. In M.O. Woodburne, editor. *Late Cretaceous and Cenozoic mammals of North America: Biostratigraphy and geochronology*. Columbia University Press, New York, NY.
- Tedford, R.H., and S.F. Barghoorn. 1993. Neogene stratigraphy and mammalian biochronology of the Española basin, northern New Mexico. In S.G. Lucas and J. Zidek, editors. *Vertebrate Paleontology in New Mexico. New Mexico Museum of Natural History and Science Bulletin* 2:159–168.
- Tedford, R.H., T. Galusha, M.F. Skinner, B.E. Taylor, R.W. Fields, J.R. Macdonald, J.M. Rensberger, S.D. Webb, and D.P. Whistler. 1987. Faunal succession and biochronology of the Arikareean through Hemphillian interval (late Oligocene through earliest Pliocene Epochs) in North America. Pages 153–210. In M.O. Woodburne, editor. *Cenozoic Mammals of North America: Geochronology and Biostratigraphy*. University of California Press, Berkeley, CA.
- Warny, S., R.A. Askin, M.J. Hannah, B.A.R. Mohr, J.I. Raine, D.M. Harwood, F. Florindo, and SMS Science Team. 2009. Palynomorphs from a sediment core reveal a sudden remarkably warm Antarctica during the middle Miocene. *Geology* 37(10):955–958.
- Wilson, R.W. 1960. Early Miocene rodents and insectivores from northeastern Colorado. *University of Kansas Paleontological Contributions—Vertebrata* 7:1–131.
- WoldeGabriel, G., D.E. Broxton, and F.M. Byers Jr. 1996. Mineralogy and temporal relations of coexisting authigenic minerals in altered silicic tuffs and their utility as potential low-temperature dateable minerals. *Journal of Volcanology and Geothermal Research* 71:155–165.
- Wood, H.E., II, R.W. Chaney, J. Clark, E.H. Colbert, G.L. Jepsen, J.B. Reeside, and C. Stock. 1941. Nomenclature and correlation of the North American continental Tertiary. *Bulletin of the Geological Society of America* 52(1):1–48.
- Woodburne, M.O. 1969. Systematics, biogeography, and evolution of *Cynorca* and *Dyseohyus* (Tayassuidae). *Bulletin of the American Museum of Natural History* 141(2):273–355.
- Woodburne, M.O. 1991. The Mojave Desert Province. In M.O. Woodburne, R.E. Reynolds, and D.P. Whistler, editors. *Inland Southern California: The Last 70 Million Years—A Self-Guiding Tour of Major Paleontologic Localities from Temecula to Red Rock Canyon: Fossils, Structure, and Geologic History. San Bernardino County Museum Association Quarterly* 38(3–4):60–77.
- Woodburne, M.O. 1996. Precision and resolution in mammalian chronostratigraphy: Principles, practices, examples. *Journal of Vertebrate Paleontology* 16(3):531–555.
- Woodburne, M.O., S.T. Miller, and R.H. Tedford. 1982. Stratigraphy and geochronology of Miocene strata in the central Mojave Desert, California. Pages 47–64. In J.D. Cooper, compiler. *Geologic Excursions in the California Desert*. Geological Society of America, Cordilleran Section 78th Annual Meeting, April 19–21, 1982, Anaheim, California, Volume and Guidebook.
- Woodburne, M.O., and R.E. Reynolds. 2010. Mammalian litho- and biochronology of the Mojave Desert Province. Pages 124–147. In R.E. Reynolds and D.M. Miller, editors. *Overboard in the Mojave: 20 million Years of Lakes and Wetlands*. Desert Studies Consortium, California State University, Fullerton.
- Woodburne, M.O., and R.H. Tedford. 1982. Litho- and biostratigraphy of the Barstow Formation, Mojave Desert, California. Pages 65–76. In J.D. Cooper, compiler. *Geologic Excursions in the California Desert*. Geological Society of America, Cordilleran Section 78th Annual Meeting, April 19–21, 1982, Anaheim, California, Volume and Guidebook.
- Woodburne, M.O., R.H. Tedford, and C.C. Swisher. 1990. Lithostratigraphy, biostratigraphy, and geochronology of the Barstow Formation, Mojave Desert, southern California. *Bulletin of the Geological Society of America* 102(4):459–477.

Nonmarine gastropods from the Temblor and Barstow formations of California

Austin S. Plyley,¹ Don L. Lofgren,² and Andrew A. Farke²

¹ Webb Schools, Claremont, California 91711; ² Raymond M. Alf Museum of Paleontology, Claremont, California 91711

Introduction

The study of non-marine gastropods from the Temblor Formation of central California and the Barstow Formation of southern California (Figure 1) has developed in two distinct ways. Barstow Formation gastropods were first studied by Dwight Taylor over 60 years ago, while non-marine gastropods from the Temblor Formation have never been described. In the late 1940's, Taylor attended Webb School of California, a secondary school in Claremont with a unique paleontology program run by Raymond Alf (whose work was honored in 1967 with establishment of the Raymond Alf Museum of Paleontology on the Webb campus). While in high school Taylor developed a keen interest in the taxonomy and biogeography of mollusks and corresponded with scientists at the Museum of Comparative Zoology at Harvard University (Kabat and Johnson, 2008), in addition to joining the shell club sponsored by the Los Angeles County Museum (Taylor letter to Lofgren, 2000). Taylor went on fossil collecting trips to Barstow with Raymond Alf and found some bones, but also found fossil snails, and his "career was set" (Taylor letter to Lofgren, 2000). These fossils were the subject of a paper in Taylor's historical geology class at Pomona College (Taylor letter to Lofgren, 2000) and later were published as a USGS Professional Paper (Taylor 1954) while Taylor was in graduate school at the University of California at Berkeley (Kabat and Johnson 2008). Taylor's 1954 USGS publication remains the most comprehensive study of a Miocene terrestrial gastropod fauna from California where ten species from the Barstow Formation were described. These included four new taxa: *Lymnaea mohaveana*, *Menetus micromphalus*, *Craterarion pachystracon*, and *Helminthoglypta alfi* (Taylor 1954). Taylor went on to a distinguished career as a paleontologist and malacologist, publishing 65 papers and describing 132 taxa (Kabat and Johnson 2008).

Terrestrial gastropods from the Temblor Formation were first reported by Zaborsky (2004) based

on fossils recovered from a multi-taxa vertebrate bone bed (University of California Museum of Paleontology locality UCMP V99563) from the uppermost part of the Temblor Formation along Monocline Ridge north of Coalinga (Figure 1). The quarry has yielded over 1,200 fossils of terrestrial vertebrates including a diverse assemblage of mammals, birds, and reptiles (Zaborsky 2004; Kelly and Stewart 2008). The site was discovered by a paleontology mitigation crew during installation of a power line tower which was part of a major power transmission project. Matrix from the quarrying operation was retained for screen-washing with the expectation that it would yield small fossils.

Over the past two decades, crews from the Alf Museum, composed primarily of students from The Webb Schools, have collected hundreds of mollusks from the Barstow Formation and two of Taylor's original sites were located and resampled. Also, the quarry matrix from UCMP V99563 (equals RAM V200915) was transferred to the Raymond Alf Museum of Paleontology (RAM) where it was sieved through screens in 2009-2010. Course fraction of the screening yielded about 4,000 gastropods. The purpose of this study is to describe these fossils and compare them to the gastropods from the Barstow Formation reported by Taylor (1954) and collected by RAM crews.

Geologic and biostratigraphic setting

The Temblor Formation is a mostly marine unit known for its richness and diversity of fossils. Terrestrial mammals are rare and are known in abundance at only two sites in the upper part of the formation (Kelly and Stewart 2008). The first was found in the early 1900's along Domingine Creek north of Coalinga and was referred to as the "Merychippus Zone" (Merriam 1915; Bode 1935) or the North Coalinga Local Fauna (Tedford et al. 1987; 2004). At the "Merychippus Zone," vertebrate fossils, including an amazing number of isolated horse teeth, were quarried from a series of conglomerate lenses in the uppermost Temblor Formation, just below the Big Blue Formation (Bode 1935). Shark teeth were also plentiful (Bode 1935). Facies analysis of upper Temblor Formation strata along Domingine Creek suggests a barrier-beach depositional setting associated with a fluvial dominated tidal inlet (Bate 1985). The uppermost sand interval of the upper Temblor Formation, which includes the "Merychippus Zone," was interpreted to represent a littoral environment



Figure 1. Map of California, with location of the Barstow Formation (A) and Temblor Formation (B) noted.

near the mouth of a river (Merriam 1915; Bode 1935). The age of the “*Merychippus* Zone” or North Coalinga Local Fauna is Middle Miocene or early Barstovian, between 15-16 myo (Tedford et al. 2004).

The bone bed (UCMP V99563/RAM V200915) located on Monocline Ridge about ten miles north of Domengine Creek (“*Merychippus* Zone”) is within strata that represent a complex mélange of shallow marine to tidal-lagoonal deposits of the upper Temblor Formation (Bartow 1996). The site is mapped as a landslide deposit and strata are vertical due to slumping (Bartow 1996). The bone producing unit is a .5 meter thick conglomeratic sandstone, consisting of gray-light green sandstone with abundant pebble sized rip-ups of green mudstone. Complete carpals, tarsals, and phalanges of mammals are common, as are isolated horse teeth and gastropods. Unidentifiable fragments are also abundant as are partial mammalian limb elements preserving either a proximal or distal end. Well preserved dentigerous elements are present but are not common (Kelly and Stewart 2008). The bone producing unit represents a fluvial deposit of considerable energy where vertebrate bone, mollusks, and mudstone rip-ups underwent limited sorting and were deposited with sandy matrix adjacent to the Pacific Ocean. The age of RAM 200915 is about early to early late Barstovian or 14.8-15.8 myo, based on the combined geochronologic ranges of its horses and camels (Kelly and Stewart 2008).

In contrast to the Temblor Formation, the Barstow Formation is composed of entirely terrestrial strata deposited within an inland basin. This fossiliferous unit is composed of about 1,000 meters of fluvial and lacustrine sediments and water lain tuff beds (Diblee 1968; Woodburne et al. 1990). The Barstow Formation is divided into three members; in ascending stratigraphic order, Owl Conglomerate Member, unnamed middle member, and unnamed upper member (Woodburne et al. 1990). The Barstow Formation is designated as the type assemblage for the Barstovian North American Land Mammal Age (Wood et al. 1941), which is subdivided into the Early Barstovian and Late Barstovian (Tedford et al. 1987; Tedford et al. 2004; Pagnac 2009). All mollusks recovered from the Barstow Formation by RAM crews, except for one specimen, are from the upper member, which is late Barstovian, or about 13.4-14.8 myo (Woodburne et al. 1990). These fossils are found in fine grained strata that represent pond or floodplain deposits of low fluvial energy, in contrast to the mollusks from the Temblor Formation locality (RAM V200915).

Materials and methods

The specimens reported here from the Barstow Formation were collected by RAM crews from 1991 to 2011, except for about two dozen specimens of *Helminthoglypta alfi* collected prior to 1970. As noted above, the great majority of Temblor Formation specimens were recovered during the screenwash process in 2009-2010 from quarry matrix.

These efforts resulted in the recovery of about four thousand gastropods. It was impractical to measure so many specimens, so for each identified species, 100 or 200 specimens were measured with digital calipers. If fewer than 100 specimens were known for any species, then the entire sample was measured. These measurements are presented in Table 1. Collections made by Taylor (1954) included two planorbid taxa, *Planorbula mojavensis* and *Menetus micromphalus*. These taxa are both discoid biconcave planorbids of about the same size and we could not confidently distinguish them. Thus, we refer to this morphotype as “planorbid similar to *Planorbula mojavensis* and *Menetus micromphalus*,” recognizing that one or both may be present in a sample from a single site. A listing of taxa found at each locality is given in Table 2 and a photo of a representative specimen for each species is provided in Figures 2-7. Photos of these species were also published by Taylor (1954; plate 1).

Gastropod species

Of the five species identified from the Barstow Formation, *Craterarion pachyostracon*, *Lymnaea mohaveana*, *Lymnaea megasoma*, *Helminthoglypta alfi*, and planorbids similar to *Planorbula mojavensis* and *Menetus micromphalus*, two were also found in the Temblor Formation (*Lymnaea mohaveana* and planorbid similar to *Planorbula mojavensis* and *Menetus micromphalus*) (Table 2). *Hawaiiia minuscula* was only found in the Temblor Formation, but has been reported from the Barstow Formation (Taylor 1954). All of these species were described by Taylor (1954) so no additional taxonomic descriptions are needed. The most abundant species at Barstow is *Craterarion pachyostracon*, and the most abundant species at the Temblor site is the planorbid similar to *Planorbula mojavensis* and *Menetus micromphalus* (Table 2). Most Barstow localities yield a single species, but locality V200025 has four taxa, sharing two with the Temblor locality (V200915). Of the species shared between formations, morphological differences are few, but measurements indicate that Barstow species are larger than the same species from the Temblor Formation (Table 1). The size difference is of uncertain significance because it could reflect a greater percentage of juvenile specimens at the Temblor site versus the Barstow localities, or fluvial sorting, or some other factor.

Craterarion pachyostracon

This genus and species is only known from a single site (RAM V200515) in the Barstow Formation, interpreted to represent a pond deposit (Lindsay 1972). The site is referred to as “the slug bed” (Lindsay 1972, Pagnac 2009, and others), and is the same “Lake Bed Horizon” reported by Taylor (1954) as his Barstow locality 3. Slugs are reported from Miocene strata in Europe but this is the earliest record of them from North America (Taylor 1954). At V200515, the slug bed is a dip slope exposure whose area is more than an acre. Gastropods and



Figure 2. *Craterarion pachyostracon* from the Barstow Formation. Scale in mm

snails are abundant at V200515, but only *C. pachyostracon* is easily collected because their thick shells are densely calcified and are found in great numbers as float. Other mollusk shells are composed of calcareous material, which is thin and weakly cemented and thus easily destroyed by erosion. These mollusks are found in the same stratigraphic unit as small vertebrate fossils, including teeth of the Miocene beaver *Mono-saulax* (Lindsay 1972).

RAM crews have visited the site many times and over 3,000 specimens have been collected. The shells have a light bronze color with smooth and wavy ventral surface and a dorsal surface covered with faint growth lines (Figure 2). Measurements are given in Table 1.

Planorbid similar to *Planorbula mojavensis* and *Menetus micromphalus*

Planorbids are common terrestrial snails in North America. As noted above, *Planorbula mojavensis* and *Menetus micromphalus* (Figure 3) are difficult to distinguish and could not be separated with confidence. This planorbid (or two planorbids) is known from about 4,000 specimens from V200915 in the Temblor Formation and nearly 200 from V200025 and V201201-02 in the Barstow Formation based on collections by RAM crews (Table 2). Taylor (1954) also reports *Planorbula mojavensis* and *Menetus micromphalus* from the slug bed (V200515) and three other sites in the Barstow Formation. To collect mollusks in addition to slugs from the slug bed would require very delicate excavation, something that has not been attempted by RAM crews. The RAM collections have a single planorbid specimen from Quarry 5 (RAM 199015), a site in the middle member of the Barstow Formation. This occurrence is the only documented gastropod found from the middle member; all others are from the upper member. Specimens have a broad size range, with the Barstow larger than those from the Temblor Formation (Table 1). Many specimens have sediment debris coating the shell, making shell details difficult to distinguish.

Lymnaea mohaveana

Lymnaea mohaveana (Figure 4) is found at V200915 in the Temblor Formation and V200025 in the Barstow Formation. Taylor (1954) also reports *L. mohaveana* from the slug bed (V200515) in the Barstow Formation. Specimens from both formations have a broad size range, but



Figure 3. *Menetus micromphalus* or *Planorbula mojavensis* from the Barstow Formation (left) and the Temblor Formation (right). Scale in mm.



Figure 4. *Lymnaea mohaveana* from the Barstow Formation (left) and the Temblor Formation (right). Scale in mm.

the Barstow specimens are, on average, about twice as large as those from the Temblor Formation (Table 1).

Lymnaea megasoma

Lymnaea megasoma (Figure 5) is much rarer than *Lymnaea mohaveana*, as the former is only known from eight specimens from V200025 in the Barstow Formation, although Taylor (1954)



Figure 5. *Lymnaea megasoma* from the Barstow Formation. Scale in mm.



Figure 6. *Hawaiiia minuscula* from the Temblor Formation. Scale in mm.

reported it from the slug bed (V200515) as well. The shell is very similar to that of *Lymnaea mohaveana*, but is slightly longer and wider (Table 1).

Hawaiiia minuscula

A single specimen of this species was reported by Taylor (1954) from the slug bed in the Barstow Formation. Forty one specimens

of *Hawaiiia minuscula* (Figure 6) are also known from the Temblor Formation (Table 2) and measurements are given in Table 1.

Helminthoglypta alfi

Taylor (1954) reported *Helminthoglypta alfi* (Figure 7) from four sites in the Barstow Formation, including the slug bed (V200515). The type locality (locality one of Taylor 1954; equals RAM V200114) is within Rainbow Basin and was relocated using photos in the RAM archives. *Helminthoglypta alfi* is also found at RAM locality V200025, a Barstow site that has yielded four species of gastropods (Table 2). Measurements are given in Table 1.



Figure 7. *Helminthoglypta alfi* from the Barstow Formation. Scale in mm.

and *Menetus micromphalus?* are aquatic species living in a pond or slow moving stream with some aquatic vegetation; *Hawaiiia minuscula* is a land snail that lived under logs, bark, stones, etc. on moist leaf mold; and *Helminthoglypta alfi* and *Craterarion pachyostracon* are land snails that lived in a fairly dry habitat, under rocks among brush and leaves, perhaps beside a stream or pond.” The fine grained strata yielding Barstow species is compatible with the environmental model of Taylor (1954), as these species underwent little or no transport from where they lived to their final resting place. In contrast, Temblor Formation species are in strata with mudstone clasts and numerous whole and fragmentary vertebrate skeletal elements. Thus, Temblor Formation gastropods underwent some sorting as they were transported and deposited by fluvial processes. This sorting may also explain size differences between the Temblor and Barstow samples.

Based on associated fossil mammals, gastropods from the upper member of the Barstow Formation are late Barstovian in age (Tedford et al. 2004; Pagnac 2009), whereas the Temblor Formation site is slightly older, early to early late Barstovian (Kelly and Stewart 2008). Exposures of the Barstow Formation and the Temblor Formation are separated by about 500 km (both areas are located on the east side of the San Andreas Fault system, so the relative latitudes of these sites apparently have remained stable since the Miocene). Also, the Temblor Formation is mostly marine, with rare nonmarine/intertidal facies, and the Barstow Formation is entirely nonmarine and deposited within an inland basin far to the south. Thus, it appears very unlikely that the two areas were within the same drainage system. The Temblor Formation and Barstow Formation gastropod faunas are quite similar despite the significant geographic separation and different

Discussion

For species found in both the Barstow and Temblor formations, specimens of shared species from Barstow are on average larger than those from the Temblor Formation (Table 1). Specimens of juveniles are common in samples from both formations, and the size difference may be partly related to the Temblor Formation specimens reflecting a higher percentage of juveniles.

Differences in depositional environment are reflected in the stratigraphic setting of the mollusk producing sites in the Barstow Formation versus the single Temblor Formation site. Taylor (1954:69) notes: “*Lymnaea mohaveana*, *Lymnaea megasoma*, *Planorbula mojavensis*,

Table 1. List of taxa and their formation, with measurements and number of whorls. Measurements in mm show mean (range). 100 specimens measured for each species except 94 for *Helminthoglypta alfi*, and 8 for *Lymnaea megasoma*.

Taxon	Major Diameter	Minor Diameter	Height	Whorls
<i>P. mojavensis</i> / <i>M. micromphalus</i> (Barstow)	6.9 (3.9-10.2)	5.9 (3.3-8.7)	3.1 (2.1-4.6)	3
<i>P. mojavensis</i> / <i>M. micromphalus</i> (Temblor)	4.8 (3.0-6.8)	6.0 (2.5-4.1)	3.1 (1.3-2.2)	3
<i>Hawaiiia minuscula</i> (Temblor)	6.7 (3.7-10.4)	5.8 (3.3-8.8)	3.5 (2.2-6.0)	4
<i>Craterarion pachyostracon</i> (Barstow)	6.3 (4.4-9.1)	3.7 (2.2-5.5)	2.4 (1.2-4.6)	N/A
<i>Helminthoglypta alfi</i> (Barstow)	9.1 (5.5-14.4)	8.0 (4.7-13.1)	5.7 (3.4-10.3)	4
	Length	Width	Length of Aperture	Whorls
<i>Lymnaea mohaveana</i> (Barstow)	17.2 (10.2-25.7)	7.4 (4.5-10.8)	7.3 (3.9-12.0)	5
<i>Lymnaea mohaveana</i> (Temblor)	7.7 (3.0-14.0)	3.6 (2.0-6.6)	4.6 (2.8-7.9)	5
<i>Lymnaea megasoma</i> (Barstow)	18.9 (15.1-22.4)	7.6 (6.2-8.6)	7.9 (6.4-10.4)	

Table 2. Number of specimens per taxon by locality.

V200915 is from the Temblor Formation, all other sites are in the Barstow Formation

	V200915	V200025	V200114	I99015	V200515	V201201-2
<i>Lymnaea mohaveana</i>	161	240				
<i>Lymnaea megasoma</i>		8				
<i>Menetus micromphalus</i> or <i>Planorbula mojavensis</i>	3971	102		1		80
<i>Craterarion pachyostracon</i>					3114	
<i>Hawaiia minuscula</i>	41					
<i>Helminthoglypta alfi</i>		9	85			

depositional setting, which indicates that similar habitats existed in both areas and that barriers to dispersal were minimal. Lack of topographic barriers is reinforced by the presence of stickleback fish in the Barstow Formation as Pacific Ocean stickleback populations apparently dispersed to the continental interior in streams with low gradients (Bell and Reynolds, 2010).

Acknowledgments

We thank E. Zaborsky and R. O'Dell of the Hollister BLM Office permits and field assistance, J. Stewart for site information, students of The Webb Schools for field and lab assistance, A. Hess and D. Silver for assistance with figures, Bob Reynolds for helpful comments, and the Mary Stuart Rogers Foundation and the David B. Jones Foundation for financial support.

Literature Cited

- Bartow, J.A. 1996. Geologic map of the west border of the San Joaquin Valley in the Panoche Creek Cantua Creek area, Fresno and San Benito Counties, California. U.S. Geological Survey Miscellaneous Investigations Series I-2430, 1:50,000.
- Bate, M. A. 1985. Depositional sequence of the Temblor and Big Blue formations, Coalinga Anticline, California. P. 69-86, in S. A. Graham (ed.), *Geology of the Temblor Formation, Western San Joaquin Basin, California*. Pacific Section, SEPM volume and Guidebook 44.
- Bell, M. A., and R. E. Reynolds, 2010. Miocene and Late Pleistocene stickleback spines from the Mojave Desert, California. *California State University, Desert Symposium Vol. 2010:162-168*.
- Bode, F. D. 1935. The fauna of the *Merychippus* zone, North Coalinga District, California. *Carnegie Institution of Washington Publication 453:65-96*.
- Dibblee, T. W. 1968. *Geology of the Fremont Peak and Opal Mountain quadrangles*. California Division of Mines and Geology Bulletin 188:1-64.
- Kabat, A. R., and R. I. Johnson. 2008. Dwight Willard Taylor (1932-2006): his life and malacological research. *Malacologia* 50:175-218.
- Kelly, T. S. and J. D. Stewart. 2008. New records of Middle and Late Miocene Perissodactyla and Artiodactyla from the western border of the San Joaquin Valley, Diablo Range, Fresno County, California. *Natural History museum of Los Angeles County, Contributions in Science* 516:1-29.
- Lindsay, E. H., 1972. Small mammal fossils from the Barstow Formation, California. *University of California Publications in Geological Sciences* 93:1-104.
- Merriam, J. C. 1915. Tertiary vertebrate faunas of the north Coalinga region of California. *Transactions of the American Philosophical Society* 22:191-234.
- Pagnac, D. C., 2009. Revised large mammal biostratigraphy and biochronology of the Barstow Formation (Middle Miocene), California. *Paleobios* 29:48-59.
- Taylor, D. W. 1954. Nonmarine mollusks from the Barstow Formation of southern California. *United States Geological Survey Professional Paper 254-C:57-80*.
- Taylor, D. W. 2000. Letter to Don Lofgren; archives of Raymond Alf Museum of Paleontology, 6pp.
- Tedford R. H., Galusha, T., Skinner, M. F., Taylor, B. E., Fields, R. W., MacDonald, J. R., Rensberger, J. M., Webb S. D., and D. P. Whistler, 1987. Faunal succession and biochronology of the Arikareean through Hemphillian interval (late Oligocene through earliest Pliocene epochs) in North America. Pp.153-210, in M. O. Woodburne (ed.), *Cenozoic mammals of North America, Geochronology and Biostratigraphy*. University of California Press, Berkeley.
- Tedford, R. H., Albright III, L. B., Barnosky, A. D., Ferrusquia-Villafranca, I., Hunt Jr., R. M., Storer, J. S., Swisher II, C. C., Voorhies, M. R., Webb S. D., and D. P. Whistler, 2004. Mammalian biochronology of the Arikareean through Hemphillian interval (late Oligocene through early Pliocene epochs). Pp. 169-231, in M. O Woodburne (ed.), *Late Cretaceous and Cenozoic mammals of North America*. Columbia University Press, New York.
- Wood, H. E., R. W. Chaney, J. Clark, E. H. Colbert, G. L. Jepsen, J. B. Reeside Jr., and C. Stock. 1941. Nomenclature and correlation of the North American continental Tertiary. *Geological Society of America Bulletin* 52:1-48.
- Woodburne, M. O., Tedford, R. H. and C. C. Swisher III, 1990. Lithostratigraphy, biostratigraphy, and geochronology of the Barstow Formation, Mojave Desert, southern California. *Geological Society of America Bulletin* 102:459-477.
- Zaborsky, E. 2004. Final report on the bone beds excavated 45/1 and 46/2 structures on Path 15. Hollister, California: Bureau of Land Management, Hollister Field Office, 10 pp.

History of the Barstow Formation cricetid record

Everett H. Lindsay¹ and David P. Whistler²

¹ Professor Emeritus, Department of Geosciences, University of Arizona, ehind@cox.net

² Curator Emeritus, Natural History Museum of Los Angeles County, dhwhistler@bendcable.com

Introduction

Cricetid rodents were first reported from Rodent Hill in the Barstow Formation by E. Raymond Hall (1930). Hall described *Peromyscus longidens*, later changed to *Copemys longidens* by Lindsay (1972). Cricetid rodents are one of the more common small mammals recorded from the Barstow Formation. When vertebrate paleontologists established North American Land Mammal Ages as a framework for North American chronology, they designated the mammal fauna from the fossiliferous tuff member of the Barstow Formation as typical for the Late Miocene interval they called Barstovian land mammal age (LMA), and suggested that the appearance of *Peromyscus* (and several other mammals) represent the beginning of Barstovian LMA (Wood, H.E. et al., 1941). Many of the rodent fossils initially named *Peromyscus*, an extant genus, have been renamed *Copemys* or *Postcopemys* (see Korth, 1998 and Lindsay & Czaplewski, 2011). The Barstovian LMA is still a key interval in North American chronology, although we now consider it middle Miocene, rather than late Miocene.

Collecting in the Barstow Fossil Beds

Fossils were first reported from the Barstow area in 1911 (Baker 1911, Merriam 1911), and Merriam (1919) identified 19 genera of fossils from the Mud Hills where the Barstow fauna is located. Baker (1911) designated five members in the stratigraphic sequence of the Mud Hills, assigning them to the Rosamond Series, and later Merriam (1919) informally assigned these deposits to the Barstow Formation. Between 1919 and 1930, more or less, Annie Alexander and Louise Kellogg from the University of California Museum of Paleontology (UCMP) were active



Cricetidae: *Neotoma magister*. Alan Cressler photo.

in building up the UCMP collection from the Mud Hills, under the direction of W.D. Matthew. About the same time (1923–1930) personnel from the Frick Laboratory of the American Museum of Natural History made extensive collections of vertebrate fossils for the Frick Laboratory. When Dick Tedford was teaching at the University of California Riverside (1960–1966) he frequently brought his students (including Dave Whistler, Bob Reynolds, George Jefferson, and many others) to the Mud Hills to develop their skills in vertebrate paleontology.

Ruben A. (“Stirt”) Stirton and Dick Tedford were developing the vertebrate fossil record of Australia in 1962–1964 where they introduced new graduate student Mike Woodburne to Australian vertebrate paleontology. Mike was looking for a dissertation topic and Dick suggested to him that the geology and paleontology of the Mud Hills would be an excellent subject. Later that field season they discovered the Alice Springs fauna in Australia, which became Woodburne’s dissertation, so when they returned to Berkeley in 1963 and one of us (EL) was looking for a dissertation topic, Mike mentioned the Barstow topic that Tedford has suggested to him. In 1964 Dick Tedford introduced me to the Mud Hills. I described my mixed communication with Dick Tedford during my first visit to the Mud Hills (summer of 1964) in my contribution to the American Museum of Natural History (AMNH) volume dedicated to Dick Tedford and edited by Larry Flynn (2003) so I won’t repeat that here. Suffice to say that Dick Tedford took me to several of his sites in Carnivore Canyon and the Rodent Hill area of the Mud Hills and that got me started. I must admit, however, that John White—who was at Berkeley on sabbatical from Long Beach State when I arrived at Berkeley—also influenced me. John pointed out that you could collect an entire fossil rodent skeleton (or a rodent fauna) in one afternoon and take it home in your pocket, whereas you might spend many days and tons more work to collect and bring a horse or a dinosaur back to the lab.

Dick Tedford’s suggestion for my dissertation was to develop a stratigraphic framework in the Mud Hills by screen washing fossil sites and placing the individual fossil sites in that framework. Claude Hibbard had developed a productive screen washing process in Meade County, Kansas, showing that large samples of small mammals could be accumulated by that method. The method had been applied with great success by many other graduate students at Berkeley, including Bill Clemens in Cretaceous deposits of Wyoming, Malcolm McKenna in Eocene

deposits of Wyoming, Arnold Shotwell in Mio-Pliocene deposits in Oregon, and Gideon (“Gid”) James in Mio-Pliocene deposits of the Cuyama area in California. Tedford believed the Barstow beds were just aching to be screen washed.

The only other time that I joined Dick Tedford in the Mud Hills was during the winter of 1964-1965 just before he left Riverside for the AMNH. Dick and his student Bob Reynolds spent a couple of bitterly cold days with Don Savage and me in the Mud Hills so that I could show Tedford and Savage what I had accomplished during my previous field season. At the end of my first field season my dissertation advisor, R.A. Stirton, was thinking I should change my dissertation topic to a study of the Republican River area in Nebraska. Dave Webb had just finished his dissertation on Clarendonian and Barstovian faunas in Nebraska and Stirt realized a follow-up on the Barstovian and Hemingfordian faunas in Nebraska would be valuable. I believe that it was Dick Tedford who convinced Stirt that I should continue my work in the Mud Hills.

Howard Hutchison joined the graduate “brigade” at Berkeley during my second year at UCB. Howard had worked in Kansas with Claude Hibbard and in Oregon with Arnold Shotwell. He pointed out that Shotwell was using screen boxes with 30-mesh screens rather than the 16-mesh screen that Hibbard, Clemens, McKenna, and others had used to collect small mammals, and he was collecting many more small teeth using the smaller screens. So I tried 30-mesh screen on the concentrate that I had brought to Berkeley from the Mud Hills and realized that during my first year at Barstow I was “salting” the Mojave River below Victorville, where I screen washed, with numerous small mammal fossils that escaped through my 16-mesh screen boxes. Thereafter, I constructed double screen boxes, with a 16-mesh screen box inside a slightly larger outer screen box with 30-mesh screen.

During the 1965 field season, graduate students Dennis Bramble and Howard Hutchison helped me screen wash and collect fossils at Barstow. I would drive a pickup truck as close to the fossil site as possible, collect and transport about 10 gunny sacks of fossiliferous sediment to the pickup with a large wheel barrel, and then drive the loaded pickup to Victorville where Bramble and Hutchison did most of the screen washing. Bill Daily befriended and helped me during my first field season in the Mud Hills. After Bill and his cousin “humped” several bags of dirt with me, they showed me that it would be much more productive to build a narrow road (for a wheel barrel) to the fossil site from the main wash, then “wheel” rather than “hump” the bags to the pickup. I usually used the “Bill Daily method” of transporting fossil matrix after that. It was Dick Tedford who pointed out, after I got my pickup stuck during my introduction to the Mud Hills, how to lower the air pressure in my tires when driving on soft sand to increase the tire surface and friction, thereby

avoiding more embarrassing stuck-in-the-sand experiences. I always carried a tire pump with me after that, and never got stuck in the sand again. Most of my collecting and screen washing in the Mud Hills was done during that second summer (1965). There were usually several trips to the Mud Hills during the subsequent years but I usually hauled several bags of matrix back to Berkeley where I screen washed the sediment in the basement of the Earth Science Building on campus rather than take screen boxes to Victorville and screen wash there.

Identifying cricetid rodents

1960s and 70s

When I finished my dissertation (1967) I had identified six species of cricetid rodents in the Barstow fauna; cricetids still represent the most abundant and diverse small mammal in the Barstow fauna. In my dissertation all of these cricetids were assigned to the genus *Miochomys* Hoffmeister 1959. They had previously been assigned to *Peromyscus*, following Hall (1930) and Clark, Dawson and Wood (1964). However, Hoffmeister (1959) had described cricetid rodents from the Niobrara fauna in Nebraska and named them *Miochomys*, arguing that they differ from the modern cricetid *Peromyscus* in several features. Some of material described by Hoffmeister, including the type, was in the UCMP collection and therefore available to me. I examined the material studied by Hoffmeister and agreed with him that the material from the Niobrara River area and Barstow differ from modern cricetids, so I assigned the Barstow cricetids to *Miochomys*.

While studying at Berkeley I took a seminar from Seth Benson, a professor in the Museum of Vertebrate Zoology (MVZ) at Berkeley, in which I reviewed a paper by E.T. Hooper (1957) evaluating variation in the mesoloph(-id) as a taxonomic character. Vertebrate paleontologists use dental features to describe changes in fossil mammal populations and Hooper was expressing caution in the application of variable features in teeth for taxonomic significance. With Dr. Benson’s blessings, I compared many of the specimens in the MVZ that had been studied by Hooper, as well as others. Fortunately, many of the skins in the MVZ had skulls preserved with the specimens, so that the teeth of the individual could be evaluated. I actually had another motive—the gender of specimens curated in the MVZ are recorded with the specimens, if known, and I was interested in seeing if any of the dental features, including size, were related to the gender of the individual. The fossil specimens available to me from Barstow could not be identified by gender. Another objective was to evaluate morphological variation in a relatively large sample (20 individuals collected from the same area during the same interval of time was my goal). As noted in the summary of that study (Lindsay, 1972, p. 71-74), none of the dental characters I examined, including size of the teeth, appeared to be related to gender. Neither fossil nor modern cricetid rodents are

sexually dimorphic, to our knowledge. I also learned that in rodents, size of the teeth alone does not reliably separate two similar species.

During the course of my perusal of the mammal collection of the MVZ it occurred to me that *Peromyscus* teeth have aligned cusps (especially the proto-loph II and the anterior arm of the hypocone in upper cheek teeth, and the entolophid and the posterior arm of the protoconid of the lower cheek teeth); these features are illustrated in Figure 2. These cusps are joined after moderate wear, thereby forming an oblique ridge that intersects at a large angle (about 70–80°) with a corresponding ridge on the occluding tooth, similar to two lines intersecting to form the letter X. Similar oblique ridges (and wear) also develop in these rodents by alignment of the anterocone and the anterior arm of the protocone on M1, along with the metalophid II of M1 and the anterior arm of the protocone of M2 in upper cheek teeth, as well as the posterior arm of the hypoconid of m1 and the metalophid I of m2 in the lower cheek teeth. Alignment of these cusps in modern *Peromyscus* form a series of oblique ridges that intersect in occlusion with similar oblique ridges (intersecting at about 70° on occluding teeth). These intersecting ridges never occur in the fossil cricetid that I was studying from the Barstow Formation. Therefore, the Barstow fossil cricetids, lacking oblique cross ridges in their cheek teeth, can be distinguished from modern *Peromyscus*, and should be given a different name.

Hoffmeister's *Miochomys* lacks the cross loph intersection of *Peromyscus*, so I assigned the Barstow cricetids to

Miochomys. Hoffmeister's (1959) diagnosis of *Miochomys* was based on the relative position of the cusps and wear on the cusps, which do not really distinguish *Miochomys* from *Copemys*, as revealed by Fahlbusch (1967). Subsequently (and, fortunately before my study of Barstow small mammals was published) I learned from Volker Fahlbusch who had been studying *Copemys* following his research on the Miocene cricetids *Democricetodon* and *Megacricetodon* in Germany, that North American *Copemys* is virtually indistinguishable from European *Democricetodon*, and that Wood's (1936) characterization of *Copemys*, based on *Copemys loxodon* from the Santa Fe Formation in New Mexico, is inadequate and inaccurate.

Fahlbusch (1967) concluded that *Democricetodon* and *Copemys* belong in the same genus, as subgenera; e.g., *Copemys (Democricetodon)* and *Copemys (Copemys)*. I agree with Fahlbusch that these two taxa are probably truly subgenera, but it seemed to me that their derivation is from a European (or Asiatic) taxon rather than a North American taxon. At that time no cricetid taxon was known in North America with features that suggest derivation for the genus *Copemys*. Wood (1936) and Wood in Clark, Dawson, and Wood (1964) suggested that the fossil taxon they called *Peromyscus* (and is now called *Copemys*) was likely derived from either *Eumys* or *Leidymys* here in North America. We now realize the record of cricetids is very poor in the Hemingfordian LMA preceding the Barstovian LMA, and none of the then-known Hemingfordian cricetid rodents resemble *Copemys*.

Therefore, I followed Fahlbusch's diagnosis (and illustrations) of *Copemys*, and assigned the cricetids from Barstow to *Copemys* rather than *Miochomys* when my work was published (1972). I continue to believe the interpretation of Fahlbusch (1967), and until recently believed that *Copemys* was probably an immigrant to North America in the middle Miocene, appearing in the Barstovian LMA.

1980s to 2010

During the 1980s new stratigraphic and paleomagnetic work was completed in the Mud Hills by Mike Woodburne, Dick Tedford, Carl Swisher, Bruce MacFadden, and Neil Opdyke (Woodburne et al., 1990; MacFadden et al., 1990). These studies included new isotopic dating and paleomagnetic data that resolved many of the earlier problems in the Mud Hills stratigraphy and Barstovian paleontology, but we still had very few fossils from below the Steepside Quarry level, which was recognized as base of the Green Hills fauna and

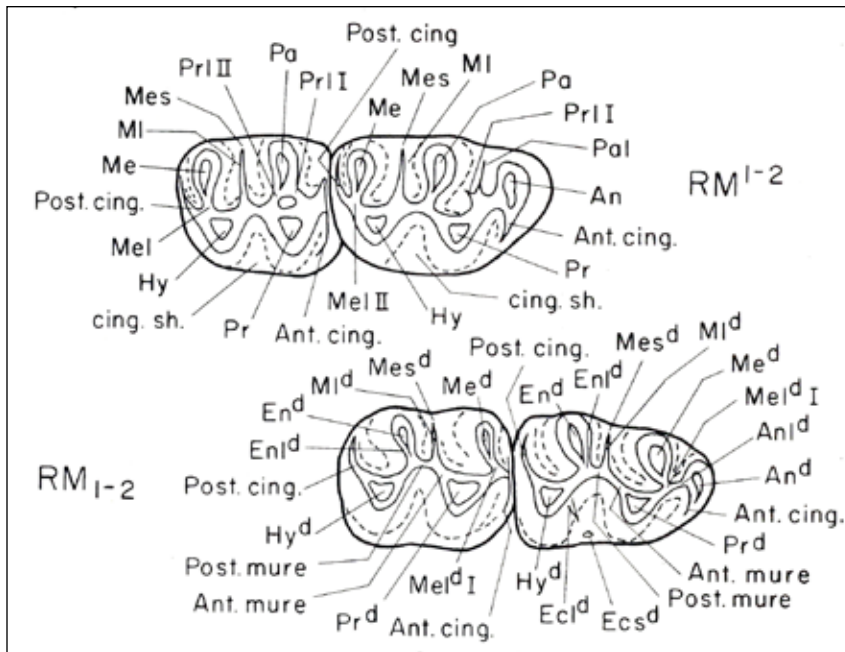


Figure 2. Cusp terminology of *Copemys*. Pa = paracond; Me = metacone; Pr = protocone; Hy = hypocone; An = anterocone; En = entocone; Pal = paralophule; Mel I = metalophule I; Mel II = metalophule II; Pr I = protolophule I; Pr II = protolophule II; An I = anterolophule; Ecl = ectoloph; En I = entolophule; Ml = mesoloph; Mes = mesostyle; lab. Cing. = labial cingulum; ling. Val. = lingual valley; Ant. Cing. = anterior cingulum; Post. Cing. = posterior cingulum; cing. Sh. = lingual cingular shelf; ant. Mure = anterior mure; Post. Mure = posterior mure; Ecs = ectostyle; (d = suffix id, which designates lower dentition). (Lindsay 1972, Fig. 40).

the beginning of Barstovian LMA. It also occurred to me that I had not sampled adequately for small samples from sediments stratigraphically below the level of Steepside Quarry, since that quarry was the lowest stratigraphic level I had sampled for my dissertation. I decided to return to the Mojave Desert to sample for small mammals in sediments below the level of Steepside Quarry. My students and I spent two summer field seasons searching for fossils in both the Cady Mountains (east of the Mud Hills) and in the Mud Hills, hoping to find fossils indicative of Hemingfordian LMA. Results of that work were published in Lindsay (1995).

We found a few more small mammal fossils, thereby extending the fossil record a bit lower stratigraphically, but none of those fossils indicated a clear Hemingfordian LMA. *Copemys pagei* was represented in most of the sites we sampled, including the Green Hills Division (earliest Barstovian) and the Rak Division (latest Hemingfordian). *Copemys tenuis* was also represented in the Second Division level. Actually, we probably created more problems than we resolved relative to the Hemingfordian–Barstovian boundary.

If one places the boundary between Hemingfordian and Barstovian LMAs as a “golden spike” at some stratigraphic level, such as Steepside Quarry, then everything collected below that level is Hemingfordian. If one places the boundary between Hemingfordian and Barstovian LMAs at the stratigraphic appearance of a fossil that by definition marks the appearance of Barstovian LMA, then that fossil must be Barstovian. Fortunately (or not), the boundaries of land mammal ages were never clarified in the formal establishment of land mammal ages (Wood et al., 1941). By convention, land mammal ages are recognized with a fossil assemblage rather than a single taxon. It seems reasonable that the boundary of Hemingfordian–Barstovian LMAs should be placed within the strata of the Mud Hills, but the boundary should be based on an assemblage of fossils, rather than a single taxon.

Meanwhile, Dave Whistler had done mitigation work for many years, related primarily to highway construction projects in southern California, as part of his job as Curator of Vertebrate Paleontology at the Natural History Museum of Los Angeles County. Dave, along with E. Bruce Lander, who supported this mitigation work through Paleo Environmental Associates, Inc. of Altadena, California, compiled and published some of the results of the work in Orange, Los Angeles, Santa Barbara, and Ventura Counties (Whistler and Lander, 2003). These projects resulted in more than 4,000 fossil vertebrate specimens from late Eocene to mid Miocene deposits in those counties. Fortunately, cricetid rodents were an important part of those fossil assemblages, especially in sequences ranging in age from the Arikareean LMA to early Hemingfordian LMA. Dave retired from the Natural History Museum of Los Angeles County, and moved to Bend, Oregon, where he volunteers at the John Day Fossil Beds National Monument. The John Day beds

have produced some of the best fossils of the Arikareean cricetid *Leidyomys*, and Dave recently studied a nice collection of cricetids from the Campbell Ranch site (Fremd and Whistler, 2009).

2011 to present

In 2011 we launched a study of Miocene cricetid rodents in hope of better understanding the taxonomy of these rodents, and their relationship to similar mammal faunas in Oregon, Montana, and Nebraska where most of the North American Arikareean and Hemingfordian faunas had been studied. When our colleague, Tom Deméré at the San Diego County Museum of Natural History heard of our project, he offered to loan us the large accumulation of cricetid rodents that he and his colleague, Steve Walsh, had collected from the Otay Formation in San Diego County. In total, we borrowed more than 1600 fossil cricetid specimens, usually isolated teeth, from four institutions: Natural History Museum of Los Angeles County, San Diego Natural History Museum, Cooper Center of Orange County, and John Day Fossil Beds National Monument. We also borrowed about 150 comparative specimens, including types and casts, from eight museums: American Museum of Natural History, Carnegie Museum of Natural History at Pittsburgh, University of Nebraska Museum, Museum of Comparative Zoology at Harvard, National Museum of Natural History (Smithsonian Institution), University of Colorado at Boulder, University of Kansas Museum, and the Natural History Museum of Los Angeles County. We question whether a larger assemblage of cricetid rodents had ever been assembled previously in North America. This study is currently active, although we don't consider that any of our existing conclusions are ready for publication.

What is most encouraging is that we recognize several distinct new taxa within the large sample of Arikareean and Hemingfordian cricetids that we have assembled. These new taxa add features that are seen in some species of *Copemys*, increasing the likelihood that a suitable ancestor for *Copemys* might be found in North America.

References

- Baker, C.L. 1911. Notes on the later Cenozoic history of the Mohave Desert region in southeastern California. California University Publications in Geological Sciences, 6:333-383.
- Clark, J.B., Dawson, M.R., and Wood, A.E. 1964. Fossil mammals from the lower Pliocene of Fish Lake Valley, Nevada. Museum of Comparative Zoology (Harvard) Bulletin, 131 (2):27-63.
- Fahlbusch, Volker 1967. Die Beziehungen zwischen einigen Cricetiden (Mamm., Rodentia) des nordamerikanischen und euroäischen Jungtertiärs. Paläontologie Zeitschrift, 41 (3/4):154-164.
- Flynn, L.J. (ed.) 2003. Vertebrate Fossils and their Context, Contributions in Honor of Richard H. Tedford. Bulletin of the American Museum of Natural History, 279: 1-659.

- Fremd, T. J and D. P. Whistler. 2009. Preliminary description of a new microvertebrate assemblage from the Arikareean (early Miocene) John Day Formation, central Oregon, in Albright, L. B. III, ed., Papers on Geology, Vertebrate Paleontology and Biostratigraphy in Honor of Michael O. Woodburne, Museum of Northern Arizona Bulletin 65, p. 159-170.
- Hall, E. R. 1930. Rodents and lagomorphs from the Barstow beds of southern California. University of California Publications in Geological Sciences, 19(13):313-318.
- Hoffmeister, D.F. 1959. New cricetid rodents [*Miochomys* and *Peromyscus kelloggae*] from the Niobrara River fauna. Journal of Paleontology, 33:696-699.
- Hooper, Emmet T. 1957. Dental patterns in the mice of the genus *Peromyscus*. Miscellaneous Publications of the Museum of Zoology, University of Michigan, 99:1-59.
- Korth, W.W. 1998. Rodents and lagomorphs (Mammalia) from the late Clarendonian (Miocene) Ash Hollow Formation, Brown County, Nebraska. Annals of Carnegie Museum, 67:299-348.
- Lindsay, E.H. 1972. Small mammal fossils from the Barstow Formation, California. University of California Publications in Geological Sciences, 93:1-104.
- Lindsay, E.H. 1995. *Copemys* and the Barstovian/Hemingfordian Boundary. Journal of Vertebrate Paleontology, 15 (2):357-365.
- Lindsay, Everett H. and Czaplewski, Nicholas J. 2011. New rodents (Mammalia, Rodentia, Cricetidae) from the Verde Fauna of Arizona and the Maxum Fauna of California, USA, early Blancan Land Mammal Age. Palaeontologia Electronica, 14 (3).
- MacFadden, Bruce J., Swisher, Carl C. III, and Woodburne, Michael O. 1990. Paleomagnetism, geochronology and possible tectonic rotation of the middle Miocene Barstow Formation, Mojave Desert, southern California. Geological Society of America Bulletin, 102:478-493.
- Merriam, J.C. 1911. A collection of mammalian remains from Tertiary beds on the Mohave Desert. California University Publications in Geological Sciences, 6:167-169.
- Merriam, J.C. 1919. Tertiary mammalian faunas of the Mohave Desert. California University Publications in Geological Sciences, 11:437a-437e, 438-485.
- Whistler, D. P. and E.B. Lander. 2003. ew late Uintan to early Hemingfordian land mammal assemblages from the undifferentiated Sespe and Vaqueros formations, Orange County, and from the Sespe and equivalent marine formations of Los Angeles, Santa Barbara, and Ventura Counties, southern California. Bulletin of the American Museum of Natural History, 13(279):231-268.
- Wood, A.E. 1936. The cricetid rodents described by Leidy and Cope from the Tertiary of North America. American Museum Novitates, 822:1-7.
- Wood, H.E., Chaney, R.W., Clark, J., Colbert, E.H., Jepsen, G.L., Reeside, J.B. Jr. and Stock, C. 1941. Nomenclature and correlation of the North American continental Tertiary. Geological Society of America Bulletin, 52:1-48.
- Woodburne, Michael O., Tedford, Richard H., and Swisher Carl C. III 1990. Lithostratigraphy, biostratigraphy, and geochronology of the Barstow Formation, Mojave Desert, southern California. Geological Society of America Bulletin, 102:459-477.

Review of *Megahippus* and *Hypohippus* from the Middle Miocene Barstow Formation of California

Bobby Gonzalez¹ and Don L. Lofgren²

¹The Webb Schools, Claremont, California 91711

²Raymond M. Alf Museum of Paleontology, Claremont, California 91711

Introduction

Skeletal remains of large anchitherine equids are rare in Miocene aged strata in North America. *Megahippus* and *Hypohippus* are both present in the Barstow Formation which crops out in the Mud Hills north of Barstow California (Figure 1). The first anchitherine remains reported from the Barstow Formation were a jaw fragment with m1-2, a fragment of an upper molar, and a few limb fragments (Merriam 1919). Anchitherine specimens described by Merriam (1919), and others collected later by crews from the University of California Museum of Paleontology (UCMP), number about 25 specimens. The largest Barstow Formation collection of large anchitherines consists of about 65 specimens recovered mainly through large scale quarrying efforts by Frick Laboratory crews from the 1920s to the 1950s, specimens now housed at the American Museum of Natural History (AMNH).

Barstow Formation field work by the Raymond M. Alf Museum of Paleontology (RAM) was initiated by Raymond Alf and students of The Webb Schools in 1936 (Lofgren and Anand 2010). Two phalanges and two metapodial fragments were recovered between 1950 and 1960. These specimens were sold to the University

of California-Riverside in the 1960s and are now at the UCMP. In 1955, Alf found an upper molar of a large anchitherine (now lost) and two years later, Webb student John Tuteur found a partial skull of a large anchitherine. This specimen was described by Tedford and Alf (1962) as a new species, *Megahippus mckennai*; the original catalog number of this specimen (RAM 6500) has been replaced by RAM 910. Concerted prospecting efforts in the Barstow Formation by RAM crews (which includes students and faculty of The Webb Schools on whose campus the RAM is located) from 1992-2012, has only resulted in the recovery of five additional specimens of large anchitherine equids.

In spite of their rarity, few specimens of *Hypohippus* and *Megahippus* from the Barstow Formation have been reported or described. Here we illustrate and briefly describe specimens of *Hypohippus* and *Megahippus* housed at the Raymond Alf Museum of Paleontology. Also, a listing of large anchitherine equids from the Barstow Formation in the collections at the American Museum of Natural History and the University of California Museum of Paleontology are listed, as most of this material has never been reported. A single specimen housed at the Natural History Museum of Los Angeles County is also noted.

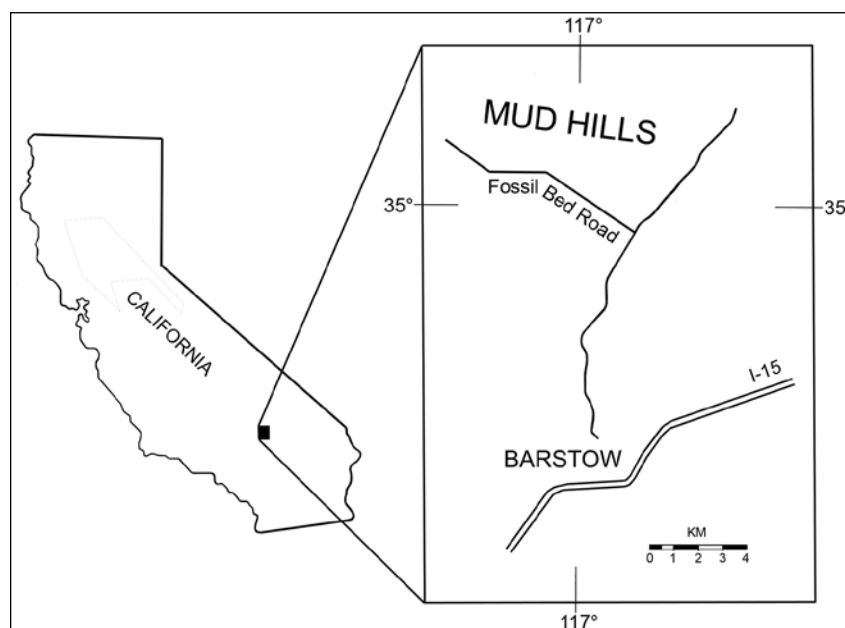


Figure 1. Location of the Barstow Formation within the Mud Hills, Mojave Desert, California (adapted from Steinen 1966).

Material and methods

All specimens listed were studied at the collections facilities in which they reside. Site visits were conducted between 2010-2012 by D. Lofgren to the University of California Museum of Paleontology, American Museum of Natural History, and Natural History Museum of Los Angeles County. Mitutoyo digital calipers were used to measure all specimens. Uncataloged specimens from the Frick collections at the AMNH are listed by their field numbers which usually include a box number (labeled BAR, for Barstow) followed by a specimen number (example, BAR 95-51). The stratigraphic context, locality or quarry, and collection date is given for each specimen if that information was available.

The stratigraphic locations of five major Frick quarries from the Barstow Formation mentioned in the text are shown in Figure 2. *Hemicyon* Quarry is also commonly referred to as the *Hemicyon* Stratum, so AMNH specimens labeled as such are from a single locality. The unnamed middle member and unnamed upper member of the Barstow Formation are not formal stratigraphic units. However, to avoid redundant text, these informal units will be referred to as the middle member of upper member.

Institutional Abbreviations—AMNH, American Museum of Natural History, New York, New York; FAM, Frick American Museum, New York, New York; LACM, Los Angeles County Museum, Los Angeles, California; RAM, Raymond M. Alf Museum of Paleontology, Claremont, California; UCMP, University of California Museum of Paleontology, Berkeley, California; UCR or RV, University of California-Riverside, Riverside, California; USNM, United States National Museum (Smithsonian), Washington D. C. **Other Abbreviations**—Ba1, Barstovian Biochron 1; Ba2, Barstovian Biochron 2; BAR, field collection crate number for FAM specimens; NALMA, North American Land Mammal Age.

Megahippus

There are two known species of *Megahippus*, *Megahippus matthewi* and *Megahippus mckennai* (MacFadden 1992). The genotypic specimen of *Megahippus* (USNM 10-16-S-13, partial palate with P2-M1, Devil’s Gulch Horse Quarry, Nebraska), selected as the holotype of *Megahippus matthewi* by McGrew (1938), was initially described as *Hypohippus matthewi* (Barbour 1914). *Megahippus matthewi* was noted as being one fourth larger than specimens of *Hypohippus affinis* from the same quarry (McGrew 1938). Other features that separate *Megahippus matthewi* and *Hypohippus affinis* are the extremely large and procumbent incisors and continuous upper premolar lingual cingula of *Megahippus matthewi* (McGrew 1938; Stirton 1940).



Figure 3. Occlusal view of RAM 910, holotype of *Megahippus mckennai*, maxilla with left and right P1-M3 and left I1-I2.

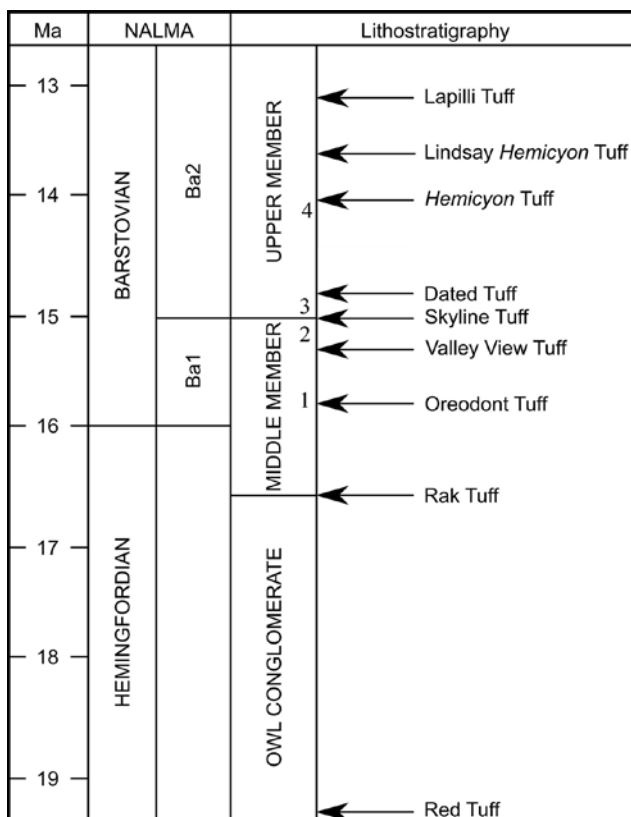


Figure 2. Geochronology and biostratigraphic subdivision of the Barstow Formation (adapted from Pagnac 2009). Stratigraphic position of the Oreodont Quarry (1), Skyline Quarry (2), May Day and New Year quarries (3), and *Hemicyon* Quarry or Stratum (4) noted by numbers. Note: Woodburne et al. (1990;fig. 5) place May Day Quarry slightly below the Skyline Tuff, at the same level as Skyline Quarry.

In the early 1960s, another species of *Megahippus*, *M. mckennai*, was described by Tedford and Alf (1962) from the Barstow Formation. The type specimen of *M. mckennai* (RAM 910) is a partial skull with both left and right P1-M3 and left I1-I2, whose incisors have the distinctive shape of *Megahippus* incisors (Figure 3). *Megahippus mckennai* is approximately 25 percent smaller than *M.*

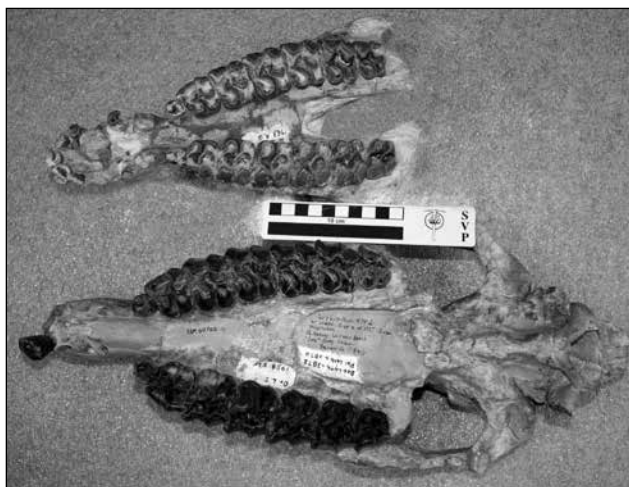


Figure 4. Ventral view of partial skull of *Megahippus mckennai* (FAM 21085) from the Barstow Formation and ventral view of the skull of *Megahippus matthewi* (FAM 60700) from the Valentine Formation of Nebraska.

matthewi (Figure 4) and also differs in having upper premolars with weaker lingual cingula (Tedford and Alf 1962).

Hypohippus

There are three main species of *Hypohippus* from western North America, *H. equinus*, *H. osborni*, and *H. affinis*, and all are restricted to Miocene strata (Osborn 1918; MacFadden 1992). Distinguishing dentigerous specimens of the three species is primarily based on both size and crown height. The teeth of *H. affinis* are the largest, *H. equinus* the smallest, and *H. osborni* intermediate in size (Matthew and Gidley 1906; Gidley 1907; Osborn 1918). Also, the cheek teeth of *H. equinus*, are lower crowned than those of *H. osborni*, and *H. affinis* has proportionately higher crowns than *H. osborni* (Matthew and Gidley 1906; Gidley 1907). There can be some difficulty in distinguishing species of *Hypohippus* based on fragmentary dentitions as *H. equinus*, *H. osborni*, and *H. affinis* represent three somewhat overlapping stages of tooth size and crown height development in a single lineage (McGrew 1938).

Differentiating Megahippus and Hypohippus in the Barstow Formation

Complete skulls or dentaries of *Megahippus* and *Hypohippus*, the largest anchitherine genera from the Barstow Formation, are easily distinguished by the large and procumbent incisors of *Megahippus* (Figure 5) (McGrew 1938; Stirton 1940, Tedford and Alf 1962). Also, the canine to first premolar diastema in both the upper and lower dentition of *Megahippus* is relatively shorter than that of *Hypohippus* (McGrew 1938; Tedford and Alf 1962; Pagnac 2005). However, specimens of large anchitherine equids from the Barstow Formation with the anterior dentition



Figure 5. Occlusal views of the partial premaxilla and maxilla of *Hypohippus affinis* (BAR 247-24; above) and *Megahippus mckennai* (FAM 21085; below). BAR 247-24 has small incisors laying on the premaxilla and left C-M3 and right C-M3. FAM 21085 has right I1-2, C-M3 and left I1-M3.

intact are fairly rare. Thus, differentiating the two genera can be difficult because specimens usually consist of either isolated postcranial elements or partial dentitions.

For the upper dentition, a character that differentiates the two genera is the greater development of lingual cingula in the upper cheek teeth of *Megahippus* compared to *Hypohippus* (McGrew 1938; Stirton 1940; Tedford and Alf 1962). Using this character, specimens of the upper dentition of large anchitherines from the Barstow Formation at the AMNH and the RAM were separated into two groups. Specimens with well-developed lingual cingula on all upper premolars were identified as *Megahippus* (Figure 6), and those with only lingual cingula on P2 were identified as *Hypohippus* (nearly all P2s of *Hypohippus* have lingual cingula). All specimens identified as *Megahippus*



Figure 6. Occlusal view of FAM 21083, left and right maxilla fragments of *Megahippus mckennai* with left P2-M2 and right P1-M3, showing lingual cingula on cheek teeth.



Figure 7. Occlusal view of Bar 247-23, right maxilla with P2-4 of *Megahippus mckennai* from Skyline Quarry, showing well-developed lingual cingula on P3-4.

based on upper premolar cingula also had large procumbent incisors (Figure 5) if the anterior upper dentition was present. Specimens identified as *Hypohippus* based on P3-M3 without lingual cingula, had smaller incisors (Figure 5). Lingual cingula were usually present in the upper molars of *Megahippus*, although less developed in comparison to the upper premolars in most cases. In contrast, specimens identified as *Hypohippus* based on incisors, did not have lingual cingula on their upper molars.

When *Megahippus* was first described, size was noted as a feature separating the new genus from *Hypohippus*, as *Megahippus matthewi* is 25% larger than *Hypohippus affinis* (McGrew 1938). This distinction between genera became problematic when *Megahippus mckennai* was described as being 25% smaller than *M. matthewi* (Tedford and Alf 1962), or approximately the same size as *Hypohippus affinis*.

We tested whether upper cheek teeth from the Barstow Formation, first identified as either *Hypohippus* or *Megahippus* based on the development of lingual cingula in the upper premolars and molars, could then be distinguished by size. Results indicate that there is a significant overlap in the size of the upper cheek teeth of the two genera from the Barstow Formation (Table 1). Thus, upper cheek teeth cannot be confidently identified as either *Hypohippus* or *Megahippus* based solely on size. In any case, both *Megahippus mckennai* and *Hypohippus affinis* are present in the Barstow Formation.

Because the size of the upper dentition of *Hypohippus* or *Megahippus* overlaps, dimensions of the lower cheek teeth of the two genera must overlap as well. Because features of the lower cheek teeth that distinguish *Hypohippus* and *Megahippus* have not been reported, we could not distinguish the lower dentition of the two genera unless incisors were present. An exception is four partial anchitherine dentaries (with cheek teeth only) from Skyline Quarry at the AMNH that are distinctly smaller than any others from the Barstow Formation (Table 2). Smaller species of *Hypohippus* are known (i.e. *H. osborni*, *H. equinus*), but a species of *Megahippus* smaller than *M. mckennai* has never been reported and seems unlikely to represent this smaller taxon. The four

Table 1. Measurements of upper dentition specimens identified as *Megahippus* or *Hypohippus* from the Barstow Formation based on incisor size and/or absence or presence of lingual cingula on P3-M3

	AMNH <i>M. mckennai</i>	RAM 910 <i>M. mckennai</i>	AMNH <i>H. affinis</i>	RAM 6904 <i>H. affinis</i>
P1 Length				
Number	5	2	4	2
Range	15.48-17.94	16.22-17.58	15.88-19.81	16.16-16.67
Mean	16.51	16.9	17.29	16.42
P1 Width				
Number	5	2	4	2
Range	11.35-13.28	13.22-14.48	12.09-14.31	12.83-13.57
Mean	12.12	13.85	13.08	13.2
P2 Length				
Number	8	2	11	2
Range	25.05-29.03	24.11-25.01	30.18-36.19	28.93-29.05
Mean	27.65	24.56	31.96	28.99
P2 Width				
Number	8	2	12	2
Range	28.04-29.52	30.30-33.33	24.47-29.18	26.26-27.62
Mean	28.76	31.82	27.14	26.94
P3 Length				
Number	10	2	12	2
Range	25.33-28.65	25.32-25.96	27.49-35.50	27.70-28.90
Mean	26.91	25.64	30.69	28.3
P3 Width				
Number	10	2	13	2
Range	31.14-33.84	35.56-36.33	26.39-32.26	26.38-27.31
Mean	32.94	35.95	29.61	26.85
P4 Length				
Number	10	2	11	2
Range	25.58-30.19	25.08-25.87	28.33-34.98	31.31-33
Mean	27.59	25.475	31.41	31.32
P4 Width				
Number	10	2	12	2
Range	33.04-36.64	35.71-41.71	29.50-33.87	27.54-27.59
Mean	34.84	38.71	31.59	27.57

Table 1 (continued)

M1 Length				
Number	7	2	4	2
Range	25.78-32.02	27.22-28.47	29.76-31.78	27.71-27.90
Mean	28.64	27.85	30.37	27.81
M1 Width				
Number	7	2	5	2
Range	33.47-35.70	36.72-36.77	32.41-35.01	28.24-30.58
Mean	34.87	36.75	33.3	29.41
M2 Length				
Number	7	2	4	
Range	24.96-28.95	26.59-27.82	28.48-30.11	
Mean	26.57	27.21	29.05	
M2 Width				
Number	7	2	4	
Range	30.47-36.88	37.46-37.91	31.10-32.57	
Mean	33.82	37.69	32.15	
M3 Length				
Number	6	2	5	
Range	20.17-25.19	20.20-21.57	21.44-25.33	
Mean	22.29	20.89	23.65	
M3 Width				
Number	6	2	5	
Range	25.62-31.31	29.24-30.39	23.31-27.52	
Mean	29.3	29.82	25.12	

Specimens measured include:

—AMNH (*M. mckennai*): BAR 279-1, BAR 279-582, FAM 21085, FAM 21083, BAR 280-596, AMNH 143242 (BAR 198-6), BAR 247-23, FAM 21081, FAM 21081.

—RAM 910, holotype of *M. mckennai*, left and right P1-M3.

—AMNH (*H. affinis*): BAR 289-862, FAM 21084, BAR 247-24, BAR 81, FAM 21087, FAM 21086, FAM 21089, BAR 268-3237, BAR 95-51, AMNH 143241, BAR 196-21.

—RAM 6904, partial maxilla of *H. affinis* with left and right P1-M1.

small dentaries from Skyline Quarry are similar in size to those of the paratype of *H. osborni* (AMNH 9395) from northwestern Colorado (Table 2). Thus, there appears to be two species of *Hypohippus* in the Barstow Formation, *H. affinis*, and a smaller one, similar in size to *H. osborni*. A review of the anchitherine specimens from Skyline Quarry indicate the presence of *Megahippus mckennai*, based on BAR 247-23, a partial maxilla (Figure 7), and *Hypohippus affinis*, based on B247-24 (Figure 5) and BAR 268-3237, both partial skulls. The only lower dentitions from Skyline Quarry, other than the four small dentaries, are two larger specimens, BAR 267-272 and BAR 251-23.

BAR 251-23 is too fragmentary for identification to genus, but BAR 267-272 has p2-4, and although unprepared, lengths of these teeth can be measured. The p2 is 28.04 mm in length, the p3 26.37 mm, and the p4 27.90 mm, dimensions much larger than the same teeth from the four smaller dentaries from Skyline Quarry (Table 2). The large partial dentary (BAR 267-272) may be *Hypohippus* or *Megahippus*, but the presence of a large species of *Hypohippus*, *Hypohippus affinis* at Skyline Quarry, is confirmed by BAR 247-24 which is the same size as *Megahippus mckennai* (Figure 5). Comparison of a small dentary from Skyline Quarry (BAR 267-282) to a dentary of *Megahippus mckennai* (BAR 296-1070) from New Year Quarry that is about the same size as *H. affinis*, illustrates the significant size difference of these dentaries (Figure 8). Since *Megahippus* and two variants of *Hypohippus* occurred together at Skyline Quarry, it appears that three species of anchitherine equids coexisted for at least a short span of time during deposition of the Barstow Formation.

Specimens of the upper dentition identified as *Megahippus mckennai* or *Hypohippus affinis* using premolar cingula and incisor size and shape, are listed below under their respective genus. For the lower dentition, most specimens of large anchitherines are identified as *Megahippus* or *Hypohippus* undifferentiated unless the incisors were present. In the UCMP and AMNH collections from the Barstow Formation, many isolated postcranial elements of large anchitherine equids are identified as either *Hypohippus* or *Megahippus*, but these identifications are questionable as a detailed comparison of postcranial elements of *Hypohippus* or *Megahippus* has not been reported. Thus, all postcranial elements of large anchitherine equids housed at the UCMP and AMNH are listed as *Megahippus* or *Hypohippus* undifferentiated.

Megahippus mckennai

Prior to this study, all specimens of *Megahippus mckennai* were thought to be from the upper member of the Barstow Formation (Woodburne et al. 1990; Tedford et al. 2004; Pagnac 2005; 2009). A review of information on specimen labels indicates that specimens of *Megahippus* are all from strata that represent the upper member of the Barstow Formation, except BAR 247-23 (Figure 7) which is from Skyline Quarry in the upper most part of the middle member (Figure 2).

RAM 910, holotype of *Megahippus mckennai*, partial skull with both left and right P1-M3 and left I1-I2 (Figure 3; measurements in Table 1); RAM locality V98004 (equals UCR locality 3695). Collected in 1957 about 30 meters below the *Hemicyon* Tuff in the upper member at about the same

stratigraphic level as Easter Quarry (Lofgren and Anand 2010).

RAM 7454, partial maxilla with 6 complete or partial teeth from heavily weathered maxilla fragment (Figure 9) collected in 2005 from RAM locality V98004. Due to heavy wear, only the P3 and P4 could be identified. Measurements of this specimen match favorably with those of *Megahippus* from the Barstow Formation, but there is overlap in size between *Hypohippus* and *Megahippus*. We list RAM 7454 here only because it is from the same locality as the holotype; it could represent *Hypohippus affinis* as well.

FAM 21080, left P1-P4, no bone connects the teeth but all appear to be from a single maxilla (no locality or collection date listed). Lingual cingula are present on all premolars.

FAM 21081, partial right maxilla with P1-P4, P1 heavily damaged (no locality or collection date listed). Lingual cingula present on P2-P4.

FAM 21083, left and right maxilla fragments with left P2-M2 and right P1-M3 with lingual cingula (Figure 6) (no locality or collection data)

FAM 21085, partial skull with right I 1-2, C, P1-M3 and left I 1-3, C, P1-M3 (Figures 4, 5) from *Hemicyon* Quarry, upper member. Has large spaulate incisors and lingual cingula are present on P3-P4 and weakly developed on the molars. Also included with this catalog number are two vertebrae fragments, the head of a femur, and a patella.

AMNH 143242 (BAR 198-6), partial skull with left and right P1- M3, *Hemicyon* Stratum near the Old Mill, 1931, upper member. The P1s, P2, and right P3 are heavily damaged, but some teeth can still be measured. Weakly developed lingual cingula are present on the molars and premolars.

BAR 280-586, maxilla with P1-M3, May Day Quarry, 1933, upper member. P2-M3 have weak, but continuous lingual cingula.

BAR 279-582, left P1-P4 and four damaged right cheek teeth, May Day Quarry, 1933, upper member. The left premolars have lingual cingula.

BAR 279-1, partial maxilla with left P3-M3 (right M2 in same box,

Table 2. Measurements of the lower dentition of selected large anchitherine equids from the Barstow Formation. The small species of *Hypohippus*, (*Hypohippus* aff. *H. osborni*) from Skyline Quarry compares favorably to *Hypohippus osborni*.

	AMNH <i>M. mckennai</i> and <i>H. affinis</i>	RAM 15061 <i>H. affinis</i>	AMNH Small <i>Hypohippus</i>	Paratype <i>H. osborni</i>
p1 Length				
Number	1	1	1	1
Range	7.33	9.06	8.75	8.55
Mean				
p1 Width				
Number	1	1	1	1
Range	6.11	7.66	5.77	6.08
Mean				
p2 Length				
Number	9	1	2	2
Range	24.71-30.63	30.34	19.28-19.93	23.61-23.62
Mean	27.56		19.61	23.62
p2 Width				
Number	8	1	2	2
Range	15.30-17.68	17.64	12.50-13.71	13.70-14.00
Mean	16.58		13.11	13.87
p3 Length				
Number	9	1	3	2
Range	23.47-30.60	26.62	18.64-21.25	24.14-24.34
Mean	27.14		20.30	24.24
p3 Width				
Number	8	1	2	2
Range	15.79-20.26	18.63	14.96-16.83	15.51-15.97
Mean	17.7		15.9	15.74
p4 Length				
Number	9	1	4	2
Range	24.14-31.36	27.28	20.42-22.12	24.71-24.93
Mean	27.98		21.24	24.82
p4 Width				
Number	8	1	3	2
Range	15.42-19.93	18.92	16.57-18.60	16.00-16.14
Mean	18.13		17.35	16.07

Table 2 (continued)

m1 Length				
Number	4	1	4	2
Range	26.00-29.80	27.71	20.65-21.90	24.34-24.89
Mean	27.78		21.47	24.62
m1 Width				
Number	3	1	2	2
Range	18.30-19.59	17.17	16.09-17.53	15.28-15.33
Mean	19.12		16.81	15.31
m2 Length				
Number	4	1	4	2
Range	25.13-28.29	27.18*	20.08-21.32	23.68-24.21
Mean	26.72		20.75	23.95
m2 Width				
Number	4	1	4	2
Range	16.47-18.49	16.19*	14.55-16.68	14.04-14.61
Mean	17.48		15.25	14.33
m3 Length				
Number	2		2	2
Range	27.11-31.95		22.98-23.09	21.15-21.61
Mean	29.53		23.04	21.38
m3 Width				
Number	2		2	2
Range	13.52-15.96		13.70-13.74	11.77-12.24
Mean	14.74		13.72	12.01

*estimate

Specimens measured include:

--*M. mckennai* and *H. affinis*: BAR 291-904, BAR 296-1070, BAR 298-1145, FAM 21092, FAM 21098, FAM 21097, FAM 21096, FAM 21090.--RAM 15061, partial dentary with p1-m2 of *H. affinis*?--Small *Hypohippus* (*Hypohippus* aff. *H. osborni*): BAR 267-282, BAR 391-3619, BAR 255, BAR 251-A.--Paratype of *H. osborni*. (AMNH 9395), left p2-m3 and right p1-m3.

uncertain if part of same maxilla), May Day Quarry, 1933, upper member. Partially prepared specimen with P3-4 prepared and M1-3 mostly covered in matrix. A lingual cingulum can be seen in some of the cheek teeth.

BAR 247-23, partial right maxilla with P2-P4 (Figure 7), Skyline Quarry, second division, 1932, middle member. This partially prepared specimen has lingual cingula on its premolars.

BAR 296-1070, partial left and right dentaries with left i1-3 and p2-m3 (m3 erupting) and right i1-3 (Figure 8), New Year Quarry, 1934, upper member. This specimen has large and wide incisors and probably represents the lower dentition of *Megahippus*.

Hypohippus affinis

Hypohippus affinis occurs in both the upper and middle members of the Barstow Formation and is the only species of the genus reported from Barstow Formation strata (Pagnac 2005; 2009). This identification is based on the large size of the Barstow anchitherine material and that Barstow Formation upper molars are transversely wide, like upper molars of *H. affinis* from the Burge Fauna (Pagnac 2005). As noted above, four specimens from Skyline Quarry (uppermost middle member) were distinctly smaller than other specimens of *Hypohippus* or *Megahippus*. These specimens are listed as *Hypohippus* aff. *H. osborni*. Based on all available information, specimens of *Hypohippus affinis* are all from strata that represent the middle and upper members of the Barstow Formation.

RAM 6904, partial maxilla with right and left P1-M1 (Figure 10; measurements in Table 1), RAM locality V94040, collected in 1993, middle member. This specimen lacks lingual cingula on P3-M1.

RAM 15061, partial dentary with p1-m2 (Figure 11; measurements in Table 2), RAM locality V94040, collected in 2012, middle member. This specimen consists of a well-preserved dentary whose m1 is unworn and m2 is erupting. The very high crown of the m1 suggests that this is *H. affinis*.

RAM 14689, premaxilla with left I1-2 and right I1-3 (Figure 12), RAM locality V95082, collected in 1998, Oreodont Quarry, middle member. Based on size, this specimen represents a large anchitherine equid, whose relatively small incisors distinguish it from *Megahippus*.

FAM 21082, palette with right P2-4 and left P2-4, P2s heavily damaged and right M1 erupting but heavily damaged, (no locality or collection data). Lingual cingula on P2s only.

FAM 21084, partial maxilla with left P2-4, *Hemicyon* Stratum, upper member. P2 has a partial lingual cingula.

FAM 21086, skull parts with tooth fragments, right P2-4, left DP?, and partial innominate, *Hemicyon* Stratum, upper member. P2 has a lingual cingula, but P3-4 do not.

FAM 21087, right maxilla with P1-M1 and isolated left M3 (no locality or collection data). P1-3 heavily damaged, M1 with anterior labial damage and no lingual cingula.

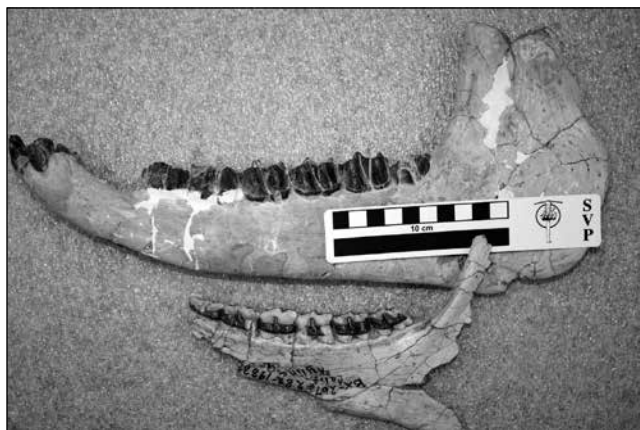


Figure 8. Labial view of Bar 267-282, left dentary fragment of *Hypohippus* aff. *H. osborni* with p2-m3 (below), and labial view of BAR 267-1070, left dentary of large anchitherine, *Megahippus mckennai* (above).

FAM 21089 (specimen tag indicates that this material may or may not represent FAM 21089), lower molar and five damaged upper teeth; three lefts and two rights (no locality or collection data). Lingual cingula damaged on all but two upper teeth and the undamaged ones have no lingual cingula

FAM 21090, left dentary with p2-4, right dentary with p2-4, two isolated incisor fragments, and astragulus (no locality or collection data). The incisors are too small to be *Megahippus* and appear to be associated with the dentaries.

AMNH 143241 (Box 196-21), maxilla with left and right P2-P4, *Hemicyon* Stratum, 1931, upper member. Has lingual cingula on P2s only.

BAR 247-24, partial skull with two loose incisors lying on diastema, left C, P1-M3 and right C, P1-M3 (Figure 5), Skyline Quarry, second division, 1932, middle member. Lingual cingula present only on P2 and incisors relatively small.



Figure 10. Occlusal view of RAM 6904, partial maxilla of *Hypohippus affinis* with left and right P1-M1.



Figure 9. Occlusal view of RAM 7454, a damaged maxilla of *Megahippus mckennai*, with P2 and P3 and four other partial teeth.

BAR 95-51, partial skull with left P1-M3 and right P2-M3; proximal phalange, north end of formation, layer #3, 1928. No lingual cingula on teeth except for P2s.

BAR 289-862, partial skull with left P1-P4 and right P1 to P3, May Day Quarry, 1934. Lingual cingula on P2s only.

BAR 96-28, partial maxilla with P2-M2 (heavily damaged), layer #3, North End, 1928, probably upper member. No lingual cingula on P3-M2 when lingual part of tooth is preserved.

BAR 268-3237, partial skull with rostrum lacking incisors and canines with left P2-P4, M1 erupting, and right P2-4, Skyline Quarry, 1933, middle member. No lingual cingula present except on P2s.

BAR 81, right maxilla fragment with P2 and damaged P3, no locality data. Lingual cingulum present on P2, but not P3.

BAR 95-54, upper left P4 or M1 or M2, north end, 1928, probably upper member. Specimen lacks a lingual cingulum so probably represents *Hypohippus*.

BAR 37 (Feb 5/24), left upper tooth but not a P2, bottom layer. Tooth lacks a lingual cingulum.

Hypohippus aff. *H. osborni*

H. affinis is the largest *Hypohippus* species and *H. osborni* is significantly smaller. Measurements of these four specimens indicate a second species of *Hypohippus* is probably present in the Barstow Formation that is about the size of



Figure 11. Labial view of RAM 15061, partial dentary of *Hypohippus affinis?* with p1-m2.



Figure 12. Occlusal view of RAM 14689, partial premaxilla of *Hypohippus affinis* with left I1-I2 and right I1-I3.

H. osborni (Table 2). All four specimens are from Skyline Quarry and are referred to *Hypohippus* aff. *H. osborni*.

BAR 391-3619, left dentary with p1-m3, Skyline Quarry, 1937.

BAR 255, right dentary with p4-m2, Skyline Quarry, 1933.

BAR 251-A, maxilla with p3-m3, Skyline Quarry, upper second division, 1932-33.

BAR 267-282, left dentary fragment with p2-m3 (Figure 8), Skyline Quarry, 1933.

***Hypohippus* or *Megahippus* undifferentiated**

RAM 9358, left dentary with p2-p3 and right dentary with p2-p4 (Figure 13), RAM locality V200511, collected in 2006, upper member.

LACM 35362, left dentary with m1-m2, Rainbow Basin.

UCMP 311371, maxilla fragment with broken roots of two teeth, approximately 20 meters above *Hemicyon* Tuff, upper member.

UCMP 21468, a few limb bones, UCMP localities 1398 and 2056.

UCMP 323131, proximal end of lateral metapodial, locality RV 6786 (RAM 5101, 5102 or 5103), bone has BAR-8 (or BAR-B) written on it.

UCMP 323129, distal end of metapodial, locality RV 6786 (RAM 5201, WS 128 written on it).

UCMP 323130, proximal phalange, locality RV 6786 (RAM 5101, 5102 or 5103).

UCMP 311420, medial phalange, locality RV 5904 (RAM 5904).

UCMP 29397, distal tibia, proximal and medial phalange, distal metapodial fragment, three proximal phalanges and two medial phalanges, medial phalange, astragalus, Rodent Hill Basin #1, 2056 or locality 1400. These specimens were in four separate specimen boxes all numbered UCMP 29397. Two locality numbers were given, 2056 and 1400.

UCMP 114794, calcaneum, locality 1398.

UCMP 35590, phalange, Site 14, 1400.



Figure 13. Labial view of RAM 9358, partial left dentary with left p2-p3 (above) and lingual view of right dentary with p2-p4 (below) of *Hypohippus* or *Megahippus*.

UCMP 80623, distal metapodial fragment, locality 1400.

UCMP 80652, distal metapodial fragment, locality 1400.

UCMP 21216, proximal and medial phalange, Coon Canyon #1, site 24, figured by Merriam (1919;fig. 29).

UCMP 21220, proximal phalange, Coon Canyon #1, site 24, locality 2056.

UCMP 21406, proximal metacarpal fragment.

UCMP 21466, medial phalange, locality 2056.

UCMP 80668, proximal metatarsal fragment, locality 2056.

UCMP uncataloged, astragalus, locality 2056.

UCMP 21214, partial maxilla with broken molar, Coon Canyon 1, locality 2056. Referred to *Megahippus mckennai* by Tedford and Alf (1962), but too fragmentary to be listed under *Megahippus*.

UCMP 21215, left dentary fragment with m1-2, locality 2060, short ravine, upper member. Figured by Merriam (1919;fig. 28) and referred to *Megahippus mckennai* by Tedford and Alf (1962). But as noted here, lower molars of *Hypohippus* and *Megahippus* can't be distinguished.

UCMP 323270 (was UCR 23270), partial m3, Webb Quarry 5 (equals RAM V94026), middle member.

UCMP specimen? (was UCR 3696-1), damaged left M1-2, UCR locality 3696, upper member. Referred to *Megahippus mckennai* by Tedford and Alf (1962), who state the teeth lack their labial and lingual borders. Specimen was not found in UCMP collections, but upper molars without the lingual tooth border cannot be assigned to either *Hypohippus* or *Megahippus* with confidence.

FAM 21091, left jaw fragment with p2-4 (no locality or collection data)

FAM 21092, right jaw fragment with p2-4, m1 erupting (no locality or collection data).

FAM 21093, left jaw fragment with p2-4 with m1 erupting (no locality or collection data).

FAM 21094, left jaw fragment with p2-3, p4 missing, m1 erupting (no locality or collection data).

FAM 21095, right jaw fragment with p2-m3, m2-3 heavily damaged and left jaw fragment with heavily damaged m3, distal radius, and assorted bone fragments (no locality or collection data).

- FAM 21096**, right jaw fragment with p2-3 (no locality or collection data).
- FAM 21097**, right jaw fragment with p2-m2 (no locality or collection data).
- FAM 21098**, right jaw fragment with p4-m3 (no locality or collection data).
- FAM 21099A**, left jaw fragment with erupting tooth (no locality or collection data).
- AMNH 143243 (BAR 198-8)**, right dentary with p2-m2 (some teeth damaged), *Hemicyon* stratum, near Old Mill, 1931, upper member.
- BAR 298-1145**, partial left dentary and symphysis, with canines erupting and p2-4, New Year Quarry, 1934, upper member.
- BAR 306-1401**, partially prepared maxilla with three fragmentary teeth, Rainbow Quarry Prospect, 1935, upper member. Teeth are too damaged lingually to determine if lingual cingula were present.
- BAR 199-21**, partial left dentary with tooth fragment, *Hemicyon* stratum, 1931, upper member.
- BAR 199-20**, left jaw with ?p2-3, *Hemicyon* stratum, 1931, upper member.
- BAR 321-1694**, left jaw fragment with p2-m1?, Leader Quarry, north end locality, 1935, upper member. Teeth are worn and heavily damaged.
- BAR 99-30**, left lower tooth (not a p2 or m3), north end of formation, layer #3, Green Hills, 1928, probably upper member.
- BAR 95-61**, upper tooth fragment with no lingual cingula, lower tooth fragments, patella, and phalange, north end of formation, 1928, probably upper member.
- BAR 96-38**, left m3 fragment, layer #3, north end, 1928, probably upper member.
- BAR 96-30**, right dentary fragment with tooth, layer #3, north end of formation, 1928.
- BAR 95-65**, incisor, layer #2, north end of formation, 1928.
- BAR 295-1049**, medial metatarsal, New Year Quarry, 1934, upper member.
- BAR 267-272**, left dentary with ?p2-4, isolated canine and incisor, Skyline Quarry, 1932, middle member. Specimen is unprepared.
- BAR 23**, upper tooth, tuff division, north of pottery house, north end of formation, 1923, probably upper member.
- BAR 52**, three lower tooth fragments (no locality or collection data).
- BAR 93-2**, three metatarsals (medial and laterals); white layer, 1927.
- BAR 94**, left and right calcaneum, astragalus, five phalanges (four proximal and one medial), left maxilla fragment with two partial teeth (probably P4-M1 or M1-2), White Operation (Rak's white layer), half mile below cabin, 1927. Upper teeth too damaged to determine if lingual cingula were present.
- BAR 291-904**, partial right dentary with p1-m3, New Year Quarry, 1934, lower 1st Division, upper member.
- BAR 407-3990**, partial tibia with distal end, New Year Quarry, 1935.
- BAR 220-20**, left and right dentary fragments in an indurated block of red sandstone, four-five right teeth and four left teeth partially exposed, layer above cabin, 1932.
- BAR 251-23**, dentary and tooth fragments, Skyline Quarry, 1932, middle member.
- BAR 280-594**, unprepared left dentary with p2-m3 and five upper deciduous premolars (two lefts and three rights) sitting on top of jaw, May Day Quarry, 1933, upper member.
- BAR 220**, proximal phalange, north end, 1932, probably upper member.
- BAR 196-31**, medial phalange, north end quarry, 1931, probably upper member.
- BAR 173**, calcaneum, lower layer, north end, 1930 probably upper member.
- BAR 280-600**, unprepared left dentary fragment with ?p2-m1, May Day Quarry, 1932, upper member.
- BAR 181-27**, left and right dentary fragments glued together to form one jaw, anterior part of dentary is a left with p2, posterior part of dentary is a right with p2-p4, north end, lower layer, 1930.
- BAR 199-10**, partially prepared right dentary fragment with six partially exposed teeth (teeth heavily worn and damaged), probably p2-m3, north end quarry (E), 1931, probably upper member.
- BAR 282-698A**, left dentary fragment with four broken teeth, May Day Quarry, upper second division, 1933, upper member.

Discussion

Megahippus and *Hypohippus* are rarely found in the Barstow Formation as over 150 trips by RAM crews to these strata since 1992 has only yielded five specimens. Our survey of the AMNH, UCMP, and LACM collections, combined with the RAM specimens, shows that the Barstow sample of large anchitherine equids equals about 100 specimens that apparently represent three taxa; *Hypohippus affinis*, *Hypohippus* aff. *H. osborni*, and *Megahippus mckennai*. Determining the stratigraphic distribution of the three taxa is limited by the large number of specimens that cannot be confidently assigned to either genus (including all postcranial specimens). Also, about 27% of AMNH/FAM specimens lack locality data, and many UCMP specimens collected early in the 20th century have locality numbers that correspond to a fairly broad geographic area (e.g. UCMP 1398, 1400, 2056). With these limitations in mind, the stratigraphic distribution of *Megahippus mckennai* is from the uppermost part of the middle member (Skyline Quarry), up to just below the *Hemicyon* Tuff (*Hemicyon* Quarry/*Hemicyon* Stratum) in the upper member. It is also reported from higher in the Barstow Formation (Pagnac 2009;fig. 3). In either case, *Megahippus mckennai* has a stratigraphic interval corresponding to the Ba2 Biochron (Figure 2). *Hypohippus affinis* occurs at least as low as Oreodont Quarry (based on RAM 14689) and it is also reported from Steepside Quarry about 35 meters below Oreodont Quarry (Pagnac 2009;fig.

3). Both occurrences are low in the middle member. *Hypohippus affinis* occurs at least as high as the *Hemicyon* stratum in the upper member (Pagnac 2009), giving the species a stratigraphic interval corresponding to the Ba1 and BA2 biochrons (Figure 2). *Hypohippus* aff. *H. osborni* only occurs in the upper most part of the middle member (Skyline Quarry), a stratigraphic interval corresponding to the Ba1 Biochron. Based on Barstow Formation specimens, *Megahippus mckennai* occurs in the late Early Barstovian-Late Barstovian, *Hypohippus affinis* in the Early-Late Barstovian, and *Hypohippus* aff. *H. osborni* in the late Early Barstovian (Figure 2).

Our reported occurrence of *Megahippus mckennai* at Skyline Quarry (BAR 247-13; Figure 7) is a stratigraphic range extension for this taxon, downward into the uppermost part of the middle member of the Barstow Formation. Previously, its lowest stratigraphic occurrence was the lower part of the upper member, as *Megahippus mckennai* is reported from May Day Quarry and New Year Quarry (Pagnac, 2009, this study). Pagnac (2009) recently proposed a new biostratigraphic zonation of the Barstow Formation, building upon the earlier efforts of Woodburne et al. (1990) and Tedford et al. (2004). In the definition and characterization of the Ba2 Biochron, the lowest occurrence of *Megahippus mckennai* was used to define the base of the *Megahippus mckennai* /*Merycodus necatus* Interval Zone (Pagnac 2009). The lowest occurrence of *Megahippus mckennai* was defined as New Year Quarry, which is about 20 meters above the Skyline Tuff (Pagnac 2009). Skyline Quarry is about one meter below the Skyline Tuff and based on BAR 247-23 (Figure 7), *Megahippus mckennai* is present. Thus, another taxon should replace *Megahippus mckennai* as the defining taxon for the base of the *Megahippus mckennai* /*Merycodus necatus* Interval Zone. Range extensions of Barstow Formation taxa are to be expected over time as new field discoveries are made and existing collections are restudied. For example, the lowest stratigraphic occurrence of *Gomphotherium* in the Barstow Formation was a tooth (FAM 20850A) from *Hemicyon* Quarry. But in 2007, an M2 of *Gomphotherium* was collected at RAM locality V98004, a site about 30 meters below the tuff that underlies *Hemicyon* Quarry (Lofgren et al. 2012).

Regionally, *Megahippus* occurs throughout the Great Plains and Great Basin, while *Megahippus mckennai* has a much more limited distribution occurring at a few sites in Nebraska and Nevada (MacFadden 1998), as well as the Barstow Formation. *Hypohippus* has a much broader distribution and is known from Florida to California, and Texas to Saskatchewan (MacFadden 1998). The closest well documented occurrences of *Hypohippus affinis* and *Hypohippus osborni* to southern California are from the Stewart Spring and Tonopah local faunas of western Nevada (MacFadden 1998), whose strata are about the same age as the Barstow Formation (Tedford et al. 2004). Interestingly, *Hypohippus affinis* and *Hypohippus osborni* are also both known from the Tonopah Local Fauna (Henshaw 1942;

MacFadden 1998), a situation similar to that of *Hypohippus affinis* and *Hypohippus* aff. *H. osborni* from Skyline Quarry (in the latter case, *Megahippus mckennai* also is present). The only other rock unit where all three occur is the Valentine Formation of Nebraska (MacFadden 1998).

One purpose of our survey of the large anchitherine equids from the Barstow Formation is to document specimens present in museum collections, which have, in some cases, remained unreported for numerous decades. It is rare that larger bodied Miocene mammals from a single stratigraphic unit receive a detailed systematic treatment; an example is the Barstow mammalian megafauna (Pagnac 2005). At the AMNH there are many well preserved specimens of a very large species of *Hypohippus* that is unofficially labeled "*Hypohippus giganteus*" from the Ash Hollow Formation in Cherry County, Nebraska. "*Hypohippus giganteus*" is significantly larger than *H. affinis*, but remains undescribed. This and other related systematic projects should be undertaken so the diversity and distribution of large anchitherine equids in North America can be more accurately documented.

Acknowledgements

We thank J. Shearer of the California Bureau of Land Management for assistance with permits, J. Meng, R. O'Leary, and J. Galkin of the AMNH and P. Holroyd and M. Goodwin from the UCMP for access to specimens, and S. McLeod and J. Harris of the LACM for access to and loan of specimens, and the Mary Stuart Rogers Foundation and the David B. Jones Foundation for financial support.

References cited

- Barbour, E. H. 1914. A new fossil horse, *Hypohippus matthewi*. Nebraska Geological Survey 4:169-173.
- Gidley, J. W. 1907. Revision of the Miocene and Pliocene Equidae of North America. Bulletin of the American Museum of Natural History 23:865-934.
- Lindsay, E. H., 1972. Small mammal fossils from the Barstow Formation, California. University of California Publications in Geological Sciences 93:1-104.
- Lofgren, D. L., and R. S. Anand, 2010. 75 years of fieldwork in the Barstow Formation by the Raymond Alf Museum of Paleontology. Pp. 169-176, in Reynolds, R. E. and D. M. Miller (eds.), Overboard in the Mojave, 20 million years of lakes and wetlands. Desert Studies Consortium, California State University, Fullerton.
- Lofgren, D. L., Hess, A., Silver, D. and P. Liskanich. 2012. Review of proboscideans from the middle Miocene Barstow Formation of California. p. 125-134, in R. E. Reynolds (ed.), Search for the Pliocene: the southern exposures. Desert Symposium Field Guide and Proceedings, California State University, Fullerton.
- Matthew, W. D. and J. W. Gidley. 1906. New or little known mammals from the Miocene of South Dakota. Bulletin of the American Museum of Natural History 22:135-153.
- MacFadden, B.J. 1992. Fossil horses, systematics, paleobiology, and evolution of the family Equidae. Cambridge University Press, Cambridge, United Kingdom, 369pp.

- Mac Fadden, B. J. 1998. Equidae, p. 537-559, in C.M. Janis, K. M. Scott, and L. L. Jacobs (eds.), Evolution of Tertiary Mammals of North America, Volume 1: Terrestrial carnivores, ungulates, and ungulatelike mammals. Cambridge University Press, Cambridge, United Kingdom.
- McGrew, P. O. 1938. The Burge Fauna, a lower Pliocene mammalian assemblage from Nebraska. University of California Publications Bulletin of the Department of Geological Sciences 24:309-328.
- Merriam, J. C., 1919. Tertiary mammalian faunas of the Mohave Desert. University of California Publications in Geological Sciences 11:437a-437e, 438-585.
- Osborn, H. F. 1918. Equidae of the Oligocene, Miocene, and Pliocene of North America. Memoir of the American Museum of Natural History 2:1-217.
- Pagnac, D. C., 2005. A systematic review of the mammalian megafauna of the middle Miocene Barstow Formation, Mojave Desert, California (PhD dissertation). University of California-Riverside. 384 pp.
- Pagnac, D. C., 2009. Revised large mammal biostratigraphy and biochronology of the Barstow Formation (Middle Miocene), California. *Paleobios* 29:48-59.
- Steinen, R. P., 1966. Stratigraphy of the middle and upper Miocene, Barstow Formation, California. (m.s.thesis): University of California-Riverside, 150 pp.
- Stirton, R. A. 1940. Phylogeny of North American Equidae. University of California Publications Bulletin of the Department of Geological Sciences 25:2165-2198.
- Tedford, R. H., and R. M. Alf, 1962. A new *Megahippus* from the Barstow Formation San Bernardino County, California. Bulletin of the Southern California Academy of Sciences 61:113-122.
- Tedford, R. H., Albright III, L. B., Barnosky, A. D., Ferrusquia-Villafranca, I., Hunt Jr., R. M., Storer, J. S., Swisher II, C. C., Voorhies, M. R., Webb S. D., and D. P. Whistler, 2004. Mammalian biochronology of the Arikarean through Hemphillian interval (late Oligocene through early Pliocene epochs). Pp. 169-231, in M. O Woodburne (ed.), Late Cretaceous and Cenozoic mammals of North America. Columbia University Press, New York.
- Woodburne, M. O., Tedford, R. H. and C. C. Swisher III, 1990. Lithostratigraphy, biostratigraphy, and geochronology of the Barstow Formation, Mojave Desert, southern California. Geological Society of America Bulletin 102:459-477.

Calico—a brief overview of mining history

Larry M. Vredenburg

Bureau of Land Management, Bakersfield, California

The story of Calico begins at Waterman mine, located four miles north of Barstow, and nine miles west of Calico. In 1876 George G. Lee, a local prospector, discovered what he thought was mercury ore. After prospecting the property he died (probably murdered) on the desert in the fall of 1879. Robert W. Waterman, a leading farmer in the San Bernardino Valley (and a future governor) and geologist John L. Porter visited the Lee property in mid-1880. In December, they found silver in samples taken from the claims, and staked out the area. Operations began at once. By summer 1881 a 10-stamp mill had been constructed, as well as a settlement. Before the mill was constructed, fabulously rich ore (reportedly assaying up to \$3,000) per ton was shipped to San Francisco for processing [anyone interested in the history of this mine should read Lingenfelter's 2012 account of these events].

News of the silver discovery made by Waterman and Porter at George Lee's old mine spread quickly; prospectors fanned out and staked hundreds of new locations. Almost daily groups of San Bernardino residents set out into the desert, and reported their finds to an eager press in Colton and San Bernardino.

On April 6th the Silver King was staked by San Bernardino residents, Frank Meacham, George Yager, Meacham's uncle; and Tom Warden and Huse Thomas, sheriff's deputies. They were grubstaked by San Bernardino County Sheriff John C. King (an uncle to Walter Knott) and Ellis Miller, the owner of Grapevine Station and ranch. The samples collected while staking this claim contained some silver, but certainly nothing

to get excited about. But in late June, Meacham's brother Charles returned to the claim with Hieronymus Hartman and Huse Thomas. High on the east end of the claim Charles broke off a sample that caught his attention. Taking out his knife he found odd blisters that could be cut like a lead bullet. It was horn silver. Recognizing his discovery, he broke off a number of samples, all which contained these "blisters." It was with this discovery the rush to the Calico Mountains began in earnest.

In October 1882 the Silver King Mine was leased to the owners of the Oro Grande mill, which was located forty miles up the Mojave River near the present location of Victorville. In January 1883, the company completed an impressive ore chute and bin at the Silver King mine, above the town of Calico. Immediately after construction of the chute, mule-drawn wagons began hauling ore through town headed to the Oro Grande mill.

In early 1884 the Oro Grande Company (the second with that name) purchased the King Mine and Oriental Company's mine and mill near Daggett. After enlarging the Daggett mill to 15 stamps, the ore wagons to Oro Grande ceased. During the period of time the Oro Grande mill was running on ore from the Silver King mine, about \$50,000 per month was produced.

By the end of 1884, the district had taken shape geographically: immediately north of Calico camp, on King Mountain, were the Silver King, Oriental, Burning Moscow, Red Cloud, and other mines. The northeast, in the vicinity of Odessa Canyon, were the mines of "East Calico;" including the Garfield, Odessa, Bismarck,

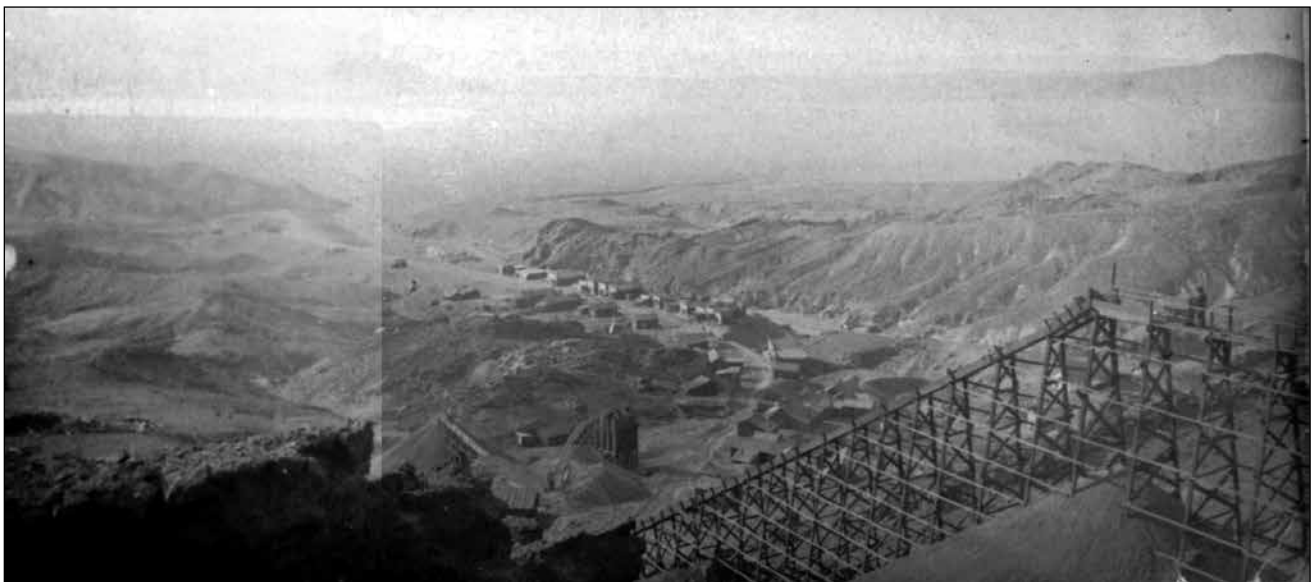


Figure 1. View of Calico from the Silver King Mine. R. V. "Penny" Morrow collection.

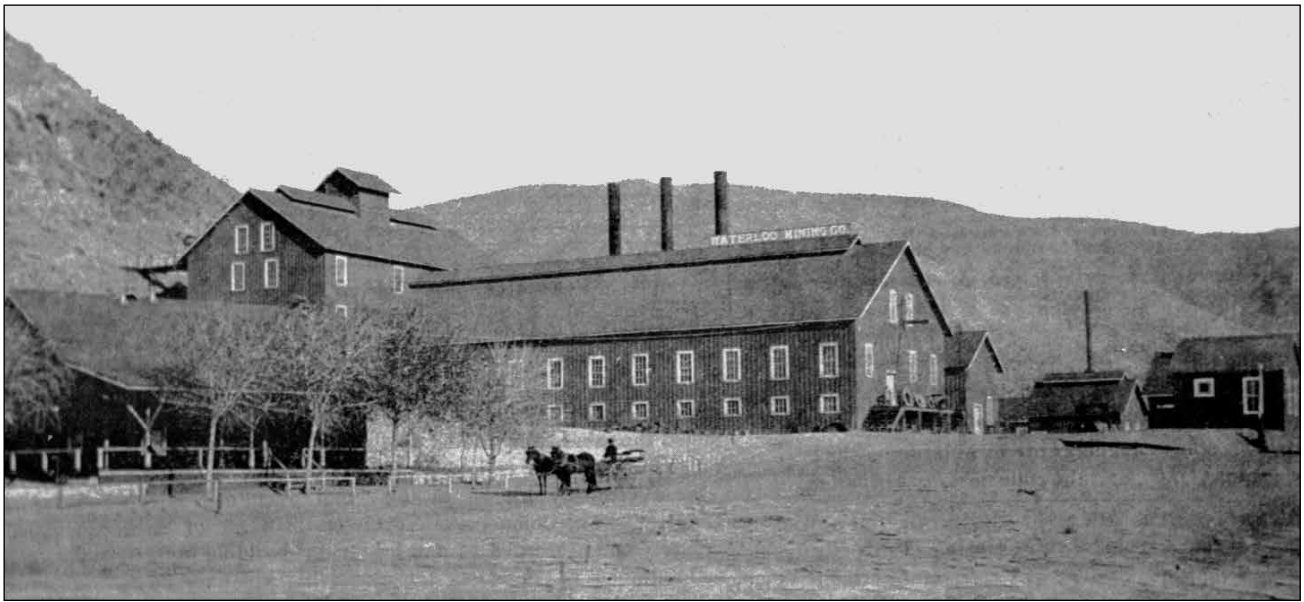


Figure 2. Mills of the Waterloo Mining Company, San Bernardino County. Mining & Scientific Press: May 12, 1894, p. 289.

Blackfoot, Thunderer and Occidental; and to the west and northwest lay “West Calico,” with ultimate development of the Waterloo, Sue, Langtry, and other mines.

It is difficult to fix a date for the beginning of Calico’s decline. As early as the first months of 1885 the mines were mostly extracting low-grade ore. The faint signs of dull times were growing obvious as 1885 passed. The King’s output of \$302,000 in 1885 was down sharply from the \$507,000 produced in 1884. During 1886 production fell to \$120,000.

In 1887 the Oro Grande Company spent \$250,000 to further enlarge the mill at Daggett to 60 stamps, but in August as it neared completion the mill burned to the ground.

In March 1888, the Oro Grande Company started work on a seven-mile, narrow-gauge railroad from Daggett to the Waterloo Mine’s ore bins. The reconstructed mill and the railroad were completed later that year. Two small locomotives would ease cars loaded with ore down the grade to Daggett and return with supplies and timbers. The completion of the line cut the cost of hauling from \$2.50 a ton (by wagon) to as little as seven cents a ton.

Not surprisingly, with the decline in the grade of ore, the economy of scale favored the corporate influence on Calico’s mining industry over individual leasees or “chloriders.” The Oro Grande Company was reorganized as the Waterloo Mining Company in February 1889. The company owned the Waterloo mines and mill and other properties, notably the Silver King Mine and its mill. The Waterloo Company built a branch of the railroad past the town to the ore bins at the Silver King Mine in 1889. Meanwhile, several properties owned by J. S. Doe and Company of San Francisco, notably the Odessa,

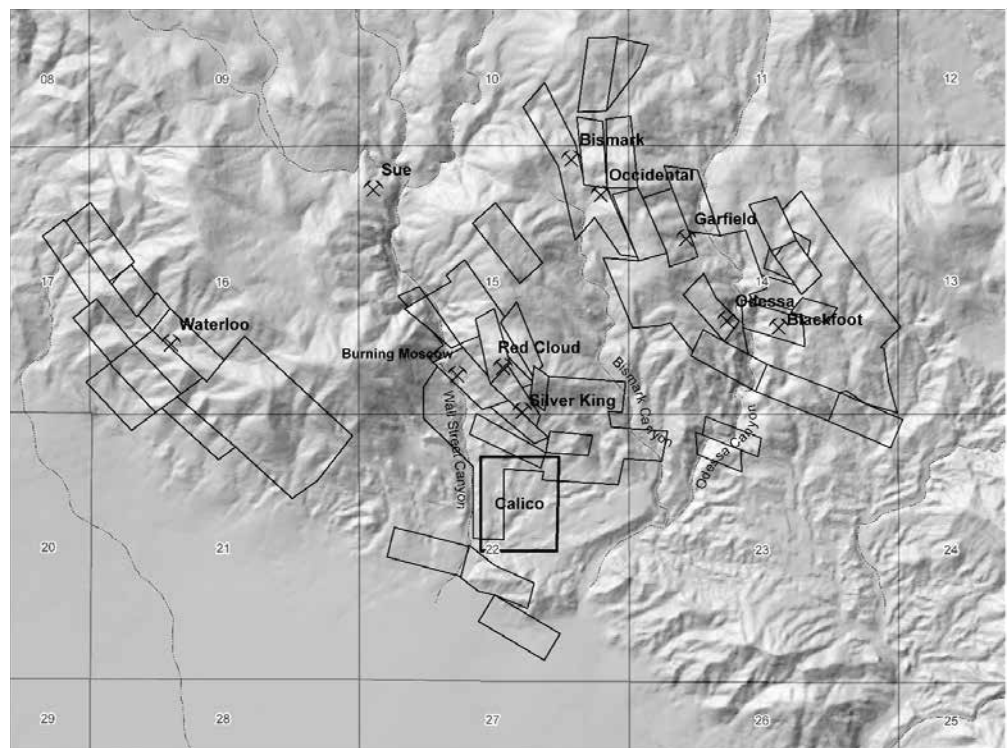


Figure 3. Calico Silver Mining District, map showing patented mining claims. Derived from BLM records.

Table 1. Patented Mining Claims of the Calico Silver Mining District						
Patent Number	Patent Date	Section	Mineral Survey	Claims	Acres	Patentee
13990	4/8/1890	14	MS 2329	Blackfoot Consolidated No. 1	14.64	Hart Samuel
14158	6/25/1888	22	MS 2371	Oregon Quartz Mine	12.64	Oro Grande Mining Co
14456	11/3/1888	16	MS 2406	Waterloo Quartz Mine	18.69	Oro Grande Mining Co
14494	11/21/1888	14	MS 2330	Blackfoot Consolidated No. 2	7.04	Hart Samuel
14495	11/21/1888	14	MS 2331	Blackfoot Consolidated No. 3	2.03	Hart Samuel, Locan, F
16827	11/19/1890	15	MS 2592	Red Cloud Quartz Mine	17.83	Doe John S
16828	11/19/1890	22	MS 2593	Gray Carbonate	7.99	Doe John S
16829	11/19/1890	14, 15	MS 2597	Thunderer Quartz Mine	19.07	Doe John S
16830	11/19/1890	14	MS 2596	Run Over Quartz Mine	20.63	Doe John S
16831	11/19/1890	10, 15	MS 2598	Occidental No. 1	17.81	Doe John S
16832	11/19/1890	10, 11, 14, 15	MS 2599	Occidental No. 2	18.112	Doe John S
16900	12/4/1890	14	MS 2595	Garfield Quartz Mine	19.68	Doe John S
17013	1/10/1891	15, 22	MS 1941	Silver King Quartz Mine	7.25	Bradley Charles T, Metcalf William H, Sanger Casper M, Wells Daniel Jr.
17689	4/20/1891	15	MS 2549	Mastodon Quartz Mine	10.63	Felt Paul
17841	5/6/1891	14, 23	MS 2544	Mountain View Quartz Mine	38.431	Oro Grande Mining Co
17841	5/6/1891	14, 23, 24	MS 2545	Snow Bird Quartz Mine	38.431	Oro Grande Mining Co
18487	8/10/1891	16	MS 2796	Gem Silver Mine	9.79	Waterloo Mining Co
18488	8/10/1891	15	MS 2641	Old Oriental Quartz Mine	20.54	Doe John S
18648	10/6/1891	16, 17	MS 2769	Illinois Quartz Mine	16.01	Waterloo Mining Co
19048	12/5/1891	23	MS 2767, MS 2771	Non-Parallel Mine, Belle Key Quartz Mine	18.23	Waterloo Mining Co
19331	1/8/1892	16, 17, 21	MS 2765, MS 2770	Daggett Quartz Mine, Compass Quartz Mine	36.4	Waterloo Mining Co
19332	1/8/1892	22	MS 2877	Millsite Quartz Mine	20.62	Doe John S
19505	1/20/1892	22	MS 2911	Try Quartz Mine	19.24	Waterloo Mining Co
19506	1/20/1892	22	MS 2888	Milwaukee Quartz Mine	20.66	Waterloo Mining Co
19507	1/20/1892	10, 11	MS 2889	Dana Quartz Mine	11.61	Waterloo Mining Co
19677	2/6/1892	16	MS 2772	Harmonial No. 1	13.84	Waterloo Mining Co
19679	2/6/1892	14	MS 2948	Ballast No. 2	11.57	Waterloo Mining Co
19680	2/6/1892	14	MS 2947	Ballast No. 1	12.53	Waterloo Mining Co
19681	2/6/1892	16, 17	MS 2795	Grant Quartz Mine	20.65	Waterloo Mining Co
19867	2/23/1892	15	MS 2887	Black Strap Quartz Mine	10.43	Waterloo Mining Co
20096	3/11/1892	15	MS 2332	Little Bonanza Quartz Mine	5.6	Bradley Charles T
20097	3/11/1892	14	MS 2945	Triangle #2	0.44	Waterloo Mining Co
20687	4/9/1892	14	MS 2965	Little Scottie No. 1	2.71	Waterloo Mining Co
20688	4/9/1892	10	MS 2836	Bullion Quartz Mine	18.94	Doe John S
21028	4/23/1892	14	MS 3005	Little Scottie No. 3	1.63	Waterloo Mining Co
21455	6/8/1892	15	MS 2333	Burning Moscow	11.68	Burning Moscow Mining Co
21855	8/12/1892	14	MS 2766	Alabama Quartz Mine	18.56	Oro Grande Mining Co, Waterloo Mining Co
21856	8/12/1892	16	MS 2773	Zephyr Quartz Mine	5.45	Waterloo Mining Co
25575	5/4/1895	15, 22	MS 2591	Oriental #2 Quartz Mine	6.351	Doe John S
25861	7/22/1895	14	MS 2109	Odessa Silver Mine	15.45	Odessa Silver Mining Co
27532	10/29/1896	15	MS 2854	Red Jacket Quartz Mine	13.195	Waterloo Mining Co

Table 1. Patented Mining Claims of the Calico Silver Mining District						
Patent Number	Patent Date	Section	Mineral Survey	Claims	Acres	Patentee
1067972	2/8/1934	15, 22, 23	MS 6040	Wall Street, Wall Street #1, Maggie, Lucille, Gray Carbonate #1, Oriental No. 3 Oriental No. 4 Gordon, Comstock Claim.	150.613	Zenda Gold Mining Co
1072292	9/19/1934	15	MS 6039	High Grade, Silver Star Mine, Rose, Red Cloud Extension	64.979	Zenda Gold Mining Co
1100614	1/4/1939	13, 14	MS 6189.	Golconda, Lookout, Richmond, J. R. Lane No. 1, J. R. Lane No. 2, Triangle, Lucy Lane.	118.733	Lane Lucy B
1116696	4/19/1943	14, 15	MS 6067,	Veto No. 1, Thunderer No. 1, Garfield No. 1, Esther, Krueger, Odessa Extension, Dragon, Alhambra.	162.897	Lane Lucy B
1117816	2/5/1944	10, 14, 15	MS 6062	Argentum No. 1, No. 2 & No. 4.	52.267	Britt Henry W
4710187	5/20/1971	16, 21	MS 6771	Nevada Quartz Mine	14.134	Burcham R L Heirs of Burcham Rose
4720002	7/29/1971	16, 17	MS 6770	Harmonia1 No.2, Lamar Lode	34.84	Mulcahy Joseph B
4720010	8/12/1971	16, 21	MS 6768	California, Colorado, Idaho, New Mexico, Washington, and Wyoming Quartz Mines	114.875	Burcham R L Heirs of Burcham Rose
4720045	11/23/1971	16	MS 6769	Silver Gem Extension Lode Mining Claim	0.149	Buch R C
4720090	3/15/1972	16, 21	MS 6771	Nevada Quartz Mine	14.134	Burcham R L Heirs of Burcham Rose
4760087	9/23/1976	6, 7, 8	MS 6777	Quad Duece I, II, IV, V, X, XII, XIII, XIV, Quad Duece 22, Pal No.'s 16,17,35,36, Langtry No.'s 1,2,4, 5, 6, Cisco No.'s 1 through 3 Lodes	433.88	Title Insurance And Trust Co
4810003	10/14/1980	22	LOT A OF MS 6818;	Shamrock No.'s 1 and 2 Millsites	2.856	Buch R C

Oriental, and Occidental–Garfield mines, were sold. The new concern was confusingly named the Silver King Mine Company, Ltd., of London. The Garfield mill, 20 stamps, was renamed the King mill.

In July 1890 the Sherman Silver Purchase Act was pushed through Congress. This law, requiring the U.S. Treasury to buy a limited amount of silver every month, gave a boost to the industry, causing the price of silver rise from 97 cents an ounce to \$1.05. The Waterloo and Silver King corporations reopened their low-grade deposits. The King Mine was shipping out 100 tons of ore a day by September, 1891, the Waterloo 50 tons. Three months later, the Silver King Company enlarged its mill (the old Garfield) from 20 to 30 stamps.

But this prosperity was short lived. The price of silver to dipped, to 88 cents in 1892. Considering it “foolhardy to exhaust the great ore bodies when the profit ... was merely nominal,” the Waterloo company closed its mine and mill in March, 1892; 120 to 150 men were idled.

It has been estimated that during the period of 1882 to 1896, a total of between \$13 and \$20 million was produced from the mines of the district.

According to Tucker and Sampson (1931), both the Zenda Mining Company and the Total Wreck Mine (Burcham Group) were active during the late 1920s and early 1930s.

Geology Overview

Barite veins usually mineralized with silver occur in a wide area including the Calico Mountains, Waterman Hills, Lead Mountain, and Mt. General. In a study of the silver ore bodies in the Calico Mining District, Weber (1971) concluded:

In early (?) Pliocene, andesite and dacite were intruded discordantly and, in parts, concordantly into a middle and late Miocene sequence of pyroclastic sediments and minor volcanic flows of the Pickhandle Formation and playa lake and fluvial sediments of the

Barstow Formation. The sequence apparently was arched gently during the intrusion.

Slightly later, fractures and faults formed in these rocks along a northwest-trending belt about four miles long and half a mile wide, and were filled with jasper, barite, silver-bearing minerals and other minerals that were derived from residual fluids of the intrusive mass. The ascending fluids also invaded, altered and mineralized permeable portions of the playa and fluvial sediments.

Bowen (1954), Dibblee (1970) and Durrell (1954) noted barite (\pm silver) mineralization is widespread and spatially associated, if not in fact genetically associated, with the Tertiary intrusion of andesite, dacite and rhyolite. These volcanics have intruded not only the Miocene sediments, but also the Precambrian Waterman Gneiss, Precambrian–Cambrian (?) Oro Grande Series (composed largely of limestone and quartzite) and Mesozoic granitics. Barite (\pm silver) veins occur in all of these rock types except the Oro Grande Series.

Out of dozens of past silver producers, several have potential for production. West of Calico, core drilling by ASARCO in the early 1970s had indicated an ore body of about 30 million tons which averages 3 ounces of silver a ton and from 7 to 15 percent barite.

References

- Anonymous, (1980) The California Comstock? Calico Silver Sparkles Again: California Mining, Volume 5 no. 3, p. 10.
- Agey, W.W. et. al. (1973) Beneficiation of Calico District, California, Silver–Barite Ores: U.S. Bureau of Mines Report of Investigations 7730, 15 pp.
- Bowen, Oliver E. (1954) Geology and Mineral Deposits of Barstow Quadrangle, San Bernardino County, California: California Division of Mines Bulletin 165.
- Dibblee, T.J. (1970) Geologic Map of the Daggett Quadrangle, San Bernardino County, California: USGS Misc. Geol. Invest. Map I 592.
- Durrell, Cordell (1954) Barite Deposits Near Barstow, San Bernardino County, California: California Division of Mines Special Report 39.
- Hensher, Alan., Vredenburg, Larry M, 1986, Ghost Towns of the Upper Mojave Desert, self-published typescript, 138 pp.
- Lefond, S.J., Barker, J.M. (1980) Borates Past, Present and Future: Society of Mining Engineers of AIME Preprint No. 80-101, Feb.
- Lingenfelter, Richard E., 2012, Bonanzas and Borrascas, Gold Lust and Silver Sharks 1848 – 1884 (Arthur H. Clark, (University of Oklahoma Press Norman Oklahoma). Pp 312 – 313
- Nadeau, Remi, 1999, The Silver Seekers, (Crest Publishers, Santa Barbara) p. 242 - 267
- Oesterling, W.A., Spurch, W.H. (1964) Minerals for Industry, Southern California, Volume III Part III: Southern Pacific Company
- Steeles, Douglas W., 1999 Treasure from the painted hills: a history of Calico, California 1882 – 1907, Greenwood Press: Connecticut.
- Tucker, W. B., Sampson, R. J., 1931, Los Angeles Field Division, San Bernardino County, California Division of Mines, Report 27 No. 3, p. 358, 362.
- Vredenburg, Larry M, 1979, The Calico Mountains GEM Resource Area Report, unpublished internal BLM document.
- Weber, Harold F. (1967) Silver Deposits of the Calico District: Mineral Information Service, Vol. 20, No.1, pp. 3-8.
- Weber, Harold F. (1967) Silver Deposits of the Calico District: Mineral Information Service, Vol. 20, No.2, pp. 11-15.
- Weber, Harold F. (1971) Gravity Fault Dislocation of Silver Ore, Calico District, San Bernardino County, California: Geol. Society of America Abstracts, Vol. 3, No.2, p. 214.
- Wright, L.A. et. al. (1953) Mines and Mineral Deposits of San Bernardino County California: California Journal of Mines and Geology, Vol. 49.

The High Road to Borate

Robert E. Reynolds

Redlands, California, rreynolds220@verizon.net

RAISING QUESTIONS: *a mysterious photograph leads to an investigation of mining roads that served the borax mines at Borate and Little Borate in the Calico Mountains between 1884 and 1898.*

“Where was this photo taken? Where is this steep road? Let’s go find it.” So spoke Ted Faye, raising several questions about wagon routes to Borate that were in use just before the turn of the last century. What was the steep road pictured in “Up the Hill” (Fig.1; Hildebrand, 1982), and why did those hulking wagons pulled by twenty mules use a direct route to Borate across steep and rugged terrain, when a smoother, albeit longer route was available?

Borax ore in the form of colemanite was first mined from Little Borate Canyon in about 1894 (Wright and others, 1953) and the deposits farther east at Borate were developed for mining by 1889 (Hildebrand, 1982). Mule teams were apparently used for hauling ore for the fourteen year period before the narrow gauge Borate and Daggett Railroad was completed in 1898 (Myrick, 1992).

“There it is!” exclaimed Ted, “that’s the Up the Hill route.” From Mule Canyon Road (View Stop 1-10, Fig. 2, this guide; Fig. 3) the High Road to Borate runs north, up a hill to the ridge top, then southeast to a point where it crosses a wash (Fig 4), then crosses Mule Canyon Road and climbs a ridge to reach the west-central portion of Little Borate Canyon (aka: Happy Hollow Camp, Hildebrand, 1982; Reynolds, 1999). Why would such an arduous route be taken when Mule Canyon Road was available? Admittedly, today’s road hadn’t been built, but there was a narrow, rutted wagon road parallel and slightly north of where Mule Canyon Road runs today. The question remains, why would there be two roads to Borate, one steeper than the other?

One possible reason is a question: How do you turn around a mule team with wagons?

Answer: You don’t. You circle them in a large loop.

Another question: How is one mule team with wagons able to pass another on a one-team-wide trail?

Answer: It doesn’t. It takes a different route—the other side of the loop.

Ted and I had just found the High Road to Borate that allowed empty wagon teams to avoid loaded wagons returning through narrow canyons from Borate. This northern route (Fig 3) gained 310 feet within half a mile (a 14% grade, steeper than planning departments allow for driveways), quite a feat for twenty mules pulling two wagons that, empty, each weighed 7,800 pounds (3.9 tons). The water in the attached 500 gallon water wagon weighed 4,000 lbs, for a total of almost 10 tons (US Borax, n.d.).



Figure 1. Up the Hill (the photographer may have exaggerated the steepness of the road).



Figure 2. View north of High Road, 2013

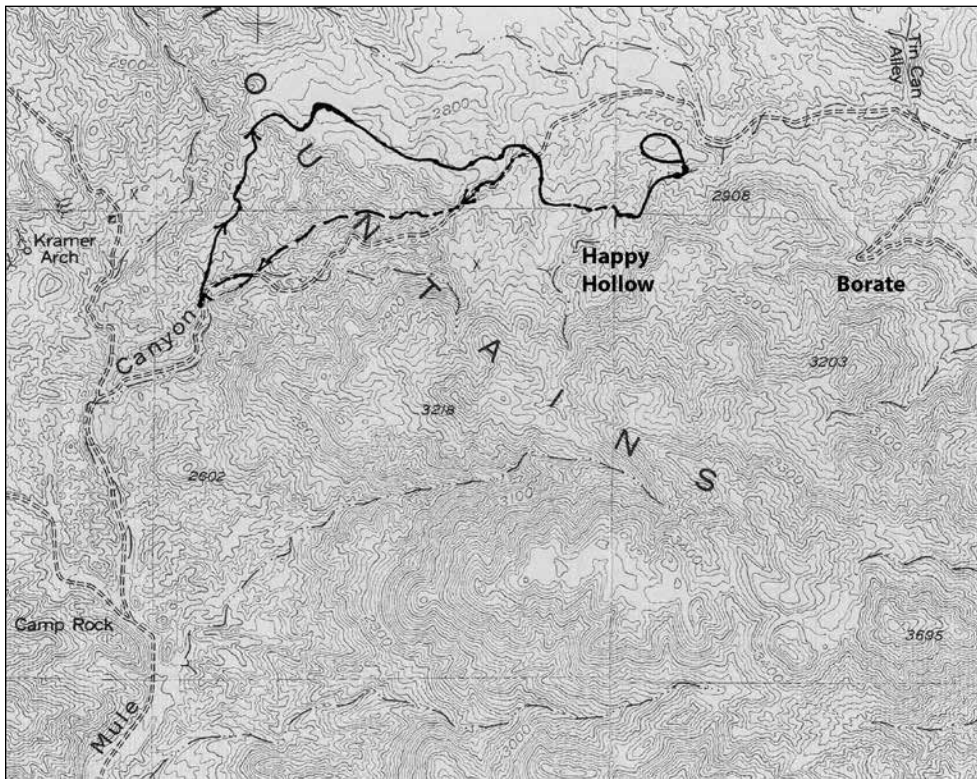


Figure 3. Map of the Mule Canyon area in the Calico Mountains showing Borate, Little Borate (Happy Hollow), the High Road (solid line) and the low road (dashed line).



Figure 4. The High Road runs eastward from the ridge top and crosses a wash to reach Little Borate Canyon.



Figure 5. View west of wagon ruts on the downhill road.

Loaded with ore, two wagons weighed a total of 73,200 pounds (36.5 tons) and probably were hard to control on down grades. Loaded teams heading west from Borate or Little Borate had to gain only 150 feet in elevation (4.5% grade) when reaching Mule Canyon summit. Downhill west of the summit (Fig. 5) was a drop of 250 feet (11% grade) until the start of the High Road was reached.

Mule teams coming from Borate with loaded wagons would stop at Camp Rock (Fig 6), and then proceed to the railhead at Daggett (Fig. 8) to unload at the Atchison, Topeka and Santa Fe Railroad (Myrick, 1992; Reynolds, 1999). Why not use a longer route with a lesser overall grade? Such

a route might start east of Yermo at Minneola, and run north to the east end of Mule Canyon, and then to Big Borate Canyon. The steepest gain in any half mile section would be 100 feet (4.2% grade). The eastern route would be about 12.8 miles in length, 4.2 miles longer than the 8.6 mile westerly run. The direct route was probably chosen based on simple economics. Mule skinnners got paid by the load, or by the trip, not by the hour, so the short but direct route was the most cost effective (Fig 6). As it was, that route required a day and a half to complete, with an overnight mule watering stop at Camp Rock (Fig 7).



Figure 6. Borax ore in wagons. The empty water wagon was hauled from Borate for refilling. Ed Pitcher, teamster, standing.

An eastern route might have been successful if a railhead had been available at Yermo. However, the Union Pacific Railroad did not reach Yermo, a town on the north bank of the Mojave River, until 1905. By then the narrow gauge Daggett and Borate Railroad was already in use, easily mined ore was becoming scarce, and prices were falling.

In an attempt to reduce cost, borax entrepreneur Francis Marion Smith tried other ways to haul ore (Hildebrand, 1982). A 110 horse-power steam tractor called Dinah was put into service in 1894 (Fig. 9), but it was not successful because of Dinah's extreme weight and costly maintenance. Dinah's trial did result in road grade improvements along Mule Canyon Road. The resulting large road cuts we can still see today probably improved the mule team efficiency, and were eventually used by the narrow gauge Borate and Daggett Railroad (Fig. 10).

The narrow gauge railroad was completed by 1898. The "last haul" (Fig. 11) shows a mule team still in use at a time when the railroad had been extended to the Bartlett (No 1) Mine in Big Borate Canyon. The railroad was designed to reach the portals of the mine adits, thereby reducing the man-power necessary to load ore, reducing the amount of lumber to support ore shoots, and greatly cutting the cost of transportation (Hildebrand, 1982). Loaded rail cars headed west (Fig. 12) over the trestle at Little Borate Canyon to the calcining plant at Marion (Fig. 13) on Calico Dry Lake, where the colemanite (calcium borate) was "calcined" (roasted) at a temperature of 1200°F, causing the colemanite to decrepitate (explode) into fine particles and fall through fine mesh screens, leaving the limestone matrix behind. This process of beneficiation concentrated the ore, allowing the high grade to be shipped Alameda, California for dissolution and final purification.

Between 1904 and 1907, ore reserves at Borate were running low and vertical shafts in the mines were in danger of collapse. Pacific Coast Borax Company moved the entire operation, locomotives, trestles, and all, to the Lila C mine in Death Valley.

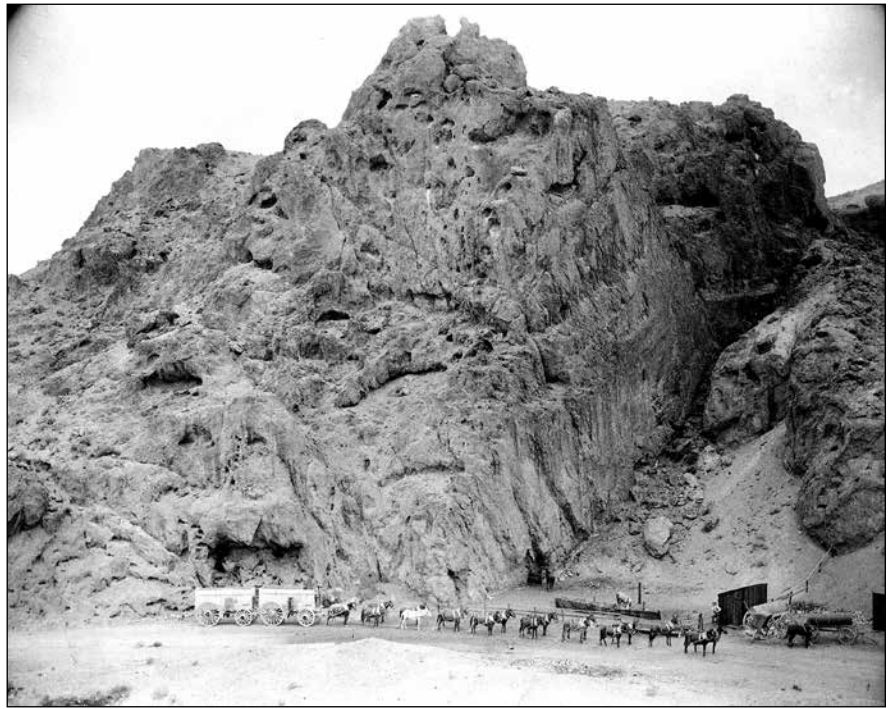


Figure 7. Teams and water wagons were exchanged at Camp Rock.



Figure 8. Borax ore is unloaded at Daggett for shipment to Alameda, California



Figure 9. The steam tractor "Dinah" passes through the road cut that we still use at Mule Canyon summit.



Figure 10. Mule Canyon summit: the downhill wagon road is on the left and the railroad grade on the right.



Figure 11. The “last haul” shows a mule team hauling freight in Big Borate Canyon; the completed narrow gauge trestle is top right.

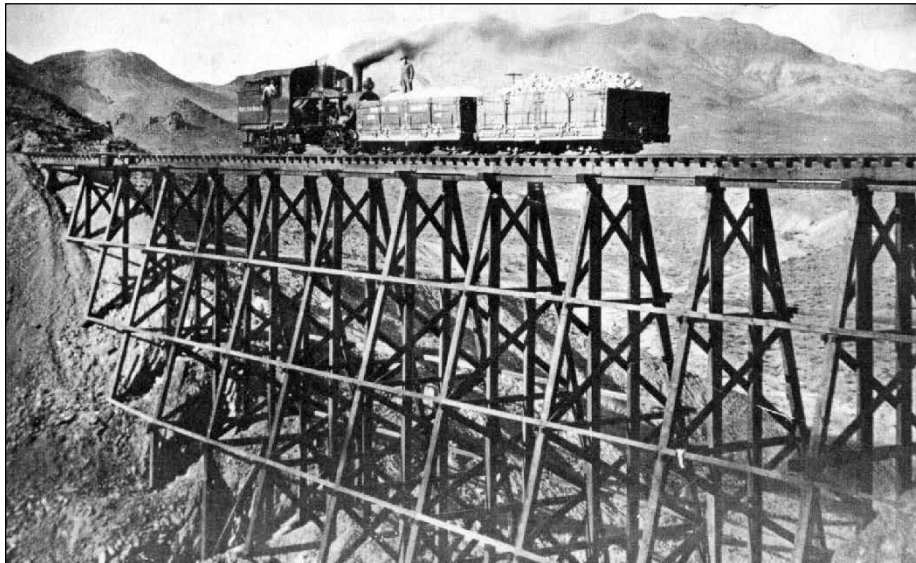


Figure 12. Locomotive hauls loaded gondolas across the trestle at Little Borate Canyon, heading toward Marion.

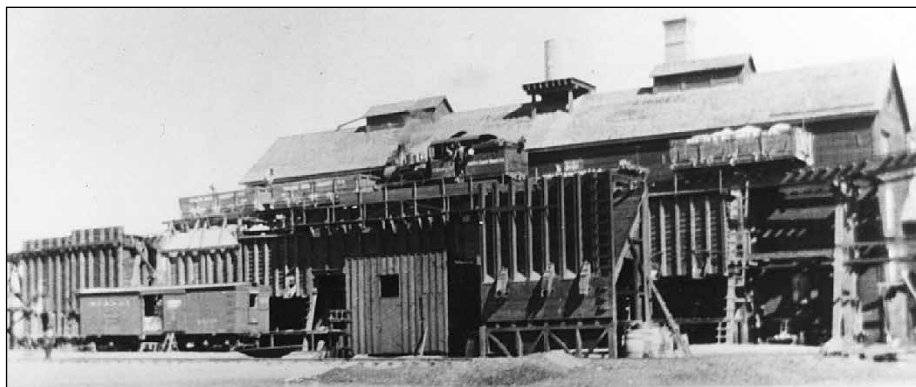


Figure 13. Ore gondolas are dumped into hoppers at the Marion plant for calcining before the concentrate is shipped to Alameda, California.

Acknowledgements: Thanks to Ted Faye for inspiration and for forwarding images from the U. S. Borax Collection at Death Valley National Park, and to the late William H. Smitheram for permission to use photos from his collections. Recent photos are by the author. I also thank George T. Jefferson for his helpful review of an earlier version of this manuscript.

References cited

Hildebrand, G. H. 1982. *Borax Pioneer: Francis Marion Smith*. San Diego, Howell-North Books, 318p.

Myrick, David F. 1992. *Railroads of Nevada and Eastern California*, vol. II. San Diego, Howell North Books, p. 455-933.

Reynolds, R.E., 1999. A walk through Borate—rediscovering a borax mining town in the Calico Mountains. *San Bernardino County Museum Association Quarterly*, vol. 46(1), p. 31.

US Borax, n.d. Borax, the twenty mule team. <http://scvhisto.ipower.com/scvhistory/borax-20muleteam.htm> accessed 02-09-2013.

Wright, L.A., R. M. Stewart, T. E. Gay and G. C. Hazenbush. 1953. *Mines and minerals of San Bernardino County, California*. *California Journal of Mines and Geology*, v. 49 (1, 2), p. 93.

Bernardino County, California. *California Journal of Mines and Geology*, v. 49 (1, 2), p. 93.

Non-vertebrate fossils in the Miocene Barstow Formation, central Mojave Desert, California

R. E. Reynolds

Redlands, CA, 92373, rreynolds220@verizon.net

The Barstow Formation is known for its succession of vertebrate assemblages (Pagnac, 2009) that define the Barstovian (Ba) Land Mammal Age of the North American Continent (NALMA). At the type locality in the Mud Hills, the sedimentary section also includes the transition from late Hemingfordian (Hh2) faunas of the Red Division (Woodburne and Reynolds, 2010) to the Barstovian (Ba) faunas. Recent research (Reynolds and others, 2010) has expanded the geographic extent of the Barstow Formation to include outcrops from Lenwood, Stoddard Valley, Calico Mountains, Daggett Ridge, Harvard, and the southern margin of the Cady Mountains northwest of Ludlow. Several of these localities produce additional Hemingfordian NALMA local faunas.

In addition to the vertebrate faunas of the Barstow Formation (Hh and Ba), multiple invertebrate taxa, track and trace impressions (ichnites), and several plant localities have been documented in the literature. Further study of these non-vertebrate fossils would help develop a complete picture of lake and stream salinity, fluctuation of shoreline, seasonality of deposition and fauna, temperature, precipitation and climate change—in the words of Ray Alf(1970), “... better to understand the ecological conditions of the upper Miocene times.”

References cited

- Alf, Raymond M. 1970. A preliminary report on a Miocene Flora from the Barstow Formation, Barstow, California. Southern California Academy of Science, 69(3-4): 183-189.
- Pagnac, D. 2009. Revised large mammal biostratigraphy and biochronology of the Barstow Formation (middle Miocene), California. *PaleoBios* 29(2): 48-59.
- Reynolds, R. E., D. M. Miller, M. O. Woodburne, L. B. Albright. 2010. Extending the boundaries of the Barstow Formation in the central Mojave Desert. *CSU Desert Symposium Volume, 2010*; p. 148-161.
- Woodburne, M. O., and R. E. Reynolds. 2010. The mammalian litho- and biochronology of the Mojave Desert Province. *CSU Desert Symposium Volume, 2010*; p. 124-147.

Scanning electron microscope (SEM) images of Miocene invertebrate fossils from the Calico Mountains courtesy John Jenkins and Robert Housley.



Midge head, showing compound eyes and antennae bases. SEM x 350.



Water mite, head-on view. SEM x 500.



Water mite, complete. SEM x 250.



Spider spinnerets with silk. SEM photo..



Dragonfly nymph trachea. SEM photo.

Selected bibliography

Arthropods: insects and spiders

- Jenkins, J. E. 1985. Miocene invertebrates from the Calico Mountains, San Bernardino County, California, *in* Geologic investigations along Interstate 15, Cajon Pass to Manix Lake, R. E. Reynolds, ed. San Bernardino County Museum, p. 142-152.
- Jenkins, J. E. 1986. Miocene Invertebrates from the Calico Mountains. *SBCMA Quarterly*, vol. 33, 42 p.
- Kirkby, R. A. 1959. Pseudomorphs after life. *Gems and Minerals*, November, p. 22-23.
- Leggitt, V.L. 2001. Three-Dimensional arthropods from microlaminated sediments of the Barstow Formation, Mojave Desert, California: *Geological Society of America Bulletin*, v. 333, no. 3, p. A54.
- Leggitt, V.L. 2003. Silicified microfossils from Black Canyon: Miocene Barstow Formation, San Bernardino County, California. *Geological Society of America, Abstracts with Programs*, 35, 495.
- Lister, K. H. 1970. Paleocology of insect-bearing Miocene beds in the Calico Mountains, California. Unpublished M. S. thesis, University of California, Los Angeles, 108 pp.
- Miller, K.B. & S.H. Lubkin. 2001. *Calicovatellus petrodytes*, a new genus and species of primitive vatelline diving beetle (Coleoptera: Dytiscidae: Hydroporinae: Vatellini) from the Miocene Barstow Formation, Southern California, USA. *Journal of Paleontology*, 75, 890-894.
- Palmer, A. R. 1957. Miocene arthropods from the Mojave Desert. U. S. Geological Survey Professional Paper 294-G, p. 237-280.
- Palmer, A.R. and A.M. Bassett. 1954. Nonmarine Miocene arthropods from California. *Science*, 120, 28-29.
- Park, L.E. 1995. Geochemical and paleoenvironmental analysis of lacustrine arthropod-bearing concretions of the Barstow Formation, southern California. *Palaios*, v. 10, p. 44-57.
- Park, L.E. and K.F. Downing. 2001. Paleocology of an exceptionally preserved arthropod fauna from lake deposits of the Miocene Barstow Formation, southern California, USA. *Palaios*, v. 16, no. 2, 175-184.
- Park, L. E. and M. A. Wilson. 1988. New interpretations of arthropod-bearing nodules from the Miocene of southern California: *Geological Society of America, Abstracts with Programs*, v. 22, p. 384.
- Pierce, W. D. 1958. Fossil arthropods of California, No. 21, Termites from Calico Mountains nodules. *Bulletin, Southern California Academy of Sciences*, vol. 57, part 1, p. 14.
- Pierce, W. D. 1959. Fossil arthropods of California, No. 22, A progress report on the nodule studies: *Bulletin, Southern California Academy of Sciences*, vol. 58, p. 72-78.
- Pierce, W. D. 1960. Fossil arthropods of California, No. 23, Silicified insects in Miocene nodules from the Calico Mountains: *Bulletin, Southern California Academy of Sciences*, vol. 59, p. 138-143.
- Pierce, W. D. and J. Gibrón, Sr. 1962. Fossil arthropods of California, No. 24, Some unusual fossil arthropods from the

Calico Mountains nodules: Bulletin, Southern California Academy of Sciences, vol. 61, part 3, p. 143.

Seiple, E. 1983. Miocene insects and arthropods in California. California Geology, California Division of Mines and Geology. November, p. 246-248.

Spencer, R. S. 2005. Paleoenvironmental and geochemical analysis of arthropod-bearing lacustrine deposits, Black Canyon, Barstow Formation, Southern California, California State University, Desert Symposium Volume, 2005: p. 91-92.

Spencer, R. S. 2006. Arthropod-Bearing Lacustrine Deposits, Black Canyon, Barstow Formation. Unpublished Master's Thesis, Loma Linda University, School of Science and Technology. 100p.

Arthropods: crustaceans

Belk, D. and F. R. Schram. 2001. A new species of anostracans from the Miocene of California: Journal of Crustacean Biology, v. 21(1), p. 49-55.

Howe, T. and M. Eby. 2006. Miocene invertebrate trackways in the Owl Canyon area, Barstow, California. CSU Desert Symposium Vol. 2006, p. 63-64.

Jenkins, J. E. 1986. Miocene invertebrates from the Calico Mountains. SBCMA Quarterly, vol. 33, 42 p.

Leggitt, V.L. 2005. Cladocerans (Branchiopoda: Anomopoda) from the Miocene Barstow Formation: San Bernardino County, California. Geological Society of America, Abstracts with Programs, 37, 368.

Leggitt, V.L. 2006. Lacustrine ostracoda and other microcrustaceans with preserved appendages from the Miocene Barstow Formation. Geological Society of America, Abstracts with Programs, 38, 64.

Palmer, A. R. 1960. Miocene copepods from the Mojave Desert, California: Journal of Paleontology, v. 34, p. 447-452.

Spencer, R. S. 2005. Paleoenvironmental and geochemical analysis of arthropod-bearing lacustrine deposits, Black Canyon, Barstow Formation, Southern California, California State University, Desert Symposium Volume, 2005: p. 91-92.

Spencer, R. S. 2006. Arthropod-Bearing Lacustrine Deposits, Black Canyon, Barstow Formation. Unpublished Master's Thesis, Loma Linda University, School of Science and Technology. 100p.

Wilkinson, I. P., P. R. Wilby, M. Williams, D. J. Siveter, A. A. Page, L. Leggitt, and D. A. Riley. 2010. Exceptionally preserved ostracodes from a Middle Miocene palaeolake, California, USA. Journal of the Geological Society, London, Vol. 167, 2010, pp. 817-825. doi: 10.1144/0016-76492009-178.

Platyhelminthes

Pierce, W. D. 1960. Silicified Turbellaria from Calico Mountains nodules: Bulletin, Southern California Academy of Sciences Bulletin, vol. 59, p. 144-148.

Gastropod shells and tests

Leslie, S.R., D.M. Miller, J.L. Wooden, and J.A. Vazquez. 2010. Stratigraphy, age, and depositional setting of the Miocene Barstow Formation at Harvard Hill, central Mojave Desert, California, in Reynolds, R.E., and Miller, D.M., ed.,

Overboard in the Mojave: Desert Studies Consortium, California State University, Fullerton, p. 85-104.

Lindsay, E. H. 1972. Small mammal fossils from the Barstow Formation, California. University of California Publications in Geological Sciences, vol. 93, 104 p. (Mentions "slug bed")

Plyley, A. S., D. L. Lofgren and A. A. Farke. 2013. Nonmarine gastropods from the Temblor and Barstow Formations of California. CSU Desert Symposium Volume, 2013 (this volume).

Taylor, D. W. 1954. Nonmarine mollusks from the Barstow Formation of southern California. United

States Geological Survey Professional Paper 254-C:57-80.

Forams and diatoms

Dibblee, T. W., Jr. 1968. Geology of the Opal Mountain and Fremont Peak quadrangles, California. California Division of Mines and Geology, Bulletin 188:64p.

Lohman, K. E. 1968. Miocene diatoms from the Black Canyon Area, In: Geology of the Fremont Peak and Opal Mountain quadrangles, California: California Division of Mines and Geology, no. 188, 64 pp.

Algal stromatolites

Caceres, Carmen and V. Pedone. 2003. Charophyte mounds in the Middle Miocene Barstow Formation, Mud Hills, California. CSU Desert Symposium Vol. 2003, p. 62.

Cole, J.M., E.T. Rasbury, G.N. Hanson, I.P. Montanez, and V.A. Pedone. 2005. Using U-Pb ages of Miocene tufa for correlation in a terrestrial succession, Barstow Formation, California. Geological Society of America Bulletin, 117, 276-287.

Leslie, S.R., D.M. Miller, J.L. Wooden and J.A. Vazquez, J.A. 2010. Stratigraphy, age, and depositional setting of the Miocene Barstow Formation at Harvard Hill, central Mojave Desert, California, in Reynolds, R.E., and Miller, D.M., ed., Overboard in the Mojave: Desert Studies Consortium, California State University, Fullerton, p. 85-104.

Pedone, V. and C. Caceres. 2001. Carbonate phytoherm mounds in the Middle Miocene Barstow Formation, Mud Hills, California. CSU Desert Symposium Vol. 2001, p. 58-60.

Reynolds, R. E., D. M. Miller, M. O. Woodburne, L. B. Albright. 2010. Extending the boundaries of the Barstow Formation in the central Mojave Desert. CSU Desert Symposium Volume, 2010; p. 148-161.

Floral remains

Alf, R.M. 1970. A preliminary report on a Miocene Flora from the Barstow Formation, Barstow, California. Southern California Academy of Science, 69(3-4): 183-189.

Reynolds, R. E. and T. A. Schweich. 2013. The Rainbow Loop Flora from the Mud Hills, Mojave Desert, California. CSU Desert Symposium Volume, 2013; this volume.

Ichnites: tracks and traces

Alf, R.A. 1966. Mammal trackways from the Barstow Formation, California. Southern California Academy of Science, 65(4): 258-264.

Leggitt, V. Leroy, 2002. Preliminary report on the stratigraphic setting and microstructure of Avian eggshell fragments from

- the Calico Mountains: Barstow Formation, Mojave Desert, California. CSU Desert Symposium Volume, 2002, p. 51-57.
- Reynolds, R.E. 1998. Flamingo egg from the Miocene sediments of the Calico Mountains, San Bernardino County, California, *in* Abstracts of Proceedings, 1998 Desert Research Symposium, J. Reynolds (ed). San Bernardino County Museum Association Quarterly, 45(1, 2), p. 106.
- Reynolds, R.E. 1999. Fossil footprints. San Bernardino County Museum Association Quarterly, 46(2): 55p.
- Reynolds, R.E. 1999. Gomphothere tracks in southern California, *in* Reynolds, R.E., 1999. Fossil footprints. San Bernardino County Museum Association Quarterly, 46(2): 31-32.
- Reynolds, R.E. 2003a. Fossil footprints in the Calico Mountains, *in* Guide to the Calicos: Calico Mining Camps and Scenic Areas, Bill Mann. Gem Books.
- Reynolds, R.E. 2003. Miocene horse tracks in California and Nevada: morphology, motion, and tribes. Western Association of Vertebrate Paleontologists, Abstracts and Program.
- Reynolds, R.E. 2004. Miocene cat tracks in the Mojave Desert of California. *Journal of Vertebrate Paleontology*, Abstracts of Papers. V. 25, 104a.
- Reynolds, R.E. 2006. Horse Hoof Prints in the Fossil Record. California State University, Desert Studies Consortium: 25-28.
- Reynolds, R. E. 2006. Imprints of horse hooves in the southwestern Neogene fossil record. Abstracts of Papers. *Jour. Vert. Paleo*, Vol. 26, Suppl. to No. 3. p. 104A.
- Reynolds, R.E. and M.O. Woodburne. 2001. Review of the Proboscidean datum within the Barstow Formation, Mojave Desert, California. *Journal of Vertebrate Paleontology*, Abstracts of Papers, 21(3): 93A.
- Reynolds, R.E., and M.O. Woodburne. 2002. Review of the Proboscidean datum within the Barstow Formation, Mojave Desert, California [abs], *in* Reynolds, R.E., (ed), 2002. Between the basins: exploring the western Mojave and southern Basin and Range Province. California State University, Desert Studies Consortium: 82-83.
- Sarjeant, W.A.S. and R.E. Reynolds. 1999. Camelid and horse footprints from the Miocene of California and Nevada *in* Reynolds, R.E., 1999. Fossil Footprints. San Bernardino County Museum Association Quarterly, 46(2): 3-20.
- Sarjeant, W.A.S., and R.E. Reynolds. 2001. Bird footprints from the Miocene of California, *in* Reynolds, R.E. (ed.), 2001. The changing face of the east Mojave Desert. California State University, Desert Studies Center: 21-40.
- Sarjeant, W.A.S., R.E. Reynolds, and M.M. Kissell-Jones. 2002. Fossil creodont and carnivore footprints from California, Nevada, and Wyoming, *in* Reynolds, R.E., (ed), 2002. Between the basins: exploring the western Mojave and southern Basin and Range Province. California State University, Desert Studies Consortium: 37-50.

Biostratigraphy

- Degans, E. T., W. D. Pierce and G. V. Chillingar. 1962. Origin of petroleum-bearing freshwater concretions of Miocene age: *Am. Assoc. Petroleum Geologists Bulletin*, v. 46, no. 8, p. 1522-1525.
- Deocampo, D. and V. Pedone. 2004. Authigenic ultrafine clays from a Miocene paleolake; paleohydrology in the Barstow Basin, California, USA: Abstracts with Programs, *Geol. Soc Am*, v. 36, no. 5, p. 472.
- Lewis, G. E. 1957. Stratigraphic paleontology of the Barstow Formation in the Barstow Syncline. California State Survey.
- Link, M. H. 1979. Lacustrine facies of the Miocene Barstow Formation, Mojave Desert, California. *Geological Society of America Abstracts with Programs*, vol. 11, p. 88.
- Pierce, W. D. 1962. The significance of the petroliferous nodules of our desert mountains. *Bulletin, Southern California Academy of Sciences* vol. 61, part 1, p. 7-14.
- Reynolds, R.E. 2000. Marker units suggest correlation between the Calico Mountains and the Mud Hills, central Mojave Desert, California, *in* Reynolds, R.E. and Reynolds, J. (eds), Empty Basins, Vanished Lakes. San Bernardino County Museum Association Quarterly, 47(2): 3-20.
- Reynolds, R. E., D. M. Miller, M. O. Woodburne, and L. B. Albright. 2010. Extending the boundaries of the Barstow Formation in the central Mojave Desert. CSU Desert Symposium Volume, 2010; p. 148-161.
- Woodburne, M. O. and R. H. Tedford. 1982. Litho- and biostratigraphy of the Barstow Formation, Mojave Desert, California, *in* Geologic excursions in the California Desert, J. D. Cooper, ed. Guidebook, 78th Annual Meeting, Geological Society of American, Cordilleran section.

Iron ore deposits of the Johnson Valley

Douglas C. Shumway and Dinah O. Shumway
TerraMins, Inc.

Introduction

In the late 1940s and early 1950s there was significant interest in identifying iron ore resources in the southern California area for national defense and in particular for the Kaiser Steel plant in Fontana, CA. The US Bureau of Mines deployed their geologists and geophysical field staffs in this effort. Kaiser Steel and US Steel were the two primary companies active in the search for iron resources in southern California. Many of the Southern California iron deposits contained significant amounts of magnetite and were identified by helicopter magnetic surveys conducted by an unknown contractor. In the early 1950s Kaiser and US Steel discovered a series of iron deposits in the Johnson Valley along the Camp Rock fault.

The Johnson Valley is located approximately 12 miles northeast of Lucerne Valley, between the Rodman and Fry Mountains (see Figures 1 & 2). The zone of iron has been called the "Lava Bed District." A large magnetic signature was identified trending along the trace of the Camp Rock fault (see Figure 3). The Camp Rock fault runs in a northwest and southeast trend and this series of iron deposits runs along the fault (see Figure 4)

Aside from its importance in the manufacture steel, iron is also a critical additive in the manufacture of cement resources. Prior to the 1980s the cement industry got much of its iron from the slag resources at the Kaiser steel plant. The quality of the slag resources was continually degraded and forced cement plants like Mitsubishi to investigate alternative iron resources.

In the mid-1990s Mitsubishi Cement Corporation (MCC) engaged consultant Paul Morton, past minerals officer for the California Division of Mines and Geology (CDMG), to conduct a regional study of all the iron deposits within hauling distance to the MCC Cushenbury Plant in Lucerne Valley. Morton engaged another retired CDMG geophysicist, Roger Chapman, to assist. This proved to be an incredible association as Chapman had worked in his early career for US Steel and, as a result, had accumulated significant information on the iron resources in the California desert. Among these documents were maps, reports, drilling data, and analysis of the deposits in the Camp Rock Valley area of the Mojave Desert.

Morton's study identified the valley along the Camp Rock fault as the most significant of the areas to conduct further investigations. The area had already been recognized by Kaiser Steel and others as a resource area, and most

of the deposits with exposure had been explored; the Bessemer was mined from 1945 to around 1949.

After assembling data from both US Steel and Kaiser Steel, two companies not in existence today, there appeared to be a structural relationship between the numerous iron deposits. All the significant iron deposits are located along the Camp Rock fault, supporting a proposition that the mineralization is at least partially controlled by earlier faulting as a zone of weakness for fluid migration into older dolomitic rocks with later displacement along the Camp Rock fault zone. Some of the deposits are offset by action on the Camp Rock fault. These deposits are listed below by the original owners:

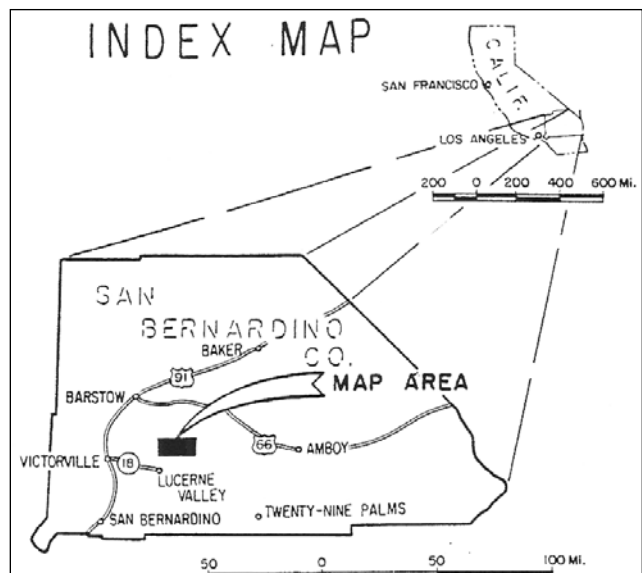


Figure 1: Location map for the Camp Rock iron deposits.

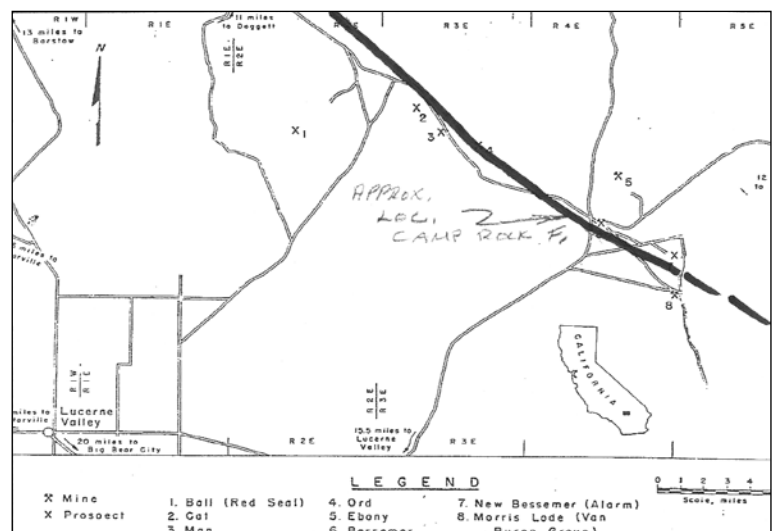


Figure 2: Location map for some of the iron deposits in the Camp Rock (Lava Bed) area

Kaiser Steel

- Morris Lode
- Bessemer

Private Property

- New Bessemer

US Steel

- Rod
- Ord
- Camp
- Fry
- Mann

Two maps accompany this report: the Camp Rock Fault Map (Figure 3) and the Aero-magnetic Map (Figure 4). The iron properties listed above occur along the trace of the Camp Rock fault.

Geology of the Camp Rock fault area

Rocks in the area are classified into four groups based upon age: 1) Paleozoic metasedimentary rocks consisting mainly of quartzites, carbonates and hornfels; 2) Triassic volcanic and porphyritic intrusives; 3) Mesozoic plutonic rocks; and 4) Tertiary-Quaternary alluvial deposits.

Three types of faults are recognized in the area: northerly pre-intrusive faults, older northeasterly striking, post-intrusive faults; and northwest striking recent faults. The Camp Rock fault belongs to the latter type and is most important, as it affects the iron ore deposits. The Camp Rock fault consists of a zone of parallel strands and has a width of about 1,000 feet. The Camp Rock fault zone strikes N 40 W and dips are vertical to steeply dipping. Evidence supports an interpretation of displacement of 13,000 feet in a right lateral direction. The Camp Rock fault actually cuts the Mann and Camp deposits to areas where the Ord and Rod deposits are located (See Figure 4).

Iron Deposits

Morris Lode

This property consists of patented and unpatented lands currently owned by HAHM International, Inc. who purchased the property from Kaiser Steel Resources. It is a shallow magnetite deposit with a strong magnetic signature. The Morris Lode area is underlain by a roof pendant of metasedimentary rocks that lies within Cretaceous quartz monzonite. The carbonate rocks adjacent to a north-striking, steeply dipping

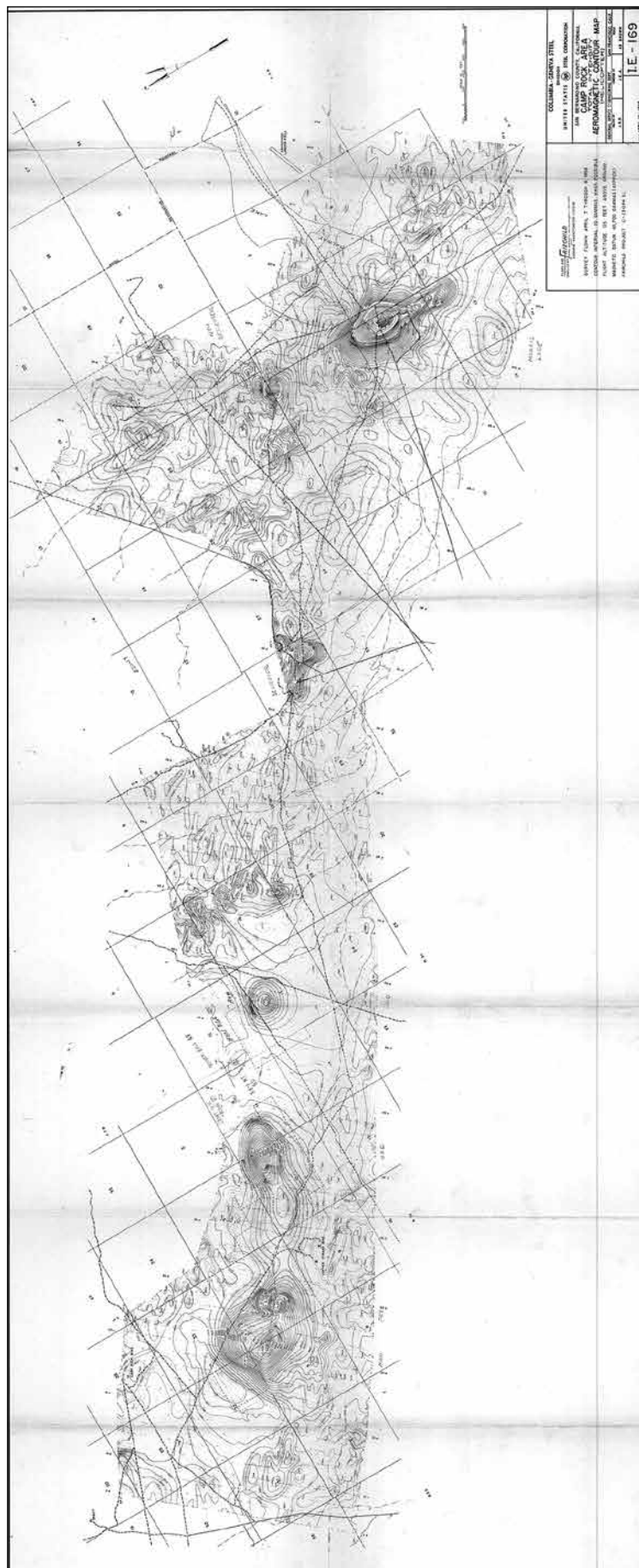


Figure 3a & 3b: Aeromagnetic map of the Camp Rock area.

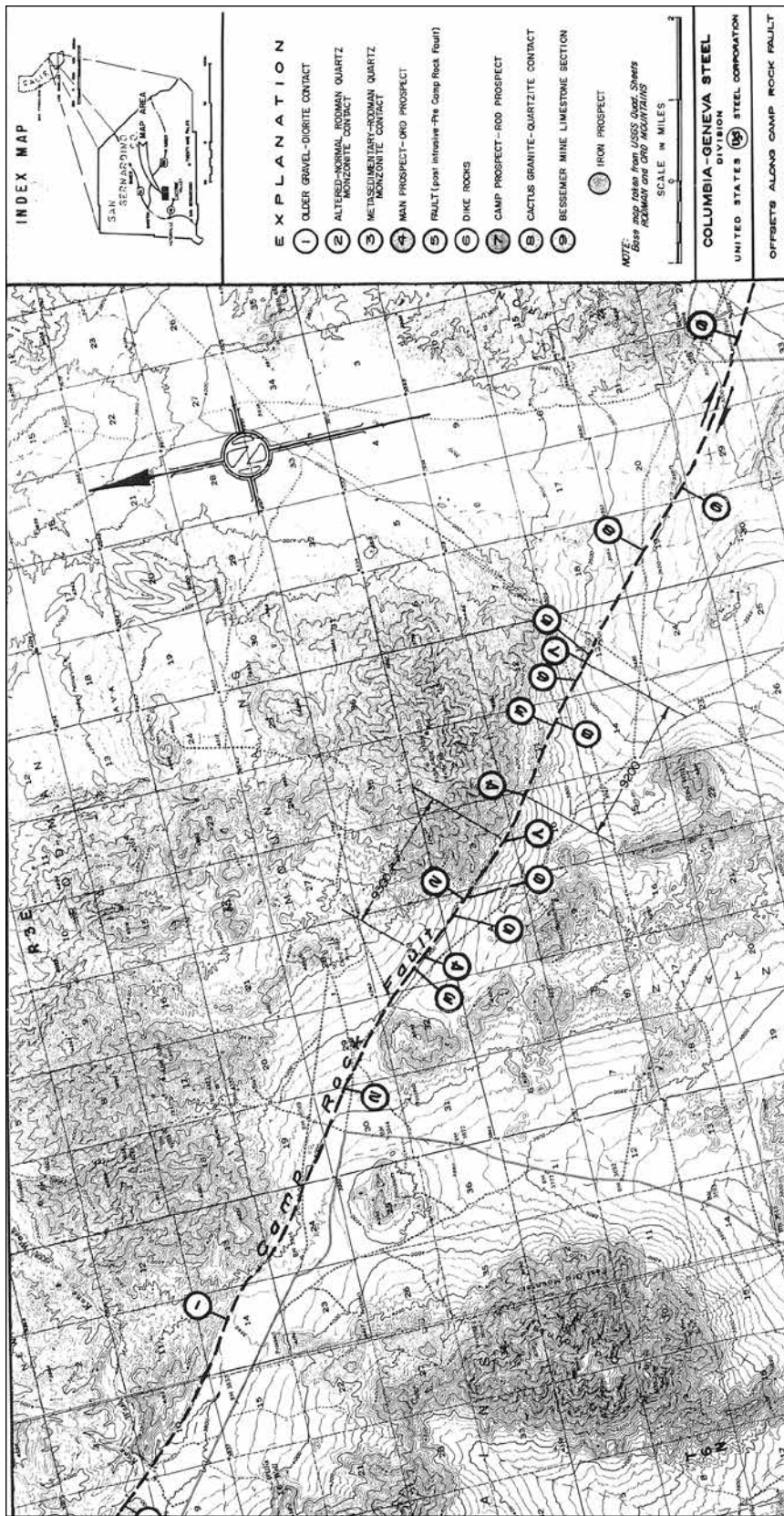


Figure 4a & 4b: Fault map of the Camp Rock area

quartz monzonite contact have been altered by contact metasomatism to an iron skarn composed mainly of magnetite, diopside, and garnet. An unmetamorphosed mass of dolomite lies adjacent to the skarn zone, on the

west, apparently in fault contact. The iron skarn within which the orebody lies is composed of light green diopside and brown garnet with scattered coarse grains of muscovite and irregular concentrations of quartz with fine pyrite.

The Morris Lode property consists of 180 acres of patented and 160 acres of unpatented lands. Exploration work on the Morris Lode indicates proven reserves of 8 million tons of magnetite/hematite ore. There are 10 million tons of inferred reserves. One drill hole shows ore from surface to 900 feet in depth. This property is permitted with San Bernardino County and has a Right of Way with the BLM.

New Bessemer

This property is located north of the Morris Lode on private patented lands. Part of the property is owned by Chevron Minerals. This magnetite/hematite occurrence trends northwest-southeast along a granite/dolomite contact. The deposit consists of a contact metasomatic zone trending east-west within a roof pendant of metasedimentary rocks of Paleozoic age occurring within batholithic rocks of quartz monzonite. There are numerous pods and stringers of ore indicating about 325,000 tons of ore. MCC conducted small drilling projects that did not indicate favorable extensions. An expanded drilling program might provide additional information.

Bessemer

The Bessemer iron mine, west of the New Bessemer, was discovered and developed by Kaiser Steel as potential feed for the Kaiser Steel Mill in Fontana in the late 1940s. This property is also owned by HAHM, Inc. The ore bearing area is underlain by dolomite, the host rock for the iron deposition, and by granite and syenite. The ore occurs as irregular to podlike bodies and as replacement veins in the dolomite near the granite contact. Magnetite is the predominant ore mineral but hematite and limonite also occur. The Bessemer area

has 14 outcrops of iron pods and stringers. All of these have been previously mined or prospected. There is an adjacent undeveloped buried deposit. Inferred reserves are about 1.5 to 2 million tons of 30 to 65% Fe. An expanded drilling program may provide additional information.

The Ebony property is 2 miles north of the Bessemer. Two orebodies occur in separate fissures along the granite-dolomite contact. Both of these have been mined and have no current economic significance. This property is not connected to the Camp Rock fault.

US Steel properties

Starting at the northwest end of the iron zone is the largest iron resource, the Mann deposit. See the accompanying maps.

Mann

The Mann deposit is a large buried deposit with 220 acres of private patented lands and 260 acres of unpatented lands. The investigator does not know if the unpatented claims are currently valid. A portion of the deposit is on Southern Pacific Railroad lands. The top of the Mann deposit is 2,400 feet below the surface. The deepest drill hole (by US Steel) was 4,038 feet deep including 1,625 feet of iron mineralization. Several drill holes and a large magnetic anomaly indicate iron reserves of over 250 million tons. This is easily the largest iron reserve in the district; however, under current economic conditions, the depth of the deposit (2,400 feet) makes it uneconomic.

Fry

The Fry deposit is immediately southeast of the Mann resource. The Fry is located on Mann patented claims. Two drill holes were completed in 1957, both approximately 4000 feet in depth. One hole showed 175 feet of magnetite at over 200 feet deep. Estimated reserves from these two drill holes are 1.5 million tons. The property was drilled by MCC, revealing that the property, as an iron resource, is limited to the development of numerous but uneconomic veins for surface mining.

The Fry revealed an unusual feature of mineralization in one drill hole of a high content of zinc and lead. Erratic amounts of sphalerite and galena, together with pyrite, were found in the lower portion of the hole. The sulfide mineralization however, is confined to the silicified and marbled limestone section of the hole.

Camp

Southwest of the Mann Deposit is the Camp prospect. A 698 foot drill hole completed in 1957 encountered no ore. Two gravity-magnetic lines were run on this prospect. The magnetic anomaly indicates either a deep-seated orebody or a less deep-seated skarn with low iron content. Another exploration hole drilled to at least 2,000 feet would provide additional information.

Rod

In addition to the regional helicopter magnetic survey, three gravity profiles were run on the Rod prospect. No drill holes were done at this site. Interpretation of magnetic, gravity and regional geology indicate a large quantity of skarn overlying the iron mineralization. Data suggest inferred reserves of 68 million tons of iron. Unfortunately, this deposit is also at depth and only a drill hole would confirm the exact depth.

Conclusion

The Lava Bed District had already been recognized by Kaiser Steel and others as a resource area, and Morton's study for MCC confirmed the importance of the district. The unique relationship of the iron deposits of the Lava Bed District is they all occur in the Camp Rock fault zone. Some of these deposits appear to offset by the Camp Rock fault. Even though the deposits are cut by the Camp Rock with maximum right lateral movement of up to 13,000 feet, the deposits are aligned along the fault indicating that it may be likely that the formation of the deposits are at least partially controlled by the zone of weakness that is the Camp Rock fault zone.

The cement plants of southern California require iron in cement manufacturing process. Their current source is the Silver Lake mine north of Baker. In 10 years this source will be closed due to expansion of Ft. Irwin military base. The only other viable source is the Baxter Mine between Barstow and Baker north of Afton Canyon. This property is owned by Cal Portland Cement and is used exclusively for Cal Portland projects. The other southern California iron properties have been mined and would require large amounts stripping to produce ore. There are iron sources in Cedar City, Utah, but shipping Utah iron into Southern California would be very costly.

The Camp Rock iron deposits are in urgent need of examination and consideration for a special resource zoning by the County of San Bernardino and the Bureau of Land Management. Such zoning might protect this resource from encroachment by the proposed expansion of the Twentynine Palms Marine Base. The exact boundary of the expansion is not known at this time; however, if the expansion continues as expected, it is entirely likely that the resources in the Camp Rock area will be completely inaccessible to development.

Morton's study identified the valley along the Camp Rock fault as the most significant of the areas to conduct further iron resource investigations. It is the opinion of the investigator that the deposits of the Camp Rock area need consideration for a special resource zoning status and further investigation.

Rock avalanche setting of the Cave Mountain (Baxter Mine) iron deposits, Afton Canyon, California

Kim M. Bishop

Dept. of Geosciences and Environment, California State University, Los Angeles

ABSTRACT—The Cave Mountain iron deposits are mined from the Baxter open pit mine which has been intermittently active from the 1930's to the present. The following three main stratigraphic units are identified in the area of the mine: 1) Mesozoic diorite, 2) Miocene fluvial and landslide deposits, and 3) Quaternary alluvial and colluvial cover. Miocene landslide deposits are intercalated with the fluvial units and are classified as rock avalanches. The Miocene fluvial and landslide sequence has been tectonically tilted southward and presently dips southward between 30 and 60 degrees. At least three landslides are present and consist of the following lithologies: Mesozoic intrusive rock, Mesozoic quartzite and metavolcanic rock, and upper Paleozoic limestone. The iron ore mineralization occurs in the stratigraphically lowest of 3 landslides and is hosted by metamorphosed porphyritic volcanic rocks. The geologic setting of the Cave Mountain iron deposits has similarities to iron deposits in the southern Avawatz Mountains 40 km to the north. Of particular note is that the iron deposits at both locations occur within Miocene rock avalanche deposits.

Introduction

The Cave Mountain iron deposits occur north of the Mojave River at the east end of Afton Canyon and have been mined from an open pit known as Baxter Mine (Fig. 1). Operations began in the 1930's and have been intermittent (Wright et al., 1953). Commercial mining activity occurred during the period of this study in January, 2013. However, buildings and some mining equipment that were present within the last few years (observable on Google Earth) have been removed.

The two most detailed studies of the geologic setting of the mine were authored by Lamey (1948) and Howard and Monroe (2000). Bob Reynolds suggested the present study because he had noted features within the host rock of the iron deposits that suggested the possibility they were involved in landslide activity, an observation not noted in previous studies. This study presents the results of approximately 4 field days work and is not considered comprehensive, although it does contain significant new observations and interpretations regarding the stratigraphy of the area.

Stratigraphy

Within the study area covering 2.5 km², the following 3 principal stratigraphic units are present: 1) Mesozoic diorite, 2) Miocene terrestrial deposits, and 3) Quaternary surficial materials. This subdivision departs substantially from previous studies in that the Miocene

terrestrial deposits, which underlie the majority of the study area, have been previously interpreted and mapped as Mesozoic and older in-place bedrock. Evidence from this study indicates that the outcrops mapped as Mesozoic and older bedrock are actually large rock avalanche landslide masses intercalated within tectonically tilted, moderately- to poorly-indurated fluvial sandstone units. As described later, the Miocene age of the sandstone and landslide sequence is based on inferred stratigraphic position relative to known Miocene sedimentary rocks.

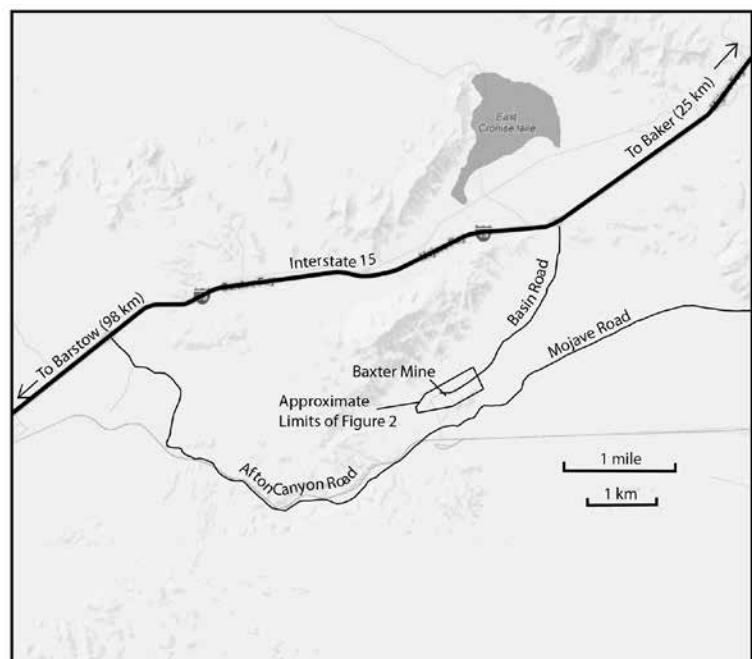


Figure 1. Location map of the Baxter Mine south of Cave Mountain.

This stratigraphic relationship needs to be more strongly confirmed.

Mesozoic diorite

Medium-grained Mesozoic diorite containing scattered felsic dikes is exposed in the northern part of the study area (Mzd in Figure 2). Exposures form a prominent west-trending ridge parallel to and just beyond the north boundary of the map area. The diorite forms mostly dark-colored outcrops and appears to extend well to the north along the east side of Cave Mountain. Also present within the unit are masses of light-colored rock that were not examined in this study and, therefore, of unknown lithology.

Miocene terrestrial sedimentary rock

A Miocene terrestrial sedimentary sequence forms the bulk of the bedrock exposed in the study area. The sequence strikes roughly east-west and dips southward at 30 to 75 degrees. Strata comprising the sequence consist of moderately to poorly lithified fluvial sandstone, conglomerate, and breccia intercalated with much thicker landslide deposits interpreted as rock avalanches. The rock avalanche landslide deposits are estimated to comprise 85 to 90 percent of the sequence volume as estimated from outcrop pattern.

Rock avalanches are catastrophic landslides that travel at rates of 100 km per hour or faster. They generally involve rock masses with volumes of 1 million cubic meters or greater (Shaller and Shaller, 1996). During emplacement, the rock within the landslide is locally

to thoroughly shattered and brecciated (Yarnold and Lombard, 1989). Thicker rock avalanches often have large volumes of intact rock within the body of the landslide that has the appearance of in-situ bedrock (Yarnold and Lombard, 1989; Bishop, 2012; 1998) Zones of concentrated shear and rock comminution are common within a few meters of the landslide base (Yarnold and Lombard, 1989). By as yet poorly understood mechanics (Shaller and Shaller, 1996), rock avalanches display low apparent friction during emplacement and are capable of moving long distances across flat surfaces. For example, a Miocene rock avalanche in the Halloran Hills 50 km northeast of the study area had a run-out distance of 40 km across a flat-lying alluvial plain (Bishop, 1998). Rock avalanches are relatively common deposits intercalated within Miocene terrestrial basins of the southwest United States (e.g., Friedmann, et al., 1994)

The overall Miocene stratigraphy at Baxter Mine, specifically the presence of rock avalanche deposits intercalated with non-metamorphosed fluvial units, is clear but the details are masked by extensive Quaternary cover including historic tailings from the mining operation. The rock comprising the landslides is relatively resistant and forms ridges and hills. These rocks are better exposed than the less resistant Miocene fluvial units. The best exposures of the Miocene units occur in the walls of the open pit mine and other areas of mine-related excavation. Importantly, the base of one of the landslide units is also well-exposed in the open pit mine. At this exposure, the landslide concordantly overlies arkose sandstone beds.

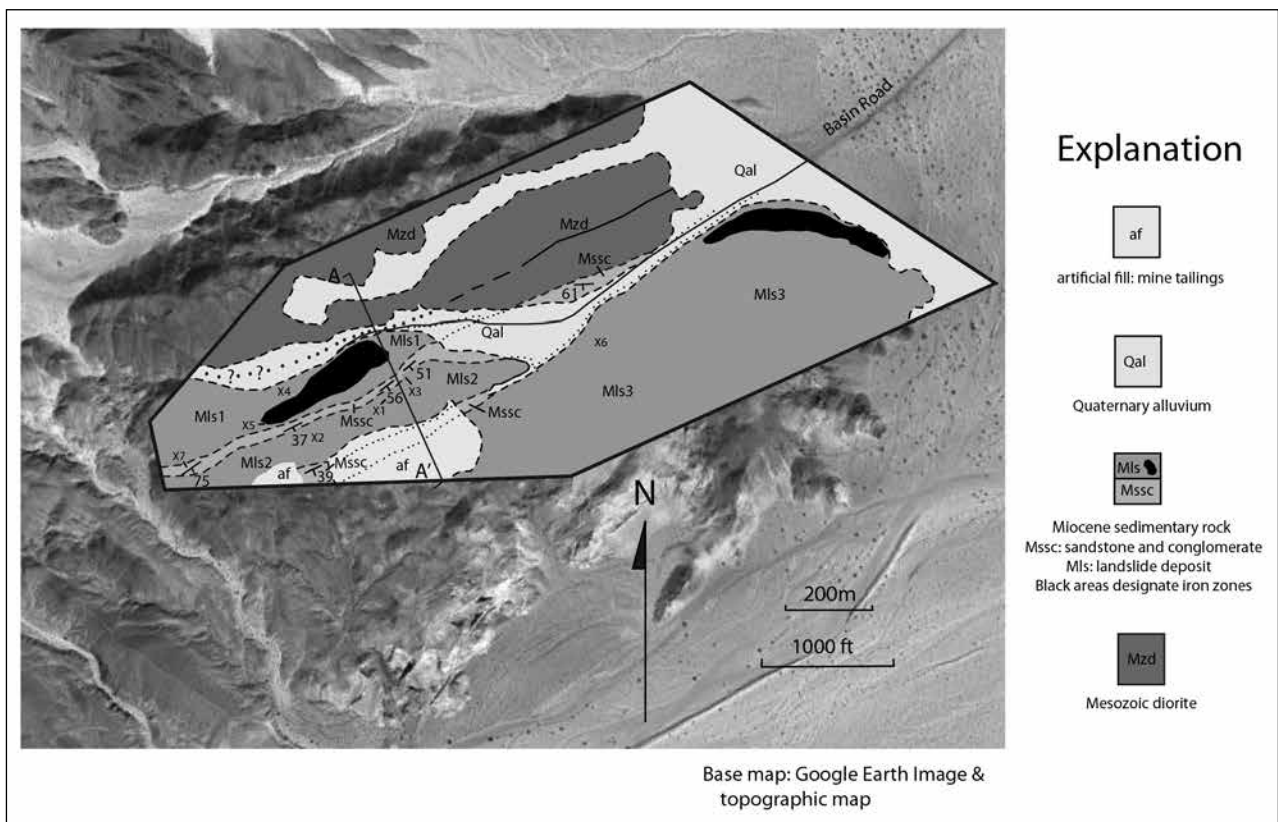


Figure 2. Geologic map. Xs on the map indicate the locations of photographs presented in the paper as figures.

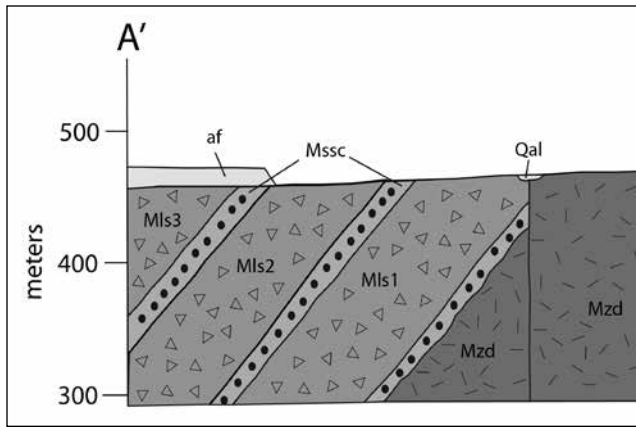


Figure 3. Geological Cross-Section A-A'.

This basal landslide exposure is key to confirming the landslide interpretation.

Figure 2 presents a geologic map and Figure 3 a cross-section of the mine area. Strike and dip symbols indicate the orientation of Miocene fluvial deposits within the section. At the strike and dip locations, the strata are well-exposed. However, because of poor exposure in most other areas the trace of geologic contacts as they trend across the map area has large uncertainty. Nonetheless, the beds of light-colored Miocene arkose exposed at different locations in the east-west direction across the central part of the map area have strikes toward one another and line up sufficiently well to assume the outcrops represent a continuous or nearly continuous unit.

The most clearly distinguished landslide unit (Mls2, Figs. 2 and 3) is deposited on the arkose mentioned above and is well-exposed in the open pit mine. This

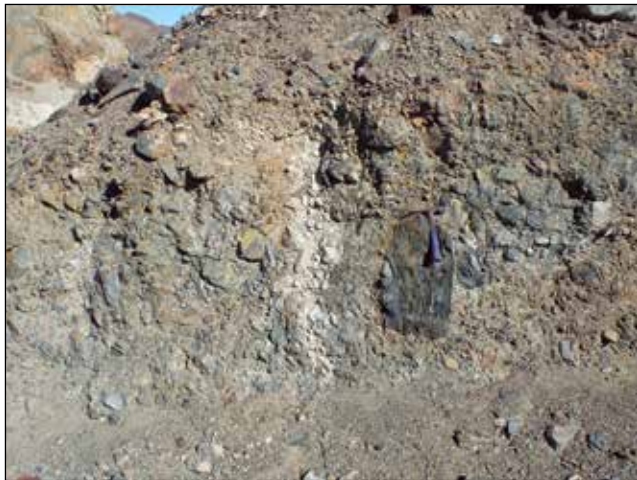


Figure 4. Breccia of landslide Mls2 exposed in the wall of the open pit mine. View toward the east. Location of the outcrop is designated with an X1 on Figure 2. Note the large clast-to-matrix ratio and lack of mixing of clasts with different lithologies. Both characteristics are common in rock avalanche deposits.



Figure 6. Base of landslide Mls2 resting on non-metamorphosed sandstone. View southwest of the southern open pit mine wall. Location of the outcrop is designated with an X3 in Figure 2. Note the irregularity of the contact and the slight mixing of landslide and substrate material.



Figure 5. Breccia of landslide Mls2 exposed in mine excavation. View toward the west. Location of the outcrop is designated with an X2 on Figure 2. Note lack of mixing of clasts with different lithologies. Also note the clasts of non-metamorphosed sandstone just to the left and above the rock hammer. The sandstone is interpreted to be substrate material incorporated into the landslide. Possibly, the sand material intruded the rock avalanche as a clastic dike during landslide emplacement and the dike then disrupted as the landslide continued moving.



Figure 7. Base of landslide Mls2 resting on non-metamorphosed sandstone. View south of the southern open pit mine wall. Location of the outcrop is designated with an X3 in Figure 2. Note the lens of sandstone substrate, slightly darker than the substrate below the rock avalanche base, entrained in the rock avalanche on the left-center of the photograph.



Figure 8. Matrix-rich breccia near the base of landslide Mls1. Location of the outcrop is designated with an X4 in Figure 2.



Figure 9. Brecciated light-colored quartzite and dark-colored iron mineralized rock in an excavation west of the open pit mine. Location of the outcrop is designated with an X5 in Figure 2.



Figure 10. Limestone breccia exposed along the north margin of landslide Mls3. View toward the southeast. Location of the outcrop is designated with an X6 in Figure 2. This exposure occurs near the base of the landslide.



Figure 11. Non-metamorphosed sandstone stratigraphically between Mls1 and Mls2. Location of the outcrop is designated with an X7 in Figure 2. View toward the east. Note the steep southward dip of the sandstone beds.

unit appears to be primarily composed of several types of Mesozoic intrusive rocks, including both felsic and mafic varieties. Throughout, the landslide unit consists of brecciated and shattered rock forming a breccia with a small percentage of matrix material and a wide variety of clast sizes from gravel to boulder (Figs. 4 and 5). The landslide has an irregular basal contact and, importantly, does not form a sharp boundary with the underlying sandstone (Fig 6). At one outcrop location, the landslide mass contains a lens-shaped mass of substrate sandstone about 1 meter above the base (Fig. 7). The sandstone lens is elongate parallel to the base and is about 0.5 m thick and 5 m long. A similar occurrence of wedges of substrate material dislodged and entrained within a rock avalanche mass has been observed by the author in rock avalanches in another area. Mls2 is estimated to be approximately 70 meters thick. An outcrop on the south side of the landslide exposes sandstone that rests depositionally on top of the landslide mass.



Figure 12. View of metavolcanic rock exposed in the north wall of the open pit mine. Note the light colored plagioclase grains within the dark fine-grained matrix. Also note the near vertical mineralized zone under the rock hammer head and just left of the handle.

Two other landslide units are inferred based mainly on their brecciated nature and outcrop location. One of the landslide units (Mls1, Fig. 2) is stratigraphically below Mls2 and includes the Baxter Mine iron ore zones present in the open pit. The other landslide is stratigraphically above Mls2 and consists of upper Paleozoic carbonate and Mesozoic intrusive rock (Mls3, Fig. 2).

The stratigraphically lowest landslide, Mls1, contains both brecciated (Fig. 8) and non-brecciated zones. The brecciated zones are typical for rock avalanche deposits in that there is a large clast-to-matrix ratio and based on the distribution of clast lithologies, the breccia was formed by fragmentation of bedrock with little to no mixing of clasts following fragmentation (Fig. 9).

Exposures of the northern contact between Mls1 and adjacent rock unit or units is not exposed. The contact is inferred to be a fault based on projection of a fault exposed in the basement rock in the east part of the map area (Fig. 2).

Mls3 (Fig. 2) is interpreted as a landslide deposit rather than in-situ bedrock based on the presence and characteristics of brecciation and its location relative to the south dipping sandstone beds to the north of the landslide mass. With regard to the landslide interpretation, the most important brecciation occurs along the landslide's north outcrop boundary, which coincides with the base of the south-dipping landslide. Similar to the breccia in the other two landslides, the breccia in Mls3 has a large clast-to-matrix ratio with little to no mixing of clasts with different lithologies (Fig. 10). Much of the landslide is not brecciated, a condition attributed here to the fact that the landslide is more than 350 meters thick. As previously mentioned, thick rock avalanche deposits have been observed to contain large volumes of intact source rock in contrast to thinner rock avalanche deposits (Bishop, 1998). (Based on the author's experience, the boundary between thick and thin rock avalanches is very roughly 100 m.)

There is good evidence that the contact between Mls3 and its substrate dips south, just as the stratigraphically underlying fluvial and landslide units do. Lamey (1948) describes two adits that were present at the time of his study. The adits were excavated toward the Mls3 mass from the north. Both adits encountered brecciated rock that, based on Lamey's lithologic description, belong to landslide Mls2. The adits extended further south than the overlying northern outcrops of the Mls3 carbonate. From this description the base of the carbonate rock (Mls3) must dip southward, a conclusion noted by Lamey (1948).

At the east end of Mls3, Mesozoic intrusive rock has been altered to iron ore (Fig 2). This ore has been prospected, but not mined. Why it has not been mined is unknown to the author, but perhaps it is of lower grade or small volume.

A Miocene age is inferred to the fluvial and landslide sequence based on the deformation of the sequence and its apparent stratigraphic relationship to known Miocene deposits to the southwest in Afton Canyon. The fluvial and

landslide sequence dips moderately to steeply southward. Quaternary strata in the Afton Canyon area are horizontal to nearly horizontal and, thus, the sequence must be older than Quaternary. More importantly, based on reconnaissance study the upper part of landslide Mls3 occurs south of the study area across the Mojave River. This landslide mass is overlain by a fourth landslide mass. In turn, this stratigraphically higher landslide is depositionally overlain by gray conglomerate that grades upward into the Miocene sequence exposed in central Afton Canyon. Thus, the fluvial and landslide units in the study area appear to form the lower part of the Afton Canyon Miocene section.

Quaternary surficial deposits

Quaternary surficial deposits include alluvium in washes and colluvium on slopes, particularly on the lower parts of slopes. Some terrace alluvium is present locally. In addition to these natural deposits, mine tailings are scattered across the site along with materials disturbed from mining excavation. These deposits cover much of the bedrock in the area, particularly in the low-lying areas. Most of these natural and anthropogenic deposits are not mappable.

Structure

The Miocene sequence is homoclinally tilted southward (Fig. 2) as determined from the geometry of bedding within the sandstone and breccia units between the rock avalanche deposits (Fig. 11). Other than being younger than the sequence, the time of tilting is unknown. The dip direction appears to be similar to that of Miocene sediments exposed further to the west and south of the Mojave River in Afton Canyon. Presumably, the tilting is related to regional deformation that also caused tilting of the Miocene units south of Afton Canyon.

Numerous small faults with offsets estimated to be on the order of up to a few meters are present within the Miocene units. Some of these faults displace the contact between the landslides and bedded deposits indicating that the faults post-date deposition of the Miocene units. They may be related to deformation that caused tilting of the depositional sequence and/or to activity of the nearby Manix fault.

A fault of unknown slip magnitude is present in the east part of the map area (Fig. 2). The outcrop pattern indicates the fault is near vertical. Projection of the fault westward suggests that it separates the Miocene strata on the south with older rock on the north, which in turn suggests the fault has a down-to-the-south component of slip. Any strike-slip component is unknown. Because the fault is parallel to the Afton Canyon fault to the south, the two may be tectonically related.

There is the possibility that one or more faults with 10's of meters or more slip are present within the map area. Indeed, the short distance from the top of the Mesozoic unit (Mzd) to the base of Mls3 at the east side of the map area and the much wider distance at the west end suggests the presence of at least one large displacement

fault oriented sub-parallel with the strike of the Miocene sequence. If there are no large faults, then the sequence would have to be positionally thin eastward at a large gradient.

Iron mineralization

The iron ore in the study area consists of magnetite and hematite with subordinate limonite (Lamey, 1948). As mentioned earlier, the iron ore occurs in two main zones within the study area (Fig 2). The western zone occurs in the stratigraphically lowest of the landslides, Mls1. The iron mineralization in Mls1 is brecciated, clear evidence that the mineralization pre-dates the landslide movement. Since the 1930's, this zone has been extensively mined (Lamey, 1948) resulting in the present-day open pit. The eastern iron ore zone is in the stratigraphically highest landslide deposit, Mls3, which consists mainly of Paleozoic limestone intruded by Mesozoic mafic plutonic rock. Given the non-metamorphosed state of the sandstone and conglomerate deposits interbedded with the landslides, the iron mineralization in Mls3 must also pre-date the landslide activity.

As observed from this study, the western ore zone in the lowest landslide mass occurs with quartzite and what is interpreted to be metavolcanic rock. The metavolcanic rock contains feldspar grains set in a dark green, fine-grained matrix (Fig. 11) and occurs in contact with the iron mineralized zone. Some iron mineralized veins cut through the metavolcanic rock (Fig. 12).

Similar appearing metamorphosed porphyritic volcanic rocks (without iron mineralization) are exposed in the Soda Mountains 12 km to the east and northeast, where metavolcanic rocks associated with quartzite are interpreted to be Jurassic (Walker and Wardlaw, 1989). Quartzite and metavolcanic rock determined to be Jurassic also occur in the Barstow area to the west and have, indeed, been correlated with the quartzite and metavolcanic sequence at the eastern end of Afton Canyon (Schermer et al., 2002).

Although prospected, the ore in the eastern mineralized zone embedded in Mls3 has been mined little, if at all. At this location iron mineralization has replaced mafic igneous rock that intrudes the Paleozoic carbonate of the landslide mass. This ore body appears to be volumetrically smaller than the ore deposits in the western zone.

All major iron mineralized zones in the southern California occur in proximity to limestone or dolomite (Carlisle et al., 1954). At most locations, the mineralization replaces carbonate rock. The interpretation from this study is that iron mineralization in both the west and east zones, which corresponds to the stratigraphically lowest and highest landslide units, respectively, replaces only igneous rock. However, the replacement in the eastern zone occurred only a few meters from limestone, thus the limestone may have been a necessary catalyst to the iron mineralization, just as it appears to have been in the

other southern California deposits. Although no evidence for the presence of limestone in the western zone (Mls1) was apparent during this study, Lamey (1948) states the following regarding the Baxter Mine area: "at practically every place where ore is exposed there is also a diorite porphyry and remnants of partially replaced limestone." From descriptions throughout his article, the diorite porphyry mentioned by Lamey (1948) is probably the rock identified in the present study as metamorphosed volcanic rock present in the landslide Mls1. Lamey (1961) also indicates there is mineralogical evidence that the iron minerals replaced carbonate minerals in the mine area.

Based on Lamey's (1961; 1948) correlation of iron mineralization with carbonate, it is puzzling that there is no evidence in the present open pit mine exposures for the presence of carbonate rock. One possible explanation is that the mineralized zone exposed at the time of Lamey's studies was, indeed, associated with carbonate and the carbonate has subsequently been entirely removed by mining. If so, the carbonate rock could have been either Paleozoic miogeoclinal rock such as is present in Mls3 or may have been Mesozoic carbonate interbedded with the metavolcanic and quartzitic rocks. South of the Baxter Mine area across the Mojave River are metavolcanic and quartzitic rocks with what appears to be interbedded carbonate. Either option is reasonable.

Regardless of whether or not limestone was present in the Mls1 zone of iron mineralization (at the open pit mine), it does not seem likely that the present proximity of the western and eastern iron mineralization zones is the coincidence of two landslides derived from widely separated source bedrock ending up close to one another. This is especially true given that the nearest known iron mineralization locality to the Cave Mountain area is 40 km distant. Rather, the simplest explanation is that the two separate landslides contain iron mineralization that formed in one area and both landslides were derived from that area. If so, then it can be inferred based on the presence of abundant Paleozoic carbonate in Mls3 that in a general sense the iron mineralization in Mls1 also formed in proximity to limestone. The importance of this issue is that if the iron mineralization in Mls1 did not form in proximity to carbonate rock, as known to the author it would be the only deposit in southern California not spatially associated with carbonate.

Similarities to southern Avawatz Mountains

The geologic setting of the iron deposits at Cave Mountain is similar to iron deposits in the southern Avawatz Mountains (often referred to as the Silver Lake district (Wright et al., 1953), 40 km to the northeast. In the Avawatz Mountains, iron ore is mined from Miocene rock avalanche deposits intercalated with fluvial sedimentary rocks (Bishop and Brady, 2006), a strikingly similar setting to the Cave Mountain deposits. Also, the iron

deposits at both localities are in proximity to Paleozoic carbonate rocks. A major difference, however, is that the iron deposits at Cave Mountain all appear to have formed within igneous rock, whereas the Silver Lake iron deposits formed within the Paleozoic carbonate.

Summary

The Cave Mountain iron deposits mined at the Baxter Mine occur in two variably brecciated landslide deposits interpreted to be rock avalanche deposits interbedded with sandstone and conglomerate. The stratigraphically lower landslide consists mainly of metamorphosed rock derived from Mesozoic volcanic and quartzose deposits and the higher landslide mainly consists of Paleozoic limestone and mafic intrusive rock. A third landslide unit, thoroughly brecciated and barren of exposed iron mineralization, lies stratigraphically between the other two landslides. Separating the landslides are non-metamorphosed fluvial arkosic sandstone and conglomeratic deposits. The entire sequence of fluvial and landslide units dips southward at 37 to 75 degrees. The sequence appears to form the base for the Miocene terrestrial sedimentary and volcanic deposits exposed in Afton Canyon to the west and in the Cady Mountains to the south. If correct, then the fluvial and landslide sequence is also Miocene.

Iron mineralization within the rock avalanches occurs within the metavolcanic rocks in the stratigraphically lowest landslide and in mafic plutonic rocks that invaded Paleozoic limestone in the highest landslide. The mineralization occurred within the source rock for the landslides, although the location for the source rock is not known. The geologic setting for the iron deposits at Cave Mountain is quite similar to those in the Silver Lake area of the southern Avawatz Mountains, 40 km to the north.

Acknowledgements

The author thanks Bob Reynolds for having suggested this study. Bob receives full credit for being the first to suggest that the iron deposits at Cave Mountain occur within landslide deposits. Thanks also go to Kevin Schmidt and Andre Ellis for thoughtful reviews and a number of helpful comments. All shortcomings are the responsibility of the author, however.

References

- Bishop, K. M., 1998, Miocene rock avalanche deposits, Halloran/Silurian Hills area, southeastern California: *Environmental and Engineering Geosciences*, vol. IV, no. 4, p. 501-512.
- Bishop, Kim M., 2012, The morphology and anatomy of a Miocene long-runout landslide, Old Dad Mountain, California: implications for rock avalanche mechanics; *in* Reynolds, R. E., ed., *Searching for the Pliocene: Southern Exposures: The 2012 Desert Symposium Field Guide and Proceedings*; California State University Desert Studies Consortium, p. 38-43.
- Bishop, K. M. and Brady, M., 2006, Stratigraphic evidence from Miocene megabreccia deposits for a regional-scale Mesozoic allochthon in the western Soda and Avawatz Mountains, eastern Mojave Desert, California; *in* Girty, G.H. and Cooper, J.D., *Using Stratigraphy, Sedimentology, and Geochemistry to Unravel the Geologic History of the Southwestern Cordillera*, Pacific Section SEPM Society for Sedimentary Geology, p. 337-254.
- Carlisle, D., Davis, D.L., Kildale, M.B., and Stewart, R.M., 1954, Base metal and iron deposits of southern California; *in* Jahns, R. H., ed., *Geology of Southern California*, California Division of Mines and Geology Bulletin 170, v. 1, p. 41-49.
- Friedmann, S.J., Davis, G.A., Fowler, T.K., Brudos, T., Burbank, D.W., and Burchfiel, B.C., 1994, Stratigraphy and gravity-glide elements of a Miocene supradetachment basin, Shadow Valley, eastern Mojave desert; *in* McGill S.F., and Ross, T.M., eds., *Geological Investigations of an Active Margin*, Geological Society of America Cordilleran Section Guidebook, p. 302-320.
- Howard, H.J. and Monroe, L., 2000, Geology and mineral deposits in the Baxter-Basin area south of Cave Mountain, San Bernardino County, California; *in* Reynolds, R.E. and Reynolds, J., eds., *Empty Basins, Vanished Lakes*; San Bernardino County Museum Quarterly, v. 47, no. 2, p. 42-46.
- Lamey, C.A., 1961, Contact metasomatic iron deposits of California: *Geological Society of America Bulletin*, v. 72, p. 669-678.
- Lamey, C.A., 1948, Cave Canyon iron ore deposits, San Bernardino County, California: *California Division of Mines and Geology Bulletin* 129, p. 59-67.
- Schermer, E.R., Busby, C.J., and Mattinson, J.M., 2002, Paleogeographic and tectonic implications of Jurassic sedimentary and volcanic sequences in the central Mojave block; *in* Glazner, A.F., Walker, J.D., and Bartley, J.M., eds., *Geologic Evolution of the Mojave Desert and Southwestern Basin and Range*; Geological Society of America Memoir 195, p. 93-115.
- Shaller, P.J. and Shaller, A.S., 1996, Review of proposed mechanisms for sturzstroms (long-runout landslides); *in* Abbott, P.L. and Seymour, D.C., eds., *Sturzstroms and Detachment Faults, Anza-Borrego Desert State Park, California*, South Coast Geological Society Annual Field Trip Guide, Book No. 24, p. 185-202.
- Walker, J. D. and Wardlaw, B.R., 1989, Implications of Paleozoic and Mesozoic rocks in the Soda Mountains, northeastern Mojave Desert, California, for late Paleozoic and Mesozoic Cordilleran orogenesis: *Geological Society of America Bulletin*, v. 101, p. 1574-1583.
- Wright, L.A., Stewart, R.M., Gay, T.E., and Hazenbush, G.C., 1953, Mines and minerals of San Bernardino County, California: *California Journal of Mines and Geology*, v. 49 (1 and 2), p. 93.
- Yarnold, J.C. and Lombard, J.P., 1989, Facies model for large rock avalanche deposits formed in dry climates; *in* Colburn, I.P., Abbott, P.L., and Minch, J., eds., *Conglomerates in Basin Analysis: A Symposium Dedicated to A.O. Woodford*, Pacific Section, Society of Economic Paleontologists and Mineralogists, p. 9-31.

Parapliohippus carrizoensis (Perissodactyla: Equidae) from early Miocene (Hemingfordian NALMA) Barstow Formation outcrops in the southwestern Cady Mountains, Mojave Desert, California

Robert E. Reynolds

Redlands, CA, rreynolds220@verizon.net

Introduction

A small fossil horse was recovered from sediments in the southwestern Cady Mountains. The specimen is referred to *Parapliohippus carrizoensis* based on upper dentition measurements and morphology. The specimen was preserved in outcrops of the lower Barstow Formation, specifically in the silicified Brown Platy Limestone (BPL) lying above the Massive Stromatolitic Limestone (MSL). The presence of this small horse reinforces the Late Hemingfordian North American Land Mammal Age (NALMA) of these Barstow Formation strata that are fault-juxtaposed against volcanic rocks of the Cady Mountains.

Stratigraphy

The specimen was preserved in the south dipping, silicified sediments of the Brown Platy Limestone (BPL) lying above the Massive Stromatolite Limestone (MSL). These two distinctive beds are part of a time-transgressive marker sequence of sediments in the lower Barstow Formation (Reynolds and others, 2010) that is also found in eastern exposures of Daggett Ridge and in the Sleeping Beauty area of the southeastern Cady Mountains (Figure 1). The time-transgressive marker sequence generally includes, from the lowest, the Massive Stromatolitic Limestone (MSL), the Brown Platy Limestone (BPL) with a silicified basal member, with the Strontium-Borate (SrB) horizon uppermost. The Peach Spring Tuff (PST; 18.8 Ma, Hillhouse and others, 2011) is present above the marker sequence at eastern Daggett Ridge and at the DuPont locality in the southeastern Cady Mountains.

Description

The fossil horse specimen was recovered from a private section of land by Terry Thorp and donated to the Jurupa Mountain

Discovery Center, Riverside, CA. The fossil horse locality in the southwestern Cady Mountains is called the “Talc Mine” area (misnomer) where clay was mined (Dibblee and Bassett, 1966a, b). The “Talc Mine” section in the southwestern Cady Mountains contains the MSL and the BPL horizons, and is located geographically between the Daggett Ridge on the west and Sleeping Beauty on the east.

Blocks contain an upper right maxillary dentition with P3/ through M3/ (Figure 2); a shattered scapula; and a proximal femur. The skeletal elements are preserved in chalcedony, making preparation of the specimen for measurements extremely difficult. All measurements were taken from surfaces exposed along fractures through the chalcedony.

The protocone visible on several upper molars appears round, and since the break exposes the basal portion of the tooth, it shows that the protocone is united with the protoconule in late wear. The dimensions of upper premolars and molars compare well with antero-posterior

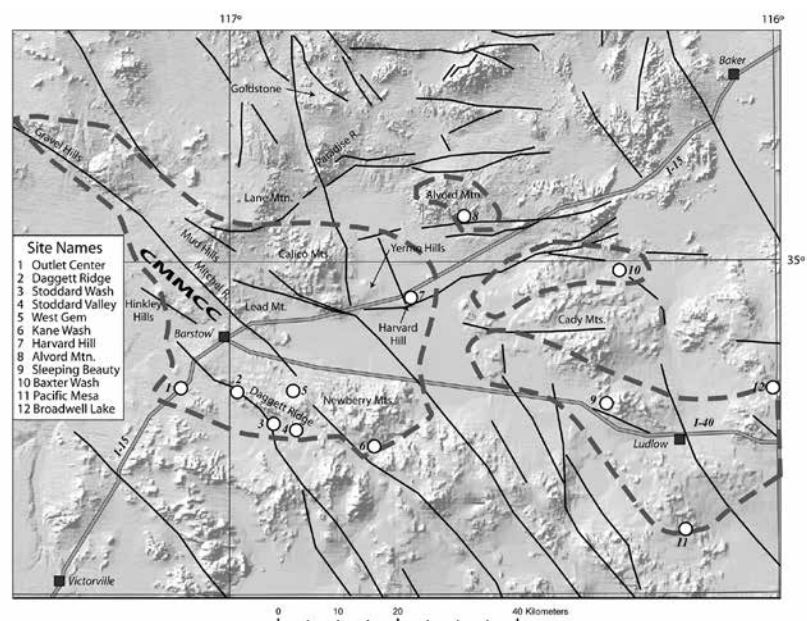


Figure 1. Location map (from Miller, 2010).

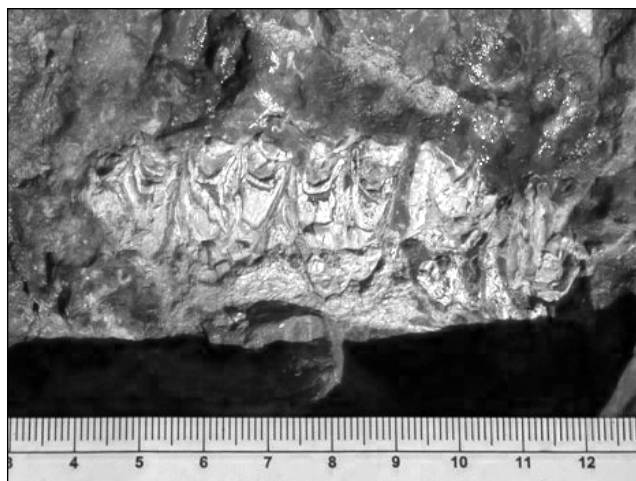


Figure 2. Right maxillary dentition of *P. carrizoensis* from the southwestern Cady Mountains. P3 and P4 are on the left, and M1, M2, M3 are to the right. Scale in mm.

and transverse dimensions listed for *P. carrizoensis* from the Hector Formation in the northern Cady Mountains (Miller, 1980; Table 4, p. 86). The slight variation in dimensions can be attributed to the fractured nature of the specimen and to "...individual variation..." (Miller 1980, p. 87).

Table 1. *Parapliohippus* dentition (measurements in mm)

Position	P3	P4	M1	M2	M3
A-P length	18.5	18.2	17.8	15.2	14.9
Tr width	16.5	14.9+	14.9	14.8	12.8

The associated scapula is crushed, but the diameter of the glenoid fossa at the proximal end is 36 mm, the width of neck is 21 mm, and the approximate length of the crushed specimen is 14 cm. An associated medial section of metapodial has a diameter of 11.2 mm. No dimensions of postcranial elements are provided for northern Cady Mountains specimens (Miller, 1980).

The status of this small horse has recently been evaluated (Kelly, 1995). *Parapliohippus carrizoensis* was initially described as *Merychippus carrizoensis* (Dougherty, 1940 and later as *Merychippus tehachapiensis* (Buwalda and Lewis, 1955). The taxonomic relations of these horses were reevaluated by Miller (1978) and Munthe (1979), who noted that *M. tehachapiensis* was a junior synonym of *M. carrizoensis*. Analysis of the facial morphology of additional specimens from the Bopesta Formation (Quinn, 1984) recognized the relation of this horse to the pliohippines, rather than to the strict merychippine lineage. Kelly (1995) noted upper cheek tooth characteristics that include: "thin enamel walls, moderate hypsodonty, and long separation of protoloph and metaloph during wear." The reevaluation by Kelly (1995) placed these fossil horses into the genus *Parapliohippus*, with a single species, *P. carrizoensis*.

This species is known from the northern Cady Mountains (Miller, 1980); the Spanish Canyon Formation of Alvord Mountain (Byers, 1960); the Red Division Fauna of the Barstow Formation (Woodburne and Reynolds, 2010); Daggett Ridge and Toomey Hills (Reynolds, 1991); the Kinnick Formation (Buwalda and Lewis, 1955) and Bopesta Formation (Quinn, 1987) of the Tehachapi Mountains; and the northern Caliente Range (Dougherty, 1940). It is considered to be a pre-Barstovian NALMA indicator (Buwalda and Lewis, 1955) and is useful for defining the late Hemingfordian (He2) NALMA between 17.5 and 16 Ma (Kelley, 1995; Tedford and others, 2004). The presence of *P. carrizoensis* from the "Talc Mine" area in the block of Barstow Formation in the southwestern Cady Mountains suggests an age between 18–16 Ma.

Discussion

Previous geologic mapping in the western Cady Mountains was conducted by Dibblee and Bassett (1966a, b). MacFadden and others (1990b), and Ross (1995) noted large amounts of clockwise rotation around a vertical axis in the Cady Mountains, in contrast to the lack of such rotation in the Mud Hills in the last 19 Ma (MacFadden and others, 1990a). The general model (MacFadden and others 1990b; Ross, 1995) indicates that paleomagnetic signatures of the Hector Formation in the northern Cady Mountains define 26° of clockwise rotation after about 16 Ma (MacFadden and others, 1990b). Consistent with their model, the left-lateral Manix and Cady faults bound the north and central portions (respectively) of the Hector block. Ross and others (1989) describe terranes of the central Mojave Desert associated with left-lateral and northwest trending faults undergoing as much as 50° of clockwise rotation after early Miocene deposition.

The DuPont Strontium Claims (Durrell, 1953), just west of Sleeping Beauty on the southeast margin of the Cady Mountains, are 14 miles east-southeast of the "Talc Mine" locality. Here, the PST lies above the other three marker horizons, and the entire section is overturned. The Southern Cady Frontal Fault places the overturned section of Barstow Formation markers against basalts and Hector Formation sediments of the central Cady Mountain Block (Bortugno and Spittler, 1986; Woodburne, 1998).

Nineteen miles west of the "Talc Mine" locality, a similar section of overturned markers MSL, BPL, SrB and PST are located at the east end of Daggett Ridge at the Columbia (Gem) Mine locality (Dibblee, 1970; Reynolds and others, 2010). Since the PST lies above the three marker horizons at the Daggett Ridge and DuPont localities, the age of those localities within this section of Barstow Formation is considered to be older than 18.8 Ma. Since *P. carrizoensis* is an indicator of the late Hemingfordian (He2), this suggests that the age of the Barstow Formation block in the southwestern Cady Mountains is somewhat younger than close counterparts located in the southeastern Cadys and at eastern Daggett Ridge.

Acknowledgements

I thank Steve Mains, Virginia Odom, and Mark Yeager from the Jurupa Mountain Discovery Center for arranging the loan of the specimen for purposes of identification. I also thank Tom Kelly for providing constructive review comments.

References cited

- Bortugno, E.J., and T.E. Spittler. 1986. Geologic map of the San Bernardino quadrangle, CDMG map 3A, Scale 1:250,000.
- Buwalda, J.P. and G.E. Lewis. 1955. A new species of *Merychippus*; United States Geological Survey Professional Paper 264-G, p. 147-152.
- Byers, P.M., Jr. 1960. Geology of the Alvord Mountain quadrangle, San Bernardino County, California: United States Geological Survey Bulletin 1089-A, p.1-71.
- Dibblee, T. W. Jr. 1970. Geologic map of the Daggett quadrangle, San Bernardino County, California, U. S. Geological Survey. Misc. Geologic Investigations, Map I-592
- Dibblee, T.W. Jr. and A.M. Bassett. 1966a. Geologic map of the Newberry quadrangle, San Bernardino County, California. U.S. Geological Survey Miscellaneous Geological Investigations Map I-461, 1:62,500.
- Dibblee, T.W. Jr. and A.M. Bassett. 1966b. Geologic map of the Cady Mountains quadrangle, San Bernardino County, California. U.S. Geological Survey Miscellaneous Geological Investigations Map I-467, 1:62,500.
- Dougherty, J.F. 1940. A new Miocene mammalian fauna from Caliente Mountain, California: Carnegie Institute of Washington Publication 514, p. 109-143.
- Durrell, C. 1953. Geological investigations of strontium deposits in southern California. California Division of Mines and Geology Special Report 32:23-36.
- Hillhouse, J.W., D.M. Miller, and B.D. Turrin. 2011. Correlation of the Miocene Peach Springs Tuff with the geomagnetic polarity time scale and new constraints on tectonic rotations in the Mojave Desert, California
- Kelly, T.S. 1995. New Miocene horses from the Caliente Formation, Cuyama Valley Badlands, California. Natural History Museum of Los Angeles County Contributions in Science 455: 1-33.
- MacFadden, B.J., N.D. Opdyke, C.C. Swisher, III, and M.O. Woodburne. 1990a. Paleomagnetism, geochronology and possible tectonic rotation of the middle Miocene Barstow Formation, Mojave Desert, California. Geological Society of America Bulletin 102: 478-493.
- MacFadden, B.J., N.D. Opdyke, and M.O. Woodburne. 1990b. Paleomagnetism and Neogene clockwise rotation of the northern Cady Mountains, Mojave Desert of Southern California. Journal of Geophysical Research 95(B4):4597-4608.
- D. M. Miller, S. R. Leslie, J. W. Hillhouse, J. L. Wooden, J. A. Vazquez, and R. E. Reynolds. 2010. Reconnaissance geochronology of tuffs in the Miocene Barstow Formation: implications for basin evolution and tectonics in the central Mojave Desert. CSU Desert Symposium Volume, 2010; p. 70-84.
- Miller, S. T., 1978. Geology and mammalian biostratigraphy of a portion of the northern Cady Mountains, California. Master's Thesis, University of California, Riverside.
- Miller, S.T. 1980. Geology and mammalian biostratigraphy of a part of the northern Cady Mountains, California. U.S. Geological Survey Open File Report 80-978:121p.
- Munthe, J. 1979. The Hemingfordian mammal fauna from the Vedder locality, Branch Canyon Sandstone, Santa Barbara County, California. Part III: Carnivora, Perissodactyla, Artiodactyla and summary. Paleobios 29:1 -22.
- Quinn, J. P., 1984. Geology and biostratigraphy of the Bopesta Formation, southern Sierra Nevada Mountains, Kern County, California. Master's Thesis, University of California, Riverside.
- Quinn, J.P. 1987. Stratigraphy of the middle Miocene Bopesta Formation, southern Sierra Nevada, California. Natural History Museum (Los Angeles), Contributions in Science 393:1-31.
- Reynolds, R.E. 1991. Hemingfordian/Barstovian Land Mammal Age faunas in the central Mojave Desert, exclusive of the Barstow Fossil Beds, in Inland Southern California: the last 70 million years, Woodburne, M.O., Reynolds, R.E., and Whistler, D.P., eds. San Bernardino County Museum Association Quarterly 38(3, 4):88-90.
- Reynolds, R. E., D. M. Miller, M. O. Woodburne, and L. B. Albright. 2010. Extending the boundaries of the Barstow Formation in the central Mojave Desert. CSU Desert Symposium Volume, 2010; p. 148-161.
- Ross, T.M. 1995. North-south directed extension and timing of extension and vertical-axis rotation in the southwestern Cady Mountains, Mojave desert, California. Geological Society of America Bulletin 107:793-811.
- Ross, T.M., B.P. Luyendyk, and R.B. Haston. 1989. Paleomagnetic evidence for Neogene tectonic rotations in the central Mojave Desert, California. Geology, 17:470-473.
- Tedford, R.H., L.B. Albright, A.D. Barnosky, I. Ferrusquia-Villafranca, R.M. Hunt, Jr., J.E. Storer, C.C. Swisher, III, M.R. Voorhies, S.D. Webb, and D.P. Whistler. 2004. Mammalian biochronology of the Arikarean through Hemphillian interval (late Oligocene through early Pliocene epochs), pp. 169-231, in Woodburne, M.O., ed., Late Cretaceous and Cenozoic Mammals of North America: Biostratigraphy and Biochronology. Columbia University Press, New York.
- Woodburne, M.O. 1998. Arikarean and Hemingfordian faunas of the Cady Mountains, Mojave Desert province, California. In D.O. Terry, Jr., H.E. LaGarry, and R.M. Hunt, Jr, eds, Depositional environments, lithostratigraphy, and biostratigraphy of the White River and Arikaree Groups (late Eocene to early Miocene, North America. Geological Society of America Special Paper 325: 197-201.
- Woodburne, M.O. and R. E. Reynolds. 2010. The mammalian litho- and biochronology of the Mojave Desert Province. CSU Fullerton Desert Studies Symposium, 2010 Desert Symposium Proceedings Volume, p. 124-147.

New mammal tracks and invertebrate ichnites from Early Miocene Barstow Formation sediments on Daggett Ridge, Mojave Desert, California

Robert E. Reynolds

Redlands, CA 92373, rreynolds220@verizon.net

ABSTRACT: Associated tracks of camels, cats, and a possible horse have been located in the early Miocene Barstow Formation on central Daggett Ridge. The medium-sized camel tracks represent the ichnospecies *Lamaichnum alfi*, while the medium-size cat tracks represent an unnamed ichnospecies of Felipeda that were probably made by *Nimravides*. The single horse print is similar in morphology to, but smaller in size than *Hippipeda araiochelata*, a Barstovian ichnospecies. This suggests a smaller taxon of horse was present in Hemingfordian Barstow Formation strata, coincident with the age of the vertebrate fauna from this part of the section. Other associated ichnites include insect casings and tufa deposited around water reeds. Fossil cat tracks have been previously reported from Daggett Ridge Basin., one of the two localities - under discussion - Daggett Ridge West is a second and new locality and its ichnites are described here.

Geologic Setting

Daggett Ridge is located in California's central Mojave Desert, south of Barstow and Daggett (see Figure 1 in Reynolds, *Parapliohippus*, this volume). Barstow Formation strata on Daggett Ridge (Dibblee, 1970; Reynolds and others, 2010) are recognized by a series of marker beds; lowest to highest: massive stromatolitic limestone (MSL), brown platy limestone (BPL), and strontium-borate horizon (SrB) (Reynolds and others, 2010). The Daggett Ridge section also contains the Peach Spring Tuff (18.8 Ma; Hillhouse and others, 2010), which occurs above the marker sequence on eastern Daggett Ridge at the Columbia [Gem] locality and below the marker sequence on western Daggett Ridge at Stoddard Cut-off (Reynolds and others, 2010). Consequently, the precise age of Miocene sediments on central Daggett Ridge is difficult to determine. The age is currently based on a single vertebrate local fauna, the Powerline locality (Reynolds, 1991; SBCM locality 1-109-2), which has produced thirteen mammalian taxa, including the early Miocene horse, *Parapliohippus carrizoensis* (Reynolds, 1991). This distinctive taxon has a known temporal range of only two million years, from 18 Ma to 16 Ma (Kelly, 1995; Reynolds, 2013).

Stratigraphy

Two localities are known to contain fossil tracks on central Daggett Ridge. In relation to the Powerline locality, the westerly location is called Daggett Ridge West (DRW), and the easterly Daggett Ridge Basin (DRB). The Powerline locality is situated on the uppermost of three

BPL marker beds. The Daggett Ridge West tracks are in the lowest of the three BPLs and just above MSL, which is approximately 100 feet stratigraphically below the Powerline locality. The Daggett Ridge Basin tracks are found in a marly limestone estimated to be 40–60 feet stratigraphically higher than the BPL marker beds within which the Powerline locality lies.

Track Descriptions

Camel tracks

The medium-sized camel tracks represent a single ichnotaxa, *Lamaichnum alfi* (Sarjeant and Reynolds, 1999; plate 2, fig. 7), known from both the Daggett Ridge West and the Daggett Ridge Basin localities. At the DRW locality, the “heart-shaped” manus (Figures 1, 3a) measures 7.5 cm in length and 5.0 cm in width. The anterior gap diminishes in the posterior quarter of the print. A small indentation suggests a posterior gap, and there is indication of a medial pocket. No claw marks are apparent (Figs. 1, 3a).

The sub-quadrate pes specimen from DRW (L 6.5 cm, W 7.0 cm; Fig 2, 3b); and from DRB (L: 7.0 cm, W: 6.0 cm; [Fig. 4a, 4b) are similar in dimensions. The anterior gap is of relatively constant width and extends to the posterior third of the print; there is a slight medial pocket. The posterior margin of the track is broadly convex with a small indentation suggesting a posterior gap. No claw marks are apparent (Figs. 1, 2, 3b; 4a). These pedial imprints are referred to *Lamaichnum alfi*. Size and morphology is comparable to the *Lamaichnum alfi* tracks from the Barstow Formation in the Mud Hills (Sarjeant and Reynolds, 1999; plate 2, fig. 7).

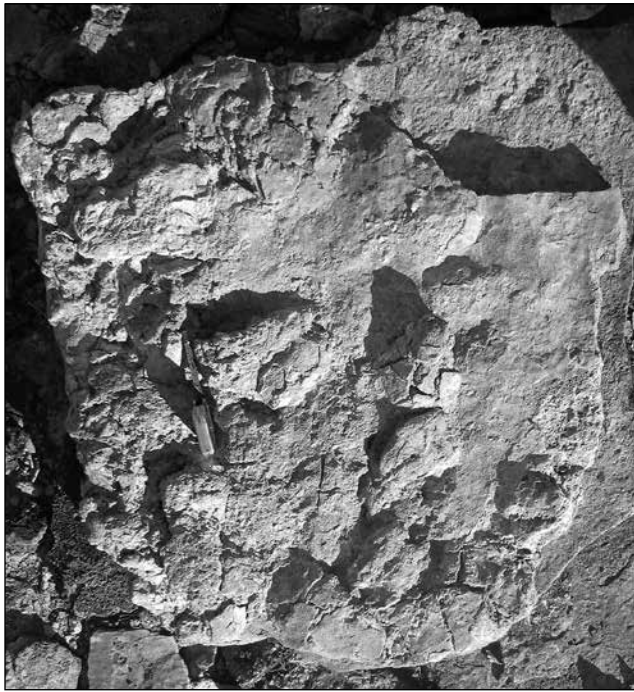


Figure 1: Camel left manus impression, referred to *Lamaichnum alfi*, from the Daggett Ridge West locality.



Figure 2: Camel left pes impression, referred to *Lamaichnum alfi*, from the Daggett Ridge West locality.

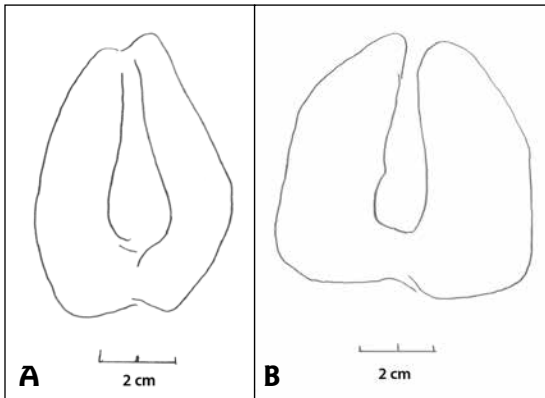


Figure 3. (a) sketch of Fig 1, camel left manus impression; (b) sketch of Fig 2, camel left pes impression,

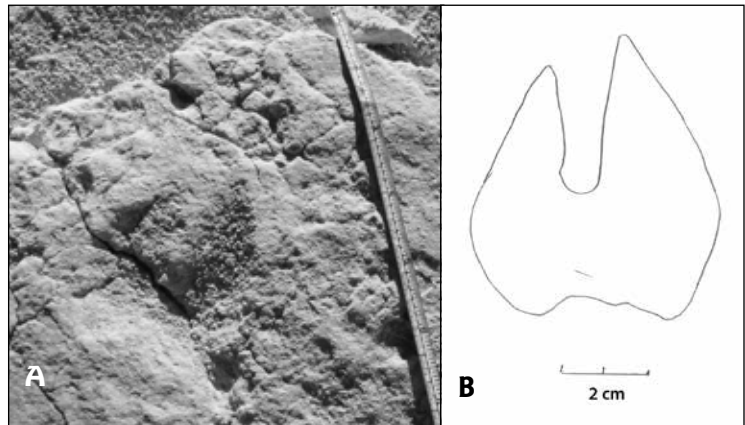


Figure 4a. (a) camel left pes impression, referred to *Lamaichnum alfi*, from the Daggett Ridge Basin locality; (b) sketch of camel left pes impression.



Figure 5. Sketch of horse track from the Daggett Ridge West locality. Morphometrics of this hoof print (L: 3.0 cm; W: 2.0 cm) suggest a small horse manus print of Hemingfordian age.

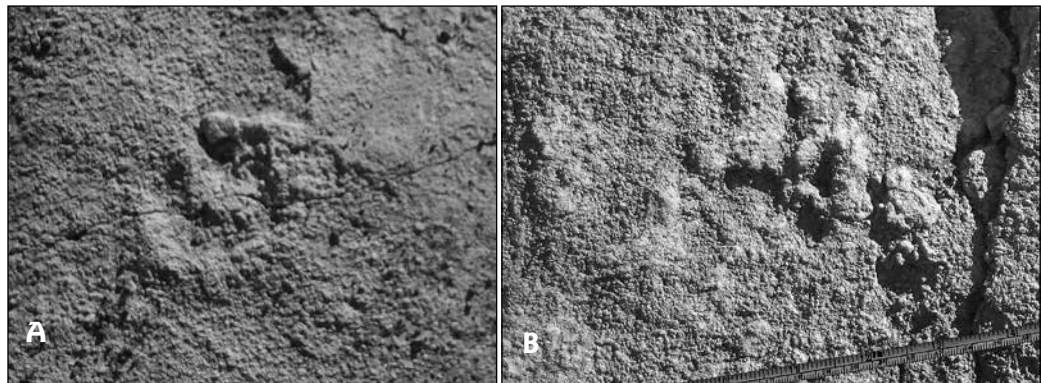


Fig 6. (a) Medium-sized cat manus impressions referred to *Nimravides hayii* from Daggett Ridge Basin (Reynolds and Milner, 2012). Manus has oval digital pads and an equidimensional bilobed metapodial pad. (b) medium-sized cat pes impressions referred to *Nimravides hayii* from Daggett Ridge Basin (Reynolds and Milner, 2012). Pes, has elongate digital pads and trilobed metapodial pads.

Horse track

A single impression at the Daggett Ridge West locality may represent the hoof of a horse. The impression (Fig. 5) is ellipsoidal, truncated posteriorly, and the morphology suggests a hind hoof. Dimensions of the impression (length: 4.0 cm; width: 3.0 cm) are 33% shorter and 22% narrower than Barstovian horse tracks from the Mud Hills (Reynolds, 2006, 2013), reinforcing a Hemingfordian age for Daggett Ridge West.

Cat tracks

Manual and pedial cat footprint impressions are present at the Daggett Ridge Basin locality. The dimensions of these tracks were previously described (manus L:6.0 cm x W: 7.0 cm; pes L: 6.5 cm x W: 5.5 cm; Reynolds, 2004; Reynolds and Milner, 2012). Digits of the manus (Fig. 6a, 7a) are oval, while digits of pes (Fig. 6b, 7b) are elongate, both being separate from the metapodial pad, the latter being bilobed in the manual print and trilobed in the pedial print. Their age is Late Hemingfordian (He2), 17.5–16.2 Ma, based on the presence of *Parapliohippus carrizoensis* at the stratigraphically lower Powerline locality. These Felipeda tracks were probably made by *Nimravides hayii*, (Browne, 2005). Since body fossils of small cats are not recorded during the late Hemingfordian (He2), the tracks

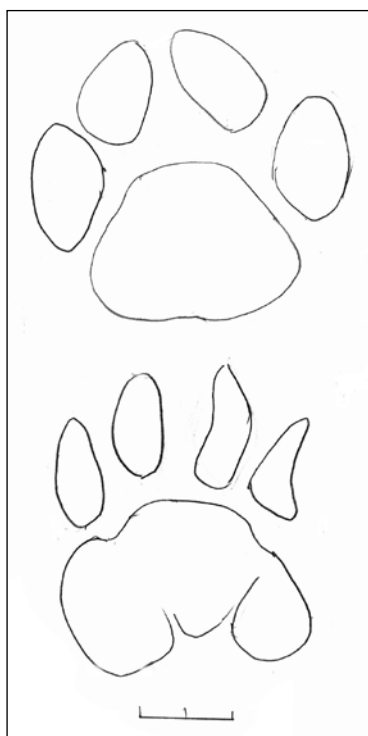


Fig 7a, 7b. Sketch of medium-sized cat print impressions referred to *Nimravides hayii* from Daggett Ridge Basin (Reynolds and Milner, 2012). Manus (a) has oval digital pads and an equidimensional bilobed metapodial pad. Pes, (b) has elongate digital pads and trilobed metapodial pads (sketches from Reynolds and Milner, 2012)

probably indicate that *Nimravides* sp. was present in western North America in latest Hemingfordian time, two million years before skeletal remains have been reported (Reynolds and Milner, 2012).

Invertebrate trace fossils

The reddish gray, fine-grained silty sandstone above the limestone at Daggett Ridge Basin contains molds of insect burrows and casts of fossil reeds. The insect burrows (Figure 8) indicate the development of soil horizons during times of stable surfaces. Such burrows are cells to house developing pupae of *Bembrix* sp. (Crabronidae) sand wasps (Eiseman and



Figure 8. Insect larval casing mold filled with sediment

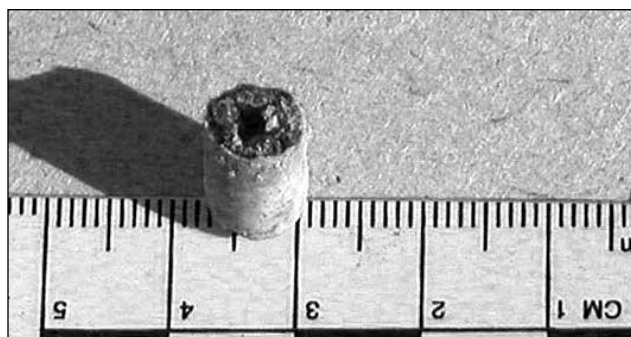


Figure 9. Tufa coating around water reed.

Charney, 2010). The tufa-coated casts of reeds (Figure 9) suggest intermittent incursion of shallow, clear, lake water or wet playas with margins that supported water reeds in a developing basin.

Summary

New tracks, trackways and nonvertebrate ichnites from two localities on Daggett Ridge amplify the biostratigraphy of the fossiliferous sedimentary section that includes the Hemingfordian Powerline locality. No exclusively Barstovian tracks or body fossils have been recovered from Daggett Ridge, suggesting that the age of Barstow Formation sediments located here are older than 16 Ma, or late Hemingfordian. (Woodburne and Reynolds, 2010).

Acknowledgements: This work was conducted under the authorization of Jim Shearer, archaeologist, Bureau of Land Management, Barstow Field Office (BLM Permit No. CA-10-00-007P). Leroy V. Leggett (Loma Linda University) brought the tracks at the Daggett Ridge Basin locality to my attention.

This study could not have been completed without the help of volunteers from the Mojave River Valley Museum (B. Hilburn, president), the Riverside Metropolitan Museum (T. Howe), and the Natural History Museum of San Diego (M. Roeder). Thanks also go to Don Lofgren, Alf Museum, Claremont, CA, for constructive comments on an earlier draft of this paper.

References

- Browne, I. 2005. A case for reassignment the reassignment of the Barstovian Felid *Pseudaelurus marshi* to the genus *Nimravides*. *Journal of Vertebrate Paleontology*, Abstracts vol. 25(3, Suppl) p. 40A.
- Dibblee, T. J., Jr. 1970. Geologic map of the Daggett quadrangle, San Bernardino County, California. USGS Misc. Geol. Investigations, Map I-592, scale 1:62,500'.
- Eiseman, C., and N. Charney. 2010. *Tracks and Signs of Insects and Other Invertebrates, a Guide to North American Species*. Stackpole Books, Mechanicsburg PA, 582 p.
- Hillhouse, J. W., D. M. Miller and B. D. Turrin. 2010. Correlation of the Miocene Peach Spring Tuff with geomagnetic polarity time scale and new constraints on tectonic rotations in the Mojave Desert, in *Extending the boundaries of the Barstow Formation in the central Mojave Desert*, R. E. Reynolds, ed. CSU Desert Studies symposium volume, p. 177-195.
- Kelly, T.S. 1995. New Miocene horses from the Caliente Formation, Cuyama Valley Badlands, California. *Natural History Museum of Los Angeles County Contributions in Science* 455, p. 1-33.
- Reynolds, R.E. 1991. Hemingfordian/Barstovian Land Mammal Age faunas in the central Mojave Desert, exclusive of the Barstow Fossil Beds, in *Inland Southern California: the last 70 million years*, M. O. Woodburne, R. E. Reynolds and D. P. Whistler, ed. San Bernardino County Museum Association Quarterly vol. 38(3, 4) p. 88-90.
- Reynolds, R. E. 2004. Miocene cat tracks from the Mojave Desert of California. Abstract, *Jour. Vert. Paleontology*, vol. 24(3, Suppl) p. 103A.
- Reynolds, R. E. 2006. Horse hoof prints in the fossil record. CSU Fullerton Desert Studies Symposium volume, pp. 25-28.
- Reynolds, R. E., and A. R. C. Milner. 2012. Early Neogene cat tracks from California and Utah. CSU Fullerton Desert Studies Symposium volume, p. 153-159.
- Reynolds, R. E. 2013. *Parapliohippus carrizoensis* (Perissodactyla: Equidae) from the early Miocene (Hemingfordian NALMA) Barstow Formation outcrops in the southwestern Cady Mountains, Mojave Desert, California. CSU Fullerton Desert Studies, this volume.
- Reynolds, R. E., D. M. Miller, M. O. Woodburne and L. B. Albright. 2010. Extending the boundaries of the Barstow Formation in the central Mojave Desert in *Extending the boundaries of the Barstow Formation in the central Mojave Desert*, R. E. Reynolds, ed. CSU Desert Studies volume, p. 148-161.
- Reynolds, R. E. and A. R. C. Milner. 2012. Early Neogene cat tracks from California and Utah in *Extending the boundaries of the Barstow Formation in the central Mojave Desert*, R. E. Reynolds, ed. CSU Desert Studies symposium volume, p. 153-159.
- Sarjeant, W.A.S. and R. E. Reynolds. 1999. Camelid and horse footprints from the Miocene of California and Nevada, pp 3-20 in *Fossil Footprints*, R.E. Reynolds, ed. San Bernardino County Museum Association Quarterly, vol. 46(2).
- Woodburne, M.O. and R. E. Reynolds, 2010. The mammalian litho- and biochronology of the Mojave Desert Province. CSU Fullerton Desert Studies symposium volume, p. 124-147.

Recognized, zoned, active and potentially active faulting in the Mojave Desert

Frank F. Jordan, Jr

California State University, Los Angeles

ABSTRACT—Large historic earthquakes centered in the Mojave Desert have focused attention on active and potentially active faulting that crosses the Mojave Province. The MW 6.4 Manix Earthquake of 1947 occurred along the Manix fault in the north-central Mojave Desert. More recently, the MW 7.3 Landers Earthquake and the MW 7.1 Hector Mine Earthquake occurred in 1992 and 1999, respectively, along northwest-striking faults in the southeastern Mojave Desert. All of these faults belong to the Eastern California Shear Zone (ECSZ). The ECSZ is recognized for the potential to produce large, if relatively infrequent, earthquakes. Portions of several northwest-striking and east-striking faults mapped within the ECSZ are included within Alquist-Priolo Earthquake Fault Zones (A-P EFZs) by the State of California. The A-P EFZs are State issued planning/building safety zones several hundred feet in width that are designed to incorporate traces of active and potentially active faulting. However, the actual surface ruptures associated with the historic earthquakes have revealed a more complicated pattern of fault rupture when compared with current fault maps, including the maps showing A-P EFZs. Geomorphology, synthetic aperture radar, Thematic Mapper imagery, and digital aerial photographic interpretation suggest that the ECSZ is more analogous in character to a large braided stream. Individual faults in the ECSZ appear more curvilinear on high-altitude imagery than is portrayed on published geologic maps. Review of various types of imagery reveals an anastomosing pattern of fault traces within the ECSZ. The more northerly directed rupture patterns of the 1992 Landers and 1999 Hector Mine earthquakes, and the cascaded pattern of fault rupture demonstrated by at least the Landers earthquake may be the result of a more northerly oriented vector component of current plate motion or a slight clockwise rotation of microplates within the shear zone. Use of digital imagery suggests that the ECSZ may extend as far southeast as the San Andreas fault near the Salton Sea, as far northwest as the Pond-Poso Creek fault northeast of Bakersfield, and as far west as the Mirage Valley-Shadow Mountain(s)-Apple Valley fault in the Adelanto, Victorville, and Apple Valley areas. The potential for fault rupture to cascade across mapped faults suggests that the seismic hazard associated with the ECSZ may currently be underestimated in maximum magnitude, duration, and areal extent. The extent of the Mojave Desert, when compared with the very limited data sets currently available regarding active faulting within the same area, points to the need to maintain continued access to the fault traces for detailed two-dimensional and three-dimensional subsurface studies and fault investigations.

Geology

The Mojave Desert block occupies a pivotal location at the heart of the southern California tectonic regime. The Mojave Desert block is bordered on the southwest by the San Andreas fault, the recognized transform boundary between the Pacific and the North American tectonic plates (Crowell, 1968, 1975), the southern Sierran block on the northwest, the Basin and Ranges province on the north and northeast, the Sonoran Desert block on the east, and the Transverse Ranges province on the south (Norris and Webb, 1976). The central and southeastern portions of the Mojave Desert are characterized by mountain ranges separated by broad alluviated valleys. Mountain ranges within the Mojave block expose Precambrian crystalline basement rocks, upper Precambrian to Paleozoic sedimentary rocks, and Mesozoic marine and

continental sedimentary rocks, which are intruded by syenitic plutonic rocks, hypabyssal volcanic rocks and granitoid batholithic rocks (Woodburne, 1991; Dokka *et al.*, 1988; Dibblee, 1967h). Surface deposits within the valley areas of the block are primarily alluvial, pluvial and lacustrine sediments of Pliocene, Pleistocene, and Holocene age. Considerable effort has been expended mapping the geology of the Mojave Desert block (*i.e.* California Department of Water Resources, 1934, 1963, 1967, 1984; Hewett, 1954; Bowen, 1954; Bader and Dutcher, 1958; Grose, 1959; Burke, 1960; Page and Moyle, 1960; Dibblee, 1960a-c, 1964a-d, 1965, 1966, 1967a-h, 1968a, 1968c, 1970, 1980; Dibblee and Bassett, 1966a-b; Kunkel, 1962; Kupfer and Bassett, 1962; Bassett and Kupfer, 1964; McCulloh, 1965; Steinen, 1966; Rogers, 1969; Hardt, 1971; Morton, 1974; Jennings, 1977; Moseley, 1978; Morton *et al.*, 1980; Miller, 1980; Williamson, 1980; May, 1981; Brown, 1981,

1984, 1986; Miller *et al.*, 1982; Burke *et al.*, 1982; Woodburne and Tedford, 1982; Woodburne *et al.*, 1982, 1990; Wells *et al.*, 1984; Bortugno and Spittler, 1986; Lambert, 1987; Howard *et al.*, 1987; Spencer, 1990a; Skirvin and Wells, 1990; Howard and Miller, 1992; Umbarger, 1992a-b; Chrisley, 1997; Cox and Tinsley, 1999; Cox and Hillhouse, 2000; Stamos *et al.*, 2001, 2004; Morton and Miller, 2003a-b, 2006; URS, 2003a-b; Mojave Water Agency, 2004; Hernandez *et al.*, 2008; Jennings *et al.*, 2010). Although a considerable body of literature exists regarding the geology of the Mojave Desert, the older mapping efforts were generally conducted prior to the 1992 Landers earthquake, with its coalescing fault rupture pattern, and prior to the 1983 Coalinga and 1987 Whittier Narrows earthquakes, which revealed the presence of blind active reverse faulting in southern California. In particular, extensive mapping in southern California was conducted in the 1960's by various agencies, including the U.S. Geological Survey (USGS), California Division of Mines and Geology [now the California Geological Survey (CGS)], the California Department of Water Resources (DWR), and the California Division of Oil and Gas [now the Division of Oil, Gas, and Geothermal Resources (DOGGR)], well before the theory of plate tectonics was entrenched into geological models (Atwater, 1970).

Faulting

Extensional normal faulting, associated with the Mojave Rift, initiated in the central Mojave Desert during the Oligocene (Dokka, 1986, 1989; Dokka and Glazner, 1982; Dokka *et al.*, 1988, 1991, 1994; Woodburne, 1991). This extensional tectonism was directed north and south, resulting in the development of generally east-striking normal faults during the Miocene, between 22 and 17 million years ago (Walker *et al.*, 1990; Woodburne, 1991; Dokka *et al.*, 1991, 1994). Local reverse faulting during this period resulted in the uplift of the Waterman Hills near Barstow some 20 to 30 vertical kilometers (Dokka *et al.*, 1988; Woodburne, 1991). Up to 90° of clockwise rotation of the blocks bounded by east-striking faults may have occurred during the Miocene (Kamerling and Luyendyk, 1979; Luyendyk and Hornafius, 1987; Luyendyk *et al.*, 1980, 1985; Carter *et al.*, 1987; Golombek and Brown, 1988; Ross *et al.*, 1989; MacFadden *et al.*, 1990a, 1990b). In addition, Valentine *et al.* (1988) documented counterclockwise rotations of certain blocks in the Mojave Desert during Cenozoic time. Also during this period, cessation of subduction and initiation of the ancestral San Andreas fault as a transform boundary began at around 20 Ma (Atwater, 1970).

North-south directed compression began to affect the Mojave Desert after approximately 13 Ma, with resultant rupture of northwest-striking faults slicing through the central and western Mojave (Garfunkel, 1974; Bartley *et al.*, 1990; Spencer, 1990b; Woodburne, 1991). Several lengthy northwest-striking and somewhat

shorter east-northeast-striking faults are recognized as traversing the central and southeastern Mojave Desert block (Jennings, 1975, 1977, 1992, 1994; Bryant, 1987, 2005; California Geological Survey, 2007; Jennings and Bryant, 2010; Jennings *et al.*, 2010; Ziony and Yerkes, 1985; Ziony and Jones, 1989). These faults were included within the southwest portion of the Neogene age Eastern California Shear Zone (ECSZ) by Dokka and Travis (1990a, 1990b) and Richard and Dokka (1992). Atwater (1992) suggested that the initiation of faulting within the ECSZ may have corresponded with the reorientation in tectonic plate motion that resulted from the capture of Baja California onto the Pacific plate and the opening of the Gulf of California around 5.5 Ma. Major mapped northwest-striking faults in the southwest portion of the ECSZ include the Helendale, Lenwood, Lockhart, Calico, Old Woman Springs, Harper Lake, Blackwater, Camp Rock, Mt. General, Gravel Hills, Homestead Valley, Emerson, Hidalgo, Mesquite Lake and Copper Mountain faults. The Death Valley, Soda-Avawatz, and Bristol-Granite Mountains fault zones define the northeast boundary of the ECSZ (Brady, 1988, 1992; Brady and Dokka, 1989; Brady *et al.*, 1989; Dokka and Travis, 1990a; Howard and Miller, 1992). Previous geologic mapping has shown these northwest striking faults to be locally discontinuous along strike and separated by relatively large spaces, particularly in-between the named fault zones.

A-P faulting

The Alquist-Priolo Earthquake Fault Zoning Act (A-P Act) has defined surface rupture along individual faults to be "active" in California if it has occurred during the Holocene epoch (approximately the last 11,300 years) and "potentially active" if it has occurred during the Pleistocene epoch (Hart and Bryant, 1997, 1999, 2003; Bryant and Hart, 2007). The definition of "potentially active" faulting, being linked legally to the definition of the Pleistocene, was formerly surface rupture that had occurred during about the last 1.8 million years. Based on the change to the start of the Pleistocene epoch (Gibbard and Head, 2009a, 2009b, 2010; Gibbard *et al.*, 2009; Finney, 2011a, b), the definition of what constitutes a "potentially active" fault has also changed to include surface rupture during the past approximately 2.6 million years. Relatively linear portions of several of the faults in the Mojave Desert are included within Alquist-Priolo Earthquake Fault Zones (A-P EFZs) by the State of California (Bryant and Hart, 2007). The A-P EFZs are designated by the State to identify faults that are considered active or suspected to be active (Bryant and Hart, 2007). In all, faulting identified as active or suspected to be active has been identified by the California Geological Survey on fifty-six 7.5 minute quadrangles covering portions of the Mojave Desert (Bryant and Hart, 2007). Portions of faults included within A-P EFZs include the Helendale, Lockhart, South Lockhart, Lenwood, Old Woman Springs, Upper and

Lower Johnson Valley, Homestead Valley, Kickapoo, Burnt Mountain, Eureka Peak, Emerson, Hidalgo Peak, Camp Rock, Gravel Hills, Calico, West Calico, Copper Mountain, Mesquite Lake, Pisgah, Bullion, Lavic Lake, Llano, Manix faults, and the Newberry Fracture Zone within the Mojave Desert, as well as the bounding San Andreas, Garlock, Pinto Mountain and North Frontal faults (Bryant and Hart, 2007). In addition to active faulting as defined by the A-P Act, the 2010 California Building Code (CBC) expanded the definition of active faulting in California to include faults that are associated with, or may potentially generate, earthquake activity (California Building Standards Commission, 2010). This definition of active faulting has been continued in the 2013 CBC (California Building Standards Commission, 2013). However, a list of active faults delineated by seismicity has not yet been generated by the State (Chris Wills, CGS, personal communication, 2012).

Seismicity

Historic movements of faults in the ECSZ occurred in 1947 along the Manix fault (Richter, 1947; Buwalda and Richter, 1948; Keaton and Keaton, 1977; Jefferson *et al.*, 1982), in 1992 on the Landers fault zone (Hauksson *et al.*, 1993; Hart *et al.*, 1993; Topozada, 1993; Treiman, 1992a-b; Goter, 1992; Goter *et al.*, 1994), and in 1999 along the Lavic Lake fault (Hart and Bryant, 1997, rev. 1999). The 1947 Manix earthquake ruptured in an east-northeast direction in the northeast portion of the ECSZ (McGill *et al.*, 1988). The 1992 Landers and 1999 Hector Mine earthquakes produced ground surface ruptures that trended in generally north-south directions in the southwest portion of the ECSZ. The movement during the Landers earthquake in particular appeared to take advantage of rupture from northwest-striking faults (Eureka Peak, Lower Johnson Valley) on to the northeast-striking Kickapoo fault, and then back onto northwest-striking faults (Emerson and Camp Rock).

Geodetics

Geodetic measurements of block motion in the Mojave Desert show the overall vector motion relative to the Pacific Plate to be oriented to the northwest (Sauber *et al.*, 1986). The more northerly trends of surface rupture produced during the most recent quakes in the northwest-striking portion of the ECSZ suggest that the current local vector of plate motion within this zone is northerly directed. This north-directed vector of plate motion has also been detected as stress changes in the crust resulting from movement along the Landers fault (Stein *et al.*, 1992; Jaume and Sykes, 1992; Harris and Simpson, 1992, 1993). If the overall vector of plate motion in this portion of the Mojave Desert is indeed northerly directed, the mapped northwest orientations of the faults in the southwest portion of the ECSZ may represent a slightly older, perhaps late Pleistocene-early Holocene vector of

plate motion. Such a change in the overall vector motion of plate movement could help to explain the orientation of both the Landers and Lavic Lake rupture patterns and the large magnitudes of the Landers (M_w 7.3) and Hector Mine (M_w 7.1) earthquakes.

Paleoseismicity

In addition to historic earthquakes and associated ground surface rupture, surficial geologic/geomorphic mapping and subsurface two-dimensional and three-dimensional paleoseismic trenching studies of faults traversing the Mojave Desert have demonstrated Holocene and late Pleistocene offset along portions of various faults. Evidence for Holocene activity has been demonstrated to have occurred on the Landers-Johnson Valley fault (Manson, 1986; Crippen, 1988; Stein *et al.*, 1992; Reynolds, 1993; Bornyasz, 1993; Herzberg and Rockwell, 1993; Sieh *et al.*, 1993; Lindvall and Rockwell, 1993; U.S. Geological Survey, 1992, 1993; Herzberg, 1996), Landers-Homestead Valley fault (Hawkins and McNey, 1979; Hill *et al.*, 1980; Hutton *et al.*, 1980; McJunkin, 1980; Manson, 1986; Reynolds, 1993a-b; Cinti *et al.*, 1993; Hecker *et al.*, 1993), Landers-Kickapoo fault (Reynolds, 1993a-b; Lazarte and Lemmer, 1993; Lazarte *et al.*, 1994; Murbach *et al.*, 1994; Sowers *et al.*, 1994), Landers-Emerson fault (Reynolds, 1993a-b; Sieh *et al.*, 1993), Landers-Camp Rock fault (Shakal, 1993), Landers-Calico fault (Hauksson, 1993; Hafner and Hauksson, 1994); Galway Lake fault (Beeby and Hill, 1975; Hill and Beeby, 1977); Helendale fault (Bryan and Rockwell, 1994, 1995), Lenwood fault (Padgett and Rockwell, 1994), Lavic Lake fault (Scientists *et al.*, 2000), North Noble Dome fault (Miller *et al.*, 1994), and Old Woman Springs fault (Houser, 1996; Houser and Rockwell, 1996). Shear in the central Mojave Desert would appear to concentrate onto the Blackwater fault in the northern Mojave Desert, based on geologic mapping and tectonic geodesy. However, Oskin and Iriondo (2004) found evidence only for Pliocene-age surface offset along the Blackwater fault. Predictions of rapid rates of Holocene-age fault slip derived solely from geodetic measurements for this critical member of the ECSZ could not be substantiated (Oskin and Iriondo, 2004).

Rubin and Sieh (1997) and Rockwell *et al.* (1993, 2000) indicated that ground surface rupturing earthquake events along faults in the ECSZ are relatively infrequent, averaging approximately 5,000 to 15,000 years between events. Utilizing terms more familiar to vulcanologists, the faults of the ECSZ lie *dormant* for long periods of time in-between short-lived spurts of *active* offset (Rubin and Sieh, 1997). Changes in local plate motion and/or local deformation of blocks can result in the re-orientation of the vector components of motion, causing the extinction of movement along individual fault branches, localized fault segments, or even an entire fault. Through time, though, changes in plate motion can take advantage of crust weakened by older faults, resulting in the

reactivation of old faults, often by movement in a different direction. For example, the Whittier and Newport-Inglewood faults are modeled as Miocene age normal faults that now exhibit right-lateral, strike-slip movement, while the Elysian Park and Puente Hills blind thrust faults are considered to have initially developed as extensional detachment faults, but now accommodate compressional low-angle thrust faulting (Dolan and Sieh, 1992a, 1992b; Dolan *et al.*, 2001).

Fault trenching represents the primary method for verifying the presence or absence of active faulting in California, as defined by the A-P Act. Fault trenching, as required to satisfy elements of the A-P Act, results in the excavation of continuous subsurface exposures to depths sufficient to reveal all available Holocene-age sediments as well as the uppermost portion of the Pleistocene-age, or older, sediments at a particular site. Although limited trenching can be excavated manually, most A-P investigations require the use of rubber-tire extendahoes, track-mounted backhoes, bulldozers, or earthmovers. These pieces of equipment are normally trucked to the appropriate locations on large flat-bed semi trucks. These trucks require adequate means of access, particularly the presence and maintenance of paved and dirt access roads. Safety concerns, most succinctly expressed in the regulations of CalOSHA, dictate that the trenches be shored to prevent collapse or benched to reduce the risk of collapse. Therefore, fault trenching often results in the production of large, deep, wide excavations hundreds to thousands of feet in length, bordered on both sides of the trench by spoil piles as long as the trench itself, ten or more feet in height and tens of feet in width. Geotechnical testing, particularly cone penetrometer testing (CPT), when coupled with continuous core geologic drilling can provide a means to identify active and potentially active faulting, but also requires the deployment of large well-equipped trucks and accompanying drill rigs. Although the State recognizes the use of geophysical methods to locate faults, the A-P Act does not permit fault identification or age determination of a fault by geophysical means alone.

SAR and Thematic Mapping

Analyses of synthetic aperture radar (SAR) image mosaics generated by EROS and the USGS (U.S. Geological Survey, 1985a-g; Sneed *et al.*, 2003) and Thematic Mapper imagery produced by the Jet Propulsion Laboratories (Ford *et al.*, 1990) revealed light-toned, generally curvilinear traces of these recognized faults in the Mojave Desert. Field mapping conducted by the author has confirmed that these lighter toned features represent energy reflected off of Pleistocene-age calcium carbonate (caliche) precipitates which have been uplifted by movements along the fault strands and subaerially exposed. The curvilinear character of the fault zones observed on the SAR images suggests that the northwest-striking portion of the ECSZ

is composed of anastomosing faults that produce a braided shear zone that transmits energy in an overall pattern similar to a large braided stream or river. This pattern of fault zone development would seem to intimate that fault rupture events in the southwest portion of the ECSZ may currently follow pathways of convenience based more on fractal physics than on repetitious characteristic events (Turcotte, 1997). The reorientation of the vector plate motion within the ECSZ from a northwesterly direction to a more northerly direction may explain the apparent anastomosing character of the shear zone. The curvilinear traces of the individual faults could be the result of clockwise rotation affecting smaller blocks in the shear zone that reflects the reorientation of the vector motion from northwest-directed to north-directed.

Southeast terminus of the ECSZ

The northwest-striking faults of the southwest portion of the ECSZ are mapped as terminating at the southeast margin of the Mojave Desert against the east-striking Pinto Mountain fault (Dibblee, 1968, 1992; Bortugno, 1986; Bortugno and Spittler, 1986; Grimes, 1986, 1987; Hopson, 1998). The California Geological Survey (CGS) currently recognizes a single active trace of the Pinto Mountain fault, which is incorporated into an Alquist-Priolo EFZ (California Geological Survey, 1988). The U.S. Geological Survey also recognized a single trace to the fault, located approximately one-half mile north of the trace mapped by the State (Dibblee, 1967d, 1967h). A fault investigation conducted by John R. Byerly, Inc. (November 17, 2009) in the Joshua Tree area documented the presence of multiple active traces of the Pinto Mountain fault across a zone over a half mile in width, stretching from the trace mapped by CGS on the south to the trace mapped by Dibblee on the north. Until 1992, only a short segment of the southeastern-most part of the Bullion fault was mapped as penetrating the Pinto Mountain fault, right-laterally offsetting the main trace of the Pinto Mountain fault by approximately 1.8 miles (Hatheway, 1975; Jennings, 1992, 1994). Surface rupture associated with the 1992 Landers earthquake revealed the presences of the active Eureka Peak and Burnt Mountain faults south of the Pinto Mountain fault. However, neither of these southern branches of the Landers fault zone was documented as offsetting the Pinto Mountain fault at their intersections. These ruptures did indicate that active faulting of the ECSZ does also traverse the eastern portion of the Transverse Ranges block. Mapping by Rymer (2000) in the southern portion of the Transverse Ranges has shown that the Burnt Mountain fault correlates with the East Wide Canyon fault and the Eureka Peak fault is coincident with the West Deception Canyon fault. These correlations suggest that at least the Landers fault zone of the ECSZ thoroughly penetrates the Transverse Ranges block to the Mission Creek branch of the San Andreas fault. Rymer (2000) also recognized the Blind Canyon and

Desolation Canyon faults in the Desert Hot Springs area, suggesting that the Landers fault zone may actually be wider than revealed by the 1992 earthquake. The pattern of aftershock seismicity generated by the 1992 Joshua Tree and Landers earthquakes provided a subsurface connection linking the Landers fault zone to the Indio Hills fault zone (Hauksson *et al.* 1993; Hart *et al.* 1993). The Indio Hills fault zone is mapped as a north-striking splay that branches off of the Mission Creek (San Andreas) fault (Bryant and Hart, 2007; Hart and Bryant, 1997, revised 1999, revised 2003; Corona and Sabins, 1993). Nicholson *et al.* (2012) modeled the active Hidden Springs branch of the San Andreas fault zone northeast of the mapped main trace of the San Andreas fault, based on three-dimensional mapping of microseismic hypocentral locations. Crowell (1992) postulated that the blocks northeast of the San Andreas fault are experiencing simple right-lateral shear “extending for an unknown distance” northeast of the San Andreas fault.

Review of digital 3D imagery rendered by Google Earth (Google, 2009–2012), Bing Maps 3D (Microsoft, 2011), and WorldWind (NASA, 2011) indicate that several northwest-trending tonal lineaments with geomorphic expressions traverse the Transverse Ranges block on trend with the Homestead Valley, Copper Mountain, Hidalgo, Mesquite Lake faults, as well as previously mapped Bullion fault. Mapping of microseismicity north of Salton Sea has revealed the presence of the Hidden Hills branch of the San Andreas fault, located northeast of the Mission Creek branch (Goter, 1988, 1992; Goter *et al.* 1994; Nicholson *et al.* 2012). Similar to the Indio Hills fault, at least four north-striking mapped splays branch off of the Hidden Hills (San Andreas) fault (Jennings, 1992, 1994; Jennings and Bryant, 2010). The California Geological Survey presented these splays as potentially active faults (Jennings, 1992, 1994; Jennings and Bryant, 2010). Microseismicity is also associated with each of these northerly-trending splays (Real *et al.* 1978; Topozada *et al.*, 2000; Goter, 1988, 1992; Goter *et al.* 1994; Nicholson *et al.* 2012). The lineaments observed crossing the Transverse Ranges appear to correspond to the northerly-striking splays of the Hidden Hills branch of the San Andreas fault. If these lineaments indeed represent the surface expressions of potentially active faults, they may represent the projection of at least the Homestead Valley, Copper Mountain, Hidalgo and Mesquite Lake faults of the ECSZ to points of connection with the San Andreas fault. This would suggest that maximum magnitudes (M_{MAX}) for earthquakes along these faults may be considerably larger than currently proposed, with longer durations, and much higher potentials for triggered slip in the event of a large earthquake along the San Andreas fault. The maximum considered earthquake (MCE) magnitude for these faults may be similar to cascaded events forecast for the San Jacinto and Elsinore fault zones (i.e. M_w 7.85) by the U.S. Geological Survey (2008), Frankel *et al.* (2008), Petersen *et al.* (2008), and the Working Group (2008).

The currently accepted fault model postulates that the northwest oriented vector of movement along the eastern portion of the ECSZ originates from the west-directed vector of movement associated with the north side of the Pinto Mountain fault (Dibblee, 1968b; Plesch and Shaw, 2002; Plesch *et al.*, 2007). The postulated connection between the Hidden Hills branch of the San Andreas fault with the southeast end of the ECSZ would provide a source of the energy required to instigate and maintain movements along the eastern portion of the ECSZ. This linkage between the Hidden Hills fault and the ECSZ would allow transference of a portion of the Pacific-North American plate transform movement through the Mojave Desert towards the Owens Valley, as postulated by Nur *et al.* (1993a, 1993b).

Northwest terminus of the ECSZ

Shear in the central Mojave Desert would appear to concentrate onto the Blackwater fault in the north-central Mojave Desert, based on geologic mapping and tectonic geodesy. Shear in the eastern Mojave Desert would appear to concentrate onto the Goldstone Lake and Soda Lake faults in the northeastern Mojave Desert, based on geologic mapping. Geologic mapping suggests the presence of corollary faults in the Basin and Range Province north of the Garlock fault zone. The corollary faults to the Blackwater, Goldstone Lake and Soda Lake faults would include the Owens Valley, Panamint Valley and Death Valley fault zones (Jennings, 1977; Jennings *et al.*, 2010). Nur *et al.* (1993a, 1993b) suggested that movement along the ECSZ propagates across the Garlock fault zone to continue into northern California along the Owens Valley fault. In the Nur *et al.* model, this movement represents a significant portion of the transform offset between the North American and Pacific plates. A portion of this plate transform offset would provide the energy to drive the Walker Lane fault zone in Nevada. However, Oskin and Iriondo (2004) only found paleoseismic evidence for Pliocene-age surface offset along the Blackwater fault. Similarly, Miller *et al.* (1994) determined that faults belonging to the Goldstone Lake fault zone don't show evidence for movement during the Holocene. Predictions of rapid rates of Holocene-age fault slip derived solely from geodetic measurements for portions of the ECSZ have not been substantiated.

Examination by the author of three dimensional digital aerial photography provided by Google Earth, Bing 3D, and World Wind reveals the presence of several well defined northwest-trending tonal lineaments with geomorphic expression projecting both southeast and northwest from the traces of the Mirage Valley and Shadow Mountain(s) faults. The lineaments southeast of the Shadow Mountains project towards, and into, the San Bernardino Mountains, crossing the North Frontal Fault Zone in the process. The lineaments northwest of Mirage Valley project towards, and into, the Tehachapi

Mountains, crossing the Garlock fault. At least one of these lineaments is coincidental with the right-lateral bend mapped in the Garlock fault near Double Mountain. Northwest-ward projecting lineaments appear to trend towards the potentially active Kern Gorge and Pond-Poso Creek faults, and an unnamed zone of northwest-striking faults that experienced ground surface rupture triggered by the 1952 Tehachapi earthquake. This zone of unnamed zone of northwest-striking faults is included within A-P EFZs by the State (Bryant and Hart, 2007).

Review of previously mapped seismicity (Real *et al.*, 1978; Topozada *et al.*, 1980; Kanamori *et al.*, 1992; Hauksson *et al.*, 1993; Goter, 1988, 1992; Goter *et al.*, 1994; Working Group, 1992, 2008; Stover and Coffman, 1993), in combination with ongoing documentation of recent microseismicity occurring within the Mojave Desert (Southern California Earthquake Data Center, 2011; National Earthquake Information Center, 2010; Southern California Seismic Network, 2011; Nicholson *et al.*, 2012) confirm that several northwest-trending, as well as northeast-trending, active faults (based on the definition of active faulting presented by the A-P Act and the CBC) traverse the western portion of the Mojave Desert. The relatively subdued geomorphology displayed in the Western Mojave, as compared with the more prominent relief and geomorphology found in the central and eastern portions of the province suggest that fault offset rates are probably a magnitude higher in the ECSZ than rates displayed by faults in the western portion of the Mojave. Utilizing the equations of Wells and Copper-smith (1994), along with the standards for determining the maximum credible earthquake (MCE) recently adopted by the California Building Standards Commission (2013) for inclusion into the 2013 CBC, maximum earthquake magnitudes between M_w 7.5 and M_w 7.8 may be expected for rupture of at least the Mirage Valley-Shadow Mountain(s) fault zone in the western Mojave Desert, which is similar to magnitudes expected for other large faults in the ECSZ. This faulting may extend southeast across the NFFZ and through the San Bernardino Mountains to connect with the SAF. Additionally, this faulting may extend northwest across the Garlock fault and through the Tehachapi Mountains to connect with active portions of the Pond-Poso Creek fault. Extension of the active Mirage Valley-Shadow Mountain(s) fault either to the southeast or northwest would significantly increase the MCE associated with the fault zone.

Western portion of the ECSZ

The Helendale fault is currently recognized as the southwest boundary of the ECSZ (Richard and Dokka, 1992). Only eight relatively short faults are recognized by the California Geological Survey, the U.S. Geological Survey, and the Southern California Earthquake Center as displaying evidence for offset during the Pleistocene epoch (Jennings, 1975, 1992, 1994; Jennings and

Bryant, 2010; Bryant, 2005; Bortugno, 1986; Ziony and Jones, 1989; Ziony and Yerkes). These faults include the Llano, Mirage Valley, Shadow Mountain(s), Blake Ranch, Spring, Leuhman/Leuman, and short, unnamed faults near California City and Cottonwood Creek (Jennings, 1992). These faults are considered potentially active by the State (Jennings, 1992, 1994; Jennings and Bryant, 2010). However, without a mapped linkage to the SAF or the ECSZ, the energy required to initiate and maintain horizontal movement along these faults remains undetermined, based on current mapping. Numerous northwest-trending lineaments have been observed on three-dimensional, digital aerial photography (presented by Google Earth, Bing 3D, and World Wind) traversing the Victorville, Adelanto, Hesperia, Apple Valley, and Baldy Mesa areas by the author and associates (Jeff Fitzsimmons, Debbie Kunath, David Gaddie). Southeastward projection of these lineaments tends to coincide with northwest-striking faults previously mapped in the San Bernardino Mountains by Sadler (1982), Brown (1986), and Meisling and Weldon (1989). The presence of these lineaments suggests that faults in the western portion of the ECSZ may link with several faults splaying off of the Mission Creek, Mill Creek, Banning, North and South Branches of the SAF in and near the San Geronio Pass.

None of these faults are included within A-P EFZs (Bryant and Hart, 2007). The Mojave Water Agency (MWA, 2004) did recognize several of these faults. Youngs (1988) mapped geophysical anomalies that also appear to coincide with the locations of mapped faults in the southern Mojave area. The MWA showed the Shadow Mountains fault extending southeast of the zone mapped by the State, eventually joining with the northeast-striking Adelanto fault. The MWA also mapped the northwest-striking Apple Valley fault coincident with a prominent scarp in Pleistocene age alluvium along the east bank of the Mojave River and generally on-trend with the projections of the mapped splays of the Shadow Mountain(s) fault, through the Town of Apple Valley. The MWA also acknowledged the need for a northwest-striking fault, the Narrows fault, to help explain the geomorphic knot produced by downcutting of the Mojave River into the igneous rock at the Narrows in Victorville, (rather than following the former Plio-Pleistocene path of the ancestral Mojave River around the basement rock to the west). The age of the older sediments west of the current river suggest that this downcutting occurred during early Pleistocene time.

Eastern portion of the ECSZ

The MWA (2004) mapped the northwest-striking Baja fault northeast of the Lake Dolores fault in the vicinity of Yermo. The southeast terminus of the mapped Baja fault is coincident with the west end of the portion of the Manix fault that ruptured in 1947. The author has observed that the northwest projection of the Baja fault is coincident

with a northwest-trending lineament visible on Google Earth, World Wind, and Bing 3D that separates Coyote Lake from Alvord Mountain.

Conclusions

The faulting mapped in the Mojave Desert has been included in the ECSZ. Portions of this faulting have been recognized as active or potentially active and included within A-P EFZs. Seismicity emanating at depth from the Mojave Desert substantiates the presence of active faulting in the ECSZ as defined by the 2010 and 2013 CBCs. Overall geodetic measurements show that tectonic blocks in the Mojave Desert are generally migrating towards the northwest, but that the blocks have experienced rotation around vertical axes as well. Geologic mapping and paleoseismic trenching have verified that portions of mapped faults in the ECSZ are active as defined by the A-P Act. Review of SAR and thematic imagery suggest that mapped straight-line faults are actually curvilinear, resulting in the braiding of the independently mapped faults into broad, anastomosing fault patterns. Review of three-dimensional digital aerial photography suggests that significantly more faulting traverses all portions of the Mojave Desert and may extend to the southeast to connect directly with the SAF. Geodetic measurements, surface mapping, seismicity, and review of the digital aerial photography also suggest that this active faulting traverses the eastern, central and western portions of the Mojave Desert, eventually connecting with active faulting recognized in Death Valley, Panamint Valley, Owens Valley and the Central Valley.

The importance of paleoseismic trenching studies conducted during the past 40 years to determine fault rupture timing and recurrence intervals cannot be over emphasized – these trenching studies provide the *primary* means of determining which faults are active and the patterns of seismic rupture through time. Physical access to sites, including access for motorized equipment (like backhoes and trackhoes) necessary for the safe and expedient excavation of the trenches, will continue to be a major necessity for geologic researchers working in the Mojave Desert in order to adequately conduct these trenching studies during the upcoming decades.

Acknowledgements

I wish to express my thanks to the shoulders upon which I stand—David Miller, Michael Rymer, Bob Reynolds, Craig Nicholson, Jerry Treiman, Egill Hauksson, Tom Dibblee, Doug Morton, Pete Sadler, Howard Brown, Tom Rockwell, James Dolan, Gary Rasmussen, Wessly Reeder, Jay Martin, Steve Wells, Marty Stout, Perry Ehlig, Jason Saleeby, Jeff Fitzsimmons, Debbie Kunath, David Gaddie, and Margaret Gooding. I am also grateful for the thoughtful review of this paper provided by an anonymous peer who helped keep my thoughts and facts straight. And a special thanks to Dr. Clarence Allen for being my inspiration.

References

- Atwater, T., 1970, Implications of plate tectonics for the Cenozoic tectonic evolution of western North America: *Geological Society of America Bulletin*, V. 84, p. 1095-1100.
- Atwater, T., 1992, Constraints from plate reconstructions for Cenozoic tectonic regimes of Southern and Eastern California: in Richard, S.M. ed., Deformation associated with the Neogene Eastern California Shear Zone, southeastern California and southwestern Arizona: San Bernardino County Museums, Special Publication 92-1, p. 1-2.
- Bader, J.S., Page, R.W., and Dutcher, L.C., 1958, Data on wells in the Upper Mojave Valley area, San Bernardino County, California: *U. S. Department of the Interior, Geological Survey, Ground Water Branch Open-File Report* (unnumbered).
- Bartley, J.M., Glazner, A.F., and Schermer, E.R., 1990, North-south contraction of the Mojave Block and strike-slip tectonics in southern California: *Science*, V. 248, p. 1398-1401.
- Bassett, A.M., and Kupfer, D.H., 1964, A geologic reconnaissance of the southeastern Mojave Desert: *California Resources Agency, Department of Conservation, Division of Mines and Geology Special Report*, SR 83, 43 p.
- Beeby, D.J., and Hill, R.L., 1975, Galway Lake fault – a previously unmapped active fault in the Mojave Desert, San Bernardino County, California: *California Geology*, V. 28, N. 10, p. 219-221.
- Bornyas, M.S., 1993, Neotectonics of the Johnson Valley fault, Mojave Desert, California: *San Diego State University, Department of Geological Sciences Senior Thesis*, 13 p.
- Bortugno, E.J. (1986). “Map showing recency of faulting, San Bernardino quadrangle, California” in Bortugno, E.J., and Spittler, T.E., compilers, 1986, Geologic map of the San Bernardino Quadrangle.” *California Resources Agency, Department of Conservation, Division of Mines and Geology Regional Geologic Map Series*, Map No. 3A, Scale 1:250,000 or 1” = 4 miles.
- Bortugno, E.J. and Spittler, T.E., compilers, 1986, Geologic map of the San Bernardino Quadrangle, California: *California Resources Agency, Department of Conservation, Division of Mines and Geology Regional Geologic Map Series*, No. 3A, Scale 1:250,000 or 1” = 4 miles.
- Bowen, O.E., Jr., 1954, Geology and mineral deposits of the Barstow quadrangle, San Bernardino County, California: *California Resources Agency, Department of Conservation, Division of Mines and Geology Bulletin*, B 165, Scale 1:62,500 or 1” = 1 mile.
- Brady, R.H., III, 1988, Southward continuation of the southern Death Valley fault zone from the Avawatz to the Bristol Mountains, San Bernardino County, California: *Geological Society of America Abstracts with Programs*, V. 20, N. 4, p. 145.
- Brady, R.H., III, 1992, The Eastern California Shear zone in the northern Bristol Mountains, southeastern California: in Richard, S.M. ed., Deformation associated with the Neogene Eastern California Shear Zone, southeastern California and southwestern Arizona: *San Bernardino County Museums, Special Publication 92-1*, p. 6-10.

- Brady, R.H., III and Dokka, R.K., 1989, the eastern Mojave shear zone: A major Tertiary tectonic boundary in the southwestern Cordillera: *Geological Society of America Abstracts with Programs*, V. 21, N. 5, p. 59.
- Brady, R.H., III, Negrini, R.M., and Robin, B., 1989, Geophysical expression and geological interpretation of botanical lineaments, eastern Soda Lake, San Bernardino County, California: in *Geology and geophysics of San Bernardino County: San Bernardino County Museum Special Report*.
- Brown, H., 1981, Stratigraphy and structure of a portion of the Bristol Mountains, San Bernardino County, California: in Howard, K., Carr, M., and Miller, D., editors, *Tectonic framework of the Mojave and Sonora Deserts, California and Arizona: U. S. Department of the Interior, Geological Survey Open-File Report, OFR 1981-0503*, p. 11-12.
- Brown, H., 1984, Correlation of metamorphosed Paleozoic strata of the southeastern Mojave Desert region, California and Arizona, discussion reply: *Bulletin of the Geologic Society of America*, B 95, p. 1482-1486.
- Brown, H.J., 1986, Stratigraphy and Paleogeographic Setting of Paleozoic Rocks in the Northern San Bernardino Mountains, California: in Kooser, M.A. and Reynolds, R.E., editors, *Geology Around the Margins of the Eastern San Bernardino Mountains: Publications of the Inland Geologic Society*, V. 1, p. 105-115.
- Bryan, K. and Rockwell, T.K., 1994, Recognition of non-brittle fault deformation in trench exposures: An example from the Helendale fault: in Murbach, D., ed., *Mojave Desert: South Coast Geological Society Annual Fieldtrip Guidebook*, p. 253-262.
- Bryan, K.A. and Rockwell, T.K., 1995, Holocene character of the Helendale fault zone, Lucerne Valley, San Bernardino County, California: *Geological Society of America Abstracts with Programs*, V. 27, p. 7.
- Bryant, W.A., 1987, Recently active traces of the Harper, Blackwater, Lockhart and related faults near Barstow, San Bernardino County, California: *California Resources Agency, Department of Conservation, Division of Mines and Geology Fault Evaluation Report FER-189*.
- Bryant, W.A., compiler, 2005, Digital database of Quaternary and Younger Faults from the Fault Activity Map of California, version 2.0: California Resources Agency, Department of Conservation, Geological Survey website: http://www.consrv.ca.gov/CGS/information/publications/Pages/QuaternaryFaults_ver2.aspx.
- Bryant, W.A. and Hart, E.W., 2007, Fault-rupture hazard zones in California, Alquist-Priolo Earthquake Fault Zoning Act with index to Earthquake Fault Zones maps, interim revision: *California Resources Agency, Department of Conservation, Geological Survey Special Publication SP 42*, 42 p.
- Burke, D.B., Hillhouse, J.W., McKee, E.H., Miller, S.T., and Morton, J.L., 1982, Cenozoic rocks in the Barstow basin area of southern California-Stratigraphic relations, radiometric ages, and Paleomagnetism: *U. S. Department of the Interior, Geological Survey Bulletin B 1529-E*, p. E1-E16.
- Buwalda, J.P., and Richter, C.F., 1948, Movement on the Manix, California fault on April 10, 1947, abstract: *Bulletin of the Geological Society of America*, V. 59, N. 12, p. 1367.
- Byers, F.M., Jr., 1960, Geology of the Alvord Mountain quadrangle, San Bernardino County, California: *U. S. Department of the Interior, Geological Survey Bulletin B 1089-A*, 71 p., Scale 1:62,500 or 1" = 1 mile.
- California Building Standards Commission, 2010, 2010 California Building Code: *California Building Standards Commission*, after the *International Code Council, Inc.*, 2006, 2006 International Building Code.
- California Building Standards Commission, 2013, 2013 California Building Code: *California Building Standards Commission*, after the *International Code Council, Inc.*, 2012, 2012 International Building Code.
- California Department of Water Resources, 1934, Mojave Rivers Investigations: *California Resources Agency, Department of Water Resources Bulletin 47*.
- California Department of Water Resources, 1963, Water wells and springs – Bristol, Broadwell, Cadiz, Danby and Lavic Valleys and vicinity, San Bernardino and Riverside Counties: *California Resources Agency, Department of Water Resources Bulletin No. 91-14*.
- California Department of Water Resources, 1967, Mojave River ground water basin investigations: *California Resources Agency, Department of Water Resources Bulletin 84*.
- California Department of Water Resources, 1984, Federal-State cooperative ground water investigations map of the Yucca Valley-Twenty-nine Palms area, California, showing reconnaissance geology and locations of wells and springs: *California Resources Agency, Department of Water Resources Map, Scale 1:62,500 or 1" = 1 mile*.
- California Division of Mines and Geology and International Conference of Building Officials, 1998, Maps of known active fault near-source zones in California and adjacent portions of Nevada: California Resources Agency, Department of Conservation, Division of Mines and Geology and International Conference of Building Officials, Scale 1" = 4 kilometers.
- California Division of Mines and Geology, March 1, 1988, Alquist-Priolo Earthquake Fault Zones Map (formerly Special Studies Zone Map), Joshua Tree North Quadrangle, Official Map: California Resources Agency, Department of Conservation, Division of Mines and Geology, Scale 1:24,000 or 1" = 2,000'.
- California Division of Mines and Geology, July 1, 1993, Alquist-Priolo Earthquake Fault Zones Map (formerly Special Studies Zone Map), Landers Quadrangle, Revised Official Map: *California Resources Agency, Department of Conservation, Division of Mines and Geology, Scale 1:24,000 or 1" = 2,000'*.
- California Geological Survey, 2007, Interactive fault parameter map of California, 2002: California Resources Agency, Department of Conservation, Geological Survey, Webpage: http://www.conservation.ca.gov/cgs/rghm/psha/fault_parameters/htm/Pages/index.aspx.
- Carter, J.N., Luyendyk, B.P., and Terres, R.R., 1987, Neogene clockwise rotation of the eastern Transverse Ranges, California, suggested by paleomagnetic vectors: *Geological Society of America Bulletin*, V. 98, p. 199-206.
- Chrisley, S.M., 1997, Geology and hydrogeology of the George Air Force Base vicinity, California: *San Jose State University*

- Master's Thesis, Paper 1563, website: http://scholarworks.sjsu.edu/etd_theses/1563.
- Cinti, F.R., Fumal, T.E., Garvin, C.D., Hamilton, J.C., Powers, T.J., and Schwartz, D.P., 1993, Earthquake recurrence and fault behavior on the Homestead Valley fault-central segment of the 1992 Landers surface rupture sequence: *Geological Society of America Abstracts with Programs*, V.25, p. 101.
- Clark, M. M., Harms, K.K., Lienkaemper, J.J., Harwood, D.S., Lajoie, K.R., Matti, J.C., Perkins, J.A., Rymer, M.J., Sarna-Wojcicki, A.M., Sharp, R.V., Sims, J.D., Tinsley III, J.C., and Ziony, J.I., 1984, Preliminary slip-rate table and map of late-Quaternary faults of California: *U.S. Department of the Interior, Geological Survey Open-File Report OFR 1984-0106*, Preliminary Report.
- Corona, F.V. and Sabins, F.F., Jr., 1993, The San Andreas fault of the Salton Trough region, California, as expressed on remote sensing data: in Reynolds, R.E. and Reynolds, J., eds., *Ashes, Faults, and Basins: San Bernardino County Museum Association Special Publication 93-1*, p. 69-75.
- Cox, B.F. and Hillhouse, J.W., 2000, Pliocene and Pleistocene evolution of the Mojave River, and associated tectonic development of the Transverse Ranges and Mojave Desert, based on borehole stratigraphy studies near Victorville, California: *U. S. Department of the Interior, Geological Survey, Open-File Report OFR 2000-0147*, 65 p.
- Cox, B.F. and Tinsley, J.C., 1999, Origin of the late Pliocene and Pleistocene Mojave River between Cajon Pass and Barstow, California: in Reynolds, R.E. and Reynolds, J., editors, *Tracks along the Mojave: A field guide from Cajon Pass to the Calico Mountains and Coyote Lake: San Bernardino County Museum Association, Quarterly*, V. 46, N. 3, p. 49-54.
- Crippen, R., 1988, Southerly continuation of the Johnson Valley fault, east of the San Bernardino Mountains, southern California: *Geological Society of America Bulletin*, V. 20, p. 152-153.
- Crowell, J.C., 1968, Movement histories of faults in the Transverse Ranges and speculations on the tectonic history of California: in *Proceedings of Conference on Geologic problems of the San Andreas fault system: Stanford University*, p. 323-341.
- Crowell, J.C., 1975, The San Andreas fault in southern California: in Crowell, J.C., ed., *San Andreas fault in southern California, a Guide to San Andreas fault from Mexico to Carrizo Plain: California Resources Agency, Department of Conservation, Division of Mines and Geology Special Report SR 118*, p. 7-27.
- Crowell, J.C., 1992, Cenozoic faulting in the Little San Bernardino – Orocopia Mountains region, southern California: in Richard, S.M. ed., *Deformation associated with the Neogene Eastern California Shear Zone, southeastern California and southwestern Arizona: San Bernardino County Museums, Special Publication 92-1*, p. 16-19.
- Dibblee, T.W., Jr., 1960a, Preliminary geologic map of the Apple Valley Quadrangle, California: *U.S. Department of the Interior, Geological Survey Mineral Investigations Field Studies Map, MF-232*, Scale 1:62,500 or 1" = 1 mile.
- Dibblee, T.W., Jr., 1960b, Geologic map of the Barstow Quadrangle, San Bernardino County, California: *U.S. Department of the Interior, Geological Survey Mineral Investigations Field Studies Map, MF-233*, Scale 1:62,500 or 1" = 1 mile.
- Dibblee, T.W., Jr., 1960c, Preliminary geologic map of the Victorville Quadrangle, California: *U.S. Department of the Interior, Geological Survey Map, MF-229*, Scale 1:62,500 or 1" = 1 mile.
- Dibblee, T.W., Jr., 1964a, Geologic map of the Lucerne Valley Quadrangle, San Bernardino and Riverside Counties, California: *U.S. Department of the Interior, Geological Survey Miscellaneous Geologic Investigations Map I-426*, Scale 1:62,500 or 1" = 1 mile.
- Dibblee, T.W., Jr., 1964b, Geologic map of the Ord Mountains Quadrangle, San Bernardino County, California: *U.S. Department of the Interior, Geological Survey Miscellaneous Geologic Investigations Map I-427*, Scale 1:62,500 or 1" = 1 mile.
- Dibblee, T.W., Jr., 1964c, Geologic map of the Rodman Mountains Quadrangle, San Bernardino County, California: *U.S. Department of the Interior, Geological Survey Miscellaneous Geologic Investigations Map I-430*, Scale 1:62,500 or 1" = 1 mile.
- Dibblee, T.W., Jr., 1964d, Geologic map of the San Gorgonio Mountain Quadrangle, San Bernardino and Riverside Counties, California: *U.S. Department of the Interior, Geological Survey Miscellaneous Geologic Investigations Map I-431*, Scale 1:62,500 or 1" = 1 mile.
- Dibblee, T.W., Jr., 1965, Geologic map of the 15-minute Hesperia Quadrangle, San Bernardino County, California: *U.S. Department of the Interior, Geological Survey Open-File Report OFR (unnumbered)*, Scale 1:62,500 or 1" = 1 mile.
- Dibblee, T.W., Jr., 1966, Geologic map of the Lavic Quadrangle, San Bernardino County, California: *U.S. Department of the Interior, Geological Survey Miscellaneous Geologic Investigations Map I-472*, Scale 1:62,500 or 1" = 1 mile.
- Dibblee, T.W., Jr., 1967a, Geologic map of the Ludlow Quadrangle, San Bernardino County, California: *U.S. Department of the Interior, Geological Survey Miscellaneous Geologic Investigations Map I-477*, Scale 1:62,500 or 1" = 1 mile.
- Dibblee, T.W., Jr., 1967b, Geologic map of the Broadwell Lake Quadrangle, San Bernardino County, California: *U.S. Department of the Interior, Geological Survey Miscellaneous Geologic Investigations Map I-478*, Scale 1:62,500 or 1" = 1 mile.
- Dibblee, T.W., Jr., 1967c, Geologic map of the Deadman Lake Quadrangle, San Bernardino County, California: *U.S. Department of the Interior, Geological Survey Miscellaneous Geologic Investigations Map I-488*, Scale 1:62,500 or 1" = 1 mile.
- Dibblee, T.W., Jr., 1967d, Geologic map of the Joshua Tree Quadrangle, San Bernardino County, California: *U.S. Department of the Interior, Geological Survey Miscellaneous Geologic Investigations Map I-516*, Scale 1:62,500 or 1" = 1 mile.
- Dibblee, T.W., Jr., 1967e, Geologic map of the Morongo Valley Quadrangle, San Bernardino County, California: *U.S. Department of the Interior, Geological Survey Miscellaneous Geologic Investigations Map I-517*, Scale 1:62,500 or 1" = 1 mile.

- Dibblee, T.W., Jr., 1967f, Geologic map of the Emerson Lake Quadrangle, San Bernardino County, California: *U.S. Department of the Interior, Geological Survey Miscellaneous Geologic Investigations Map I-190*, Scale 1:62,500 or 1" = 1 mile.
- Dibblee, T.W., Jr., 1967g, Geologic map of the Old Woman Springs Quadrangle, San Bernardino County, California: *U.S. Department of the Interior, Geological Survey Miscellaneous Geologic Investigations Map I-518*, Scale 1:62,500 or 1" = 1 mile.
- Dibblee, T.W., Jr., 1967h, Areal geology of the western Mojave Desert, California: *U.S. Department of the Interior, Geological Survey Professional Paper PP 522*, Scale 1:125,000 or 1" = 2 miles.
- Dibblee, T.W., Jr., 1968a, Geologic map of the Twentynine Palms Quadrangle, San Bernardino County, California: *U.S. Department of the Interior, Geological Survey Miscellaneous Geologic Investigations Map I-561*, Scale 1:62,500 or 1" = 1 mile.
- Dibblee, T.W., Jr., 1968b, Evidence of major lateral displacement on the Pinto Mountain fault, southeastern California: *Geological Society of America Special Paper SP 115*, p. 322.
- Dibblee, T.W., Jr., 1968c, Geology of the Opal Mountain and Fremont Peak Quadrangles, California: *California Resources Agency, Department of Conservation, Division of Mines and Geology Bulletin 188*, 64 p., Scale 1:62,500 or 1" = 1 mile.
- Dibblee, T.W., Jr., 1970, Geologic map of the Daggett Quadrangle, San Bernardino County, California: *U.S. Department of the Interior, Geological Survey, Miscellaneous Geological Investigations Map, I-592*, Scale 1:62,500 or 1" = 1 mile.
- Dibblee, T.W., Jr., and Bassett, A.M., 1966a, Geologic map of the Newberry Quadrangle, San Bernardino County, California: *U.S. Department of the Interior, Geological Survey Miscellaneous Geologic Investigations Map I-461*, Scale 1:62,500 or 1" = 1 mile.
- Dibblee, T.W., Jr., and Bassett, A.M., 1966b, Geologic map of the Cady Mountains Quadrangle, San Bernardino County, California: *U.S. Department of the Interior, Geological Survey Miscellaneous Geologic Investigations Map I-467*, Scale: 1:62,500 or 1" = 1 mile.
- Dibblee, T.W., Jr., 1992, Geology and inferred tectonics of the Pinto Mountain fault, Eastern transverse ranges, California: *in Richard, S.M. ed., Deformation associated with the Neogene Eastern California Shear Zone, southeastern California and southwestern Arizona: San Bernardino County Museums, Special Publication 92-1*, p. 28-31.
- Dokka, R.K., 1983, Displacements on late Cenozoic strike-slip faults of the central Mojave Desert, California: *Geology*, V. 11, p. 305-308.
- Dokka, R.K., 1986, Patterns and modes of early Miocene crustal extension, central Mojave Desert, California: *in Mayer, L., ed., Extensional tectonics of the southwestern United States: A perspective on processes and kinematics: Geological Society of America Special Paper 208*, p. 75-95.
- Dokka, R.K., 1989, The Mojave Extensional Belt of southern California: *Tectonics*, V. 8, p. 363-390.
- Dokka, R.K. and Glazner, A.F., 1982, Aspects of early Miocene extension of the central Mojave Desert: *in Cooper, J.D., compiler, Geologic Excursions in the California Desert: Geological Society of America, Cordilleran Section 78th Annual Meeting Volume and Guidebook*, p. 31-45.
- Dokka, R.K. and Travis, C.J., 1990a, Late Cenozoic strike-slip faulting in the Mojave Desert, California: *Tectonics*, V. 9, p. 311-340.
- Dokka, R.K. and Travis, C.J., 1990b, Role of the eastern California shear zone in accommodating Pacific-North American plate motion: *Geophysical Research Letters*, V. 17, p. 1323-1326.
- Dokka, R.K., Henry, D.J., Ross, T.M., Baksi, A.K., Lambert, J., Travis, C.J., Jones, S.M., Jacobson, C., McCurry, M.M., Woodburne, M.O., and Ford, J.P., 1991, Aspects of the Mesozoic and Cenozoic geologic evolution of the Mojave Desert: *Geological Society of America, Annual Meeting Guidebook*, p.
- Dokka, R.K., Henry, D.J., Sella, G.F., Ford, J.F., MacConnell, D.F., McCabe, C., Neuffer, P., and Quinones, R., 1994, Critical events in the Late Mesozoic-Cenozoic geologic history of the Mojave Desert - Off Limits in the Mojave Desert: Field Trip Road Log: *in Reynolds, R.E., ed., Off Limits in the Mojave Desert, field trip guidebook and volume for the 1994 Mojave Desert Quaternary Research Center filed trip to Fort Irwin and surrounding areas: San Bernardino County Museum Association Special Publication 94-1*, p. 3-30
- Dokka, R.K., McCurry, M., Woodburne, M.O., Frost, E.G., and Okaya, D., 1988, Field Guide to the Cenozoic crustal structure of the Mojave Desert: *in This Extended Land, geological journeys in the southern Basin and Range: Weide, D.L. and Faber, M.L., eds., Geological Society of America, Cordilleran Section*, p. 21-44.
- Dolan, J.F., and Sieh, K., 1992a, Tectonic geomorphology of the northern Los Angeles Basin: Seismic hazards and kinematics of young fault movement: *in Ehlig, P.L. and Steiner, E.S., eds., Engineering geology field trips, Orange County, Santa Monica Mountains, Malibu: Association of Engineering Geologists, Southern California Section, 35th Annual Meeting, Guidebook and Volume*, p. B-20 to B-25.
- Dolan, J.F., and Sieh, K., 1992b, Structural style and tectonic geomorphology of the northern Los Angeles Basin: Seismic hazards and kinematics of young fault movement: *in Ehlig, P.L. and Steiner, E.A., eds., 1992, Engineering geology field trips, Orange County, Santa Monica Mountains, Malibu: Association of Engineering Geologists, Southern California Section, 35th Annual Meeting, Guidebook and Volume*, p. B-26 to B-28.
- Dolan, J.F., Gath, E.M., Grant, L.B., Legg, M., Lindvall, S., Mueller, K., Oskin, M., Ponti, D.F., Rubin, C.M., Rockwell, T.K., Shaw, J.H., Treiman, J.A., Walls, C., and Yeats, R.S., 2001, Active faults in the Los Angeles metropolitan region: *Southern California Earthquake Center, SCEC Special Publication Series, No. 001*, 47 pages.
- Finney, S.C., 2011a, Formal definition of the Quaternary System/Period and redefinition of the Pleistocene Series/Epoch: *Episodes* 33, p. 159-158.
- Finney, S.C., 2011b, Formal definition of the Quaternary System and redefinition of the Pleistocene Series by the International Commission on Stratigraphy." *in Reynolds, R.E., compiler, "Abstracts of Proceedings - The 2011 Desert Studies*

- Symposium: *in* Reynolds, R.E., ed., The Incredible Shrinking Pliocene – The 2011 Desert Symposium Field Guide and Proceedings: *California State University Desert Studies Consortium*, p. 127.
- Frankel, A., Petersen, M., Mueller, C., Haller, K., Wheeler, R., Leyendecker, E., Wesson, R., Harmsen, S., Cramer, C., Perkins, D., and Rukstales, K., 2002, Documentation for the 2002 Update of the National Seismic Hazard Maps: *U.S. Department of the Interior, Geological Survey Open-File Report OFR 2002-0420*.
- Ford, A.P., Dokka, R.K., Crippen, R.E., and Blom, R.G., 1990, Faults in the Mojave Desert as revealed from enhanced Landsat images: *Science*, V. 248, p. 1000-1003.
- Garfunkel, Z., 1974, Model for the late Cenozoic tectonic history of the Mojave Desert, California, and for its relation to adjacent regions: *Geological Society of America Bulletin*, V. 85, p. 1931-1944.
- Gibbard, P. and Head, M.J., 2009a, The definition of the Quaternary System/Period and the Pleistocene Series/Epoch: *Quaternaire* V. 20, N. 2, p. 125-133.
- Gibbard, P. and Head, M.J., 2009b, IUGS ratification of the Quaternary System/Period and the Pleistocene Series/Epoch with a base at 2.58: *Quaternaire* V. 20, N. 4, p. 411-412.
- Gibbard, P.L. and Head, M.J., 2010, The newly-ratified definition of the quaternary System/Period and redefinition of the Pleistocene Series/Epoch, and comparison of proposals advanced prior to formal ratification: *Episodes* 33, p. 159-163.
- Gibbard, P.L., Head, M.J., Walker, M.J.C., and the Subcommittee on Quaternary Stratigraphy, 2009, Formal ratification of the Quaternary System/Period and the Pleistocene Series/Epoch with a base at 2.58 Ma: *Subcommission of Quaternary Stratigraphy, Journal of Quaternary Science*, V. 25, p. 96-102.
- Golombek, M.P. and Brown, L.L., 1988, Clockwise rotation of the western Mojave Desert: *Geology*, V. 16, p. 126-130.
- Google Earth, 2009-2012, *Google*.
- Goter, S.K., 1988, Seismicity of California, 1808-1987: *U.S. Department of the Interior, Geological Survey Open-File Report OFR 1988-0286*, Scale 1:1,000,000 or 1" = 16 miles.
- Goter, S.K., 1992, Southern California Earthquakes: *U.S. Department of the Interior, Geological Survey Open-File Report OFR 1992-0533*, Scale 1:380,000 or 1" = 6 miles.
- Goter, S.K., Oppenheimer, D.H., Mori, J.J., Savage, M.K., and Masse, R.P., 1994, Earthquakes in California and Nevada: *U.S. Department of the Interior, Geological Survey Open-File Report OFR 1994-0647*, Scale 1:1,000,000 or 1" = 16 miles.
- Grimes, G., 1986, Sediments adjacent to a portion of the Pinto Mountain fault in the Yucca Valley area of San Bernardino County, California: *in* Kooser, M.A. and Reynolds, R.E., eds., *Geology around the Margins of the Eastern San Bernardino Mountains: Publications of the Inland Geological Society*, V.1, p. 75-76.
- Grimes, G.J., 1987, Geology at the convergence of the Pinto Mountain fault and Morongo Valley fault, southern California: California State University at Los Angeles Master of Science thesis, 102 pages, Scale 1:12,000 or 1" = 1,000'.
- Grose, L.T., 1959, Structure and petrology of the northeast part of the Soda Mountains, San Bernardino County, California: *Geological Society of America Bulletin*, V. 70, p. 1509-1548.
- Hafner, K. and Hauksson, E., 1994, Aftershocks of the 1992 M_w 7.3 Landers Earthquake Sequence in the Barstow Daggett for Irwin area: *in* Reynolds, R.E., ed., *Off Limits in the Mojave Desert*, field trip guidebook and volume for the 1994 Mojave Desert Quaternary Research Center filed trip to Fort Irwin and surrounding areas: *San Bernardino County Museum Association Special Publication 94-1*, p. 38-40.
- Hardt, W.F., 1971, Hydrologic analysis of Mojave River Basin, California, using electric analog model: *U.S. Department of the Interior, Geological Survey Open-File Report OFR 1972-0157*.
- Harris, R.A. and Simpson, R.W., 1992, Changes in static stress on southern California faults after the 1992 Landers earthquake: *Nature*, V. 360, p. 251-254.
- Harris, R.A. and Simpson, R.W., 1993, Stress caused by the 1992 Landers Earthquake: *in* Reynolds, R.E., compiler, *Landers: Earthquakes and Aftershocks: San Bernardino County Museum Association Quarterly*, V. 40, N. 1, p. 61-64.
- Hart, E.W. and Bryant, W.A., 1997, Fault-rupture hazard zones in California, Alquist-Priolo Earthquake Fault Zoning Act with index to Earthquake Fault Zones maps: California Resources Agency, Department of Conservation, Division of Mines and Geology Special Publication SP 42, 34 p.
- Hart, E.W. and Bryant, W.A., 1997, revised 1999, Fault-rupture hazard zones in California, Alquist-Priolo Earthquake Fault Zoning Act with index to Earthquake Fault Zones maps, revised with supplements 1 and 2 added 1999: California Resources Agency, Department of Conservation, Division of Mines and Geology Special Publication SP 42, 38 p.
- Hart, E.W. and Bryant, W.A., 1997, revised 2003, Fault-rupture hazard zones in California, Alquist-Priolo Earthquake Fault Zoning Act with index to Earthquake Fault Zones maps, revised with supplements 1, 2 and 3 added 2003: California Resources Agency, Department of Conservation, Division of Mines and Geology Special Publication SP 42, 40 p.
- Hart, E.W., Bryant, W.A., and Treiman, J.A., 1993, Surface faulting associated with the June, 1992, Landers earthquake, California: *California Geology*, V. 46, N. 1, p. 10-16.
- Hart E.W., Bryant, W.A., Kahle, J.E., Manson, M.W., and Bortugno, E.J., 1988, Summary Report: Fault Evaluation Program 1986-1987, Mojave Desert and other areas: California Resources Agency, Department of Conservation, Division of Mines and Geology Open-File Report OFR 88-1LA, 49p. with plates.
- Hatheway, A.W., 1975, Terminus of the Pinto Mountain fault, near Twentynine Palms, California: *Geological Society of America Abstracts with Programs, Cordilleran Section, 71st Annual Meeting*.
- Hauksson, E., 1993, The Barstow Sequence: Aftershocks of the 1992 M_w 7.3 Landers Earthquake: *in* Reynolds, R.E., compiler, *Landers: Earthquakes and Aftershocks: San Bernardino County Museum Association Quarterly*, V. 40, N. 1, p. 52-55.
- Hauksson, E., Hutton, K., and Jones, L.M., 1992, Preliminary report on the 1992 Landers earthquake sequence in southern

- California: *in* Landers earthquake of June 28, 1992, San Bernardino County, California, Field Trip Guidebook: *Association of Engineering Geologists, Southern California Section*, p. 23-31.
- Hawkins, H.G., and McNey, J.L., 1979, Homestead Valley earthquake swarm, San Bernardino County, California: *California Geology*, V. 32, N. 10, p. 222-224.
- Hecker, S., Fumal, T.E., Powers, T.J., Hamilton, J.C., Garvin, C.D., and Schwartz, D.P., 1993, Late Pleistocene-Holocene behavior of the Homestead Valley fault sequence-1992 Landers, CA surface rupture: *EOS AGU Fall supplement*, p. 612.
- Herzberg, M., 1996, The neotectonic history of the Johnson Valley fault, San Bernardino County, California: *San Diego State University*, Department of Geological Sciences Master's Thesis, 68 p.
- Herzberg, M. and Rockwell, T.K., 1993, Timing of past earthquakes on the northern Johnson Valley fault and their relationship to the 1992 rupture: *EOS AGU Fall supplement*, p. 612.
- Hernandez, J.L., Brown, H.J., and Cox, B.F., 2008, Geologic Map of the Victorville 7.5' Quadrangle, San Bernardino County, California: A Digital Database, version 1.0: *California Resources Agency, Department of Conservation, Geological Survey Preliminary Geologic Map website*: http://www.conservation.ca.gov/cgs/rghm/rghm/preliminary_geologic_maps.htm.
- Hewett, D.F., 1954, General geology of the Mojave Desert region, California: *in* Jahns, R.H., ed., *Geology of Southern California: California Resources Agency, Department of Conservation, Division of Mines Bulletin B 170*, Ch. II.
- Hill, R.L., and Beeby, D.J., 1977, Surface faulting associated with the 5.2 magnitude Galway Lake earthquake of May 31, 1975: Mojave Desert, San Bernardino County, California: *Geological Society of America Bulletin*, V. 88, p. 1378-1384.
- Hill, R.L., Pechmann, J.C., Treiman, J.A., McMillan, J.R., Given, J.W., and Ebel, J.E., 1980, Geologic study of the Homestead Valley earthquake swarm of March 15, 1979: *California Geology*, V. 33, N. 3, p. 60.
- Hopson, R.F., 1998, Quaternary geology and neotectonics of the Pinto Mountain fault, Mojave Desert, southern California: *California Geology*, V. 51, N. 6, p. 3-13.
- Houser, C.E., 1996, Tectonic geomorphology and Quaternary history of the Old Woman Springs fault, San Bernardino County, California: *San Diego State University*, Department of Geological Sciences Master's Thesis, 81 p.
- Houser, C.E., and Rockwell, T.K., 1996, abstract, Tectonic geomorphology and paleoseismology of the Old Woman Springs fault, San Bernardino County, California: *Geological Society of America*, Cordilleran Section, Abstracts with Programs, p. 76.
- Howard, K.A., and Miller, D.M., 1992, Late Cenozoic faulting at the boundary between the Mojave and Sonoran blocks: Bristol Lake area, California: *in* Richard, S.M., ed., *Deformation associated with the Neogene eastern California shear zone, southwestern Arizona and southeastern California: San Bernardino County Museum Association Special Publication 92-1*, p. 37-47.
- Howard, K.A., Kilburn, J.E., Simpson, R.W., Fitzgibbon, T.T., Detra, D.E., and Raines, G.L., 1987, Mineral resources of the Bristol/Granite Mountains Wilderness Study Area, San Bernardino County, California: *U. S. Department of the Interior, Geological Survey Bulletin*, B 1712-C, 18 p.
- Hutton, L.K., Johnson, C.E., Pechmann, J.C., Ebel, J.E., Given, J.W., Cole, D.M., and German, P.T., 1980, Epicentral locations for the Homestead Valley earthquake sequence, March 15, 1979: *California Geology*, V. 33, N. 5, p. 110-114.
- Jaume, S.C. and Sykes, L.R., 1992, Changes in state of stress on the southern San Andreas fault resulting from the California earthquake sequence of April to June 1992: *Science*, V. 258, p. 1325-1328.
- Jefferson, G.T., Keaton, J.R., and Hamilton, P., 1982, Manix Lake and the Manix Fault: *San Bernardino County Museum Association Quarterly*, V. 24, N. 3/4, p. 1-47.
- Jennings, C.W., 1975, Fault map of California with locations of volcanoes, thermal springs, and thermal wells: *California Resources Agency, Department of Conservation, Division of Mines and Geology Geologic Data Map Series*, CDM No. 1, Scale 1:750,000 or 1" = 12 miles.
- Jennings, C.W., 1977, Geologic Map of California: *California Resources Agency, Department of Conservation, Division of Mines and Geology Geologic Data Map Series*, CDM No. 2, Scale 1:750,000 or 1" = 12 miles.
- Jennings, C.W., 1992, Preliminary fault activity map of California: *California Resources Agency, Department of Conservation, Division of Mines and Geology Open-File Report*, OFR 92-03, Scale 1:750,000 or 1" = 12 miles.
- Jennings, C.W., 1994, Fault activity map of California and adjacent areas with locations and ages of recent volcanic eruptions: *California Resources Agency, Department of Conservation, Division of Mines and Geology California Geologic Data Map Series*, CDM No. 6, Scale 1:750,000 or 1" = 12 miles.
- Jennings, C.W., with modifications by Gutierrez, C., Bryant, W., Saucedo, G., and Wills, C., 2010, Geologic map of California: *California Resources Agency, Department of Conservation, Geological Survey Geologic Data Map No. 2*, Scale 1:750,000 or 1" = 12 miles. Accessed at: <http://www.quake.ca.gov/gmaps/GMC/stategeologicmap.html>.
- Jennings, C.W. and Bryant, W.A., 2010, with assistance from Saucedo, G., Fault activity map of California: *California Resources Agency, Department of Conservation, Geological Survey Geologic Data Map series*, CDM No. 6, Scale 1:750,000 or 1" = 12 miles. Accessed at: <http://www.quake.ca.gov/gmaps/FAM/faultactivitymap.html>.
- Kamerling, M.J. and Luyendyk, B.P., 1979, Tectonic rotations of the Santa Monica Mountains region, western Transverse Ranges, California, suggested by paleomagnetic vectors: *Geological Society of America Bulletin*, V. 90, p. 1331-1337.
- Kanamori, H., Thio, H.-K., Dreger, D., Hauksson, E., and Heaton, T., 1992, Initial investigation of the Landers, California earthquake of 28 June 1992 using TERRAScope: *Geophysical Research Letters*, V. 19, p. 2267-2270.
- Keaton, J.R. and Keaton, R.T., 1977, Manix fault zone, San Bernardino County, California: *California Geology*, V. 30, p. 177-186.

- Kunkel, F., 1962, Reconnaissance of ground water in the western part of the Mojave Desert region, California: *U.S. Department of the Interior, Geological Survey Hydrologic Investigations Atlas HA-31*.
- Kupfer, D.H., and Bassett, A.M., 1962, Geologic reconnaissance map of part of the southeastern Mojave Desert, California: *U.S. Department of the Interior, Geological Survey Mineral Investigations Field Studies Map, MF-205, Scale 1:125,000 or 1" = 2 miles*.
- Lambert, J.R., 1987, Middle Tertiary structure and stratigraphy of the southern Mitchell Range, San Bernardino County, California: *Louisiana State University, Department of Geology and Geophysics Master's Thesis*.
- Lazarte, C.A., Bray, J.D., Johnson, A.M., and Lemmer, R.E., 1994, Surface breakage of the 1992 Landers Earthquake and its effect on structures: *Bulletin of the Seismological Society of America*, V. 84, p. 547-561.
- Lindvall, S.C. and Rockwell, T.K., 1993, Recurrent Holocene faulting along the Johnson Valley portion of the 1992 Landers earthquake surface rupture: *Geological Society of America Abstracts with Programs*, V. 25, p. 70.
- Luyendyk, B.P. and Hornafius, J.S., 1987, Neogene crustal rotations, fault slip, and basin development in southern California: *in* Ingersoll, R.V. and Ernst, W.G., eds., *Cenozoic Basin Development of Coastal California: Prentice-Hall*, p. 259-283.
- Luyendyk, B.P., Kamerling, M.J., and Terres, R., 1980, Geometric model for Neogene crustal rotations in southern California: *Geological Society of America Bulletin*, V. 91, p. 211-217.
- Luyendyk, B.P., Kamerling, M.J., Terres, R.R., and Hornafius, J.S., 1985, Simple shear of southern California during Neogene time suggested by paleomagnetic declinations: *Journal of Geophysical Research*, V. 90, B14, p. 12,454-12,466.
- MacFadden, B.J., Opdyke, N.D., Swisher, C.C., III, and Woodburne, M.O., 1990a, Paleomagnetism, geochronology and possible rotation of the middle Miocene Barstow Formation, Mojave Desert, California: *Geological Society of America Bulletin*, V. 102, p. 478-493.
- MacFadden, B.J., Opdyke, N.D., and Woodburne, M.O., 1990b, Paleomagnetism and Neogene clockwise rotation of the northern Cady Mountains, Mojave Desert of southern California: *Journal of Geophysical Research*, V. 95, B4, p. 4597-4608.
- Manson, M.W., 1986, Fault evaluation report for the Homestead Valley fault, Johnson Valley fault, and associated faults, San Bernardino County: *California Resources Agency, Department of Conservation, Division of Mines and Geology, Fault Evaluation Report FER 180, 10 p*.
- May, S.R., 1981, Geology and mammalian paleontology of the Horned Toad Hills, Mojave Desert, California: *University of California, Riverside, Department of Earth Sciences Master's Thesis*.
- McCulloh, T.H., 1965, Geologic map of the Nebo and Yermo Quadrangles, San Bernardino County, California: *U.S. Department of the Interior, Geological Survey, Open File Report (unnumbered), Scale 1:24,000 or 1" = 2,000'*.
- McGill, S.F., Murrey, B.C., Maher, K.A., Lieske, J.H., Jr., Rowan, L.R., and Budinger, F., 1988, Quaternary history of the Manix fault, Lake Manix Basin, Mojave Desert, California: *San Bernardino County Museum Association, Quarterly Volume XXXV, Numbers 3 and 4*.
- McJunkin, R.D., 1980, Strong-motion data for the Homestead Valley earthquake swarm, San Bernardino County, California, 15 March 1979: *California Geology*, V. 33, N. 1, p. 11-13.
- Meisling, K.E., and Weldon, R.J., 1989, Late Cenozoic tectonics of the San Bernardino Mountains, Southern California: *Geological Society of America Bulletin*, V. 101, N. 1, p. 106-128.
- Microsoft, 2011, Bing Maps 3D: *Microsoft Corporation Website: <http://maps.live.com/default.aspx?v=2&cp=44.023938--99.71&style=h&lvl=4&tilt=-89.875918865193&dir=0&alt=7689462.6842358>*.
- Miller, D.M., Howard, K.A., and John, B.E., 1982, Preliminary geology of the Bristol Lake region, Mojave Desert, California: *in* Cooper, J.D., ed., *Geologic excursions in the Mojave Desert: Geological Society of America Cordilleran Section, 78th Annual Meeting, Volume and Guidebook*, p. 91-100.
- Miller, D.M., Yount, J.C., Schermer, E.R., and Felger, T.J., 1994, Preliminary assessment of the recency of faulting at southwestern Fort Irwin, north-central Mojave Desert, California: *in* Reynolds, R.E., ed., *Off Limits in the Mojave Desert, field trip guidebook and volume for the 1994 Mojave Desert Quaternary Research Center field trip to Fort Irwin and surrounding areas: San Bernardino County Museum Association Special Publication 94-1*, p. 41-52.
- Miller, S.T., 1980, Geology and mammalian biostratigraphy of a part of the northern Cady Mountains, California: *U.S. Department of the Interior, Geological Survey Open-File Report OFR 1980-0978, 121 p*.
- Mojave Water Agency, January 2004, Geology of Mojave River Groundwater Basin: *in* *Mojave Water Agency, 2004 Regional Water Management Plan, V. 1: Report, Chapter 3*, p. 10.
- Morton, D.M., 1974, Geologic, fault and major landslide and slope stability maps: *in* Fife, D.L., Rogers, D.A., Chase, G.W., Chapman, R.H., and Sprotte, E.C., 1976, *Geologic hazards in southwestern San Bernardino County, California: California Resources Agency, Department of Conservation, Division of Mines and Geology Special Report SR 113, Scale 1:48,000 or 1" = 4,000'*.
- Morton, D.M. and Matti, J.C., 1993, Tectonic synopsis of the San Gorgonio Pass and San Timoteo Badlands areas, southern California: *San Bernardino County Museum Association, Spring Quarterly*, V. 40, N. 2, p. 3-14.
- Morton, D.M. and Miller, F.K., 2003a, Preliminary geologic map of the San Bernardino 30' X 60' quadrangle, California: *U.S. Department of the Interior, Geological Survey Open-File Report OFR 2003-0293, Scale 1:100,000 or 1" = 1.5 miles*.
- Morton, D.M. and Miller, F.K., 2003b, Preliminary geologic map of the San Bernardino 30' X 60' quadrangle, California: *in* Morton, D.M. and Miller, F.K., 2006, *Geologic map of the San Bernardino and Santa Ana 30' X 60' quadrangles, California: U.S. Department of the Interior, Geological Survey Open-File Report OFR 2006-1217, Version 1.0, Scale 1:100,000 or 1" = 1.5 miles*.

- Morton, D.M. and Miller, F.K., 2006, Geologic map of the San Bernardino and Santa Ana 30' X 60' quadrangles, California: *U.S. Department of the Interior, Geological Survey Open-File Report OFR 2006-1217*, Version 1.0, Scale 1:100,000 or 1" = 1.5 miles.
- Morton, D.M., Miller, F.K., and Smith, C.C., 1980, Photo reconnaissance maps showing young looking fault features in the southern Mojave Desert, California: *U.S. Department of the Interior, Geological Survey Miscellaneous Field Studies Map MF-1051*.
- Moseley, C.G., 1978, Geology of a portion of the northern Cady Mountains, Mojave Desert, California: *University of California, Riverside Department of Earth Sciences Master's Thesis*.
- Murbach, D., Rockwell, T.K., and Bray, J.D., 1999, The relationship of foundation deformation to surface rupture and near-surface faulting resulting from the 1992 Landers earthquake: *Earthquake Spectra*, V. 15, N. 1, p. 121-144.
- National Aeronautics and Space Administration [NASA], April 27, 2011, WorldWind, version 0.6.805.15357: *National Aeronautics and Space Administration Website: worldwind.arc.nasa.gov*.
- National Earthquake Information Center, 2010, Earthquake Hazards Program, Earthquake Search: *U.S. Department of the Interior, Geological Survey Webpage: http://earthquake.usgs.gov/earthquakes/eqarchives/epic/*
- Nicholson, C., Plesch, A., Shaw, J., and Hauksson, E., 2012, poster, Upgrades and improvements to the SCEC Community Fault Model: Increasing 3D fault complexity and compliance with surface and subsurface data: *Southern California Earthquake Center Annual Meeting, Meeting Program*, p. 19.
- Norris, R.M. and Webb, R.W., 1976, Geology of California: *John Wiley & Sons, Inc.*, 378 p.
- Nur, A., Hagai, R., and Beroza, G.C., 1993a, The nature of the Landers-Mojave earthquake line: *Science*, V. 261, p. 201-203.
- Nur, A., Hagai, R., and Beroza, G.C., 1993b, Landers-Mojave earthquake line: A new fault system?: *GSA Today*, V. 3, p. 253, 256-258.
- Oskin, M. and Iriondo, A., 2004, Large-magnitude transient strain accumulation on the Blackwater fault, Eastern California shear zone: *Geology*, V. 32, N. 4, p. 313-316.
- Padgett, D.C. and Rockwell, T.K., 1994, Paleoseismology of the Lenwood fault, San Bernardino County, California: in Murbach, D., ed., *Mojave Desert: South Coast Geological Society Annual Fieldtrip Guidebook*, p. 222-238.
- Page, R.W., and Moyle, W.R., 1960, Data on water wells in the eastern part of the middle Mojave Valley area, San Bernardino County, California: *California Resources Agency, Department of Water Resources Bulletin 91-3*.
- Petersen, M.D., Frankel, A.D., Harmsen, S.C., Mueller, C.S., Haller, K.M., Wheeler, R.L., Wesson, R.L., Zeng, Y., Boyd, O.S., Perkins, D.M., Luco, N., Field, E.H., Wills, C.J., and Rukstales, K.S., 2008, Documentation for the 2008 Update of the United States National Seismic Hazard Map: *U.S. Department of the Interior, Geological Survey Open-File Report OFR 2008-1128*, 128 pgs., Webpage: <http://pubs.usgs.gov/of/2008/1128/>
- Plesch, A., and Shaw, J. H., 2002, SCEC 3D Community fault model for southern California: *EOS Transactions of the American Geophysical Union*, V. 83, N. 47, Fall Meeting Supplement, Abstract S21A-0966, and <http://structure.harvard.edu/cfma>.
- Plesch, A., Shaw, J.H., Benson, C., Bryant, W.A., Carena, S., Cooke, M., Dolan, J.F., Fuis, G., Gath, E., Grant, L., Hauksson, E., Jordan, T.H., Kamerling, M., Legg, M., Lindvall, S., Magistrale, H., Nicholson, C., Niemi, N., Oskin, M.E., Perry, S., Planansky, G. Rockwell, T., Shearer, P., Sorlien, C., Suess, M.P., Suppe, J., Treiman, J., and Yeats, R., 2007, Community Fault Model (CFM) for Southern California: *Bulletin of the Seismological Society of America*, V. 97, N. 6, p. 1793-1802.
- Proctor, R.J., 1973, Major earthquakes and recently active faults in the southern California region: in Moran, D.E., Slosson, J.E., Stone, R.O., and Yelverton, C.A., eds., *Geology, seismicity and environmental impact: Association of Engineering Geologists Special Publication*, Scale 1:125,000 or 1" = 2 miles.
- Real, C.R., Topozada, T.R. and Parke, D.L., 1978, Earthquake epicenter map of California, 1900-1974: California Resources Agency, Department of Conservation, Division of Mines and Geology Map Sheet MS 39, Scale 1:1,000,000 or 1" = 16 miles.
- Reynolds, R.E., 1992, Quaternary movement on the Calico Fault, Mojave Desert, California, in Richard, S.M. ed., *Deformation associated with the Neogene Eastern California Shear Zone, southeastern California and southwestern Arizona: San Bernardino County Museums, Special Publication 92-1*, p. 64-65.
- Reynolds, R.E., compiler, 1993a, Landers: Earthquakes and Aftershocks: San Bernardino County Museum Association Quarterly, V. 40, N. 1, p. 70-72.
- Reynolds, R.E., 1993b, Road Guide: in Reynolds, R.E., compiler, Landers: Earthquakes and Aftershocks: San Bernardino County Museum Association Quarterly, V. 40, N. 1, p. 7-39.
- Richard, S.M. and Dokka, R.K., 1992, Introduction: in Richard, S.M. ed., *Deformation associated with the Neogene Eastern California Shear Zone, southeastern California and southwestern Arizona: San Bernardino County Museums, Special Publication 92-1*, p. v.
- Richter, C.F., 1947, The Manix (California) earthquake of April 10, 1947: *Bulletin of the Seismological Society of America*, V. 37, p. 171-179.
- Rockwell, T.K., Schwartz, D.P., Sieh, K.E., Rubin, C., Lindvall, S., Herzberg, M., Padgett, D., and Fumal, T., 1993, Initial paleoseismic studies following the Landers earthquake: Implications for fault segmentation and earthquake clustering: *EOS AGU Fall supplement*, p. 67.
- Rockwell, T.K., Lindvall, S., Herzberg, M., Murbach, D., Dawson, T., and Berger, G., 2000, Paleoseismology of the Johnson Valley, Kickapoo, and Homestead Valley faults: Clustering of earthquakes in the Eastern California Shear Zone: *Bulletin of the Seismological Society of America*, V. 90, N., p. 1200-1236.
- Rogers, T.H., 1969, Geologic map of California, Olaf P. Jenkins edition, San Bernardino Sheet: *California Resources Agency, Department of Conservation, Division of Mines and Geology*, Scale 1:250,000 or 1" = 4 miles.

- Ross, T.M., Luyendyk, B.P., and Haston, R.B., 1989, Paleomagnetic evidence for Neogene tectonic rotations in the central Mojave Desert, California: *Geology*, V. 17, p. 470-473.
- Rubin, C.M. and Sieh, K., 1997, Long dormancy, low slip rate, and similar slip-per-event for the Emerson fault, eastern California shear zone: *Journal of Geophysical Research*, V. 102, p. 15,319-15,333.
- Rymer, M.J., 2000, Triggered surface slips in the Coachella Valley area associated with the 1992 Joshua Tree and Landers, California, earthquakes: *Bulletin of the Seismological Society of America*, V. 90, N. 4, p. 832-848.
- Sadler, P.M., 1982, Geology of the NE San Bernardino Mountains, San Bernardino County, California: *California Resources Agency, Department of Conservation, Division of Mines and Geology*, Open-File Report OFR 82-18 L.A., Scale 1:24,000 or 1" = 2,000'.
- San Bernardino County, 1994, San Bernardino County Official Land Use Plan, General Plan Geologic Hazard Overlays: *San Bernardino County Land Use Services Department Maps*, Scale 1:24,000 or 1"=2,000'.
- San Bernardino County, 2007, San Bernardino County Land Use Plan, General Plan, Geologic Hazard Overlays, C Series: *San Bernardino County Land Use Services Department Maps*, Scale 1:14,400 or 1"=1,200'.
- San Bernardino County, 2010, San Bernardino County Land Use Plan, General Plan, Geologic Hazard Overlays, C Series: *San Bernardino County Land Use Services Department Map*, Scale 1:14,400 or 1"=1,200'.
- Sauber, J., Thatcher, W., and Solomon, S.C., 1986, Geodetic measurements of deformation in the central Mojave Desert, California: *Journal of Geophysical Research*, V. 91, p. 12,683-12,693.
- Scientists from the USGS, SCEC and CDMG, 2000, Preliminary report on the 16 October 1999 M 7.1 Hector Mine, California, earthquake: *Seismological Research Letters*, V. 71, p. 11-23.
- Shakal, A.F., 1993, Strong-motion records from the June 28, 1992 Landers Earthquake: in Reynolds, R.E., compiler, Landers: Earthquakes and Aftershocks: San Bernardino County Museum Association Quarterly, V. 40, N. 1, p. 40-43.
- Sieh, K., Jones, L., Hauksson, E., Hudnut, K., Eberhart-Phillips, D., Heaton, T., Hough, S., Hutton, K., Kanamori, H., Lilje, A., Lindvall, S., McGill, S., Mori, J., Rubin, C., Spotila, J., Stock, J., Thio, H.K., Treiman, J., Wernicke, B., and Zachariasen, J., 1993, Near-field investigations of the Landers earthquake sequence, April to July, 1992: *Science*, V. 260, p. 171-176.
- Skirvin, T.W. and Wells, S.G., 1990, Late Cenozoic structure, geomorphology and landscape evolution of the Old Dad Mountain area, California: in Reynolds, R.E., Wells, S.G., and Brady, R.H., III, compilers, At the end of the Mojave: Quaternary studies in the eastern Mojave Desert: San Bernardino County Museum Special Report, p. 73-88.
- Sneed, M., Ikehara, M.E., Stork, S.V., Amelung, F., and Galloway, D.L., 2003, Detection and measurement of land subsidence using Interferometric synthetic aperture radar and global positioning system, San Bernardino County, Mojave Desert, California: U.S. Department of the Interior, Geological Survey, Water-Resources Investigations Report WRI 03-4015.
- Stein, R.S., King, G.C.P., and Lin, J., 1992, Change in failure stress on the southern San Andreas fault system caused by the 1992 magnitude = 7.4 Landers earthquake: *Science*, V. 258, p. 1328-1332.
- Southern California Earthquake Center, 2010, Community Fault Model: Harvard University website: <http://structure.harvard.edu/cfm/>.
- Southern California Earthquake Data Center, 2011, Southern California Catalogs, 1932 - Present* Earthquake Catalog: Southern California Earthquake Center, website: http://www.data.scec.org/catalog_search/date_mag_loc.php.
- Southern California Seismic Network, 2011, Earthquakes: Southern California Seismic Network Website: <http://www.scsn.org/earthquakes.html>.
- Sowers, J.M., Unruh, J.R., Lettis, W.R., and Rubin, T.D., 1994, Relationship of the Kickapoo fault to the Johnson Valley and Homestead Valley faults, San Bernardino County, California: *Bulletin of the Seismological Society of America*, V. 84, p. 528-536.
- Spencer, J.E., 1990a, Geologic map of southern Avawatz Mountains, northeastern Mojave Desert region, San Bernardino County, California: U.S. Department of the Interior, Geological Survey Miscellaneous Field Studies Map MF-2117, Scale 1:24,000 or 1" = 2,000'.
- Spencer, J.E., 1990b, Late Cenozoic extensional and compressional tectonism in the southern and western Avawatz Mountains, southeastern California: in Geological Society of America Memoir 176, p. 317-333.
- Stamos, C.L., Martin, P., Nishikawa, T., and Cox, B.F., 2001, Simulation of ground-water flow in the Mojave River Basin, California: U.S. Department of the Interior, Geological Survey Water-Resources Investigations Report WRI 2001-4002, version 1.1.
- Stamos, C.L., Huff, J.A., Predmore, S.K., and Clark, D.A., 2004, Regional water table (2004) and water-level changes in the Mojave River and Morongo ground-water basins, southwestern Mojave Desert, California: U.S. Department of the Interior, Geological Survey Scientific Investigations Report SIR 2004-5187.
- Steinen, R.P., 1966, Stratigraphy of the middle and upper Miocene Barstow Formation, San Bernardino County, California: University of California, Riverside, Department of Earth Sciences Master's Thesis.
- Stover, C.W. and Coffman, J.L., 1993, Seismicity of the United States, 1568-1989: (revised), U.S. Department of the Interior, Geological Survey Professional Paper PP 1527.
- Topozada, T.R., 1993, The Landers-Big Bear earthquake sequence and its felt effects: *California Geology*, V. 46, N. 1, p. 3-9.
- Topozada, T., Branum, D., Petersen, M., Hallstrom, C., Cramer, C., and Reichle, M., 2000, Epicenters of and areas damaged by M \geq 5 California Earthquakes, 1800-1999: California Resources Agency, Department of Conservation, Division of Mines and Geology Map Sheet MS 49, Scale 1:1,500,000 or 1" = 24 miles.
- Townley, S.D. and Allen, M.W., 1939, Descriptive catalog of earthquakes of the Pacific Coast of the United States 1769 to

- 1928: Bulletin of the Seismological Society of America, V. 29, N. 1, p. 1-297.
- Turcotte, D.L., 1997, Fractals and Chaos in Geology and Geophysics: Cambridge University Press, 398 p.
- Treiman, J.A., 1992a, Eureka Peak and Burnt Mountain faults – two “new” faults in Yucca Valley, San Bernardino County, California: in Landers earthquake of June 28, 1992, San Bernardino County, California, Field Trip Guidebook: Association of Engineering Geologists, Southern California Section, p.19-22.
- Treiman, J.A., 1992b, Eureka Peak and related faults: Joshua Tree South and Yucca Valley South Quadrangles, San Bernardino and Riverside Counties, California: California Resources Agency, Department of Conservation, Division of Mines and Geology Fault Evaluation Report FER-230, 15 p.
- Umbarger, K.E., 1992a, Quaternary geology of the Spy Mountain region, Landers Quadrangle, San Bernardino County, California: California State University, Los Angeles, Geology Department Master’s Thesis.
- Umbarger, K.E., 1992b, Quaternary geology of the Spy Mountain region, Landers Quadrangle, San Bernardino County, California: in Reynolds, R.E., compiler, Old Routes to the Colorado: San Bernardino County Museum Association Special Publication 92-2, p. 34-39.
- United States Geological Survey, 1985a, Radar image mosaic of the Bakersfield Quadrangle, synthetic-aperture radar imagery, x-band near range, west look, Scale 1:250,000 or 1” = 4 miles.
- United States Geological Survey, 1985b, Radar image mosaic of the Death Valley Quadrangle, synthetic-aperture radar imagery, x-band near range, west look, Scale 1:250,000 or 1” = 4 miles.
- United States Geological Survey, 1985c, Radar image mosaic of the Kingman Quadrangle, synthetic-aperture radar imagery, x-band near range, west look, Scale 1:250,000 or 1” = 4 miles.
- United States Geological Survey, 1985d, Radar image mosaic of the Los Angeles Quadrangle, synthetic-aperture radar imagery, x-band near range, west look, Scale 1:250,000 or 1” = 4 miles.
- United States Geological Survey, 1985e, Radar image mosaic of the Needles Quadrangle, synthetic-aperture radar imagery, x-band near range, west look, Scale 1:250,000 or 1” = 4 miles.
- United States Geological Survey, 1985f, Radar image mosaic of the San Bernardino Quadrangle, synthetic-aperture radar imagery, x-band near range, west look, Scale 1:250,000 or 1” = 4 miles.
- United States Geological Survey, 1985g, Radar image mosaic of the Trona Quadrangle, synthetic-aperture radar imagery, x-band near range, west look, Scale 1:250,000 or 1” = 4 miles.
- United States Geological Survey, 1992, Pattern of surface ruptures associated with the June 28, 1992, Landers earthquake: EOS Transactions of the American Geophysical Union, AGU, V. 73, p. 357-358.
- United States Geological Survey, 1993, The 1992 Landers earthquake and surface faulting: Earthquakes and Volcanoes, V. 24.
- United States Geological Survey and California Geological Survey, 2002, Quaternary fault and fold database for the United States, U.S. Department of the Interior, Geological Survey Webpage: <http://earthquake.usgs.gov/regional/qfaults/>.
- United States Geological Survey and California Geological Survey, 2006, Quaternary fault and fold database for the United States, U.S. Department of the Interior, Geological Survey Webpage: <http://earthquake.usgs.gov/regional/qfaults/>.
- United States Geological Survey, 2007, 2002 National Seismic Hazard Maps – California Fault Parameters: U.S. Department of the Interior, Geological Survey Webpage: http://gldims.cr.usgs.gov/webapps/cfusion/Sites/qfault/qf_web_search_res.cfm.
- United States Geological Survey, 2008, Documentation for the 2008 Update of the United States National Seismic Hazard Maps: Appendix I. Parameters for Faults in California: U.S. Department of the Interior, Geological Survey Webpage: <http://pubs.usgs.gov/of/2008/1128/>.
- United States Geological Survey, 2009, Earthquake Search: U.S. Department of the Interior, Geological Survey Earthquake Hazards Program, Earthquake Center website: <http://neic.usgs.gov/neis/epic/epic.html>.
- URS Corporation, March 13, 2003a, Mojave River Transition Zone recharge project, Phase I report, Transition Zone hydrogeology: URS Corporation for the Mojave Water Agency, 112 p.
- URS Corporation, June 13, 2003b, Mojave River Transition Zone recharge project, Phase II report, Groundwater supply and demand in the Transition Zone: URS Corporation for the Mojave Water Agency, 117 p.
- Valentine, M.J, Brown, L., and Golombek, M. 1988, Counterclockwise Cenozoic rotations of the Mojave Desert: *Geological Society of America, Cordilleran Section 84th Annual Meeting Abstracts with Programs*, V. 20, p. 239.
- Walker, J.D., Bartley, J.M., and Glazner, A.F., 1990, Large-magnitude Miocene extension in the central Mojave Desert: Implications for Paleozoic to Tertiary paleogeography and tectonics: *Journal of Geophysical Research*, V. 95, p. 557-569.
- Wells, D.L. and Coppersmith, K.J., 1994, New empirical relationships among magnitude, rupture length, rupture width, rupture area, and surface displacement: *Bulletin of the Seismological Society of America*, V. 84, N. 4, p. 974-1002.
- Wells, S.G., McFadden, L.D., Dohrenwend, J.C., Bullard, T.F., Feilberg, B.F., Ford, R.L., Grimm, J.P., Miller, J.R., Orbock, S.M., and Pickle, J.D., 1984, Late Quaternary geomorphic history of the Silver Lake area: An example of the influence of climatic changes on the desert piedmont evolution in the eastern Mojave desert, California: *Geological Society of America, Field Trip Guidebook, Annual Meeting*, p. 69-87.
- Williamson, D.A., 1980, The geology of a portion of the eastern Cady Mountains, Mojave Desert, California: *University of California, Riverside Department of Earth Sciences Master’s Thesis*.
- Woodburne, M.O., 1991, The Mojave Desert Province: in Woodburne, M.O., Reynolds, R.E., and Whistler, D.P., eds., Inland Southern California: The last 70 Million Years: *San Bernardino County Museum Association Quarterly*, V. 38, N. 3 & 4, p. 60-77.

- Woodburne, M.O. and Tedford, R.H., 1982, Litho and biostratigraphy of the Barstow Formation, Mojave Desert, California: in Cooper, J.D., compiler, *Geologic Excursions in the California Desert: Geological Society of America, Cordilleran Section 78th Annual Meeting Volume and Guidebook*, p. 65-76.
- Woodburne, M.O., Tedford, R.H., and Miller, S.T., 1982, Stratigraphy and geochronology of Miocene strata in the central Mojave Desert, California: in Cooper, J.D., compiler, *Geologic Excursions in the California Desert: Geological Society of America, Cordilleran Section 78th Annual Meeting Volume and Guidebook*, p. 47-64.
- Woodburne, M.O., Tedford, R.H., and Swisher, C.C., III, 1990, Lithostratigraphy, biostratigraphy, and geochronology of the Barstow Formation, Mojave Desert, southern California: *Geological Society of America Bulletin*, V. 102, p. 459-477.
- Working Group on the Probabilities of Future Large Earthquakes in Southern California, 1992, *Future Seismic Hazards in Southern California, Phase I: Implications of the 1992 Landers earthquake sequence: California Resources Agency, Department of Conservation, Division of Mines and Geology Report*.
- 2007 Working Group on California Earthquake Probabilities, 2008, *The Uniform California Earthquake Rupture Forecast, Version 2 (UCERF 2): U.S. Department of the Interior, Geological Survey Open-File Report OFR 2007-1437*, website: <http://pubs.usgs.gov/of/2007/1437/>; *California Resources Agency, Department of Conservation, Geological Survey Special Report SR 203; Southern California Earthquake Center contribution No. 1138; Southern California Earthquake Center Webpage: http://www.wgcep.org/ucerf/*
- Youngs, L.G., 1988, Aeromagnetic Map of the San Bernardino Quadrangle: *California Resources Agency, Department of Conservation, Division of Mines and Geology, Regional Geophysical Map Series, No. 3D, Scale 1:250,000 or 1" = 4 miles*.
- Zachariasen, J. and Sieh, K., 1995, The transfer of slip between two en echelon strike-slip faults: A case study from the 1992 Landers earthquake, southern California: *Journal of Geophysical Research*, V. 100, p. 15,281-15,301.
- Ziony, J.I., and Jones, L.M., 1989, Map showing the Quaternary faults and 1978-1984 seismicity of the Los Angeles region, California: *U.S. Department of the Interior, Geological Survey Miscellaneous Field Studies Map MF-1964, Scale 1:250,000 or 1" = 4 miles*.
- Ziony, J.I. and Yerkes, R.F., 1985, Evaluating earthquake and surface-faulting potential: in Ziony, J.I., ed., *Evaluating earthquake hazards in the Los Angeles region – an earth-science perspective: U.S. Department of the Interior, Geological Survey Professional Paper PP 1360*, p. 43-91.

Vegetation lineaments near Pearblossom, CA: possible indicators of secondary faulting subparallel to the San Andreas Fault

David K. Lynch¹ and Frank Jordan²

¹ U. S Geological Survey; ² California State University Los Angeles

ABSTRACT—A cluster of twenty-four vegetation lineaments on Holcomb Ridge near Pearblossom, California were identified on Google Earth imagery. They ranged in length from 0.21 to 2.29 km (mean 0.8 km). The cluster is roughly 13 km long by 2 km wide, and is approximately 3 km north of the San Andreas Fault (SAF). The cluster and the VLS are subparallel to the SAF. None of the lineaments coincide with faults in the USGS and CGS databases, although one falls along a suspected or concealed fault identified by Dibblee. Seismicity (1932-2011) in the cluster is uncorrelated with the veg lines. Several lineaments are crossed by the California aqueduct. A few are coincident with elongated metamorphic units mapped by Dibblee as Precambrian marble pendants, dolomite and mica schist. Field reconnaissance revealed a number of low scarps and offset channels on several of the veg lines. These veg lines presumably trace out relatively shallow, long-lasting moisture sources, though where they correlate with marble, soil chemistry or Jointing may also play a role. If these veg lines mark the surface traces of faults, they may indicate the presence of a heretofore unrecognized region of localized lithospheric fracture associated with forebergs of the SAF. Work is underway to determine whether they are active faults.

1. Introduction

Vegetation lineaments (VLS) often mark the surface traces of faults, especially in the desert (Rymer et al. 2002; Treiman et al. 2012). Gouge and different rocks across the fault plane act as aquatards to inhibit subsurface water flow. Water accumulates uphill of the fault and rises to or near the surface. With moist soil closer to the surface, plants grow more readily, producing VLS. VLS may be either discrete strips of enhanced vegetation or relatively abrupt ~linear boundaries to ground cover (Lynch 2005; 2007; 2012). VLS can also be produced in a number of ways that are unrelated to faulting. For example, VLS are found in valleys along streams and at boundaries in rocks such as dikes cutting granitic rocks.

While VLS are most evident on major faults, any fault in a vadose zone of fractured material reaching to the water table can also produce them, including secondary faulting of a plate boundary and forebergs. A foreberg is a narrow ridge of tectonically-produced hills rising up to 100 m above the surrounding alluvial fans. They are usually subparallel to the major controlling faults and often are associated with positive flower structures generated by uplift and deformation (Bayarsayhan et al. 1996; Bayasgalen et al. 1999).

The main topographic feature in the area is Holcomb Ridge, a NW trending spine of late Cretaceous granodiorite with embedded linear metamorphic units (Dibblee 2002; Morton and Miller 2006). It is bounded on the south by the San Andreas Fault and to the north by the Cajon Valley Fault (Kenney 1999). Though most prominent east of Big Rock Creek, Holcomb Ridge appears to have lower elevation extensions reaching as far west as Pearblossom. The area is part of a regional restraining bend in the SAF (Hill and Dibblee 1953). The SAF strikes N63W while the

relative direction between the Pacific and North American Plates is 315°, a difference of 18° from the SAF's strike. Weldon (1986), Weldon et al. (1993), Kenney (1999) and Kenney and Weldon (2004) discuss the late Quaternary deformation of rocks and dynamics of this area. Holcomb Ridge would appear to be a foreberg, because it is an elongated, perhaps anticlinal structure that is subparallel to the SAF.

In this paper we describe some newly recognized VLS and possible foreberg-style faulting north of the SAF on the north slopes of Holcomb Ridge near Pearblossom, California in Los Angeles County. Several of them are crossed by the California aqueduct. Preliminary field investigations show evidence for faulting along the VLS.

2. Aerial imaging and spatial setting

While surveying secondary fault structures along the SAF on Google Earth, we came across a cluster of ~ 24 VLS (Figures 1–3 & Appendix 1), 23 of which are draped over the northern flank of Holcomb Ridge and its northwesterly extension of low hills. Searches for 50 km north and south along the SAF revealed no similar structures. The VL cluster is subparallel to the SAF, and ~3 km north of it. It is roughly 13 km long by 2 km wide. The bearing of the cluster's long axis is ~297° (N63W), the same as the SAF's strike of N63W in this area. Excluding VL14 that bears NE, the VLS mean headings averaged $304^\circ \pm 11^\circ$ (1σ), or N56W, consistent with the SAF's strike. VLS ranged in length from 0.21 to 2.29 km (mean 0.8 km). None of the VLS coincide with faults in the USGS and CGS databases, although VL15 clearly falls along a suspected or concealed fault identified by Dibblee (2002). The VLS fall in the Valermo and Juniper Hills 7.5' quadrangles. VL1, VL2, VL5 & VL17 are crossed by the Pearblossom discharge line (an

underground section of the California Aqueduct) and were associated with faulting by the California Department of Water Resources in documents in the 1960's and 1970s (Dow 1967; 1969).

According to the California State Water Project report (1974),

During excavation of the discharge lines, a number of vertical to steeply dipping faults and shears were exposed, varying from 12 inches to 25 feet in width. The fault system within this area crosses the discharge lines roughly subparallel to the San Andreas fault zone. Although numerous faults are present in the foundation rock of the plant and discharge lines, they are not considered active, but a major quake along the San Andreas zone could cause some movement.

Trench excavation logs noted a number of shear zones and gouge planes. In these reports, VLS in the vicinity were identified as marking fault traces on aerial photos. Even today, VL2 is apparent where it crosses the disturbed soil of the aqueduct south of the Pearblossom pumping plant (Figure 3).

Many of the VLS occur in thin patches of Holocene sediments overlying sparsely exposed medium to fine grained massive Mesozoic quartz-monzonite/granodiorite. Several VLS (9,10,18 & 21) are precisely coincident with elongated metamorphic units mapped by Dibblee (2002) as Paleozoic limestone or dolomite marble pendants and mica schist. Morton and Miller (2006) map the country rock as monzonite and the linear metamorphic units as Paleozoic marble. Based on

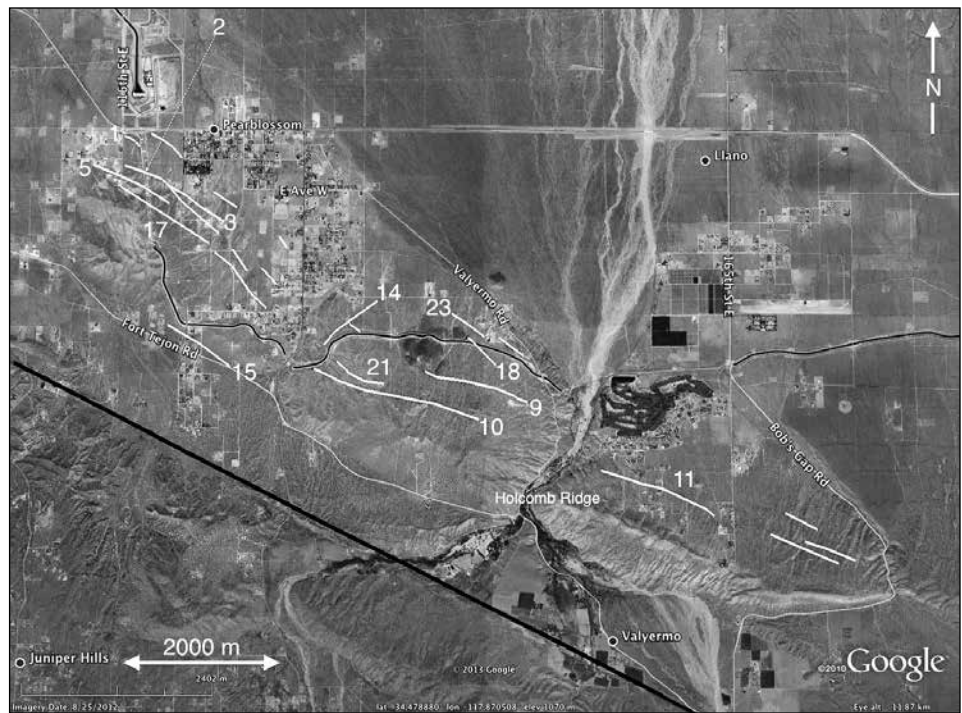


Figure 1. Pearblossom Vegetation Lineaments (white lines) marked on Google Earth imagery. The thick black line is the main trace of the San Andreas Fault. VLS mentioned in the text are labeled (see Appendix I for full list). Holcomb Ridge trends parallel to the San Andreas Fault and is dissected by Big Rock Creek. Image is 13 km wide.



Figure 2. Google Earth image of vegetation lineament VL11 in Crystallaire, CA between Valvermo Rd and 165th St. E

recent earthquake relocations for 1932-2011, the VLS did not appear to be correlated with seismicity.

When elevation profiles on Google Earth are examined, many but not all of the VLS are associated with subtle topographical structures, often slope breaks or small scarps. These findings were confirmed in the field. We note, however, that scarps, like VLS, can be caused by



Figure 3 Google Earth image of an underground section of the California Aqueduct crossing VL2. The ground was scraped clean during construction and VL2 has reestablished itself in the disturbed soil. At the left are twin chevron-shaped outcrops uphill (toward the bottom of the picture) of VL2. Field investigations found them to be fine-grained granitic rock. The apices of the chevrons are parallel to the VL. The northern terminations of the outcrops coincide with the VL. North of the VL, no outcrops are present, and only eroded and deposited grus is found.

faults and by underlying rock, for instance by differential erosion of contrasting rock types. They can also be caused by groundwater sapping.

3. Field investigations

Several field surveys were conducted in 2012 and 2013 to search for evidence of stream offsets, topographical features and evidence of recent activity. Real-time GPS and imagery available on a smart phone verified the locations of the VLs. It was not always possible to easily recognize the VLs *in situ* because visibility was impeded by the larger plants. Additionally, the edges of the lineaments are not sharply defined.

The VLs' contrast is due entirely to denser plant growth and larger plants, not to localized soil color differences. This was evident, especially where dirt roads crossed the VLs and no color contrast was seen. While tall trees (2-4 m height) like California Juniper (*Juniperus californica*) and Joshua (*Yucca brevifolia*) were prominent, most of

the plants defining the VLs consisted of low shrubs and grass. The plants were generally much darker than the surrounding light colored tan and gray soil.

Many—but not all—VLs were found to be coincident with subtle topographical structures like scarps and ridges, usually rounded and with low relief. In some cases, the topography may have been controlled by differential weathering of bed rocks rather than tectonic movement. This was observed near some metamorphic bodies, e.g. VL10.

While all the VLs were visited, detailed surveys were only done on VL2 and VL11. Both were clearly evident on aerial photos and were mostly on natural, undisturbed terrain. VL2 was of particular interest because it was crossed by the aqueduct and was visible as a continuous VL on either side (Figure 3). VL9, VL10, VL21, VL18 and VL23 also appear to be crossed by or intersect the aqueduct at other locations.

VL2: Unlike many of the VLs, VL2 was clearly visible in the field (Figure 4). A number of fine-grained aplite-



Figure 4. Vegetation lineament VL2 running horizontally across the image, view looking SSW. Top: wide angle view, aqueduct just off the left side of the picture. Bottom: Enlarged view.

like outcrops trending down hill terminated at the VL, below which was only finer grained grus from weathered monzonite. Where the VLs are roughly perpendicular to the direction of channel flow, a few offset channels were found, usually but not always right lateral (Figure 5). Additionally, several topographic features were found parallel to VL2, most notable being two chevron-shaped outcrops whose apices were parallel to the VL and whose northern ends terminated on the VL (left hand side of Figure 3).

VL11: This lineament was in much denser vegetation than in the vicinity of VL2 and visibility was limited by the large number of tall Juniper trees. While there was some evidence of right lateral offset channels, no systematic conclusions could be drawn. VL11 coincides with a linear metamorphic unit (VL2 did not) and scattered cobbles of marble were found that confirmed previous geologic mapping. VL11 obliquely crosses W Ave Y-8 but no soil color variations were found in the dirt road. The lineament arguably splits into two strands. The main (south) strand occurs on a small slope break and the north strand coincides with an eroded scarp about 3 meters high (Figure 6). VL9 and VL11 together were mapped as a possible single fault by Morton and Miller (2006).

VL3: Based on bioturbation and exploratory trenching where VL3 crosses 121st Street E and road construction exposes a ~1 meter high cut, we found what appeared to be thin O and A soil horizons (few mm) consisting of light colored, tan granitoid Holocene grus. Below the grus was a few cm of reddish unconsolidated Pleistocene B-horizon soil that overlaid well indurated brown B horizon soil. The cleaned road cut at VL3 showed possible evidence of strike slip motion (Figure 7). On either side of a “disturbed” zone that appeared to be centered on the lineament, there were distinct soil color differences with approximate Munsell hues of 10YR northeast of the disturbed zone juxtaposed against hues of 7.5YR southwest of the zone. Additionally, a number of low furrows in a bench cut were roughly parallel to the lineament, perhaps indicating joints or fractures in the well indurated soil.

4. Discussion

In view of their clustering and common trend subparallel to the SAF, we believe these VLs are related and probably have a common origin, perhaps tectonic. These VLs presumably trace out relatively shallow and persistent moisture sources, though where



Figure 5. Right lateral jog in channel wall immediately downhill from VL2. Displacement ~2 m.

they correlate with marble, soil chemistry or interface fracturing may encourage plant growth.

The actual number of VLs is subject to interpretation. Several of the VLs appear to line up and may represent through-going features. For example, VLs 10, 11 and 13 may be a single structure. The same is true of VL9 and VL19, and perhaps VL5 and VL22. Weaker VLs were also present but not cataloged here.

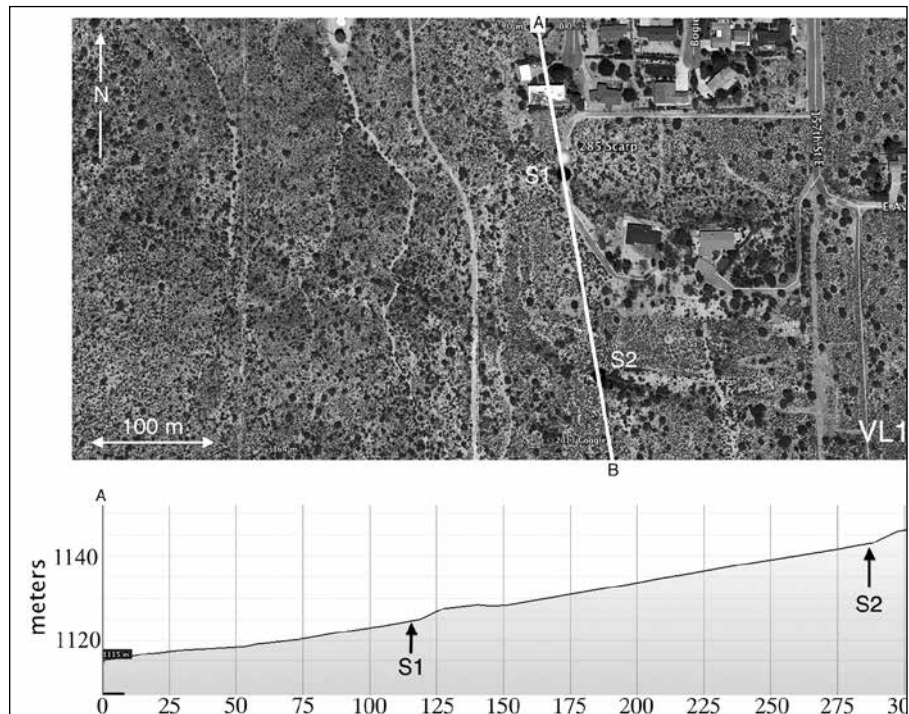


Figure 6. Elevation profile across two segments of VL11. Scarp S1 is very prominent in the field, and was a persistent feature upslope that may be part of a pressure ridge. Scarp S2 is evident but subtle. Both occur on the down hill side of the VL, which is typical of topographic structures coinciding with the VLs. Imagery and elevation data from Google Earth.

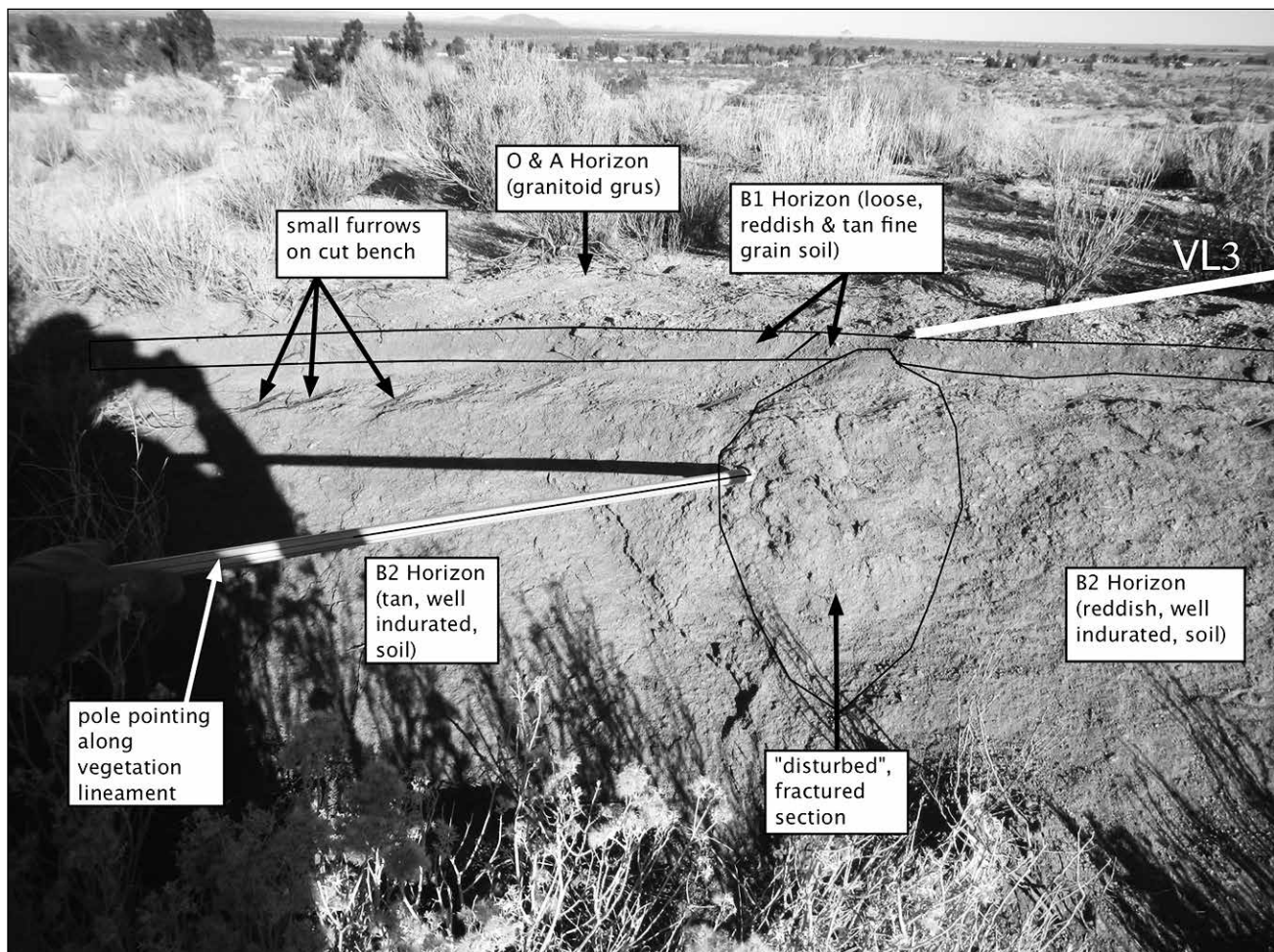


Figure 7. Exploratory trench across VL3 that revealed contrasting soils across the center of the VL, and an array of small furrows parallel to the VL. The thick, dark ~horizontal line is the shadow of a broom handle.

A number of faint VLs are found to the east in an adjacent area bounded roughly by Bob's Gap Rd, Pearblossom Hwy, 263rd St E and Holcomb Ridge Rd. These VLs rather suspiciously run more or less E-W and some are coincident with dirt roads. We have not included these VLs in this study, as they appear to be fundamentally different from the Pearblossom VLs.

5. Summary and Conclusions

We have described a cluster of vegetation lineaments (VLs) on Holcomb Ridge that are subparallel to the San Andreas Fault. These VLs may mark the surface traces of a number of secondary faults on forebergs, or alternatively, may mark rock boundaries that control near-surface water persistence. Most occur on or near slope breaks and some coincide with previously mapped linear metamorphic units of marble and schist. There is some indication of right lateral offset channels but no clear picture has yet emerged as to direction of motion, if any. An exploratory trench across one VL showed evidence of strike-slip faulting in the form of different subsurface soil colors on either side of the lineament and fracture zones coincident the VLs. All of the VLs are near the California Aqueduct

and several of them are crossed by it. In this early study, we could not assess their current state of activity.

To extend this work, two projects seem reasonable: 1) trenching across selected lineaments to expose soil and rock morphology possibly indicative of faulting, and 2) obtaining high resolution lidar DEMs to search for subtle features like offset channels, scarps and ridges, displaced rock units, etc.

Acknowledgments

The authors are indebted to Dave Miller (USGS) for many suggestions that improved the paper. We also thank Jerry Treiman (CGS), Jon Matti (USGS), John Tinsley (USGS) and Daniel Ponti (USGS) for helpful discussions on the lineaments and assistance in locating historical documents. Kenneth W. Hudnut (USGS) provided valuable assistance in the field.

References

- Bayarsayhan, C., A. Bayasgalan, B. Enhtuvshin, Kenneth W. Hudnut, R. A. Kurushin, Peter Molnar and M. Ölziybat, 1996. 1957 Gobi-Altay, Mongolia, earthquake as a prototype for southern California's most devastating earthquake, *GEOLOGY*, 24 no. 7 p. 579-582

- Bayasgalan, A., J. Jackson, J. Ritz and S. Carretier, 1999 "Fore-berg' flower structures, and the development of large intra-continental strike-slip faults: the Gurvan Bogd fault system in Mongolia, *J of Structural Geology*, 21, 1285-1302
- Dibblee, T. W., 2002. Geological map of the Valyermo quadrangle, Los Angeles County, California. Dibblee Geological Foundation, Map DF-80, scale 1:24,000.
- Dow, Ralph C. 1967
- Dow, Ralph C. 1969
- Florensov, N. A., and V. P. Solonenko (Eds.), *The Gobi-Altai Earthquake* (in Russian), Akad. Nauk USSR, Moscow, 1963 (English translation, U.S. Dept. Commerce, Washington, D.C., 424 pp., 1965).
- Hill, M. L. and Dibblee, T. W., 1953, San Andreas, Garlock, and Big Pine faults, California—a study of the character, history, and tectonic significance of their displacements: *Geological Society of America Bulletin*, v. 64, no. 4, p. 443-458.
- Kenney, Miles, D., 1999 Emplacement, offset history and recent uplift of basement within the San Andreas Fault System, northeastern San Gabriel Mountains, California [PhD thesis]; University of Oregon, 279p
- Kenney, Miles D. and Ray Weldon 2004 The Holcomb Ridge-Table Mountain fault slide: ramifications for the evolution of the San gabriel fault into the San Andreas fault, in *Breaking Up, the 2004 Desert Symposium Field Trip*, R.E. Reynolds,(ed), 57-63 <http://biology.fullerton.edu/dsc/pdf/2004breakingup.pdf>
- Lynch, David K. 2005 Line of Macomber Palms, Earth Science Picture of the Day, 26 October 2005 <http://epod.usra.edu/blog/2005/10/line-of-macomber-palms.html>
- Lynch, David K. 2007 San Andreas Fault in the Salton Trough, Earth Science Picture of the Day, 5 June 2007, <http://epod.typepad.com/blog/2007/06/san-andreas-fault-in-the-salton-trough.html>
- Lynch, David K. 2012 Vegetation Lineaments, Earth Science Picture of the Day, 18 July 2012 <http://epod.usra.edu/blog/2012/07/vegetation-lineaments.html>
- Morton, D.M., and Miller, F.K., 2006, Geologic map of the San Bernardino and Santa Ana 30' x 60' quadrangles, California, with digital preparation by Cossette, P.M., and Bovard, K.R.: U.S. Geological Survey Open-File Report 2006-1217, scale 1:100,000, 199 p., <http://pubs.usgs.gov/of/2006/1217>.
- Rymer, M. J., Seitz, G. G., Weaver, K. D., Orgil, A., Faneros, G., Hamilton, J. C., Goetz, C., 2002 Geologic and paleoseismic study of the Lavic Lake fault at Lavic Lake Playa, Mojave Desert, Southern California, *Bul. Seismo. Soc. Am.* 92: 1577 - 1591
- Treiman, Jerome A, Florante G. Perez and William A. Bryant, 2012 Utility of combined aerial photography and digital imagery for fault trace mapping in diverse terrain and vegetation regimes, in *Digital Mapping techniques '10 Workshop proceedings*, David R. Soller (ed), USGS Open-file Report 2012-1171, http://pubs.usgs.gov/of/2012/1171/pdf/usgs_of2012-1171-Treiman_p15-28.pdf
- Weldon, R. J., II, 1986, *The Late Cenozoic Geology of Cajon Pass, Implications for Tectonics and Sedimentation along the San Andreas Fault* [Ph.D. Thesis] Pasadena, California, California Institute of Technology, 400 pages including 12 unpublished map plates.
- Weldon, R. J., Meisling, K. E., and Alexander, J., 1993, A Speculative history of the San Andreas fault in the central Transverse Ranges, in, Powell, R. E., Weldon, R. J., and Matti, J. eds., *The San Andreas fault system; displacement, palinospastic reconstruction, and geologic evolution*, *Geological Society of America*, Memoir 178, p. 161-178.

Appendix I

Presented here is a list of the vegetation lineaments discussed in the paper, their names and locations, and Google Earth imagery of them.

Table A1: Pearblossom Vegetation Lineaments

name	center lat	center long	length(km)	mean bearing (°)
VL1	34.505170	-117.921466	0.24	308
VL2	34.501200	-117.919239	0.66	293
VL3	34.497318	-117.911652	0.91	303
VL4	34.496861	-117.912879	0.94	313
VL5	34.496112	-117.916550	1.39	303
VL6	34.497968	-117.907794	0.37	303
VL7	34.490814	-117.905671	0.36	326
VL8	34.492934	-117.895455	0.20	325
VL9	34.476176	-117.871588	1.40	287
VL10	34.478827	-117.883209	2.29	287
VL11	34.464039	-117.845510	1.59	291
VL12	34.456893	-117.821727	0.69	290
VL13	34.457047	-117.825379	0.96	293
VL14	34.482700	-117.891228	0.92	50
VL15	34.480851	-117.911175	1.00	303
VL16	34.504851	-117.916490	0.27	309
VL17	34.499972	-117.290762	1.14	297
VL18	34.480127	-117.870983	0.53	314
VL19	34.482868	-117.889217	0.21	305
VL20	34.488895	-117.901351	0.31	318
VL21	34.477012	-117.888793	0.70	295
VL22	34.488253	-117.905263	1.01	317
VL23	34.483249	-117.872979	0.56	306
VL24	34.460160	-117.825651	0.46	297

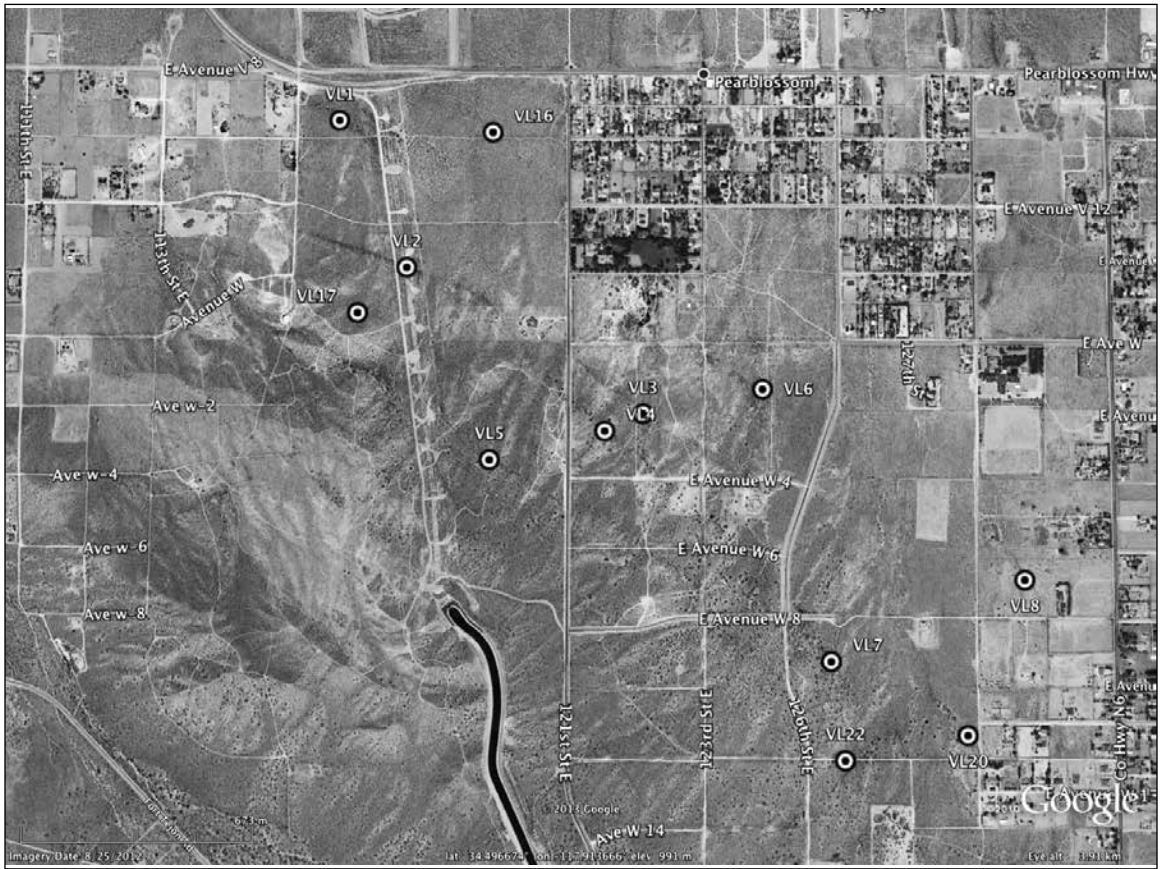


Figure A-1.

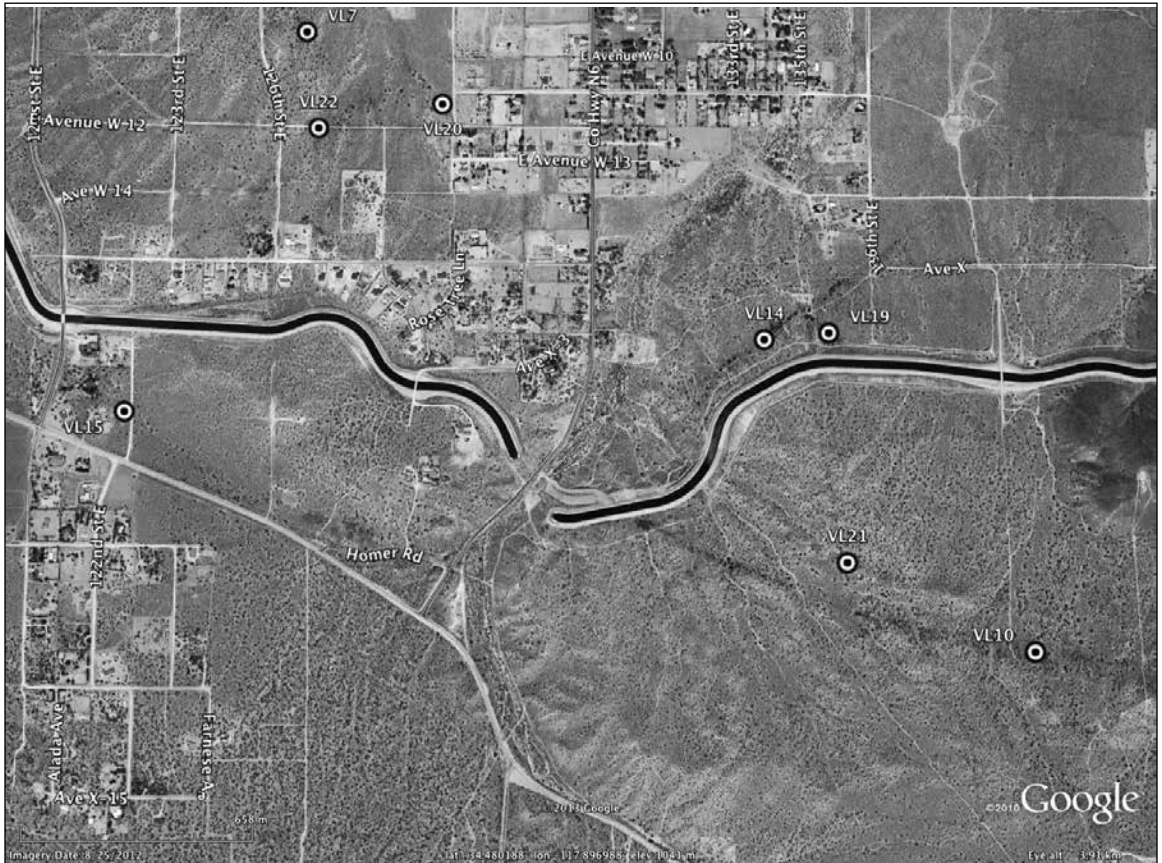


Figure A-2.



Figure A-3



Figure A-4.

Population dynamics of the Joshua tree (*Yucca brevifolia*): twenty-three-year analysis, Queen Valley, Joshua Tree National Park

James W. Cornett

JWC Ecological Consultants, P.O. Box 846, Palm Springs, California 92263, jwcornett@aol.com

One of the most recognizable desert plants is the Joshua tree, *Yucca brevifolia*. Large size, dagger-like leaves and endlessly varying silhouettes make the Joshua tree visually unique. It is the only native tree found on Mojave Desert flatlands, the ecologically dominant component in many regions and one of seven plant species for which an American national park has been named. It has become the symbol of the California deserts (Cornett, 1999). For these reasons populations of *Y. brevifolia* were monitored for more than twenty years at ten, one-hectare study sites located in California, Nevada, Utah and Arizona. This paper describes the results of twenty-three years of monitoring one Joshua tree population located in Queen Valley, Joshua Tree National Park, California.

The Queen Valley study site was located on an alluvial plain surrounded by low hills and mountains. Drainage occurred to the northwest, into nearby Lost Horse Valley. Soil was a mix of sand and silt. Site elevation was 1,362 meters above sea level. At the inception of the study *Y. brevifolia* was considered to be dominant and likely accounted for the greatest biomass of any plant species. Listed in estimated decreasing order of ground cover were the following perennial plant taxa found within the site boundaries: *Hilaria rigida*, *Ephedra aspera*, *Coleogyne ramosissima*, *Yucca brevifolia*, *Eriogonum fasciculatum*, *Stipa speciosa*, *Ambrosia salsola*, *Sporobolus contractus*, *Atriplex canescens*, *Tetradymia stenolepis*, *Lycium cooperi*, *Yucca schidigera*, *Cylindropuntia echinocarpa*, *Opuntia basilaris* and *Echinocereus mojavensis*. Taxonomic nomenclature follows *The Jepson Manual* (Baldwin et al., 2012).

A wildfire passed through the project site on July 1, 2006, consuming most perennial plant species including many Joshua trees. In January of 2013, nearly seven years later, *Yucca brevifolia* accounted for the most ground coverage followed by *Ambrosia salsola*, *Atriplex canescens* and perennial bunch grass species.

From 1990 through 2013 Joshua trees within the Queen Valley study site were monitored in most years with regard to dimensions, vigor and reproductive status. Forty-four living trees were present in 1990 representing both mature and immature individuals. Based upon leaf cluster status, 26 of the 44 trees were considered to be enlarging, 12 were stable, and 6 were declining. By 2013 *Y. brevifolia* numbers had declined to 12, an approximately 73% decrease. Of the

12 living trees remaining on-site in 2013, 5 were considered enlarging, 4 were stable and 3 were declining.

The Geo Fire of 2006 was responsible for the destruction of numerous Joshua trees. However, tree numbers and vigor were already in decline in March of 2006 when the annual analysis was conducted. From December 1990 to March of 2006 tree numbers had declined from 44 to 36, an approximate decrease of 18%. Of those 36 trees 16 were considered to be enlarging, 15 were stable and 5 were declining.

This data indicates the population of *Yucca brevifolia* within the Queen Valley study site was declining in both numbers and vigor from 1990 to 2013. The Geo Fire intensified the rate of decline. The results compliment a twenty-year analysis of a Joshua tree population at Upper Covington Flat in the western portion of Joshua Tree National Park (Cornett, 2009). The population on the Upper Covington Flat site declined by a similar pre-fire percentage, 16%, in twenty years. Taken together these results may indicate a gradual decline in Joshua tree numbers and vigor within Joshua Tree National Park. Changes in climate associated with global warming may explain declines in Joshua tree populations at these two study sites (Cole et al., 2011).

I thank the Garden Club of the Desert and Joshua Tree National Park Association for providing financial support for this research.

Literature Cited

- Baldwin, G. G., D. H. Goldman, D. J. Keil, R. Patterson, T. J. Rosatti and D. H. Wilken, editors. 2012. *The Jepson manual: vascular plants of California, second edition*. University of California Press, Berkeley.
- Cole, K.L., K. Ironside, J. Eischeid, G. Garfin, P. B. Duffy and C. Toney. 2011. Past and ongoing shifts in Joshua tree distribution support future modeled range contraction. *Ecological Adaptations* 21(1):137-149.
- Cornett, J. W. 1999. *The Joshua Tree*. Nature Trails Press, Palm Springs, California.
- Cornett, J. W. 2009. Population Dynamics of the Joshua Tree (*Yucca brevifolia*): Twenty Year Analysis, Upper Covington Flat, Joshua Tree National Park. California State University, Desert Studies Consortium, Abstracts 2009 Desert Symposium.

Kelso Dunes mining claim validity examination

Gregg Wilkerson

Bureau of Land Management, Bakersfield Field Office

ABSTRACT—Platinum was reported to exist in economic concentrations in a portion of the Kelso Dunes, beginning in 1967. The mining claimant was Mineral Extractors, Inc. They located 846 placer mining claim over an area of 4,220 acres. Almost all of the Kelso Dunes geomorphic feature was included in this claim block. The Kelso Dunes were proposed for a Wilderness Study Area (WSA number COCA 250) and later withdrawn from mineral entry by Public Land Order (PLO) 5224 in 1972. Mineral Extractors, Inc. submitted a plan of operations (POO) to BLM which they named the “J&P Project” in 1989. As part of its review of that POO, BLM conducted a mining claim validity examination to determine if a discovery of a valuable mineral deposit had been made on any of the claims. This examination was conducted under authority of 43 Code of Federal Regulations, Sections 3802 and 3891. It was completed in February, 1992.

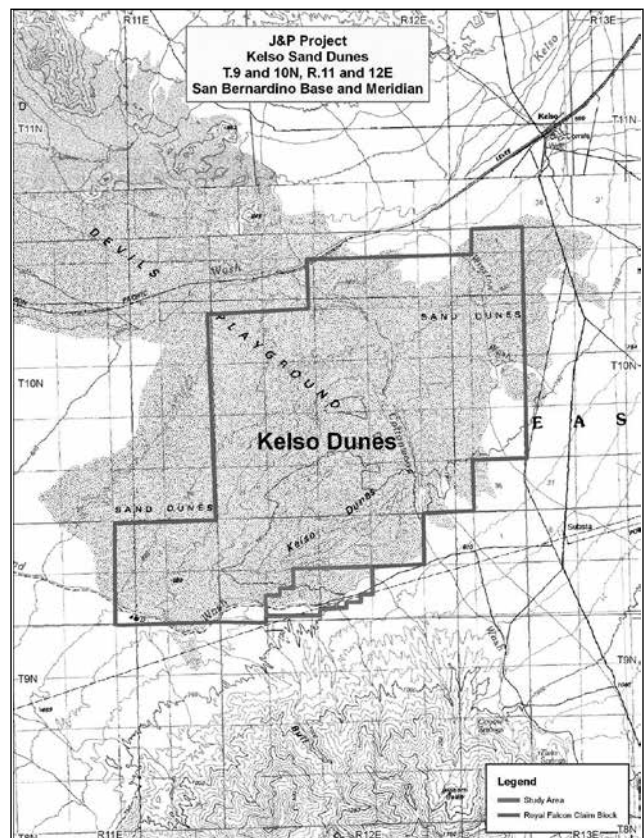
The geologic model for the platinum ore was wind-concentrated bands of black sand in sections of the Kelso sand dunes. Samples were collected from 42 Placer Mining Claims (PMCs) included in P&J’s POO. The concentrations of iron, titanium, gold, silver and Platinum Group Metals (PGMs) in these samples was evaluated using several methods and laboratories, including Bondar-Clegg Laboratories and the U.S. Bureau of Mines. The value of sand for iron oxide pigments was also evaluated. Dry magnetic mineral concentrates processed by the J&P Project plant contained no detectible PGMs and only traces of gold (0 to 0.00014 troy oz/ton Au). As a consequence of this determination, the POO for the J&P project was never approved by BLM.

Location and access

Kelso Dunes is a 52,000 acre dune field in the eastern Mojave Desert, some 35 miles south of Baker, California and roughly 50 miles west of the Nevada border. The Dunes make up the southeastern extent of a larger dune field known as the Devil’s Playground. The dune field is along the Mojave River Wash in a valley surrounded by the Granite Mountains to the south, the Providence Mountains to the east and the Kelso mountains to the north. To the west, the dune field is partially surrounded by the Bristol Mountains. Our study area is on the south margin of the Kelso Dunes adjacent to Devils Playground Wash.

Access to the site is from the east by a well graded dirt road that connects to the Kelbaker paved road. Art Parker, the claimant, often arrived at the mine site by a Beechcraft propjet or a small propeller driven light plane. The landing strip used is the widened west end of the dirt access road from the Kelbaker road. From the mine site, all travel into the sand dunes had to be by foot or, in the claimants situation by ORV or rubber tired loader, as they had grandfather rights/uses up to the time the claims were declared null and void in 1993.

Unless otherwise noted, all information in this article comes from the report by Evans and others, 1992.



Location map for the Kelso Dunes and the J&P Project.

Abbreviations

BLM = U.S. Bureau of Land Management
 CFR = Code of Federal Regulations
 IMP = Interim Management Plan
 PGM = Platinum Group Metals
 PLO = Public Land Order
 PMC = Placer Mining Claim
 POO = Plan of Operations
 WSA = Wilderness Study Area
 MEL = Mineral Extractors Inc.

Physiography

Kelso Dunes form peaks, hollows, and low ridges in a complex topography over 3,000 feet above sea level. Almost all the dune area is underlain by eolian sand, although some alluvial materials and igneous rock outcrops do occur. The taller dunes at Kelso are in three discontinuous east-northeast trending ridges, increasing in height to the south where peaks are several hundred feet above the other surrounding dunes. Hill 949 T is the tallest and largest dune in our study area, about four miles long and 550 feet high.

Throughout our study area there are many smaller traverse dunes which occur at lower elevations. Many of the transverse dunes have steep slip faces and broad rounded crests that curve downward before breaking off sharply. The morphology and geology of the dune field in our study area is typical of the lower slopes of the active dunes throughout the region. Within the subject area, as throughout the dune field, a combination of wind, vegetation, and moisture has produced various transverse dune forms. The southern part of our study area is marked by Devils Playground Wash. Most of the sand at Kelso Dunes was derived from western sources; however, some sand is derived from the mountains around the basin in which the Devil's Playground occurs.

Kelso Dunes comprise about 52,000 acres in the eastern Mojave Desert, some 35 miles south of Baker, California and roughly 50 miles west of the Nevada border. The dunes make up the southeastern extent of a larger, less prominent dune field known as the Devil's Playground. The dunes are in a valley surrounded by the Granite Mountains to the south, the Providence Mountains to the east and the Kelso Mountains to the north. To the west, the dune field is partially surrounded by the Bristol Mountains. Yeend and others (1984) suggest that the broad dune valley is a graben and the surrounding mountains are bound by displaced high-angle faults that resulted from Basin and Range deformation. Kelso Dunes is the most prominent dune field in the Mojave Desert and among the tallest dunes in the world. The age of the dunes is questionable. Yeend and other (1984) postulated that the dunes are likely to be 100,000 to 1 million years old.

Sharp (1966) has a more conservative estimate of several thousand to 20,000 years old.

Climate

Kelso Dunes and environs are in an arid climate with hot, dry, and windy summers, and cool and windy winters. Maximum rainfall is about 4.5 in/yr, minimum rainfall about 2.5 in/yr, and average rainfall about 3.5 in/yr. Temperatures range from around a low of 32°F in the winter to a high of at least 115°F in the summer. As the area is arid and windy the evaporation rate is high. Mild winds blow most every afternoon, but strong persistent winds from the northwest and west peak during spring and even during early fall. Wind velocities are not well known, but can blow from a few miles per hour to as much as 60 or more miles per hour. As Kelso Dunes is in a valley nearly surrounded by mountains the direction of winds must be irregular. The configuration and shape of the sand dunes provides strong evidence for crosswinds. Winds of only several miles per hour will cause movement of silt and very fine sand grains. During strong winds, blowing silt and sand become a real problem for workers and goggles are necessary. In spite of the vigorous arid climate a mineral operation was viable for most of any year.

History

The following historical summary is a compilation of information obtained from Art Parker in a Retrospective Summary J&P Project, and correspondence sent to BLM by Parker and his associates. It is not intended to be a complete history of the operation, but a summary of important events in the development of Mineral Extractor's property at Kelso Dunes.

Prior to 1967, the subject claims were owned by William Glass. In 1964, Mr. Glass made some initial contacts with Irimaru Company, Ltd., of Japan, who wished to purchase the iron concentrates contained within the dune sand. A preliminary report entitled "A Tentative Plan for Development of Kelso Placer Iron Deposit, California, U.S.A." was prepared by Anzaki of Irimaru in 1965. The report states that 230,000,000 tons of iron sand concentrate reserves, with an Fe content of 65%, were available for processing, at an initial investment of \$22,000,000.

Upon Mr. Glass's apparent failure to file assessment work affidavits for the subject claims in "1965 or 66", Bob Jernberg and Art Parker "adversely located" over Glass's locations and acquired ownership of the mining property. In 1967, Jernberg and Parker (J&P) developed a prototype sand plant to extract the magnetic fraction of the dune sands. Eriez Magnetics conducted initial testing, and determined that a 70% Fe product recovery was possible.

In the fall of 1967 and early in 1968, Mineral Extractors, Inc. (MEI) set up a prototype mine plant on the south side of the dunes to extract the magnetic black sands.

This plant was designed to produce 3,500 tons per day of black sand for a pig iron plant to be “located at Kelso.” The equipment to be utilized in the plant included a hopper, dryer, two Eriez magnetic separators, a conveyor, Cat, grader, front-end loader, four sand buggies, oil tank, and a single trailer. A watchman was hired and was present until the project was suspended in 1994.

During the spring of 1968 (Feb–June), the plant produced about 40 tons per day of black sand, operating from 8 and 16 hours per day. During the years 1968–1972 (according to assessment work affidavits), MEI constructed 26 miles of access roads, drilled a water well, conducted surveys, operated the mine, conducted core drilling, development, research, and feasibility studies. Parker states that in 1968, all of the equipment was moved off the dunes, except for the raw sand hopper and a portion of the dryer. In 1970, negotiations were underway to supply the “Hughes Corporation” with high grade iron ore for drill bit manufacture.

During the years 1972–1977, Sandia Metals, Ken Meadows, Valley Agri-Services, Metals Western, and Bonneville/Rockwell were testing the Kelso black sands, selling some of the “precious metal products” and working to improve precious metal recovery. MEI produced about 1,800 tons of black sand during this period. In 1972–73, MEI installed a bigger firebox which increased the plant capacity to 36–40 tons of black sand per two-shift day. In 1975, MEI acquired a big dryer, capable of drying enough sand to yield 350 tons of black sand per day. In 1976, the new dryer broke and was replaced. In 1977, the mine plant was moved to its present location, new feed and production hoppers were installed, and 2 additional conveyors were acquired. During this period, the water tank and 11-mile water line were installed.

The plant continued to operate from 1977–1981 “or 1982”, with one shift per day, off and on over a 7 to 8 month “season” each year. Production with the new dryer was about 4 tons of black sand per shift. The tailings were not returned to the dunes, but were “dumped” east of the current plant site.

Between 1982–1988, the plant produced only “test amounts”, for a total production of about 200 tons of black sand. In 1989–90, MEI returned to its 7–8 month, one shift per day, “season,” producing about 300 tons of black sand.

Historic grandfathered uses

Under 43 United States Code (U.S.C.) 1782(c) of the Federal Land Policy and Management Act of 1976 (FLPMA), as guided by the BLM Interim Management and Policy Guidelines (IMP), the BLM should not allow any activity to impair the wilderness characteristics of the Kelso Dunes Wilderness Study Area (WSA), unless activities are continuing in the same manner and degree as were occurring on October 21, 1976 (passage of the FLPMA). These activities have been called grandfathered uses by the BLM. At the time, an analysis (Environmental

Assessment) was made by BLM and the conclusion reached that

The operator’s (Parker and others) level of activity to date, appears to be a logical progression of activity since the passage of the FLPMA as provided at I.B.6. of the IMP, and is consistent with the manner and degree clause in section 603(c) of the FLPMA, and therefore, the requirements of the IMP have been met.

Mineral Extractors Inc. had filed a timely vested rights reclamation petition with San Bernardino County under the California State Surface Mine and Reclamation Act (SMARA1). The county approved MEL’s reclamation plan and vested the operation at 4 tons of magnetic concentrate per day. MEL claimed valid existing rights to impair the WSA in the conduct of their proposed operations. But the BLM had not verified “grandfathered uses” to support continuation of existing levels of operation, or logical progression under the “manner and degree” criteria to support proposed operations. Under the procedures in place at the time, the Plan of Operations was to be reviewed under the IMP as a result of valid rights rather than grandfathered uses because the right to mine in the area segregated from the mining laws by the WSA was contingent primarily on whether the mining claims are valid. Hence there arose a need for BLM to conduct a mining claim validity examination.

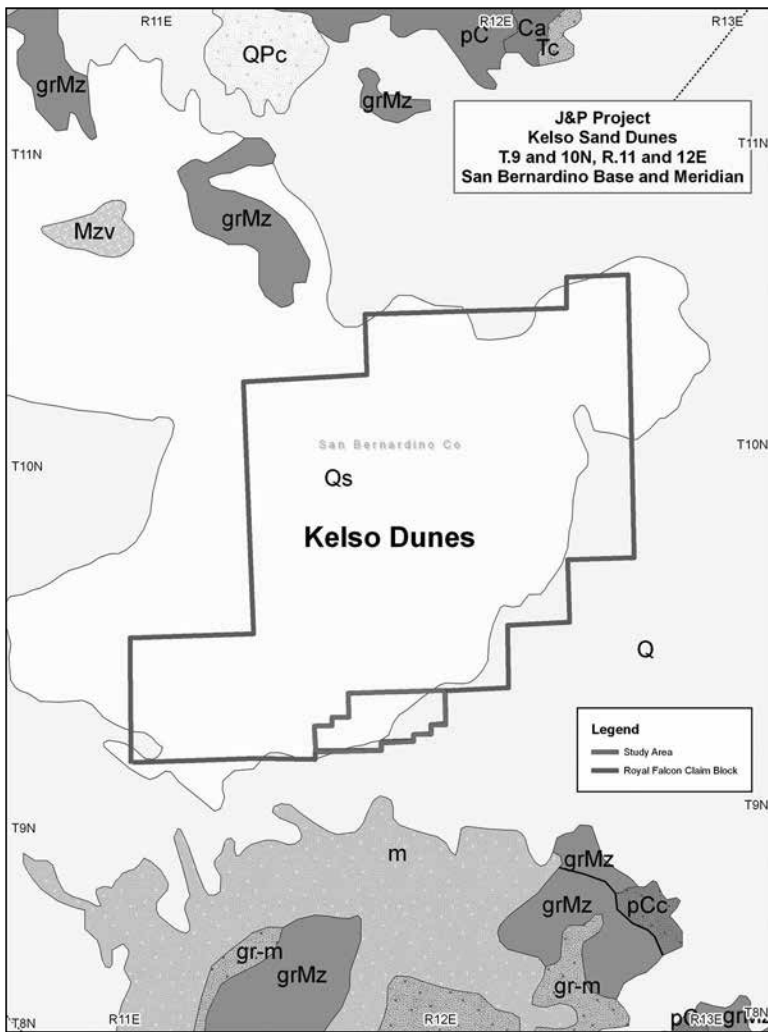
The Bureau did recognize a certain level of grandfathered activity did exist for the purpose of evaluating the environmental impacts from the BLM sampling program. This was addressed through an Environmental Assessment (EA). That analysis basically stated that the level of activity in the BLM-proposed in-sampling program for the examination of the property was much less than those which Mineral Extractors had been conducting since October 21, 1976, the date of passage of the FLPMA.

Geology

Kelso Dunes is made up of a complex topography of peaks, hollows and low ridges that surround four larger ridges. Dunes are made up almost entirely of eolian sand. Yeend and others (1984) identified six separate geologic units at Kelso Dunes. The geologic units that are described below are very similar to the units described by Yeend and others (1984) with the exception of some minor unit boundary changes which can be seen in Map M-2. There is only one general area throughout the entire dune field where all of the units are exposed. The area is in the southeast corner of the dunes near Cottonwood Wash (See Map M-2). Below are descriptions of the units throughout Kelso Dunes which are separated into Igneous, Eolian, and Alluvial units.

Igneous Rock Units

The oldest and the stratigraphically lowest unit in the map area is granodiorite (Tg). This unit has only two visual



Geologic map of the Kelso dunes. Q = quaternary sediments, Qs = Quaternary sand, grMz = Mesozoic granite, QPc = Quaternary-Pliocene conglomerate, pC = Precambrian metamorphic, Ca = Carboniferous andesite, Tc = Tertiary conglomerate, MZv = Mesozoic volcanic, gr-m = undifferentiated granite and metamorphic. pCc = PreCambrian conglomerate.

The **Sand Sheet** unit (Os) is stratigraphically the lowest of the eolian units. It consists of coarse to fine grained, 3- to 6-foot sheets of predominately quartz-rich eolian sand. The sand grains are moderate to well sorted and well rounded. The unit is exposed on the surface along the western half and the north-east portion of the mapped area (see Map M-2). Vegetative cover is moderate to heavy and most plentiful along Cottonwood Wash and the lower elevations because of higher moisture.

Stratigraphically above the sand sheet unit is the **Stable Dunes** unit (Osd). This unit consists of medium to fine grained predominately quartz sand. The sand grains are well sorted and well rounded. Vegetative cover is medium to heavy and is scattered throughout the unit as large grass patches (see Plate P-2, C). The stable dunes unit extends from the center to the eastern boundary of the mapped area (see Map M-2).

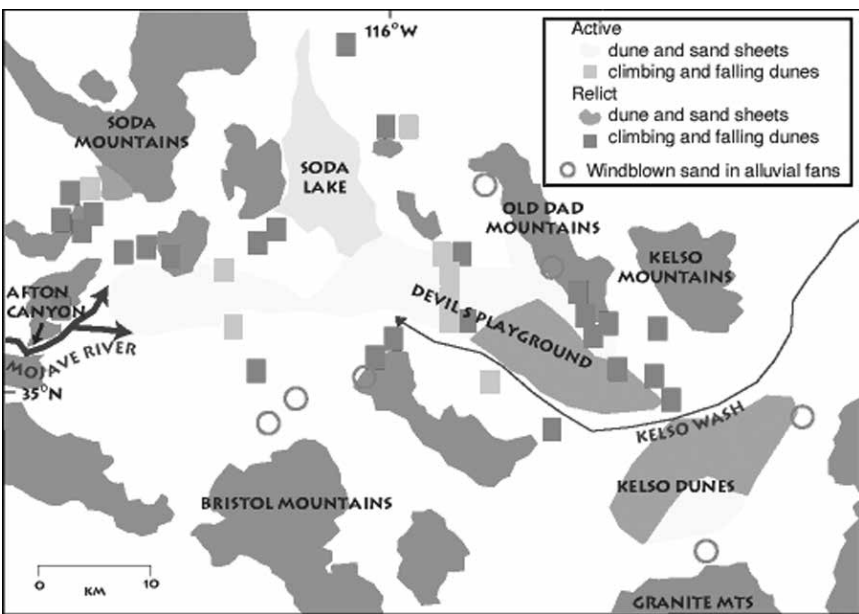
The highest stratigraphic unit throughout the dune field is the **Active Dunes** (Oad). This unit consists of very fine grained predominately quartz sand. There are several distinct dune forms throughout the active dunes. The dune forms include domes, barchans and traverse dunes and can be identified from great distances (see Plates P-2, A-C; P-3, A). The major differences between the active dunes (Oad) and the other two eolian units (Osd and Os) is that the active dunes have less vegetation, due to the continuous movement or migration of sand grains. Locally, heavier black sand grains are seen at the surface of

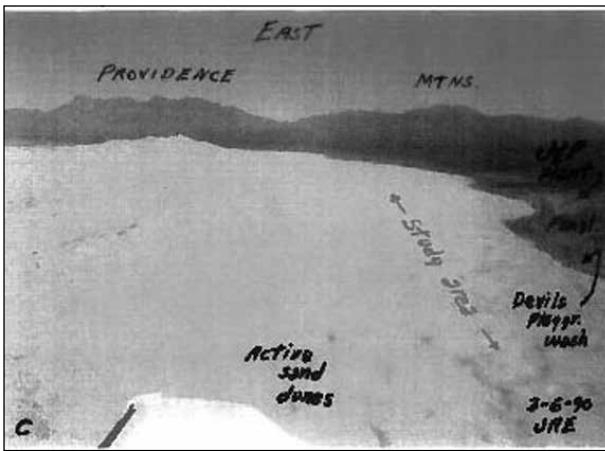
surface exposures. The two exposures are in the form of small knobs located just east of Cottonwood Wash (see M-2).

Eolian Units

Three eolian units were identified throughout the dune field. The units appear in the form of broad flat sand sheets (Os), vegetative supported sand dunes (Osd), and active sand dunes (Oad).

Sand types in the Kelso Dunes. From U.S. Geological Survey <http://geomaps.wr.usgs.gov/parks/mojave/kelsomap.html>, adapted from Lancaster, N., 1995, Kelso Dunes, in Reynolds, R.E. and Reynolds, J., ed., Ancient Surfaces of the East Mojave Desert: San Bernardino County Museum Association, p.47-51.





Aerial photograph of study area. View is to the east, toward the Providence Mountains.

the Oad dunes because the lighter quartz grains have been blown away from the area.

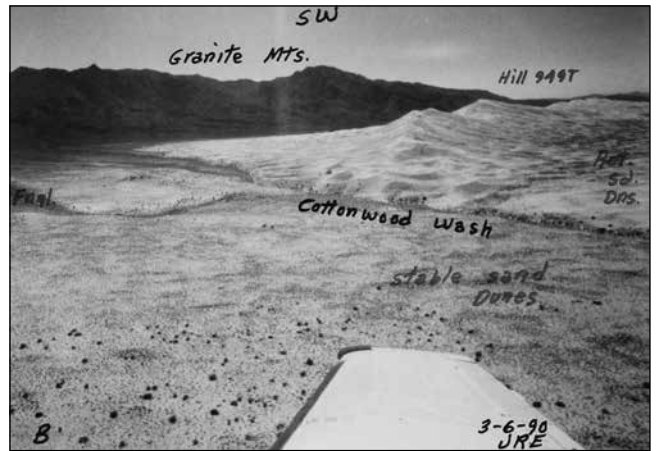
Alluvial Units

There are two alluvial units in the mapped area. The older of the two units is a fanglomerate/alluvial fan (Of). This unit is stratigraphically lower than the eolian units described above. The fanglomerate consists of sand, gravel and boulder sized igneous rock fragments that originated from the surrounding mountain ranges. Moderate to heavy vegetation is associated with the unit (see Plate P-2, 8 & C). It is exposed at the surface along the northeast and southeast boundaries of the mapped region (see M-2). The other alluvial unit (Qal) is found mainly along the modern drainages within the dune field (Map M-2). The material ranges from sand to gravel size and is mostly well rounded and poorly sorted. In some areas, boulder sized material is present. There are several modern drainages throughout the region. The drainages are easily recognized because of the heavy vegetation that fills them (See Plate P-2, 8&C).

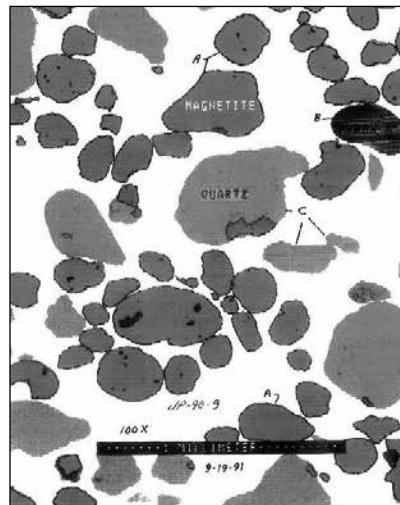
Sampling and sample processing

It was clear from the start of the J&P project that the magnetic mineral fraction of the dune sand was only a small portion of the dune sand itself and that the fraction could vary over distance by significant amounts. Therefore bulk properties of the dune sand were measured for weight, volume, moisture, swell, mineralogy, and grain textures and sizes. There was a possible precious metal content in the magnetite fraction which was mostly magnetite. The high iron environment required special consideration for selection of any analytical testing method.

Twenty-two bulk samples were taken from the PMC corners and central PMC areas of the claims included in Parker's POO. Samples were collected from the top 3 feet of sand with Parker's rubber tired Cat 966C front end loader. The Plan of Development called for mining only the top three feet of sand. The Kelso Dune sands contain discontinuous zones of high magnetic concentrations, interspersed with zones of low magnetic mineral



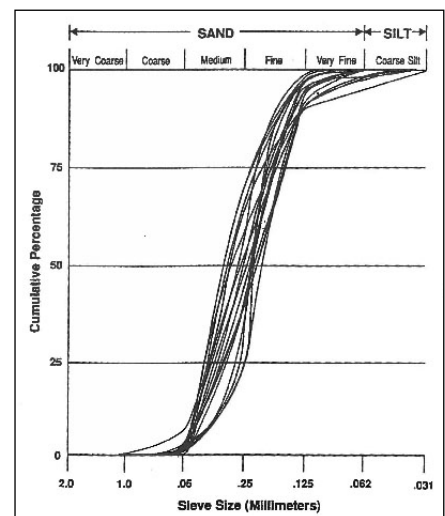
Aerial photograph of the Kelso Dunes. View is to the southwest, toward the Granite Mountains. Hill 949T is in the top left. Cottonwood Wash separates active sand dunes to the upper right from stable sand dunes on the lower left.



Drawing of a scanning electron microscope image of sand grains in BLM sample JP-90-9. The image was taken with a JEOL JSM-T300 scanning microscope. Image is courtesy of J.J. Sjoberg, Bureau of Mines, Reno, Nevada. A= magnetite and ilmenite, B= CA-Fe silicates, C= quartz and plagioclase.

concentrations. The zones vary in areal extent and depth. A bulk front end loader was used for sampling in the order to obtain at least 2 cubic yards per sample to account for zonations in the material. The bulk sampling also was representative of the low percentage of magnetic concentrate in the dune sands. In addition, this sampling method reflected the historic mining practice used by Parker.

A summary of the bulk physical testing follows:



Sorting curves for natural dune sand samples from the Kelso dunes.

- Smoothed over Cat 966C wheel loader bucket content is 2.36 cubic yards
- Dry dune sand weighs 106 pounds per cubic foot
- Dry dune sand weights 2,862 pounds per cubic yards
- Dry dune sand weighs 1.43 tons per cubic yard
- An 85 gallon steel drum of magnetite concentrate weighs about one-ton
- Moisture content of the upper 3 feet of dune sand was from 0.21 to 3.46 percent
- Percent moisture averaged 1.60 percent
- Swell factor for damp sand in the top 3 feet of dune sand is 10 percent
- Wheel loader bucket contents are 2.15 cubic yards of dry sand
- Wheel loader bucket content of dry sand is 3 tons (6,000 pounds)

After determining bulk physical properties our next step was to process bulk samples through a magnetic separation process to simulate Parker's plant processing procedures. To do that, BLM mineral examiners used the Parker plant as the testing laboratory for their study.

BLM plant test for processing magnetic concentrate

During plant sample testing, the first-stage magnetic separator (25 pole unit) was used. The magnetic concentrates were removed directly by hand, through a small door at the base of the separator unit. Bulk processed sand was discharged by conveyor to the tailings pile for return to the mine site. The magnetic concentrates were subsequently weighed, analyzed for mineral character and grain size, and sealed for assay.

The plant was able to process 6,000 pounds of bulk sand in an average of 16 minutes. Sample throughput times varied from about 11 minutes to about 20 minutes. Sample throughput times represent the capacity of the current, in-place system, to process sand from the subject deposit. The system throughput capacity is fixed, adjustable only through the drying circuit. Samples were taken in mid-summer, and probably represent the median for moisture content, a critical factor in throughput time.

Weight of magnetic concentrates

Just as throughout the entire dune field, black sand is visible at the surface in the J&P project area, and most visible in the active dune unit. It is mainly concentrated along the windward side of the dunes ridges. Weight of black sand concentrate recovered from each BLM sample varied significantly. Weights ranged from 20.92 to 182.85 pounds. Of the 22 samples collected, 12 samples were from 25 to 50 lbs, three samples from 51 to 75 lbs, five samples from 76 to 100 lbs, one sample from 101 to 125 lbs, and one sample from 176 to 200 lbs. In terms of percent concentrate, 13 samples had less than 1

percent concentrate; eight samples had between 1 and 2 percent, and one sample had over 3 percent. Weight per unit volume of the magnetic concentrate from the BLM samples ranged from 1.93 tons per cubic yard to 2.32 tons per cubic yard.

On microscopic analysis of the magnetic concentrate, it was noted that many grains of the magnetic concentrates are attached to other grains, mainly quartz and feldspar. Because these grains are connected they become part of the magnetic concentrate and are recovered by magnetic separation, reducing the sample weight per unit volume.

Magnetic concentrate mineralogy

Scanning electron microscopic observation of the magnetic concentrates showed that from about 58 to 80 percent is magnetite, 10 to 15 percent quartz, 10 to 15 percent feldspar, and about 5 to 8 percent ilmenite, sphene, hornblende, garnet, apatite, pyroxenes, rutile, and epidote.

Magnetic concentrate texture

Sieve analysis showed that the size of the grains of magnetic concentrate ranged from 0.05 to 0.0625 mm (medium to very fine). The majority of the grains was magnetite and passed through the 0.250 screen and remained on the 0.125 screen (fine sand). Concentrates were very well sorted with grains well rounded to subrounded. Grains are spherical to sub-prismoidal in shape. All magnetite grains are rounded to well rounded.

Analytical testing and results

Bondar-Clegg, Inc. testing for the BLM

A split for each of the 22 magnetic concentrate samples stored in the BLM Folsom Minerals Lab was made in that lab on August 22, 1990, by J.R. Evans. Results from the testing by Bondar-Clegg showed no platinum group elements or gold above 0.002 troy ounces per ton (detection limits) in the magnetic concentrate.

Chemical testing of magnetic concentrates through the J & P staff for themselves

On several occasions, Art Parker had told J.R. Evans that "standard assayers with standard methods cannot determine PGM in my magnetic concentrates". Parker also told BLM staff that his own customized assay methods would work, but that they were confidential.

The confidential methods were investigated in 1990 and 1991 when BLM staff visited Parker's laboratory and the laboratory of his assayer, AST lab of Scottsdale Arizona. The owner of AST labs was Siegfried Bremer. Parker's procedures involved a smelting method and an acid-resin-fire assay method. Bremer described his assay theory and methods for determination of the precious metals (PGM) and precious metal elements (PGE), or "clusters" as he called them. Bremer said he could detect both PGM and PGE using his assay methods, but contended this does not necessarily mean that standard assays will show the presence of PGE, or that they are

commercially recoverable. He also said that if PGM were present, they should be detectable by fire assay, Atomic Absorption (AA), or induced coupled polarization (ICP) methods. However, according to Bremer's assay theory, these standard methods would only work if the PGE's are broken from their "molecular" or "cluster" bond to a metallic bond before they are detectable by standard assay methods. Bremer indicated that if he identified PGM, then BLM should also be able to detect them. However, any PGE which are not in metallic or ionic bonds, but rather "molecular" bonds, must be broken down to atoms (metal) before they are detectable by normal analytical means. He said the way to break down the "molecules" is by means of the vacuum electron beam furnace. He uses a furnace of Lleibold (Company of Degussa Corp.) in Hanover, Germany.

Bremer discussed briefly his spectrophotometric methods. He used one or half-ton fire assay preparation with the same fluxes as recommended by Beamish (1977) for iron ore. Bremer takes the lead button from the fusion and runs a portion of it at high voltage spark for PGM. For PGE, the lead button, or a part of it is run in the DC Arc Plasma on the spectrograph.

Chemical testing of magnetic concentrate through the Bureau of Mines for the BLM

To verify the Parker/Bremer assay process, on August 23, 1990, Evans and Waiwood took three samples to Ken G. Broadhead, Bureau of Mines, Reno. These samples had been collected at Parker's Twentynine Palms lab during their visit to observe Henderson's procedures in July 1990.

Sample #1, iron matte (Y2 square inch ±); broken off a large dinner plate sized iron billet made by Parker in an induction furnace in his lab at Twentynine Palms; collected 7-30-90. Parker indicated these plates contained PGM.

Sample #2, gold-bearing residue from nitric acid processing; collected 7-31-90.

Sample #3, gold fragment (100 microns) in residue from sample #2; collected 7-31-90

No PGM were detected in #1 above. Numbers 2 and 3 were not tested for PGM because no PGM were considered to be present after Henderson's processing.

On January 23, 1991, in the BLM Minerals lab at Folsom, California, Evans packaged a random scoop sample of magnetic concentrates from each of the 22 samples collected by the BLM during June, 1990. On January 24, 1991, Evans took the samples to K.G. Broadhead at the Bureau of Mines lab in Reno. The Bureau determined bulk density for all samples, mineralogy for JP-90-5 and 5A, PGM and gold for all samples, result of assay using copper as a collector for PGM, and a sample assay run with a known amount of platinum. Results of the Bureau of Mines tests are summarized below:

1. There was a significant variance in bulk density as a result of various quartz and feldspar content. Fibrous material (burnt organic matter) was present in all samples. In mining only the top three feet of sand, a certain amount of grass and vegetation is to be expected in the samples.
2. Upon one-half ton fire assay preparation with ICP finish, no platinum, palladium, or rhodium was found to be present at detection limits of the analytical process (0.003 troy ounce per ton).
3. Recovery was excellent for known amounts of platinum introduced as a standard.
4. The copper collector test was disappointing and inconclusive. High copper content of the HN03 solution could not be run because of background interference.

On April 19, 1991, Evans went to the Bureau of Mines Reno lab to meet with Ken Broadhead where the April 11 and 12, 1991, trip to Bremer's AST lab in Scottsdale, AZ, and future PGM testing was discussed. Evans left a cut piece of the copper-iron bar from sample JP-90-11 and a cut piece of the lead "bar" from sample JP-0-5A~ for appropriate PGM tests. These bars were developed during the BLM trip to Parker slab on April 8 and 9, 1991.

No gold or PGM were detected in any of the materials described above. Copper-iron bars, such as the one developed from BLM sample JP-90-11, are said to be marketable by Parker, along with magnetic concentrates. Because of the statement, a polished surface of the JP-90-11 bar was examined carefully by scanning electron microscope even though no PGM were detected by ICP analysis of the copper and iron zones.

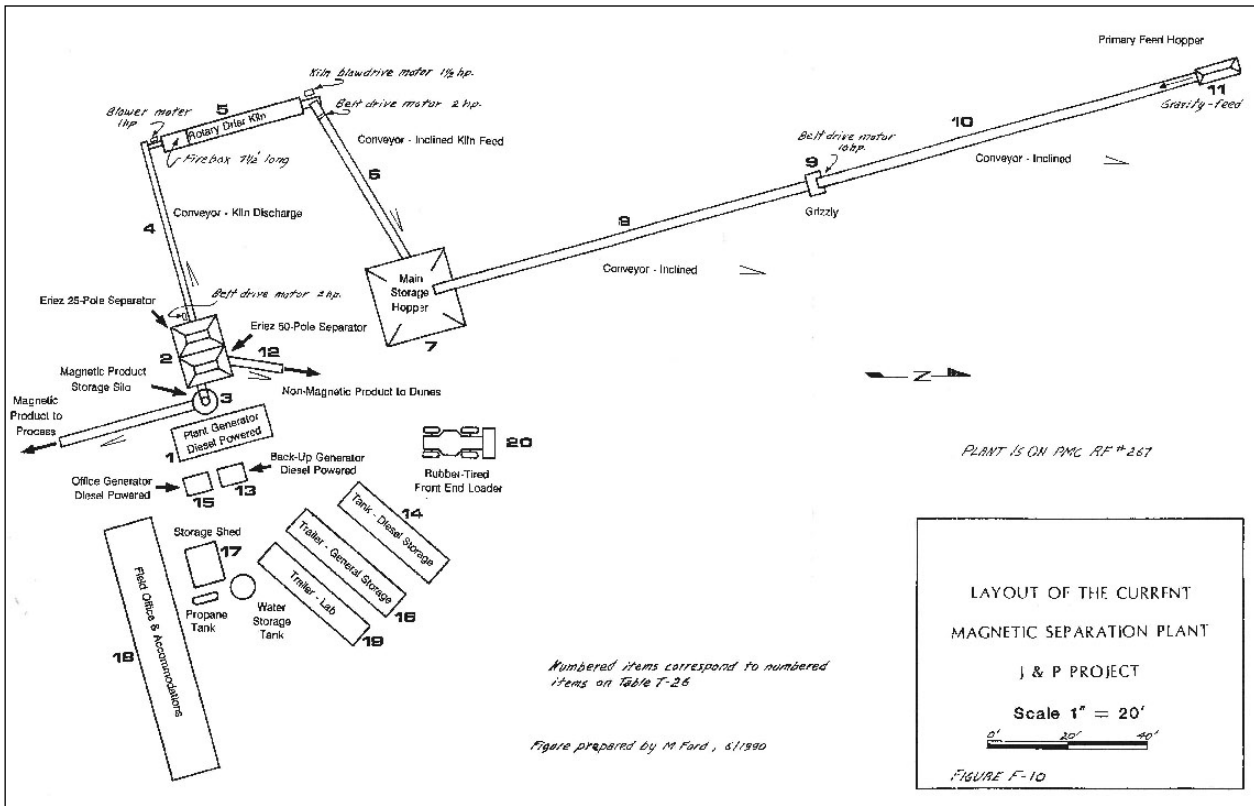
Four metals phases were identified. Copper phase A was most abundant because of the copper added during fluxing of the 5-assay ton sample. No PGM spectra or phases were detected during the microscopic examination.

Parker's mining and plant processing procedures

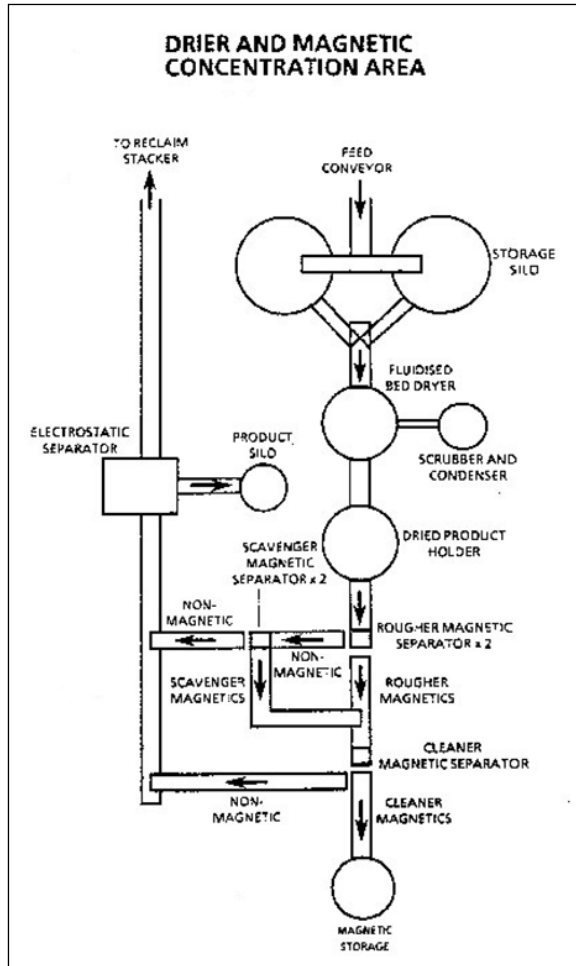
The J&P processing plant was located on the southern margin of Kelso Dunes, approximately 8.8 airline miles south-southwest of Kelso Train Depot. The J&P plant used a magnetic concentration process to extract magnetic minerals from bulk placer sand dune deposits.

The mine plant consisted of a primary feed hopper, conveyor system, grizzly, main storage hopper, rotary drier kiln, two-stage magnetic separator unit, and a magnetic product storage silo. Material from the top 3 feet of sand was delivered to the plant by a rubber tired front-end loader, Cat 966C, using a 3 cubic yard bucket.. The loader operator mined sand from dunes in close proximity to the processing plant, typically within a radius of 2,000 feet.

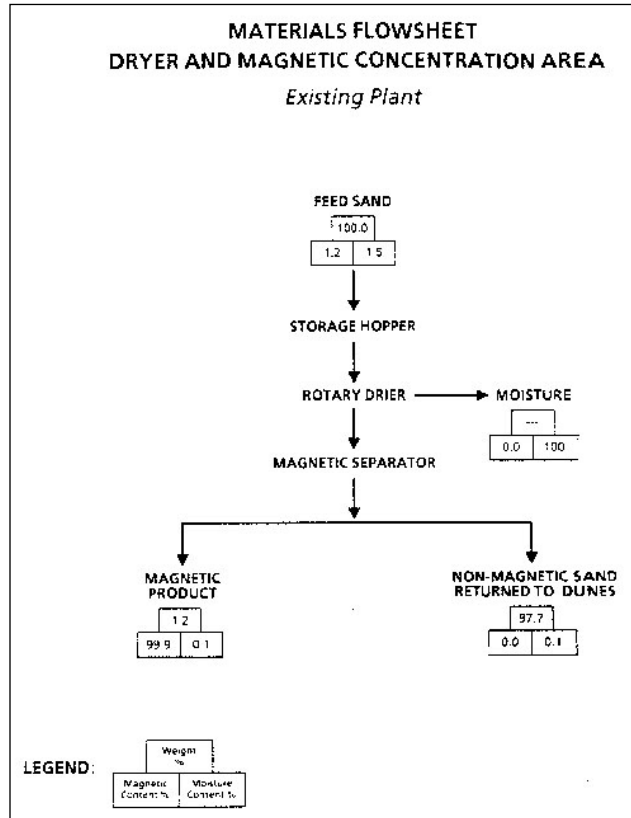
The front-end loader was driven to the mining area to load the bulk sand independently, then transported the material to the plant for processing. At the plant, sand was



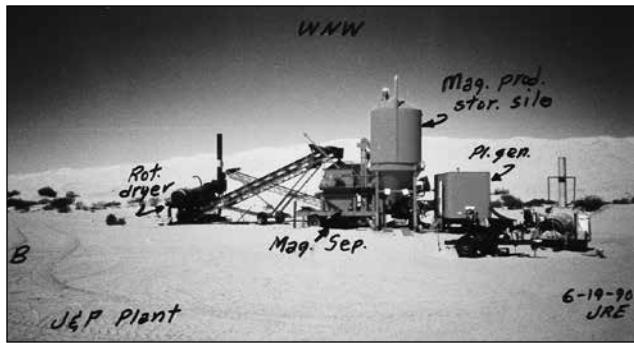
Schematic of the separation plant layout.



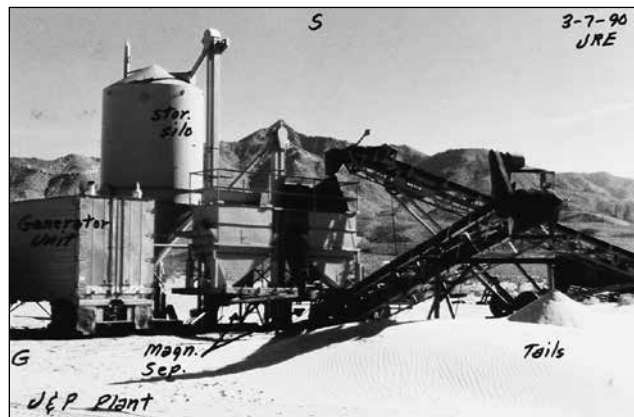
Schematic of the dryer and magnetic concentrator configuration.



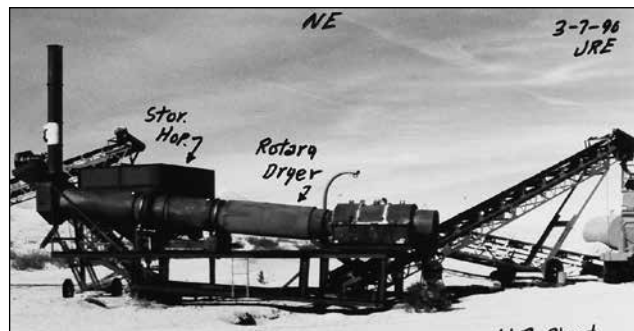
Material flow sheet for dryer and magnetic concentrator.



J.P. Project processing plant showing rotary drier, magnetic separation unit, and magnetic concentrate storage silo. Photo taken 6/19/1990 by J. R. Evans.



J.P. Project processing plant, showing conveyors, magnetic separation unit, and magnetic concentrate storage silo and generator unit. Photo taken 3/7/1990 by J.R. Evans.



J.P. Project processing plant rotary drier.

dumped into the primary feed hopper for direct feed onto the conveyor system. The material then passed through a minus one-inch grizzly, which separated the wood, plant material, and cow chips from the sand. The cleaned sand was carried by conveyor to the main storage hopper for through-feed by conveyor into the rotary drier kiln. Upon entering the kiln, the material was heated to 150 degrees to dry the sand and possibly increase its magnetic attraction. The dried material was transported by conveyor from the rotary drier kiln through a star feeder, and into a two-stage Eriez magnetic separation unit.

The first-stage separator, Eriez Model D.F.H. 25, contained a 25 pole Hi Speed magnetic drum concentrator which is intended to separate pure magnetite grains

from the bulk sand at 800 to 10,000 gauss. This stage was designed to recover 95% of the contained magnetite along with magnetite locked in silica and ilmenite grains and ferro-titanium minerals. This unit operated at drum peripheral speed of 800 feet per minute.

The second-stage separator, Eriez Model D.F.H. 50, contained a 50 pole Hi Speed magnetic drum concentrator which was intended to separate clean magnetite from the sand. It produced a high grade concentrate low in silica and titania. This stage was designed to operate at 12,000 foot per minute drum speed to obtain increased "magnetic agitation" and pronounced centrifugal force for maximum rejection of the iron-bearing silica and ilmenite particles which were not as magnetic.

After the bulk sand was processed through the magnetic separator unit, the tailings were discharged by conveyor to a tailings pile, for eventual return to the mine site. The magnetic material was typically transferred by elevator from the two-stage magnetic separator unit into the magnetic product storage silo.

Reclamation and environmental mitigation costs

In order to ensure that reclamation and environmental mitigation considerations and costs were considered as part of the economic analysis of the claims, a separate reclamation and environmental costs (REC) analysis was made. For the J&P Project, reclamation and environmental costs included the cost to provide any compensation for the loss of habitat for the Desert Tortoise (if the tortoise were to be affected by the operation), a species that had, in 1991, been placed on the threatened species list by the United States Fish and Wildlife Service. Additional REC costs included the costs to assure adequate reclamation of the access road, mine plant site, and disturbed dune areas.

Gold and PGM resources

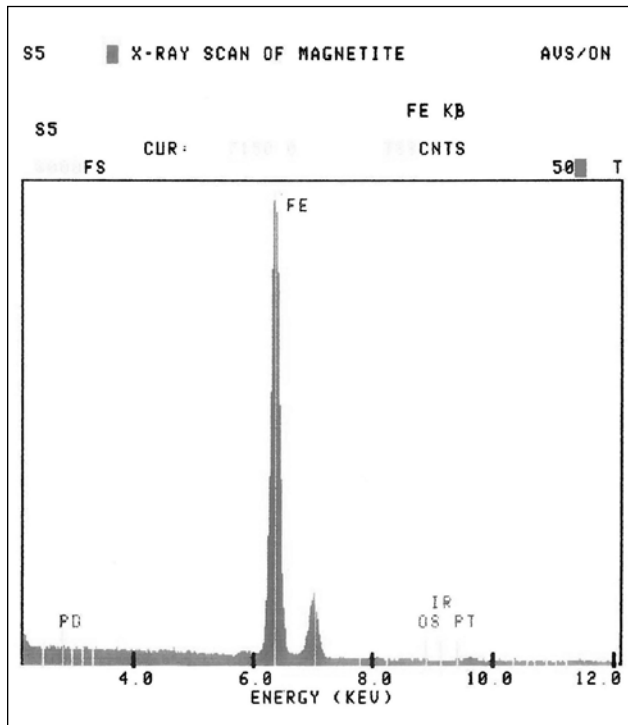
For purposes of BLM's investigation, gold and PGM resources on the J&P claim block were those that can be developed from magnetic concentrates processed through the J&P Project plant. Any gold or PGM that might be recovered by wet-gravity separation was not considered. BLM staff did not make any tests for free gold or PGMs. Presence of free PGM in the Kelso Dune sand is highly unlikely. Free gold in very minor amounts does occur in the region surrounding the J&P claim block according to the Bureau of Mines. In 1982 they sampled from an area about 750 ft. north of the J&P Project plant. Nine samples weighing from 9 to 17.5 pounds were taken at about equal distances along a line 400 ft. west of the 750 ft. point (see Munts, 1983, location map, p.51). A wet-gravity separation using a Wilfley table in a laboratory environment was made of pulverized materials crushed from these samples. Samples showed from zero to 0.00014 troy ounce per ton free gold, and from about one-tenth to one percent of

magnetic concentrates (Munts, 1983, Tables 3 and 5, p. 53 and 59).

About 250 ft. east of the 750 ft. point, a pit was dug and 24 grid samples of several pounds each were taken from about 3 feet of damp sand. They were also separated by wet-gravity means. The magnetic fraction was from about 3 to 13 grams. Free gold was from zero to as much as 285 milligrams. Most of the gold fraction was below 25 milligrams (see Muntz, 1983, Figures 9 and 10, p. 47 and 48). Sample weight fractions for both magnetic concentrates and free gold varied widely, laterally and vertically. Parker has said from the beginning of this study that real PGM and gold values were in the magnetic concentrate portion of the dune sand, specifically within the magnetite itself. Testing done for BLM by Bondar-Clegg, Inc., and the Bureau of Mines Research laboratory at Reno, Nevada. These analytical studies showed no detectable PGM or gold in the samples BLM or Bureau of Mines staffs collected. Parker had always claimed that the methods he used or subscribed to are the only way to detect PGM in the Kelso Dune sands. BLM staff could not accept Parker's thesis and arrived at the conclusion that the magnetic concentrate and copper-iron bars that Parker indicated he could market for PGM do not contain either PGM or gold. Therefore, the BLM mineral examiners concluded that no gold or platinum resources occur in the magnetic concentrate of the Kelso Dunes sand.

Conclusions and recommendations

Iron resources, gold, and platinum group elements were not found within the limits of the Placer Mining Claims



X-ray scan of a magnetite grain from the Kelso Dunes collected from BLML sample JP-90-9. There are no Platinum Group Metal lines in the spectra.

(PMC's) investigated by BLM in sufficient quantities and/or qualities to constitute a discovery of a valuable mineral deposit.

As no discovery was found to exist on any of the PMC's in the Parker claim block, all 10-acre tracts were classified by BLM as non-mineral in character. BLM staff recommended that a contest complaint be initiated against the PMCs.

Hearing and appeals

The technical investigation of the Parker PMC's led the California State Office of BLM to determine that the Hope #86 to #89, Jemberg #37 to #50 and Royal Falcon #231 to #279 placer mining claims invalid for want of discovery of a valuable mineral deposit. Upon being informed of BLM's decision, the claimants appealed it. The Chief of Adjudication and Records, Robert Naurt, issued a complaint on April 16, 1992. It became Contest number CACA 29673-B. The hearing judge for this complaint agreed with BLM and declared the mining claims BLM staff had examined to be null and void for want of a discovery of a valuable mineral deposit. The hearing judge was not impressed by the claimants "black box" methods of processing the black sands to recover PGMs.

This judicial action voided the claims in the study area (red in location map) and the J&P operation plant was subsequently dismantled in 1993.

But there were hundreds of claims outside the study area in the Royal Falcon claim block (blue on the location map). The claimants continued to pay maintenance fees on their claims for six more years. In 1999 the claimants failed to do assessment under a small miner's waiver or pay the maintenance fees. The fee was \$100 per claim, so holding hundreds of them meant they were paying thousands of dollars a year, and getting nothing in return. By 1999 the California Desert Protection Act of 1994 was being implemented, and the prospects for them getting a permit to mine was dimmer than ever. So the Kelso Dune platinum project a project that began in 1967, came to a slow end.

The Kelso Dunes platinum project legacy

The effect of the Kelso Dunes J&P project was to galvanize anti-mining feelings during development of the California Desert Plan and during debates for what became the California Desert Protection Act of 1994. Even though BLM eventually found the J&P project claims to be invalid, the possibility that a mining operation on the Kelso Dunes *might* be permitted caused several angry articles to be written in Southern California newspapers. Many thousands of other mines and mineral collecting sites in the California Desert District were also closed by the 1994 legislation. In part that was because of fears that J&P-like projects *might* be approved in those other areas.

Selected references

- Ammen, C.W., 1984, Recovery and refining of precious metals: Van Norstrand Reinhold Co., New York, 328 p.
- Analytical Chemistry of the platinum-group metals (symposium), 1972: Journal of the South African Chemical Institute, vol. 25, no. 3, p. 155-319 (multiple authors and titles).
- Anzaki, T., January, 1967, A tentative plan for development of Kelso placer iron deposits, California, U.S.A., Technical Advisor, Irimaru Co., Ltd., Tokyo, Japan, 24 pp.
- Anzaki, T., December, 1965, A tentative plan for development of Kelso placer iron deposits, California, U.S.A., Technical Advisor, Irimaru Co., Ltd., Tokyo, Japan, 24 pp.
- Baba, Suresh P., and Leonard, Joseph W., 198~, Coal; in SME Mineral Processing Handbook, N.L. Weiss, Ed., Society of Mining Engineers, AIME, New York, N.Y, Table 2, pp. 25-2.
- Baglin, E.G., Gomes, J.M., Carnahan, T.G., and Snider, J.M., 1985, Recovery of platinum, palladium, and gold from Stillwater complex floatation concentrate by roasting-leaching procedure: Bureau of Mines Report of Investigation RI 8970, 12 p
- Barker, J.C., Thomas, D.L., and Hawkins, D.B., 1985, Analysis of sampling variance from certain platinum and palladium deposits in Alaska: Bureau of Mines Report of Investigation RI 8948, 26 p.
- Barry, W.L., 1982, Bureau of Mines practice in fire assaying-Reno Research Center, Reno, NV: Bureau of Mines Open File Report OPR 130-82,18 p.
- Beamish, F.E., and Van Loon, J.C., 1977, Analysis of noble metals; Academic Press, New York, NY, 327 p.
- Benbow, John, Iron oxide pigments: Construction adds a touch of colour, in Industrial Minerals, March, 1989, pp 21-41.
- Bennet, R.L., 1985, Iron ore: Characteristics of iron ore and agglomerates as related to furnace use; in SME Mineral Processing Handbook, N.L. Weiss, Ed., Society of Mining Engineers, AIME, New York, N.Y, pp. 20-2 to 20-4.
- Brown, Erwin C., 1973, Pigments and Fillers, in United States Mineral Resources, U.S. Geological Survey, Professional Paper 870, pp. 527-536.
- Bugbee, E.E., 1940, A textbook of fire assaying, 3rd ed.: Colorado School of Mines Press, Golden Colo., 314 p.
- Carmichael, Robert S., Ed., 1989, Practical handbook of physical properties of rocks and minerals; magnetic properties of minerals and rocks, CRC Press, Inc., Boca Raton, Florida, Section IV, pp.299-358.
- Clark, William B., June 1970, Platinum: California Division of Mines, Mineral Information Service, p. 115-122.
- Cousens, D.R., French, D.H., Ramsden, A.R., Griffin, W.L., Ryan, C.G., and Sie, S.H., February 1989, Application of the proton microprobe to the partitioning of platinum group elements in sulfide and oxide phases: Minpet 89, Mineralogy-Petrology Symposium, The Australian Institute of Mining and Metallurgy, Sydney, NSW, Australia, p. 45-49.
- Das Sarma, B., Sen, B.N., and Chowdhury, A.N., 1966, Studies on geochemistry of platinum: Economic Geology, vol. 61, p. 592-597.
- Dikeou, James T., 1980, Cement in: Mineral Facts and Problems, U.S. Bureau of Mines, Bulletin 671, pp. 148, 150.
- Entrekin, C.H., and Clarkson, D.S., June 1986, EB refining promises super clean metal production, Met. Prog., vol. 129, no. 7, p. 35-39.
- Evans, James R., R.M, Waiwood, M. Leverette, and M. Ford, 1992, Valid Existing Rights Determination (VERD) for 42 Placer Mining Claims of Mineral Extractors, Inc (J&P Project), Kelso Dunes, San Bernardino County, California. Mineral Report on file with the Bureau of Land Management, California Desert District, Moreno Valley, California.
- Folk, R.L., 1974, Petrology of sedimentary rocks; Hemphill Publishing, Austin, TX., 78703, 178 p.
- Frye, Keith, 1981, Encyclopedia of earth sciences, Volume IVB: The Encyclopedia of Mineralogy, Hutchinson Ross Publishing Company, Strousberg, Penna., page 662.
- Ginzburg, S.J., Ezerskaya, N.A., Prokof'eva, I.V., Fedorenko, N.V., Shlenskaya, V.I., and Bel'skii, N.K., 1972, Analytical chemistry of platinum metals, English translation of Russian book by Israel Program for Scientific Translations, 1975, Jerusalem; Halsted Press, John Wiley and Sons, New York, NY, 673 p. (Translated by N. Kamer, ed. by P. Shelnitz.
- Haffty, J., and Riley, L.B., and Gass, W.O., 1977, A manual on fire assaying and determination of the noble metals in geologic materials: U.S. Geological Survey Bulletin 1445, 58 p.
- Haffty, J., and Riley, L.B., 1968, Determination of palladium platinum, and rhodium in geologic materials by fire assay and emission spectroscopy: Talanta, vol. 15,p111-117.
- Heady, H.H., and Broadhead, K.G., 1977, Assaying ores, concentrates, and bullion; revision of Information Circular 7695: Bureau of Mines Information Circular, IC 8714r, 26 p.
- Jenkins, Olaf P., 1948, Iron resources of California, Department of Natural Resources, Division of Mines, Bulletin 129, pp. 304.
- Johnson, Wilton, 1989, Cement, U.S. Bureau of Mines, Mineral Yearbook, 28 pp.
- Jolly, Janice L. W., and Collins, Cynthia T., 1980, Iron oxide (in two parts) 2. Natural iron oxide pigments-location, production, and geological description, U.S. Bureau of Mines, Information Circular 8813, 79 pages.
- Jones, Thomas S., 1978, Iron oxide (in two parts), 1. Fine-particle iron oxides for pigment, electronic, and chemical use, U.S. Bureau of Mines, Information Circular 8771, 58 pages.
- Kackman, A.H., and Brown, A.W., 1985, Portland Cement; in SME Mineral Processing Handbook, N.L. Weiss, Ed., Society of Mining Engineers, AIME, New York, N.Y, pp. 26-1 to 20-52.
- Kallmann, S., 1987, A survey of the determination of the platinum group elements: Talanta, vol. 34, no. 8, p. 677-698.
- Klinger, F.L., 1980, Iron ore in: Minerals Yearbook, United States Department of the Interior, Bureau of Mines, Volume I, pp. 405-427.
- Kloebenstein, J.A., August 1990, Platinum group metals-1989, Bureau of Mines Minerals Yearbook: Washington D.C., U.S. Government Printing Office, 11 p.

- Logan, C.A., 1918, Platinum and allied metals in California: California Division of Mines and Geology, Bulletin 85, 120 p.
- Mickelsen, Donald P., September, 1990, Iron oxide pigments In: Minerals Yearbook, 1989, U.S. Bureau of Mines, 9 pages.
- Muntz, S.A., 1983, Mineral resources of the Kelso Dunes Wilderness Study Area (BLM No. CDCA-060-250), San Bernardino County, California: U.S. Bureau of Mines Open File Report MLA 107-83,16 p.
- Nonferrous Metal, and Data Collection and Coordination Branches, Bureau of Mines Mineral Industry Surveys, Monthly-Gold and Silver.
- Nonferrous Metal, and Data Collection and Coordination Branches, Bureau of Mines Mineral Industry Surveys, Quarterly-Platinum Group Metals.
- Platinum, Palladium, and Gold and their alloys: Newark, New Jersey, Englehardt Industries, Inc., Baker Platinum Division, 15 p.
- Puhr, Francis, Schwartzkopf, Florian, Thompson, Robert B., and Dahlstrom, Donald A., 1983, Thickening, Filtering, and drying: 4. Drying; in SME Mineral Processing Handbook, N.L. Weiss, Ed., Society of Mining Engineers, AIME, New York, N.Y, pp. 9-35.
- Rapp, J.S., Silva, M.A., Higgins, C.T., Martin, A.C., and Burnett, J.L., 1990, Mines and mineral producers active in California 1988-1989, California Division of Mines and Geology, Special Publication 103, pp. 57.
- San Miguel, A.F., 1967, Magnetite-ilmenite recovery from Parker/Jernberg sand: Eriez Manufacturing Company Technical Report, Erie, Pa., 14 p.
- Sastry, K.V.S., 1985, Sampling and Testing: Pelletizing Characteristics; in SME Mineral Processing Handbook, N.L. Weiss, Ed., Society of Mining Engineers, AIME, New York, N.Y, pp. 30-108 to 30-115.
- Saul, A.B., Gray, C.H., Evans, J.A., 1960-1962, Mines and mineral resources of Riverside County, California, California Division of Mines and Geology, unpublished report with map.
- Sharp, A.P., 1966, Kelso Dunes, Mojave Desert, California: Geological Society of American Bulletin, v. 77, pp. 1045-1074. 152
- Shepard, O.C., and Dietrich, W.F., 1940, A textbook of fire assaying: McGraw-Hill Book Co., Inc., The Maple Press Co., York, PA., 277 p.
- Singleton, Richard H., and Davis, Charles L., 1980, Cement in: Minerals Yearbook, Metals and Materials, U.S. Bureau of Mines, Volume I, pp 161-188.
- Sober, J., and Gomes, J.M., May 1981, Platinum group metals in alluvial deposits, northern and southern California: California Division of Mines and Geology, California Geology, p. 91-98.
- Smith, E.A., 1913, The sampling and assay of the precious metals; Neill and Co., Ltd., Edinburgh, Scotland, 460 p.
- Soothing, D.M., and Page, N.J., 1986, International strategic minerals inventory summary report-platinum group metals: U.S. Geological Survey Circular 930-E, 34p.
- Tyler, P.M., and Santmyers, R.M., 1931, Platinum: Bureau of Mines Information Circular IC 6389, 69 p.
- U.S. Bureau of Mines, 1987, An appraisal of Minerals availability for 34 commodities: iron ore, Bulletin 692, pp. 126-137.
- U.S. Bureau of Mines, Iron are, in: Commodity Data Summaries, 1976, pp. 82-83.
- U.S. Bureau of Mines, Iron are, in: Mineral Commodity Summaries, 1991, pp. 80-81.
- Watson, Ian, Asst. Ed., Iron oxide pigments-Colourful competition between natural and synthetic, in Industrial Minerals, August, 1979, pp. 43-51.
- White, M.G., January 9, 1990, Recovery of precious metals from complex ores: United States Patent No. 4,892,631, United States Patent Office, 8 p.
- Wright, T.L., and Fleisher, M., 1965, Geochemistry of the platinum metals: U.S. Geological Survey Bulletin 1214-A, 24 p.
- Wright, Lauren A., Stewart, Richard M., Gay, Thomas E., Jr., and Hazenbush, George. C., 1953, Mines and mineral deposits of San Bernardino County, California, Department of Natural Resources, Division of Mines, Vol. 49, No.2, pp.86-99.
- Yeend, W., Dohrenwend, J.C., Roger, S.U., Smith, R.G., Simpson, R.W., Jr., and Muntz, S.R., 1984, Mineral resources and mineral resource potential of the Kelso Dunes Wilderness Study Area (CDCA-250), San Bernardino County, California: U.S. Bureau of Mines and U.S. Geological Survey, Open File Report 84-647, 19p.

Dinosaur and arthropod tracks in the Aztec Sandstone of Valley of Fire State Park, Nevada

Heather M. Stoller,¹ Stephen M. Rowland,² and Frankie D. Jackson³

¹ Department of Geoscience, University of Nevada, Las Vegas Las Vegas, NV 89154-4010, stollerh@unlv.nevada.edu

² Department of Geoscience, University of Nevada, Las Vegas Las Vegas, NV 89154-4010, steve.rowland@unlv.edu

³ Department of Earth Sciences, Montana State University, Bozeman, MT 59717-3480, frankiej@montana.edu

ABSTRACT—We provide the first published descriptions and preliminary interpretations of dinosaur tracks and arthropod tracks and burrows within the Aztec Sandstone of Valley of Fire State Park. Such tracks have so far been discovered at three sites within the park. One tracksite contains poorly preserved, tridactyl, grallatoroid undertracks, six of which form a trackway. The scorpionoid ichnogenus *Paleohelcura* also occurs at this site, along with a network of burrows that we tentatively attribute to burrowing colonial insects. Another site consists of a cross-section exposure with a disturbed zone of laminae that we interpret to have resulted from a tridactyl dinosaur foot penetrating dry sand. The third tracksite contains a puzzling trackway consisting of five, small, left, tridactyl footprints and no right footprints. Research on Aztec Sandstone tracks within the park is ongoing.

Introduction

The Aztec Sandstone is a Lower-Middle Jurassic, eolian sandstone exposed in southern Nevada and southeastern California. It is correlative with—and was originally contiguous with—the Navajo Sandstone of southern Utah and northern Arizona (Marzolf, 1993; Marzolf and Anderson, 2005). The Navajo Sandstone has yielded a diverse assemblage of vertebrate and invertebrate trace fossils, including at least four ichnotaxa attributed to dinosaurs (Faul and Roberts, 1951; Baird, 1980; Lockley and Hunt, 1995; Rainforth and Lockley, 1996; Hamblin and Bilbey, 1999; Smith and Santucci, 2001; Irmis, 2005; Lockley, 2005; Loope, 2006; Ekdale et al., 2007; Milàn et al., 2008; Milner et al., 2012), as well as a small number of body fossils (Winkler et al, 1991; Parrish and Falcon-Lang, 2007; Sertich and Loewen, 2010). Aztec Sandstone exposures in the Mescal Range of eastern California (Fig. 1) have also yielded a diverse assemblage of vertebrate tracks (Reynolds, 2002; Reynolds, 2006a, 2006b; Reynolds and Mickelson, 2006). Most of the Mescal Range tracks, including the only dinosaur tracks known to occur in California, have been collected and repositied in the San Bernardino County Museum and the Natural History Museum of Los Angeles County, to protect them from illegal collectors (Springer et al., 2009). Some of these Mescal Range tracks are prominently on display in the dinosaur exhibit of the Natural History Museum of Los Angeles County.

In contrast to the trace-fossil-rich Navajo Sandstone, and the exposures of the Aztec Sandstone in the Mescal Range, southern Nevada's exposures of the Aztec Sandstone have historically been much less productive. Rowland and Mercadante (2007) reported the occurrence

of the mammaloid ichnogenus *Brasilichnium* in the Aztec Sandstone of Valley of Fire State Park, but prior to 2012, no other reports of fossils in the Aztec Sandstone of southern Nevada had been published. That situation has recently changed quite dramatically. Several vertebrate and invertebrate tracksites are now known in the Aztec Sandstone of Red Rock Canyon National Conservation Area (RRCNCA), near Las Vegas (Rowland et al., 2012). A few years before fossil tracks were discovered in RRCNCA, one of us (FJ), while teaching a Montana State University field paleontology course in Valley of Fire State Park, discovered a variety of fossil tracks in the Aztec Sandstone within the park.

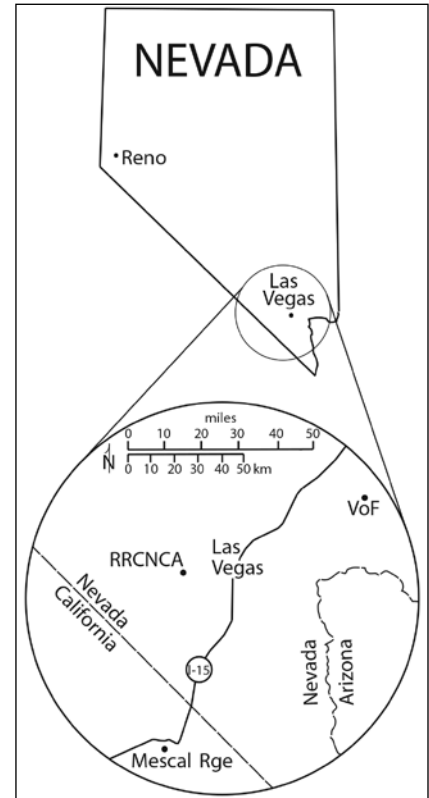


Figure 1. Locations where tracks have been reported in the Aztec Sandstone. VoF = Valley of Fire State Park; RRCNCA = Red Rock Canyon National Conservation Area.

These were briefly mentioned, but not described or figured, in Bonde et al. (2012).

The purpose of this paper is to provide descriptions and preliminary interpretations of three dinosaur tracksites in Valley of Fire State Park (Fig. 1), along with descriptions of the arthropod tracks and burrows that occur at one of the sites. Synapsid tracks, including *Brasilichnium* and at least one additional mammaloid ichnogenus, will be described in one or more future papers. Precise locations of the tracksites are not disclosed, at the request of the park supervisor.

Tracksite UNLV-AZ-001

Tracksite UNLV-AZ-001 is a peninsula of bedrock, approximately 10 m wide and 20 m long with about 1.7 m of relief, in a sandy wash (Fig. 2). The strata dip 11° to the west. Six poorly preserved, tridactyl undertracks form a northward-oriented trackway, with a seventh track alongside, also pointed northward (Fig. 3). Individual tracks are approximately 12 cm long and approximately 10 cm wide (Fig. 4), although most of them are too indistinct for precise measurement. The stride is 52 cm, and the trackway width is 18 cm. The most distinct track (second from left in Fig. 3) is a right footprint in which the impressions of digits III and IV are preserved in positive epirelief, while the impression of digit II is missing (Fig 4).

These tracks are interpreted to be undertracks, transmitted through some thickness of sediment and impressed into moist sand. Experiments by Manning (2004) showed that moisture content between 2-24% by weight is needed in sand to preserve distinct surface dinosaur tracks. Below 2% the sand is not sufficiently cohesive for distinct tracks to form, and above 24% moisture the sand is gloppy, and it flows under its own weight, also preventing the development of distinct tracks.

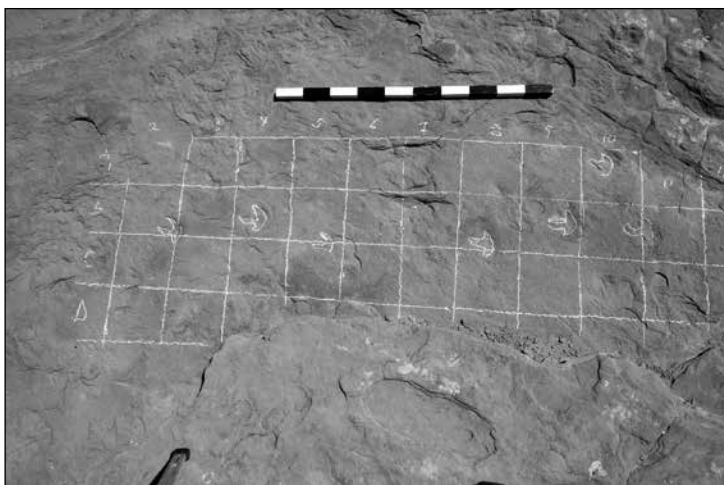


Figure 3. Chalked grid and outlined tridactyl tracks at Tracksite UNLV-AZ-001. Squares are 20 cm by 20 cm. Black and white scale is 1 m long, calibrated in decimeters. Detail of second track from left is shown in Figure 4.

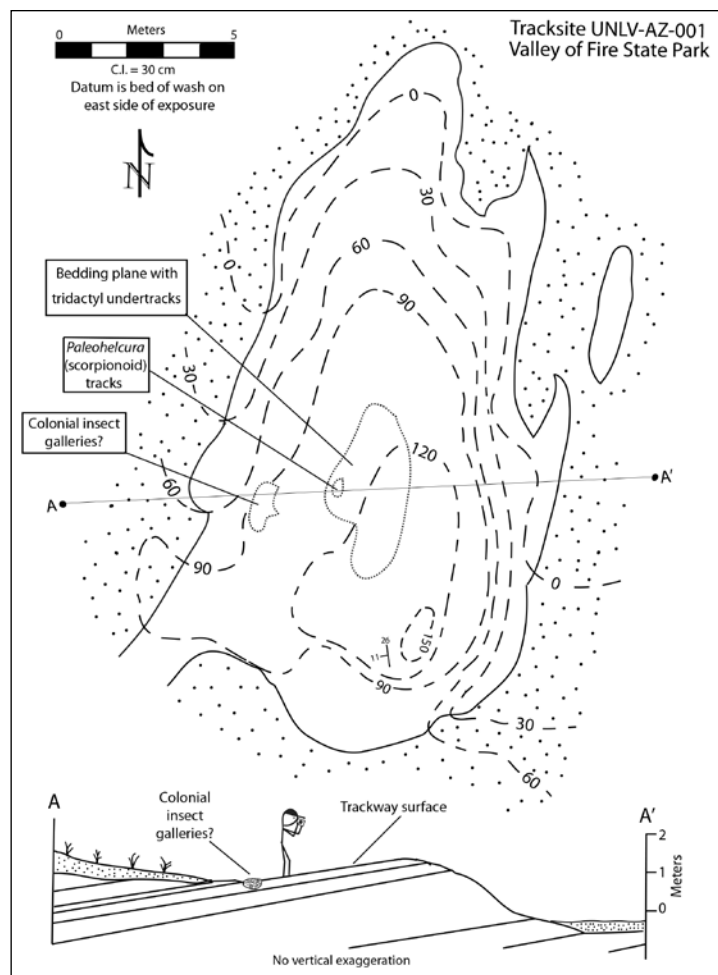


Figure 2. Map and cross-section of Tracksite UNLV-AZ-001.

Similar moisture constraints would have existed in the subsurface. The positive epirelief of the two digits shown in Figure 4 may be the result of moist sediment adhering to the bottoms of the digits as the dinosaur's foot exited the substrate.

The trackway surface also contains two types of arthropod trace fossils. One of these (Fig. 5) belongs to the ichnogenus *Paleohelcura*, which is well known in the Navajo Sandstone, and also in Permian sandstones of western North America (Brady, 1947; Lockley and Hunt, 1995; Lockley, 2002). *Paleohelcura* is commonly attributed to scorpions (Brady, 1947; Lockley and Hunt, 1995; Lockley, 2002).

The *Paleohelcura* tracks are certainly surface tracks (in contrast to the dinosaur tracks at this site). Experiments by McKee (1947) suggest that such delicate tracks can be made only in loose, dry sand. They may have been preserved by the dampening of the trackway surface, perhaps by dew, imparting cohesion and a slightly closer packing to the sand grains. This close packing is retained, even after subsequent drying and burial by loose, dry sand, thus creating a parting interface that

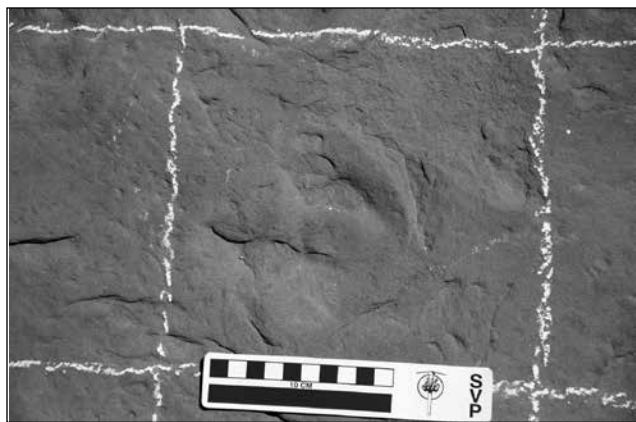


Figure 4. Dinosaur undertrack at Tracksite UNLV-AZ-001.

facilitates later exposure of the trackway surface, as described by McKee (1944).

The other arthropod trace fossils at this tracksite, which belong to an unknown or undescribed ichnotaxon, we tentatively attribute to burrowing colonial insects (Fig. 6). These consist of a network of variously oriented, tubular, sand-filled burrows, round in cross-section, and about 8 mm in diameter. These burrows are conspicuously more resistant to erosion than is the surrounding

matrix, resulting in small knobs of resistant burrow-fill on the exposed bedding plane (Fig. 6). This burrow network occurs in a distinct, irregularly-shaped area, approximately 2 m long and 1 m wide.

The foregoing interpretations imply that the scorpions that left the *Paleohelcura* tracks were present at this site prior to the dinosaurs that created the undertracks. By the time the dinosaurs walked here, the *Paleohelcura*-bearing surface was buried under sand.

The size and morphology of the dinosaur tracks, poorly preserved though they are, place them in the ichnogenus *Grallator*, a common ichnogenus of the Navajo Sandstone (Lockley and Hunt, 1995). The *Grallator* trackmaker was a carnivorous, bipedal theropod (Thulborn, 1990).

Tracksite UNLV-AZ-002

Tracksite UNLV-AZ-002 is on the side of a large, overturned, allochthonous block. Unlike the bedding-plane exposures occurring at tracksites UNLV-AZ-001 and 003, the exposure at this site is a cross-section of bedding that contains multiple zones of disrupted laminae. One of these disrupted zones is illustrated in Figure 7. It is approximately 9 cm wide at the top, decreasing in width downward.

The morphology of this disturbed zone of sandstone, with a central downfold at the bottom, marginal upfold, and deeply scalloped lower boundary, closely matches features described by Loope (2006, Fig. 5) from the Navajo Sandstone, which he interpreted to be tracks of small, theropod dinosaurs in dry sand. The three panels of Figure 8 show our interpretation of the zones of disrupted laminae at Tracksite UNLV-AZ-002.

Tracksite UNLV-AZ-003

Like Tracksite UNLV-AZ-002, Tracksite UNLV-AZ-003 is on the side of a large allochthonous block of sandstone. However, in this case the tracksite is a bedding-plane exposure in which the trackway surface has been tilted a few degrees beyond vertical. Fourteen poorly preserved, very small tracks occur on this bedding plane, all of which are pointed in the same direction. At least five of the tracks lie in a recognizable trackway (Fig. 9).

Figure 10 is a photograph and sketch of the most distinct track at this site. It is about 5 cm long and 5 cm wide, with a strongly asymmetrical divarication of digits. The digits are distinct, but impressions of claws are not present. Assuming that the angle of divarication between digits II and III is greater than the angle between digits III and IV (which is demonstrably the case at an Aztec Sandstone tracksite in RRCNCA), we identify the track

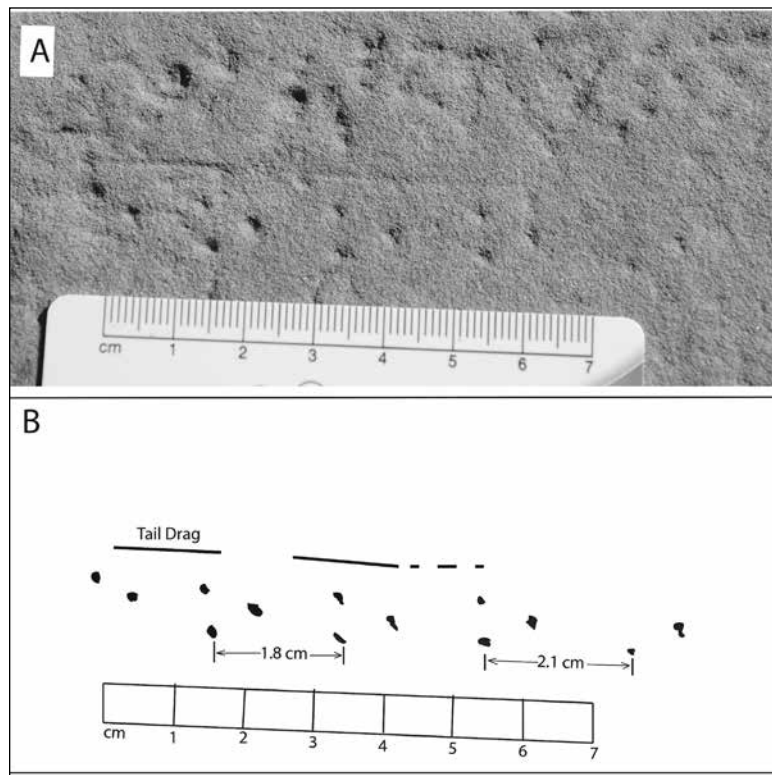


Figure 5. Photo (A) and sketch (B) of the trace fossil *Paleohelcura*, which is generally interpreted to be the track of a scorpion, at Tracksite UNLV-AZ-001. One characteristic pattern of *Paleohelcura*, as represented here, is consecutive sets of three pits, with each set arranged in an approximate equilateral triangle, as occur just above the scale in "A," and drawn in "B." Portions of four stride cycles are clearly represented, with strides ranging from 1.8 cm to 2.1 cm. The intermittent linear impression, which may or may not be present in *Paleohelcura*, is interpreted to represent a tail-drag mark. The pattern of pits above the tail-drag line is too irregular to interpret. According to Brady (1947), based on studies of living scorpions, this pattern indicates that the animal was moving from right to left.

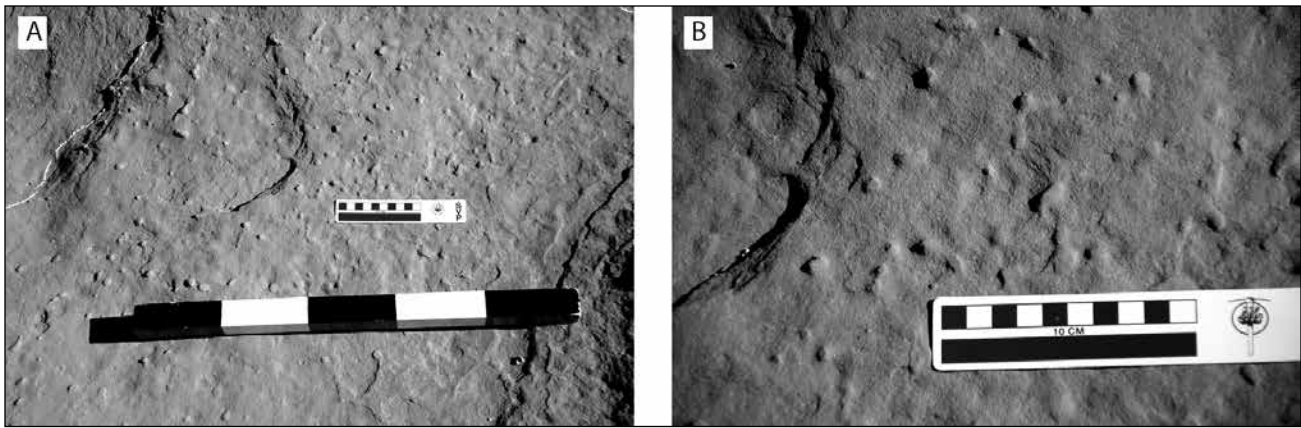


Figure 6. Burrows tentatively attributed to burrowing colonial insects. A. View of dense occurrence of burrows. Black and white scale is 0.5 m long. B. Detail of burrows, showing that burrow-fill is more resistant than the surrounding matrix. Tracksite UNLV-AZ-001.

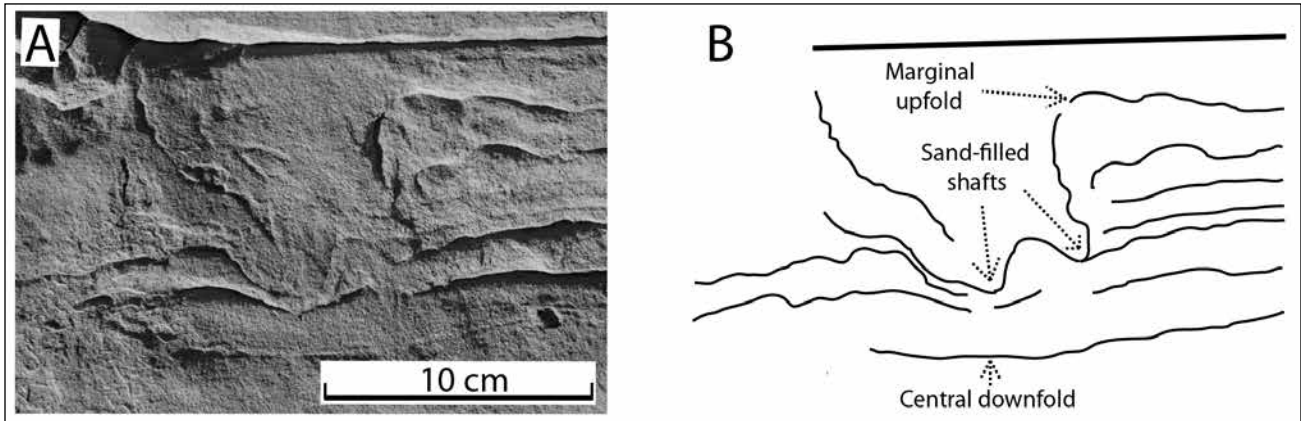


Figure 7. Photograph (A) and sketch (B) of a cross-section-exposure of strata at Tracksite UNLV-AZ-002, showing a zone of disrupted laminae that we interpret to be the result of the penetration of a dinosaur's foot into dry sand. Because the block of rock is upside down, this photograph has been printed upside down, to restore the original orientation of the laminae.

in Figure 10 as a left footprint. The average spacing from one track to the next is 18.7 cm (Fig. 9). At this time we do not assign the tracks at this site to an ichnogenus.

A surprising aspect of the trackway shown in Figure 9 is that all of the tracks that are distinct enough to show digits (including some that are adjacent to each other), display the same smaller-angle-on-the-left asymmetry, which is to say that they are all left feet.

There are at least three possible explanations for this one-legged trackway. One possibility is that moist sand was patchily distributed when this animal walked here. As discussed above, moist sand is necessary for distinct surface tracks to be preserved. If the animal was straddling the boundary between a patch of moist sand and a patch of dry sand, stepping in moist sand with its left foot and dry sand with its right foot, one can imagine a scenario in which the left tracks would be preserved while the right tracks would not be preserved.

Arguing against the patchy-moist-sand hypothesis, however, is the complete lack of any hint of right footprints. If the track was made by a small tridactyl dinosaur, which is our working hypothesis, the trackway would not be very wide (e.g., Fig. 3); it's unlikely that the animal's narrow trackway would

exactly straddle the boundary between moist and dry sand for five stride cycles, such that the left tracks would be preserved and the right tracks would not be preserved. Also, such a distribution of moist and dry sand would be unlikely, except perhaps at the boundary between an interdune area and the sloping face of a dune. There is no conspicuous sedimentological evidence of a change in paleoslope at this site.

The second possibility is that the animal was walking horizontally or diagonally across a relatively steeply

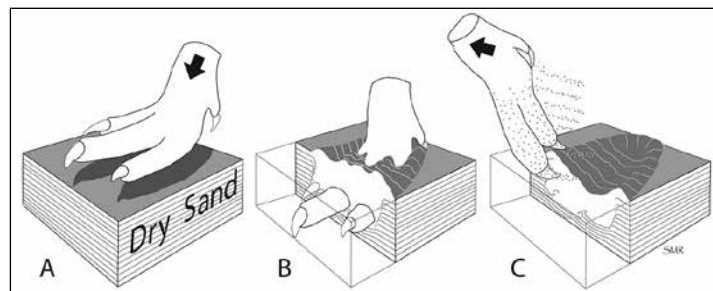


Figure 8. Interpretation of the origin of zones of disrupted laminae at Tracksite UNLV-AZ-002. A. Right foot of theropod dinosaur immediately prior to penetration into dry sand. B. Foot has penetrated into the dry sand, causing the central downfold, disruption of laminae, and scalloped lower boundary of zone of disrupted laminae. C. Foot has exited the sand, resulting in marginal upfold; loose, dry sand has filled the space where foot had been. Compare with Figure 7.

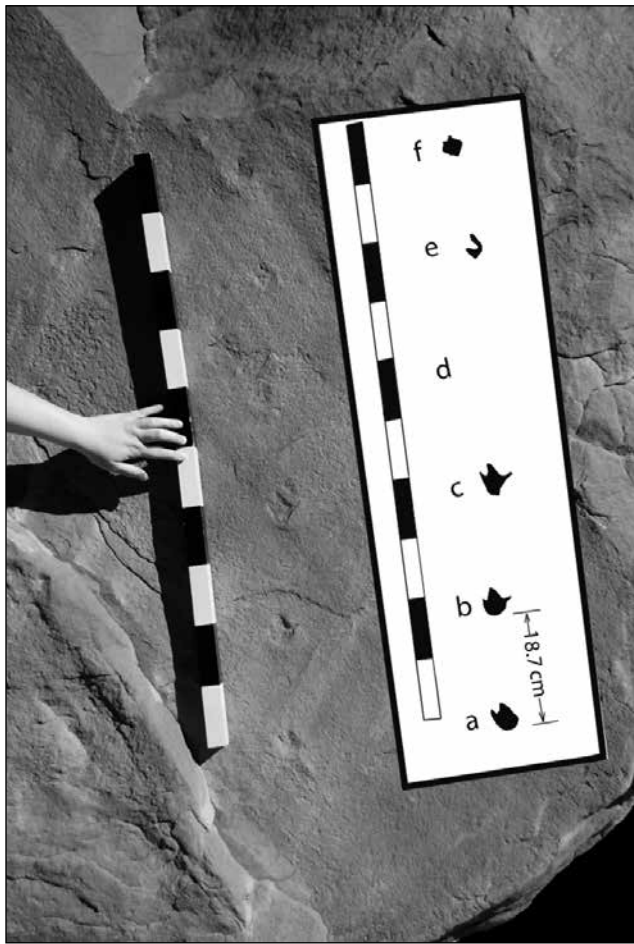


Figure 9. Photograph and drawing of Tracksite UNLV-AZ-003, which occurs on the steep, overturned face of an allochthonous block of sandstone that tumbled down from higher elevation. The trackway consists of five tracks, all of which we interpret to be left footprints. Track “d” is missing, although the surface is somewhat disturbed in the area where it should be. Scale is 1 m long, calibrated in decimeters.

sloping surface. In such a situation the foot on the upslope side of the animal’s body would sink deeper into the sand than would the foot on the downslope side. Thus, a layer at the appropriate depth could record undertracks from the upslope foot, and none from the downslope foot.

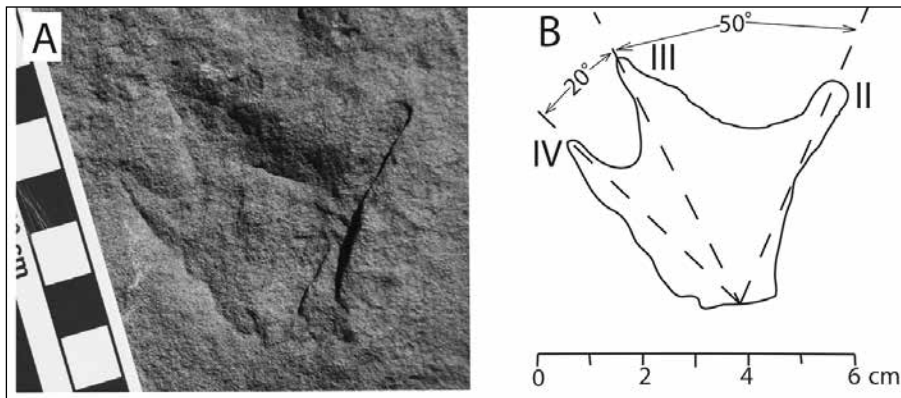


Figure 10. Photograph (A) and drawing (B) of the most distinct track at Tracksite UNLV-AZ-003. This track is Track “c” of Figure 9. Digit numbers are based on the observation at an Aztec Sandstone site in RRCNCA that, in asymmetrical tracks, the divarication angle between digits III and IV is smaller than the divarication between digits II and III, which implies that this is a left footprint.

The third possibility is that this animal was hopping on one foot, due to an injury.

Additional study of the morphology of the other tracks at this site, as well as the sedimentology of the track-bearing layer, will be undertaken to test these three hypotheses.

Conclusion

It is now apparent that dinosaurs and arthropods (in addition to synapsids) inhabited the Jurassic dunefield desert that is now represented by the Aztec Sandstone. The three tracksites described in this paper display some of the variety of preservation we might expect to find at other dinosaur tracksites within Valley of Fire State Park and elsewhere in southern Nevada. Our study of tracks and trackways in the Aztec Sandstone is ongoing.

Acknowledgments

This research in Valley of Fire State Park was conducted under a research permit to SMR. We thank Park Supervisor Jim Hammonds and Regional Manager Russ Dapsauski for their support of this research.

References cited

Baird, D.1980. A prosauropod dinosaur trackway from the Navajo Sandstone (Lower Jurassic) of Arizona, in *Aspects of Vertebrate History: Essays in Honor of Edwin Harris Colbert*, L.L. Jacobs, ed. Flagstaff, Museum of Northern Arizona Press, p. 219-230.

Bonde, J.W., Varricchio, D.J., Bryant, G., and Jackson, F.D. 2012. Mesozoic vertebrate paleontology of Valley of Fire State Park, southern Nevada, in *Field Trip Guide Book: 71st Annual Meeting of the Society of Vertebrate Paleontology*, Paris Las Vegas, Las Vegas, Nevada November 2-5, 2011, J.W. Bonde and A.R.C. Milner, eds. Nevada State Museum Paleontological Papers Number 1, p. 108-126.

Brady, L.F. 1947. Invertebrate tracks from the Coconino Sandstone of northern Arizona. *Journal of Paleontology*, v. 21, p. 466-472, pls. 66-69.

Ekdale, A.A., Bromley, R.G., and Loope, D.B. 2007. Ichnofacies of an ancient erg: a climatically influenced trace fossil association in the Jurassic Navajo Sandstone, southern Utah, USA, in *Trace Fossils: Concepts, Problems, Prospects*, W. Miller III, ed. Amsterdam, Elsevier, p. 562-574.

Faul, H., and Roberts, W.A. 1951. New fossil footprints from the Navajo(?) Sandstone of Colorado. *Journal of Paleontology*, v. 25, p. 266-274.

Hamblin, A.H., and Bilbey, S.A. 1999. A dinosaur track site in the Navajo-Nugget Sandstone, Red Fleet Reservoir, Uintah County, Utah, in *Vertebrate Paleontology of Utah*,

- D.D. Gillette, ed. Utah Geological Survey Miscellaneous Publications, p. 51-57.
- Irmis, R.B. 2005. A review of the vertebrate fauna of the Lower Jurassic Navajo Sandstone in Arizona, in *Vertebrate Paleontology of Arizona*, R.D. McCord, ed., Mesa Southwest Museum Bulletin Number 11, p. 55-71.
- Lockley, M.G. 2002. A guide to fossil footprints of the world. Denver, Lockley-Peterson, 124 p.
- Lockley, M.G. 2005. Enigmatic dune walkers from the abyss: Some thoughts on water and track preservation in ancient and modern deserts. *Canyon Country (Museum of Moab)*, v. 54, p. 43-51.
- Lockley, M.G., and Hunt, A.P. 1995. Dinosaur tracks and other fossil footprints of the western United States. New York, Cambridge University Press, 338 p.
- Loope, D.B. 2006. Dry-season tracks in dinosaur-triggered grainflows. *PALAIOS*, v. 21, p. 132-142.
- Manning, P.L. 2004. A new approach to the analysis and interpretation of tracks: examples from the dinosauria, in *The Application of Ichnology to Palaeoenvironmental and Stratigraphic Analysis*, D. McIlroy, ed. Geological Society, London, Special Publication 228, p. 93-123.
- Marzolf, J.E. 1993. Palinspastic reconstruction of Early Mesozoic sedimentary basins near the latitude of Las Vegas: Implications for the early Mesozoic Cordilleran cratonal margin, in *Mesozoic Paleogeography of the Western United States II*, G. Dunn, and K. McDougall, eds. Pacific Section SEPM, Book 71, p. 433-462.
- Marzolf, J.E., and Anderson, T.H. 2005. Lower Mesozoic facies and crosscutting sequence boundaries: Constraints on displacement of the Caborca terrane, in *The Mojave-Sonora megashear hypothesis: Development, assessment, and alternatives*, T.H. Anderson, J.A. Nourse, J.W. McKee, and M.B. Steiner, eds. Geological Society of America Special Paper 393, p. 283-308, doi: 10.1130/2005.2393(10).
- McKee, E. D. 1944. Tracks that go uphill. *Plateau*, v. 16(4), p. 61-72.
- McKee, E. D. 1947. Experiments on the development of tracks in fine cross-bedded sand. *Journal of Sedimentary Petrology*, v. 17, p. 23-28.
- Milà, J., Loope, D.B, and Bromley, R.G. 2008. Crouching theropod and Navahopus sauropodomorph tracks from the Early Jurassic Navajo Sandstone of USA. *Acta Palaeontologica Polonica*, 53(2): 197-205.
- Milner, A. R. C., Birthisel, T. A., Kirkland, J. I., Breithaupt, B. H., Matthews, N. A., Lockley, M. G., Santucci, V. L., Gibson, S. Z., DeBlieux, D. D., Hurlburt, M., Harris, J. D., and Olsen, P. E. 2012. Tracking Early Jurassic dinosaurs across southwestern Utah and the Triassic-Jurassic transition, in *Field Trip Guide Book: 71st Annual Meeting of the Society of Vertebrate Paleontology*, Paris Las Vegas, Las Vegas, Nevada November 2-5, 2011, J.W. Bonde and A.R.C. Milner, eds. Nevada State Museum Paleontological Papers Number 1, p. 1-107.
- Parrish, J.T., and Falcon-Lang, H.J. 2007. Coniferous trees associated with interdune deposits in the Jurassic Navajo Sandstone Formation, Utah, USA. *Palaeontology*, 50(4), p. 829-843.
- Rainforth, E.C., and Lockley, M.G. 1996. Tracks of diminutive dinosaurs and hopping mammals from the Jurassic of North and South America, in *The Continental Jurassic*, M. Morales, ed. Museum of Northern Arizona Bulletin 60, p. 265-269.
- Reynolds, R.E. 2002. California dinosaur tracks: inventory and management, in *Between the Basins: Exploring the Western Mojave Desert and Southern Basin and Range Province*, R.E. Reynolds, ed. Fullerton, California State University Desert Studies Consortium, p. 15-18.
- Reynolds, R.E. 2006a. Way out west: Jurassic tracks on the continental margin, in *The Triassic-Jurassic Terrestrial Transition*, J.D. Harris et al., eds. New Mexico Museum of Natural History and Science Bulletin 37, p. 232-237.
- Reynolds, R.E. 2006b. Jurassic tracks in California, in *Making Tracks Across the Southwest*, R.E. Reynolds, ed. Fullerton, California State University Desert Studies Consortium, p. 19-24.
- Reynolds, R.E., and Mickelson, D.L. 2006. Way out west: preliminary description and comparison of pterosaur ichnites from the Mescal Range, Mojave Desert, California, in *The Triassic-Jurassic Terrestrial Transition*, J.D. Harris et al., eds. New Mexico Museum of Natural History and Science Bulletin 37, p. 226-230.
- Rowland, S.M., and Mercadante, J. 2007. Gregarious behavior recorded in the tracks of a Jurassic therapsid. *Journal of Vertebrate Paleontology*, v. 27, Supplement to no. 3, p. 137A.
- Rowland, S.M., Saines, M., and Stoller, H. 2012. Discovery of dinosaur tracks and arthropod tracks in the Aztec Sandstone (Lower Jurassic), Red Rock Canyon National Conservation Area, Las Vegas, Nevada, in *Search for the Pliocene: the Southern Exposures*, Desert Symposium Field Guide and Proceedings, R.E. Reynolds, ed. Fullerton, California State University Desert Studies Consortium, p. 182-183.
- Sertich, J.J.W., and Loewen, M.A., 2010. A new basal sauropodomorph dinosaur from the Lower Jurassic Navajo Sandstone of southern Utah. *PLoS ONE* 5(3): e9789. doi:10.1371/journal.pone.0009789.
- Smith, J.A., and Santucci, V.L. 2001. Vertebrate ichnostratigraphy of the Glen Canyon Group (Jurassic) in Zion National Park, Utah, in *The Changing Face of the East Mojave Desert*, R.E. Reynolds, ed. Fullerton, California State University Desert Studies Consortium, p. 15-19.
- Springer, K.B., Chiappe, L., Sagebiel, J.C., Scott, E. 2009. Preserving California's only dinosaur trackways by collection—an unprecedented opportunity for public protection and interpretation of fossil specimens from federal land, in *Proceedings of the Eighth Conference on Fossil Resources*, S.E. Foss et al., eds. St. George, Utah, p. 26-27.
- Thulborn, T. 1990. Dinosaur tracks. London, Chapman and Hall, 410 p.
- Winkler, D.A., Jacobs, L.L., Congleton, J.D., and Downs, W.R. 1991. Life in a sand sea: biota from Jurassic interdunes. *Geology*, v. 19, p. 889-892.

New records of fish from southern exposures of the Imperial Formation of San Diego County, California

Mark A. Roeder

Department of Paleontology, San Diego Natural History Museum, maroeder1731@aol.com

Introduction

In eastern San Diego County, outcrops of the Imperial Group consist of upper Miocene and Pliocene marine mudstones, siltstones and sandstone that preserve evidence of incursions of the ancient Gulf of California and subsequent entry of the Colorado River into the Salton Trough.

Fossil marine invertebrates (microfossils, corals, clams, snails, sand dollars, sea urchins) of the Imperial Group are well documented (Kew 1914, 1920; Dickerson 1918; Vaughan 1917a, 1917b; Hanna 1926; Deméré and Rugh 2005; Stump 1972; Stump and Stump, 1972; Powell 1984, 1987, 1988, 1995; McDougal 2008; Watkins 1990a, 1990b). Except for the record of *Carcharocles megalodon* (large extinct great white shark) by Hanna (1926), little is known of the fossil fishes of the Imperial Group. Recent collecting by paleontologists from Anza Borrego Desert State Park and the San Diego Natural History Museum has yielded new records. Deméré (2005) and Roeder (2005) summarized records known at that time. This article documents those records and newer discoveries of fossil fish from the Imperial Group. The information on environmental, ecological, and biogeographical aspects of related modern fish taxa used in the taxonomic accounts was taken from Allen and others, 2006; Compagno and others, 2005; Ebert 2003; Eschmeyer and Herald 1983; Goodson 1976, 1988; Miller and Lea, 1976; Robins and Ray, 1986; Thomson and McKibben 1986; Thomson and others, 1987.

Fossil fish

Imperial Group

All of the upper Miocene and Pliocene marine sediments in the Anza Borrego Desert Region and adjacent regions were once referred to as the Imperial Formation. Later paleontological and stratigraphic investigations by Winkler and Kidwell (1996) elevated this formation to group status and the members (or subunits) to formational ranking.

Latrania Formation

Introduction: Based on the presence of fossil corals and sea urchins in sandstones of Latrania Formation, this basal rock unit of the Imperial Group was probably deposited in clear and warm marine offshore waters of the ancestral Gulf of California on the western edge of the

Salton Trough. The age of this rock unit has been estimated at 5.12 to 6.27 million years old (Dorsey and others, 2011; Jefferson and others, 2012).

Sharks and Rays (Chondrichthyes): In addition to the record of *Carcharocles megalodon* (Hanna, 1926), teeth of either *Odontaspis* or *Carcharias* (sand tiger shark), *Galeocerdo rosaliaensis* (extinct tiger shark), *Isurus* cf. *I. oxyrinchus* (shortfin mako), *Carcharodon*, cf. *Myliobatoidea* (bat stingray), *Balistidae* (triggerfishes), cf. *Semicossyphus* (sheephead), and *Sphyræna* cf. *S. sphyræna* (great barracuda) have been recovered from the Latrania Formation (Table 1). The majority of these fossils were discovered in outcrops in and around the Coyote Mountains in eastern San Diego County and western Imperial County.

Today, there are three species of odontaspids in western hemisphere marine waters, *Carcharias taurus* (sand tiger shark), *Odontaspis ferox* (ragged tooth shark), and *Odontaspis noronhai* (bigeye sandtiger). *Carcharias taurus* is a shallow water shark found in the warm temperate and tropical waters of the Atlantic, Mediterranean, and Indo west Pacific, but not in the central and eastern Pacific. *Odontaspis ferox* is present in shallow to deep waters in the Gulf of California, off southern California, and other isolated coastal areas in the world. *Odontaspis noronhai* is a very rare form found in warm, deep seas worldwide. The lingual (inside) enamel surfaces of *C. taurus* and the fossil odontaspid teeth have fine striations from the root to the tip of the tooth. The fossil teeth may be *C. taurus*, but teeth of *O. ferox* and *O. noronhai* and other fossil odontaspid species need to be examined to determine the species. First, the identification of tooth type (medial, symphyssial, alternate, anterior, intermediate, lateral, and posterior) and position in the jaw needs to be determined (Applegate 1965; Purdy and others 2001). Second, tooth characters such as tooth size, the presence and absence of striations on lingual surfaces, the morphology of lateral cusps, size and shape of transverse groove, morphology of cutting edge, angle of the labial recurvature of tooth tip of the Latrania Formation odontaspid needs to be examined (Purdy and others, 2001). Third, these characters in the Latrania Formation teeth need to be compared with similar characters in the living odontaspids and as well as other fossil odontaspid species for determination of species. *Carcharias taurus* is known from the Pliocene Yorktown Formation of the Lee Creek Mine in North



Figure 1. *Galeocерdo rosaliaensis* (extinct tiger shark) tooth, Latrania Formation.

Carolina (Purdy and others 2001). Rare teeth of *Odonaspis ferox* are known from the middle Miocene Pungo River Formation of the Lee Creek Mine (Purdy and others, 2001).

Galeocерdo rosaliaensis (extinct tiger shark) was described by Applegate (1978) from the Tirabuzon Formation (= Gloria Formation of Applegate 1978; Landin and others, 2000) near Santa Rosalia, Baja California Sur, Mexico (Figure 1). The Tirabuzon Formation is thought to be early to middle Pliocene in age (Ortlieb and Colletta, 1984). Applegate (1978) described this extinct species as a transitional form between the extinct Late Miocene tiger shark (*Galeocерdo aduncus*) and the modern tiger shark (*Galeocерdo cuvier*).

Within Carcharhinidae (requiem sharks), the genus *Carcharhinus* makes up over half of the species of this family. In the northwestern Atlantic Ocean, there are at least 14 species of *Carcharhinus*, while in the eastern Pacific, there are at least 16 species and in the Gulf of California, nine species (Kato et al. 1967; Applegate 1978). Fossil teeth of *Carcharhinus* have been reported from the middle Miocene of California and Baja California (Mitchell 1965; Deméré and others, 1984). From the middle to upper Pliocene Tirabuzon Formation at Santa Rosalia, Baja California Norte, Mexico, Applegate (1978) identified nine species of *Carcharhinus* from fossil teeth. The single *Carcharhinus* tooth recovered from the Latrania Formation may be assigned to a modern species or a fossil species as more comparative material becomes available. Based on tooth shape, teeth of *Carcharhinus* can be differentiated into lower and upper teeth. The upper teeth are usually larger, broader and more triangular in shape than the lower, which are smaller and more spike-like. The single fossil Latrania Formation *Carcharhinus* tooth was an upper tooth. As with the odontaspids, teeth of all known species of *Carcharhinus* need to be examined

for diagnostic tooth characters for identification of fossil Latrania Formation tooth to species level.

Recently, research on fossils of *Carcharodon* (white shark) from the Upper Miocene-Pliocene Pisco Formation of Peru suggest that the modern great white shark (*Carcharodon carcharias*) is not descended from the large extinct great white shark, *Carcharocles megalodon*, but instead evolved from the broad-tooth mako, *Carcharodon hastalis*. This species includes a transitional form, *Carcharodon hubbelli* which is late Miocene (6-8 Ma years) in age (Ehret, D.J. and others, 2012). The Latrania Formation may have two extinct white sharks that are not related, *Carcharocles megalodon* and possibly *Carcharodon hubbelli*.

Today, the shortfin mako (*Isurus oxyrinchus*) is found in coastal marine waters in the Gulf of California and worldwide in all temperate and warm seas. Fossil shortfin mako teeth are known from the middle Miocene Pungo River Formation and Pliocene Yorktown Formation of the Yorktown Formation of Lee Creek Mine, North Carolina (Purdy and others, 2001), and the Pliocene San Diego Formation.

A preliminary analysis of over 300 individual jaws of the modern California bat stingray (*Myliobatis californicus*) revealed that morphology of teeth is highly variable and “transcends virtually all supposed generically distinct dental patterns of other myliobatid rays” (Welton and Zinsmeister, 1980). Bat stingray-like rays in the northwestern Atlantic Ocean are assigned to at least three genera, *Aetobatus*, *Myliobatis*, *Rhinoptera*, while in the eastern Pacific such rays are assigned to *Pteromylaeus*, *Myliobatis*, and *Rhinoptera*. Because of this high degree of morphological variation, the Latrania Formation ray teeth can be identified only to the superfamily level.

Bony Fish (Osteichthyes): The family Balistidae is sometimes split into two families, filefishes (one or more families) and triggerfishes (one family). Triggerfishes are deep-bodied and compressed fishes with three dorsal spines. The first dorsal spine can be locked in the upright position deterring predators from attempting to swallow this fish. Triggerfishes are found in the Atlantic, Pacific and Indian Oceans with seven genera with 35 species (Nelson 1976). They occur in warm seas over rocky areas and reefs, but a few are found over soft bottoms. In the northwestern Atlantic Ocean, there are six species of triggerfishes, while in the Gulf of California there are only two species. Until more comparative material becomes available, the Latrania Formation triggerfish “canine” teeth will be assigned to the subfamily, Balistinae (triggerfishes).

Semicossyphus pulcher (California sheephead) lives today in coastal waters from Monterey, California to Guadalupe, Island, north-central Baja California, Mexico, and in the Gulf of California. The pharyngeal teeth of this large labrid fish are very distinctive and diagnostic. Fossil sheephead teeth are known from the Pliocene San Diego Formation.

From the Latrania Formation, a single jaw tooth of a great barracuda was found. Today, the great barracuda (*Sphyraena sphyraena*), which can reach 6.5 feet (2 meters) in length, is found in all tropical seas except the eastern Pacific. Smaller barracudas, 2-3 feet (1 meter), are found in the eastern Pacific (two or three species) and western Atlantic (three species).

Today, most of the sharks and fishes from the Latrania Formation would be considered as offshore marine species.

Deguyunos Formation—Mud Hills Member

Introduction: Overlying the Latrania Formation, the Mud Hills Member of the Deguyunos Formation has a record of two kinds of sharks. The Mud Hills Member consists of mudstones that chronicle the Colorado River entering the Salton Trough and building its delta. The Mud Hills Member consists of mudstones that were deposited in the distal end of prodelta (outermost delta) environment of the ancient Colorado River (Winkler and Kidwell 1996; Dorsey 2005) The age of this rock unit has been estimated at 4.49 to 5.12 million years old (Dorsey and others 2011, Jefferson and others 2012).

Sharks and Rays (Chondrichthyes): From the Mud Hill Member, Roeder (2007) identified two sharks (Centrophoridae-gulper sharks, and an identified species). The first tooth appears to be from a gulper shark (Family Centrophoridae). Gulper sharks, related to the modern dogfish (genus *Squalus*), are mainly a group of deepwater marine bottom-dwelling sharks. Today, these small-bodied (1 meter or less) sharks are found almost worldwide from cold temperate to tropical seas, except in the northeast Pacific and high latitudes. To date, about 16 species have been placed in two genera, *Centrophorus* and *Deania*. Although one species has been recorded in depths as shallow as 50 m, most are found in waters between 1000–1500 m deep.

The second tooth is not identifiable at this time.

Deguyunos Formation—Yuha Member

Introduction: The shallow marine Yuha Member of the Deguyunos Formation was deposited in a delta front paleoenvironment and contains extensive fossil oyster beds. This unit represents a coarsening up sedimentary sequence from the mudstones of the Mud Hills Member and has at dated at approximately 4.35-4.49 million of years old (Dorsey 2005).

Sharks and Rays (Chondrichthyes): From the Yuha Member of the Deguyunos Formation, there are records of *Heterodontus*

(horn shark), either *Odontaspis* or *Carcharias* (sand tiger), *Carcharodon* sp. (white shark), *Carcharhinus* sp. (large requiem shark), cf. *Myliobatoidea* sp. (bat stingray) and Istiophoridae (billfishes).

Presently, in the eastern Pacific, there are three species of horn shark, *Heterodontus* (*francisci*, *mexicanus*, *quoyi*) and, surprisingly, there are no species in the western Atlantic Ocean. Until more comparative material becomes available, the Yuha Member horn shark tooth cannot be speciated.

As with the Latrania Formation odontaspids, the fossil sand tiger teeth from the Yuha Member need to be compared to modern odontaspids and Pliocene species from the Yorktown Formation of the Lee Creek Mine of North Carolina (Purdy and others, 2001).

The *Carcharodon* teeth may be the modern species, the white shark (*Carcharodon carcharias*).

The single *Carcharhinus* tooth recovered (Figure 2) may be assigned to a modern species or a fossil species as more comparative material becomes available.

As stated earlier, the ray teeth recovered can be only assigned to the superfamily level, Myliobatoidea.

Bony Fish (Osteichthyes): The single billfish partial vertebra could only be assigned to the family Istiophoridae (billfishes).

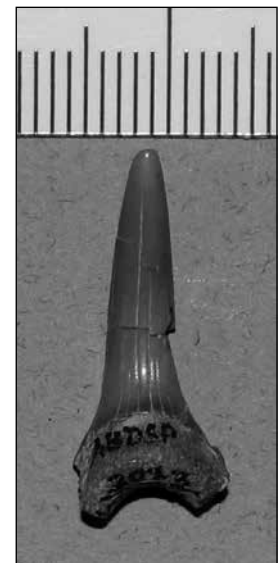


Figure 2 *Carcharias* or *Odontaspis* (sand tiger shark) ABDSP 2043 /V5885, anterior? tooth Yuha Member of the Deguyunos Formation

Table 1. Fossil Fishes from the Imperial Group

Scientific Name	Common Name	Latrania Fm.	Imperial Group		
			Mud Hills Member	Yuha Member	Camelhead Member
cf. <i>Semicossyphus</i>	sheephead	X			
<i>Sphyraena</i> cf. <i>S. sphyraena</i>	great barracuda	X			
<i>Balistinae</i>	triggerfish	X			
Istiophoridae	billfish			X	
<i>Heterodontus</i>	horn shark	X			
Centrophoridae	gulper shark		X		
<i>Carcharias</i> or <i>Odontaspis</i>	sand tiger shark	X		X	
<i>Carcharocles megalodon</i>	extinct great white shark	X			
<i>Carcharodon</i>	white shark	X ¹		X ²	
<i>Galeocerdo rosaliaensis</i>	extinct tiger shark	X			
<i>Isurus</i> cf. <i>I. oxyrinchus</i>	shortfin mako	X			
<i>Carcharhinus</i>	requiem shark	X		X	
Myliobatoidea	eagle ray	X			
Unidentified shark	shark		X		
Teleosts	bony fishes				X

X¹ may be extinct species *Carcharodon hubbelli*
 X² may be modern species *Carcharodon carcharias*

Deguyunos Formation-Camels Head Member

Introduction: The very shallow marine Camels Head Member of the Deguyunos Formation was deposited in muddy tidal flats. This unit represents a fining up sedimentary sequence from the Yuha Member and has been dated approximately 4.25-4.35 million of years (Dorsey 2005; Dorsey and others 2011; Jefferson and others 2012).

The presence of fossiliferous claystones with burrowing marine animals, wavy bedded sandstones and foraminifers (microfossils) suggests a depositional environment similar to what we find today in the broad tidal flats surrounding the lower Colorado River delta (Dorsey 2005).

Bony Fish (Osteichthyes): From the Camels Head Member, there are poorly preserved and not identifiable bony fish scales and bones.

Discussion

In over 100 years of collecting fossils in the Imperial Group, only a handful of shark, ray, and bony fish fossils have been collected from the Imperial Group. This paucity may be a consequence of the fact that fossil fish remains are naturally rare in Imperial Group rocks. Also, this may be the result of a collecting bias, since the Imperial Group rocks have not received the same level of attention, such as field collecting activities (surface collecting, bulk sampling and water screening of sediments) as the more paleontologically interesting Palm Spring Group and other terrestrial rock units in the Anza Borrego Desert area. Recent work by Roeder (2012) at two localities in northern exposures of the Imperial Formation in the Palm Springs area of Riverside County, has yielded relatively diverse fossil fish faunas by bulking sampling of sediments, water screening of these sediments, and picking the concentrates with the aid of a microscope. The upper Miocene Super Creek locality (6.2-6.5 million years) has yielded at least 17 species of bony fishes while the Pliocene Willis Palm locality (3.0-3.1 million years) has yielded five species of sharks and rays and four species of bony fish (Roeder 2012).

In spite of smaller sample size from the southern exposures of the Imperial Group, several interesting conclusions can be made about the emerging fossil fish faunas of this area.

First, like the fossil mollusks and corals from the Imperial Group, there are fossil species of marine fish that today are not present in the eastern Pacific, but have representatives living in the Caribbean Sea and elsewhere such as great barracuda, the gulper shark, and possibly the odontaspids. During the Late Miocene, the Central American Seaway existed across what is today Panama, until closure and elevation of the Isthmus in the middle Pliocene. Before that time, the Central American Seaway allowed the free exchange of waters and marine organisms between the Pacific and Atlantic Oceans.

Second, with more recovered fish fossils, and the known biostratigraphic and paleomagnetic age control for rock units of the Imperial Group this information may be used in the future to address broad scale topics dealing with the evolution of, similar to the research conducted on fossil sharks of the Pisco Formation of Peru (Erlet, D.J. and others, 2012). Researchers may be able to trace the evolutionary history of certain groups of fossil fish through time like the white sharks within the Imperial Group rocks. In the Latrinia Formation, we have one lineage of fossil white shark, the large extinct *Carcharocles megalodon* and possibly another lineage represented by *Carcharodon* that may be in the *Carcharodon hastalis-Carcharodon hubbelli-Carcharodon carcharias* (modern white shark) lineage (Erlet, D.J. and others, 2012).

Third, the fish remains from the southern exposures of the Imperial Group chronicle the fish faunas in several marine depositional environments of the ancestral Gulf of California from 4.2 to 6.3 million years ago. Recent work by Roeder (2012) in northern exposures of the Imperial Formation in the Palm Springs area has shown that fish remains recovered from that area consisted of Gulf of California, southern California, and Caribbean species.

Fourth, most fish species have certain environmental requirements (e.g., substrate, water temperature, and water depth), and these fossils may help in reconstructing the depositional environments of the rock units that they are found in. For example the fossil gulper shark tooth from the Mud Hills Member of the Deguyunos Formation, based on environmental information on modern gulper sharks which are usually found in waters exceeding 1000 meters in depth, indicates that this portion of this rock unit was deposited in fairly deep marine water.

Acknowledgments

I would like to thank Tom Deméré, Curator, and Kesler Randall, Collections Manager, of the Department of Paleontology at the San Diego Natural History Museum, and Lyndon Murray and George Jefferson (retired) of the Stout Research Center, Anza-Borrego Desert State Park, for bringing to my attention fossil shark and bony fish specimens from southern exposures of the Imperial Group in their care. Also I would like to thank the paleontological field crews of the same institutions for their recent collections of fossil fish material, especially Mr. Jerry Hughes and other volunteers who collected most of the material from the Yuha Member of the Deguyunos Formation. Special thanks to Mr. Bob Reynolds for making the guidebook possible.

References

- Allen, L.G., Pondella, D.J., II, and M.H. Horn, (eds.), 2006. The Ecology of Marine Fishes: California and adjacent water. *University of California Press*, Berkeley. 660p.
- Applegate, S.P., 1965. Tooth terminology and variation in sharks with special reference to the sand shark, *Carcharias taurus*

- Rafineque: *Natural History Museum of Los Angeles County, Contributions in Science*, Volume 88, p.3-18.
- Applegate, S.P., 1978. Phyletic Studies; Part 1; Tiger Sharks. *Revista*, Volume 2 Number 1, Universidad Nacional Autonoma de Mexico, p. 55-61.
- Compagno, L., Dando, M. and S. Fowler, 2005. Sharks of the World. *Princeton Field Guides*. Princeton University Press. Princeton and Oxford. 368 p.
- Deméré, T.D., 2005. The Imperial Sea: Marine Geology and Paleontology in Jefferson, G.T., and L. Lindsay, editors, *Fossil Treasures of the Anza-Borrego Desert*, Sunbelt Publications, San Diego, p. 29-41.
- Deméré, T. A., Roeder, M. A., Chandler, R. M., and J. A. Minch, 1984. Paleontology of the Middle Miocene Los Indios Member of the Rosarito Beach Formation, Northwestern Baja California in Minch, J. A. and J. R. Ashby, editors, *Miocene and Cretaceous Depositional Environments, Northwestern Baja California, Mexico*. Published by the Pacific Section, American Association of Petroleum Geologists, Los Angeles. Volume 54, p. 47-56.
- Deméré, T.D., and N.S. Rugh, 2005. Invertebrates of the Imperial Sea in Jefferson, G.T., and L. Lindsay, editors, *Fossil Treasures of the Anza-Borrego Desert*, Sunbelt Publications, San Diego, p.41-69.
- Dickerson, R.E., 1918. Mollusca of the Carrizo Creek beds and their Caribbean affinities. *Geological Society of America Special Paper 29*: p.1-48.
- Dorsey, R., 2005. Stratigraphy, Tectonics, and Basin Evolution in the Anza Borrego Desert Region in Jefferson, G.T., and L. Lindsay, editors, *Fossil Treasures of the Anza-Borrego Desert*, Sunbelt Publications, San Diego, p.89-104.
- Dorsey, R., Housen, B.A., Janecke, C.M., Fanning, C.M., and A.L.F. Spears, 2011. Stratigraphic record of basin development within the San Andreas fault system: Late Cenozoic Fish Creek-Vallecito basin, southern California. *Geological Society of America Bulletin* 123 (5,6), p. 771-793.
- Ebert, D. A., 2003. Sharks, Rays and Chimaeras of California. California Natural History Guide No. 71 *University of California Press*. Berkeley and Los Angeles, London. 285p.
- Ehret, D. J., MacFadden, Jones, B.J., Devries, D.S., Foster, T.J., and R. Salas-Gismondi, 2012. Origin of the white shark *Carcharodon* (Lamniformes: Lamnidae) based on recalibration of the Upper Neogene Pisco Formation of Peru. *Palaeontology*, Volume 55, Issue 6, p. 1139-1153.
- Eschmeyer, W. N. and E. S. Herald, 1983. A Field Guide to Pacific Coast Fishes of North America. *The Peterson Field Guide Series*, Houghton Mifflin Company, Boston. 336p.
- Goodson, G., 1985. Fishes of the Atlantic Coast. *University of Stanford Press*. Stanford. 202p.
- Goodson, G., 1988. Fishes of the Pacific Coast. *University of Stanford Press*. Stanford. 267p.
- Hanna, G.D., 1926. Paleontology of Coyote Mountain, Imperial County, California. *Proceeding of the California Academy of Sciences*, 4th Series 14:427-503.
- Jefferson, G.T., Lynch, D., Murray, L.K., and R. E. Reynolds, 2012. Searching for the Pliocene: Field Trip Guide to the southern exposures, Day 2 in Reynolds, R.E., ed., *Wild, scenic and rapid: a trip down the Colorado River trough*. California State University Desert Studies Symposium p. 83.
- Kato, S., Springer, S., and M. H. Wagner, 1967. Field Guide to Eastern Pacific and Hawaiian Sharks. *U. S. Fish and Wildlife Service, Bureau of Commercial Fisheries*. Washington, D.C. Circular No. 271. 47p.
- Kew, W.S.W. 1914. Tertiary echinoids of the Carrizo Creek region in the Colorado Desert, California University Publications, *Bulletin of the Department of Geology*, 8:39-60.
- Kew, W.S.W. 1920. Cretaceous and Cenozoic Echinoidea of the Pacific coast of North America. University of California *Publications of the Geology Department*, 12(20):32-137.
- Landin-Ochoa, L., Ruiz, J., Calmus, J., Perez-Segura, E., and F. Escandoin 2000. Sedimentology and Stratigraphy of the upper Miocene El Boleo Formation, Santa Rosalia, Baja California, Mexico. *Revista Mexicana de Ciencias Geologicas*, Volume 17, Number 2, p. 83-93. Universidad Nacional Autonoma de Mexico.
- McDougall, K.A., 2008. Late Neogene marine incursions and the ancestral Gulf of California, in Reheis, M.C., Hershler, R., and Miller, D.M., eds., Volume Late Cenozoic Drainage History of the Southwestern Great Basin and Lower Colorado River Region: Geologic and Biotic Perspectives, Geological Society of America Special Paper 439, p. 353-371.
- Miller, D. J. and R. N. Lea, 1976. Guide to the Coastal Fishes of California. *Fish Bulletin* 157. California Department of Fish and Game. 249p.
- Mitchell, E.D. 1965. History of Research at Sharktooth Hill, Kern County, California. *Kern County Historical Society*.
- Nelson, J. S., 1976. Fishes of the World. *A Wiley-Interscience Publication*. John Wiley and Sons. New York, London, Sydney, and Toronto. 416p.
- Ortlieb, L., and B. Colleta. 1984. Sintesis Cronoestratigrafica sobre el Neogeno y el Cuaternario marino de la Cuenca de Santa Rosalia, Baja California Sur, Mexico, in Malpica-Cruz, V., Celis-Gutierrez, S., Guerrero-Garcis, J., and L. Ortlieb, eds., *Neotectonics and sea level variation in the Gulf of California area, a symposium*: Mexico, D.F. Universidad Nacional Autonoma de Mexico, Instituto de Geologia, Contributions volume, p. 241-260.
- Powell, C. L II, 1985. Bivalve molluscan paleoecology of northern exposures of the marine Neogene Imperial Formation in Riverside County, California. *Western Society of Malacologists Annual Report*, August 1985. Volume 17 for 1984.
- Powell, C. L II, 1987. Correlation between sea level events and deposition of marine sediments in the proto-Gulf of California during the Neogene. *Geological Society of America*, Abstracts with program, 19(7): p.809
- Powell, C. L II, 1988. The Miocene and Pliocene Imperial Formation of Southern California and its molluscan fauna. *Western Society of Malacologists*. San Diego, California. Annual Report, Volume 20, p. 11-18.
- Powell, C. L II, 1995. Preliminary report on the Echinodermata of the Miocene and Pliocene Imperial Formation in southern California. In Remeika, P., and A. Sturz 1995, eds., Paleontology and geology of the western Salton Trough Detachment, Anza-Borrego Desert State Park, California. Field Trip

- Guidebook and volume for the 1995 *San Diego Association of Geologist's* field trip to Anza-Borrego Desert State Park, Volume 1.
- Purdy, R.K. and others, 2001. In Ray, Clayton E. and D.J. Bohaska, eds., *Geology and Paleontology of the Lee Creek Mines, North Carolina*. III, *Smithsonian Contributions to Paleobiology*. 90:71-202.
- Robins, C. R. and G. C. Ray. 1986. A Field Guide to Atlantic Coast Fishes of North America. *The Peterson Field Guide Series*. Houghton Mifflin Company, Boston. 354p.
- Roeder, M.A., 2005. Fossil Fishes of the Anza-Borrego Region in Program and Abstracts for *Fossil Treasures of the Anza-Borrego Desert*. Anza-Borrego Institute, California State Parks, and Sunbelt Publications, San Diego. p. 16-17.
- Roeder, M.A., 2007. A late Miocene record of a fossil gulper shark (Family Centrophorus) from the Mud Hills Member of the Deguynos Formation, Lycium Wash, Fish Creek basin, Anza-Borrego Desert State Park, San Diego County, California. In Reynolds, R.E., ed., *Wild, scenic and rapid: a trip down the Colorado River trough*. California State University Desert Studies Symposium p. 83.
- Roeder, M.A., 2012. New records of fish from northern exposures of the Imperial Formation of Riverside County, California. In Reynolds, R.E., ed., *Searching for the Pliocene: Southern Exposures*. California State University, Desert Studies, The 2012 Desert Research Symposium, p. 53-64.
- Stump, T.E., 1972. Stratigraphy and paleontology of the Imperial Formation in the western Colorado Desert. Master of Science Thesis, San Diego State University, 132 pp.
- Stump, T.E. and Stump, J.D., 1972. Age, stratigraphy, paleoecology, and Caribbean affinities of the Miocene fauna of the Gulf of California depression. *Geological Society of America*. Special Paper 4((3):243.
- Thomson, D. A., Findley, L. T. and A. N. Kerstitch. 1987. Reef fishes of the Sea of Cortez. *University of Arizona Press*. Tucson.
- Thomson, D. A. and N. McKibben, 1986. Gulf of California Fishwatcher Guide. *Golden Puffer Press*. 75p.
- Vaughan, T.W., 1917a. The reef-coral fauna of Carrizo Creek, Imperial County, California and its significance. U. S. Geological Survey Profession Paper 98T:335-387.
- Vaughan, T.W., 1917b. Significance of reef coral fauna at Carrizo Creek, Imperial County, California. *Washington Academy of Science journal* 7:194.
- Watkins, R., 1990a. Pliocene channel deposits of oyster shell in the Salton Trough region, California. *Palaeogeography, Palaeoclimatology, Palaeoecology*. 79:249-262.
- Watkins, R., 1990b. Paleoecology of a Pliocene rocky shoreline. *Palaios*. 5:167-175.
- Welton, B.J. and W.S. Zinmeister, 1980. Eocene Neoselachians from the Meseta Formation, Seymour Island, Antarctic Peninsula. Natural History Museum of Los Angeles County. *Contributions in Science*. 329:1-10.
- Winkler, C.D. and S.M., Kidwell, 1996. Stratigraphy of a marine rift basin. In Field Conference Guidebook and Volume for the American Association of Petroleum Geologists Annual Convention, Pacific Section 73:295-336.

Hydrographic significance of fishes from the Early Pliocene White Narrows Beds, Clark County, Nevada

Gerald R. Smith,¹ Robert E. Reynolds,² and Joseph D. Stewart³

¹University of Michigan Museum of Zoology, Ann Arbor, MI 48109, grsmith@umich.edu

²Redlands, CA, 92373

³Natural History Museum of Los Angeles County, 900 Exposition Boulevard, Los Angeles, CA 90007

Introduction

Fish fossils were preserved in Pliocene sediments deposited in Muddy Valley, Glendale Basin, Clark County, Nevada (Schmidt and others, 1996; Pederson, 2003), an extensional valley of the southeastern Great Basin. The White Narrows unit, incised into the upper Muddy Creek Formation, was carefully described and informally named in U.S.G.S. Open-File Report 96-521 by Dwight Schmidt and others in 1996 and placed in a broader biostratigraphic context by Reynolds and Lindsay (1999). Bohannon (1984) and Howard and John (1987) described sedimentary and tectonic relationships of the east-tilted fault blocks of the extensional basins and their sharp separation at the west-dipping Grand Wash fault zone from drainages of the adjacent Colorado Plateau (Faulds and others, 2003; Spencer and Pearthree, 2003) (Fig. 1).

Hunt (1956) described the existence of aggradational drainages of the upper Colorado River on the Colorado Plateau, isolated from Great Basin drainages in the Miocene. Evidence for Miocene drainage isolation was further documented by Lucchitta (1979, 1990) and summarized by Lucchitta and Jeanne (2003). Early Pliocene timing of the onset of the spillover and through-flowing Colorado River was established by Spencer and Pearthree (2003), Spencer and others (2003), Castor and Faulds (2003), and Dorsey (2012). Effects of these drainage relations on fish distributions was explored by Miller and Hubbs (1960), Smith (1966), and Spencer and others (2008).

Geologic setting

Muddy Valley, lying south of the Caliente Caldera Complex, offers important clues to the tectonic history of the Basin and Range Province. The Caliente Caldera Complex formed between 24 and 13 Ma (Rowley and others, 1995) during an episode of subduction that preceded crustal extension in the Basin and

Range Province; volcanic quenching roughly coincided with the beginning of crustal extension. Dated ash-flow tuffs found within sediments that filled newly formed basins constrain the timing of basin formation and filling (Taylor and others, 1989). Flat-lying sediments, including those in Muddy Valley, formed during or after the tectonic extension. Thus, flat-lying sedimentary deposits south of the Caliente Caldera Complex are younger than about 10 million years. Ash-flow tuffs in Muddy Valley are derived from volcanism in southern Idaho, where volcanism continued after decline of activity in the Caliente Caldera

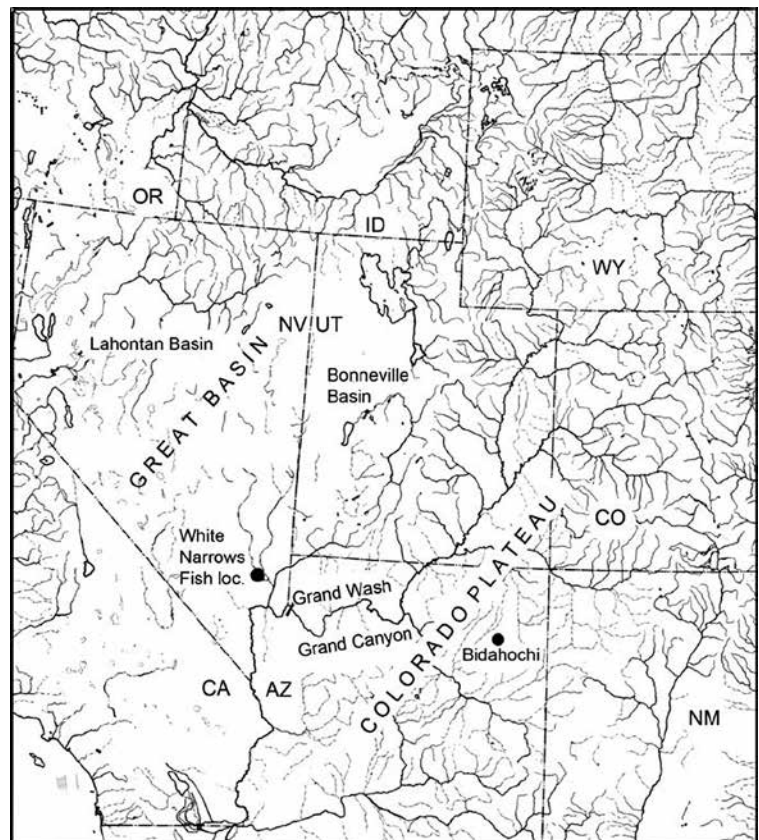


Fig. 1. Location of the White Narrows fish samples, SBCM L3313, Clark County, Nevada, and the closest related Mio-Pliocene fauna in the Bidahochi Formation, Navaho County, Arizona. Four White Narrows species have relationships in the Great Basin, *Siphateles*?, the plagioprotein (*Lepidomeda*?), *Pantosteus*, and *Archoplites*. Three species *Ptychocheilus*, *Orthodon/Evomus*, and *Catostomus latipinnis* were originally related to Bidahochi and Colorado Plateau forms. *Rhinichthys* is widespread in both areas.

Complex (Perkins and Nash, 2002). After extension, meandering drainages became cohesive, drainage courses were further altered by latest Tertiary tectonics, and the Virgin and Colorado river systems developed.

Muddy Creek Formation: The Muddy Creek Formation was deposited in a series of small basins that coalesced into a single large basin that now includes a 5,000 square mile area bounded by Henderson on the southwest, Mesquite on the northeast, Coyote Spring Valley on the northwest, and the Grand Wash Cliffs on the southeast (Longwell and others, 1965; Lucchitta, 1979). The Muddy Creek Formation sits unconformably on the Horse Spring Formation and on the red sandstone unit of Bohannon (Bohannon, 1984; Wallin and others, 1993). The timing of crustal extension that caused tilting of the Horse Spring Formation is constrained by deposition of flat-lying Muddy Creek sediments. The youngest date on the Horse Spring Formation is 15.9 Ma. Structural tilting ended before the deposition of the Muddy Creek Formation where early dates are as old as 11.6 Ma (Beard, 1993) or 10.4 Ma (Wallin and others, 1993).

Deposition in Muddy Basin continued at least until the time of flows of the Fortification Basalt member of the Muddy Creek Formation. Dates on the Fortification Basalt, south of Henderson, range from 4.9 to 5.85 Ma (Lucchitta, 1979; Anderson, 1978; Damon and others, 1978). Dates near the top of the Muddy Creek Formation are 5.9 Ma at Table Mountain (D. L. Schmidt, personal communication to R. E. Reynolds, 1992) and 4.73 Ma from the north side of Grand Wash (Reynolds and others, 1986). A description of the Muddy Creek Fm. (Schmidt and others, 1996) includes two members, the Red Claystone (Tmr) and the Green Claystone (Tmg).

Biostratigraphic age control (Reynolds and Lindsay, 1999). Stock (1921) assigned a Miocene age to the Muddy Creek Formation near the type area at Overton, Nevada, based on scant vertebrate remains, including horse and camels. Ted Galusha from the AMNH Frick Labs discovered a robust Muddy Creek fauna at Juanita Springs in Arizona, southwest of Mesquite, Nevada (Robert Evander written communication to R. E. Reynolds via R. H. Tedford, 1997). The Hemphillian camel *Alforjas* sp. (SBCM L2745-133) was found west of Mesquite, Nevada, and *Neotragoceras* sp. (SBCM L2743-32) came from within Mesquite. *Aelurodon validus*, *Indarctos* sp. (AMNH repository), *Alforjas* sp., and *Neotragoceras* sp. (SBCM repository), restricted to the Hemphillian North American Land Mammal Age (NALMA), are found at localities in the middle and upper portions of the section in eastern exposures of the Muddy Creek Formation (Robert Evander written communication to R.E. Reynolds via R.H. Tedford, 1997).

White Narrows formation (informal designation): A White Narrows fauna was recovered west of Glendale, Nevada (Reynolds and Lindsay, 1999). This fauna contains gastropods, ostracods, fish, frog, and toad that suggest a marshland habitat.

Temporally restricted rodent taxa include six known only from the Hemphillian NALMA and three known only from the Blancan NALMA. This suggests that the basal White Narrows unit (Schmidt and others, 1996) was deposited around 4.7 Ma at the beginning of the Blancan NALMA (Woodburne and Swisher, 1995; Bell and others, 2004). The fishes (SBCM repository L-3313) that are the subject of this paper were recovered from Starvation Flat, 13 miles northwest of the White Narrows Fauna locality and 2.5 miles northwest of the outcrop of the Tuff of Dead Man Wash.

The Tuff of Dead Man Wash is found within White Narrows marls (Twg) exposed along Hwy 168 between Starvation Flat and the community of Moapa. This volcanic ash compares chemically to other ashes from southeastern Nevada and falls within a range of 5.56 Ma from Arrow Canyon, Nevada and to 4.64 Ma from Wildcat Wash, Nevada (pers. comm. to Reynolds via David Miller from Elmira Wan, 2007).

The age of the fossil fauna corresponds well with the age of the 4.64 Ma ash from Wildcat Wash. The latter is located in northeastern Clark County, Nevada, 4.5 miles west of the Tuff of Dead Man Wash outcrop and three miles south of the fossil fish locality at Starvation Flat, north of Highway 168.

The relatively consistent dates suggested by the vertebrate fauna from the upper portion of the White Narrows formation (4.8 - 4.7 Ma) and the dates of the Tuff of Dead Man Wash (4.64 Ma) suggest that deposition of the White Narrows formation within a graben was after the local cessation of Muddy Creek deposition (5.9 Ma at nearby Table Mountain) and contemporaneous with the last phases of Muddy Creek deposition to the south (4.73 Ma at north Grand Wash; Reynolds and others, 1986).

Pederson 2003 concluded that most of the regional sediments were deposits that originated in the Caliente volcanoes to the north, with no evidence of Colorado River sediments from the Colorado Plateau a few miles to the east. Lower Colorado River tributary integration (House and others, 2007) suggests that a series of lakes developed along the lower Colorado River after 5.6 Ma, 100 miles south of Glendale, Nevada, below the mouth of Grand Canyon to Mojave Valley (Bullhead City to Needles). Lake drainage divides were then breached and basins were filled after 5.6 Ma and before 4.1 Ma. The large fish vertebra in White Narrows sediments, a Colorado River Pikeminnow (*Ptychocheilus lucius*) about 1.5 m long, suggests nearby large fluvial habitat such as the Colorado River. This species is found only in the Colorado River and its several largest tributaries today.

Paleontology

Reynolds and Lindsay (1999) documented a White Narrows mammalian fauna including seven murid rodents, *Paronychomys* cf. *P. lemredfieldi*, *Copemys* cf. *C. vasquezi* (*Antecalomys vasquezi* of Korth, 1998)

Repomys cf. *R. gustleyi*, *Peromyscus valensis*, (*Antecalomys valensis* of Korth, 1998) *Calomys (Bensonomys)* cf. *C. coffeyi* (Martin et al, 2002), *Calomys (Bensonomys)* cf. *C. arizonae* (Martin et al, 2002), *Neotoma (Paraneotoma)* cf. *N. vaughni*; and four heteromyid rodents *Dipodomys gidleyi* (*Prodipodomys* sp. of Dalquest and Carpenter, 1986), *Oregonomys* cf. *O. sargenti*, *Perognathus* sp., and *Prodipodomys* sp. Fossils of one or two species of shrews were also identified. The collections reported here (SBCM L3313) also include an unprepared rabbit jaw, possibly *Hypolagus*, in addition to the fishes. Mammals indicate an earliest Blancan fauna, later than the earliest Blancan Panaca Formation from Meadow Valley Wash, which dates about 4.95 Ma (Lindsey and others, 1999; Reynolds and Lindsay, 1999; Mou, 2011). The White Narrows faunas may be older than the Glens Ferry fauna at Hagerman (Mead, 1998; Ruez, 2009).

Mead and Bell (2001) reported pelvic and limb bones of two species of toads (*Bufo*), fragmentary jaw bones of a phrynosomatid lizard, jaw fragments of a night lizard (*Xantusia*), and a vertebra of a colubrid snake from the White Narrows sediments in Moapa Valley, 8 miles above the confluence of the Muddy River and Meadow Valley Wash. On the basis of these amphibians and reptiles, Mead and Bell (2001) interpreted the environment to be sub-humid, becoming cooler and drier with riparian vegetation and oak-juniper woodland. Schmidt and others reported evidence of a marl lake and fluvial sediments.

Fishes

The Starvation Flat locality was discovered by Bob Reynolds and collected by Dwight Schmidt in 1992. Two localities that produced the specimens reported here (SBCM L3313) are from yellow sands associated with gray silts near the base of the White Narrows unit as mapped and understood by Schmidt, Page, and Workman (1996).

The White Narrows fish fauna includes at least eight species in three families, Cyprinidae (minnows), Catostomidae (suckers), and sunfish (Centrarchidae). The present fauna in the basin includes no sunfish, but the basin now has genera and species of minnows and suckers not yet sampled from the Pliocene. Three species in the fauna probably originated on the Colorado Plateau—the Colorado River Pikeminnow, a Blackfish, and the Flannelmouth Sucker—would have gained access to the White Narrows area with the arrival of the upper Colorado River about 5.3 Ma (Dorsey 2012). Speckled Dace are genetically and morphologically variable in both the upper and lower Colorado River basins. Two species, Desert Suckers and a spinedace, are in the modern fauna of the lower Colorado River drainage in the Great Basin. Two species, the Tui Chub (*Siphateles*) and sunfish (*Archoplites*) are found north and west of the White Narrows area in Miocene and modern faunas.

Family Cyprinidae, minnows

Ptychocheilus lucius, Colorado River pikeminnow (Fig. 2)

The fossils include one large vertebra (L3313-2), matching only *Ptychocheilus* in its large size (25.7 mm in lateral diameter) and its texture of small pits. It is a fused first-plus-second centrum of the vertebral column (Fig. 2 a), of the Weberian apparatus (part of the fish hearing mechanism). The vertebra (referred to in Dwight Schmidt's field notes) is largest in its (lateral) diameter; its identification as a *Ptychocheilus* is supported by its large size and the small sizes of the dorsal, ventral, and lateral pits and fossae. It is a dorsoventrally compressed anterior pair of Weberian vertebra 13 mm long. No other western North American freshwater fish has bony vertebrae approaching this large size. (The next largest western fish is the Razor-back Sucker, with vertebrae up to 1.5 cm in diameter and with unfused first and second centra.) The White Narrows *Ptychocheilus* would have been about 1.5 m long. The second White Narrows fossil of this species is an anterior fragment of a cyprinid left cleithrum (L3313-1) with the elongated dimensions of *Ptychocheilus*, and not *Gila*, which is smaller; *Gila* has a less pronounced lateral ridge between two planes of the bone. *Ptychocheilus* is widely distributed in the west from Middle Miocene to recent and from the Ringold Formation, Washington, to the Bidahochi Formation, Arizona (Smith and others, 2002; Spencer and others, 2008).

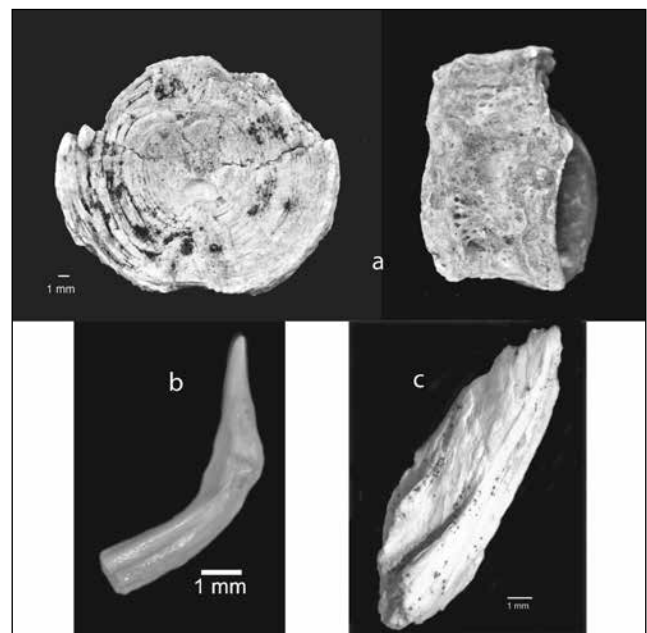


Fig. 2. *Ptychocheilus*, vertebral centrum, pectoral fin hemitrich, and fragment of cleithrum: a, fused first and second centra of a large Pikeminnow (SBCM L3313-2), anterior (left image) and left lateral (right image), the slender disc of first centrum mostly obscured by diagenetic alteration; b, hemitrich of pectoral fin ray (SBCM L3313-37); c, fragment of angle of left cleithrum of *Ptychocheilus*, anterolateral view (SBCM L3313-1).

***Siphateles*, tui chub (Fig. 3)**

Numerous cyprinid pharyngeal teeth (SBCM L3313-50) and one distinctive median fin-ray base among the White Narrows fossils have traits most similar to those of *Siphateles bicolor* (Tui Chubs). Teeth of Tui Chubs are distinctive in being relatively oval near the base, not flattened in cross-section. The posterior teeth have flattened grinding surfaces, exposing dentin rimmed by enamel, as seen from the dorsal aspect; these grinding surfaces are often concave as seen from the side of the tooth, with a blunt hook at the distal point of each tooth (Fig. 3; Smith and others 2009). Several vials of over 100 tooth fragments (SBCM L3313-41) include many teeth like those in Fig. 3 as well as many unidentified fragments.

Teeth of plagopterines and Speckled Dace differ from *Siphateles* in being more flattened not oval in cross-section, with a concave blade rather than a flattened grinding surface directed dorsally (toward the basioccipital pad). Teeth of *Gila* are relatively long and straight with weak or no grinding surfaces. They occur in two rows and are ovoid to slightly flat postdorsally.

The fossil median-fin hemitrich (Fig. 3 k) is distinctive among western cyprinids in having a prominent head with a short process, a deep anterior notch between the head and the shaft, a deep longitudinal groove on the mesial side of the shaft, and no special ornamentation on the mesial side of the shaft.

Siphateles is known from Pliocene to recent localities on the east side of the Sierras from Manix Lake to Fort Rock Lake (Smith and others 2009). The record in the White Narrows fauna is east of previously known localities, but related to their presence in Lahontan drainages 200 mi to the west and northwest.

***Orthodon* or *Evomus*, blackfish (Fig. 4)**

Specimens of a left and right pelvic basiptyrgia (Fig. 3 a-c, SBCM L3313-3) and a basal half of a median lepidotrich (Fig. 3 d, SBCM L3313-4) are identified as cyprinid bones by the orientation of the fin-support processes. The

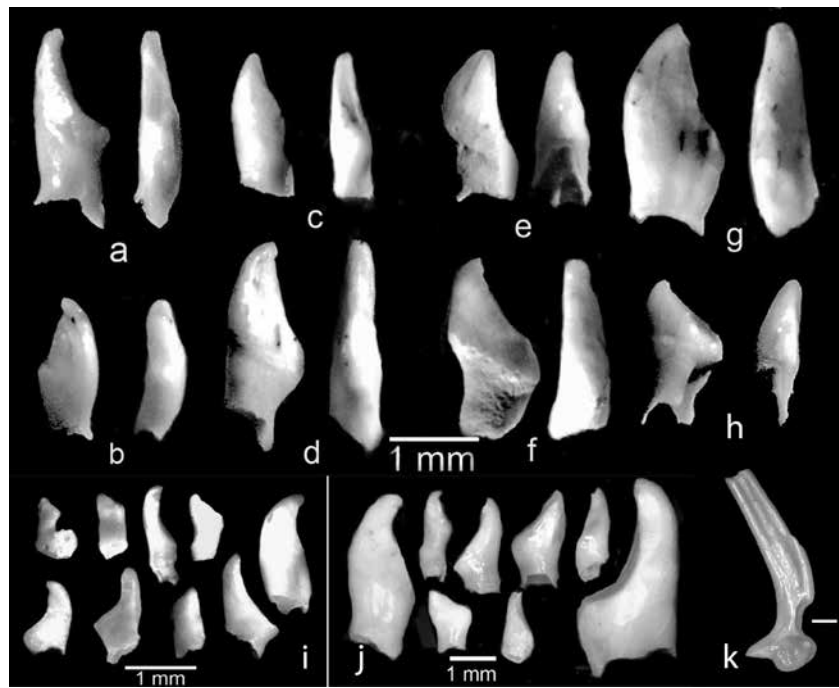


Fig. 3. *Siphateles*? a-h, image pairs of eight pharyngeal teeth with robust cross-section and grinding surface diagnostic of *Siphateles* (SBCM L3313-50, part); i, nine teeth, and j, eight teeth with sizes and shapes most like *Siphateles* (SBCM L3313-50, part); k, last rudimentary ray or first principal fin ray hemitrich with deep notch between head and shaft, most like the left dorsal or right anal fin ray bases of *Siphateles* (SBCM L3313-50, part).

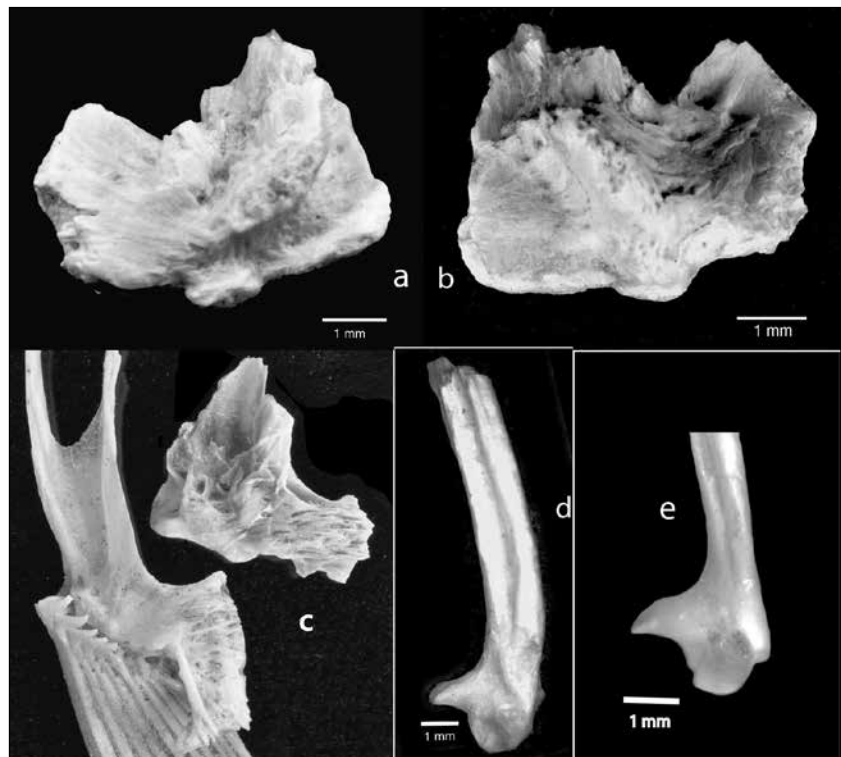


Fig. 4. *Orthodon* (or *Evomus*?), pelvic basiptyrgia and dorsal hemitrichs: a, fragmentary right basiptyrgium of *Orthodon* or *Evomus*, (dorsal view, left, ventral view, right); b, left basiptyrgium and pelvic fin rays of *Orthodon macrolepidotum*, UMMZ 179936, CA, and fragment of left basiptyrgium of *Orthodon* or *Evomus*, White Narrows (SBCM L3313-3), dorsal views; c, base of left first principal dorsal hemitrich of *Orthodon*? or *Evomus*? (SBCM L3313-4) (left image) and base of first principal dorsal hemitrich of *Orthodon macrolepidotum* (UMMZ 179936, CA).

basipterygia are distinctive enough to rule out the genera *Ptychocheilus* and *Gila*. They match the complex articulating surfaces, processes, and angles of *Orthodon* (Fig. 3 c) more than other western genera. Left hemitrichs of last rudimentary or first principal dorsal rays of *Orthodon* or *Evomus* are compared in Fig. 3 d and 3 e. One fragment of a distal part of a dentary with the mental foramen (SBCM L3313-75) may represent a Blackfish. Specimens of other bones similar to *Orthodon* are known from the Bidahochi formation, from which they were named *Evomus* by Uyeno and Miller (1965) (Spencer and others 2008). *Orthodon* is otherwise known from the Sacramento drainage and from Miocene and Pliocene fossils on the Snake River Plain (Smith and others 1982). Comparative basipterygia of *Evomus* have not yet been seen. These fossils do not match other cyprinid taxa in the Lower Colorado River Basin, so their similarity to *Orthodon*, a relative of *Evomus*, from the Bidahochi Formation, is suggested.

***Rhinichthys*, speckled dace(?) (Fig. 5)**

Questionable specimens of these small cyprinids appear in the form of extremely small pharyngeal arches and teeth, a fragment of a dentary, and an anterodorsal corner of an opercle. Pharyngeal arch (SBCM L3313-44) has a minor row of two teeth in addition to the major (ventral) row of four teeth, as in *Rhinichthys*. Plagopterin have four or five teeth in the major row and two teeth in the minor row, possibly similar to the fossils. The postventral corner of the pharyngeal arch of SBCM L3313-44 is prominently offset from the tooth-bearing anterior part of the arch, as in *Rhinichthys* but not plagopterin. Several of the teeth are similar to *Rhinichthys* and plagopterin in having a slightly convex blade rather than a grinding surface on the contact margin of the tooth (SBCM L3313-43, 44). The anterior fragment of a left dentary (SBCM L3313-44 part) has a flat oral surface and lacks sensory pores, as in *Rhinichthys*. The fragment of the opercle (SBCM L3313-75) has a deep notch at the anterodorsal corner above the condyle as in Speckled Dace.

Rhinichthys osculus is distributed in Pacific drainage streams from southwestern Canada to the Mexican border. The Colorado River forms are moderately distinctive and variable within and between the upper and lower basins, but the mtDNA haplotypes have been transferred by stream capture to neighboring drainages, including the southern Bonneville Basin and the streams in the Los Angeles Basin (Smith and Dowling 2008).

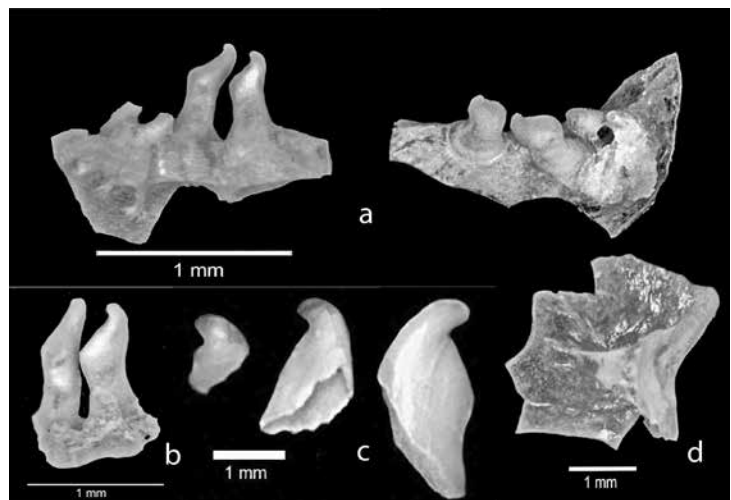


Fig. 5. *Rhinichthys*? Pharyngeal arches and teeth (SBCM L3313): a, dorsal (left) and mesial (right) views of a small minnow with two rows of teeth and an ascending process with a large angle at its base and nearly right angle to tooth bearing process (SBCM L3313-44), traits of *Rhinichthys*; b, two small attached teeth, possibly *Rhinichthys* (SBCM L3313-45); c, three isolated teeth with convex blade as in larger *Rhinichthys* SBCM L3313-43 part; d, anterodorsal corner of opercle (SBCM L-3313-75) with deep notch at hyomandibular socket as in *Rhinichthys*.

***Lepidomeda*(?), spinedace (Fig. 6)**

A single pelvic spine, 7 mm long (SBCM L3313-66) (Fig. 6) bears the unmistakable ends, grooves, and ray-like structure of the spines diagnostic of the Plagopterini or Spinedace. Spines are a unique feature of this closely-related cluster of North American species endemic to the lower Colorado River drainage in the Great Basin. The group currently ranges through the Gila, Virgin, White,

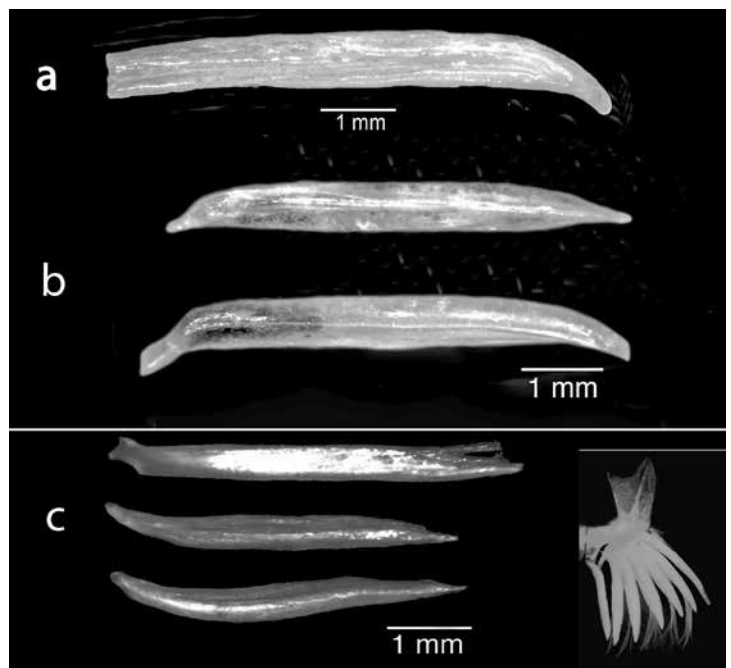


Fig. 6. Plagopterins: Pelvic spines of spinedace: a, one pelvic spine, possibly *Lepidomeda*, White Narrows formation, Clark County, Nevada (SBCM L3313-66); b, two spines, possibly *Lepidomeda*, Ellensburg Formation, Washington, South Dakota State Museum SDSM 86761, collected by Kevin Meeks; and c, *Lepidomeda albivallis*, UMMZ 212753, cleared and stained, three spines, and inverted image of pelvic girdle with seven spines, from Clark County, Nevada.

and Little Colorado river drainages. Three genera, *Plagopterus*, *Meda*, and *Lepidomeda*, bear dorsal and pelvic spines and diagnostic osteology, so distinctive as to be ranked as a family, subfamily, or tribe by early authors (Miller and Hubbs, 1960). The fossil spine is slender, as in *Lepidomeda*, and bears the distinctive autotomous distal end, slightly curved and attenuate proximal end, longitudinal groove, and slight curvature of that genus. Rudimentary fin rays emerge from near the distal end in intact forms (Fig. 6).

Spineless relatives are found in the Bonneville and upper Snake River drainages (Dowling et al. 2002). Hydrographic connections to the Northwest through the Great Basin are also indicated by the presence of the only other known fossil plagopterin spines in the Miocene Ellensburg Formation of Washington, of Clarendonian Land Mammal Age (Smith et al. in prep.).

Cyprinidae indet.

Unidentified cyprinid (and other) vertebrae (SBCM L3313-5, 6, 27, 34, 35).

One cleithral fragment, possibly cyprinid (SBCM L3313-7).

Catostomidae

Catostomus cf. *C. latipinnis*, flannelmouth sucker (Fig. 7)

A left dentary and a palatine are the most representative bones of *Catostomus* from the White Narrows. The fossil dentary (SBCM L3313-26) (Fig. 7, c, d) is compared with a recent dentary of *Catostomus latipinnis* (Fig. 7, a, b) with less than satisfactory morphological matches, but the fossil is readily distinguished from other catostomids found nearby—*Xyrauchen texanus* and *Catostomus insignis*—by the angle between the proximal and distal parts of the bone and the length and shape of the distal process. A fossil palatine (SBCM L3313-26) also diverges slightly from *Catostomus latipinnis*, but is a better match with the processes and angles of that species than with *Catostomus insignis* (Fig. 7 e, f), the unusual *Xyrauchen texanus*, and *Pantosteus* sp. (Fig. 8, see next). The sample also includes a 3 mm fragment of a right maxilla of *Catostomus* (SBCM L3313-60) and a 2.5 mm fragment of a pharyngeal with bases of six teeth (SBCM L3313-74).

Distributions of the two species of *Catostomus* suggest that *C. latipinnis* originated on the Colorado Plateau as the sister to *C. insignis* in the Great Basin waters of the Colorado River. *Catostomus insignis* is now restricted to the Gila River but was formerly as far north as the Virgin River; it is not known from the Grand Canyon. *Catostomus latipinnis* is known from Pliocene sediments in the Bidahochi area. It extended its range downstream in the Colorado River. *Xyrauchen texanus*, which is known

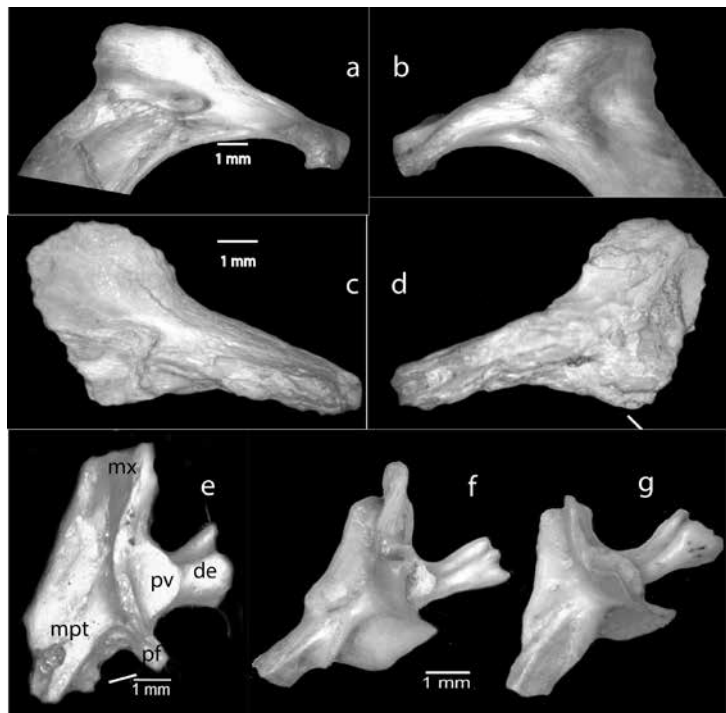


Fig. 7. *Catostomus* cf. *C. latipinnis*. a, b, *Catostomus latipinnis* left dentary, UMMZ 182423, a mesial view, b, lateral view; c, d, *Catostomus* cf. *C. latipinnis*, White Narrows formation (SBCM L3313-8), c, mesial view, d, lateral view; e, right palatine, (SBCM L3313-26), showing concave ventrolateral face diagnostic of *Catostomus*, and the long maxillary process (mx), extension of the prevomer flange (pf) from the prevomer facet (pv) to the mesopterygoid process (mpt); the dermethmoid process (de) is distinctively short; f, *Catostomus latipinnis*, right palatine, UMMZ 182423; g, *Catostomus insignis* right palatine, UMMZ 162742.

from Pliocene sediments in southern California (Hoetker and Gobalet 1999), extended its range upstream in the Colorado River, after the upper and lower basins became connected through the Grand Canyon.

Pantosteus cf. *P. clarkii*, desert sucker (Fig. 8)

Pantosteus (mountain suckers) are represented by a diagnostic dentary and a small vertebra, 4.8 mm in diameter. The dentary is readily recognizable as *Pantosteus* by the approximate right angle of the proximal vs. distal halves of the bone, the low coronoid process, and the wide symphyseal ends of the bone, extending sharply mesial from the axis of the bone (Smith and others, in press). The vertebra is the disc-shaped first vertebra in the column, recognized by the multiple pores (lateral, dorsal, and ventral). The fossil sample also includes a fragment of a dorsal hyomandibula (SBCM L3313-56) with the diagnostic posterodorsal keel of *Pantosteus*.

Pantosteus comprises about a dozen species that inhabit moderate-gradient streams from southwest Canada to central Mexico and from the Black Hills of South Dakota to the Willamette River in Oregon. The White Narrows fossil is most like *P. clarkii*, but shares some traits with *P. santaanae* of the Los Angeles basin and *P. plebeius* of the Rio Grande and Pacific drainages in Mexico. The White Narrows mountain sucker is identified as a new species related to *Pantosteus clarkii*, *P. discobolus*, and *P.*

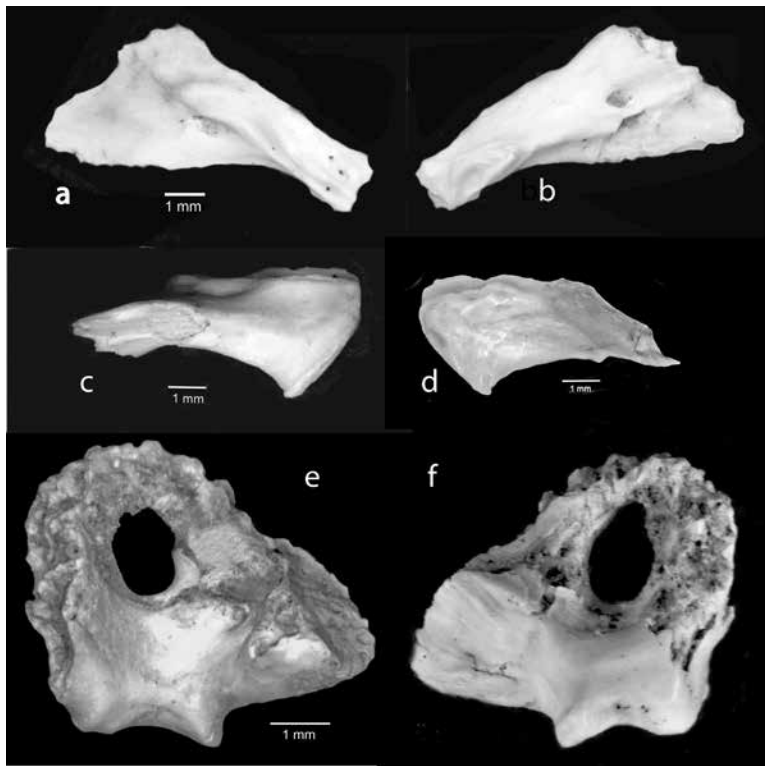


Fig. 8. *Pantosteus* sp. a-d, right dentary (SBCM L3313-23): a, lateral view, b, mesial view, c, posteroverventral view, and d, anterodorsal view; e, lateral view, and f, mesial view of left mesocorocoid (SBCM L3313-10).

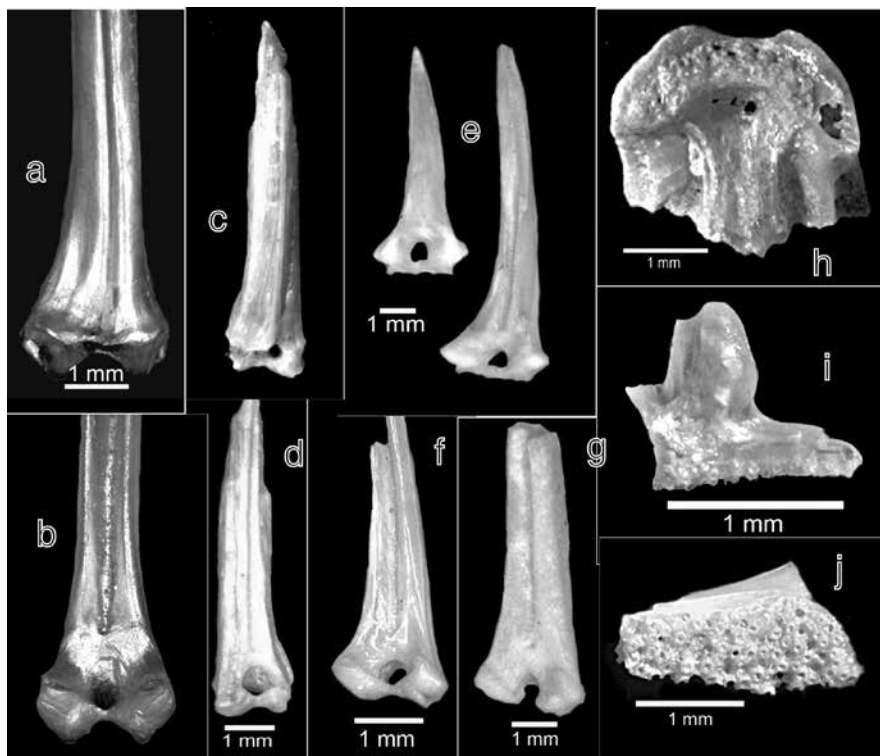


Fig. 9. *Archoplites* sp. a-b, *Archoplites interruptus* UMMZ 179978, Mendocino Co., CA: a, dorsal spine, anterior view; b, dorsal spine, posterior view. c-j, *Archoplites* sp., White Narrows formation: c, (SBCM L3313-11), median spine, anterior view; d, median spine, posterior view; e, (SBCM L3313-30 part), two median spines, posterior view; f, (SBCM L3313-30 part), median spine, posterior view; g, (SBCM L3313-30 part), median spine, posterior view; h, (SBCM L-3313-90), prevomer, ventral view; i, (SBCM L3313-59), median fragment of right premaxilla, posterior view; j, (SBCM L3313-59), mesial fragment of left premaxilla, posterior view.

santaanae in a revision of fossil and recent *Pantosteus* by Smith and others (in press).

Family Centrarchidae

Archoplites sp., western sunfish (Fig. 9, c-j)

Archoplites is represented in the SBCM collections by dozens of fragments of median spines (Figs. 9 c-g) (SBCM L3313-30 part), a prevomer (Fig. 9 h) (SBCM L3313-90), fragments of premaxillae (Figs. 9 i, j) (SBCM L3313-48), and numerous fragments of serrated edges of bones of the opercular series (SBCM L3313-51). The median spines have an enclosed foramen for articulation with their supporting pterygiophores (except where the basal bridge is abraded), a posterior groove, and basal processes for muscle attachment and anterior-posterior movement as in *Archoplites*, and paired proximal posterior processes (Fig. 9). *Plagopterus* and *Lepidomeda* are the only dorsal-spined fishes now native to the White Narrows region. *Plagopterus* has a transverse anteroventral ridge above the articulation and *Lepidomeda* has an open, not closed articulating foramen. (Both

have pelvic spines as in Fig. 6.) The fossil prevomer (SBCM L3313-90) has convex-forward margins of the tooth patch (Fig. 9 h) like *Lepomis*, unlike the posteriorly-straight tooth patch of recent *Archoplites interruptus* of the Sacramento drainage or Miocene and Pliocene *A. taylori* of the Snake River Plain, but the short median processes and wide tooth patches of the premaxillae (Fig. 9 i, j) and serrations of the facial bones identify the White Narrows fossils as *Archoplites*. The White Narrows fossils are geographically remote from its relatives in California, Oregon, Washington, Idaho, Nevada, and Utah. It is part of a much broader range in the Miocene and Pliocene than the present relict populations in the Sacramento drainage.

Summary

Eight identifiable kinds of fishes have been identified from the yellow sands at the base of the stratigraphic unit that Dwight Schmidt and others (1996) named

the White Narrows beds, at the top of the Muddy Creek Formation at Starvation Flat, Clark County, Nevada. Mammals (Reynolds and Lindsay 1999) and reptiles and amphibians (Mead and Bell 2001) from this unit were estimated biostratigraphically to be at the boundary of the Hemphillian and Blancan North American Land Mammal ages, 4.9–4.3 Ma.

White Narrows fishes are mainly Great Basin forms, but three or four species had probable origins on the Colorado Plateau. They are known from the Bidahochi area in the late Miocene and Pliocene (Uyeno and Miller, 1965; Spencer and others, 2008)—Flannelmouth Sucker, Pikeminnow, Blackfish, and possibly Speckled Dace. These probably arrived in the White Narrows area via the Colorado River spillover (Spencer and Pearthree, 2003) from the plateau to the Great Basin at 5.3 Ma (Dorsey 2012). The Colorado Pikeminnow, Speckled Dace, and Flannelmouth Sucker occupy the Colorado River drainage today. A form of Blackfish (*Orthodon* or *Evomus*) lived in the Bidahochi drainage and the Snake River Plain in the Miocene and lives only in the Sacramento River Drainage today.

Two of the fish species, a plagiopetrid spine dace, (*Lepidomeda*?) and a mountain sucker (*Pantosteus* cf. *P. clarkii*) live downstream from the fossil site in the Virgin, White, Gila, and Little Colorado river drainages today.

Two White Narrows species no longer live in the area: The Tui Chub (*Siphateles bicolor*?) lives in the eastern Great Basin and Klamath drainage, with a rich Miocene to Pleistocene fossil record on the east side of the Sierras (Smith and others 2009). The sunfish, *Archoplites*, was widespread in Miocene and Pliocene drainages from northern Nevada and northwestern Utah, across the Snake River Plain to Oregon and Washington; it lives now only in the Sacramento drainage.

The distributions of these lineages of fish are consistent with a pattern of drainage isolation, with connections between the Colorado River on the Colorado Plateau and the Snake River in the Miocene, followed by transport through the Colorado River spillover across the Grand Wash trough to the Great Basin in the earliest Pliocene (Spencer and Pearthree 2003).

Fishes of the Colorado River drainage now divide into two geographic groups, an Upper Basin Colorado Plateau fauna and a lower Colorado Great Basin fauna. Geminant pairs and two separate evolutionary radiations suggest long isolation by the uplifted plateaus at the Grand Canyon before reconnection of the drainages in the early Pliocene (Lucchitta, 1979). Bluehead Sucker, Flannelmouth Sucker, and Humpback Chub, originally on the Colorado Plateau, contrast with the Desert Sucker, Sonora Sucker, five species of spinedace, Moapa Dace, pupfish (*Cyprinodon*), and four species of splitfins (Goodeidae), in the Lower Colorado drainage in the Great Basin. (Few species—strong swimmers or littoral inhabitants—colonized through Grand Canyon and across both upper and lower basins in the past 5 million years.)

The fauna indicates a wetter environment in the early Pliocene than today, with abundant standing water, high gradient to low gradient streams, and a nearby large river. Small sunfish live in warm, low-energy waters, small mountain suckers inhabit cool mountain streams with moderate gradient and current. Small Speckled Dace and spinedace inhabit a wide range of small, low-energy fluvial habitats. Mid-sized Tui Chubs, Blackfish, and *Catostomus* suckers were probably generalists in both large standing waters and streams. The most important habitat indicator is the Colorado Pike Minnow, which because of its huge size (about 1.5 m) and body shape, indicates proximity to a large fluvial environment like the Colorado River both at White Narrows and in the Bidahochi lake.

Acknowledgements

Eric Scott, curator of paleontology at the San Bernardino County Museum, facilitated the loan of fossil specimens for this study. Nate Carpenter and Ev Lindsey assisted with field reconnaissance and answered many questions. John Megahan of the University of Michigan Museum of Zoology helped with the figures. We thank William J. Kilday for his extensive efforts in processing most of the fossils and Nate Carpenter for his helpful review of the manuscript.

References

- Anderson, R.E., 1978, Geologic map of the Black Canyon 15' Quadrangle, Mojave County, Arizona and Clark County, Nevada: U.S. Geological Survey Geologic Quadrangle Map GQ-1394, scale 1:62,500.
- Beard, S.L., 1993, Tertiary stratigraphy of the South Virgin Mountains, southeast Nevada, and the Grand Wash Trough, northwest Arizona, in Sherrod, D.R. and Nielson, J.E., editors, U.S. Geological Survey Bulletin 2053, p. 29–32.
- Bell, C.J., Lundelius, E.L. Jr., Barnosky, A.D., Graham, R.W., Lindsay, E.H. Ruez, D.R. Jr., Semken, H.A., Jr., Webb, S.D., and Zakrzewski, R.J., 2004, The Blancan, Irvingtonian, and Rancho Labrean Mammal Ages, in Woodburne, M.O., ed., *Cenozoic Mammals of North America, Geochronology and Biostratigraphy*: Berkeley, University of California Press, p. 232–314.
- Bohannon, R.G., 1984, Nonmarine sedimentary rocks of Tertiary age in the Lake Mead region, southeastern Nevada and northwestern Arizona: U.S. Geological Survey Professional Paper 1259, 72 p.
- Bohannon, R.G., Grow, J.A., Miller, J.J., and Blank, R.H., Jr., 1993, Seismic stratigraphy and tectonic development of Virgin River depression and associated basins, southeastern Nevada and northwestern Arizona: *Geological Society of America Bulletin* v. 105, p. 501–520.
- Buising, A.V., 1992, The Bouse Formation and bracketing units, southeastern California and western Arizona, in Reynolds, R.E., compiler, *Old Routes to the Colorado*: San Bernardino County Museum Special Publication v. 92-2, p. 103.
- Castor, S.B., and Faulds, J.E., 2003, Post-6 Ma limestone along the southeastern part of the Las Vegas Valley Shear Zone,

- southern Nevada, in Young, R.A., and Spamer, E.E., editors, *Colorado River Origin and Evolution: Grand Canyon Association Monograph 12*, p. 77-79.
- Czaplewski, N. J., 1990, The Verde local fauna: small vertebrate fossils from the Verde Formation, Arizona: *San Bernardino County Museum Association Quarterly*, v. 37, no. 3, 39 p.
- Dalquest, W.W., and Carpenter, R.M., 1986, Dental characters of some fossil and recent kangaroo rats with description of a new species of Pleistocene *Dipodomys*: *Texas Journal of Science*, v. 38, no. 3, p. 251-264.
- Damon, P. E., Shafiqullah, M. J., and Scarborough, R. B., 1978, Revised chronology for critical stages in the evolution of the lower Colorado River: *Geological Society of America, Abstracts with Programs* v. 10, no. 3, p. 101-102.
- Dorsey, R., 2012, Earliest delivery of sediment from the Colorado River to the Salton Trough at 5.3 Ma: evidence from Split Mountain Gorge: *Desert Symposium 2012*, p. 88-93.
- Dowling, T.E., Tibbets, C.A., Minckley, W.L., and Smith, G.R., 2002, Evolutionary relationships of the plagiopeterns (Teleostei: Cyprinidae) from Cytochrome B sequences: *Copeia* 2002, p. 665-678.
- Farrell, J.M., and Pederson, J.L., 2001, Finding the pre Grand Canyon Colorado River: Petrology of the Muddy Creek Formation north of Lake Mead: *Rocky Mountain and South-Central Sections, GSA*. 2001, Abstracts.
- Faulds, J.E., Price, L.M., and Wallace, M.A., 2003, Pre-Colorado River paleogeography and extension along the Colorado Plateau-Basin and Range boundary, northwestern Arizona, in Young, R.A., and Spamer, E.E., editors, *Colorado River Origin and Evolution: Grand Canyon Association Monograph 12*, p. 93-99.
- Gardner, L.R., 1968, The Quaternary geology of the Moapa Valley, Clark County, Nevada: Pennsylvania State University, Ph.D. dissertation, 162 p.
- Hoetker, G.M., and Gobalet, K.W., 1999, Fossil Razorback Sucker (Pisces, Catostomidae, *Xyrauchen texanus*) from southeastern California: *Copeia*, 1999, p. 755-759.
- House, K.P., Pearthree, P.A., and Perkins, M.E., 2007, Stratigraphic evidence for the role of lake-spillover in the inception of the lower Colorado River in southern Nevada. *CSU Desert Symposium volume 2007*, p. 38 - 49.
- Howard, K.A., and John, B.E., 1987, Crustal extension along a rooted system of imbricate low-angle faults: Colorado River extensional corridor, California and Arizona, in Coward, J.F., and Hancock, P.L., editors, *Continental Extensional Tectonics: Geological Society Special Publication 28*, p. 299-311.
- Hunt, C.B., 1956, *Cenozoic Geology of the Colorado Plateau*: U.S. Geological Survey Professional Paper 279, 99 p.
- Korth, W.W., 1998, Rodents and lagomorphs (Mammalia) from the Late Clarendonian (Miocene) Ash Hollow Formation, Brown County, Nebraska: *Annals of Carnegie Museum*, v. 67, no. 4, p. 299-348.
- Lindsay, E.H., Mou, Y., Downs, W., Pederson, J. Kelly, T., Henry, C., and Trexler, J., 1999, Resolution of the Hemphillian/Blancan boundary in Nevada: *Journal of Vertebrate Paleontology*, v. 19, p. 59.
- Longwell, C. R., Pampeyan, E. H., Bowyer, Ben and Roberts, R. J., 1965, *Geology and mineral deposits of Clark County, Nevada*: Nevada Bureau of Mines, Bulletin 62, 218 p.
- Lucchita, Ivo, 1979, Late Cenozoic uplift of the southwestern Colorado Plateau and adjacent lower Colorado River region, in McGetchin, T.R., and Merrill R.B., editors, *Plateau uplift - mode and mechanism: Tectono Physics*, v. 61, p. 63-95.
- Lucchitta, I., and Jeanne, R.A., 2003, Geomorphic features and processes of the Shivwits Plateau, Arizona, and their constraints on the age of western Grand Canyon, in Young, R.A., and Spamer, E.E., editors, *Colorado River Origin and Evolution: Grand Canyon Association Monograph 12*, p. 65-69.
- Martin, R. A., Goodwin, H. T., and Farlow, J. O., 2002, Late Neogene (late Hemphillian) rodents from the Pipe Creek Sinkhole, Grant County, Indiana: *Journal of Vertebrate Paleontology*, v. 22, no. 1, p. 137-151.
- Mead, J.I., Sankey, J.T, McDonald, H.G., 1998. Pliocene (Blancan) herpetofauna from the Glenns Ferry Formation, southern Idaho, in Akersten, W., McDonald, H., Meldrum, D., and Flint, M., editors: *Idaho Museum of Natural History Miscellaneous Paper 36*, p. 94-109.
- Mead, J.I., and Bell, C.J., 2001, Pliocene Amphibians and Reptiles from Clark County, Nevada: *Southern California Academy of Sciences Bulletin* 100(1), p. 1-11.
- Miller, R.R., and Hubbs, C.L. 1960. The spiny-rayed cyprinid fishes (Plagiopeterni) of the Colorado River System: *Miscellaneous Publications of the University of Michigan Museum of Zoology* 115, 39 p.
- Mou, Yun. 2011. Cricetid rodents from the Pliocene Panaca Formation, southeastern Nevada, USA: *Palaeontologia Electronica* v. 14, 31A, 53 p.
- Pederson, Joel L., 2008. The mystery of the pre-Grand Canyon Colorado River—Results from the Muddy Creek Formation. *GSA Today*, Vol 18, No. 3, pp. 4-10.
- Reynolds, R.E., and Lindsay, E.H., 1999. Late Tertiary Basins and Vertebrate Faunas along the Nevada/Utah Border, in Gillette, D. D. editor, *Vertebrate Paleontology in Utah*. *Miscellaneous Publications of the Utah Geological Survey*, 99-1, p. 469-478.
- Reynolds, S.J., Florence, F.P., Welty, J.W., Roddy, M.S., Currier, D.A., Anderson, A.V., Keith, S.B., 1986, *Compilation of radiometric age determination in Arizona*: Arizona Bureau of Geology and Mineral Technology, Bulletin 197, 258 p.
- Rowley, P.D., Nealey, L.D., Unruh, D.N., Snee, L.W., Mehnert, H.H., Anderson, R.E., and Gromme, C. S., 1995, Stratigraphy of Miocene Ash-flow Tuffs in and near the Caliente Caldera Complex, southeastern Nevada and southwestern Utah: *U.S. Geological Survey, Bulletin* 2056B: p. 47-88.
- Rowley, P.D. and Shroba, R.R., 1991, *Geologic map of the Indian Cove Quadrangle, Lincoln County, Nevada*: U.S. Geological Survey, Map GQ-1701, scale 1:24,000.
- Rowley, P.D., Shroba, R.R., Simonds, P.W., Burke, K.J., Axen, G.J., and Olmore, S.D., 1994, *Geologic map of the Chief mountain Quadrangle, Lincoln County, Nevada*: U.S. Geological Survey, Map GQ-1781, scale 1:24,000.

- Ruez, D.R., Jr., 2009. Revision of the Blacn (Pliocene) mammals from Hagerman Fossil Beds National Monument, Idaho. *Journal of the Idaho Academy of Science*, 45(1): 1-143.
- Schmidt, D.L., Page, W.R., and Workman, J.B., 1996. Preliminary geologic map of the Moapa West Quadrangle, Clark County, Nevada: U.S. Geological Survey, O.F.R. 96-521, scale 1:24,000.
- Smith, G.R. 1966. Distribution and evolution of the North American catostomid fishes of the subgenus *Pantosteus*, genus *Catostomus*. *Miscellaneous Publications of the University of Michigan Museum of Zoology* 129: 1-133.
- Smith, G.R., Reynolds, R.E., Serrano, R.J. 2009. Recent records of fossil fish from eastern Owens Lake, Inyo County, California. *Desert Symposium 2009*: 177-183.
- Smith, G.R., and Dowling, T.E., 2008, Correlating hydrographic events and divergence times of speckled dace (*Rhinichthys Teleostei*, *Cyprinidae*), in the Colorado River drainage, in Reheis, M., Hershler, R., Miller, D., editors, *Late Cenozoic Drainage History of the Southwestern Great Basin and Lower Colorado River Region: Geologic and Biotic Perspectives*. *Geological Society of America Special Publication* 439: p. 301-317.
- Smith, G.R., Swirydczuk, K., Kimmel, P.G., and Wilkinson, B.H., 1982, Fish biostratigraphy of late Miocene to Pleistocene sediments of the western Snake River Plain, Idaho, in B. Bonnicksen and R.M. Breckenridge, editors, *Cenozoic Geology of Idaho*: Idaho Bur. Mines and Geol. Bull. 26, p. 519-542.
- Smith, G.R., Stewart, J.D., Carpenter N.E., 2013. New fossil and recent Mountain Suckers and evolution of *Pantosteus* (*Teleostei*, *Catostomidae*) in Western United States. *Occasional Papers of the University of Michigan Museum of Zoology* (in press).
- Spencer, J.E., and Pearthree, P.A. 2003, Headward erosion versus closed-basin spillover as alternative causes of Neogene capture of the ancestral Colorado River by the Gulf of California, in Young, R.A., and Spamer, E.E., editors, *Colorado River Origin and Evolution: Grand Canyon Association Monograph* 12, p. 215-219.
- Spencer, J.E., Peters, L., McIntosh, W.C., Patchett, P.J., 2003, $^{40}\text{Ar}/^{39}\text{Ar}$ geochronology of the Hualapai Limestone and Bouse Formation and implications for the age of the Lower Colorado River, in Young, R.A., and Spamer, E.E., editors, *Colorado River Origin and Evolution: Grand Canyon Association Monograph* 12, p. 89-92.
- Spencer, J.E., Smith, G.R., and Dowling, T.E., 2008, Middle to Late Cenozoic geology, hydrography, and fish evolution in the American Southwest, in Reheis, M., Hershler, R., and Miller, D., editors, *Late Cenozoic Drainage History of the Southwestern Great Basin and Lower Colorado River Region: Geologic and Biotic Perspectives: Geological Society of America Special Paper* 439: p. 279-299.
- Stock, Chester, 1921, Later Cenozoic mammalian remains from Meadow Valley Region, southeastern Nevada: *American Journal of Science*. v. 2, p. 250-264.
- Tedford, R.H., Skinner, M.F., Fields, R.W., Rensberger, J.M., Whistler, D.P., Galusha, Ted, Taylor, B.E., MacDonald, J.R., and Webb, S.D, 2004, Faunal succession and biochronology of the Arikaarean through Hemphillian interval (late Oligocene through earliest Pliocene epochs) in North America in Woodburne, M.O. editor, *Cenozoic Mammals of North America — Geochronology and Biostratigraphy*: Berkeley, University of California Press, p. 153-210.
- Wallin, E.T., Duebendorfer, E.M., and Smith, E.I., 1993, Tertiary stratigraphy of the Lake Mead Region: PN 33-35, in U.S. Geological Survey Bulletin 2053, 250 p.
- Uyeno, T., and Miller, R.R., 1965, Middle Pliocene cyprinid fishes from the Bidahochi Formation, Arizona: *Copeia* 1965, p. 28-41.
- Woodburne, M.O. and Swisher III, C.C., 1995, Land mammal high-resolution geochronology, intercontinental overland dispersal, sea level, climate and vicariance: *Geochronology, Time Scales, and Global Stratigraphic Correlation*, SEPM Special Publication No. 54, p. 335-364.

The terror bird, *Titanis* (Phorusrhacidae), from Pliocene Olla Formation, Anza-Borrego Desert State Park, southern California

Robert M. Chandler,¹ George T. Jefferson,² Lowell Lindsay,² and Susan P. Vescera²

¹Biological and Environmental Science, Georgia College, Milledgeville, Georgia 31061

²Department of Parks and Recreation, Colorado Desert District Stout Research Center, Borrego Springs, California 92004

ABSTRACT—During the Great American Biotic Interchange that took place after the formation of the Panamanian Land Bridge, *Titanis walleri* (family Phorusrhacidae, known as terror birds) entered southern-most North America during the mid-Pliocene. Specimens of these 2 m-tall, 150 kg flightless birds are known from Florida, and a single specimen from the gulf coast of Texas. Unfortunately, most are postcranial remains and no premaxillae are known. The anterior-most part of a premaxilla (beak), ABDSP(LACM) 6747/V26697, from the Olla Formation, 3.7 Ma, Anza-Borrego Desert State Park, was recently re-identified as *Titanis* and is comparable to the South American *Patagornis marshi*. The specimen was previously assigned to *Aiolornis incredibilis*. This new identification is important for several reasons: 1) it represents a significant geographic range extension for the genus; 2) it may represent the oldest known *Titanis* remains from the US; and 3) it reinforces the tropical aspect of the paleoenvironment of the Pliocene Epoch ancestral Colorado River deltaic deposits within the Salton Trough, California.

Introduction

Titanis is a member of the family Phorusrhacidae, commonly called terror birds. The family includes numerous genera and species (de Alvarenga and Höfling 2003) that range through a major part of the Cenozoic Era, 62 to about 2 Ma. All are South American in distribution except for a single taxon *Titanis walleri* (Brodkorb 1963) from North America. *T. walleri* is considered a valid genus distinguished from other taxa on the slender character of the tarsometatarsus (de Alvarenga and Höfling 2003).

The Phorusrhacidae entered North America via the Panamanian Land Bridge as part of the Great American Biotic Interchange (Webb 1985).

The first phorusrhacid fossils were found in Florida by scuba diver Ben Waller in 1962, hence the specific nomen *Titanus walleri* (Brodkorb 1963). While diving in the Santa Fe River, Gilchrist County, Florida, Waller recovered a tarsometatarsus and Digit III, proximal phalanx. A comparable Digit III, proximal phalanx, was found later in a gravel pit along the Nueces River, San Patricio County near Corpus Christi, Texas (Baskin 1995). Fewer than 50 specimens of *T. walleri* have been reported from the US, and all but the Texas specimen are from four localities in Florida. Most are post cranial elements, and no premaxillae are known (Chandler 1994; de Alvarenga and Höfling 2003; Gould and Quitmyer 2005). The age and identity of these materials have been the subject of discussion and controversy (Gould and Quitmyer 2005), and have an estimated age range from <5 to 2.2–1.8 Ma (McFadden et al. 2007).

The *Titanis* sp. from ABDSP represents a significant range extension from the previously known paleogeographic distribution on the Texas gulf coast and Florida. And, it better constrains the age range of *Titanis* in North America.

Abbreviations are: ABDSP = Anza-Borrego Desert State Park; LACM = Los Angeles County Museum of Natural History. We thank Lyn Murray for his critical review and helpful comments.

Material and occurrence

The *Titanis* sp. premaxilla, ABDSP(LACM) 6747/V26697 (field locality TD 1073), was found by G. Davidson Woodard in 1961. Woodard worked as a geologist with Ted Downs of the Los Angeles County Museum. The specimen was recovered from the lower part of the Olla Formation (Cassiliano 2002) exposed in the Fish Creek/Vallecito Creek Basin of the southern part of ABDSP. The Olla Formation is typified by packages of ancestral Colorado River, well sorted, medium-grained quartzose deltaic sandstone that are interbedded with apparently locally derived packages of poorly sorted, feldspathic fluvial sandstone (Winker 1987). The specimen was recovered from the fluvial part of the formation. It was mapped within the stratigraphic section by Downs as within CZ 23.7 (collecting zone, or CU collecting units of Cassiliano 1999). This horizon falls within reversed subchron C2Ar (4.18–3.58 Ma), and based on the magnetostratigraphy of Dorsey et al. (2011) the interpolated age is 3.7 Ma.

The phorusrhacid identity of the ABDSP specimen was first recognized by Chandler (pers. comm. 2009,

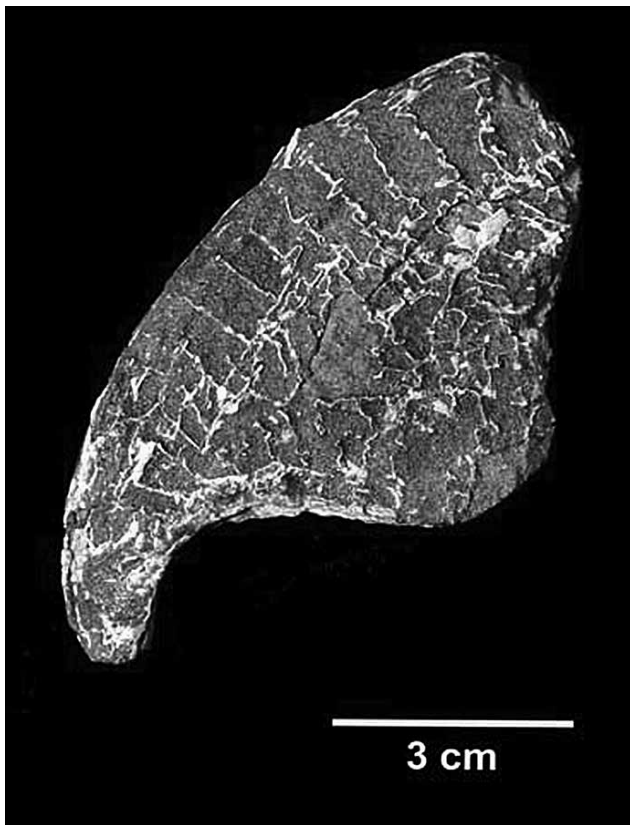


Figure 1. Left lateral view of the anterior portion of premaxilla ABDSP(LACM) 6747/V26697 (image from Jefferson 2006, Jefferson et al. 2012, photographed by B. Marrs).

Jefferson et al. 2012). The specimen (Fig. 1) represents only the anterior-most portion of the premaxilla, and was described in detail by Howard (1972) who placed it the genus *Teratornis*. The specimen largely consists of the permineralized internal portion of the premaxilla with culmen and exposed trabeculae, lacking much cortical bone which apparently has been weathered away. ABDSP (LACM) 6747/V26697 measures 90.8 mm in length, 55.4 mm in height, and 27.5 mm in maximum width across the palate. The specimen is triangular in vertical cross section, with a relatively sharp dorsal crest and flat sides. It exhibits a chord (arc) of the partial culmen (exposed premaxilla) that is identical to that in *Patagornis marshi* (previously *Phororhacos inflatus*, Andrews 1899). ABDSP (LACM) 6747/V26697 has a complete bony palate, not an open, vaulted premaxilla like *Aiolornis*, to which it was referred by Campbell (1999). The specimen has an internal morphology, as revealed in coronal scan (L. Witmer pers. comm. 2009), that is identical in construction to a beak like *Patagornis* with an open space or chamber inside.

The premaxilla, ABDSP (LACM) 6747/V26697, and a wing bone, ABDSP (LACM) 1318/V3803 that was recovered from the Pleistocene Hueso Formation, were both placed in the genus *Teratornis* by Howard (1963, 1972). An additional *Teratornis* specimen, ABDSP(IVCM) 519/V5660, was reported by Jefferson (1995). In 1999 the genus *Teratornis* was divided into two genera and all specimens from ABDSP that were previously assigned to *Teratornis*

(Howard 1963, 1972; Jefferson 1995, 2006) were placed in the new genus *Aiolornis* by Campbell et al. (1999). It should be noted that the premaxilla is about 2.5 Ma older than other materials assigned to *Aiolornis* from ABDSP. All of the above specimens except ABDSP (LACM) 6747/V26697 remain assigned to *Aiolornis incredibilis*.

Discussion

The ABDSP specimen at 3.7 Ma falls within the estimated temporal range for *Titanis*, <5 to 2.2–1.8 Ma (McFadden et al. 2007). The estimate for a maximum age of <5 Ma is based on the Texas specimen, which was recovered from late Pleistocene sediments, ca. 13 ka BP. However, it has a rare-earth-element signature of early Pliocene materials and may have been re-worked from older deposits transported from upstream and mixed with the Pleistocene deposit (McFadden et al. 2007). The materials from Florida sites are estimated to be between 2.2 and 1.8 Ma (McFadden et al. 2007). Most of those specimens were recovered from a mid-channel accumulation, SF1A, but are traceable to in-place sediments of SF1B. The proximal humerus, UF 137839, was found at SFB1 and is Blancan NALMA in age. ABDSP (LACM) 6747/V26697 is the only specimen from North America that has a well supported date, and may be the oldest record.

The Arroyo Diablo and Olla formations, which are stratigraphically lateral equivalents (Winker 1987; Cassiliano 2002), yield a fossil wood assemblage that includes tropical taxa such as *Persea podadenia* (avocado) and *Washingtonia* sp. (fan palm) (Remeika 2006). Although vertebrate remains from these stratigraphic units are rare, they include tropical wetland forms such as Gomphotheriidae (elephant-like gomphothere) and subtropical taxa such as *Hesperotestudo* (giant tortoise) and *Pumelia novaceki* (iguana). These and *Titanis* reinforce the idea that the Pliocene fossil record from ABDSP exhibits a tropical to subtropical paleoenvironment not unlike the southern-most US, proximal to the Gulf of Mexico and Mexico at that time.

References

- Andrews, C. W. 1899. On the extinct birds of Patagonia, I. The skull and skeleton of *Phororhacos inflatus* Ameghino. Transactions of the Zoological Society of London 15(3):55-86.
- Baskin, J. A. 1995. The giant flightless bird *Titanis walleri* (Aves: Phorusrhacidae) from the Pleistocene coastal plain of south Texas. Journal of Vertebrate Paleontology 15 (4): 842-844.
- Brodkorb, P. 1963. A giant flightless bird from the Pleistocene of Florida. Auk 80(2):111-115.
- Campbell, K. E., Jr., E. Scott, and K. B. Springer 1999. A new genus for the incredible teratorn (Aves: Teratornithidae). In Avian Paleontology at the Close of the 20th Century: Proceedings of the 4th International Meeting of the Society of Avian Paleontology and Evolution, edited by S.L. Olson, Smithsonian Contributions to Paleobiology 89:169-175.
- Cassiliano, M. 2002. Revision of the stratigraphic nomenclature of the Plio-Pleistocene Palm Spring Group (new rank),

- Anza-Borrego Desert, southern California. Proceedings of the San Diego Society of Natural History 38:1-30.
- Chandler, R. M. (1994). The wing of *Titanis walleri* (Aves: Phorusrhacidae) from the late Blancan of Florida. Bulletin of the Florida Museum of Natural History, Biological Sciences, 36: 175-180.
- de Alvarenga, H., and E. Höfling 2003. Systematic revision of the Phorusrhacidae (Aves: Ralliformes). Papeis Avulsos de Zoologica 43(4):55-91.
- Dorsey, R. J., B. A. Housen, S. U. Janecke, C. M. Fanning, and A. L. F. Spears 2011. Stratigraphic record of basin development within the San Andreas fault system: Late Cenozoic Fish Creek-Vallecito basin, southern California. Geological Society of America Bulletin 123(5,6):771-793.
- Gould, G. C., and I. R. Quiltymer 2005. *Titanis walleri*: bones of contention. Bulletin of the Florida Museum of Natural History 45(4):201-229.
- Howard, H. H. 1963. Fossil birds from the Anza-Borrego Desert. Los Angeles County Museum Contributions in Science 73:1-33.
- Howard, H. H. 1972. The incredible teratorn again. The Condor 74(3):341-344.
- Jefferson, G. T. 1995. An additional avian specimen referable to *Teratornis incredibilis* from the early Irvingtonian, Vallecito-Fish Creek Basin, Anza-Borrego Desert State Park, California. In *Paleontology and Geology of the western Salton Trough Detachment, Anza-Borrego Desert State Park, California*, edited by P. Remeika and A. Sturz, Field Trip Guidebook and volume for the 1995 San Diego Association of Geologist's field trip to Anza-Borrego Desert State Park, Volume 1:94-96.
- Jefferson, G. T. 2006. The fossil birds of Anza-Borrego. In *The Fossil Treasures of the Anza-Borrego Desert*, edited by G.T. Jefferson and L. Lindsay, Sunbelt Publications, San Diego, California p. 151-158.
- Jefferson, G. T., L. K. Murray, and S. D. Keeley 2012. The Pliocene fossil record of Anza-Borrego Desert State Park, western Salton Trough, California. In *Search for the Pliocene: the Southern Exposures*, edited by R.E. Reynolds, California State University Desert Studies Consortium, The 2012 Desert Research Symposium pp. 77-87.
- McFadden, B., Labs-Hochstein, J. Hulbert, and J. Baskin 2007. Revised age of the late Neogene terror bird (*Titanis*) in North America during the Great American Interchange. *Geology* 35(2):123-126.
- Webb, S. D. 1985. Late Cenozoic mammal dispersals between the Americas. In *The Great American Biotic Interchange, Topics in Geobiology*, Plenum Press, 4:357-386.
- Witmer, L. (pers. comm.) 2009. Department of Biomedical Sciences, College of Osteopathic Medicine, Ohio University, Athens, Ohio.
- Winker, C. D. 1987. Neogene stratigraphy of the Fish Creek-Vallecito section, southern California: implications for early history of the northern Gulf of California and Colorado delta. Doctoral Dissertation, University of Arizona, Tucson 494 p.

Persistent drought lowers estimated survival in adult Agassiz's desert tortoises (*Gopherus agassizii*) in Joshua Tree National Park: a multi-decadal perspective

Jeffrey Lovich,¹ Charles B. Yackulic,¹ Jerry Freilich,² Mickey Agha,¹ Meaghan Meulblok,¹ Kathie Meyer,³ Terence R. Arundel,¹ Jered Hansen,¹ Michael Vamstad,⁴ and Stephanie Root⁴

¹ U.S. Geological Survey, Southwest Biological Science Center, 2255 North Gemini Drive, MS 93-94, Flagstaff, AZ 86001 (corresponding author jeffrey_lovich@usgs.gov)

² National Park Service, Olympic National Park, North Coast & Cascades Science Learning Network, 600 East Park Ave, Port Angeles, WA 98362

³ 19233 Stratford Way, Apple Valley, CA. 92308

⁴ National Park Service, Joshua Tree National Park, 74485 National Park Drive, Twentynine Palms, CA 92277-3597

Deserts are model ecosystems for studying the effects of limited and unpredictable inputs of precipitation on wildlife (Noy-Meir, 1973). This is particularly true for herbivorous species, like the federally threatened Agassiz's desert tortoises (*Gopherus agassizii*), that are reliant on annual plant production for survival. Germination and productivity of annual plants in the Mojave Desert is tightly coupled with precipitation quality and quantity (Beatley 1967, 1974). Precipitation is highly variable both within and among years, occurring in infrequent and discrete events.

Longevity is one trait that organisms can use to cope with stochastic environmental conditions. Simply stated,

if environmental variation results in concomitantly variable reproductive success, selection will favor reduced reproductive output, greater longevity, and a longer reproductive lifespan (Murphy 1968, Schaffer 1974). The desert tortoise is a long-lived species with an estimated generation time of about 25 years (Edwards et al. 2004) and longevity exceeding 50 years (Germano 1992). Data from long-term studies are needed to accurately measure survivorship and demographic parameters in long-lived species but they are rarely available due to associated logistical and funding constraints (Tinkle 1979).

We analyzed data collected from a population of desert tortoises at a 2.59 km² study plot in the Sonoran

Desert ecosystem of Joshua Tree National Park from 1978-2012 providing a 34 year (≈ 1.4 tortoise generations) perspective on estimated survival and demography in this long-lived species. The study site, was established in 1978 (Barrow 1978) in the Pinto Basin and is known as the Barrow Plot. Systematic transect-based, mark-recapture surveys were conducted during 10 years from 1978-2012 to locate living and dead tortoises (Figure 1). We acquired winter precipitation data (October-March) from WestMap, a fine scale climate mapping program that uses PRISM (Parameter-elevation Regressions on Independent Slopes Model) data to project regional climate. PRISM uses a digital elevation model of topography and nearest point measurements of climate data to generate estimates of monthly climate parameters, including precipitation: (http://www.cefa.dri.edu/Westmap/Westmap_home.php). To test hypotheses about the effects of multiyear drought on survival we calculated covariates based on average annual estimated precipitation in the prior year, the prior 2 years and the



Figure 1. The carcass of a female Agassiz's desert tortoise encountered on 8 May, 2012 at the Barrow Plot in Joshua Tree National Park. The anterior is facing the right side of the photograph. The tortoise was first marked as ID number 88 in 1993 and equipped with a radio transmitter as shown by the traces of epoxy on the shell. The cause and date of death is unknown but bite marks consistent with scavenging or predation by a mammalian carnivore are visible near the edge of the shell between the 12 to 2 o'clock positions (if the anterior of the shell is considered to be 12 o'clock).



Figure 2. Tortoise body parts contained in a single coyote (*Canis latrans*) scat found in Joshua Tree National Park. Note the juvenile tortoise foot in the center. Other parts include adult toe nails and forelimb scales, and various shell scutes. The tortoises may have been preyed upon or scavenged by the coyote. Scale under the petri dish is 1 cm.

prior 3 years. We used only survivorship data collected from 1991-2012 in the analysis but included data back to 1978 for population size and demographic comparisons. Additional details on our estimated survivorship analyses will be published elsewhere.

Point estimates of adult (≥ 18 cm shell length) annual survivorship ranged from 0.64 to almost 1. High estimated survival was observed from 1978-1996 but decreased from 1997-2002, concurrent with persistent drought. The best model relating estimated survivorship of tortoises over time was based on three year moving average estimated winter precipitation, a possible result of exaptations of the species (Morafka and Berry 2002) that buffer against shorter-term environmental variation, but not persistent drought. Studies conducted elsewhere in the range of Agassiz's desert tortoise also show that populations experience high mortality after two or more years of drought (Longshore et al. 2003, Peterson 1994).

Only one tortoise found in 2012 exhibited symptoms consistent with upper respiratory tract disease. Disease was rarely observed in earlier surveys suggesting that it was not a significant factor affecting estimated survivorship. In contrast, some live and many dead tortoises found in 2012 showed signs of predation or scavenging by mammalian carnivores. Coyotes preyed upon radio-telemetered tortoises from 1997-1999. Coyote scats examined from the site confirmed their role as tortoise predators and scavengers in 2012 (Figure 2). However, a majority of dead tortoises found in 2012 exhibited characteristics that were consistent with death by dehydration and starvation.

Predation rates may have been exacerbated by drought when carnivores switched from preferred prey including

rabbits and small rodents to tortoises, as noted in previous studies (Woodbury and Hardy 1948, Peterson 1994). Climate change modeling suggests that the Joshua Tree region will be subjected to longer duration droughts in the future and that the habitat may become unsuitable for continued tortoise survival (Barrows 2011). Our results showing wide fluctuations in estimated survival and decreasing tortoise density over time may be early signals of that possible outcome.

Literature cited

- Barrow, J. 1979. Aspects of ecology of the desert tortoise *Gopherus agassizi*, in Joshua Tree National Monument, Pinto Basin, Riverside County, California. Proc. Symp. Desert Tortoise Council 1979: 105-131.
- Barrows, C.W. 2011. Sensitivity to climate change for two reptiles at the Mojave-Sonoran Desert interface. Journal of Arid Environments 75:629-635.
- Beatley, J.C. 1967. Survival of winter annuals in the northern Mojave Desert. Ecology 48:745-750.
- Beatley, J.C. 1974. Phenological events and their environmental triggers in Mojave Desert ecosystems. Ecology 55:856-863.
- Edwards, T., Schwalbe, C., Swann, D., Goldberg, C. 2004. Implications of anthropogenic landscape change on inter-population movements of the desert tortoise (*Gopherus agassizii*). Conservation Genetics 5:485-499.
- Germano, D.J. 1992. Longevity and age size relationships of populations of desert tortoises. Copeia 1992:367-374.
- Longshore, K.M., Jaeger, J.R., Sappington, J.M., 2003. Desert tortoise (*Gopherus agassizii*) survival at two eastern Mojave Desert sites: death by short-term drought? J. Herpetol. 37:169-177.
- Morafka, D.J., Berry, K.H. 2002. Is *Gopherus agassizii* a desert-adapted tortoise, or an exaptive opportunist? Implications for tortoise conservation. Chelonian Conservation and Biology 4:263-287.
- Murphy, G.I. 1968. Pattern in life history and the environment. The American Naturalist 102: 391-403.
- Noy-Meir, I. 1973. Desert ecosystems: environment and producers. Annual Review of Ecology and Systematics 4:25-51.
- Peterson, C.C. 1994. Different rates and causes of high mortality in two populations of the threatened desert tortoise *Gopherus agassizii*. Biological Conservation 70:101-108.
- Schaffer, W.M. 1974. Optimal reproductive effort in fluctuating environments. The American Naturalist 108:783-790.
- Tinkle, D.W. 1979. Long-term field studies. BioScience 29:717.
- Woodbury, A.M., Hardy, R. 1948. Studies of the desert tortoise, *Gopherus agassizii*. Ecol. Monogr. 18:145-200.

Changes in the paleogeographic distribution of *Mammut* in the southwestern United States and northwestern Mexico during the Pliocene and Pleistocene epochs

George T. Jefferson

Department of Parks and Recreation, Colorado Desert District Stout Research Center, Borrego Springs, California 92004

Introduction

In North America, the family Mammutidae (mastodons) is comprised of two genera, *Zygodolophodon* (junior synonym *Miomastodon*) and *Mammut* (junior synonym *Pliomastodon*). *Zygodolophodon*, which is also known from the Old World, first appears in North America during the late Hemingfordian (early Miocene) North American Land Mammal Age (NALMA) and ranges into the Clarendonian NALMA (early late Miocene) (Lambert and Shoshani 1998). *Zygodolophodon* is the ancestor of *Mammut* which first appears during the Clarendonian NALMA. *Zygodolophodon* and *Gomphotherium* (a genus in the closely related family Gomphotheriidae) are known from the Barstow Formation (Lofgren et al. 2012), Barstovian NALMA (middle Miocene) of the central Mojave Desert. *Mammut* was widespread across the US during the Clarendonian and Hemphillian NALMAs (latest Miocene and earliest Pliocene) (Lambert and Shoshani 1998). *Mammut* (reported as *Pliomastodon vexillarius*) and the gomphotheres *Rhynchotherium* are known from late Hemphillian NALMA age deposits in the Horned Toad Hills, western Mojave Desert (May et al. 2011).

Within the southwestern US and northwestern Mexico significant shifts in the paleogeographic distribution of *Mammut* have occurred over the past approximately 5 myr (million years duration). This period encompasses the Pliocene and Pleistocene Epochs, and Blancan (~5 to ~1.4 Ma [Megaannum, million years ago]), Irvingtonian (~1.4 Ma to ~240 ka [kiloannum, thousand years ago]) and Rancholabrean (~240 to ~11 ka) NALMAs (Bell et al. 2004; Sanders et al., 2009). Such paleogeographic shifts may have resulted from climate driven changes of the paleoenvironment that redistributed the preferred habitat of *Mammut*. Such changes also may result from regional geological processes that affect relevant habitat, competition with species of the Gomphotheriidae, or adaptation to the appearance and/or disappearance of other large herbivorous taxa in the region or a combination of these events.

A standard assumption, based on their low-crowned lophodont-cusped dentitions, is that Mammutidae and Gomphotheriidae were primarily browsing herbivores. However, it is inferred that mastodons fed on woody vegetation in mesic wetland environments; whereas,

gomphotheres were mixed feeders of tropical and subtropical wetlands (Newsom and Muhlbachler 2006).

Search methods and data sources

In order to quantify changes in the paleogeographic distribution of *Mammut*, Pliocene and Pleistocene fossil vertebrate assemblage data sets (see below) were searched to provide a list of all reported occurrences of Mammutidae within the far western US and northwestern Mexico. These assemblage data were queried using the following nested criteria: 1. all assemblages (sites, localities and/or local faunas) that contain the taxa Mammutidae, ? *Mammut* sp., cf. *Mammut* sp., *Mammut* sp., *Mammut* sp. cf. *M. americanum* or *Mammut americanum*; 2. the Blancan, Irvingtonian and Rancholabrean NALMAs, and 3. assemblages that fall within the target geographic region of Arizona, southern California (Inyo to Santa Barbara Counties and south), Nevada, Baja California del Norte and north western Sonora, Mexico. Age and paleogeographic distribution data for Gomphotheriidae of Blancan and Irvingtonian NALMAs were also collected for the region.

For the purposes of this discussion, the target region (southwestern US and northwestern Mexico) is subdivided into three broad geographic and presumably paleo-biotic provinces where: 1. coastal locations are defined as those that fall west of the southern California coastal ranges and Peninsular Range, and that are adjacent to the Pacific Ocean; 2. inland/montane locations that fall within the mountain and valley areas between the coastal province (1) and inland deserts province (3); and 3. desert locations that fall within the southern Great Basin, the Mojave and Sonoran Deserts (the Colorado Desert is included as part of the Sonoran Desert).

This report includes assemblage data retrieved from the following Stout Research Center archival sources (amended/revised versions of published documents and unpublished data tables are in italics):

(revised 10 January 2008). Northwestern Mexico; <CAN-MEX data.wpd>, incomplete and in preparation, data tables on file Colorado Desert District Stout Research Center Library archive.

(revised 09 May 2012). Catalogue of late *Quaternary vertebrates from Nevada*, amended data for Jefferson, G.T., H.G.

McDonald, and S. Livingston (2004), <Nevada Paleontology-Occ Paper working.wpd>, data tables on file Colorado Desert District Stout Research Center Library archive.
(revised 14 May 2012). *A Catalogue of Blancan and Irvingtonian Vertebrates and Floras from Southern California, Nevada, Utah, and Northwestern Mexico*, <Early Quaternary data and references.wpd>, in preparation, data tables on file Colorado Desert District Stout Research Center Library archive.
(revised 18 May 2012). *Catalogue of Blancan and early Quaternary vertebrate fossils from Arizona*, <Arizona early Quaternary 18 May 2012.doc>, in preparation, data tables on file Colorado Desert District Stout Research Center Library archive.
(revised 25 May 2012). *Catalogue of late Quaternary Vertebrates from California*; <California data and references.doc>, amended data for Jefferson 1991a and 1991b, data tables on file Colorado Desert District Stout Research Center Library archive.
(revised 25 May 2012). *A Catalogue of late Quaternary and Holocene Vertebrates from Arizona*, <Arizona late Pleistocene catalogue.doc>, data tables on file Colorado Desert District Stout Research Center Library archive.

Locality data list

Within the target region, a total of 59 assemblages were found to include remains identified as ? *Mammut* sp., cf. *Mammut* sp., *Mammut* sp., *Mammut* sp. cf. *M. americanum*, *M. americanum*, and Mammutidae or Gomphotheriidae. These locations and assemblages are:

Andrade's Ranch

Regional location: Sonoran Desert, Pima County, Arizona
Relative age: age uncertain
Source: Hay (1927)
Note: This record has not been verified.

Barrel Springs, Palmdale: SBCM 09.1.1; UCRV 7681 (UCMP)

Regional location: Mojave Desert, San Bernardino County, California
NALMA: late Irvingtonian
Age estimate: approximately 800 ka
Sources: Reynolds (1989a, 1989b)

Beverly Boulevard and Kilkea Drive, Los Angeles: LACM 236, 2034

Regional location: coastal, Los Angeles County, California
NALMA: ? Rancholabrean
Source: Miller (1971)

Beverly Hills

Regional location: coastal Los Angeles County, California
NALMA: ? Rancholabrean
Source: J.P. Quinn (pers. comm. 1985)

Borrego Badlands: ABDSP (numerous locations), F:AMNH, LACM

Regional location: Sonoran Desert, San Diego County, California
NALMA: Irvingtonian
Age estimate: 1.2 Ma to ca. 650 ka; Matuyama and Brunhes Chrons, Bishop Tuff
Sources: ABDSP collections data, Howard (1963), Remeika (1992), Remeika and Jefferson (1993), Reynolds and Remeika

(1993), Remeika et al. (1995), Remeika and Beske-Diehl (1996), Lutz et al. (2006)

California Oaks Road: SBCM (numerous locations)

Regional location: inland/montane, Riverside County, California
NALMA: early-late Irvingtonian
Age estimate: Kansan and Yarmouthian, 0.85 to 0.65 Ma, Bishop Tuff
Sources: Reynolds et al. (1990), Reynolds et al. (1991), Pajak (1993, 1994), Pajak et al. (1996)

Camarillo: LACM(CIT) 586

Regional location: coastal, Ventura County, California
NALMA: ? Rancholabrean
Source: LACM collection data

Carlsbad: SDSNH

Regional location: coastal, San Diego County, California
NALMA: early Rancholabrean
Age estimate: 200 ka
Source: Burge (2008)

Carlsbad, Robertson Ranch: SDSNH

Regional location: coastal, San Diego County, California
NALMA: early Rancholabrean
Age estimate: 120 to 220 ka
Source: Burge (2008)

Cerros Negros Wash, Redington: UALP 65

Regional location: Sonoran Desert, Pinal County, Arizona
NALMA: Rancholabrean
Radiometric date: 12,000 ± 300 rcy
Sources: Haynes (1968), Saunders (1970), Lindsay and Tessman (1974), Lindsay (1978), Agenbroad (1984), Harris (1985)

Chandler Sand Pit, Rolling Hills Estates: LACM 1087

Regional location: coastal, Los Angeles County, California
NALMA: Rancholabrean
Age estimate: ¹⁸O substage 5e (130-120 ka)
Sources: Miller (1971), Langenwalter (1975), Jefferson (1989)

Corona Gravel Pit: UCRV (UCMP)

Regional location: inland/montane, Riverside County, California
NALMA: late Blancan
Age estimate: 1.5 Ma
Source: Raposa (1985), M.O. Woodburne (pers. comm. 1986)

Corona, Santa Ana River: UCRV 8601 (UCMP)

Regional location: inland/montane, Riverside County, California
NALMA: Rancholabrean
Source: M.O. Woodburne (pers. comm. 1986)

Consolidated Rock Company, Alameda Street near 26th Street, Los Angeles: LACM 1157

Regional location: coastal, Los Angeles County, California
NALMA: ? Rancholabrean
Source: Miller (1971)

Coso Mountains (Haiwee Reservoir, Olanche, South Coso Mountains): LACM 1106, 1182, 4102, 4556- 59, 4591-95; LACM(CIT) 131, 248, 285; USGS

Regional location: desert, Inyo County California
NALMA: Blancan IV
Radiometric date: 3.2 ± 0.2 to 2.6 ± 0.1 Ma, Ka/A volcanics

Sources: Stock (1932), Wilson (1932), Schultz (1937), Kurtén and Anderson (1980), Savage and Russell (1983), Lundelius *et al.* (1987) Repenning (1987), White (1988)

Cypress and Slauson Avenues, Hyde Park: LACM 1266; USNM
Regional location: coastal, Los Angeles County, California
NALMA: ? Rancholabrean
Sources: Hay (1927), Miller (1971)

Diamond Valley, Hemet (East Side Reservoir Project, Domenigioni Valley, Valley of the Mastodons):
SBCM (2581 localities)

Regional location: inland/montane, Riverside County, California

NALMA: late Rancholabrean

Radiometric dates: 46 to 41 ka, 41,490 ± 1,380 to 13,200 rcy

Sources: Springer *et al.* (1998, 2007), Springer *et al.* (2009a, 2009b), Anderson *et al.* 2002), Sagebiel *et al.* (2004, 2005)

Edwards Air Force Base: SBCM 01.155.7, 12, 28-9, 32, 166-7, 173-4, 176, 181, 184-5, 187, 194, 200-1, 205, 237-7, 258-9, 298-300, 307, 313-4, 323, 327, 349-50, 01.155.372

Regional location: Mojave Desert, San Bernardino County, California

NALMA: Irvingtonian

Source: Reynolds (1989b)

Note: Data for Irvingtonian taxa only includes localities above the elevation of Lake Thompson high stand.

Emery Borrow Pit, Ralph Clark Regional Park, Fullerton:
LACM 3536-3537, 4178, 7053-7054, 7088-7089; RCIC LC 22, 47

Regional location: coastal, Orange County, California

NALMA: ? late Irvingtonian

Sources: Kurtén and Anderson (1980) Roeder (1988), Conkling and Edwards (1989), Jefferson (1989), Babilonia (2004), Crowe (2008)

Fairbanks Ranch South: SDSNH

Regional location: coastal, San Diego County, California

NALMA: late Irvingtonian or early Rancholabrean

Age estimate: 400 to 200 ka

Source: Deméré (pers. comm. 1999)

Fourth and Mesa Streets, San Pedro: LACM 7138

Regional location: coastal, Los Angeles County, California

NALMA: ? Rancholabrean

Source: LACM collections data

Gaviota Pass:

Regional location: coastal, Santa Barbara County, California

NALMA: ? Rancholabrean

Source: Hay (1927)

Glendale, Muddy River Basin: UALP

Regional location: Mojave Desert, Clark County, Nevada

NALMA: Rancholabrean

Age estimate: late Wisconsinian, ? <33,000 yr

Sources: Van Devender and Tessman (1975), Lundelius *et al.* (1983), Kurtén and Anderson (1980), Harris (1985), Heaton (1990), FAUNMAP (1994), Holman (1995)

Note: Report of *Mammuth* sp. by Heaton (1990) has not been documented.

Goleta: SBMNH

Regional location: coastal, Santa Barbara County, California

NALMA: ? Rancholabrean

Source: R.S. Gray (pers. comm. 1987)

Gypsum Ridge: MCAGCC

Regional location: Mojave Desert, San Bernardino County, California

NALMA: early Irvingtonian

Age estimate: pre-Olduvai, between 2.0 and 1.7 Ma

Source: Wagner (2000, 2002, 2004, 2006)

Hicks Canyon: LSA Associates, Riverside, California

Regional location: coastal, Orange County, California

NALMA: Rancholabrean

Source: S. Conkling (pers. comm. 1996)

Imperial Highway, La Habra: LACM 1052

Regional location: coastal, Los Angeles County, California

NALMA: Rancholabrean

Age estimate: Wisconsinian

Source: Miller and DeMay (1942), Miller (1971)

La Cienega Boulevard, 455 near Colgate Avenue, Los Angeles:
LACM

Regional location: coastal, Los Angeles County, California

NALMA: Rancholabrean

Source: E. Scott (pers. comm. 1989)

La Mirada, Coyote Creek: LACM 6689

Regional location: coastal, Orange County, California

NALMA: late Rancholabrean

Radiometric dates: 10,690 ± 360, 8,550 ± 100 rcy

Sources: Miller (1971), Kurtén and Anderson (1980), Welton and Finger (1981)

Los Angeles Brick Yard Number 3, Mission Road and Daly Street, Los Angeles: LACM 2032; UCMP 1377

Regional location: coastal, Los Angeles County, California

NALMA: Rancholabrean

Sources: Hay (1927), Miller (1971)

Lehner Ranch: UALP 14

Regional location: Sonoran Desert, Cochise County, Arizona

NALMA: late Rancholabrean

Radiometric dates: 11,600 ± 400 to 10,900 ± 450 rcy (numerous dates)

Sources: Haury *et al.* (1959), Lance (1959), Mehringer and Haynes (1965), Martin (1967), Haynes (1968), Saunders (1970), Lindsay and Tessman (1974), Lindsay (1978), Mead *et al.* (1979), Kurtén and Anderson (1980), Agenbroad (1984), Haynes and Stanford (1984), Harris (1985), Jefferson (1989), Mead (1991), Stanford (1999)

Manchester and Airport Boulevards, Los Angeles: LACM 1180, 4942

Regional location: coastal, Los Angeles County, California

NALMA: Rancholabrean

Source: Miller (1971)

Manning Rock, Irwindale: LACM 1807

Regional location: coastal, Los Angeles County, California

NALMA: ? Rancholabrean

Source: LACM collection data

Metro Rail Hollywood Tunnel: LACM 6297, 6298, 6299

Regional location: coastal, Los Angeles County, California

NALMA: Rancholabrean

- Source: Paleo Environmental Associates (1994 Metro Rail mitigation report and site records on file at G.C. Page Museum, Natural History Museum of Los Angeles County)
- Murrieta/Temecula:** SBCM (numerous locations); USGS M1476
Regional location: inland/montane, Orange County, California
NALMA: latest Irvingtonian or early Rancholabrean
Sources: Repenning (1987), Reynolds and Reynolds (1991), Reynolds et al. (1991), Bowden and Scott (1992), Scott (1992), Pajak (1993, 1994), Pajak et al. (1996)
- Naco:** UALP 68 (Navarette = Naco #1, Leikem = Naco #2)
Regional location: Sonoran Desert, Cochise County, Arizona
NALMA: late Rancholabrean
Radiometric dates: $9,250 \pm 300$, $8,980 \pm 270$ rcy
Sources: Haury et al. (1959), Lance (1959), Saunders (1970), Lindsay and Tessman (1974), Kurtén and Anderson (1980), Agenbroad (1984), Harris (1985), Connin et al. (1998), Stanford (1999)
- Newport Bay Mesa, Newport Beach:** LACM 1066-1067, 1100, 1240, 3877
Regional location: coastal, Orange County, California
NALMA: Rancholabrean
Relative age: ^{18}O substage 5e (130-120 ka)
Sources: Miller (1971), Reynolds (1976), Hudson and Brattstrom (1977), Kurtén and Anderson (1980), Jefferson (1989)
- Oro Grande, Adelanto/George Air Force Base:** SBCM 01.114.4
Regional location: Mojave Desert, San Bernardino County, California
NALMA: late Irvingtonian
Age estimate: 0.7 to 0.45 Ma
Source: Reynolds (1989b)
- Outfall Sewer, Rodeo and Kelley, Culver City:** LACM 3367
Regional location: coastal, Los Angeles County, California
NALMA: ? Rancholabrean
Source: LACM collection data
- Pearland, Palmdale:** LACM(CIT) 589
Regional location: Mojave Desert, Los Angeles County, California
NALMA: Irvingtonian
Source: Reynolds (1989b)
- Prescott SW:** ? Charlott Hall Museum
Regional location: inland/montane, Yavapai County, Arizona
NALMA: ? Rancholabrean
Source: B. Morgan (pers. comm. 1994)
- Point Sal:** LACM 4938; SBCC; SBMNH (?= UCMP V71018)
Regional location: coastal, Santa Barbara County, California
NALMA: ? Rancholabrean
Source: R.S. Gray (pers. comm. 1987)
- Rancho La Brea:** LACM 1724 (Hauser and 8th Streets), 1814 (La Brea Boulevard and Sycamore Avenue), 1870 and 7247 (Wilshire Boulevard and Curson Avenue), 1933 and 6909 (Hancock Park), 4204 and 6910 (Wilshire Boulevard, Mutual Benefit Building), 4590 (Stanley and 8th Streets), 6911 and 7027 (Wilshire Boulevard, Prudential Building); UCMP 1058-1061, 2050-2053, 3874
Regional location: coastal, Los Angeles County, California
NALMA: Rancholabrean
Relative age: Wisconsinan, in part early Holocene
- Radiometric dates: numerous determinations, U/Th and rcy ≥ 40 to 9 ka
Sources: Merriam (1910), Miller (1910, 1925), Kellogg (1912), Stock (1913, 1925), Chandler (1916a, 1916b), Dice (1925), Merriam and Stock (1932), Howard (1930, 1936, 1962), Compton (1934, 1937), Miller and Howard (1938), Miller and DeMay (1942), Savage (1951), Brattstrom (1953), Marcus (1960), Miller (1971), Akersten et al. (1979), Cox (1979), Swift (1979, 1989), Kurtén and Anderson (1980), Rea (1980), Jefferson (1989), LaDuke (1983), Marcus and Berger (1984), Shaw and Quinn (1986), Scott (1997), Jefferson and Tejada-Flores (1993), Spencer et al. (1999, 2003), Harris et al. (2003), Harris (2007), Feranec et al. (2008), Trayler and Dundas (2009)
- Reno:** UCMP 1072
Regional location: inland/montane, Storey County, Nevada
Relative age: age uncertain
Source: UCMP collections data
Note: Identification of *Mammut* has not been confirmed. The locality may be the same as West 7th Street, Reno (Tuohy 1986) that does not contain *Mammut*.
- Salt Creek, Laguna Niguel:** NHFOC, RCIC LC
Regional location: coastal, Orange County, California
NALMA: ? Rancholabrean
Source: Jefferson (1989)
- San Buenaventura:**
Regional location: coastal, Ventura County, California
NALMA: ? Rancholabrean
Source: Hay (1927)
- Santa Barbara Coast:**
Regional location: coastal, Santa Barbara County, California
NALMA: ? Rancholabrean
Source: Hay (1927)
- Santa Susana Pass, Chatsworth:** LACM 1406
Regional location: inland/montane, Los Angeles County, California
NALMA: ? Rancholabrean
Source: LACM collections data
- Santa Ana River, Thompson Sand Pit:** RMM; R. Kirkby private collection, Rubidoux, California
Regional location: inland/montane, Riverside County, California
NALMA: ? Rancholabrean
Source: R. Kirkby (pers. comm. 1965)
- Solana Beach:** UCMP V63073
Regional location: coastal, San Diego County, California
NALMA: ? Rancholabrean
Source: UCMP collections data
- SR 54 Mastodon:** SDSNH
Regional location: coastal, San Diego County, California
NALMA: Rancholabrean I
Age estimate: 400 to 150 ka
Radiometric dates: 335 ± 35 and 196 ± 15 ka U/Th
Source: Repenning (1987) Deméré et al. (1995)
- Tecopa (Lower Tecopa):** LACM; UCRV (numerous locations)
Regional location: desert, Inyo County, California
NALMA: Blancan V

Age estimate: >2.1 Ma, below Type C, Huckleberry Ridge tephra
Sources: James (1985), Repenning (1987), Woodburne and Whistler (1992), Whistler and Webb (1999, 2000), Morrison, (1999), Larsen (2000)

Note: The reported presence of *Mammuthus* sp. in this assemblage is not consistent with a Blancan age assignment, Upper and Lower Tecopa faunal lists possibly contain mixed ages. See Tecopa (Upper Tecopa) below.

Tecopa (Upper Tecopa): SSU, USGS M1089

Regional location: desert, Inyo County, California

NALMA: Irvingtonian II

Age estimate: <0.6 Ma, above Pearlette O ash

Source: James (1983, 1985), Hillhouse (1987), Repenning (1987), Reynolds (1991), Larsen (2000), McDaniel and Jefferson (2003)

Note: See Tecopa (Lower Tecopa) above. Faunal lists possibly contain taxa of mixed ages.

Tijuana River Valley: SDSNH

Regional location: coastal, San Diego County, California

NALMA: ? Rancholabrean

Source: SDSNH collections data

The Lakes, Thousand Oaks:

Regional location: inland/montane, Ventura County, California

NALMA: Irvingtonian

Source: Turner and Lander (2005)

Tremaine and 8th Streets, Los Angeles: LACM 1198

Regional location: coastal, Los Angeles County, California

NALMA: ? Rancholabrean

Source: Miller (1971)

Yuma County:

Regional location: Sonoran Desert, Yuma County, Arizona

NALMA: ? Rancholabrean

Source: Hutchison (1967)

Valley Wells: SBCM 01.001.031, 01.001.032

Regional location: Mojave Desert, San Bernardino County, California

NALMA: late Blancan

Age estimate: >2.1 Ma

Source: Reynolds and Jefferson (1971, 1988), Reynolds et al. (1991)

Ventura:

Regional location: coastal ?, Ventura County, California

NALMA: ? Rancholabrean

Source: Hay (1927)

Note: Location is uncertain; in part included with San Buenaventura (above) and Santa Paula (Jefferson 1991a); possibly Ventura UCMP 65287.

Wanis View Estates: SDSNH

Regional location: coastal, San Diego County, California

NALMA: Rancholabrean

Source: Wagner and Randall (2003), Randall et al. (2004)

William Lyon's Homes, Moorpark: LACM, SBM

Regional location: inland/montane, Los Angeles County, California

NALMA: Irvingtonian

Source: Lander (2007), Wagner et al. (2007)

Locality information and taxonomic lists for the University of California Museum of Paleontology (UCMP) collections were compiled (Jefferson 1991a, 1991b) from the Taxonomic Information Retrieval (TAXIR) computer data base. Locality and taxonomic data from the Vertebrate Paleontology Section collection at the Los Angeles County Museum of Natural History were recovered from TAXIR and revised following examination of the collection. Collections at the Ralph Clark Park Interpretive Center, Riverside Municipal Museum, San Bernardino County Museum, San Diego Society of Natural History, and Colorado Desert District Stout Research Center also were examined. Data lists were revised as new information were reported and published.

Institutional names are abbreviated as follows: ABDSP = Anza-Borrego Desert State Park, Colorado Desert District Stout Research Center (DSRC), Borrego Springs, California; CC = Cooper Center, Fullerton, California; F:AMNH American Museum of Natural History, New York, New York; LACM = Natural History Museum of Los Angeles County, California; LACM(CIT) = California Institute of Technology (collections transferred to LACM); MCAGCC = Marine Corps Air Ground Combat Center, Twentynine Palms, California; NHFOC = Natural History Foundation Orange County, California; RCIC LC = Ralph Clark Park Interpretive Center, Los Coyotes, Fullerton, California; RMM = Riverside Municipal Museum, Riverside, California; SBCM = San Bernardino County Museum, Redlands, California; SBM = Santa Barbara City Museum, Santa Barbara City College, Santa Barbara, California; SBMNH = Santa Barbara Museum of Natural History, Santa Barbara, California; SDSNH = San Diego Society of Natural History, San Diego, California; SSU = Sonoma State University, Shoshone Museum, California; SWM = Southwest Museum, Pasadena, California; UALP = University of Arizona Laboratory of Paleontology, Tucson, Arizona; UCMP = University of California Museum of Paleontology, Berkeley, California; UCRV (Geology Museum, University of California, Riverside (collections transferred to UCMP); USGS = United States Geological Survey, Denver, Colorado; USNM = United States National Museum, Washington DC.

Analysis

The number of southwestern records for *Mammut* (all taxonomic iterations) during the Blancan and Irvingtonian NALMAs is low (N = 16) relative to a total of N = 59 (two assemblages are of uncertain age). These pre-Rancho-labrean NALMA locations are scattered across inland/intermontane and desert paleogeographic provinces of the target region. Whereas, Rancho-labrean NALMA localities (N= 42) seem to be concentrated along the California coast (N = 32). Although these numbers are not statistically significant, they exhibit distinct patterns (Fig. 1).

Blancan NALMA records of *Mammut* are rare, and no coastal or inland/intermontane province sites are known.

Three occurrences are reported from the northeastern deserts of southern California; in the Coso Mountains (type locality of *Pliomastodon cosoensis*), at Valley Wells (reported as cf. *Mammut* sp.), and a report of Gomphotheriidae or Mammutidae from Tecopa. *Mammut* is a monotypic genus, and if the taxonomic assignments are correct for these records (Schultz 1937; Reynolds and Jefferson 1971, 1988; Kurtén and Anderson 1980; Reynolds et al. 1991) likely represent *M. americanum*. Fragmentary postcranial and dental materials of *Mammut* may be difficult to distinguish from Blancan NALMA Gomphotheriidae (e.g. *Cuvieronius*). Therefore the identity of some reported materials needs to be verified.

The Blancan NALMA paleogeographic distribution pattern for *Mammut* contrasts with that for the Gomphotheriidae ($N > \text{or} = 18$) within the target region. Sixteen locations from the desert province and two assemblages from inland/montane areas are known to yield gomphotheres (reported as Gomphotheriidae, cf. *Cuvieronius* sp. or *Cuvieronius* sp.). However, no Blancan NALMA coastal province sites within the target region have yet to yield gomphotheres.

Thirteen *Mammut* sp. (likely *M. americanum*) and *M. americanum* are reported from Irvingtonian NALMA assemblages (Fig. 1). However, because morphologically similar gomphotheriid genera such as *Cuvieronius* or *Stegomastodon* also occur in Irvingtonian NALMA assemblages, some identifications that are based on incomplete material may be in error. Most of the Irvingtonian NALMA records are divided between the inland/intermontane province ($N = 5$), and desert California ($N = 6$) locations. Only two coastal province locations are known, and one of these is listed as “late Irvingtonian or early Rancholabrean”.

There are five reported gomphotheres from the target region during the Irvingtonian NALMA, four are from deserts (identified as *Cuvieronius* sp. or *Stegomastodon* sp.), and a single account (identified as Gomphotheriidae) from an inland/montane province site. There are no known Irvingtonian NALMA coastal province assemblages that yield gomphotheres.

The majority of *Mammut* locations (all taxonomic iterations combined) from the target region are from the Rancholabrean NALMA ($N = 42$) (Fig. 1). Confirmation of Rancholabrean NALMA assemblages must be based on the presence of the Eurasian immigrant *Bison*, or established by radiometric or other independent dating methods as being less than about 240 ka (Sanders et al., 2009). Twenty two sites that yield taxa of Mammutidae from the target region do not contain *Bison* and otherwise have not been dated. These are designated as “? Rancholabrean” in the above Data List. Where so noted, most locations are in latest Pleistocene deposits (e.g. the numerous sites in coastal Los Angeles County), and are herein reasonably included in the Rancholabrean NALMA age sample. The accounts of *Mammut* sp. from Pima

County, Arizona (Hay 1927), and Reno, Nevada have not been verified.

A majority (76%) of Rancholabrean NALMA sites are located along the California coast ($N = 32$). Four sites are known from inland/intermontane California. These include one of the most prolific *Mammut* locations within the target region, Diamond Valley, Riverside County (Springer et al. 1998, 2007; Springer et al. 2009b; Anderson et al. 2002; Sagebiel et al. 2004, 2005). Within the deserts of the target region ($N = 6$), 2 sites are reported from Nevada, one at Glendale near the Colorado River corridor, and one from Reno in the Great Basin of central western Nevada. Four sites are located in the Sonoran Desert of Arizona. Two of these, Lehner Ranch and Naco, are associated with human procurement activities (Stanford 1999).

An apparent shift is observed in the paleogeographic distribution of *Mammut* from pre-Rancholabrean to Rancholabrean NALMA sites, where most early sites are located in inland areas and not on the California coast. The numbers of inland/montane and desert locations for *Mammut* are essentially the same for the Irvingtonian and Rancholabrean NALMAs (Fig. 1). Although these numbers are likely affected by collecting bias. Clearly, coastal California has experienced greater sub-surface exposure and observation due to recent human development than inland/montane and desert provinces. However, it is argued that human development is of insufficient magnitude to be entirely responsible for the observed pattern. This assertion is supported by the fact that the most diverse and abundant Rancholabrean NALMA assemblages from the desert province, Manix Lake, California (Jefferson 2003, the Manix assemblage spans the Rancholabrean/Irvingtonian NALMA boundary) and Tule Springs, Nevada (Springer et al. 2009a) do not contain *Mammut*. Although, R. Rowe (Spurr 1903) reported the discovery of “mastodon” remains from Las Vegas Valley, the presence of *Mammut* has been discounted and the taxon has not been found in recent extensive surveys (Scott pers. comm. 2012). Furthermore, the total number of Irvingtonian NALMA desert and inland/montane province locations, when compared to coastal sites, is 11/2 (18%), and for Rancholabrean NALMA sites from these same provinces this ratio is 42/32 (76%). If there were a bias due to coastal development, similar elevated numbers of Irvingtonian NALMA sites would also be expected in the coastal province. This is not observed.

Discussion and speculation

The apparent replacement of *Cuvieronius* by *Mammut* that occurred between the Blancan and Irvingtonian NALMAs in the desert province of the target region probably resulted from the onset of Pleistocene climatic conditions. Glacial-interglacial climate changes occurred throughout the Pleistocene on an approximately 100 kyr (thousand years duration) cycle. In the target region, these

are characterized by glacial/interglacial fluctuations in average annual temperatures of about 4° C, increases (glacial) and decreases (interglacial) in precipitation, and general north (interglacial) and south (glacial) or up (interglacial) and down (glacial) elevation shifts in paleobotanic associations and habitats. During the Pliocene Epoch, climatic conditions were relatively stable or equitable, warmer and more humid.

Within the southwestern deserts, records for *Cuvieronius* significantly outnumber *Mammuthus* during the Blancan NALMA. However, during the Irvingtonian NALMA, records for the same province show an increase in *Mammuthus* over *Cuvieronius*. Temporal resolution at the NALMA level is relatively poor, and the Blancan NALMA lasted 3.6 myr encompassing the beginning of the Pleistocene Epoch. It appears that the spread and increase of *Mammuthus* reflects the inability of gomphotheres to adapt to the onset of cooler and less equitable Pleistocene conditions at about 2.6 Ma, within the Blancan NALMA. *Cuvieronius* is known from late Pleistocene (Rancholabrean NALMA) localities in the tropical Americas (Kurtén and Anderson 1980). The southern range restriction of gomphotheres does not necessarily indicate any competition with *Mammuthus* at that time, but that the mastodons were better adapted to local Pleistocene environments.

However, the marked change in the abundance and paleogeographic distribution of *Mammuthus* in the coastal province, between the Irvingtonian and Rancholabrean NALMAs (Fig. 1), apparently was not a result of adaptation/s to Pleistocene climate-driven paleoenvironmental changes. Glacial/interglacial cycles predated the beginning of the Rancholabrean NALMA by about 2.3 myr. Coastal and inland provinces offered more wetland and riparian habitats that were presumably suitable to *Mammuthus* (Springer et al. 1998, 2007; Springer et al. 2009b; Anderson et al. 2002; Sagebiel et al. 2004, 2005), but these conditions were also present during the Irvingtonian NALMA. Given that paleoclimate-driven ecological conditions apparently do not account for the increased numbers of locations that yield *Mammuthus* in the coastal province during the Rancholabrean NALMA, what does?

Bison immigrated from Eurasia no later than about 240 ka, and is the defining taxon for the Rancholabrean NALMA (Savage 1951). Scott (2009) argued that the arrival of *Bison* in sub-arctic North America contributed to the late Pleistocene megafaunal extinction by competing for available forage and disrupting the ecological patterns of large herbivores. Apparently there was no direct ecological link between *Mammuthus* and *Bison*. *Mammuthus* was a browser and *Bison* primarily a grazer (Akersten et al. 1988), and both *Bison* and *Mammuthus* exhibit similar coastal and inland/montane paleogeographic distributions during the Rancholabrean NALMA (Jefferson 1988; Jefferson and Goldin 1989; Scott 2002). However, the introduction of *Bison* may have caused a

Table 1. Number of *Mammuthus* locations plotted by NALMA and province.

Age	Desert	Inland/Intermontane	Coastal	Total
Blancan	3	0	0	3
Irvingtonian	6	5	2	13
Rancholabrean	6	4	32	42

disruption to large herbivore guild ecosystems (Scott 2009) that may have had an effect on *Mammuthus* distribution. For example, as a grazer, *Bison* probably competed with *Mammuthus* and *Equus*, also grazers, and its presence may have affected the ecology of large mixed-feeder herbivores such as *Camelops* (Akersten et al. 1988).

Bison seems to have been restricted to marginal and riparian habitats within the desert province (Scott 2002). *Camelops* was more abundant in the desert province in comparison to coastal areas during the Rancholabrean NALMA (Jefferson 1988). It is reasonable to conjecture that *Camelops* may have intensified browsing behavior in desert riparian habitats at the beginning of the Rancholabrean NALMA in response to a competition with *Bison* for graze on open ground. A cascade effect may have begun, whereby an unprecedented and increasing reliance on browse in such habitats then placed *Camelops* (Akersten et al. 1988) in direct competition with *Mammuthus*. Although this reasoning may explain the decreased numbers of *Mammuthus* in the desert areas, it fails to account for the Rancholabrean NALMA increase in numbers in coastal habitats.

Acknowledgements

I thank the following scientists who provided information and/or access to collections under their care: M. Rivin, CC; L. Babilonia, RCIC LC; W.R. Daily and M.O. Woodburne, UCRV; T.A. Deméré and K. Randall, SDSNH; R.S. Gray, SBM; J.H. Hutchison, UCMP; E.H. Lindsay, UALP; C. Repenning, USGS; R.E. Reynolds, LSA; E. Scott, SBCM; L. Barnes and D.P. Whistler, LACM; and R.H. Tedford, AMNH. S.A. McLeod, LACM, accessed information from the LACM and UCMP TAXIR data base. L.K. Murray of the DSRC and R.E. Reynolds reviewed the manuscript and provided helpful comments and suggestions.

References

- Agenbroad, L.D. 1984. New world mammoth distribution. In Quaternary Extinction, a Prehistoric Revolution, ed. P.S. Martin and R.G. Klein, 90-108, University of Arizona Press, Tucson.
- Akersten, W.A., T. Foppe, and G.T. Jefferson 1988. New source of dietary data for extinct herbivores. *Quaternary Research* 30(1):92-97.
- Akersten, W.A., R.L. Reynolds and A.E. Tejada-Flores 1979. New mammalian records from the late Pleistocene of Rancho La Brea. *Bulletin of the Southern California Academy of Sciences* 78(29):141-143.

- Anderson, R.S., M.J. Power, S.J. Smith, K. Springer, and E. Scott 2002. Paleocology of a middle Wisconsin deposit from southern California. *Quaternary Research* 58:310-317.
- Babilonia, L. 2004. Ralph Clark Regional Park: an untapped treasure trove of Pleistocene Fossils. Southern California Academy of Sciences, Abstracts to Papers 103(supplement to 2):26.
- Bell, C.J., E.L. Lundelius Jr., A.D. Barnosky, R.W. Graham, E.H. Lindsay, D.R. Ruez Jr., H.A. Semken Jr., S.D. Webb, and R.J. Zakrzewski 2004. The Blancan, Irvingtonian, and Rancho-labrean Mammal Ages. *In* Late Cretaceous and Cenozoic Mammals of North America, edited by M.O. Woodburne, Columbia University Press, New York, p. 232-314.
- Bowden, J.K., and E. Scott 1991. New record of *Smilodon fatalis* (Leidy), 1868 (Mammalia; Carnivora; Felidae) from Riverside County, California. Abstracts of Proceedings 6th Annual Mojave Desert Symposium, San Bernardino County Museum Association Quarterly 39(1):22.
- Brattstrom, B.H. 1953. The amphibians and reptiles from Rancho La Brea. *Transactions of the San Diego Society of Natural History* 11(14):365-392.
- Burge, M. 2008. Development yields second Pleistocene gem. *Union-Tribune*, San Diego, California, 14 April 2008.
- Chandler, A.C. 1916a. Notes on *Capromeryx* material from the Pleistocene of Rancho La Brea. University of California Publications, Bulletin of the Department of Geology 9(10):111-120.
- Chandler, A.C. 1916b. A study of the skull and dentition of *Bison antiquus* Leidy, with special reference to material from the Pacific coast. University of California Publications, Bulletin of the Department of Geology 9(11):121-135.
- Compton, L.V. 1934. New bird records from the Pleistocene of Rancho La Brea. *Condor* 36(5):221-222.
- Compton, L.V. 1937. Shrews from the Pleistocene of the Rancho La Brea asphalt. University of California Publications, Bulletin of the Department of Geological Sciences 24(5):85-90.
- Conkling, S.W., and S.H. Edwards, Jr. 1989. A floral and faunal analysis of Clark Regional Park La Habra Formation: Rancho-labrean, Orange County, California. Abstracts of Proceedings 1989 Mojave Desert Quaternary Research Symposium, San Bernardino County Museum Association 36(2):55.
- Connin, S.L., J. Betancourt, and J. Quade 1998. Late Pleistocene C₄ plant dominance and summer rainfall in the southwestern United States from isotopic study of herbivore teeth. *Quaternary Research* 50:179-193.
- Cox, S.M. 1979. Preliminary census of the Ursidae from Rancho La Brea. Southern California Academy of Sciences Abstracts to Meetings 79:45.
- Crowe, M.K. 2008. Survey of the Pleistocene Camelidae material of Ralph B. Clark Regional Park Interpretive Center, Orange County, California. Bulletin Southern California Academy of Sciences, Abstracts Annual Meeting, California State University, Dominguez Hills 107(2):139.
- Deméré, T.A., R.A. Cerutti, and C.P. Majors 1995. State Route 54 Caltrans, District 11 paleontological mitigation program, final report. Prepared for Caltrans, District 11, Document on File Colorado Desert District Stout Research Center Archives 50 p.
- Dice, L. R. 1925. Rodents and Lagomorphs of the Rancho La Brea deposits. Carnegie Institute of Washington Publications 349:119-130.
- FAUNMAP 1994. Graham, R.W., E.L. Lundelius, M.A. Graham, R.F. Stearley, E.K. Schroeder, E. Anderson, A.D. Barnosky, J.A. Burns, C.S. Churcher, D.K. Grayson, R.D. Guthrie, C.R. Harrington, G.T. Jefferson, L.D. Martin, H.G. McDonald, R.E. Morlan, H.A. Semken, Jr., S.D. Webb, and M.C. Wilson 1995. FAUNMAP: a database documenting late Quaternary distributions of mammal species in the United States. *Illinois State Museum Scientific Papers* 25(1-2):1-690.
- Feranec, R.E., E. Hadley, and A. Paytan 2008. Intra-tooth variation in isotope values of late Pleistocene bison (*Bison*) and horse (*Equus*) reveals seasonal resource competition at Rancho La Brea. *Journal of Vertebrate Paleontology* 28(3):76A.
- Harris, A.H. 1985. Late Pleistocene Vertebrate Paleocology of the West. University of Texas Press, Austin 293 p.
- Harris, J. 2007. Late Pleistocene environment at Rancho La Brea. *Journal of Vertebrate Paleontology* 27(3):87A.
- Harris, J., J. Coultrain, J. Cerling, and T. Ehlinger 2003. Trophic relationships of late Pleistocene mammals from Rancho La Brea. *Journal of Vertebrate Paleontology*, Abstracts 23(3):59A.
- Haury, E.W., E.B. Sayles, and W.H. Wasley 1959. The Lehner mammoth site, southeastern Arizona. *American Antiquity* 25(1)2-30.
- Hay, O.P. 1927. The Pleistocene of the western region of North America and its vertebrated animals. Carnegie Institute of Washington Publication 322(B):1-346.
- Haynes, C.V. Jr. 1968. Geochronology of late Quaternary alluvium. *In* Means of Correlation of Quaternary Successions, edited by R.B. Morrison and H.E. Wright Jr., University of Utah Press, Salt Lake pp. 591-631.
- Haynes, G., and D. Stanford 1984. On the possible use of *Camelops* by early man in North America. *Quaternary Research* 22(2):216-230.
- Heaton, T. 1990. Quaternary mammals of the Great Basin: extinct giants, Pleistocene relics, and Recent immigrants. *In* *Causes of Evolution: A Paleontological Perspective*, edited by R.M. Ross and W.D. Allmon, University of Chicago Press pp. 422-465.
- Hillhouse, J.W. 1987. Late Tertiary and Quaternary geology of the Tecopa Basin, southeastern California. US Geological Survey, Miscellaneous Investigations Series Map I-1728.
- Holman, A. 1995. Pleistocene Amphibians and Reptiles in North America. Oxford University Press, New York.
- Howard, H. 1930. A census of the Pleistocene birds of Rancho La Brea from the collection of the Los Angeles Museum. *Condor* 32(1):81-88.
- Howard, H. 1936. Further studies upon the birds of the Pleistocene of Rancho La Brea. *Condor* 38(1):32-36.

- Howard, H. 1962. A comparison of prehistoric avian assemblages from California. Los Angeles County Museum of Natural History, Contributions in Science 58:1-24.
- Howard, H. 1963. Fossil birds from the Anza-Borrego Desert. Los Angeles County Museum Contributions in Science 73:1-33.
- Hudson, D.M., and B.H. Brattstrom 1977. A small herpetofauna from the late Pleistocene of Newport Beach Mesa, Orange County, California. Bulletin of the Southern California Academy of Sciences 76(1):16-20.
- Hutchison, J.H. 1967. Rancholabrean vertebrate faunas of western North America. Manuscript on file University of California, Berkeley, Paleontology Seminar 250.
- James, B. 1983. Death Valley mammoth expedition 1982-1983, late Pleistocene mammoths from the Death Valley Tecopa Lake Beds. Manuscript on file California State University, Sonoma, Department of Geology 8 p.
- James, B. 1985. Late Pliocene (Blancan) nonmarine and volcanic stratigraphy and microvertebrates of Lake Tecopa, California. Masters Thesis, Department of Geological Sciences, University of California, Riverside 89 p.
- Jefferson, G.T. 1988. Late Pleistocene large mammalian herbivores: implications for big game hunters in southern California. In *Desert Ecology 1986: A Research Symposium*, edited by R.G. Zahary, Southern California Academy of Sciences and the Desert Studies Consortium pp. 15-35.
- Jefferson, G.T. 1989. Late Cenozoic tapirs (Mammalia: Perisodactyla) of western North America. Natural History Museum of Los Angeles County, Contributions in Science 406:1--1.
- Jefferson, G.T. 1991a. A catalogue of late Quaternary vertebrates from California: part one, nonmarine lower vertebrate and avian taxa. Natural History Museum of Los Angeles County, Technical Report 5:1-59.
- Jefferson, G.T. 1991b. A catalogue of late Quaternary vertebrates from California: part two, mammals. Natural History Museum of Los Angeles County Technical Reports 7:1-129.
- Jefferson, G.T. 2003. Stratigraphy and paleontology of the middle to late Pleistocene Manix Formation, and paleoenvironments of the central Mojave River, southern California. In *Paleoenvironments and Paleohydrology of the Mojave and Southern Great Basin Deserts*, edited by Y. Enzel, S.G. Wells, and N. Lancaster, Geological Society of America, Special Paper 368:43-60.
- Jefferson, G.T., and J. Goldin 1989. Seasonal migration of *Bison antiquus* from Rancho La Brea. *Quaternary Research* 31:107-112.
- Jefferson, G.T., H.G. McDonald, and S. Livingston. 2004. Catalogue of late Quaternary vertebrates from Nevada. Nevada State Museum Occasional Papers 6:1-84.
- Jefferson, G.T., and A. Tejada-Flores 1993. The late Pleistocene record of *Homotherium* (Felidae: Machairodontinae) in the southwestern United States. *PaleoBios* 15(1-4):37-46.
- Kellogg, L. 1912. Pleistocene rodents of California. University of California Publications Bulletin of the Department of Geology 7(8):151-168.
- Kurtén, B. and E. Anderson 1980. Pleistocene Mammals of North America. Columbia University Press, New York 442 p.
- LaDuke, T.C. 1983. The fossil snake fauna of Pit 91, Rancho La Brea, Los Angeles County, California. Masters Thesis, Department of Zoology, Michigan State University, East Lansing 56 pp.
- Lambert, D., and J. Shoshani 1998. Proboscidea. In *Evolution of Tertiary mammals of North America*, edited by Jamis, C.M., K.M. Scott, and L.L. Jacobs, Cambridge University Press, Cambridge, U.K. 1:606-621.
- Lance, J.F. 1959. Faunal remains from the Lehner Mammoth Site. *American Antiquity* 25:35-39.
- Lander, B. 2007. Fossil mastodon remains recovered from The Lakes parcel, Thousand Oaks, Ventura County, California. Report submitted by Paleo Environmental Associates to R.D. Turner ArchaeoPaleo Resource Management, Inc., on file Department of Parks and Recreation, Colorado Desert District Stout Research Center, Borrego Springs, California 3 p.
- Langenwalter, P.E., II. 1975. Chordates: the fossil vertebrates of the Los Angeles and Long Beach Harbors region. In Kennedy, G.L., Paleontologic record of areas adjacent to the Los Angeles and Long Beach Harbors, Los Angeles County, California, Marine Studies of San Pedro Bay, California, Part 9 Paleontology, edited by D.F. Soule and M. Oguri, Allan Hancock Foundation and Sea Grants Programs, University of Southern California, Publication USC-SG-4-75:36-54.
- Larsen, D. 2000. Sedimentology and stratigraphy of the Plio-Pleistocene Lake Tecopa beds, southeastern California: a work in progress. In *Empty Basins, Vanished Lakes*, edited by R.E. Reynolds and J. Reynolds, San Bernardino County Museum Association Quarterly 47(2):56-62.
- Lindsay, E.H. 1978. Late Cenozoic vertebrate faunas, southeastern Arizona. New Mexico Geological Society Guidebook, 29th Field Conference, Land of Cochise pp. 269-275.
- Lindsay, and Tessman 1974. Cenozoic vertebrate localities and faunas in Arizona. *Journal of the Arizona Academy of Science* 9:3-24.
- Lofgren, D.L., A. Hess, D. Silver, and P. Liskanich. 2012. Review of proboscideans from the Middle Miocene Barstow Formation of California. In *Searching for the Pliocene: Southern Exposures*, edited by R.E. Reynolds, California State University Desert Studies Center pp. 125-134.
- Lundelius, E.L., Jr., T. Downs, E.H. Lindsay, H.A. Semken, R.J. Zakrzewski, C.S. Churcher, C.R. Harrington, G.E. Schultz, and S.D. Webb 1987. The North American Quaternary sequence. In *Cenozoic Mammals of North America, Geochronology and Biostratigraphy*, edited by M.O. Woodburne, University of California Press, Berkeley pp. 211-235.
- Lundelius, E.L., Jr., R.W. Graham, E. Anderson, J. Guilday, J.A. Holman, D.W. Steadman, and S.D. Webb 1983. Terrestrial vertebrate faunas. In *Late Quaternary Environments of the United States: Volume 1, The Late Pleistocene*, edited by S. Porter, University of Minnesota Press 1:311-353.
- Lutz, A.T., R.J. Dorsey, B.A. Housen, and S.U. Janecke 2006. Stratigraphic record of Pleistocene faulting and basin evolution in the Borrego Badlands, San Jacinto fault zone,

- southern California. Geological Society of America Bulletin 118 (11/12):1377-1397.
- Marcus, L.F. 1960. A census of the abundant large Pleistocene mammals from Rancho La Brea. Los Angeles County Museum Contributions in Science 38:1-11.
- Marcus, L.F. and R. Berger 1984. The significance of radio-carbon dates for Rancho La Brea. *In* Quaternary Extinctions a Prehistoric Revolution, edited by P.S. Martin, and R.G. Klein, University of Arizona Press, Tucson pp. 159-183.
- Martin, P.S. 1967. Prehistoric overkill. *In* Pleistocene Extinctions, the Search for a Cause, edited by P.S. Martin and H.E. Wright, Jr. Yale University Press, New Haven pp. 75-120.
- May, S.R., M.O. Woodburne, E.H. Lindsay, L.B. Albright, A. Sarna-Wojcicki, E. Wan, and D.B. Wahl 2011. Geology and mammalian paleontology of the Horned Toad Hills, Mojave Desert, California. *Palaeontologia Electronica* 14(3):154; 28A:63p; palaeo-electronica.org/2011_3/11_may/index.html.
- McDaniel, G.E., Jr., and G.T. Jefferson 2003. A late Pleistocene proboscidean site in the Death Valley Tecopa Lake Beds near Shoshone, California. Manuscript on file BLM, DPR Colorado Desert District Stout Research Center, Borrego Springs, and Shoshone Museum, Shoshone, California 13 p.
- Mead, J.I. 1991. Late Pleistocene and Holocene molluscan faunas and environmental changes in southwestern Arizona. In *Beamers, Bobwhites, and Blue Points, Tributes to the Career of Paul W. Parmalee*, edited by J.R. Purdue, W.E. Kipple, and B.W. Styles, Illinois State Museum Scientific Papers 23, and the University of Tennessee, Department of Anthropology Report of Investigations 52:215-226.
- Mead, J.I., C.V. Haynes, and B.B. Huckell 1979. A late Pleistocene mastodon (*Mammuth americanum*) from the Lehner Site, southeastern Arizona. *Southwestern Naturalist* 24(2):231-238.
- Mehringer, P.J. and C.V. Haynes 1965. The pollen evidence for the environment of Early Man and extinct mammals at the Lehner Mammoth Site, southeastern Arizona. *American Antiquity* 31:17-23.
- Merriam, J.C. 1910. New Mammalia from Rancho La Brea. University of California Publications, Bulletin of the Department of Geology 5(25):391-395.
- Merriam, J.C. and C. Stock 1932. The Felidae of Rancho La Brea. Carnegie Institute of Washington Publications 422:1-232.
- Miller, A.H. 1910. Fossil birds from the Quaternary of southern California. *Condor* 12(1):12-15.
- Miller, A.H. 1925. The birds of Rancho La Brea. Carnegie Institute of Washington Publications 349:63-106.
- Miller, L. H. and I. DeMay 1942. The fossil birds of California, an avifauna and bibliography with annotations. University of California, Publications in Zoology 47(4):47-142.
- Miller, L.H., and H. Howard 1938. The status of the extinct condor-like birds of the Rancho La Brea Pleistocene. University of California, Los Angeles, Publications in the Biological Sciences 1(9):169-176.
- Miller, W.E. 1971. Pleistocene vertebrates of the Los Angeles Basin and vicinity (exclusive of Rancho La Brea). Los Angeles County Museum of Natural History, Science Series 10:1-124.
- Morrison, R.B. 1999. Lake Tecopa: Quaternary geology of Tecopa Valley, California, a multimillion-year record and its relevance to the proposed nuclear-waste repository at Yucca Mountain, Nevada. *In* Cenozoic Basins of the Death Valley Region, edited by L.A. Wright and B.W. Troxel, Geological Society of America Special Paper 333:301-344.
- Newsom, L.A., and M.C. Muhlbachler 2006. Mastodon (*Mammuth americanum*) diet foraging patterns based on dung deposits. *In* First Floridians Last Mastodons: the Page-Ladson Site in the Aucilla River, edited by S.D. Webb and E. Simons, Springer Press pp. 263-331.
- Pajak, A.F., III 1993. The second record of *Tapirus* from the Temecula Valley, southern California, and biostratigraphic implications. *San Bernardino County Museum Association Quarterly, Abstracts* 40(2):30-31.
- Pajak, A.F., III 1994. Proboscideans and xenarthrans from the Temecula Basin, Riverside County, California. *Journal of Vertebrate Paleontology* 14(3):41A.
- Pajak, A.F., III, E. Scott, and C.J. Bell 1996. A review of the biostratigraphy of Pliocene and Pleistocene sediments in the Elsinore Fault Zone, Riverside County, California. *PaleoBios* 17(2-4):28-49.
- Randall, K.A., H.M. Wagner, B.O. Riney, and M.A. Roeder 2004. A late Pleistocene (Rancholabrean) vertebrate assemblage from Oceanside, San Diego County, California. *Southern California Academy of Sciences, Abstracts to Papers* 103(supplement to 2):23.
- Raposa, R. 1985. Mastodon bones found in Corona. *The Press Enterprise, Local Monday, December 30 pp.* B1-3.
- Rea, A.M. 1980. Late Pleistocene and Holocene turkeys in the southwest. *In* Papers in Avian Paleontology Honoring Hildgarde Howard, edited by K.E. Campbell, Natural History Museum of Los Angeles County, Contributions in Science 330:209-224.
- Remeika, P. 1992. Preliminary report on the stratigraphy and vertebrate fauna of middle Pleistocene Ocotillo Formation, Borrego Badlands, Anza Borrego Desert State Park, California. Abstracts of Proceedings 6th Annual Mojave Desert Symposium, San Bernardino County Museum Association Quarterly 39(1):25-26.
- Remeika, P., and S. Beske-Diehl 1996. Magnetostratigraphy of the western Borrego Badlands, Anza-Borrego Desert State Park, California: implications for stratigraphic age control. *In* Sturzstorms and Detachment Faults Anza-Borrego Desert State Park California, edited by P.L. Abbott and D.C. Seymour, South Coast Geological Society Annual Field Trip Guide Book Number 24:209-220.
- Remeika, P., and G.T. Jefferson 1993. The Borrego local fauna: revised basin-margin stratigraphy and paleontology of the western Borrego Badlands, Anza-Borrego Desert State Park, California. *In* Ashes, Faults and Basins, edited by R.E. Reynolds and J. Reynolds, San Bernardino County Museum Association Special Publication MDQRC 93(1):90-93.
- Remeika, P., G.T. Jefferson, and L.K. Murray 1995. Fossil vertebrate faunal list for the Vallecito-Fish Creek and Borrego-San Felipe Basins, Anza-Borrego Desert State Park and vicinity, California. *In* Paleontology and Geology of the Western Salton Trough Detachment, Anza-Borrego Desert State Park,

- California, edited by P. Remeika and A. Sturz, San Diego Association of Geologists, Field Trip Guidebook 1:82-93.
- Repenning, C.A. 1987. Biochronology of the microtine rodents of the United States. *In* Cenozoic Mammals of North America, edited by M.O. Woodburne, University of California Press, Berkeley p. 237-268.
- Reynolds, R.E. 1989a. Mid-Pleistocene faunas of the west-central Mojave Desert. *In* The West-Central Mojave Desert: Quaternary Studies Between Kramer and Afton Canyon, edited by R.E. Reynolds, San Bernardino County Museum Association Special Publication, Redlands, California pp. 44-48.
- Reynolds, R.E. 1989b. Paleontologic monitoring and salvage Imperial Irrigation District transmission line Riverside and Imperial Counties, California: final report. Prepared for Mission Power Engineering Company, by San Bernardino County Museum, Manuscript on File Natural History Museum of Los Angeles County 169 p.
- Reynolds, R.E. 1991. The Shoshone zoo: a Rancholabrean assemblage from Tecopa. *In* Crossing the Borders: Quaternary Studies in Eastern California and Southwestern Nevada, edited by R.E. Reynolds, San Bernardino County Museum Association Special Publication, Redlands, California pp. 158-162.
- Reynolds, R.E., L.P. Fay, and R.L. Reynolds 1990. California Oaks Road: an early-late Irvingtonian Land Mammal Age fauna from Murrieta, Riverside County, California. Abstracts and Proceedings 1990 Mojave Desert Quaternary Research Symposium, San Bernardino County Museum Quarterly 37(2):35-36.
- Reynolds, R.E., and G.T. Jefferson 1971. Late Pleistocene vertebrates from Valley Wells, Mojave Desert, California. Geological Society of America, Abstracts with Programs 3(2):183.
- Reynolds, R.E., and G.T. Jefferson 1988. Timing of deposition and deformation in Plio-Pleistocene sediments at Valley Wells, eastern San Bernardino County, California. *In* This Extended Land: Geological Journeys in the Southern Basin and Range, edited by D. Weide, and M. Faber, Geological Society of America Guidebook pp. 218-220.
- Reynolds, R.E., G.T. Jefferson, and R.L. Reynolds 1991. Sequence of vertebrates from the Plio-Pleistocene sediments at Valley Wells, San Bernardino County, California. *In* Crossing the Borders: Quaternary Studies in Eastern California and Southwestern Nevada, edited by R.E. Reynolds, San Bernardino County Museum Association Special Publication, Redlands, California pp. 72-77.
- Reynolds, R.E., and P. Remeika 1993. Ashes, Faults and Basins: the 1993 Mojave Desert Quaternary Research Center Field Trip. *In* Ashes, Faults and Basins. edited by R.E. Reynolds and J. Reynolds, San Bernardino County Museum Association Special Publication 93-1:3-33.
- Reynolds, R.E. and R.L. Reynolds 1991. Late Pleistocene faunas of Lake Thompson. *In* Inland Southern California: the Last 70 Million Years, compiled by M.O. Woodburne, R.E. Reynolds, and D.P. Whistler, San Bernardino County Museum Association Quarterly 38(3&4):114-115.
- Reynolds, R.L. 1976. New record of *Antilocapra americana* Ord, 1818, in the late Pleistocene fauna of the Los Angeles Basin. Journal of Mammalogy 57(1):176-178.
- Roeder, M.A. 1988. Quaternary distribution of *Gasterosteus* species in southern California. Abstracts of Proceedings 1988 Mojave Desert Quaternary Research Symposium, San Bernardino County Museum Association 35(3-4):28.
- Sagebiel, J., K. Springer, C. Austin, and E. Scott. 2004. The use of GIS technology to characterize faunal changes through time and space across a depositional basin. Journal of Vertebrate Paleontology 24(3):107A
- Sagebiel, J., K. Springer, C. Austin, and E. Scott. 2005. The use of GIS technology to interpret Pleistocene fauna and flora in a depositional basin. Western Association of Vertebrate Paleontologists, Abstracts for the Meeting, Natural History Museum of Los Angeles County 9 p.
- Sanders, A.E., R.E. Weems, and L.B. Albright, III 2009. Formalization of the middle Pleistocene "Ten Mile Hill beds" in South Carolina with evidence for placement of the Irvingtonian-Rancholabrean boundary. *In* Papers on Geology, Vertebrate Paleontology, and Biostratigraphy in Honor of Michael O. Woodburne, edited by L.B. Albright III, Museum of Northern Arizona Bulletin 65:363-369.
- Saunders, J.J. 1970. The distribution and taxonomy of *Mammuthus* in Arizona. Masters Thesis, University of Arizona 230 p.
- Savage, D. 1951. Late Cenozoic vertebrates of the San Francisco Bay region. University of California Publications, Bulletin of the Department of Geological Sciences 28(10):215-314.
- Savage, D.E., and D.E. Russell 1983. Mammalian Paleofaunas of the World. Addison-Wesley Publishing Company, Reading, Massachusetts 432 p.
- Schultz, J.R. 1937. A late Cenozoic vertebrate fauna from the Coso Mountains, Inyo County, California. Carnegie Institute of Washington Publication 487:77-109.
- Scott, E. 1992. First record of *Arctodus simus* (Cope), 1879 (Mammalia; Carnivora; Ursidae) from Riverside County, California. Abstracts of Proceedings 6th Annual Mojave Desert Symposium, San Bernardino County Museum Association Quarterly 39(1):27.
- Scott, E. 1997. A review of *Equus conversidens* in southern California, with a report on a second, previously-unrecognized species of Pleistocene, small horse from the Mojave Desert. Journal of Vertebrate Paleontology 17(3):75A.
- Scott, E. 2002. Late Pleistocene distribution of *Bison* in the Mojave Desert, southern California and Nevada. Journal of Vertebrate Paleontology 22(Supplement to Number 3):104A.
- Scott, E. 2009. Extinctions, scenarios, and assumptions: Changes in latest Pleistocene large herbivore abundance and distribution in western North America. Quaternary International, doi:10.1016/j.quaint.2009.11.003.
- Shaw, C.A., and J.P. Quinn 1986. Rancho La Brea: a look at coastal southern California's past. California Geology 39(6):123-133.
- Spencer, L., B. Van Valkenburgh, and J.M. Harris. 1999. Taphonomy at Rancho La Brea: a work in progress. Journal of Vertebrate Paleontology 19(3):77A.
- Spencer, L., B. Van Valkenburgh, and J.M. Harris. 2003. Taphonomic analysis of large mammals recovered from the Pleistocene Rancho La Brea tar seeps. Paleobiology 29(4):561-575.

- Springer, K.B., E. Scott, L.K. Murray. 1998. Partial skeleton of a large individual of *Mammuth americanum* from the Domenigoni Valley, California. *Journal of Vertebrate Paleontology*, Abstracts 18(3):79A.
- Springer, K.B., E. Scott, L.K. Murray. 2007. The Diamond Valley Lake local fauna: late Pleistocene vertebrates from inland southern California. *Journal of Vertebrate Paleontology* 27(3):151A.
- Springer, K.B., E. Scott, J.C. Sagebiel, and C.R. Manker 2009a. The Tule Springs local fauna: late Pleistocene vertebrates from upper Las Vegas Wash, Clark County, Nevada. 8th Conference on Fossil Resources, Saint George, Utah pp. 108-109.
- Springer, K.B., E. Scott, J.C. Sagebiel, and L.K. Murray 2009b. Diamond Valley Lake local fauna: late Pleistocene vertebrates from inland southern California. *In* Papers on Geology, Vertebrate Paleontology, and Biostratigraphy in Honor of Michael O. Woodburne, edited by L.B. Albright III, Museum of Northern Arizona Bulletin 65:217-236.
- Spurr, J.E. 1903. Descriptive geology of Nevada south of the fortieth parallel and adjacent portions of California. *US Geological Survey Bulletin* 208:1-229.
- Stanford, D. 1999. Paleoindian archaeology and late Pleistocene environments in the plains and southwestern United States. *In* Ice Age Peoples of North America, edited by R. Bonnicksen and K.L. Turner, Oregon State University Press, Center for the Study of the First Americans pp. 218-339.
- Stock, C. 1913. *Nothotherium* and *Megalonyx* from the Pleistocene of southern California. University of California Publications, Bulletin of the Department of Geology 7(17):341-358.
- Stock, C. 1925. Cenozoic gravigrade edentates of western North America with special reference to the Pleistocene *Megalonychinae* and *Mylodontidae* of Rancho La Brea. Carnegie Institute of Washington Publications 331:1-206.
- Stock, C. 1932. *Hyaenognathus* from the late Pliocene of the Coso Mountains of California. *Journal of Mammalogy* 13(3):263-266.
- Swift, C.C. 1979. Freshwater fish of the Rancho La Brea deposit. Abstracts, Annual Meeting of the Southern California Academy of Sciences 88:44.
- Swift, C.C. 1989. Late Pleistocene fishes from the Rancho La Brea deposit, southern California. *Bulletin of the Southern California Academy of Sciences* 88(3):93-102.
- Traylor, R.B. and R.G. Dundas 2009. American mastodon (*Mammuth americanum*) in the Rancho La Brea collection of the University of California Museum of Paleontology. *Current Research in the Pleistocene* 26:184-186.
- Tuohy, D.R. 1986. Nevada's fossil elephants. *Nevada Archaeologist* 5(2):8-19.
- Turner, R.D., and E.B. Lander 2005. *Mammuth americanum* from part of former Jungland site, The Lakes parcel, Thousand Oaks, Ventura County, California. Western Association of Vertebrate Paleontologists, Abstracts for the Meeting Natural History Museum of Los Angeles County pp. 10-11.
- Van Devender, T.R., and N.T. Tessman 1975. Late Pleistocene snapping turtles (*Chelydra serpentina*) from southern Nevada. *Copeia* 2:249-253.
- Wagner, H.M. 2000. A new late Pliocene-early Pleistocene vertebrate fauna from the Mojave Desert, San Bernardino County, California. Western Association of Vertebrate Paleontology meeting at Flagstaff, Arizona, 3 March 2000.
- Wagner, H.M. 2002. Magnetic stratigraphy of the late Pliocene-early Pleistocene mammal-bearing deposits from Gypsum Ridge, San Bernardino County, California. *In* Between Basins: Exploring the Western Mojave and Southern Basin and Range Province, ed. R.E. Reynolds, Abstracts 2002 Desert Symposium, California State University, Desert Studies Consortium and LSA Associates Inc., Riverside, California p. 83.
- Wagner, H.M. 2004. The Gypsum Ridge local Fauna, an early Pleistocene vertebrate assemblage from Twentynine Palms, San Bernardino County, California. Southern California Academy of Sciences, Abstracts to Papers 103(supplement to 2):23.
- Wagner, H.M. 2006. Report to accompany the newly catalogued paleontological collections from Gypsum Ridge - Contract No. M67399-05-P-0155. Unpublished 12 p.
- Wagner, H.M., and K.A. Randall 2003. A late Pleistocene (Rancholabrean) vertebrate fauna from the Wanis View Estates housing project, Oceanside, northwestern San Diego County, California. *Journal of Vertebrate Paleontology* Abstracts of Papers 23(3):107A.
- Wagner, H.M., E.B. Lander, M.A. Roeder, D.R. Prothero, and G.E. McDaniel Jr. 2007. A new Irvingtonian land mammal assemblage from the Saugus Formation, Moorpark, Ventura County, California. Southern California Academy of Sciences Bulletin, Abstracts of Papers 143, 106(2):141.
- Welton, B.J., and K.L. Finger 1981. Geology and paleontology of the West Coyote oil field. *In* 1981 Tour and Guide to Petroleum Research and Production Facilities, the Geology of the Eastern Puente Hills, Northern Los Angeles Basin, and the Coastal Geomorphology of Southwestern Orange County, California, edited by M.S. Woyski, National Association of Geology Teachers Far Western Section pp. 15-18.
- Whistler, D.P., and S.D. Webb. 1999. A new stenomyline camelid from the latest Blancan of the Tecopa Lake Beds, California. *Journal of Vertebrate Paleontology* 19(3):84A.
- Whistler, D.P., and S.D. Webb. 2000. Fossil vertebrates of the Plio/Pleistocene Tecopa Lake beds, Inyo County, California. *In* Empty Basins, Vanished Lakes, edited by R.E. Reynolds and J. Reynolds, San Bernardino County Museum Association Quarterly 47(2):63-64.
- White, J.A. 1988. The Archaeolaginae (Mammalia, Lagomorpha) of North America, excluding *Archaeolagus* and *Pantolax*. *Journal of Vertebrate Paleontology* 7(4):425-450.
- Wilson, R.W. 1932. *Cosomys*, a new genus of vole from the Pliocene of California. *Journal of Mammalogy* 13:150-154.
- Woodburne, M.O., and D.P. Whistler 1992. The Tecopa lake beds. *In* Crossing the Borders: Quaternary Studies in Eastern California and Southwestern Nevada, compiled by R.E. Reynolds, San Bernardino County Museum Association Special Publication, MDQRC 91:155-157.

Halloran Springs and pre-Columbian turquoise trade

Sharon Hull and Mostafa Fayek

Department of Geological Sciences, University of Manitoba, Winnipeg, Manitoba, Canada

ABSTRACT: Halloran Springs has been interpreted as a possible turquoise resource area for the pre-Columbian inhabitants of the American Southwest evident by the presence of prehistoric quarries, ancient camps, hammerstones, scrapers, ceramic sherds, petroglyphs, as well as a Paiute legend that tells of the prehistoric Desert Mojave and their encounter with distant peoples that came to mine turquoise. The ability to geochemically link turquoise artifacts with their geological source allows us to reconstruct ancient turquoise trade/exchange networks and investigate the relationship of the peoples that were involved in and affected by the movement of commodities along these routes. To achieve this goal, we developed a method to identify the geological source of turquoise artifacts using the isotope ratios of hydrogen ($^2\text{H}/^1\text{H}$) and copper ($^{65}\text{Cu}/^{63}\text{Cu}$) and the microanalytical abilities of a secondary ion mass spectrometer (SIMS). We established a comparative database that contains the isotopic fingerprints of 22 turquoise resource areas. We are currently analyzing turquoise artifacts from archaeological sites across the American Southwest and the Great Basin region, identifying their geological source, and developing a digital archive so we can investigate turquoise trade routes and patterns of turquoise procurement. Here we show geochemical evidence that turquoise from Halloran Springs was obtained by the Ancestral Puebloan of the San Juan Basin in northwestern New Mexico; the Virgin River Ancestral Puebloan in the Moapa Valley, Nevada and southern Utah; and the Fremont in central Utah.

Introduction

Turquoise was used by pre-Columbian North Americans over the millennia and was a significant symbol of wealth and status. In some cases, it was transported over hundreds of kilometres from its point of origin to the archaeological sites where the artifacts were recovered (Hull 2012; Hull and Fayek 2012; Hull et al. 2013; Hull et al. 2008; Roberts et al. 2013). In principal, the further a commodity was moved from its geological source, the more it was considered an *exotic* or *luxury* item. Considering the hardships of ancient mining and the distance between the turquoise deposits and home communities, turquoise must have been as valuable to the early inhabitants of the American Southwest as silver was to the colonial societies of New Spain. In this paper, we discuss the geochemical evidence that links turquoise from Halloran Springs, located near Baker, California in the Mojave Desert, to four diverse archaeological sites. In addition, we compare the source data from Crescent Peak, near Searchlight, Nevada; Mineral Park, near Kingman, Arizona; and two turquoise resource areas near Tonopah, Nevada, Royston Hills and Lone Mountain; with similar archaeological sites in our database (Figure 1; Table 1).

In 1897, the first news of turquoise deposits in the region of the Mojave Desert was reported when a local prospector, T. C. Basset, discovered turquoise at Halloran Springs (Figure 1). He filed a claim for the Stone Hammer Mine and reported evidence of prehistoric mining (Berkholz 1960; Nazelrod 1977). Intrigued by the discovery, Gustave Eisen from the California Academy of Sciences

explored and documented the mines during an expedition in 1898 (Eisen 1898). The area was later investigated and surveyed by Malcolm J. Rogers of the San Diego Museum during expeditions in 1926 and 1928 (Rogers 1929). The turquoise deposits around Halloran Springs displayed evidence of heavy exploitation with many ancient quarries, hammerstones, scrapers, ceramic sherds, camps, and petroglyphs (Jenson 1985; Leonard and Drover 1980; Rogers 1929; Weigand 1982; Weigand and Harbottle 1993). Although historic turquoise mining has destroyed much of the evidence of ancient mining, independent modern-day miners still follow the ancient tunnels to find turquoise. Many of these prehistoric tunnels have been *mucked-out* (Figure 2); this is where an individual or small group of historical miners remove or muck-out the softer sediments that filled the adits and tunnels when they were abandoned (Nazelrod 1977). Hammerstones and other stone tools were recovered scattered throughout the soft sediments (Figure 3). The largest incident of an area that was mucked-out was reported to Malcolm J. Rogers (1929); it was where workers cleared out a prehistoric quarry that was nine meters long, and over three meters wide and deep. Artifacts such as native tortoise shells, an elk scapula, and stone tools were recovered in the debris.

Although the region has been inhabited by the Desert Mojave and historically by the Paiute, the style of the recovered artifacts was more similar to Ancestral Puebloan artifacts than the artifacts of the local populations. This led researchers to propose that the turquoise was mined by the Ancestral Puebloan;

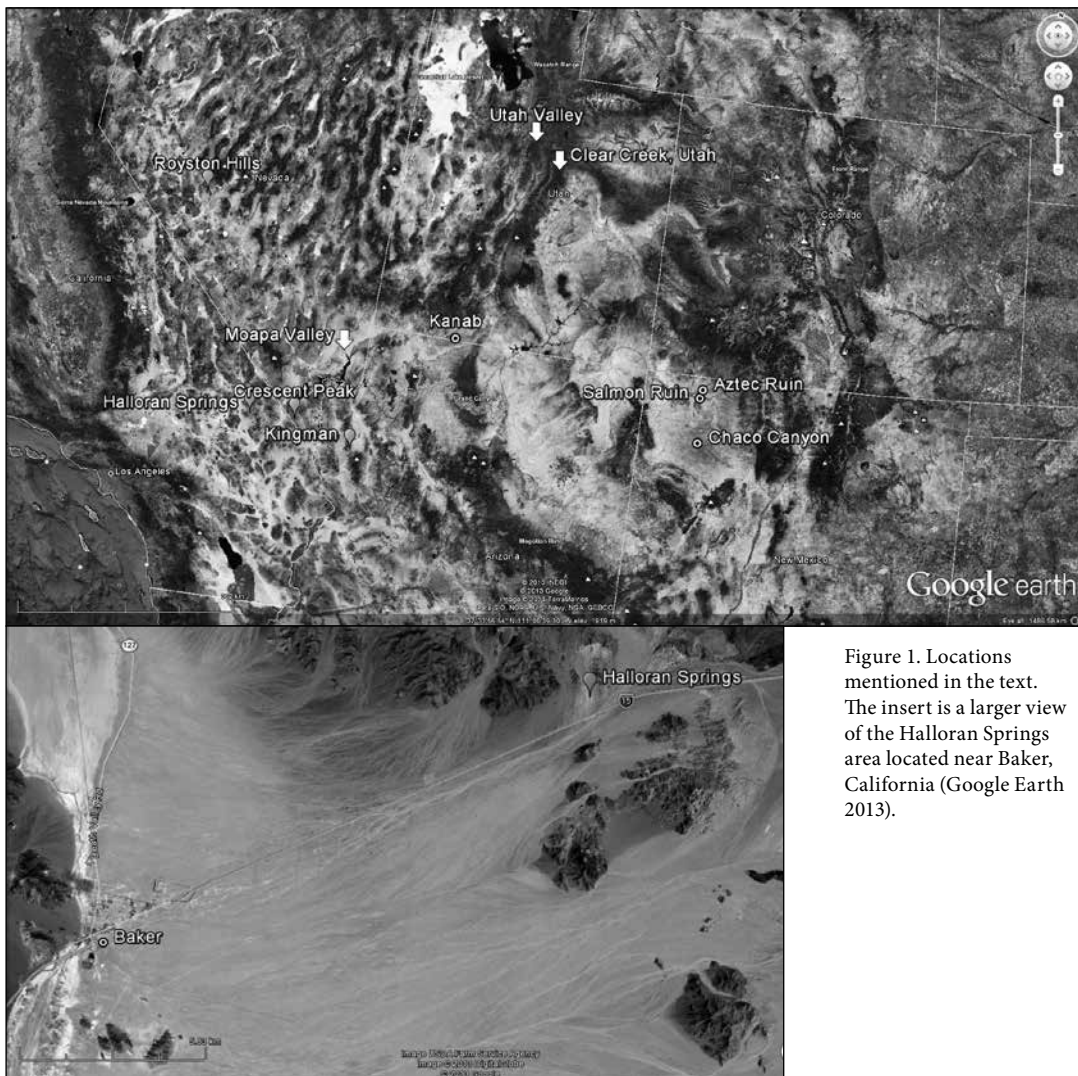


Figure 1. Locations mentioned in the text. The insert is a larger view of the Halloran Springs area located near Baker, California (Google Earth 2013).

formally known as the Anasazi (e.g., Jenson 1985; Leonard and Drover 1980; Rafferty 1990; Roberts and Ahlstrom 2012). In addition to the Puebloan style artifacts, a legend was told to Dr. Eisen by a member of the Paiute that spoke about an ancient people from a distant land that came and lived contemporaneously with the Desert Mojave while they extracted the blue-green stone (Berkholz 1960). The concept of a long-distance trade network that included shell, turquoise, salt, and cotton that linked the western desert region with the American Southwest was proposed by Margaret Lyneis (1986) suggesting that the lowland Virgin Puebloans played an important role as intermediaries in the network. Kevin Rafferty (1989) suggested that not only were the lowland Virgin Puebloans involved in trade networks but were directly tied to the extensive Chacoan trade system that may have connected the Ancestral Puebloans with Mesoamerica. Now that we have the ability to geochemically link turquoise artifacts to their geological source, we are able to investigate the propositions of Puebloan peoples obtaining turquoise from Halloran Springs and other western desert regions. We present preliminary data that support models suggesting that the Ancestral Puebloan obtained

turquoise through long-distance direct acquisition and/or turquoise trade routes from Halloran Springs and other desert resource areas. The Fremont from several sites in central Utah were also in possession of turquoise from these resource areas suggesting that there were diverse groups of miners and possibly multiple trade routes that existed across these regions.

Turquoise provenance studies

Turquoise is a supergene mineral that forms in the fractures of igneous, sedimentary, and metamorphic rocks by drawing its elemental constituents from the surrounding host rock (Morrissey 1968; Northrop 1975; Pogue 1974). The majority of turquoise deposits are associated with copper porphyry intrusive bodies, including many of the key economic copper deposits in the American Southwest and the Great Basin region of Nevada (Anthony et al. 1977; Arrowsmith 1974; Hull 2012; Morrissey 1968; Sigleo 1970). The mineral turquoise, $\text{Cu}(\text{Al}, \text{Fe}^{3+})_6(\text{PO}_4)_4(\text{OH})_8 \cdot 4\text{H}_2\text{O}$, varies in color from almost white to light blue, dark blue and dark green, with all shades in between.

Table 1. Turquoise Resource Areas Linked to Archaeological Sites.

Turquoise Resource Area	Amount	Archaeological Site	Affiliation	Location
Halloran Springs	1	Aztec Ruin	Ancestral Puebloan – affiliated with Chaco Canyon	Northern San Juan Basin, north-western New Mexico
Halloran Springs	1	Yamashita Y3 (26CK6446)	Ancestral Puebloan – Virgin Branch	Moapa Valley, northwest of Las Vegas, Nevada
Halloran Springs	3	Eagle’s Watch (42KA6165)	Ancestral Puebloan – Virgin Branch	Near Kanab, south-central Utah
Halloran Springs	1	Kay’s Cabin (42UT813)	Fremont	Near Utah Valley, central Utah
Crescent Peak, near Searchlight, NV	1	Pueblo Bonito	Ancestral Puebloan – Chaco Canyon	Central San Juan Basin, New Mexico
Crescent Peak, near Searchlight, NV	1	Salmon Ruin	Ancestral Puebloan – affiliated with Chaco Canyon	Northern San Juan Basin, north-western New Mexico
Crescent Peak, near Searchlight, NV	1	Steve Perkins (26CK2072)	Ancestral Puebloan – Virgin Branch	Moapa Valley, northwest of Las Vegas, Nevada
Mineral Park, near Kingman, AZ	1	Salmon Ruin	Ancestral Puebloan – affiliated with Chaco Canyon	Northern San Juan Basin, north-western New Mexico
Mineral Park, near Kingman, AZ	1	Eagle’s Watch (42KA6165)	Ancestral Puebloan – Virgin Branch	Near Kanab, south-central Utah
Mineral Park, near Kingman, AZ	2	Five Finger Ridge	Fremont	Near Clear Creek Canyon, Utah
Royston & Lone Mountain, near Tonopah, NV	6	Marcia’s Rincon	Ancestral Puebloan – Chaco Canyon	Central San Juan Basin, New Mexico
Royston & Lone Mountain, near Tonopah, NV	1	Pueblo Bonito	Ancestral Puebloan – Chaco Canyon	Central San Juan Basin, New Mexico
Royston & Lone Mountain, near Tonopah, NV	1	Salmon Ruin	Ancestral Puebloan – affiliated with Chaco Canyon	Northern San Juan Basin, north-western New Mexico
Royston & Lone Mountain, near Tonopah, NV	1	Kay’s Cabin (42UT813)	Fremont	Utah Valley, central Utah

The first attempt to identify the provenance regions of turquoise artifacts was to compare the color and other visual similarities between the artifacts and turquoise source samples (Mathien 1981). Unfortunately, the color and other visual similarities are subjective and range within a single turquoise deposit. As a result, researchers attempted to develop a technique to identify turquoise provenance regions by using trace and rare earth element patterns. Once a similar trace element profile was established between a source and an artifact, the researcher had evidence that could support relationships and connections between the known provenance area and the unknown artifact sample. The assumption here is that the

chemical variation within discrete compositional groups is less than the variation between compositional groups, also known as the provenance postulate (Weigand et al. 1977). The provenance postulate is the underlying basis for provenance-based studies of archaeological materials and allows researchers to examine relationships and connections between the known provenance area and the unknown artifact sample. Because the trace and rare earth element concentrations in turquoise are largely governed by the geology of turquoise deposits, the chemistry of the supergene fluids, and the weathering of turquoise, trace element analysis of turquoise could not satisfactorily differentiated between all of the turquoise resource areas.



Figure 2. A view of a turquoise deposit at Halloran Springs with an insert showing a tunnel that was *mucked out* by a modern-day miner. The photographs were taken by the authors and used with permission.



Figure 3. These stone tools were recovered from the soft sediments that were *mucked out* from the turquoise deposit in Figure 2. The photographs were taken by the authors and used with permission.

As a result, we used hydrogen and copper isotope ratios to define turquoise resource areas (Hull 2012; Hull and Fayek 2012; Hull et al. 2008).

Method

To link turquoise artifacts to their geological source, we developed the technique that uses the isotope ratios of hydrogen ($^2\text{H}/^1\text{H}$) and copper ($^{65}\text{Cu}/^{63}\text{Cu}$) and the micro-analytical abilities of a secondary ion mass spectrometer (SIMS). We established a comparative database that contains the isotopic *fingerprints* of 22 turquoise resource areas. Once the hydrogen and copper isotope ratios of the artifacts were measured, they were compared to the fingerprints in the comparative database. The identification of turquoise resource areas for artifacts that plotted in overlapping resource distribution patterns was resolved by measuring the centroid of the artifact with the centroid of the overlapping resource distribution patterns and selecting the resource area with the shortest distance. We have identified the geological source of turquoise artifacts

recovered from archaeological sites across the Greater Southwest and the Great Basin region (Hull 2012; Hull and Fayek 2012; Hull et al. 2013; Hull et al. 2008; Roberts et al. 2013).

For turquoise provenance studies, SIMS has shown to be the least destructive technique for measuring isotope ratios. SIMS allows analyses of solid samples (i.e. the ability to focus the primary ion beam on clear turquoise grains) with a spatial resolution on the scale of a few micrometres, relatively simple sample preparation, and short analysis times. For hydrogen, isotope analysis times in turquoise are less than 12 minutes (Liu et al. 2010). The sample preparation and SIMS analysis is relatively non-destructive to the sample, which is important when analyzing archaeological artifacts. Once the artifacts have been analyzed they can be returned to museum or other archaeological collections (Hull 2012; Hull and Fayek 2012; Hull et al. 2008).

For SIMS analyses, turquoise source samples are cut into 1 mm to 1 cm pieces and prepared in epoxy mounts. Large artifacts (<2 cm, e.g. pendants) are mounted in

phenol rings, and turquoise source samples and small artifacts (<6 mm, e.g. beads) are mounted in drilled-out 25 mm diameter aluminum mounts using Buehler 'Epoxy' epoxy resin. Mounts are polished using various grit (600–2400) SiC sandpaper and 1–15 µm diamond polishing compounds. Polishing is the most destructive part of the procedure and care is taken with the positioning of the artifact in the epoxy so that any areas that are relatively flat are exposed, lessening the impact of the polishing. The polished mounts are washed with a dilute soap solution, rinsed in deionized water, cleaned with ethanol, and placed in an oven at 60 °C for 20 minutes to remove absorbed water. Reflected-light photomaps of each mount are made to identify the regions devoid of inclusions and alteration. A ~200 Å thick Au coat is sputter-deposited on the sample mount surfaces to ensure a surface conductivity of 5–10 ohms/cm.

Mounts are placed in stainless steel sample holders and the entire assembly is placed in the SIMS and held at high vacuum for a minimum of eight hours prior to the start of analysis. During the measurement of isotopic ratios by SIMS, a beam of primary ions (a few µm in diameter) is focused on the solid sample surface, thus obtaining a localized spot analysis. Atoms, ions and molecules are removed by the primary beam, a phenomena referred to as sputtering. The ions are extracted, focused and accelerated by a secondary ion beam through a slit and into a mass spectrometer. During the SIMS analysis, an intrinsic mass dependent bias is introduced, which is referred to as instrumental mass fractionation (IMF) and typically favors the low mass isotope. The greatest contributor to the IMF is the ionization process dependent upon sample characteristics such as chemical composition. This is referred to as compositionally dependent fractionation or matrix effects (Riciputi et al. 1998). Therefore, accurate isotopic SIMS analysis requires correction for IMF by standardizing the IMF using mineral standards that are compositionally similar to the unknown samples. SIMS results from the standard are compared to its accepted isotopic composition in order to compute a correction factor that is applied to the unknown samples measured during the same analysis session (Riciputi et al. 1998). To calibrate the mass bias, standards with known iron contents and δ⁶⁵Cu and δD isotopic values are analyzed during the same analytical session as the samples.

The D/H and ⁶⁵Cu/⁶³Cu isotopic measurements are performed with a Cameca IMS-7F ion microprobe installed in the University of Manitoba in 2006. Positive secondary ions are produced by an O⁺ beam with impact energy of 22.5 keV. The samples and standards are analyzed using 40 nA, 12.5 kv O⁺ primary beam focused on a ~50 µm spot. The largest contrast (400 µm) and field (1800 µm) apertures, in conjunction with 150 µm image field and an energy bandpass of ±25 eV, are used to maximize sensitivity. The secondary column high voltage is set to 10 kV. For D/H isotopic measurements, the secondary ion mass spectrometer is operated at a mass resolution of

~800 to separate H²⁺ from D⁺. Interferences for ⁶⁵Cu/⁶³Cu isotopic measurements are resolved by offsetting the sample high voltage by -50 V (e.g. 9950 V), while maintaining the electrostatic analyzer in the secondary column at 10 kV.

Hydrogen and copper isotopic compositions are reported as delta (δ) values in units of per mil (parts per thousand) relative to the standard, Vienna Standard Mean Ocean Water (V-SMOW) for hydrogen and NIST976 for copper such that:

$$\delta_A = [(R_A - R_{std}) / R_{std}] \times 10^3$$

where R_A and R_{std} are the absolute ratios of ²H/¹H (D/H; D=deuterium) or ⁶⁵Cu/⁶³Cu in the sample (turquoise) and the standard (V-SMOW or NIST976), respectively. The absolute ²H/¹H ratio of V-SMOW is 155.76 × 10⁻⁶ and the absolute ⁶⁵Cu/⁶³Cu ratio of NIST976 is defined as 4.4563 × 10⁻¹.

Results

Turquoise artifacts that originated from Halloran Springs included one sample from an Ancestral Puebloan site, Aztec Ruin, in northwestern New Mexico; one from a Virgin Puebloan site, Yamashita Y3, in the Moapa Valley, Nevada; three from a Virgin Puebloan site, Eagle's Watch, near Kanab in southern Utah; and one from a Fremont site, Kay's Cabin, in central Utah (Figure 1; Table 1). Crescent Peak (Figure 1; Table 1) turquoise was linked to three sites included in this study; each site is represented by one sample. These artifacts were recovered in two Ancestral Puebloan sites in the San Juan Basin, Pueblo Bonito and Salomon Ruin; and the Steve Perkins site, a Virgin Puebloan site in the Moapa Valley. Turquoise that originated from Mineral Park included one sample from Salmon Ruin, one from the Eagle's Watch site, and two from a Fremont site near Clear Creek Canyon in central Utah, the Five Finger Ridge site (Figure 1; Table 1). Turquoise from the two turquoise resource areas near Tonopah, Royston and Lone Mountain, were recovered from Kay's Cabin, Pueblo Bonito, and Salmon Ruin; each site represented by one sample. Six turquoise samples from Royston and Loan Mountain were recovered from a cluster of small sites located near Marcia's Rincon in Chaco Canyon.

Turquoise and ancient trade routes

Although geochemical provenance techniques are an excellent tool to identify the provenance region *where* a natural resource was originally obtained, these data must be used in conjunction with other archaeological evidence to investigate *how* (e.g., exchange, trade, or direct acquisition) and *why* (the use and meaning to the end user) a resource was obtained. However by linking point A to point B, the data can lend support to current hypotheses and models, suggest the investigation of areas that are linked by archaeological materials, and point to references

about the relationships of communities that show similar turquoise procurement strategies.

Our data support the proposition that the Virgin Puebloan settlement of Lost City, located in the Moapa Valley (Figure 1), may have represented an important hub in pan-southwestern trade and may have been responsible for sponsoring mining expeditions that ventured to western turquoise resource areas (Rafferty 1990). The evidence of extensive turquoise quarrying from Halloran Springs (Jenson 1985; Leonard and Drover 1980; Rogers 1929; Weigand 1982; Weigand and Harbottle 1993) suggests a large labor investment for the miners who obtained turquoise from this region. The presence of the Virgin Puebloans, who occupied areas in southern Nevada, northern Arizona, and parts of southern Utah (Ahlstrom and Roberts 2008:130), suggest they may have been responsible for some of the turquoise mining at Halloran Springs. However, it is important to consider that the turquoise resource areas may have been exploited by other culture groups, such as the Fremont (Table 1) or the Hohokam (Sigleo 1975) contemporaneously with the Virgin Puebloan or at different time periods.

Kevin Rafferty (1990) suggested that the inhabitants of Lost City were exploiting turquoise from Halloran Springs, Crescent Peak, and the Sullivan mine near Boulder City, Nevada. Lost City phase ceramics have been identified in west central Nevada (Harrington 1926), east central Nevada (Harrington 1928), Las Vegas Valley (Lyneis 2000), and the Halloran Springs area (Leonard and Drover 1980; Rogers 1929) suggesting that they may have expanded into or were trading with the inhabitants of turquoise resource areas. The transport of turquoise, cotton, shell from the Pacific Coast and the Gulf of California, and salt from the lower Virgin River (Harrington 1925; Lyneis 1986), would have been a lucrative business for any traders willing to transport these commodities over the hundreds of kilometers to a regional center, such as Chaco Canyon. Some trade/exchange models include a group of middle-men or a group of long-distance traders that may have been responsible for the transport of the exotic commodities from the western regions to the San Juan Basin. Steadman Upham (1982) proposed that long-distance trade was controlled and conducted by the elite suggesting that long-distance traders were either controlled by or were members of the upper echelon of the Ancestral Puebloan hierarchy. In exchange for luxury items, the occupants of the western frontier may have received non-material resources such as ideology and religious concepts to reaffirm their status from the elite in Chaco Canyon (Rafferty 1990:13).

Our data show that turquoise from Halloran Springs, Crescent Peak, Kingman, and Royston Hills was transported to the San Juan Basin. Turquoise from Halloran Springs and Crescent Peak was recovered from archaeological sites in the Moapa Valley and turquoise from Halloran Springs and Kingman was recovered from the Eagle's Watch site (Figure 1; Table 1) possibly representing

nodes on a route funneling trade items between the San Juan Basin and the western desert region (Roberts et al. 2013). Turquoise from the Fremont sites in central Utah was obtained from Halloran Springs, Kingman, and the Royston Hill (Figure 1; Table 1). These sites are located on or near the main prehistoric trade routes that follow the historic Spanish Trail that connected California and New Mexico (Roberts et al. 2013). Although our sample size is small, our data allows us to investigate overall trade routes establishing the foundation for future studies. As we analyze additional artifacts, these relationships will become more apparent.

There are three essential points to consider with regards to provenance studies of any archaeological material: 1) the data obtained will only be as good as the reference database used for comparison (Lee 2004:302); 2) the research will always be a work-in-progress (Hull 2012); and 3) limitations may be identified as more samples are tested (e.g., turquoise alteration: Abdu et al. 2011; Hull 2006). For the first consideration, we established the comparative database that contains 22 turquoise resource areas representing deposits in Arizona, Baja California, southeastern California, Colorado, Nevada and New Mexico (Hull 2012; Hull and Fayek 2012). For some of the turquoise resource areas, we have analyzed multiple samples from different sites within a single locale and many of the provenance samples were analyzed several times over a two year period to test for reproducibility (Hull 2012). We will continue to add the isotope signatures of turquoise resource areas to the comparative database as provenance samples become available and the data from every analyzed turquoise artifact will also be maintained in our digital archive. As the isotopic signatures of newly analyzed turquoise resource areas are added to the database, it is possible that some of them may overlap with existing distribution patterns. The data from turquoise artifacts previously analyzed will be reviewed as more turquoise resource areas are isotopically characterized.

Conclusion

In this paper, we showed that Halloran Springs was a resource area for the Fremont, and the Virgin and Ancestral Puebloans. How the turquoise ended up in the sites is still under investigation. The development and collapse of many turquoise trade networks must have played out over the centuries within the larger framework of trade structures. Trade structures are very organized and continue over long periods of time, providing the background for trade networks that are more fluid and constantly changing through time (Weigand 1994:27). For example, Chaco Canyon may have been a principal trade center participating in the trade networks within the Greater Southwest, especially in the movement of turquoise. However when the significance of Chaco Canyon as a trade center declined, the development and importance of another trade center, such as Paquimé after A.D. 1300,

may have filled the void. Trade within the Greater Southwest may have been briefly affected by these types of changes, but the trade structure endured over time. Trade networks, on a much smaller scale, are local agreements and exchange alliances between communities that came and went within the trade structures (Weigand 1994:27).

Ancient long-distance trade networks were an important avenue for the movement of goods; however they also served other purposes. Information of distant regions would have traveled along these networks providing the foundation for migration (Duff 1998:33) and the diffusion of ideas. They were also avenues of social interaction (Irwin-Williams 1977:142) and that would blend social, political, ritual, and economical aspects. Early European explorers reported an impressive amount of trade in the American Southwest and the long distances that were travel by foot (Ford 1983:712). Nomadic groups were also reported as bringing trade items to regional centers (e.g., Pecos and Taos) for trade (Ford 1983:712). Scheduled trade festivals would have been a means that brought many groups of people (e.g., sedentary agriculturalists and nomadic hunter and gatherer groups) and different trade items together. The mechanisms responsible for the movement of turquoise across the American Southwest were probably as diverse as the cultural groups that lived there.

Future consideration for this research are: 1) the expansion of the turquoise comparative database by geochemically characterizing more turquoise resource areas, 2) the continuation of testing the isotopic homogeneity of each turquoise deposit, 3) testing the technique for additional limitations (e.g., weathering) and how to overcome these restrictions, and 4) the analyses of more artifacts and the reconstruction of pre-Columbian turquoise trade routes. The long-term goal of this research is to map the movement of turquoise across large regions and through time to evaluate hypotheses about trade structures and networks that covered this vast expanse of territory over a period of two thousand years. In conjunction with other evidence, it will be possible to discern more about the relationships between the cultures that coveted this blue-green mineral and participated in these trade structures.

References

- Abdu, Yassir A., Sharon K. Hull, Mostafa Fayek, and Frank C. Hawthorn
2011 The Turquoise-chalcosiderite $\text{Cu}(\text{Al}, \text{Fe}^{3+})_6(\text{PO}_4)_4(\text{OH})_8 \cdot 4\text{H}_2\text{O}$ Solid-Solution Series: A Mössbauer Spectroscopy, XRD, EMPA and FTIR Study. *American Mineralogist* 96:1433-1442.
- Ahlstrom, Richard V. N. and Heidi Roberts
2008 Who Lived on the Southern Edge of the Great Basin? In *The Great Basin: People and Place in Ancient Times*, eds., Catherine S. Fowler and Don D. Fowler, pp. 128-135. School for Advance Research Press, Santa Fe, New Mexico.
- Anthony, John W., Sidney A. Williams, and Richard A. Bideaux
1977 *Mineralogy of Arizona*. University of Arizona Press, Tucson, Arizona.
- Arrowsmith, Rex
1974 Introduction. In *The Turquoise. A Study of Its History, Mineralogy, Geology, Ethnology, Archaeology, Mythology, Folklore, and Technology*. Glorieta, New Mexico. Originally published 1915, Memoirs of the National Academy of Sciences Vol. XII, Part II, Washington D.C.
- Berkholz, Mary Frances
1960 Toltec Mojave Desert Mine of the Ancients. *Science of Man* Dec 1960:10-11.
- Duff, Andrew I.
1998 The Process of Migration in the Late Prehistoric Southwest. In *Migration and Reorganization: The Pueblo IV Period in the American Southwest*, ed., Katherine Spielman, pp. 31-52. Anthropological Research Papers No. 51. Arizona State University, Tempe, Arizona.
- Eisen, Gustav
1898 Long Lost Mines of Precious Gems are Found Again, Located in the Remotest Wiles of San Bernardino County and Marked by Strange Hieroglyphics. *The San Francisco Call*: March 18 and 27, San Francisco.
- Ford, Richard I.
1983 Inter-Indian Exchange in the Southwest. In *Southwest*, ed., Alfonso Ortiz, pp. 711-722. Handbook of North American Indians Vol. 10, Smithsonian Institute, Washington D. C.
- Harrington, Mark R.
1925 The "Lost City" of Nevada. *Scientific American*, July:14-17.
1926 Another Ancient Salt Mine in Nevada. *Indian Notes* 3(4):221-232. Museum of the American Indian, Heye Foundation, New York, New York.
1928 Tracing the Pueblo Boundary in Nevada. *Indian Notes* 5(2):235-240. Museum of the American Indian, Heye Foundation, New York, New York.
- Hull, Sharon
2012 *Turquoise and Exchange and Procurement in the Chacoan World*. Unpublished PhD dissertation, University of Manitoba, Winnipeg, Manitoba.
2006 *Using Hydrogen and Copper Stable Isotopes to Source Turquoise*. Unpublished M.A. thesis, Eastern New Mexico University, Portales, New Mexico.
- Hull, Sharon and Mostafa Fayek
2012 Cracking the Code of Pre-Columbian Turquoise Trade Networks and Procurement Strategies. In *Turquoise in Mexico and North America: Science, Conservation, Culture and Collections*, eds. J.C.H. King, M. Carocci, C. Cartwright, C. Mc Ewan, and R. Stacey, pp. 29-40. Archetype Publications in Association with the British Museum, London.
- Hull, Sharon, Timothy D. Maxwell, Mostafa Fayek, and Rafael Cruz Antillón
2013 *Chasing Beauty: Evidence for Southwestern U. S. Turquoise in Mexico*. Paper presented at the Society for American Archaeology, Honolulu, Hawaii.

- Hull, Sharon, Mostafa Fayek, Frances J. Mathien, Phillip Shelley, and Kathy Roler Durand
2008 A New Approach to Determining the Geological Provenance of Turquoise Artifacts Using Hydrogen and Copper Stable Isotopes. *Journal of Archaeological Science* 35:1355-1369.
- Irwin-Williams, Cynthia
1977 A Network Model for the Analysis of Prehistoric Trade. In *Exchange Systems in Prehistory*, eds., Timothy K. Earle and Jonathan E. Ericson, pp. 141-151. Academic Press, New York, New York.
- Jenson, William A.
1985 *Prehistoric Turquoise Mining in the Turquoise Mountain Region, Northeast Mojave Desert, California*. Unpublished M.A. thesis, California State University, San Bernardino, California.
- Lee, C. W.
2004 The Nature of, and Approaches to, Teaching Forensic Geoscience on Forensic Science and Earth Science Courses. In *Forensic Geoscience: Principles, Techniques, and Applications*, eds., K. Pye and D. J. Croft, pp. 301-312. Geological Society of London, London.
- Leonard III, N. Nelson and Christopher E. Drover
1980 Prehistoric Turquoise Mining in the Halloran Springs District, San Bernardino County, California. *Journal of California and Great Basin Anthropology* 2:245-256.
- Liu, Rong, Sharon Hull, and Mostafa Fayek
2010 A New Approach to Measuring D/H Ratios with the Cameca IMS-7F. *Journal of Surface and Interface Analysis* 43(1-2):458-461.
- Lyneis, Margaret
1986 A Spatial Analysis of Anasazi Architecture, A.D. 950-1150, Moapa Valley, Nevada. *The Kiva* 52(1): 53-74.
2000 Life at the Edge: Pueblo Settlements in Southern Nevada. In *The Archaeology of Regional Interaction: Religion, Warfare, and Exchange across the American Southwest and Beyond*, ed., Michelle Hegmon, pp. 257-274. Proceedings of the 1996 Southwest Symposium. University Press of Colorado, Boulder, Colorado.
- Mathien, Frances Joan
1981 Neutron Activation of Turquoise Artifacts from Chaco Canyon, New Mexico. *Current Anthropology* 22:293-294.
- Morrissey, Frank
1968 *Turquoise Deposits of Nevada*. Report 17, Mackay School of Mines, University of Nevada, Reno, Nevada.
- Nazelrod, Ed
1977 Recent Developments in the Turquoise Mountains of California. *Lapidary Journal* December 1977:1982-1988.
- Northrop, Stuart A.
1975 *Turquois and Spanish Mines in New Mexico*. University of New Mexico Press, Albuquerque, New Mexico.
- Pogue, Joseph
1974 *The Turquois. A Study of Its History, Mineralogy, Geology, Ethnology, Archaeology, Mythology, Folklore, and Technology*. Glorietta, New Mexico. Originally published 1915, *Memoirs of the National Academy of Sciences* Vol. XII, Part II, Washington D.C.
- Rafferty, Kevin
1990 The Virgin Anasazi and the Pan-Southwestern Trade System, A.D. 900-1150. *Kiva* 56:3-24.
1989 The Anasazi Abandonment and the Numic Expansion: a Reply to Ambler and Sutton. *North American Archaeologist* 10(4):311-329.
- Riciputi, Lee R., Bruce A. Paterson, and Robert L. Ripperdan
1998 Measurement of Light Stable Isotope Ratios by SIMS: Matrix Effects for Oxygen, Carbon, and Sulfur Isotopes in Minerals. *International Journal of Mass Spectrometry* 178:81-112.
- Roberts, Heidi, Sharon Hull, and Mostafa Fayek
2013 *Sourcing Turquoise Artifacts from Seven Archaeological Sites in the Eastern Great Basin*. Paper presented at the Society for American Archaeology, Honolulu, Hawaii.
- Roberts, Heidi and Richard V.N. Ahlstrom
2012 Gray, Buff, and Brown. In *Meetings at the Margins: Prehistoric Cultural Interactions in the Intermountain West*, ed. David Rhode, pp. 211-228. The University of Utah Press, Salt Lake City, Utah.
- Rogers, Malcolm J.
1929 *Report of an Archaeological Reconnaissance in the Mohave Sink Region*. San Diego Museum of Man Archaeological Papers 1(1), San Diego.
- Sigleo, Anne Marguerite Colberg
1970 *Trace-element Geochemistry of Southwestern Turquoise*. Unpublished M.S. thesis, University of New Mexico, Albuquerque, New Mexico.
1975 Turquoise Mine and Artifact Correlation for Snaketown Site, Arizona. *Science* 189:459-460.
- Upham, Steadman
1982 *Politics and Power: An Economic and Political History of the Western Pueblo*. Academic Press.
- Weigand, Phil C.
1982 Sherds Associated with Turquoise Mines in the Southwest USA. *Pottery Southwest* 9(2):4-6.
1994 Observations on Ancient Mining within the Northwestern Regions of the Mesoamerican Civilization, with Emphasis on Turquoise. In *In Quest of Mineral Wealth: Aboriginal and Colonial Mining and Metallurgy in Spanish America*, eds., Alan K. Craig and Robert C. West, pp. 21-35. *Geoscience and Man* 33.
- Weigand, Phil C. and Garman Harbottle
1993 The Role of Turquoises in the Ancient Mesoamerican Trade Structure. In *The American Southwest and Mesoamerica: Systems of Prehistoric Exchange*, eds., Jonathan E. Ericson and Timothy G. Baugh, pp. 159-177. Plenum Press, New York, New York.
- Weigand, Phil C., Garman Harbottle, and Edward V. Sayre
1977 Turquoise Sources and Source Analysis: Mesoamerica and the Southwestern U.S.A. In *Exchange Systems in Prehistory*, eds., Timothy K. Earle and Jonathan E. Ericson, pp. 15-34. Academic Press, New York, New York.

Weathering climatic change: signs of prehistoric peoples

Amy Leska

American Rock Art Research Association (ARARA), Lompoc, CA 93438, festuned@gmail.com

Adaptation plays a central role in all human history. Native American cultures have been called “primitive” and their environments “marginal.” Yet these descriptors do not convey the heartiness and depth of culture that existed for thousands of years. Rock art sites, along with other material culture, lend insight into the adaptations of hunter-gatherer societies that lived in the Mojave Desert. Exploring off the beaten tracks may lead a person to some of these signs—a pot shard, a stone tool flake, stone circles, or perhaps one of the many rock art sites in the Mojave Desert.

Rock art sites harken back to earlier eras. Continuous human occupation in the Mojave Desert began with the Clovis people during the Terminal Pleistocene approximately 10,000 years ago. Most recently, the Desert Mohave Indians (Hokan speakers) in the Lower Colorado River region, the Chemehuevi Indians (Numic speakers) in eastern and central portions, and the Vanyume Serrano (Takic speakers) closer to the San Bernardino Mountains occupied the Mojave Desert (Christensen, 2010). In historic times pioneers, miners, and other settlers arrived and pushed native groups out of their homelands. While Native Americans lived off the land, various flora and fauna provided food, shelter, and clothing, and the landscape was dynamic and sacred.

Rock art sites tell us that people were in a particular place for a specific reason. The styles of rock art suggest a time and a culture and are part of the artifact record. Rock art is a form of symbolic communication and gives us an indication of how the land was used. It is understood in context of its placement in the landscape. Possible explanations of how rock art functioned are territory or trail markers, ceremonial or meeting places, solstice markers, rites of passage, or decoration. Ultimately they occur where people have spent time be it for sacred and/or secular activities. Some rock art sites may belong to a constrained time period while others may have been revisited over an extended period of time, the imagery evolving along the way. Sometimes elements blend and merge, making categorization difficult.

Most likely the rock art tradition in the Mojave Desert began during the mid to late Holocene. An estimate for the inception of the Western Archaic Tradition of petroglyphs is 4000 years ago (Christensen, et al., 1999) which falls into this climatic period. Much of the rock art found in the Mojave Desert has been assigned to this tradition. The boundaries of the Western Archaic Tradition extend well beyond the Mojave Desert into eastern Oregon/southern Idaho, western New Mexico/Colorado,

and northern Mexico. The Great Basin Abstract style typifies the Western Archaic Tradition and is the largest style within the desert’s geographic borders. The common style indicates a common culture throughout the region and extends across the whole of Nevada and into all of its surrounding states including the Mojave Desert. It is expressed as a diverse array of abstract elements: circle variations, straight lines, and enclosed geometric designs produced by pecking, abrading, scratching, and painting (Christensen, et al., 1999). The word tradition here refers to the practice of creating rock art with an inventory of traits which is passed on from generation to generation along with its meanings or purposes.

Before this time, the Clovis people, the only Paleo-Indian complex in the Mojave Desert (10,000-8,000 BP), were highly mobile pursuing a big game economy. During the Holocene, groups began to develop into more culturally and technologically distinct populations (Sutton et al., 2007). The early Holocene brought drier conditions and climatic swings that would have thinned the herds and affected the reliability of assorted flora. The mid Holocene groups (8,000-3,000 BP) had broader diets and developed milling tools like the mortar and pestle indicating more reliance on hard seeds like mesquite pods. By the end of the mid Holocene, climatic conditions became hotter and drier and the population decreased due to environmental stresses (Jones and Klar, 2007). The archaeological record thins out; few sites date to 3000-2000 BC (Sutton, et al., 2007). The Late Holocene marked a time of cooler and wetter conditions, and several new cultural complexes emerged. Cultural complexes are classified by point typology, and later, ceramics, basketry.

In rock art, characteristic elements suggest cultural origins and distribution. Within the geographic region of the Western Archaic Tradition are areas with a varying iconography and a unique style. These rock art styles are described by elements or expressions that are distinctive to that region. The Grapevine or Colorado River style borders the Lower Colorado River and includes symmetrical and geometric designs such as enclosed crosses. In the Great Basin Abstract and the Grapevine styles, a minimal number of zoomorphic and anthropomorphic figures occur and are usually expressed as sheep, lizards, and digitated stick figures.

Since no reliable absolute dating technique has been developed for petroglyphs, archeologists connect them to other material culture when possible which can enhance our understanding of rock art. Designs on baskets are compared to rock art elements, and diagnostic points or

other datable artifacts give clues to the age of a rock art site when they are associated. For example, the few pictographs in the Cinder Cone Lava Beds tend to be connected to temporary habitation areas or milling features. Considering that the production method of pigments involves grinding and mixing, a similar activity to food preparation, and that some pictograph motifs also appear on Chemehuevi basketry or Mohave women's face paint, women could have been the creators of pictographs in the eastern Mojave Desert (Christensen and Dickey, 1996). A petroglyph depicting a bow and arrow would be no older than 1800 years, whereas a petroglyph depicting the atlatl could be thousands of years old. Horse and rider depictions are clearly historic.

Trade and social complexity increased in the Late Holocene, as did evidence of ritual activities like producing rock art, especially in regards to hunting. Researchers have long connected extensive petroglyph sites in the Coso Range—Big and Little Petroglyph Canyons—to increase rituals in regards to hunting (Grant, Baird, Pringle, 1968, Gilreath and Hildebrandt, 2008). These petroglyphs are stylized and often representational. These sites depict pattern-bodied anthropomorphs amongst large herds of uniquely styled Coso big horn sheep. They are distinctive for their unique depiction of the bighorn sheep: boat shaped bodies with horns that drape over each side of the head so that the animal faces the viewer straight on. Depictions of both atlatls and bows and arrows suggest rock art production over a depth of time. The Coso style is found in highly concentrated sites in the Coso and Argus Ranges (Christensen, et al. 1999).

Newberry Cave, another significant ceremonial site, dates to the Late Archaic around 3500 BP (Davis and Smith, 1981). It is the only site in California where split twig figurines have been found, and painted depictions of split twig figurine-type ungulates grace the walls in a color matching the paint on artifacts recovered from the cave. The pictographs are definitely part of the artifact assemblage. Obsidian found in Newberry Cave was sourced to southern Nevada and the Coso Range and is evidence of long-distance trade (Leska, 2009). The split twig figurines demonstrate a connection to the Grand Canyon in Arizona where the majority of split twig figurine sites are found. This site is evidence of a distinctive cultural complex with established trade routes and social complexity.

By 1 AD, agriculture appeared in the eastern Mojave Desert. A petroglyph near Black Mountain has been interpreted as rows of corn. The more efficient bow and arrow emerged around 200 AD replacing the atlatl, and the environment was more productive allowing more permanent structures like wickiups and pithouses to develop. Seven hundred years later the ancestral Puebloan, or Anasazi, was present in northeastern Mojave. By the time they began mining turquoise north of Halloran Springs in 1000 AD, they had also experienced the onset of the Medieval Climatic Anomaly which began around 800 AD. This

major environmental change brought drought leading to environmental deterioration and causing a sharp population decline as the land could not sustain as many people. Protohistoric cultural complexes developed out of this period around 1100 AD, and these people are believed to be the ancestors of present cultural groups. Ground figures along the Colorado River fit into the category of rock art and depict mythological characters of the Mohave Indians (von Worlhof, 2004).

The lives of Native Americans were closely tied to their environment. A recent study based on extensive recording of the rock art of the Cinder Cone Lava Beds in the Mojave Preserve concludes that most of the petroglyph panels occur along trails connected to seasonal rounds to collect resources from Cima Dome, Silver and Soda Lakes, Devil's Playground and the Clark Mountains. The water sources of the Cinder Cones are limited to ephemeral tanks and potholes, and only a few springs. There are no toolstone resources, and only small vegetal microenvironments. Therefore, subsistence migration is a likely explanation for the number of rock art sites here (Christensen, 2010).

Lastly, the Little Ice Age (1400-1875 AD) brought temperatures that are half a degree Celsius cooler than now. More winter precipitation ended the drought and allowed juniper woodlands to gradually expand. Rather than an extended, steady cold period, the LIA had major fluctuations that lasted decades (Jones and Klar, 2007). However, some archaeologists believe that in general the LIA also caused crop failures, decimated fish populations, and led to more disease and political and social conflict (Sutton, et al, 2007). Towards the end of the LIA, explorers like Friar Francisco Garces (1776) and Jedediah Smith (1826) began to travel through the Mojave Desert and interact with the Native Americans ultimately spelling the end of their traditional subsistence on the landscape.

Through the study of rock art and other cultural artifacts, we can piece together a deep prehistory for Native Americans in the Mojave Desert and discern the essence of desert life. Groups were able to develop subsistence strategies, extensive trade routes, social structures, and ceremonial rituals while persevering and even prospering through climatic fluctuations. Each climatic variation brought changes to the environment and to the availability of natural resources requiring cultural adaptations for the population to endure. People continued to find a variety of food sources, develop more efficient tools, and expand their material culture reflecting more and more sophisticated societies. The rock art tradition developed early; an enduring sign of how early people weathered climatic changes, persisting to the present.

References

- Christensen, Don D., 2010, "Context and Rock Art in the Cinder Cone Lava Beds, Eastern Mojave Desert, California," *in* *American Indian Rock Art*, Vol. 36:171-181.

- Christensen, Don D., Dickey, Jerry, 1996, 'The Pictographs of the Eastern Mojave Desert of California and Nevada: An Initial Investigation' *in* Pacific Coast Archaeological Society Quarterly, Vol. 32, Numbers 2&3, Spring & Summer, pgs. 1-81.
- Christensen, Don D., Dickey, Jerry, and Lee, David, 1999, "Regional Variation in Rock Art Styles in the Southern Great Basin: A View from the West Mojave," *in* American Indian Rock Art, Vol. 25:69-80.
- Davis, CA and Smith, GA, 1981, Newberry Cave, San Bernardino County Museum Association, Redlands, CA.
- Gilreath, A. and Hildebrandt, W.R. 2008, Coso Rock Art within its Archaeological Context *in* Journal of California and Great Basin Anthropology, Vol. 28:1-22,
- Grant, C., Baird, JW., and Pringle, JK., 1968, Rock Drawings of the Coso Range, Inyo County, California. Maturango Museum Publication No. 4, Banning, California.
- Jones, Terry L, and Klar, Kathryn A., 2007, 'Colonization, Culture, and Complexity,' *in* California Prehistory: Colonization, Culture, and Complexity, AltaMira Press, pgs. 299-315.
- Leska, Amy, 2009, "Newberry Cave, Mojave Desert, California: A Fresh Look at Newberry Cave and Its Paintings," *in* American Indian Rock Art, Farmington, NM, Vol. 35:131-146.
- Sutton, Mark Q., Basgall, Mark E., Gardner, Jill K., Allen, Mark W., 2007, 'Advances in Understanding Mojave Desert Prehistory,' *in* California Prehistory: Colonization, Culture, and Complexity, AltaMira Press, pgs. 229-245.
- Von Werlhof, Jay, 2004, "Spirits of the Earth: That They May Know and Remember," Imperial Valley College Museum Society, Ocotillo, CA.

Sites I would like to see: historic Native American refugee sites in southern California

Frederick W. Lange, Ph.D., RPA
hormiga_1999@yahoo.com

Prologue

Last year at this conference, I presented a paper entitled “Sites I would like to see: ‘moonshine still’ sites in the California desert” (Lange 2012). Moonshine still sites were a type of site that, from reading historical accounts, I knew existed, but not a single one had ever been recorded at any of the California Historical Resources Information System (CHRIS) information centers. Here we are, 12 months later, and still no one has recorded a moonshine site! So, while we continue to wait for the first moonshine site to be recorded, I want to present another category of “sites I would like to see” for your consideration: Native American refugee sites.

Many of you know that between 1769 and 1924, significant numbers of native peoples were forced to abandon emerging urban centers such as San Diego and to retreat to the hills, unless they chose the option of crossing into Mexico (as many did). In the surrounding hills, they lived much as they had lived in the pre-European past, while invaders of various skin colors and ethnic affiliations expropriated their traditional lands. Tens of thousands of these displaced native peoples, families and individuals, refugees in their own land, eked out an existence in the continually shrinking rural zones of the state; their physical traces would be highly significant sites in terms of tracing the transition from being survivors of the foreign invasions to preserving at least certain elements of their traditional cultures. The California Historical Resources Information System (CHRIS) has recorded a wide range of archaeological sites and historic period miners, dust bowlers, and homesteaders, but so far as I am aware, as absent as the moonshiners, not a single Native American refugee site; these sites represent what Robert Ascher (1974) designated “the inarticulate of history”, those who did not write about themselves, and who were not written about by others.

As will be seen below, two unique individuals (Delfina Cuero and Tom Lucas) have written about themselves (with the help of Anglo biographers). However, the archaeological vestiges of the sites they occupied during their lengthy status as refugees (particularly Delfina Cuero) are still “off the radar.” or perhaps just misidentified as the following example may demonstrate.

In the surveys I had done and the reports I had read, I had never come across a site specifically characterized as a Historic Indian Refugee Site. Perhaps a bias exists. Soon

after I had read Delfina Cuero’s account, I participated in a field visit with a representative of a state agency to a project location where there was a small rockshelter with a fire-blackened roof. The chronology of use of the site was inconclusive, and I suggested, based on my then recent reading of Delfina Cuero’s life story, the potential of it having been a short-term refugee site; my suggestion was abruptly rejected by the agency representative, and my appetite was whetted for pursuing another “Sites I Would Like to See” episode.

Introduction

As a young graduate student at the University of Wisconsin-Madison in 1967, I had the good fortune to take an ethnohistory seminar from Professor David A. Baerreis. He was one of the pioneers in the application of the methodology of ethnohistory to archaeology and had written (1961:58) that “It is indeed this methodological consideration, the appraisal of the factors involved in coordinating a multifaceted approach that enhances the significance of the study.” My masters thesis (Lange 1968), which I developed under Dr. Baerreis’s tutelage, was an ethnohistoric analysis of historic burials of mid-19th century Native Americans along the banks of the Wisconsin River. Like the southern California native refugees, their Wisconsin brethren were beyond the margins of the 19th century European societies that had over-run their traditional lands.

Based on the intellectually stimulating Wisconsin experience, I was sold on the methodology, as Frederica de Laguna (1960:200) expressed it “that archaeological, ethnological, and historical data, if combined and analyzed together, can give a deeper insight than any one type of material or methodology alone.”

Ethnohistory had been one of my “signature” methodologies throughout my career, beginning in Wisconsin (Lange 1968); then in Barbados (Lange 1972, 1974, 1976; Handler and Lange 1978, 1979; Handler, Orser, and Lange 1979; Corrucini, Handler, Mutaw, and Lange 1982; Lange and Handler 1977, 1980a, 1980b, 1985, 2006; Lange and Carlson 1985), and then in Nicaragua (Lange 2004). Thus, continuing this type of research was a natural step in my work in California (2006, 2012). Arriving in California in mid-2003, I began to search for historical accounts that would promote the application of the ethnohistorical approach (c.f. Baerreis 1961) to the study of the Native

American sites, regions, and peoples with which I was becoming involved through my participation in cultural resource management investigations. I have continued to seek research opportunities where history and archaeology merge and support one another, whether it is searching for moonshine stills or Native American refugee sites.

Perhaps a couple of years after I arrived in the Golden State, I stumbled across a small work entitled “Delfina Cuero: Her Autobiography, An Account of Her Last Years and Her Ethnobotanic Contributions” (Shipek 1991). This account of Mrs. Cuero’s life, and another autobiography that I discovered at almost the same time, that of Tom Lucas (Cline 1984) introduced me to the oppressive conditions under which the California Indians lived as their traditional lands steadily filled with an increasing flood of Anglo-Americans, Europeans, Mexicans, and Asians in the late 19th and the early 20th centuries. The waves of foreign settlers pushed the native peoples ever closer to the margins of their traditional lands and beyond, even forcing many of them into Mexico, because prior to 1924 many “Native Americans” had no status as American citizens. As Florence Shipek wrote, the Native Americans had been “pushed into the rocks.”

My cultural work with the San Manuel Band of Mission Indians has included the cultural resources section of the Environmental Overview for the reservation (2012-2013) and native monitor training for the Water Valley Substation Project between Kramer Junction, Barstow, and Victorville in the High Desert (2012). In these two visible contexts, the brutal reduction of the Serranos’ previous traditional lands from hundreds of thousands of acres to less than 1,000 (Figure 1) acres brought Shipek’s phrasing to life.



Figure 1. San Manuel Band of Mission Indians reservation in relation to Native American tribal territories of southern California. Adapted from Bean, 1978: 576; Bean and Shipek 1978:551; Bean and Smith 1978:538.

In this article, I use the date of the founding of the first Spanish Mission in California (the San Diego de Alcalá Mission in San Diego, 1769) as a benchmark for the changes in the Native American world that Delfina Cuero (member of the *Diegueño* tribe) and Tom Lucas (member of the *Kwaaymii* tribe) came to know, in varying degrees. In addition to the 1769 benchmark, I have also calculated the number of generations (a generation averages about 25 years—from the birth of a parent to the birth of a child) that have passed from 1769 to the present, in witness to the rapid disintegration of traditional Native American lifeways.

A footnote from the Coronado Expedition and Southern California—1542

While I used the 1769 founding of the first Spanish mission in California as a benchmark, the assault on native lifeways and lives had, however, probably been going on for at least two centuries before the San Diego Mission opened its gates—in the immediate pre-mission and mission period in California, this assault was fueled by microscopic germs that were invisible until various diseases violently affected Delfina Cuero’s and Tom Lucas’s ancestors (cf. Ramenofsky 1987).

Though the first wave of European impact based on germs was well-hidden, the second wave consisted of foreign immigrants who were much more visible. By 1910 the increasing Anglo and Asian populations of San Diego were filling Mission Valley with small farms, just as the urban areas filled with houses and businesses. The breakdown in traditional land-holding patterns created a large refugee population and the Indians gradually moved out of the coastal regions.

Moving into the mountains and surrounding valleys, they were technically “squatting” because by then they did not then own the lands they had traditionally occupied.

As they had to move seasonally in search of food, they were not even permanently in one squatting location on a year-round basis. By 1920, only 150 years (6 generations) after the founding of the San Diego de Alcalá, most of the Indians had abandoned the San Diego/Mission Valley area. One of these, and representing many thousands more, was Delfina Cuero.

Delfina Cuero, a brief profile

Delfina Cuero’s autobiography describes the life of a refugee people of which she was a part, always on the move in the canyons, valley, and hills on both sides of the international border (Figure 2). Her story describes the basic elements of the refugee people that are the same traits that archaeologists attempt to

identify through the interpretation of artifacts: settlement pattern, social organization, material culture, and technology.

Living in Mexico because she could not prove she had been born in the United States, Delfina searched for any written record that might have been made by someone for whom her father had worked. Unfortunately, no church records exist for the Diegueño Indians between 1900 and 1919, the time during which she might have been baptized.

In addition to the Indians on the reservations of San Diego County, there were non-reservation Indians camped throughout Lakeside, El Cajon, Monte Vista, Jamacha, Otay, and in all the mountain valleys of the San Diego back country. Indians had lived in Mission Valley and various places around San Diego. These locations have been independently confirmed by non-Indian old-timers in San Diego. Sadly, the Catholic Church in El Cajon, which had charge of the Indians from 1900 on, was destroyed by fire in 1917 and the existing baptismal records were burned.

When Florence Shippek was visiting the Campo region in the 1970s, she took an old woman from the Jamul-Barrett-Dulzura area to the Jamacha area where Delfina had been born. The old woman took her directly to an old grove of trees and indicated that there once had been a little Indian house that had been Delfina Cuero's birthplace. When we are discussing the impacts of large development projects such as solar farms and transmission corridors that impact large amounts of traditional

lands, many Native American talk about landscape size areas and focus less on particular locations. However, as the above example demonstrates, some Native Americans have a keen sense for the history of particular locations as well.

Tom Lucas, a brief profile

Delfina Cuero's early life was much more difficult and itinerant than was Tom Lucas's. For multiple reasons, primarily gender, education, and economic opportunities, Tom Lucas did not experience the profound poverty and dislocation experienced by Delfina Cuero. He was born in the mountains of southern California in the winter of 1903, 134 years (5.5 generations) after the founding of the Mission San Diego de Alcalá, at the Laguna Indian Reservation. He was, according to Cline (1984:1) the last *Kwaaymii* baby to be born, although this assertion is somewhat difficult to confirm. As she wrote, the 1860 smallpox outbreak that preceded his birth and the 1918 influenza epidemic that succeeded his birth had taken a heavy toll of the *Kwaaymii* people. The permanent *Kwaaymii* settlement was located where the Lucas Ranch is today at Mt. Laguna, California. Originally, there were three main villages there; the largest was called *Iahkaay*, which means wooded area across a meadow. It is estimated, according to oral tradition, that as many as several hundred persons may have inhabited this village at a single time. Three quarters of a mile south of *Iahkaay* was the village of *Kwaaymii*, the last occupied village and

the village in which Tom Lucas was born; out of the three original villages, only a small number of people remained and all lived in the village that had taken the name of the tribe, *Kwaaymii*. About one quarter mile southeast of the *Kwaaymii* village was the *Wiihanull* (flat rock) village. About 1825 (a brief 56 years and 2 generations after the founding of the San Diego de Alcalá Mission) some ill fate befell *Wiihanull* and all the residents died suddenly. It was speculated that they died from food poisoning and, as a child, Tom was warned to stay away from the location of the old village. To be clear within the context of this paper, these were seasonal villages in the traditional pattern, not refugee camps.

Tom Lucas's biographer (Cline 1984:12) also noted that until the beginning of the invasion by the Anglos in the middle of the 19th century, most *Kwaaymii* migrated to the desert in the winter (Figure

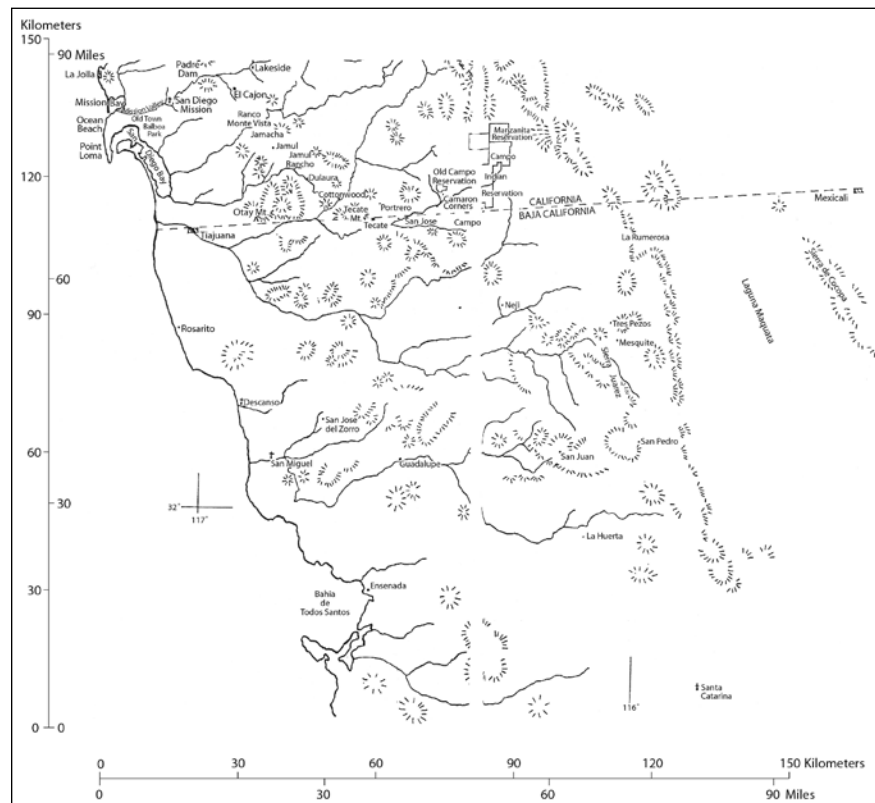


Figure 2. Territory known and traversed by Delfina Cuero (*Diegueño*). Adapted from *Delfina Cuero* by Florence Connelly Shippek, 1981, p. 106.

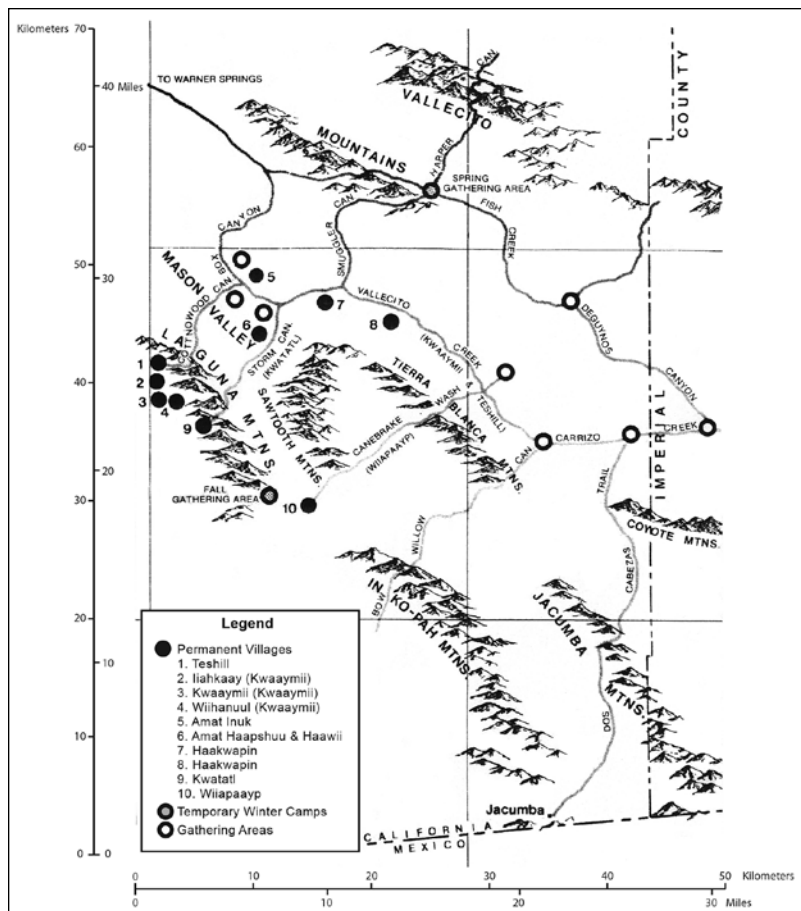


Figure 3. Territory known and traversed by Tom Lucas (*Kwaaymii*). Adapted from *Just Before Sunset*, Lora L. Cline. Tombstone, AZ: LC Enterprises (1984) p. 13.

3). By the time Tom was born, however, the invasions and dislocations began, and some residents of each village or family stayed behind to try and protect their traditional lands, villages, and houses. Many dishonest Anglos, portrayed the temporary abandonment of villages sites during the Natives’ traditional “seasonal round” as permanent abandonments and illegally appropriated temporarily vacant lands. In pre-European times, the Native Americans respected each others’ properties even when the occupants were not there, and it was also common to leave subsistence tools such as manos and metates from year to year, rather than lugging them along. The arrival of the Europeans and Asians rapidly changed these centuries and probably millenia old settlement and subsistence patterns based on tribal traditions of trust.

The search for historic Native American refugee sites

These massive dislocations, seen through the eyes of Delfina Cuero and Tom Lucas, remind us of the many thousands of others who are not memorialized in biographies or autobiographies, but who created a large refugee population that, it occurred to me, had created an unknown quantity of archaeological sites that were now invisible on the landscape—Ascher’s (1974:11) “inarticulate of history.” From what I had read, I was certain that

such sites existed; archaeological surveys were simply failing to identify refugee behavior in the site types that had been developed on the DPR 523 forms. Would it be possible to discern between sites representative of traditional patterns of seasonal transhumance and refugee sites? Four possible avenues of investigation might focus on (1) sites dateable to the period of dislocation (1769–1930); (2) sites in eco-niches that are outside the pattern of seasonal transhumance (sites dating to the period of dislocation that are in locations completely devoid of natural subsistence resources); and the direct historical approach (Steward 1942) applied to (3) ranches and farms where native refugees are known to have lived temporarily, and (4) contact period villages whose locations are known. Here is an opportunity to apply the ethnohistoric methodology and to begin to construct a model of what such refugee sites might look like.

Why search for Native American refugee sites?

Identification of such sites is an effort worth pursuing. These Historic Native American Refugee sites are the opportunity to document the southern California version of one of the greatest tragedies in

American history. Within slightly more than a century since the founding of the first Spanish Mission in Upper California, the cultures established and maintained for thousands of years by Native American peoples had rapidly disappeared because of disease and competition for land and other resources.

- (1) Sites dateable to the period of dislocation (1769–1930). Until the late 19th century, both the Kwaaymii and the Kumeyay followed a transhumant seasonal collecting and gathering subsistence pattern that probably differed little from the patterns of their prehistoric ancestors. Delfina Cuero recalled (Shipek 1991:9): that there were many Kumeyay villages all through Mission gorge, up the canyon, and in Lakeside and El Cajon valleys “...My mother and father went to one village, and then the next one, and on and on. After they had to leave their own place, they lived around wherever there was work or wild food to be gathered” (Shipek 1991:24). Cline (1984:42-43) noted that once the Indian lands were divided into allotments, their subsistence opportunities were much more limited. The natives were forced to try new adaptive techniques such as herding cattle and raising crops, but they were given little training. Many natives abandoned their traditional lands for more remote allotments or

reservations, or in many cases such as that described by Delfina Cuero, they became refugees, rootless, wandering, and "...trying to hold on to the only life they had known, or wanted to know" (Cline 1984:43). Delfina Cuero's account contributes additional data that would be useful to an archaeologist in identifying a refugee habitation sites. As she noted, "Maxwell (a local Anglo rancher who helped Native Americans when he could) gave us a little place where we could stay while we worked for him, a place to build our seamy ?ewa" [little Indian house of willows and other brush]. As she described it, "the men put up two posts and tied a beam between them with fibers stripped from yucca leaves. The reeds or brush were tied to the beam. It looked kind of like a small pup tent. Then the men put up four posts to make a square ramada beside the house" (Shipek 1991:25).

According to Cline (1984), before the Spanish, European, and Oriental invasions, Kwaaymii houses were circular. In the mountains they used support poles of either pine or juniper, anchored in the ground to depths of 35-40 cm (about 15 inches).

When the Indians were told to leave a place, Delfina Cuero's family generally just headed farther into the mountains. Soon they would be told that they had to move again. They would pack up everything they had, a few *sa.kay* (ollas) and baskets of dried food if they had been lucky and found enough food to dry for the winter, a few small stone tools, bows and arrows, *xampu* [a throwing stick for hunting rabbits], and what little clothing they had. They packed everything on a small burro that her father had and moved on.

She also noted that they always carried some grinding stones and some other tools with them. On the other hand, she noted that a lot of stones you could pick up any place and make what you needed. These locally available rocks are called "expedient tools" by the archaeologist. These lithic artifacts from the refugee period would be indistinguishable from lithic artifacts from the past 7,000 years.

Of particular note in the above account is the lack of any metal pots, pans, tools, or other Anglo artifacts that would signal that the former residents and owners of the ceramic ollas, stone tools, and grinding stones actually were refugees in the modern world.

- (2) Sites with artifacts such as projectile points made from glass or porcelain rather than from traditional lithic sources (or rattles made from tin cans rather than turtle shells, etc.). From time to time archaeologists encounter examples of historic glass that have been "flaked" into projectile points (arrowheads), just as chalcedony, obsidian, chert, and other lithics were flaked in the prehistoric period (Brunzell 2007). These traditional tools made from modern materials probably reflect individuals or small populations who were

occupying refugee locations or who had been otherwise cut off from traditional source material networks.

Christensen et al. (2001) noted two interesting glass artifacts found in the course of the Granite Mountains archaeological survey. "A purple glass fragment ... was found at CA-SBR-9826/H in the southern Providence Mountains that had incised intersecting diagonal lines and parallel lines on both sides" (Christenson 2001:23). A Cottonwood Triangular projectile point flaked from green glass was found in an upland basin (CA-SBR-9527). None of the artifacts was collected for further evaluation, but they, along with glass beads, indicate a post-contact Native American occupation of the region, perhaps by refugee peoples.

Given the presence of glass items and written accounts, the area did have an historic period Native American occupation. This site may be an indication of that. CA-SBR-8176, a prehistoric cave site also has a definite prehistoric component with a grinding stone and ceramic sherds.

Tom Lucas was reported to have made bows and arrows, pottery, pipes, rattles, fire drills, and game sticks; again, there appear to have been no modern materials utilized, but Lucas's autobiography does note that an uncle of his father's worked for the Bureau of Indian Affairs, and was paid in metal tools rather than currency.

- (3) Sites in eco-niches that are outside the pattern of seasonal transhumance (sites dating to the period of dislocation that are in locations completely devoid of natural subsistence resources, and contact period seasonal native villages whose locations are known from historic documentation). These sites would be larger than the average refugee site and contain a more complete cultural assemblage than refugee sites since, as Delfina Cuero described, the material culture transported from one refugee site to the next was minimal. Nonetheless, they may also provide a standard of material acculturation that could be compared with possible refugee sites. For example, Parkman (1989) reported on the testing and excavation of villages, campsites, and food producing locations of an ethnographic Kumeyaay settlement that was possibly called *Pilcha*.
- (4) Ranches and farms where native refugees are known to have lived temporarily. Like Delfina Cuero's and Tom Lucas's birth places, most of these locations are specific and would be prime candidates for ethnohistory projects; however, the potential presence of unknown traditional features, burials, and ceremonial artifacts might make investigation difficult, if not impossible. Nonetheless, the historic value of these sites is immeasurable; the voices of the people who lived on them were stilled many decades ago.

Summary

Native American historic refugee sites provide an opportunity to apply the ethnohistoric methodology to this tragic moment in history and to address the issue of what such refugee sites might look like and what we might learn from them. Has a Native American refugee site ever been recorded as such in the DPR annals of California archaeology? Would we be capable of recognizing one if we came across it during a survey? As noted at the beginning of this article, for much of my professional career I have made the case for the application of the ethnohistory method. Although I had previously pursued ethnohistoric research in California (Lange 2006, 2012), the theme of Native American refugee sites offers a significant opportunity to demonstrate the value of the ethnohistoric approach to archaeological research.

In the present paper, the historical evidence has alerted us to the potential to identify the sites of a population that had become refugees in their homeland. The historical documentation from two little-read memoirs (at least outside the Native American and anthropological communities) may help some of us to redirect our field recording and to be sensitive to the possibility of refugee sites in our survey areas.

Many of the basic characteristics of Native American settlements in southern California have been recalled in the personal profiles of Delfina Cuero and Tom Lucas. Delfina Cuero's settlement patterns described more of a mobile refugee pattern, while Tom Lucas's pattern traced the transition from the last era of stable Native American villages, to the migrations that began as the rate of loss of traditional lands increased.

The fact that no Native American refugee site has been recorded as such is *prima facie* evidence that those that still exist are being confused with protohistoric and prehistoric sites. And yet, population statistics alone suggest that archaeologists have walked past or over many refugee period sites and that many more remain to be found. The descriptions of Delfina Cuero's movements and Tom Lucas's early life place a heavy emphasis on the continuity of use of traditional tools made from traditional materials. Mention of clothing raises the possibility that the presence of buttons and military insignia in an otherwise Native American context might lead to a well-founded assumption that the site was a refugee site. The same may be true of sites with traditional style artifacts made from modern materials such as window and bottle glass. Four possible scenarios for defining such refugee sites have been given to help guide future research and recordation.

In the case of both prehistoric and historic artifacts in the same location, the tendency may be to define the site as multi-component, or two separate occupations. The archaeologist need also consider that the combination of artifacts represents a Native American refugee site. These are sites I would like to see. Please let me know when you submit the form to the information center.

References cited

- Ascher, Robert
1974 Tin*Can Archaeology. *Historical Archaeology* 8: 7-16.
- Baerreis, David A.
1961 The ethnohistoric approach and archaeology. *Ethnohistory* 8:49-77.
- Bean, Lowell John
1978 Cahuilla. In *California*, edited by R.F. Heizer, pp. 555-587 *Handbook of North American Indian*, vol. 8, W.C. Sturtevant, general editor, Smithsonian Institution, Washington, D.C.
- Bean, John Lowell and Florence C. Shippek
1978 Luiseño. In *California*, edited by R. Heizer, pp. 550-563. *Handbook of North American Indians*, vol. 8. W.C. Sturtevant, general editor. Smithsonian Institution, Washington D.C.
- Bean, John Lowell and Charles R. Smith
1978 Serrano. In *California*, edited by R. Heizer, pp. 570-574. *Handbook of North American Indians*, vol. 8. W.C. Sturtevant, general editor. Smithsonian Institution, Washington D.C.
- Brunzell, David
2007 Trade In the Mojave: taking a stab at flaked glass. In *Wild, Scenic, & Rapid. 2007 Desert Symposium*, and *Abstracts From Proceedings*. California State University, Desert Studies Consortium, and LSA Associates, Inc.
- Christensen, Don D., Jerry Dickey, and David Lee
2001 The Granite Mountains Archaeological Survey: Prehistoric Land Use. *PCAS* 37(2) 1-78.
- Cline, Lora L.
1984 Just Before Sunset. *Tombstone, Arizona*: LC Enterprises.
- Corruccini, Robert., Jerome S. Handler, Robert. Mutaw, and Frederick W. Lange.
1982 "A Slave Skeletal Population from Barbados, West Indies: Implication for the Biological History of American Blacks," *American Journal of Physical Anthropology* (12):443-459.
- Handler, Jerome.S. and Frederick.W. Lange.
1978 *Plantation Slavery in Barbados: An Archaeological and Historical Investigation*. Cambridge: Harvard University Press. 368 pp.
- Handler, Jerome S. and Frederick W. Lange
1979 "Plantation Slavery on Barbados, West Indies," *Archaeology* 32:45-52.
- Handler, Jerome S., Charles.E. Orser, Jr., and FrederickW. Lange
1979 "Two Necklaces and Carnelian Beads from a Slave Cemetery in Barbados, West Indies," *Ornament* 4:15-18.
- Laguna, Frederica de.
1960 The Story of a Tlingit Community: A Problem in the Relationship Between Archaeological, Ethnological, and Historical Methods. Washington, D.C.: Bureau of American Ethnology Bulletin 172.
- Lange, Frederick W.
1968 "The Bigelow Site (47-Pt-29): An Ethnohistoric Analysis of the Historic Artifacts," *Wisconsin Archeologist* 50:215-255.

- 1972 "An Archaeological Investigation of the Domestic Life of Plantation Slaves in Barbados, West Indies," 37th annual meeting, Society for American Archaeology, Miami.
- 1974 "Slave Mortuary Practices, Barbados, West Indies," *Actas, XLI Congreso Internacional de Americanistas (Mexico)* 2:477-483.
- 1976 "Slave Mortuary Practices, Barbados, West Indies," *Actas, XLI Congreso Internacional de Americanistas (Mexico)* 2:477-483.
- 2004 *Planteamientos Iniciales Sobre El Impacto Indirecto de Las Enfermedades de los españoles, y la Falta de Identificación de Sitios Protohistóricos e Históricos en Nicaragua y Centroamérica. Ponencia preparada para el Ciclo de Conferencias "Leyendo el Pasado" organizado para celebrar el 107 aniversario del Museo Nacional de Nicaragua, y Rendir Homenaje a Doña Leonor Martínez de Rocha al Cumplirse 5 años de su Fallecimiento. Palacio Nacional de la Cultura, Museo Nacional de Nicaragua, Instituto Nicaragüense de Cultura, 26 Agosto.*
- 2006 *Ethnographic Analogy and the Mesquite Regional Landfill Project. 20th Annual Desert Studies Symposium, Desert Studies Center, Zzyzx, California.*
- 2012 *Sites I would Like to See: Moonshine Stills in the California Desert. Desert Research Symposium, pp. 171-177.*
- Lange, Frederick W. and Jerome S. Handler.
 1977 "Mortuary Patterns of Plantation Slaves in Barbados," 9th Conference of the Association of Caribbean Historians, Cave Hill, Barbados.
- 1980a "The Newton (Barbados) Slave Cemetery: Patterns, People, When and Where the Twain do Meet," in symposium, "Every Man's Proper House and Home: Archaeological Perspectives on the Mentalite of Earlier Generations," 13th annual meeting, Society for Historical Archaeology, Albuquerque.
- 1980b "The Application of the South Ceramic Formula on Barbados, West Indies," 13th annual meeting, Society for Historical Archaeology, Albuquerque.
- 1985 "The Ethnohistorical Approach to Slavery" in *The Archaeology of Slavery and Plantation Life*. T. Singleton (ed.). New York: Academic Press, pp. 15-29.
- 2006 "On Interpreting Slave Status from Archaeological Remains." *The African Diaspora Archaeology Network, June 2006 Newsletter*. <http://www.diaspora.uiuc.edu/news0606/news0606.html>.
- Lange, Frederick W. and Shawn B. Carlson.
 1985 "The Distribution of European Earthenware on Barbadian Plantations" in *The Archaeology of Slavery and Plantation Life*. T. Singleton (ed.). New York: Academic Press, pp. 97-11
- Parkman, E. Breck
 1989 *Pilcha: A Kumeyaay Settlement in the Cuyamaca Mountains. PCAS 25:3 pp. 25-45.*
- Ramenofsky, Ann
 1987 *Vectors of Death: The Archaeology of European Contact*. Albuquerque: University of New Mexico Press.
- Shipek, Florence
 1991 *Delfina Cuero: Her Autobiography. An Account of Her Last Years and Her Ethnographic Contributions*. Menlo Park, CA: Ballena Press.
- Steward, Julian
 1942 *The Direct Historical Approach to Archaeology. American Antiquity 7:337-343.*

Owlshead GPS Project

Randy Banis

BLM Desert Advisory Council (DAC), RBanis@SundanceMediaCom.com

Background and History

As an early adopter of using Global Positioning System (GPS) devices for navigating roads and trails in California's desert back country, I became a member of the Bureau of Land Management (BLM) 2001/02 West Mojave Plan (WEMO) Route Survey Team that pioneered the use of pro-level GPS devices to collect data for routes on public lands.

I adapted the survey's methodology for use with ordinary consumer GPS devices and in 2003 organized a volunteer route survey for BLM lands west of Death Valley. The data we collected was used by BLM to designate motorized back country roads and trails in the Northern and Eastern Mojave Plan (NEMO).

Meanwhile, off highway vehicle (OHV) users were falling into old mine shafts because they drove off a designated trail, and scores of OHV routes were being closed because so many others were also not staying on the legal trails.

My call to action was the tragic and unnecessary death of six year-old Carlos Sanchez in a remote and lonely part of Death Valley National Park in August 2009. His mother had been simply following the lines on her new, state-the-art GPS unit, which directed her for several miles down a wilderness wash that was closed long ago, until becoming stuck in the middle of nowhere.

After spending several days stranded in the 115 degree heat without food and water, young Carlos perished. Luckily, his mother was rescued by park rangers just shy of her own death.

That same month I wrote a white-paper entitled "Off Highway Route Information Initiative for the 21st Century" wherein I described the need to make official route data available to consumer GPS users in the general



public. I asserted this would help GPS-enabled OHV users to stay on designated routes and thereby: a) reduce the environmental impact of motorized use; b) improve OHV safety; and c) preserve the existing opportunities for motorized users.

In November 2009 I met with teams from the BLM State Office and Off-Highway Motor Vehicle Recreation Division of California State Parks and I discovered that both had previously embarked on similar efforts with little success. I learned of the challenges presented by deficiencies in existing data, system architecture requirements, and staff resources.

I concluded that such an effort could only realistically be done by a non-governmental organization through funding from grants. Fortunately, Friends of Jawbone took interest and in 2010 received an Education & Safety grant from the California Off Highway Motor Vehicle Recreation (OHMRV) program to develop the project for the greater Jawbone Canyon area.

I assembled a small production force of digital experts who collaborated on a innovative strategy to deliver agency formatted agency route data to end users with ordinary, consumer GPS devices. After considerable research and analysis of agency route data, we settled on a unique suite of alternative and open source solutions including PostGIS, TileMill, Mapnik, Quantum GIS, Linux web and database servers, and Apple workstations.

We christened our effort "The Owlshead GPS Project" in the memory of young Carlos, as the site of his passing was the Owlshead Mountains. The project's logo features first the owl, which represents wisdom and guidance, and second, a direction arrow pointing out the correct way go.

OwlsheadGPS.com went live on January 1, 2012 and has guided more than 2,000 OHV users in the first year. As a result, the Owlshead GPS Project has received a second OHMVR program grant to expand coverage from the current 1.2 million acres to 25 million acres ranging from north of Death Valley south to the International Border. The expansion will occur during 2013 and will make use of the technology and methods developed in the first phase of the project.



Deficiencies and need

Recent route designation efforts by land management agencies in California have resulted in uncertainty among the public regarding legal motorized travel on public lands. Many of these new designation actions have not yet yielded updated maps and trail signs for the public. In some areas the route designations have been successfully challenged in court, resulting in great confusion among OHV users over the current legal route network.

Most map resources used by the public are inaccurate from the standpoint of OHV route designation. These include the base maps for GPS devices, USGS maps, and agency issued maps, i.e. Desert Access Guides, many of which are still sold. Recently some offices have produced OHV route maps but usually they cover smaller, more intensive use areas and do not include connecting routes from other offices or agencies.

Although the use of GPS technology and the internet among the public has increased exponentially, the route data that is offered by existing resources still often depicts as open routes that have been designated as closed to motorized travel. Printed maps are only a snap-shot in time and unless regularly updated become outdated shortly after they are printed. Printed maps are lessening in popularity among the public, while electronic guidance is increasing in use.

Therefore, we must educate OHV users via the devices and methods they already own and use, which include computers and GPS enabled devices. Yet, outside of OwlsheadGPS.com there does not exist a central repository of currently designated routes for motorized travel freely and readily available in digital format via the internet.

The consequences of a motoring public that does not adhere to the designated route network are damage to resources, route closures, and a loss of recreational and other opportunities for the public. In some cases, the consequences impact public safety.

OwlsheadGPS.com is a ground-breaking response to each of these troubling deficiencies in public information. In addition to serving traditional OHV recreation, the project assists with other recreational activities that depend on motorized access, such as hunting, gem and mineral collecting, camping, wildlife watching, history seeking, star gazing, and solitude seeking.

Goals

Off-route travel increases an OHV user's exposure to dangerous mining hazards such as open shafts and pits, contaminated soils, and unmaintained road surfaces. It can also quickly lead to ground conditions that are well beyond an OHV user's riding skill, often resulting in disorientation and getting lost. The project teaches OHV safety by providing

a useful tool that will better assist users to travel on designated routes.

Environmental resources are negatively impacted, sometimes critically, by off-route travel. Habitat can be fragmented, soils can be marred, and cultural resources damaged or destroyed due to off-route travel. This project teaches greater environmental responsibility by encouraging users to remain on designated routes, and by providing a tool for easily doing so.

Private property, particularly that adjacent to public lands, regularly suffers from undesigned OHV use. For some OHV users, trespass occurs because they are unaware of the designated routes and legal riding areas in which to operate. This project teaches greater respect for private property by assisting users to remain on designated routes.

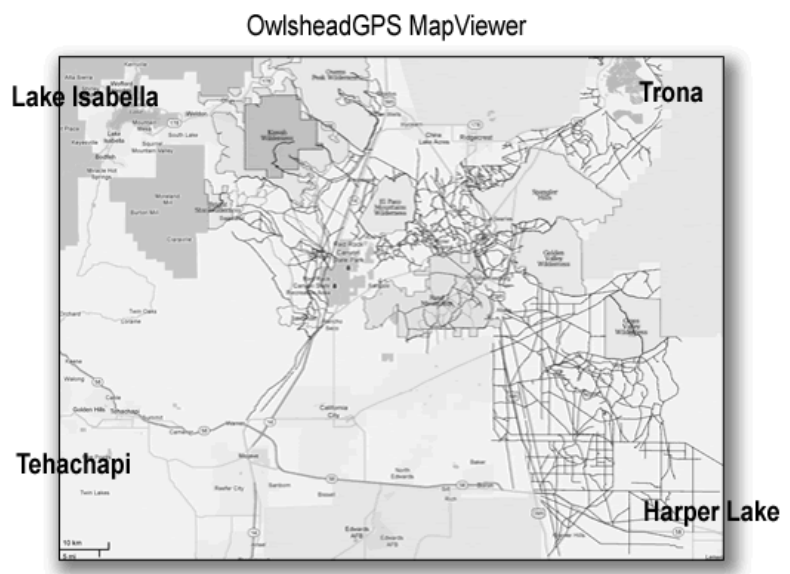
Therefore, the goals of the Owlshead GPS Project are:

- To enhance the safety of OHV users by providing official designated OHV route information;
- To protect sensitive biological and non-biological resources by encouraging on- route travel by OHV users; and
- To sustain the public's existing OHV recreation opportunities through increased compliance with route designations.

Project area

The OwlsheadGPS Project is a pilot program with a limited project area. Currently, the project area is a 1.5 million acre rectangle of public and private land in the greater Jawbone Canyon area. This is the same area covered by the popular Friends of Jawbone OHV Trail Map. The area extends from south of Tehachapi in the southwest to Lake Isabella in the northwest, and Harper Lake in the southeast to Trona in the northeast.

The OwlsheadGPS Project includes only routes that are within this Project Area. The route data is the same



across the MapViewer, the GPS Maps, and the downloadable route files. Agencies participating in this pilot phase of the program include BLM, Sequoia National Forest, and California City.

In 2013 the Owlshead GPS coverage area will expand to 25 million acres and will include the motorized route networks of:

- BLM’s NEMO, Western and Eastern Colorado Desert (WECO), Northern and Eastern Colorado Desert (NECO) and remaining WEMO
- San Bernardino National Forest
- Angeles National Forest
- Inyo National Forest
- Death Valley National Park
- Mojave National Preserve

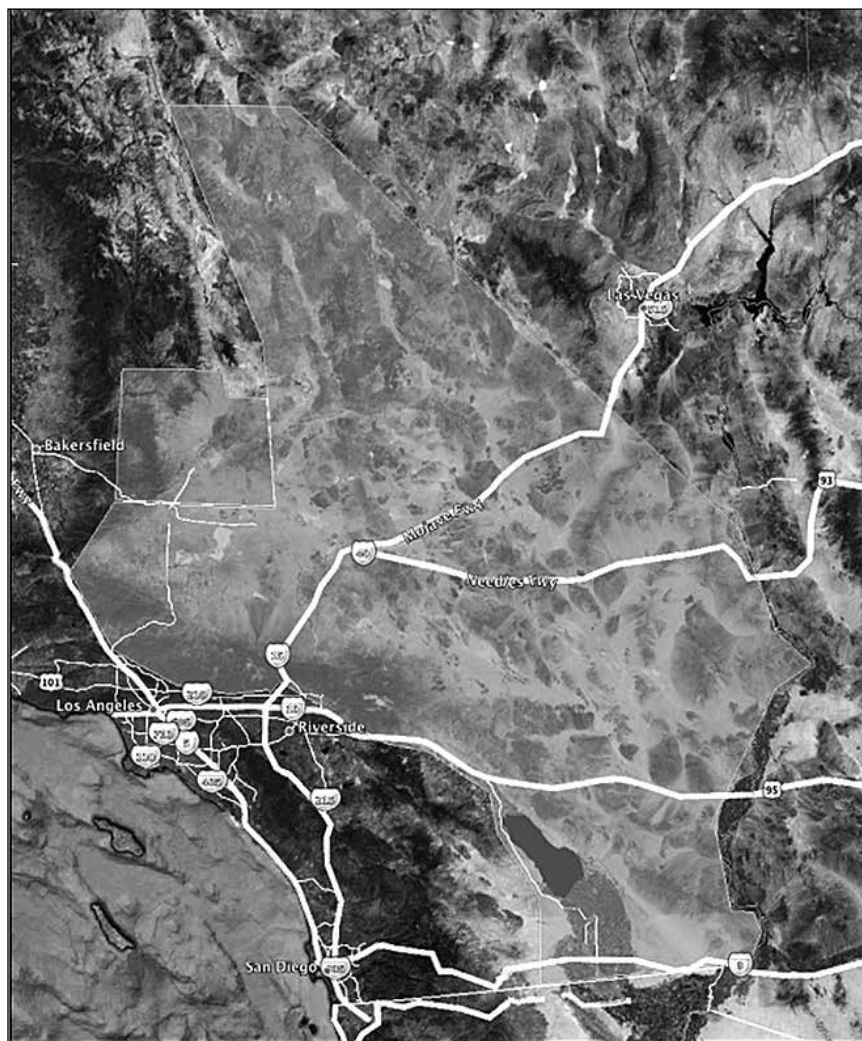
The image below compares the current Owlshead GPS Project coverage area (purple) and the second phase coverage area (green).

Tour of OwlsheadGPS.com

The OwlsheadGPS.com website provides three products of interest to GPS and computer users:



- A MapViewer tool to view the designated OHV route network
- A GPS Map that can be installed on most Garmin GPS devices
- Downloadable OHV routes files for computers & GPS devices

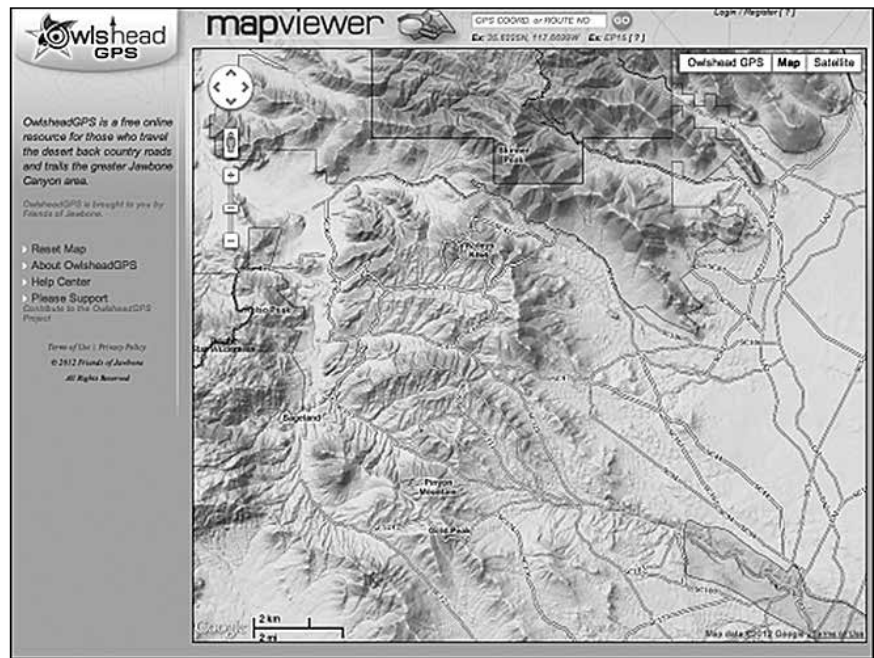


Visitors can also find a wealth of extra content and user support documentation to help enhance their use of the website and its products.

I. MapViewer

- Uses the familiar Google Maps interface
- Routes for full size OHVs are in green; single track trails are yellow
- Search by route number or GPS coordinates
- Up to nine zoom levels
- OHV areas are highlighted in magenta
- Permit-only areas are highlighted in blue
- Wilderness areas are highlighted in tan
- Interface is locked to the project area so users do not get lost
- Users can reset the map via link on right sidebar menu
- MapViewer uses all open source software and tools
 - Full Street View support via the Google PegMan
- Four backgrounds are available to the user:

- Features only
- Roads, highways & features
- Topographic
- Satellite
- Clicking on a route:
 - encloses the route, endpoint-to-endpoint, in a blue bounding box
 - launches a popup balloon that includes:
 - Route Number
 - Managing agency
 - Recommended vehicle type
 - Links to download the route in GPX and KML formats
 - includes links to Help articles with more information



2. GPS Map Installer for Garmin GPS Devices

The OwlsheadGPS GPS Map Installer for Garmin GPS Devices enables many Garmin GPS owners to easily follow the OHV route network while they travel. Visitors can download this free Windows PC application that will install an OHV route map of the project area on most Garmin GPS devices.



3. Download OHV Route Files to computer

Users can download OHV routes files to their computer in both the common GPX or KML files formats. The GPS Exchange, or GPX format, is supported by many popular consumer computer GPS mapping programs, such as National Geographic Topo, Maptech Terrain Navigator Pro, and Garmin Basecamp. The KML format is also widely supported, particularly by Google Earth and Google Map

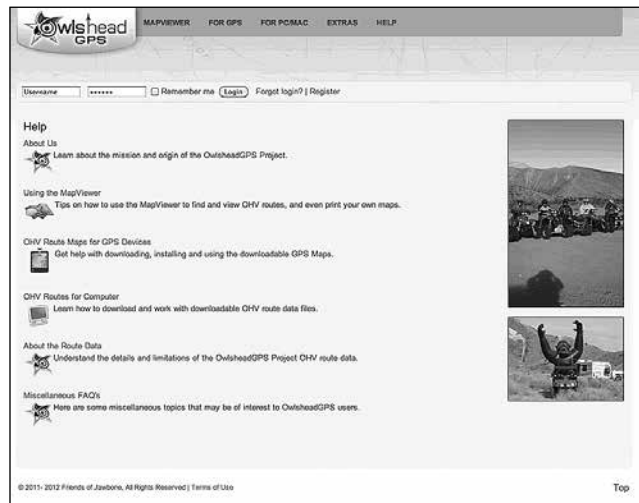
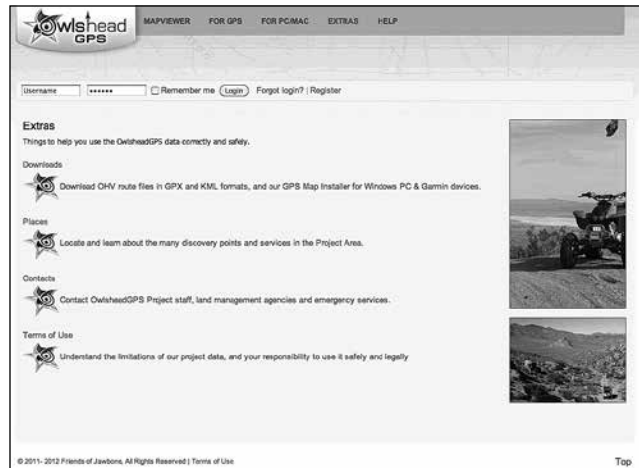
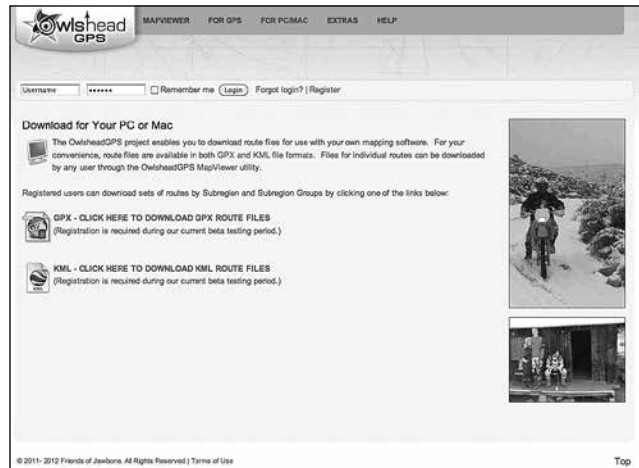
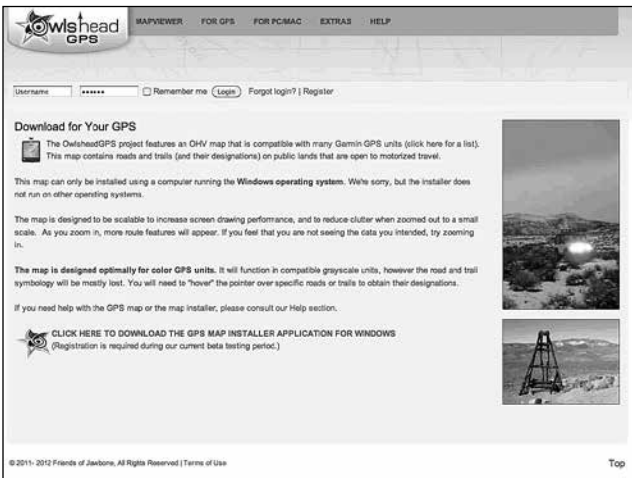
tools. Users of most GPS devices can download and use these route files in their route and track libraries.

4. Extras

The Extras menu provides direct links to:

- Download OHV route files and the GPS Map Installer
- A directory of places including:
 - Area hospitals
 - Discovery Points
 - OHV Open Riding Areas
 - Hiking trails
 - Towns with full service
 - Fuel
 - Restaurants
 - Lodging
 - Museums and visitor centers





- Contacts to:
 - OwlsheadGPS Project staff
 - Emergency contacts
 - Land management agencies
- Terms of Use, including a privacy policy, data disclaimer and agency specific supplemental language.
- Help Resources. A robust Help section in support of the MapViewer, GPS Map and OHV route files. Help resources include:
 - About Us
 - Using the MapViewer
 - OHV Route Maps for GPS Device
 - OHV Routes for Computer
 - About the Route Data
 - Miscellaneous FAQs



Recent meteorite falls in California

R. S. Verish

Meteorite-Recovery Lab, P.O. Box 463084, Escondido, CA 92046

This short paper presents a summary of previous research and results of recovery efforts for two meteorite falls that occurred in California in 2012. We present no original research. Instead, we report on the results of our fieldwork which was greatly aided by NOAA NEXRAD Doppler weather radar.

ABSTRACT—In 2012 two meteorite falls were recovered in the state of California. The meteorites recovered from the first fall were formally named “Sutter’s Mill” and were found to be very rare and continue to be of extreme interest to scientists. Many specimens have been donated to research. The second fall, so far, has only resulted in six stones being recovered (for a total of 363 grams), and has not been formally named, but is provisionally called “Novato.” It is an Ordinary Chondrite classified as “L6 breccia”. This writer was a member of search teams in which meteorites were recovered for both of these California falls. The events leading-up to the rapid recovery of these meteorites, only days after their fall, was only made possible through the utilization of Doppler weather radar data. The development of this new technique marks the advent of a new era in meteorite-recovery.

Introduction

The recovery of meteorites from a “witnessed fall” (where the bolide event was observed by various eyewitnesses) is an extremely rare event. Since 1900, the number of recognized meteorite falls is about 700 for the whole Earth. That’s roughly seven per year. Of those 700 falls, 100 of them occurred in the US. That averages to one per year. Prior to 2012, only two meteorite falls were recorded for the entire state of California. [6] Two meteorite-fall recoveries in the same year is a statistical anomaly that begs for an explanation. And that explanation is Doppler weather radar.

But before an explanation of how this radar is used to recover meteorites is described, an explanation of how this cosmic debris arrived to Earth from the Asteroid Belt of our solar system is in order. This explanation comes from the meteorites themselves. By examining the stones recovered from these two latest California meteorite falls, we’ve learned that they’re both chondritic breccias. By studying their petrology, we’ve learned that great forces are at work to bring these rocks to Earth, mostly the gravitational influences of Jupiter and our Sun. The sheer number of asteroids confined to the Asteroid Belt results in collisions. These impacts result in asteroidal debris, called meteoroids. Some of these meteoroids will have their newly formed orbits perturbed by Jupiter and Mars. Some of those meteoroids will take a new path that essentially has them falling into the Sun. As these meteoroids are pulled into the Sun, they must cross the orbital path of the earth. Some of these meteoroids will encounter the earth. When a meteoroid enters Earth’s atmosphere it doesn’t produce a meteor like the kind that is made by dust particles from comets, which are commonly seen. When a meteoroid enters the atmosphere it produces a huge fireball, which is a much rarer event. It is the observing of this event that is

the start of the process to determine where any surviving meteorites may have landed. [11]

The passage of these (asteroidal debris) meteors through Earth’s atmosphere creates a very bright fireball. During this fireball phase a great deal of the original mass is vaporized in a process called ablation. During descent, the ever thickening atmosphere results in such a rapid deceleration that the bolide eventually reaches what is called, the retardation point and whatever mass is still surviving fragments into many pieces. The smaller fragments are immediately slowed down by atmospheric drag, while the larger pieces retain some of their momentum and will keep traveling down range, but will be the first pieces to land on the ground. [9][10] This post-luminous phase where the surviving fragments decelerate to sub-sonic speeds is called “dark-flight.” This is why sonic booms can still be generated during the dark-flight portion of the descent. The smaller fragments, which were quickly stopped by friction with the atmosphere, will eventually rain down to Earth over a longer period of time. It is at this point in the meteorite fall event (below 15 km altitude) that the NOAA-NWS-NEXRAD



Figure 1. Bolide breakup over Novato, California – 2012 October 17th [5]. Image taken by Bob Moreno of Santa Rosa, CA – from high school.

Doppler-radar stations can first detect these falling masses. [3]

Although both of these California meteorite-fall events are termed witnessed falls (because the fireball-meteor event was seen and recorded by various eyewitnesses), no meteorites were actually seen to land on the ground. But by examining Doppler weather radar imagery data (the same data-sets used by meteorologists to remotely-sense clouds and precipitation) meteoriticists were able to pinpoint and predict where meteorites most likely landed. Once the fall-zone had been delineated, the media was contacted. The media would, in turn, inform their readers and viewers of the possibility that meteorites could have landed on their property, and would request their help in the recovery of these meteorites by looking for any out-of-place, black rocks. Through the Internet, word was spread that Doppler weather radar had detected falling objects. Volunteers arrived very quickly to the fall-zone. Meteorite-recovery teams were rapidly formed and deployed. In a matter of a few days, if not just hours, meteorites were found by searchers and property owners in the very area directly under these Doppler radar reflections. These meteorite finds were intensively examined and were determined to be so pristinely fresh that they were conclusively associated to their respective bolide events.

Sutter's Mill

A meteoroid the size of a van collided with Earth over California's Sierra Nevada range on the morning of 2012 April 22, at 7:51 PDT. The passage of this meteor through the Earth's atmosphere created a bright fireball that was seen all over Nevada and into California. A loud boom followed by a rumble was reported over a wide region roughly centered over Placerville. Classically this loud boom is attributed to the fragmentation event that occurs at the retardation point, but a sonic boom can also be generated anywhere along the dark-flight path prior to the bolide going subsonic. NOAA-NWS-NEXRAD Doppler-radar stations swept their beam over this area at different altitudes and at different times recorded meteorites of various size raining down to the ground. Near historic



Figure 2: Sutter's Mill #12 (CM breccia) found by Monika Waiblinger Verish. In-situ image by Robert Verish © 2012

Coloma in El Dorado County, ear-witnesses reported hearing the meteorites fluttering through the air shortly after experiencing the initial sonic boom. The recovered meteorites form a 12km by 3km distribution ellipse that includes Sutter's Mill, the discovery site where gold was first recognized by James Marshall in January of 1848. [7]

The initial discovery finds

Meteorite-hunter Robert Ward recovered the first stone two days after the meteorites had landed on the ground. He found it near the entrance way to Henningsen-Lotus Park. This first find weighed 5.5 grams. Later that same day, meteor astronomer Dr. Peter Jenniskens of the SETI Institute and NASA Ames Research Center found 4 grams of a crushed meteorite in the parking lot of that same park. And still later that same day, a third stone (5 grams) was found by meteorite-hunter Brien Cook. These were the only finds made before the first rain-storm soaked the strewn-field. Storms during the next two days slowed the recovery effort, but after that a steady stream of meteorite recoveries were made, until June of 2012, and since then, no additional finds have been reported. So far, 77 finds have been reported and verified, and with another 10 finds still awaiting formal verification, the total known weight will still be just less than 1kg. [5] Results from analysis of this meteorite have shown that there is a difference in the composition of the stones that were exposed to rainwater, compared to the first three pristine finds. This shows that a speedy meteorite-recovery effort, which is made possible when aided by immediate analysis of NOAA Doppler-radar, is crucial to obtaining optimal scientific results.

Sutter's Mill finds by members of the Meteorite-Recovery Lab

The twelfth Sutter's Mill find (SM#12) was found by my wife, Moni Waiblinger Verish, on 2012 April 29. This 17.5 gram whole individual stone was found on the property of Merv de Haas, with the prior understanding that anything found would be donated to researchers via the principal investigator at NASA-Ames. This find still represents the southern-most extent of the Sutter's Mill strewn-field.

This stone has since been sectioned and distributed to a wide variety of researchers. Because this stone was 100% fusion-crust, researchers had hoped that its interior would still be pristine, but there were still signs of alteration from being exposed to rainwater. Nevertheless, samples from this stone were used to determine that Sutter's Mill is characterized as a carbonaceous chondrite type-CM regolith breccia. [7] This means that researchers now have a sample of what astronauts would encounter when they land on the surface of this asteroid, the parent-body for the Sutter's Mill meteorite.

"Novato" (provisional)

On 2012 October 17th at 19:44:44 PDT (2012 October 18, 02:44 UT) a car-sized meteoroid entered Earth's atmosphere producing a very bright fireball-meteor which



Figure 3: Novato “N04” (L6 breccia) – not in-situ. Image taken 2012-11-11 by author.

was witnessed by many people throughout California. Numerous observers caught the blazing bolide on cell phone cameras and videos. [12] The bolide also created a loud sonic boom that was also reported by ear-witnesses in the San Francisco Bay Area. After hearing of these reports, Peter Jenniskens, head of the CAMS (Cameras for Allsky Meteor Surveillance) project, which is jointly run by NASA and the SETI (Search for Extraterrestrial Intelligence) Institute, immediately reviewed the videos from his allsky-camera-system. [7] The CAMS team captured two views of the fireball track, one by the 20-camera station at Ames, the other by a single-camera station at San Mateo College, but because the fireball was so bright and the track was so close to the camera network, the images were overexposed. This is why preliminary results were delayed, and why the ground path was twice revised. Nevertheless, the CAMS project put out a public call for information on possible meteorite sightings soon after fireball reports started to appear on the American Meteor Society website. [2]

Other researchers, trying to use the data set of Doppler radar images, had their own problems. The evidence for a meteorite fall that they were looking for in the radar data was obfuscated by a multitude of weather-related reflections. No longer an exercise in science, instead it became more of an art, trying to glean anything useful from the data that was available. [3]

These same researchers then turned to triangulating the recordings from seismic monitoring systems in order to trace the flight-path of the bolide before it went sub-sonic. They were successful in their efforts, but the results neither confirmed which radar reflections were meteorite-related, nor corroborated the results of the NASA-SETI-CAMS system. For the first few days of the meteorite-recovery effort, field workers were faced with having to cover a broad area. [11]

This writer was one of those field workers. At the time of the Novato fall, this writer was conducting meteorite recovery in the Battle Mountain strewn-field in northern Nevada. Upon confirming that this new fall had been

detected by Doppler weather radar, I departed Battle Mountain for the San Francisco Bay Area. [3]

The recovery of the first Battle Mountain meteorite is pertinent to the Novato fall. The first find from the Battle Mountain (BaM) fall was made by this writer on 2012 September 1. Upon reporting this find, I pointedly gave credit to the researchers at Galactic Analytics who had shared with me (and their other clients) the results of their analysis of the NOAA-NexRad Doppler weather radar. It soon became public knowledge that these researchers had predicted a specific spot where a meteorite could have landed, which ended up being less than 300 meters from where I eventually made the first BaM find. This fact was still fresh in the public’s mind when the Novato fall occurred one month later, resulting in a huge turnout of volunteer field workers, and a great deal of attention was drawn to Doppler weather radar.

The San Francisco Bay Area fireball event gained immediate media attention, but was destined to be short-lived. What kept this event in the public’s eye was that it serendipitously occurred just days before the peak of the annual Orionid meteor shower. Because the news media had already planned to have segments aired when the meteor shower occurred, they punched up those segments by going back to the fireball event. They used that earlier fireball footage, and made unfounded attempts to link the two events, even though numerous astronomers and bloggers posted comments that the fireball was going the opposite direction from the Orionid radiant.

The first find from the fall in Novato, CA

Three days after the fireball sightings were first reported, and after reading an article about the October 17 loud bolide in the San Francisco Chronicle, homeowner Lisa Webber, wife of a minister at the Novato Presbyterian Church, found the space rock on October 20. She remembered hearing a sound on her roof the night the meteor was reported and went searching outside her house, whereupon she found a 2.2 ounce (63 gram) stone that to her looked out-of-place. She contacted Peter Jenniskens at NASA-Ames. Jenniskens and Webber’s neighbors Luis Rivera and Leigh Blair inspected the house’s roof and found a small dent consistent with the rock having hit it from a southwest direction. No other fragments were recovered from this property.

Because all of the following is a matter of public record, I would be remiss if I did not explain my involvement with the events that unfolded:

For some reason that is still not clear, someone convinced Dr. Jenniskens that the stone he obtained from Lisa Webber was not a meteorite. When I had read this puzzling news, I contacted Brien Cook, who had recently found the second stone (Novato02). He had also read the same article and had thrown his specimen aside, figuring that his find wasn’t a meteorite either. I told him that I wasn’t so sure, not having seen either of these two stones firsthand. I suggested that, just to be sure,

he should cut his specimen so that we could have a type specimen sent to Dr. Alan Rubin at UCLA. Dr. Rubin had already contacted me and notified me that he was already prepared and waiting for a specimen to identify and classify. Not too much later, Brien posted images of the type-specimen he cut, and the numerous flecks of metal grains made it very obvious to everyone that his find was a meteorite. I forward the image to Dr. Jenniskens, but his reply to me was that he had already given the stone (uncut) back to Lisa Webber. Now, in somewhat of a panic and because it was nearby, I drove over to the Webber residence. I was greeted by Pastor Webber and was informed that Lisa had already given the stone to her next-door neighbor's son, Glenn Rivera. With the reverend's blessings, I went over to his next-door neighbor, the Luis Rivera house. I introduced myself to Leigh Blair, and explained that it was my contention that her son, Glenn Rivera, had a stone that was most likely a meteorite. She invited me in, introduced me to Glenn, and promptly handed me the stone, and I even more promptly confirmed that it was, indeed, a meteorite. I contacted Dr. Jenniskens, who was already in route, but was stuck in rush-hour traffic. We were invited to stay for dinner, and that evening we all shared in the celebration of having confirmed the recovery of Novato01, California's fourth fall. [1]

"Novato #4" find by this author

The largest mass recovered, as of this writing, is Novato04 (N04). The initial stone recovered had a mass of 96 grams, but subsequent fragments from this stone so far found bring the total weight to ~107 grams. The initial mass was found by this writer on 2012 October 27th. The subsequent fragments took several more days to be recovered. The original N04 stone was obviously larger before it impacted the pavement, possibly twice as large. The original N04 stone produced an impact feature in an asphalt-covered parking lot about 60 feet (18.5m) from where the 96 gram N04 fragment was found. All of the subsequently recovered fragments were found within this radius. When the original N04 stone impacted the parking lot asphalt it produced a shallow penetration hole. During the impact process, the top layer of asphalt was overturned and lay next to the hole. Pulverized fragments of chondritic debris were found in this mini-crater. [12]

The "bottom" side of the Novato04 stone was the side that was in contact with the gutter when it was found. This

side of the stone is a flat, freshly-broken surface. Because it has no fusion-crust covering it, the entire interior is exposed in cross-section. As a consequence, the bottom side has the most rust-spots, most likely because that side was sitting in rainwater after one of the storms that occurred between the time of the fall and when it was found. Given that the N04 stone has so few scratches, it is assumed that the bottom side is the side that made the initial impact with the asphalt, producing the shallow divot. As a consequence, an unknown amount of chondritic material from the bottom side was pulverized in the process, but after multiple attempts, only ~10grams of small fragments have been recovered. [13]

Novato04 is two meteorites in one stone. One half is composed of monomict breccia clasts of equilibrated (L6) chondritic parent material set in the other half, which is a shock-darkened impact melt.[14] It is my observation that the patches of fusion crust are of two types, as well. It is my assertion that each type of fusion crust was derived locally from the melting of the immediate, underlying mineralogical composition and that there was no mixing of these different melts prior to the crust solidifying. This assertion is based upon the following observations. The patches of fusion crust in contact with the chondritic clasts look similar to the fusion crust seen on other fresh chondrites, whereas the smaller patches of fusion crust in contact with the black shock-darkened lithology appear to have been more viscous before they solidified. The patches of fusion crust in contact with the chondritic material look larger because they appear to have adhered better to that portion of the stone, whereas the smaller patches of fusion crust in contact with the black lithology appear to have had more difficulty adhering to that portion of the meteorite even though they look to have a higher degree of viscosity, much like a drop of molten solder that is in need of more flux. The fusion crust derived from the lighter-colored chondritic groundmass adheres like glaze on a ceramic. The darker-colored lithology is lacking a "flux" that would allow the fusion-crust to adhere better. This patchy fusion crust is not at all common on chondritic stones and was the prime reason for complicating this meteorite's initial identification. [1]

Credit for the recovery of Novato 04 must be shared with Marc Fries and Rob Matson of Galactic Analytics for their prescient analysis of the NOAA NexRad Doppler

Table 1: List of "Novato" Field ID# (N##) - Meteorites Recovered

ID#	Mass	Finder	Location	Date	Notes
N01	63 g	Lisa Webber	38.1090° N, 122.6105°W	2012Oct 20	Struck house
N02	65.9g	Brien Cook	38.0941° N, 122.5683° W	2012Oct 22	Found in street
N03	79.0g	Jason Utas	38.1152° N, 122.5640° W	2012Oct 27	Found in turning lane of street
N04	107g	Bob Verish	38.1217° N, 122.5670° W	2012Oct 27	Struck pavement—many fragments
N05	24.3g	Jason Utas	38.1195° N, 122.5720° W	2012Nov02	Found by street—many fragments
N06	23.7g	Kane family	38.0768° N, 122.5692° W	2012Nov11	Found in parking lot

weather radar. On their website Marc made available images depicting pertinent radar reflections and areas on the ground where meteorites may have landed. [3] This was crucial because the area under the flight path of the bolide was too vast for the number of volunteer field-workers to affect a speedy recovery. In personal communication with Rob Matson, he hinted that one of the radar reflections depicted in the on-line image had underneath it another reflection at a much lower (1km) altitude, which he found very intriguing. He suggested that, if he had to prioritize search areas, he would start under that reflection. [11] They identified this particular radar return with the label KMUX 0239 3.6deg03. It took me three more days of searching, but I finally found N04. And when plotted on a map, the spot where N04 was found turned-out to be only 700 m from where KMUX 0239 3.6deg03 was plotted.

It could be argued that there is no way to confirm this N04 find is related to any one particular radar return, especially since there were two more finds made in this general area.[15] For that matter, it could be said that this is all a coincidence. But the fact that this recovery was a repeat of my prior feat at Battle Mountain only a month earlier that same summer speaks less of a coincidence and more of a trend in the making. And possibly, two meteorite-falls occurring in the same year in the same state is not so much of a statistical anomaly, but more an indication of a future trend, as well.

Addendum

As this paper was being written, two more bolides were witnessed to fall in California, were accompanied by sonic booms, and were detected on NOAA NexRad Doppler weather radar. [8] Although there have been no meteorites recovered, as of the submission of this paper, it is clear that the pace of detecting these events and that the interest in making recoveries has not waned. [4]

Conclusion

The number of meteorite falls on record in California was doubled in 2012. This marked increase is due in large part to the recognition that meteorite falls were inadvertently being recorded by meteorologists. The use of NOAA-NWS Doppler weather radar data for remotely sensing falling bolide debris marks the advent of a new era in meteorite-recovery. This expertise is particularly effective when coupled with allsky-camera-network astrometry, but has been shown to reduce recovery time even when used by itself when weather conditions are optimal. Reducing the time interval from meteorite fall to meteorite recovery is crucial to obtaining optimal scientific results.

References

- [1] Ainsworth, B., 2012, It's a Meteorite - Again, Cupertino Patch, 25 Oct. 2012, <http://cupertino.patch.com/articles/it-s-a-meteorite-again#photo-11893318> (January, 2013)
- [2] Fries, M. Fries, J. 2012. Weather Radar Detection of Meteorite Falls – Rapid Recovery of the Sutter's Mill Fall. *Meteorite*, Nov 2012, Vol. 18, no. 4, pp. 10
- [3] Fries, M. 2012. Personal communication.
- [4] Fries, M. 2013. Galactic Analytics: CA-17-jan-2013-1321-UTC (bolide). <http://www.galacticanalytics.com/ca-17-jan-2013-1321-utc/> (January, 2013)
- [5] Gilmer, M. 2012. Sutter's Mill California Meteorite Fall - Tally of Known Finds. <http://www.galactic-stone.com/pages/lotus> (January, 2013)
- [6] Grady, M.M. 2000. *Catalogue of Meteorites*. – 5th ed.
- [7] Jenniskens, P. and 69 coauthors. 2012. Radar enabled recovery of the Sutter's Mill meteorite, a carbonaceous chondrite regolith breccia. *Science*, 21 Dec. 2012: Vol. 338 no. 6114, pp.1583-1587. DOI: 10.1126/science.1227163
- [8] Lunsford, R. 2013. California-Nevada Fireball January 17, 2013. <http://lists.meteorobs.org/pipermail/meteorobs/2013-January/015814.html> (January, 2013)
- [9] Norton, O. Richard, 1998. *Rocks from Space*. ed. 2. pp. 60
- [10] Norton, O. Richard, 2012. *The Cambridge Encyclopedia of Meteorites*. pp.33
- [11] Matson, R. 2012. Personal communication.
- [12] Ross, D. 2012. The Latest Worldwide Meteor/Meteorite News: Breaking News - CA Fireball Meteor 17OCT2012 <http://lunarmeteoritehunters.blogspot.jp/2012/10/breaking-news-ca-fireball-meteor.html> (December, 2012)
- [13] Verish, Bob. 2012. Bob's Findings: The Recovery of the "Novato" Meteorite that Fell on 2012 October 18, 02:44 UT (Oct. 17, 19:44 PDT). An on-line article in "Meteorite-Times" on, 29 Oct 2012 21:17:27 at <http://www.meteorite-times.com/bobs-findings/the-recovery-of-the-novato-meteorite-that-fell-on-2012-october-18-0244-ut-oct-17-1944-pdt/> (January, 2013)
- [14] Verish, R. 2012. Classification for Novato (name pending approval). A post to the "Meteorite-List" on, 29 Oct 2012 21:17:27 <http://www.mail-archive.com/meteorite-list@meteoritecentral.com/msg108950.html> (January, 2013)
- [15] Wikipedia. 2013. Novato meteorite. http://en.wikipedia.org/wiki/Novato_meteorite (January, 2013)

Acknowledgements

This author would like to thank Michael Gilmer of Galactic Stone & Ironworks, as well as Marc Fries and Rob Matson of Galactic Analytics for their help in reviewing this article.

Abstracts

from the 2013 Desert Symposium

Robert E. Reynolds, editor

Petrochemistry of a rare earth occurrence within the northern New York Mountains of southern Nevada

Suzanne M. Baltzer,¹ David R. Jessey,² and Robert M. Housley³

¹Geological Sciences, California State University, Los Angeles, 5151 State University Drive, Los Angeles, CA 90032-8580, smbaltzer@gmail.com; ²Geological Sciences, California Polytechnic University-Pomona, Pomona, CA 91768; ³Division of Geological and Planetary Sciences, California Institute of Technology, Pasadena, CA, 91125

The northern New York Mountains, southern Clark County, Nevada contain anomalous concentrations of rare earth elements within a Proterozoic (1.6-1.8 Ga) orthogneiss. The host for the mineralization is a weakly alkaline granite, however, the highest rare earth concentrations occur in close proximity to the contact between granite and a more mafic intrusive phase varying in composition from granodiorite to diorite.

Four rare earth-bearing minerals have been identified. Small amounts of rare earths occur within the abundant fluorapatite of large aggregates that frequently enclose smaller grains of the other phosphates. Much higher concentrations of rare earth are present within monazite-Ce and xenotime. The monazite-Ce also contains significant amounts of lanthanum, neodymium, and thorium. Xenotime, in contrast, is enriched in gadolinium, dysprosium, and erbium. A thorium mineral species also contains small amounts of rare earth. The mineralization generally occurs as pods and disseminations within the host granite, however, some veining particularly of monazite was noted in thin section. Zoning of REEs and thorium within individual grains was common.

Alteration consists of widespread Na-metasomatism, in which k-spar has altered to albite and sodium clays, and more localized chloritization. The latter appears most commonly within breccia zones that likely were created by faulting. The relationship of the alteration to the rare earth mineralization remains enigmatic. Although some mineralization is present in areas of intense alteration other pods of rare earth mineralization have no associated alteration. The relationship is complicated by a Mesozoic copper-bearing intrusive near the north end of the New York Mountains. Fluid circulation associated with that event could account for some or all of the alteration associated with the rare earth mineralization.

Geologic reinterpretation of Paleozoic and Mesozoic "bedrock" at the east end of Afton Canyon, San Bernardino County, California

Kim M. Bishop

Department of Geosciences and Environment, California State University, Los Angeles

Rock exposed at the east end of Afton Canyon from Baxter iron mine on the north to a point a few km south of the Mojave River consist primarily of the following rock 4 suites: 1) non-metamorphosed, poorly- to moderately-lithified, fluvial sandstone and conglomerate; 2) Mesozoic intrusive rock; 3) metamorphosed volcanic rock and quartzite; and 4) upper Paleozoic miogeoclinal limestone intruded by Mesozoic mafic plutonic rock. These rock suites occur in east-west trending elongate units that are intercalated with one another along south to southwest dipping contacts.

Each of the crystalline units is brecciated, in some cases throughout and in others only locally. The units not brecciated throughout are the thickest. An important observation is that whether or not a unit is entirely brecciated, the northern edge of the unit where it contacts another unit is brecciated. Where these northern contacts are well-exposed, the breccia is seen to be more finely comminuted relative to other brecciated areas within the unit.

Previously, the Mesozoic and Paleozoic crystalline rocks have been interpreted as in-situ bedrock. However, the geometry of the units and the nature of the brecciation in these units lead to the interpretation that the entire package of units formed from the 4 rock suites is a tilted sequence of fluvial sandstone and conglomerate intercalated with rock avalanche landslide deposits.

Strong support for the landslide interpretation is provided by exposures in the Baxter open pit mine. In the south wall of the pit is an exposure of the contact between one of the sandstone units and a stratigraphically overlying brecciated Mesozoic intrusive rock unit. The contact is irregular and there is intermingling of substrate and landslide fragments. A meter above the contact is a lenticular mass of sandstone entrained within the Mesozoic rock. The contact's characteristics are unlike tectonic faults, but quite similar to known rock avalanche/substrate contacts.

The south- to southwest-tilted fluvial and landslide sedimentary package is probably Miocene in age. The highest landslide unit, which is south of the Mojave River and consists of metamorphosed Mesozoic volcanic and quartz sandstone rock, caps the package and is

conformably overlain by gray conglomerate interpreted to be the lower part of the Miocene terrestrial sedimentary and volcanic sequence exposed further west in Afton Canyon. Thus, the fluvial/landslide sequence appears to be the base of the Miocene section in the northern Cady Mountains.

Under the assumption that the crystalline Paleozoic and Mesozoic rock units are in-situ bedrock, several studies have utilized these units as markers for Paleozoic and Mesozoic paleogeographic reconstructions. Because the travel distance of these units as Miocene landslides is unknown, caution should be utilized in their use for such reconstructions.

Lithology, age, and paleomagnetic characteristics of the lower tuffaceous sequence in the Spanish Canyon Formation, Alvord Mountain, California

David C. Buesch, David M. Miller, and John W. Hillhouse

U.S. Geological Survey, 345 Middlefield Road, Menlo Park, California 94025

The 100-m thick, Miocene, Spanish Canyon Formation (SCF) can be traced about 9 km in the Alvord Mountain area, California, allowing for sampling of well-exposed stratigraphic sections for lithology, interpretation of paleo-environmental indicators, paleomagnetic properties, and geochronology. The SCF contains five lithostratigraphic sequences: (1) lower tuffaceous sequence, (2) lower arkosic sandstone and tuffaceous sequence, (3) upper tuffaceous sequence, which is primarily formed by the Peach Spring Tuff (18.78 ± 0.02 Ma from Ferguson and others, 2013), (4) upper arkosic sandstone sequence, and (5) olivine basalt lava and arkosic sandstone sequence. The lower tuffaceous sequence is well exposed in most locations, and was conformably deposited (with minor local channels) on either the Clews Formation or the Alvord Peak basalt. The 5- to 20-m thick, lower tuffaceous sequence represents the first main influx of tuffaceous material into the depositional basin. Most lower tuffaceous rocks have various amounts of pyroclastic grains including sanidine, plagioclase, quartz, and biotite fragments and (typically altered) glass shards and pumice clasts, and epiclastic grains including volcanic lithic clasts and fragments of plutonic or metamorphic bedrock including strained quartz, plagioclase, biotite, hornblende, and epidote. Typically, the lower tuffaceous sequence contains the following bedsets (from bottom to top): (1) fine-grained tuffaceous sandstone and/or ash or fine-grained pumiceous tuff, (2) very fine-grained, white ash that locally has interbedded thin, fine- to medium-grained tuffaceous sandstone, (3) tuffaceous sandstone, and (4) an erosionally resistant, pumiceous tuff or tuffaceous sandstone. Locally, one or two sequences of fine ash and tuffaceous sandstone occur above bedset #4. Interbedded with some of these deposits (especially bedset #2) are thin partings of mudstone. Many of the tuffaceous beds have

a tabular or very broadly lenticular geometry. Several deposits, especially the very fine-grained, white ash beds (bedset #2) locally have long, low-angle cross beds. Some of the ash might have been deposited as fallout tephra and some coarser-grained tuff beds as ignimbrites. However, the tabular to broadly lenticular beds, many with local mudstone partings, also are consistent with deposition in a broad, low-relief fluvial plain or shallow lacustrine environment.

Near the base of the lower tuffaceous deposits (between the bedsets #1 and #2) is a nonwelded to partially welded, gray ignimbrite, referred to informally as the “gray tuff”. The gray tuff is in the type section for the SCF as described by Byers (1960), and it occurs in several exposures at the base of bedset #2. Samples of the gray tuff and the overlying, pumiceous tuff or tuffaceous sandstone (bedset #4 and informally referred to as the “white tuff”) were analyzed to determine the paleomagnetic polarity and position within the Geomagnetic Polarity Time Scale (Hillhouse and Miller, 2011). Samples of the gray tuff and pumiceous tuff or tuffaceous sandstone (bedset #4) from the type section, as well as a newly measured sample of the very fine-grained, white ash (bedset #2) from 2.5 km to the southeast, are normally polarized and are correlated to the lower part of the upper normal-polarity part of chron C6 that ranges in age from 18.75 Ma to 19.72 Ma. The newly acquired age of the gray tuff from the type section is 19.6 ± 0.2 Ma using zircon U-Pb dating techniques. We analyzed 38 zircon grains from the sample, 22 grains are magmatic and from the chamber that produced the tuff, and 16 grains ranging in age from Cretaceous to Neoproterozoic are detrital or picked up during eruption processes.

We conclude that the lower part of the SCF is early Miocene in age, about 19.6 Ma, and represents deposition on a low-relief fluvial plain or shallow lake. The repeated influx of fine-grained ash beds and especially the more abundant tuffaceous sandstone or pumiceous tuff indicates deposition at the time of frequent local felsic eruptions.

References

- Byers, F. M., 1960, Geology of the Alvord Mountain Quadrangle, San Bernardino County, California: U. S. Geol. Surv. Bull. 1089-A, 71 p.
- Ferguson, C.A., McIntosh, W.C., and Calvin F. Miller, C.F., 2013, Silver Creek caldera—The tectonically dismembered source of the Peach Spring Tuff: Geology, v. 41, p. 3-6, first published on October 19, 2012, doi:10.1130/G33551.1.
- Hillhouse, J.W., and Miller, D.M., 2011, Magnetostratigraphy and tectonic rotation of the Miocene Spanish Canyon Formation at Alvord Mountain, California: in Reynolds, R.E., ed., “The Incredible Shrinking Pliocene”, California State University Desert Studies Consortium, p. 49-52.

An examination of the surface rupture gap associated with the 1992 Landers event south of the Johnson Valley Fault, San Bernardino County, California

David J. Crane

Chevron Oil, david.crane@chevron.com

The 1992 M_v7.3 Landers earthquake resulted in an 85 km long surface rupture, measuring up to 5 meters of right lateral slip along a north-south trending series of en echelon faults that lay to the east of the San Bernardino Mountains. Centered in Section 25 of T1N, R5E (SBBM) is a 5 km long ground rupture gap associated with this event. It lies where the surface trace of the Johnson Valley fault (JVF) projects southward, crossing perpendicular to the Pinto Mountain Fault (PMF), near the town of Yucca Valley, California. Here, the PMF delineates the northern edge of the East Transverse Range province and the southern edge of the Mojave Block. In contrast to the regional strike-slip faulting style common to the Mojave Block, field mapping in the crystalline outcrop in the gap region found an unusually unique family of faults, curvilinear about a vertical axis. Field evidence suggests, however, no slip occurred along these curvilinear faults during or following the Landers event. At the northern border of Section 25 this family of faults strike N20°W and rotate eastward in a progressive arc to a strike of N70°W where last seen at the eastern section boundary. Average dips range between 60° to 80° NE. Offsets in aplitic dikes cut by these faults and slickensided textures indicate the curvilinear faults are high-angle dip-slip. Results from Coseismic Interferogram analysis suggest warping of the regional stress field occurred within the gap region consistent with the curvilinear fault traces and implies the curvilinear faults likely parallel and mimic local warping of the rock stresses brought about by differences in the relative motion between the PMF and JVF.

Moderate to strong-seismic activity monitored over a fifteen year period during and following the Landers event shows inactivity to a depth of 3 km beneath the gap region. This leads to suggest ground rupturing south of the epicenter during the Landers event was arrested by the warping of the stress field within the gap region. This being the case, surface ruptures expressed on the Long Canyon, Burnt Mountain, and Eureka Peak Faults south of the gap region may result as sympatric movement following the initial event shock and may not have connection to the JVF, the site of the epicenter.

At depths greater than 3 km, a majority of seismic activity lie north of a plane plunging 77° N that originates at the surface trace of the PMF. This is consistent with the under-thrusting and uplifting of the Mojave Block by the East Transverse Range province along the surface trace of the PMF. Under-thrusting and uplift is also supported by the presence of high-angle reverse faults (newly named Sawtooth fault) along the central axis of the Sawtooth Range located juxtaposition and west of Section

25 and borders the PMF to the north. Field relationships imply warping within the gap region occurred with the activation of the San Andreas Fault and rotation of the East Transverse Range province, thus suggesting a late Neogene to Holocene age.

The area between the gap region and the JVF appears to be undergoing extension and pull apart. This is supported by the northeast-southwest strikes exhibited by the southern-most surface expressions in the JVF suggesting the gap region is tectonically locked.

Desert Survivors backpacking photographic potpourri

Robert Davis

www.riskingtoofar.com

Desert Survivors is an all-volunteer, non-profit organization committed to experiencing, sharing and protecting desert wilderness. Desert backpacking is one of this activity of this organization. These trips usually have a specific focus such as backcountry travel skills, wilderness monitoring, plants, animals, or archaeology. This talk will have photographs from the eastern Mojave Desert of arachnids, insects, reptiles, snakes and big mammals. There will be photographs of unusual and common plants, archaeological artifacts and structures, interesting rocks and geological formations, water sources, and scenic landscapes. Trips to find unusual plant locations and other remote sites will be discussed.

A summary of Pleistocene Lake Manly

Jeffrey Knott,¹ Lewis Owen,² Michael Machette,³ Ralph Klinger,⁴ and Kurt Frankel⁵

¹CSU Fullerton Dept. of Geological Sciences, Fullerton, CA; *jknott@fullerton.edu*, ²University of Cincinnati Dept. of Geology, Cincinnati OH, ³Retired, U.S. Geological Survey, Denver, CO, ⁴U.S. Bureau of Reclamation, Denver, CO, ⁵Deceased, Georgia Tech

Lake Manly is the name of the ancient lake that occupied Death Valley during glacial times. The existence of Lake Manly was suggested as early as 1885 and the long-standing hypothesis is that during the Last Glacial Maximum (LGM; about 20,000 years ago) Death Valley was filled by a deep lake. Lake Manly and other lakes and rivers in southeastern California were important dispersal pathways for pupfish and other animals. The debate over Lake Manly's size and age continues today; however, Lake Manly as a measure of past climate is of paramount importance. Death Valley is presently very hot and evaporation rates are very high, so it makes sense that a long-lived lake in Death Valley must represent a much cooler and wetter climate.

Over the last few decades, a number of studies have focused on the age of both Lake Manly and alluvial deposits throughout Death Valley. Combining these individual studies provides better insight into the history of Lake Manly. The Badwater core, drilled through the Death

Valley salt pan at about 80 m below sea level (bsl), determined that at the LGM Lake Manly was both shallow and saline. Alluvial fan deposits found 37 m bsl on Hanaupah fan with no evidence of lake erosion are ~70,000 years old. Similar deposits are found at 25 m bsl near Mormon Point, and <25,000 year old alluvial fans are found at 21 m bsl in southern Death Valley. The Beatty Beach bar complex, at 46 above sea level in north-central Death Valley, was dated at ~25,000 year by both radiocarbon and optically stimulated luminescence and at >100,000 years by cosmogenic nuclides. It seems plausible that the radiocarbon- and luminescence-dated materials may have been deposited much later and are therefore erroneous. Alluvial-fan deposits that overly the bar complex have been dated at ~70,000 years, indicating that the bar complex may be older than previously thought. In combination, these data indicate that during the LGM, Death Valley was a shallow, saline lake less than 60 m deep, much less than originally hypothesized.

So, how old are the prominent lake deposits around Death Valley? Cosmogenic nuclide surface exposure dates of lake gravels at Hanaupah fan are 130,000 years old; dated boulders at the Beatty Beach bar complex and near Artists Drive are >109,000 years old. In addition, fossil ostracodes from the Badwater core shows that Lake Manly was a freshwater lake ~140,000-180,000 years ago. Collectively, these data support the interpretation that the surface of Lake Manly was as high as 46 m above sea level ~140,000-180,000 years ago, which is coincident with the pre-Tahoe glaciation in the Sierra Nevada and Marine Isotope Stage VI in the oceans.

Earthshine

David K. Lynch

Thule Scientific

Earthshine (“ash light”, “ashen light”, “earthlight”, “ashen glow”, “Moonglow” or “old Moon in the new Moon’s arms”) (Figures 1-3) is sunlight reflected from the Earth to the dark side of the Moon, then back again to Earth¹⁻³ (Figure 4). Its origin was first explained by Leonardo da Vinci⁴ in the Codex Leicester between 1506 and 1510 (Figure 5). Earthshine has found a number of uses



Figure 1. Earthshine, new crescent and Venus in evening twilight.



Figure 2.. New crescent and earthshine dropping below local horizon.



Figure 3. Earthshine and new crescent taken through a small telescope. Image was taken using High Dynamic Range (HDR) photography and the sunlit limb has been digitally sharpened.

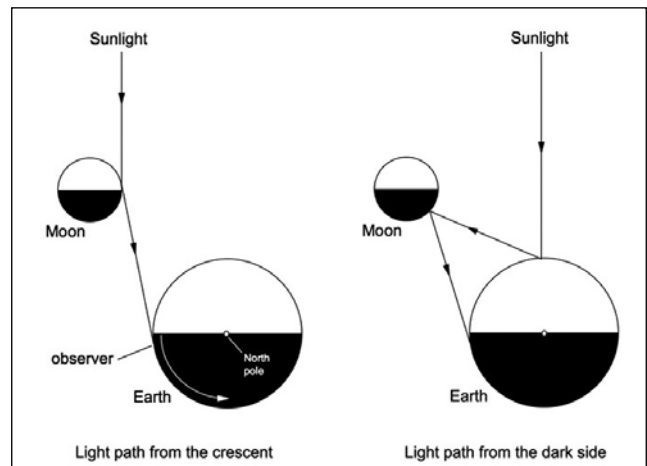


Figure 4. Left: Geometry of earthshine. Light from the sunlit crescent is scattered directly from the lunar surface to the observer. Right: Earthshine is sunlight reflected from the Earth to the dark side of the Moon, then back again to the observer on Earth.

including monitoring global cloud cover^{5,6}, and searching for extraterrestrial planets and life^{7,8}. It is also well represented in literature, art and folklore⁹.

Lunar crescents go hand-in-hand with earthshine. Both being faint and seen in twilight, many of the same factors that influence crescent visibility also affect earthshine

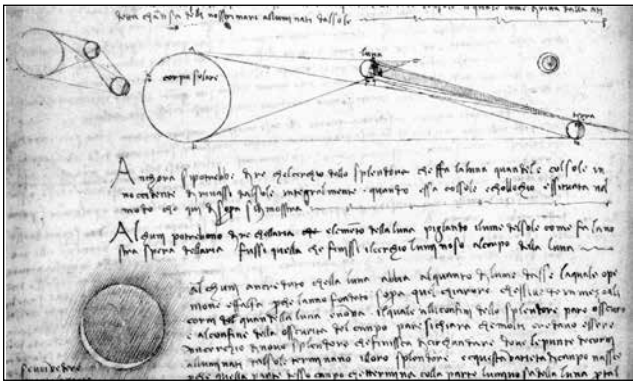


Figure 5. Page from Leonardo da Vinci's notebook giving the first correct explanation of the earthshine.

visibility. While much has been written about crescent visibility¹⁰⁻¹³ because of its religious importance, relatively little work has been done on earthshine visibility. In this paper I set forth a simple model of the earthshine using new lunar surface scattering functions that account for cratering and roughness.

References

1. Minnaert, M. G. J., 1954 *The Nature Of Light And Colour in the Open Air*, Dover, NY, originally published in 1939 in Dutch: *Licht en kleur in het landschap*.
2. Lynch, D.K. and W. Livingston 2001 *Color and Light in Nature* (2nd Edition), Cambridge University Press, Cambridge UK (2001) ISBN 0 521 77284 2 (hardback), 0 521 77504 3, now available from Thule Scientific, Topanga USA (2010) ISBN 978-0-9779935-1-5 (hardback)
3. Qiu J, Goode PR, Palle E, Yurchyshyn V, Hickey J, Rodriguez PM, Chu MC, Kolbe E, Brown CT, Koonin SE (2001). "Earthshine and the Earth's albedo: 1. Earthshine observations and measurements of the lunar phase function for accurate measurements of the Earth's Bond albedo". *Journal of Geophysical Research-Atmospheres* **108** (D22): 4709.
4. da Vinci, Leonardo, Codex Leicester (Sheet 2A, folio 2r), handwritten between 1506 and 1510.
5. Montanes-Rodriguez, P., E. Palle, P.R. Goode, J. Hickey, S.E. Koonin, 2005 "Globally integrated measurements of the Earth's visible spectral albedos", *Astrophys. J*, 629, 1175-1182,
6. Palle, E., P.R. Goode, P. Montanes-Rodriguez and S.E. Koonin, 2004 "Changes in the Earth's reflectance over the past two decades", *Science*, 304, 1299-1301, 2004a.
7. Ford, E. B., Turner, E.L. & Seager, S. (2001) "Characterization of extrasolar terrestrial planets from diurnal photometric variability" *Nature*, Volume 412, Issue 6850, pp. 885-887 <http://www.nature.com/nature/journal/v412/n6850/full/412885a0.html>
8. Sterzik, Michael F., Stefano Bagnulo & Enric Palle "Biosignatures as revealed by spectropolarimetry of Earthshine" *Nature* 483, 64-66 (01 March 2012)
9. Brunner, B. *Moon: A Brief History*, Yale University Press pp304 (2011)
10. Schaefer, B. E., 1988: "Visibility of the Lunar Crescent", *Quarterly Journal of the Royal Astronomical Society*, Vol. 29, pp. 511-523.

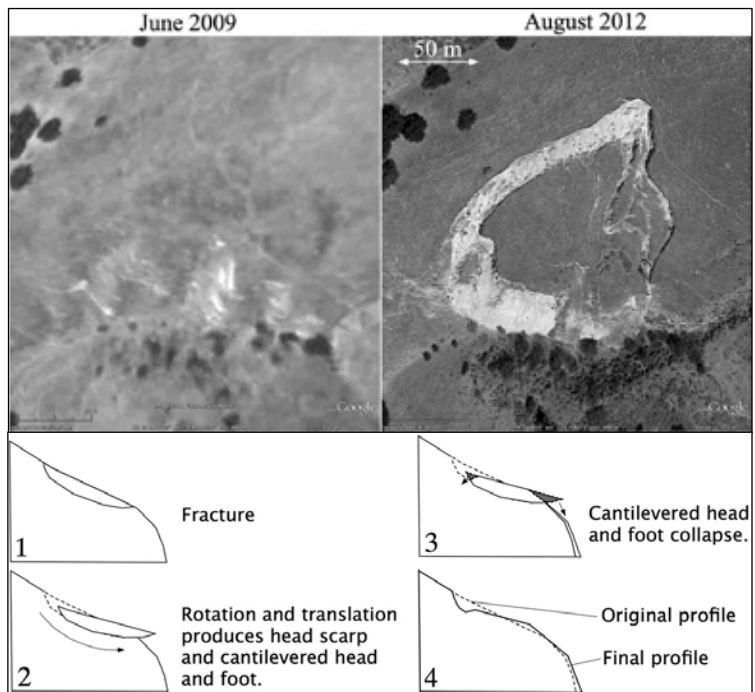
11. Schaefer, B. E., Ahmad, I. A., Doggett, L. E., 1993: "Records for Young Moon Sightings", *Quarterly Journal of the Royal Astronomical Society*, Vol. 34, pp. 53-56.
12. Ilyas, M., 1994: "Lunar Crescent Visibility Criterion and Islamic Calendar", *Quarterly Journal of the Royal Astronomical Society*, Vol. 35, pp. 425-461.
13. Doggett, L. E., Schaefer, B. E., 1994: "Lunar Crescent Visibility", *Icarus*, Vol. 107, pp. 388-403.

The Cheeseboro Ridge Landslide

David K. Lynch¹ and John R. Bayless²

¹Thule Scientific, ²First Point Scientific

Sometime between June 2009 and Aug 2012 a small landslide (120 m x 180 m) took place on a north-facing slope of Cheeseboro Ridge in the Santa Monica Mountains National Recreation Area near Agoura, CA. The slide is in south dipping (~35 degrees) Late Miocene Monterey (Modelo) Formation, a light gray-tan siltstone/claystone and shale. Visually, the light-colored rock contrasts sharply with the darker dense surface vegetation allowing clear delineation of different parts of the slide. Based on the unvegetated main scarp (vertical and 5.3m high), and sharp, near-vertical secondary scarps, it probably occurred after April 2012, the last major rain in the area. Much of the slide remained intact as it moved, though many transverse tension cracks are present. The overall direction of displacement was southerly, and parallel to the local bedding. Comparing field photos with those from Google Earth, the slide seemed to be actively creeping in late Jan 2013. Based on field observation and modeling, it appears to be a rotational rockslide that produced cantilevered sections that collapsed during the slide.



Architecture and nature—the desert is resilient when untouched but fragile when touched

Ilaria Mazzoleni and Berenika Boberska

berenika_b@hotmail.com

Luminous, fossilized network of an inhuman intelligence, of a radical indifference, —the indifference not merely of the sky, but of the geological undulations, where the metaphysical passions of space and time alone crystallize. Here the terms of desire are turned upside down each day, and night annihilates them. But wait for the dawn to rise, with the awakening of the fossil sounds, the animal silence.

AMERICA – Jean Baudrillard

The desert has always been a fascination to architects. The extreme beauty of this extreme environment: the vastness of space, the rarefied air and sharp light, colors, the mineral drama of fossilized time, the silence. To design thinkers the desert has always been about space and time —at its most luminous and pure. “Extraordinary Luminescence” is how Rayner Banham described the quality of light refracted by the salt flats in *Scenes in America Deserta*.

This very poetic inspiration is followed by a non-knowledge, in scientific terms, about the real desert environment. For example very few projects are inspired by the extreme diversity or the teeming nocturnal life of the desert. Humans have an anthropocentric understanding of the world while in order to inhabit such a space we would need to put ourselves in a different mindset. Helping creative thinkers in making that switch is science.

This paper presents two examples of a different approach, which invites science at the very inception of design process.

1. Biomimicry. Design inspired by the nature in terms of natural resources, performance, behavior, adaptation, but also spatial and atmospheric qualities. *The Desert Lizard Project*.

2. Touching the landscape lightly. How can we find ways to inhabit such a landscape, not only physically but also poetically and culturally? Learning from desert plant strategies: *The Tumbleweed Project. Scattered Readings*.

Given the continuous rise in population, designers are finding it more and more urgent to define how to inhabit fragile environments in appropriate ways. While starting from opposite point of view, collaboration between disciplines such as biology (observing) and design (making), requires first and foremost a semantic adjustment as well as flexible understanding (open mindedness) which is not common to everyone. However, in the complex world in which we live in, it is extremely necessary to bridge this gap and start the conversation. Sharing knowledge amongst the same field is only partially useful; interdisciplinary explorations between science and the creative fields is a must!

Plant derived mineral bodies as ecological, geobiological, and climatic indicators: a look at New Mexico plant communities

K. Morgan Edel,^{1,2} M. N. Spilde,³ and P. J. Boston,^{1,2}

¹ Earth & Environmental Sciences Dept., New Mexico Institute of Mining & Technology, Socorro, NM 87801 ; ² National Cave & Karst Research Institute, Carlsbad, NM 88222 ; ³ Institute of Meteoritics, University of New Mexico, Albuquerque, NM 87131

Phytoliths (or bioliths) are biologically produced minerals made by certain plants and provide mechanisms for plant structure and protection from predation. These siliceous and calcareous biogenic minerals are liberated from the plant during decay and are deposited in the surrounding soils and sediments. Depending on mineral durability, the phytoliths remain in the environment long after the plants, providing a biosignature of past ecological conditions. Aeolian and hydrological events can transport these biominerals away from their native habitat to other locations including caves. Deposition of these biominerals in caves allows their preservation to continue without the destructive effects of UV radiation, extreme climate fluctuations, weather events, or changes in moisture.

Today, New Mexico has many diverse ecosystems ranging from desert shrublands/grasslands, riparian zones, to forests and woodlands whose plant communities differ based on elevation and available moisture. Some New Mexican species have ranges that also extend into neighboring deserts and are included in plant assemblages of the Sonoran, Mojave, and Great Basin deserts. In this study, plants from riparian areas, desert scrubland, mixed conifer and ponderosa forest were collected to make a library of their biominerals. All plant samples were ashed in a muffle oven at 500-600 C for 2-4 hours depending on sample type. Biominerals were identified from the ash by optical microscopy, scanning electron microscopy (SEM), and energy dispersive spectral analysis (EDS). Sediment samples were collected from sections of Fort Stanton Cave/Snowy River, Lincoln County, NM, then sorted by particle size, and the biominerals were separated using heavy liquid floatation with sodium polytungstate (SPT). Results show a diversity of morphologies and both siliceous and calcareous minerals.

Very limited biomineral research has been done in New Mexico, thus our efforts are significantly increasing the available data. The results of our studies can be useful in comparison with other desert and mountain ecosystems. Calcic phytoliths are very understudied in all environments, and interestingly were observed in almost every plant that we have analyzed. Clearly, more study on calcium mineralogy and plant function is needed, especially in arid land species.

Silica phytoliths were also present in a lot of the study plants. Although better understood than calcic bodies, more study on the function of silica in desert and other arid land plants is necessary. In addition, mineral availability in the environment may be a limiting factor on

whether plants can make these biominerals in the first place. Further, identifying biominerals from cave flood deposits can reveal the hydrogeological history and other geomorphological processes of significance to today's environmental issues including climate change and hydrological resources.

U-Pb SHRIMP-RG dating of fault-related opals from the Eastern California Shear Zone

Perach Nuriel,¹ Kate Maher,¹ and David M. Miller²

¹ Department of Geological and Environmental Sciences, Stanford University, CA 94305, USA; ² U. S. Geological Survey, 345 Middlefield Road, MS-973, Menlo Park, CA 94025, USA

Absolute time constraints for fault activity are of fundamental importance in active fault systems in order to estimate long-term slip-rates and earthquake recurrence intervals required for seismic-hazard assessments. Here we present a novel methodological approach for direct dating of paleoearthquakes using *in situ* U-Pb SHRIMP-RG (Sensitive High Resolution Ion Microprobe – Reverse Geometry) analyses of syntectonic opal precipitates in fault segments within the Eastern California Shear Zone (ECSZ). The Mojave Desert fault segments within the ECSZ are ideal faults to investigate the long-term history because of the need for improved constraints on long-term strain accumulation rates.

We documented and sampled fault-related opals from 5 different fault exposures within the northwest-striking Camp Rock (near Daggett Ridge) and the east-striking Cave Mountain (near Alvord Mountain) fault systems. Faults displaying several meters of horizontal displacement and visible slickenlines are either coated or filled with opal material, ranging from 0.5 to 10 cm thick. Individual outcrops are from 2 to 15 meters long, and exhibit highly brecciated and sheared bands within the opal coating and filling material that can be traced along the faults. Opal samples are characterized by high U concentrations and are thus favorable for *in situ* dating.

Preliminary U-Pb results suggest that the two fault systems were active between 1.5 and 0.2 Ma. Additional analyses of syntectonic opals, taken from several sites, and from additional faults in each system can potentially provide a long-term record of the deformational history of the fault systems and contribute to our understanding of how strain is being distributed over a geological time scale.

Sex behind closed doors: high genetic diversity found in the clonal Mojave Desert moss *Syntrichia caninervis* using microsatellite markers

Amber Paasch,¹ Kirsten Fisher,¹ Brent Mishler,² and Lloyd Stark³

¹California State University, Los Angeles, 5151 State University Drive, La Kretz 351, Los Angeles, CA 90032, aepaasch@gmail.com; ²University of California, Berkeley; ³University of Nevada, Las Vegas

Syntrichia caninervis is the dominant biotic crust bryophyte in the Mojave Desert, and because of its sex ratios, is an anomaly in the plant world. This extreme arid-dwelling moss is dioicous, and reduces production of sexual organs under stressful climate conditions, i.e., high temperatures and low precipitation. When sex is expressed, the ratio between males and females is skewed. The cause is unknown, but females seem to be more tolerant of high temperatures and low precipitation than males. These sex ratios differ between elevations, with the highest elevation populations having a ratio of 14 females to 1 male, and no male sex expression observed in the more stressful lower elevation populations, indicating that sexual reproduction is infrequent. Lack of sex expression can mean lack of sexual reproduction, which could lead to a loss of genetic diversity, ultimately impacting the desert ecosystem. To assess genetic diversity between sex expressing and sexless populations of *S. caninervis*, samples from two sex-expressing sites and two sexless sites at the eastern and western edges of the Mojave Desert were collected. Eight novel microsatellite markers we developed were used to genotype ninety-six plants from each population. A total of 185 haplotypes were identified, with haplotype diversity, mean alleles per locus, number of multilocus genotypes, genotype diversity and clonal evenness being high at each site. AMOVA analysis shows *S. caninervis* has high levels of differentiation and restricted gene flow between populations. Genetic diversity was not lower in the absence of sex expression. These data represent the first characterization of genetic diversity in *S. caninervis*. Understanding the genetic structure of this unique species is helping to clarify the impact of asexual reproduction on genetic diversity in desert mosses.

Mapping plant responses to channel-water input in on a disturbed Mojave Desert alluvial fan

Aimee Roach, Miguel Macias and Darren R. Sandquist

Department of Biological Science, California State University, Fullerton, 800 N State College Blvd, Fullerton, CA 92834

Water is a precious resource in the harsh climate of the Mojave Desert. Complex networks of alluvial drainage channels (washes) guide rainwater down from desert mountains, providing water to plants throughout desert bajadas. However, roads, railroads, and other anthropogenic features cut across the natural landscape, creating

barriers to the even distribution of water to plants from the alluvial channels. In addition, railroad culverts consolidate and channel large amounts of water from upslope, creating large channels down-slope from the railroad. Such changes in water distribution can potentially alter the biotic community structure of the area immediately surrounding these channels, with plants near the channel edges growing larger due to more water availability than plants growing away from the channel margins. The physiological responses of plants at various distances around both anthropogenically impacted and non-impacted washes were examined by measuring the pre-dawn water potential, stomatal conductance, and sap flow of *Larrea tridentata* individuals at three alluvial channels in the Mojave National Preserve. In this study, land survey-grade GPS devices were used to accurately map the positions of the sampled plants as well as the study channel margins. Using the geospatial analysis technique of kriging, the measured physiological responses were used to interpolate water potential, stomatal conductance, and sap flow values of un-sampled plants around the study area channels. This method can be used to predict plant responses across the alluvial fan landscape based on channel distribution and their disturbance.

Tracks of dinosaurs, synapsids, and arthropods in the Aztec Sandstone of Southern Nevada: a progress report

Heather M. Stoller and Stephen M. Rowland

Department of Geoscience, University of Nevada, Las Vegas, Las Vegas, NV 89154-4010, stollerh@unlv.nevada.edu, steve.rowland@unlv.edu

The Aztec Sandstone (Lower-Middle Jurassic) is a 700-m-thick, sand-dune-desert deposit. Until very recently, southern Nevada exposures of the Aztec Sandstone have yielded few fossil tracks, although correlative strata in eastern California and Utah are quite fossiliferous. That situation has changed dramatically within the past two years, and now approximately twenty separate Aztec tracksites are known in southern Nevada. Most of these sites have been reported to us by observant, backcountry hikers and rockclimbers who have become attentive to the presence of fossil tracks. Most of the recently discovered tracksites occur in Red Rock Canyon National Conservation Area (RRCNCA), immediately west of Las Vegas, although several are located in Valley of Fire State Park, and one is in the Gold Butte area. Here we present a progress report of our ongoing systematic study of tracks in the Aztec Sandstone of southern Nevada.

Dinosaur tracks occur at eight of the sites, sometimes in combination with arthropod and/or synapsid tracks. The dinosaur tracksites are widely variable in terms of preservation and animal behavior. One site consists of a single, well-preserved footprint; another tracksite consists of a distinct trackway of seventeen closely-space tracks; another consists of multiple trackways, oriented in various

directions, in which the individual footprints are very far apart; and a fourth tracksite consists of dozens of poorly preserved undertracks, most of which are oriented in the same direction. Other dinosaur tracksites display variable numbers of tracks in variable states of preservation. All of the dinosaur tracks are relatively small—fourteen cm or less in length—and are inferred to have been made by small, bipedal, carnivorous, theropod dinosaurs.

We have found three types of non-dinosaur, mammaloid tracks. The most abundant of these are assigned to the ichnogenus *Brasilichnium*. Two other types of non-dinosaur vertebrate tracks are not yet identified and may belong to undescribed ichnotaxa. The trackmakers of *Brasilichnium* and the other mammaloid tracks were probably therapsids (“protomammals”).

Arthropod tracks are present at several sites. These include several examples of the scorpionid track *Paleohelcura*, some of which display a tail drag and some do not. The ichnogenus *Octopodichnus*, possibly made by a tarantula-size arachnid, is present at only one of our sites. *Paleohelcura* and *Octopodichnus* are well-known Permian and Mesozoic arthropod tracks.

Additional tracksites will almost certainly be discovered. As we develop a better understanding of the variety, relative abundance, and stratigraphic distribution of fossil tracks in the Aztec Sandstone, we will be better able to reconstruct the structure of the Jurassic desert ecosystem in which the trackmakers lived.

Foraging behavior of kangaroo rats at artificial seed trays revealed by giving-up densities and remote cameras

D. Tennant and P. Stapp

California State University, Fullerton, Department of Biological Sciences, Fullerton, CA, 92831. dylantee@csu.fullerton.edu

Behavioral ecologists are sometimes forced to use indirect approaches to understand foraging decisions of secretive animals, such as rodents. Many foraging experiments have measured rates of seed removal by rodents in artificial trays to estimate giving-up densities (GUDs), but few studies have investigated the diversity of species visiting the trays, the number of individual visitors, and amount of time they spend in the tray. Foraging activity of the desert kangaroo rat (*Dipodomys deserti*) was documented at seed trays in the Mojave Desert in summer 2012. We used Reconyx PC800 IR-flash wildlife cameras to quantify how rates of seed removal were affected by amount of seed provided, number of foragers, and duration of foraging bouts. The number and frequency of visits were affected by variation in initial seed densities in seed trays: foragers made more visits more often to richer patches. Higher seed densities resulted in higher rates of seed removal and longer durations of first visit. Foragers were able to remove >70% of the seeds in a tray over the course of the night in three out of the four treatments. All of these results

emphasize the efficiency with which kangaroo rats forage. Furthermore, our results suggest that additional, essential information can be gathered from the use of applying new technology to long-standing methodologies.

Picacho and the Cargo Muchachos—gold, guns, and geology of eastern Imperial County, California

Carole L. Ziegler and Todd A. Wirths

San Diego Association of Geologists, cziegler@swccd.edu

The San Diego Association of Geologists has recently celebrated their 40th anniversary with the publication of their latest guidebook, *Picacho and the Cargo Muchachos—Gold, Guns, and Geology of Eastern Imperial County, California*. This guidebook covers an area that has been somewhat neglected for the past few decades in the literature, as it sits in a rather remote corner of the southeastern California desert. However, the region is probably the site of the first attempt at gold mining in North America, in a district known as Potholes. Today, one of the largest gold mines in the U.S., New Gold’s Mesquite Mine, is operating nearby.

Mining has always come with a rough and tumble crowd and some of that history is also reprised here with recent and past articles, including a personal visit with Ernie Mendivil, the great-grandson of José Maria Mendivil who, in 1861, discovered gold at what is now known as the Picacho Mine.

The guidebook is dedicated to Dr. Gary Girty, Professor of Geology at San Diego State University, who has been carrying out extensive research in the Picacho area along with his many graduate students. This research has culminated in a spectacular geologic map of the area, of which a version is found in the guidebook, and presents the newly described Copper Basin Fault found within the Picacho State Recreation Area.

